

Cover Page



Universiteit Leiden



The handle <http://hdl.handle.net/1887/39834> holds various files of this Leiden University dissertation.

Author: Bruin, G. de

Title: Chemical tools to monitor and control human proteasome activities

Issue Date: 2016-06-01

Chemical tools to monitor and control human proteasome activities

PROEFSCHRIFT

ter verkrijging van

de graad van Doctor aan de Universiteit van Leiden,

op gezag van Rector Magnificus prof. mr. C.J.J.M. Stolker,

volgens het besluit van het College voor Promoties

te verdedigen op 1 juni 2016

klokke 13:45 uur

door

Gerjan de Bruin

geboren te Nunspeet in 1988

Promotiecommissie

Promotor	Prof. dr. H.S. Overkleeft Prof. dr. G.A. van der Marel
Co-promotor	Dr. B.I. Florea
Overige leden	Prof. dr. C. Driessen, Kantonsspital St. Gallen, Zwitserland Prof. dr. M. Groll, Technische Universität München, Duitsland Prof. dr. H. Ovaa Prof. dr. J. Brouwer Dr. A.F. Kisselev, Dartmouth Medical School, Verenigde Staten Dr. C.R. Berkers, Universiteit Utrecht

Table of contents

Chapter 1	7
General introduction	
Chapter 2	15
Tools and strategies to monitor and quantify proteasome activities	
Chapter 3	35
A set of activity-based probes to visualize human (immuno)proteasome activities	
Chapter 4	63
Systematic analyses of substrate preferences of 20S proteasomes using peptidic epoxyketone inhibitors	
Chapter 5	93
Structure-based design of either β 1i or β 5i specific inhibitors of human immunoproteasomes	
Chapter 6	137
Development of β 1i and β 5i selective activity-based probes	
Chapter 7	153
Development of an inhibitor and activity-based probe selective for β 5c	

Chapter 8	177
Development of an inhibitor and activity-based probe selective for β 1c	
Chapter 9	185
Towards β 2 selective inhibitors with reduced basicity	
Chapter 10	211
A native-PAGE FRET assay that reports on mammalian proteasome core particle composition	
Chapter 11	235
Enantioselective synthesis of adamantylalanine and carboranylalanine and their incorporation into the proteasome inhibitor bortezomib	
Chapter 12	255
Summary and future prospects	
Samenvatting	275
List of publications	283
Curriculum Vitae	286

CHAPTER 1

General introduction

The proteasome

Proteasomes are multi-catalytic, multi-protein complexes that are found in all eukaryotic cells and are responsible for the majority of intracellular protein degradation. Proteins destined for degradation are tagged with a polyubiquitin chain, which is recognized by the 19S caps of 26S proteasomes (Figure 1A).¹ Following ubiquitin-chain removal and unfolding, the protein is translocated to the 20S core particle (CP), in which the proteolytic activity resides. 20S CPs consist of four heptameric rings, two outer α -rings and two inner β -rings, of which β 1, β 2, and β 5 are catalytically active (Figure 1A).² The peptide backbone of the protein substrate is aligned in the β -subunit binding channel and the amino acid side chains (indicated by P) interact with the substrate binding pockets (indicated by S), which define the substrate specificity of the β -subunits (Figure 1A). The active β -subunits have an active site N-terminal threonine residue, which coordinates to a water molecule (Figure 1B).³ The threonine hydroxyl group attacks the scissile peptide bond, resulting in cleavage of the peptide bond under formation of a proteasome substrate ester bond which is cleaved through attack of an activated water molecule.

In vertebrates, all cells express the constitutive proteasomes (cCP) of which the active subunits are termed β 1c, β 2c, and β 5c. The substrate-binding channel C-terminal of the scissile peptide bond of a substrate is termed the non-primed site and the N-terminal part is termed the primed site. The substrate binding pockets of the active subunits differ in size, hydrophobicity and charge, which result in varying substrate specificities. The non-primed substrate binding pockets are considered to be determinative for the substrate preferences of the active β -subunits. β 1c preferentially cleaves after C-terminal acidic amino acids and is therefore termed caspase-like, β 2c prefers basic amino acids at P1 and is therefore termed trypsin-like and β 5c is chymotrypsin-like, since it cleaves preferentially after hydrophobic amino acids. Part of the peptides generated by proteasomes are loaded onto major histocompatibility complex class I (MCH-I) and presented on the cell surface to cytotoxic T-cells. Lymphoid tissues

and cells that are exposed to inflammatory cytokines express an additional proteasome type, namely the 20S immunoproteasome (iCP) in which $\beta 1c$, $\beta 2c$, and $\beta 5c$ are replaced by $\beta 1i$, $\beta 2i$, and $\beta 5i$.⁴ These immunoproteasome subunits exhibit slightly changed substrate specificities and produces peptides with higher affinity for MHC-I. Cortical thymic epithelial cells express a third proteasome type, namely the thymoproteasome (tCP) which play an important role in positive T-cell selection.⁵ tCPs contain the same catalytic active subunits as iCPs, with the exception that $\beta 5i$ is replaced by $\beta 5t$.

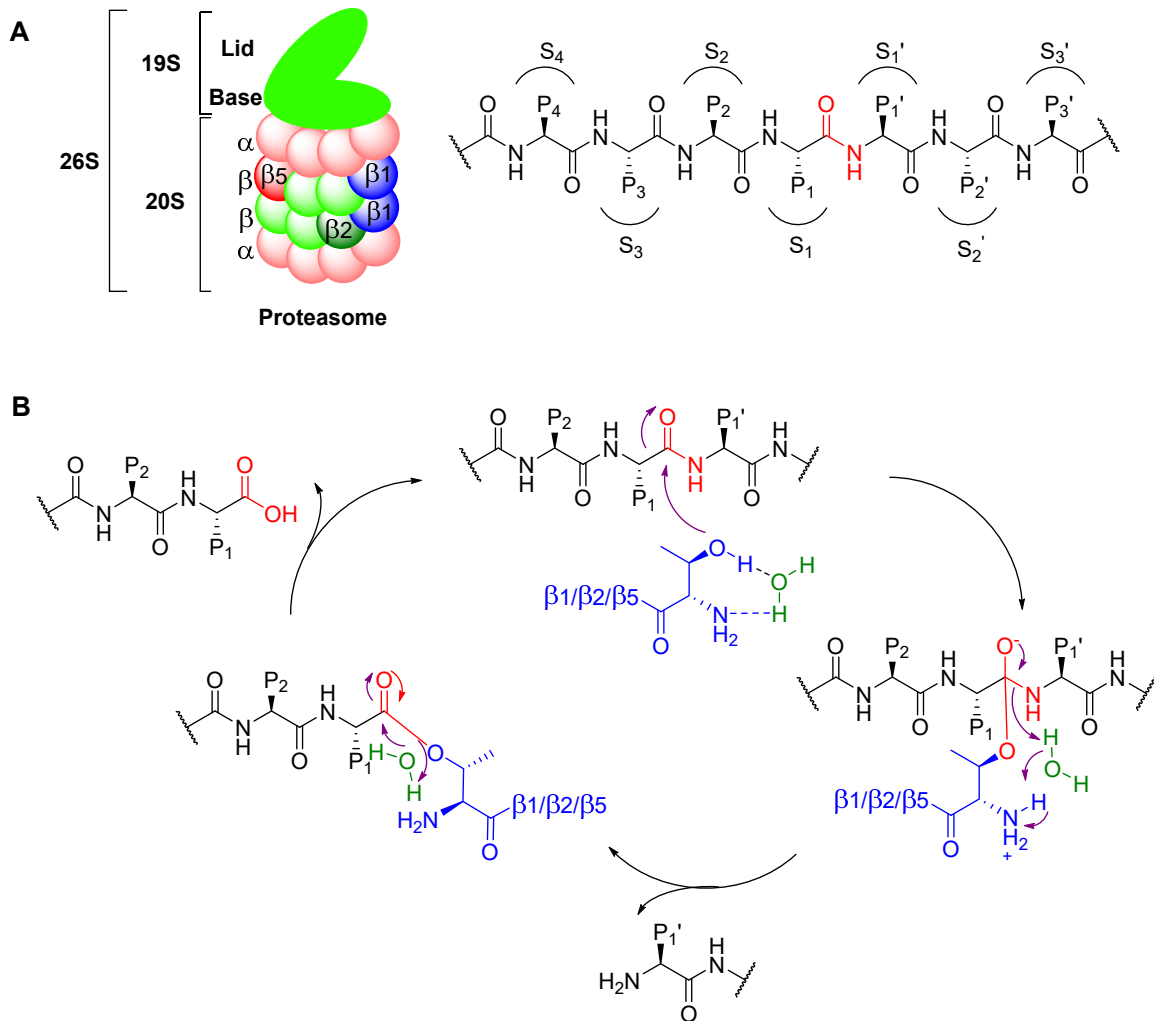


Figure 1. The proteasome. A) Schematic representation of the 26S proteasome and the substrate binding channel. B) Catalytic mechanism of peptide bond hydrolysis by the proteasome. 'P' indicates position with respect to the scissile peptide bond, 'S' indicates position of substrate binding pocket. Prime indicates primed sites. Red: scissile peptide bond, blue: active site threonine.

Proteasome inhibitors

Proteasomes are important drug targets in the field of oncology and immunology. Proteasome inhibitors are currently used or in development for the treatment of various cancers (such as multiple myeloma and mantle cell lymphoma) and several auto-immune diseases.⁶⁻⁸ The last decades, several proteasome inhibitors (PIs) have been discovered from nature and numerous have been synthesized for drug discovery purposes. PIs are often N-terminally capped di-, tri- or tetrapeptides with a C-terminal electrophilic trap, also termed warhead.⁹ The peptide part of the inhibitor interacts with the non-primed part of the substrate binding channel, thereby positioning the warhead close to the catalytic active threonine residue. When the inhibitor is sufficiently stabilized by the substrate binding channel, the warhead may react to the active site threonine residue, in a reversible or irreversible fashion depending on the nature of the warhead. The mechanisms of four widely used warheads are depicted in Figure 2, namely aldehydes, boronic acids (both reversible), epoxyketones and vinyl sulfones (both irreversible).

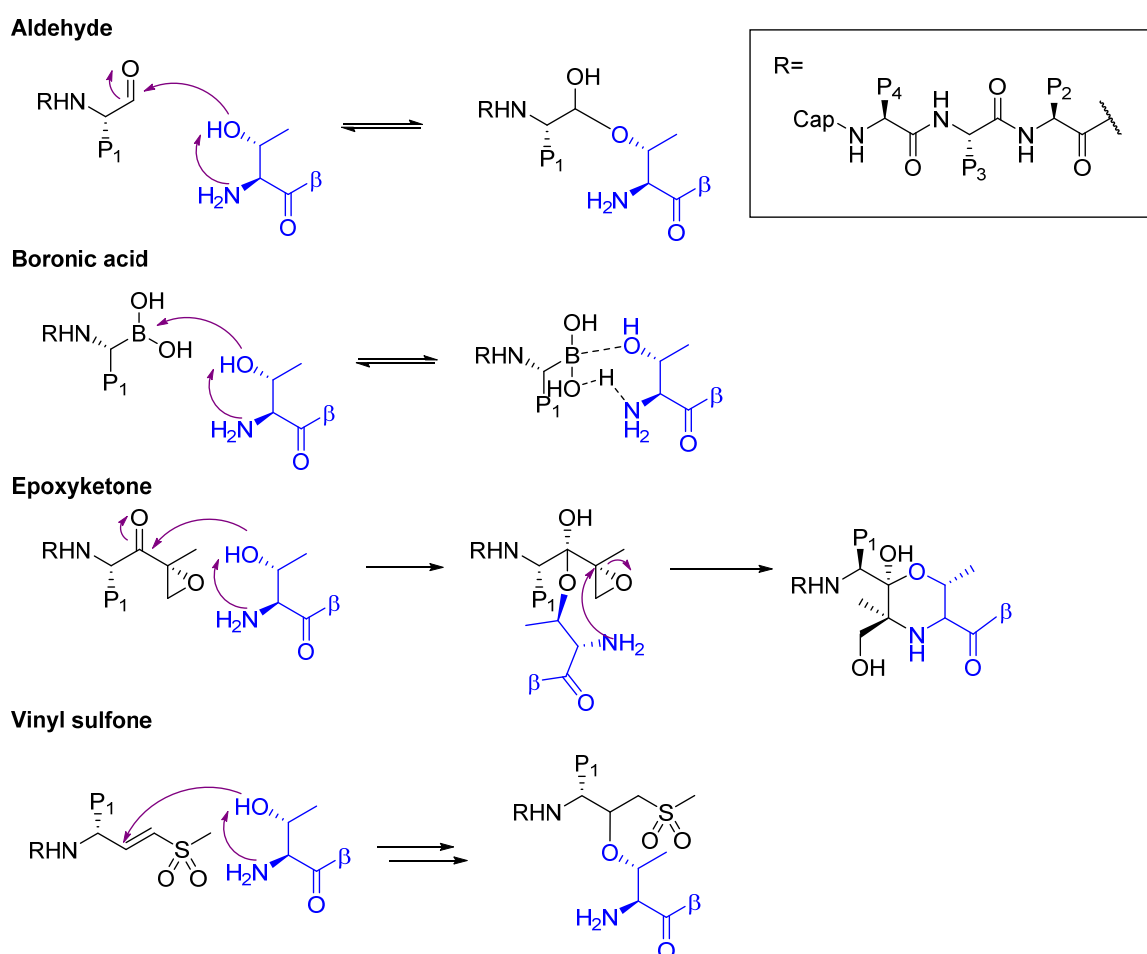


Figure 2. Mechanisms of aldehyde, boronic acid, epoxyketone and vinyl sulfone electrophilic traps.

Aldehydes form a hemiacetal with the N-terminal threonine residue of active proteasome subunits. However, the main disadvantage of aldehydes is their cross-reactivity towards cysteine proteases.¹⁰ Boronic acids are found in various clinical drugs and candidates, and form a tetrahedral adduct with the active site threonine.¹¹ The clinical drug carfilzomib is equipped with an epoxyketone, which react irreversibly with the active site threonine residue by forming a morpholine adduct.¹² Epoxyketones are highly specific for proteasomes and no off-targets have been found to date. Vinyl sulfones have initially been used as cysteine protease inhibitors, but were found to also inhibit the proteasome. The hydroxyl moiety of the active site threonine reacts irreversibly with the vinyl sulfone via a conjugate addition.¹³

In the last decades, many proteasome inhibitors have been synthesized with the aim to obtain PIs that can be used as drugs or research tools. In particular, much research has been directed to the discovery of subunit selective inhibitors. Proteasome inhibitors can also be equipped with a reporter group, such as biotin or a fluorescent moiety. The resulting activity-based probes (ABPs) can report on the proteasome activity. Proteasome targeting ABPs can be used in competitive activity-based protein profiling (ABPP) to screen for new proteasome inhibitors, to quantify the relative amount of proteasomes in a given samples and to provide insight in proteasome composition.

Aim and outline of this thesis

This thesis describes the development of multiple subunit-selective proteasome inhibitors and ABPs that can be used to determine the role of the individual proteasome subunits in biological processes such as antigen presentation and cancer. Moreover, an ABPP assay is described that enables rapid assessment of the activity of all catalytic active subunits of the cCP and iCP. Furthermore, an ABPP-fluorescence resonance energy transfer (FRET)-based assay is described that provides insight in proteasome composition.

Chapter 2 provides a comprehensive overview of the ubiquitin-proteasome system and tools to monitor and quantify proteasome activity. Two main strategies that are employed to assay proteasome activity are substrate hydrolysis and ABPP. Both approaches are explained in detail and methods based on these strategies are discussed.

Chapter 3 describes the development of an ABP cocktail that enables full resolution of all catalytic active subunits of human cCPs and iCPs on SDS-PAGE. This ABP cocktail can be used in competitive ABPP to screen for new proteasome inhibitors and to quantify the relative amounts of individual proteasome subunits in for instance primary patient cells. This chapter also describes a complete set of subunit selective inhibitors. The development of $\beta 5i$, $\beta 1i$, $\beta 5c$ and $\beta 1i$ selective inhibitors are described in the following chapters.

Chapter 4 provides a systematic analysis of the substrate preference of yeast proteasomes (γ CP) and human cCPs and iCPs. For this study, only proteinogenic amino acids were used in order to determine the natural substrate preferences of proteasome subunits. A series of tri- and tetrapeptide epoxyketones bearing different amino acids at P1, P2 and P3 were synthesized. Crystal structures of these inhibitors bound to γ CPs were determined, revealing important insights which were further exploited to develop subunit selective inhibitors, as is described in the following chapters.

Chapter 5 describes the design and synthesis of β 5i and β 1i selective inhibitors. Based on murine proteasome crystal structures it was reasoned increasing the steric bulk at P1 would result improved β 5i selectivity. Various non-proteinogenic bulky amino acids were incorporated, of which only cyclohexylalanine provided increased β 5i selectivity. Using a similar strategy, a highly selective β 1i inhibitor was discovered. The β 5i and β 1i selective inhibitors could be used to completely inhibit β 5i or β 1i in cell lysates and living cells, without co-inhibition of the other subunits. Both β 5i and β 1i selective inhibitors were equipped with a fluorescent group and the resulting ABPs were highly selective for the corresponding subunits, as is described in **chapter 6**.

In contrast to β 5i, β 5c prefers large residues at P3 and small residues at P1, as was hypothesized from murine proteasome crystal structures. **Chapter 7** describes the synthesis of a small library of inhibitors with large, non-proteinogenic amino acids at P3 and leucine or alanine at P1. It was found that the combination of bicyclohexylalanine at P3 and alanine at P1 provided the highest β 5c selectivity. Eventually, a β 5 selective inhibitor was developed that can be used to completely inhibit β 5c in cell lysates and living cells, without co-inhibition of the other subunits. In addition, an ABP that is selective for β 5c over β 5i was synthesized.

Based on the finding that aspartic acid at P1 provides β 1c selectivity, as described in chapter 4, in **chapter 8** the development of a potent and selective β 1c inhibitor and ABP is described. This inhibitor can be used to inhibit β 1c in cell lysate, however, not in intact cells since the compound proved to be cell impermeable.

Basic residues at P1 and P3 induce β 2c/ β 2i selectivity. LU-102, the most selective and potent β 2c/ β 2i inhibitor known to date, showed impaired activity in living cells compared to cell lysates. This reduction in activity is likely caused by loss of cell permeability as result of its net positive charge at physiological pH. **Chapter 9** describes the incorporation of basic amino acids with reduced basicity in peptide vinyl sulfone proteasome inhibitors in order to identify a β 2c/ β 2i selective inhibitor with improved cell permeability. The enantioselective synthesis of several lysine analogues and their incorporation into proteasome inhibitors is described. All synthesized inhibitors showed severe loss of activity compared to LU-102.

Chapter 10 describes a gel-based FRET assay to provide insight in proteasome composition. In addition to cCPs and iCPs, mixed proteasomes (mCPs) exist, in which constitutive- and immunoproteasome subunits are incorporated. With the aid of the subunit selective inhibitors and ABPs described in the previous chapter specific FRET signals between different subunit pairs could be measured, which indicate the presence of mCPs. This method provides rapid insight in the types of mCPs that are present in any crude cell lysate.

Chapter 11 describes the enantioselective synthesis of adamantylalanine and carboranylalanine and their incorporation at the P2 position of bortezomib. The resulting compounds proved to be potent proteasome inhibitors and displayed high off-rates and slight β 5i selectivity.

Chapter 12 provides a summary of this thesis and points at directions for further research.

References

1. Hershko, A. & Ciechanover, A. The ubiquitin system. *Annu. Rev. Biochem.* **67**, 425-79 (1998).
2. Löwe, J. et al. Crystal structure of the 20S proteasome from the archaeon *T. acidophilum* at 3.4 Å resolution. *Science* **268**, 533-9 (1995).
3. Marques, A.J., Palanimurugan, R., Matias, A.C., Ramos, P.C. & Dohmen, R.J. Catalytic mechanism and assembly of the proteasome. *Chem. Rev.* **109**, 1509-1536 (2009).
4. Groettrup, M., Kirk, C.J. & Basler, M. Proteasomes in immune cells: more than peptide producers? *Nat. Rev. Immunol.* **10**, 73-8 (2010).
5. Murata, S., Takahama, Y. & Tanaka, K. Thymoproteasome: probable role in generating positively selecting peptides. *Curr. Opin. Immunol.* **20**, 192-6 (2008).
6. Zhang, J., Wu, P. & Hu, Y. Clinical and marketed proteasome inhibitors for cancer treatment. *Curr. Med. Chem.* **20**, 2537-51 (2013).
7. Dou, Q.P. & Zonder, J.A. Overview of proteasome inhibitor-based anti-cancer therapies: perspective on bortezomib and second generation proteasome inhibitors versus future generation inhibitors of ubiquitin-proteasome system. *Curr. Cancer Drug Targets* **14**, 517-36 (2014).
8. Kisselev, A.F. & Groettrup, M. Subunit specific inhibitors of proteasomes and their potential for immunomodulation. *Curr. Opin. Chem. Biol.* **23**, 16-22 (2014).
9. Kisselev, Alexei F., van der Linden, W.A. & Overkleeft, Herman S. Proteasome inhibitors: an expanding army attacking a unique target. *Chem. Biol.* **19**, 99-115.
10. Rentsch, A. et al. Synthesis and pharmacology of proteasome inhibitors. *Angew. Chem. Int. Ed.* **52**, 5450-5488 (2013).
11. Groll, M., Berkers, C.R., Ploegh, H.L. & Ovaas, H. Crystal structure of the boronic acid-based proteasome inhibitor bortezomib in complex with the yeast 20S proteasome. *Structure* **14**, 451-456 (2006).
12. Groll, M., Kim, K.B., Kairies, N., Huber, R. & Crews, C.M. Crystal structure of epoxomicin:20S proteasome reveals a molecular basis for selectivity of α' , β' -epoxyketone proteasome inhibitors. *J. Am. Chem. Soc.* **122**, 1237-1238 (2000).
13. Bogoy, M. et al. Covalent modification of the active site threonine of proteasomal β subunits and the *Escherichia coli* homolog HsIV by a new class of inhibitors. *Proc. Natl. Acad. Sci.* **94**, 6629-6634 (1997).

CHAPTER 2

Tools and strategies to monitor and quantify proteasome activities

Introduction

The ubiquitin-proteasome system (UPS) degrades 80 to 90% of all proteins inside eukaryotic cells.¹ Proteins destined for degradation are tagged with a polyubiquitin chain.² In the first step of events leading to protein ubiquitination, ubiquitin (Ub), a small (8 KDa) protein, reacts with ATP to form the C-terminal mixed anhydride, ubiquitin-AMP (Figure 1). This process is catalysed by E1 Ub-activating enzymes that subsequently react with ubiquitin-AMP to form a ubiquitin C-terminal thioester involving an E1 active site cysteine thiol. Next and through trans-esterification, Ub is transferred to E2 Ub-conjugating enzymes. E3 ubiquitin ligases bind simultaneously to a specific combination of a substrate and an E2-Ub and catalyse the formation of an isopeptide bond between the ϵ -amine of a substrate lysine and the C-terminus of Ub (Figure 1). The human genome encodes for two E1-activating enzymes, dozens of E2-conjugating enzymes and hundreds of E3 ligases, which together ensure tight regulation of ubiquitin signalling. Poly-Ub chains can be formed by sequential ligations of Ub to either Lys6, 11, 27, 29, 33, 48 or 63 of an Ub residue attached to a substrate. Of these assemblies, Lys48 poly-Ub chains serve as a signal for degradation by proteasomes, which are multi-catalytic, multi-subunit protease complexes responsible for protein degradation.³ Alternative poly-Ub chains serve to guide a number of physiological processes unrelated to protein degradation. Proteasomes are composed of a 20S core particle (CP) that is capped by one or two 19S regulatory particles (RPs). RPs recognise poly-Ub chains, remove these and promote unfolding and translocation of the substrate into the hollow-cylindrical shaped CP, where protein degradation takes place (Figure 1). Proteins are processed into 3-12 amino acid peptides, which can be further degraded by aminopeptidases into single amino acids.⁴ About 1% of the proteasome-generated peptide pool is further trimmed to 8-9 amino acid peptides by downstream aminopeptidases, followed by transport to the endoplasmic reticulum (ER), where the peptides are loaded on major histocompatibility complex class I (MHC-I) molecules

and presented on the cell surface for immune surveillance. As such, proteasomes are key players in adaptive immunity and proteasome products presented by MHC-I report on, for instance, the presence of infecting viruses.⁵ CPs are C2-symmetrical protein complexes composed of 28 individual subunits assembled in four heptameric rings. The two outer α -rings interact with the regulatory particles and two inner β -rings harbour the proteolytic activity, which in eukaryotic proteasomes reside in three catalytically active β -subunits. Each active β -subunit possesses an N-terminal, catalytically active threonine residue, the hydroxyl moiety of which acts as the nucleophile in hydrolysis of the scissile peptide bond.⁶ In constitutive proteasomes, which are present in all tissues, the catalytic subunits are termed β 1c (caspase-like, cleaving preferentially after acidic residues), β 2c (trypsin-like, cleaving preferentially after basic residues) and β 5c (chymotrypsin-like, cleaving preferentially after hydrophobic residues). Next to cCPs, lymphoid tissues and cells that are exposed to the inflammatory cytokines interferon- γ (IFN- γ) and tumour necrosis factor- α (TNF- α) express immunoproteasomes (iCPs), in which β 1c, β 2c and β 5c are replaced by β 1i (branched amino acid preferring, BrAAP), β 2i (trypsin-like) and β 5i (chymotrypsin-like), respectively.⁷

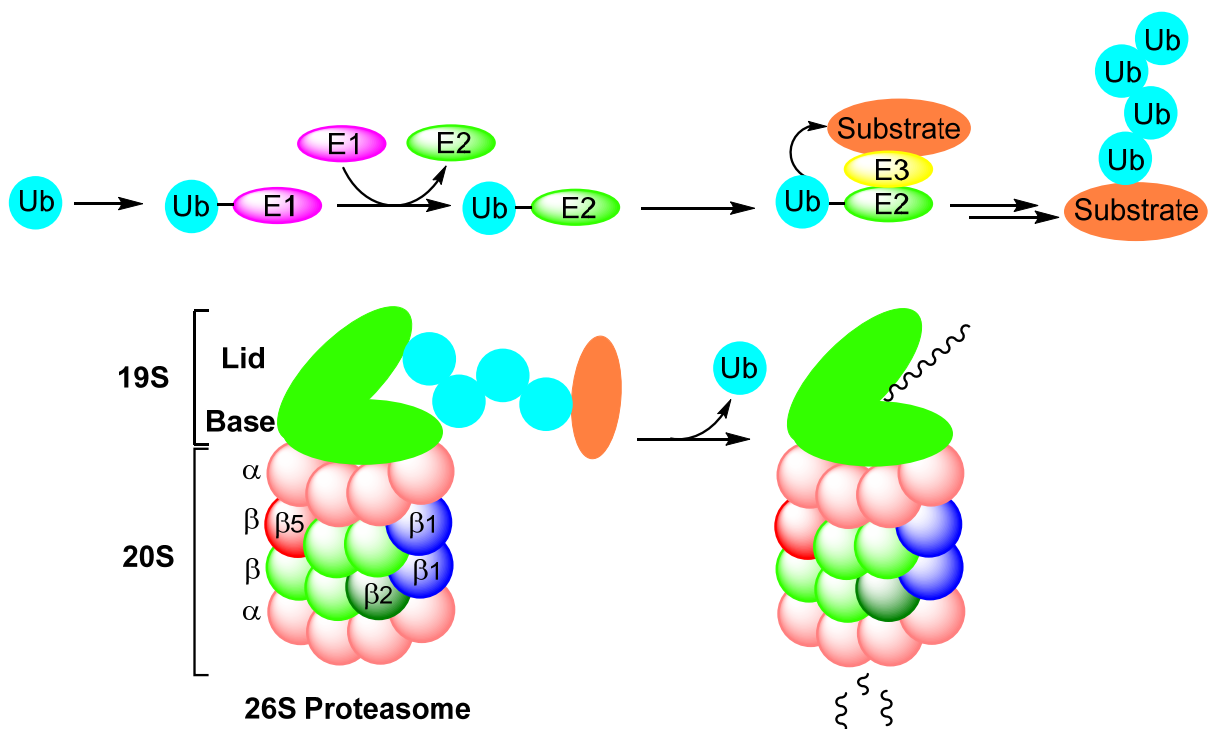


Figure 1. Schematic representation of ubiquitination of a substrate and subsequent recognition, deubiquitination and degradation by the 26S proteasome.

Whereas the substrate specificities of $\beta 2i$ and $\beta 5i$ largely resemble those of their constitutive proteasome counterparts, $\beta 1i$ prefers hydrophobic residues, as opposed to the acidic residues favoured by $\beta 1c$. As a result, compared to cCPs, iCPs predominantly produce peptides with basic and hydrophobic C-termini. Since MHC-I preferentially binds peptides with a hydrophobic residue at P1, iCPs may be superior to cCPs in supporting MHC-I-mediated antigen presentation.^{5, 8, 9}

In cortical thymic epithelial cells a third proteasome type is expressed, namely the thymoproteasome (tCP). tCPs are identical to iCP particles, with the exception that $\beta 5i$ is replaced by $\beta 5t$.¹⁰ Compared to $\beta 5i$ and $\beta 5c$, the substrate pocket of $\beta 5t$ is more hydrophilic and thus the chymotryptic activity of the proteasome is reduced.^{11, 12} tCPs generate peptide pools that have low affinity for MHC-I, and in this way are thought to promote positive selection of T-cells, one of the physiological functions of the thymus.¹³

Proteasomes are important drug targets for the treatment of cancer and autoimmune diseases.¹⁴ The peptide boronic acids, bortezomib (Velcade)¹⁵ and ixazomib (Ninlaro)¹⁶ as well as the peptide epoxyketone, carfilzomib (Kyprolis)¹⁷ are used clinically for the treatment of multiple myeloma and in some cases also mantle cell lymphoma. Myeloma cells excrete large amounts of immunoglobulins, and the numerous and continuously occurring errors in immunoglobulin synthesis and folding put a high burden on the UPS. For this reason, myeloma cells are particularly sensitive to proteasome inhibitors.¹⁸

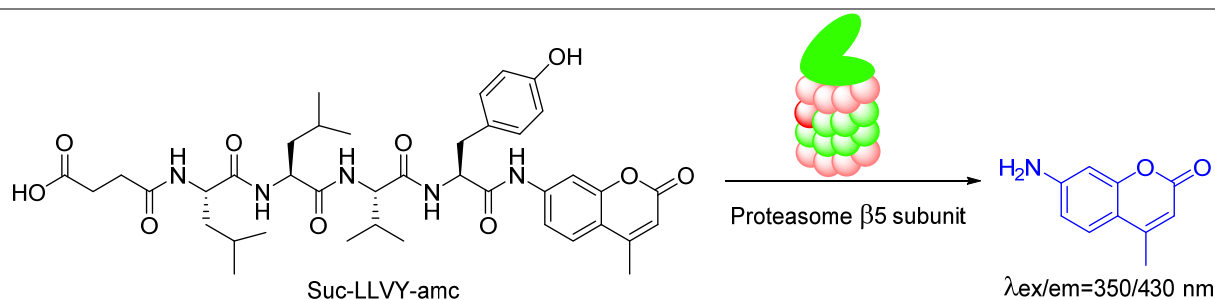
Elucidation of the physiological roles of proteasomes, as well as the development of proteasome inhibitors, necessitates tools and techniques that allow measurement of the activity of the individual catalytic β -subunits. In the past two decades, several methods have been developed to study proteasome activity. These methods rely either on hydrolysis of (fluorogenic) substrates or on covalent modification of the active site threonine by activity-based probes. This chapter provides an overview of these methods with a focus on recent developments.

Substrate hydrolysis assays

Substrate based probes have been widely used to monitor the activity of proteolytic enzymes. Such probes consist of a recognition sequence (usually a tri- or tetrapeptide) and a C-terminal reporter group that produces a measurable signal upon cleavage by the enzyme.¹⁹ In the past decades numerous fluorogenic, luminogenic and quenched substrate oligopeptides have been developed. In the following section relevant examples of these proteasome probes are given.

Fluorogenic substrates

Fluorogenic proteasome substrates generally are tri- or tetrapeptides, the N-terminus of which is capped and the C-terminus of which contain a fluorogenic reporter group. Upon enzymatic hydrolysis, the reporter group becomes fluorescent. Various fluorophores have been used in proteasome substrates, such as 7-amino-4-methylcoumarin (AMC or amc) and 2-naphthylamine (NA or na). Of these, AMC has the highest fluorescence quantum yield and is thus most widely applied. Proteasomes were discovered some three decades ago, and at that time it was not known that proteasomes harbour three different catalytic subunits. To obtain insight in the cleavage preferences of proteasomes, its proteolytic activities were determined using fluorogenic substrate peptides. Based on these studies, the activities of the proteasome were designated as chymotrypsin-like (Z-GGL-na hydrolysis), trypsin-like (Z-D-ALR-na hydrolysis) and peptidylglutamyl-peptide-hydrolyzing (PGPH, Z-LLE-na hydrolysis), which were later termed as $\beta 5c/\beta 5i$, $\beta 2c/\beta 2i$ and $\beta 1c$ respectively.^{20, 21} Another catalytic activity, which did not process these substrates, was found to hydrolyse after Leu or Ala of PAL or PAA containing substrates and was therefore designated as branched- or small neutral amino acid preferring (BrAAP or SNAAP) and later termed $\beta 1i$.²⁸ Since then, substrates for each catalytic activity have been optimized and Table 1 shows the fluorogenic substrates currently used to monitor the activity of individual proteasome subunits. Suc-LLVY-amc is the substrate of choice to monitor the activity of $\beta 5c$ and $\beta 5i$.²² Z-GGL-amc and Suc-AAF-amc can also be used for this purpose, however, those are hydrolysed much slower.²³



Subunit	Preferred	Other
$\beta 1c$	Ac-nLPnLD-amc	Ac-GPLD-amc; Z-LLE-na; Z-LLE-amc*
$\beta 1i$	Ac-PAL-amc*	
$\beta 2c/\beta 2i$	Ac-RLR-amc	Boc-LRR-amc; Z-ARR-amc; Bz-FVR-amc; Bz-VGR-amc Boc-LSTR-amc, Ac-KQL-amc*
$\beta 5c/i$	Suc-LLVY-amc*	Z-GGL-amc, Suc-AAF-amc
$\beta 5c$	Ac-WLA-amc*	
$\beta 5i$	Ac-ANW-amc*	

Table 1. Substrates to monitor proteasome subunit activities. The hydrolysis of Suc-LLVY-amc is shown as an example. *These substrates are also available as (peptide)₂-R110 substrates.

Suc-LLVY-amc is also hydrolysed by other chymotrypsin-like enzymes such as calpain, however, in cytosolic HeLa extract, non-proteasomal hydrolysis contributed to only 5% of total hydrolysis of this substrate.²³ Recently, substrates have been described that are hydrolysed selectively by β 5c (Ac-WLA-amc) or β 5i (Ac-ANW-amc).²⁴⁻²⁶ These substrates have been used to identify selective β 5c inhibitors²⁵ and to quantify the relative amount of β 5c and β 5i.²⁴

The catalytic activity of β 1c was initially monitored by Z-LLE-na.²⁰ Cleavage of this substrate releases 2-naphtylamine, which is less fluorescent than AMC and fluoresces at a different wavelength, requiring different filter sets. Furthermore, Z-LLE-na is also hydrolysed at the Leu-Glu bond. To overcome some of these problems, NA was replaced by AMC, however the resulting substrate Z-LLE-amc was cleaved about 600 times slower than the original substrate.²⁷ Kisselev and co-workers found that the standard caspase substrate Ac-YVAD-amc is hydrolysed 50 times faster than Z-LLE-amc, indicating that β 1c is caspase-like rather than PGPH.³⁷ However, this substrate was cleaved much slower than standard substrates for the chymotrypsin- and trypsin-like sites and, in addition, Ac-YVAD-amc is also hydrolysed N-terminally of the Asp-amc bond.²⁷ Using positional scanning libraries with Asp at P1, two substrates were identified that exhibited fast Asp-amc hydrolysis, without competing cleavage of other peptide bonds: Ac-nLPnLD-amc and Ac-GPLD-amc (with the former being the most rapidly processed). Ac-nLPnLD-amc is therefore the most optimal substrate currently available to monitor β 1c activity. The S1 pocket of β 1i is more hydrophobic compared to β 1c due to two point mutations: R45L and T20V.¹² Therefore, substrates used to monitor the caspase-like activities of the proteasome are not hydrolysed by β 1i. To monitor β 1i activity, Ac-PAL-amc was developed.²⁶ This substrate showed negligible hydrolysis by β 1c and can therefore be used to selectively monitor β 1i activity in presence of β 1c.^{25, 29}

Several substrates with R-amc bonds (Boc-LRR-amc; Z-ARR-amc; Bz-FVR-amc; Bz-VGR-amc; Boc-LSTR-amc) can be used to monitor the trypsin-like activities (β 2c/ β 2i). However, K_m values for these substrates are rather high (>500 mM), and the substrates furthermore suffer from low specific activity.²³ Positional scanning of fluorogenic peptide libraries led to the development of Ac-RLR-amc, which specific activity is much higher, and for which the 26S proteasome has a much lower K_m value.^{18, 30} Ac-KQL-amc, with a basic substituent at P3, represents an alternative substrate to monitor β 2c and β 2i activity.²⁵

In recent years, rhodamine 110 (R110) substrates have become commercially available and are a useful alternative to AMC substrates. R110 fluoresces at a higher wavelength ($\lambda_{ex/em}=490/520$) and R110 substrates are more sensitive and suffer less from background fluorescence caused by additives present in the sample. The R110 fluorophore features two amines, each of which is modified to contain an oligopeptide. Relevant R110-based fluorogenic proteasome substrates are (Suc-LLVY)₂-R110 (reporting on β 5c and β 5i), (Ac-KQL)₂-R110 (reporting on β 2c and β 2i), (Z-LLE)₂-R110 (reporting on β 1c), (Ac-PAL)₂-R110 (reporting on β 1i), (Ac-ANW)₂-R110 (reporting on β 5i), and (Ac-WLA)₂-R110 (reporting on β 5c).

Fluorogenic substrates are often used on purified proteasomes. Their use in crude cell extracts is more complicated due to partial hydrolysis of the substrates by other enzymes.²³ This especially holds true for those substrates used to monitor the trypsin-like activities of the proteasome. In whole cell extracts, these substrates are processed in large parts by proteases (trypsin) other than proteasomes. Non-proteasomal hydrolysis is much less pronounced in cytosolic preparations (prepared using digitonin as detergent), but still accounts for up to 25% of total hydrolysis. Non-specific hydrolysis can be further reduced by partial proteasome purification via ultracentrifugation. Altogether, proper controls to account for non-proteasomal substrate hydrolysis have to be applied when fluorogenic substrates are used on cell extracts.^{23, 24, 31, 32}

Luminogenic substrates: Proteasome-Glo assay

As an alternative to fluorogenic substrates, luminogenic peptides can be used to detect and quantify proteasome activities.³³ As with fluorogenic peptides, luminogenic peptides can be used both to report on the activity of purified proteasomes and on crude tissue extracts containing proteasome activities, and in fact luminogenic peptides can often be applied in situations where fluorogenic peptides fall short. In what has become known as the 'proteasome-Glo assay', peptide-luciferin conjugates (specifically, Suc-LLVY-aminoluciferin, Z-LRR-aminoluciferin and Z-nLPnLD-aminoluciferin), which upon hydrolysis release the luciferase substrate aminoluciferin, are applied (Figure 2).³³ A single buffer containing digitonin, a peptide-luciferin conjugate, and luciferase is added to intact cells. Digitonin permeabilizes the cell membrane and after a short incubation time, luminescence can be measured directly. The Proteasome-Glo assay represents a major advance compared to fluorescent assays since it is not only faster and more convenient, but also significantly more sensitive, allowing a 20-fold reduction of the amount of cells.³³ Notwithstanding this, serine protease inhibitors need sometimes to be included in the assay, for instance when proteasome trypsin-like activities are subject of study. Moreover, background luminescence cannot be avoided in specific cell lines when probing for either chymotrypsin-like or trypsin-like activities. Inhibition of chymotrypsin-like or trypsin-like proteasome activities prior to conducting a proteasome-Glo assay lowers the amount of background labeling, but also makes the assay somewhat cumbersome.³⁴

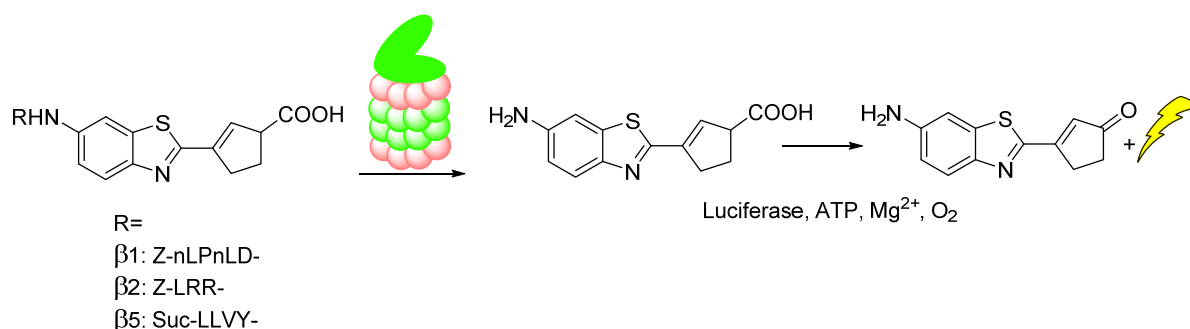


Figure 2. Proteasome-Glo assay. Peptide-aminoluciferin substrates are hydrolysed by the respective proteasome subunits, releasing aminoluciferin, which is consumed by luciferase to generate light.

Capture proteasome assay

As is evident from the above sections, measuring proteasome activities, especially trypsin-like activities, in crude cell extracts is complicated by the presence of other proteases. One way to overcome this problem is the capture-proteasome-assay (CAPA), in which the proteasome content of a cell lysate is captured on an anti- $\alpha 2$ antibody (MCP21) coated plate (Figure 3).³⁵ After a washing step, proteasome activities are readily measured using standard fluorogenic substrates (specifically, Suc-LLVY-amc, Z-LLE-amc and Boc-LRR-amc). Constitutive proteasomes, immunoproteasomes and mixed proteasomes ($\beta 5i$ or $\beta 5i\text{-}\beta 1i$)³⁶ could be captured from HEK-293 cells and various proteasome inhibitors were evaluated for their potency and selectivity for these proteasome subtypes. The capture assay can be conducted in a 96-well format, which allows screening of compound libraries on proteasome inhibitor content in a high-throughput format. Moreover, the capture assay eliminates the need for pre-purified proteasomes and, since no other proteases should bind the immobilized antibody, provides a more reliable measurement of especially the trypsin-like activities.

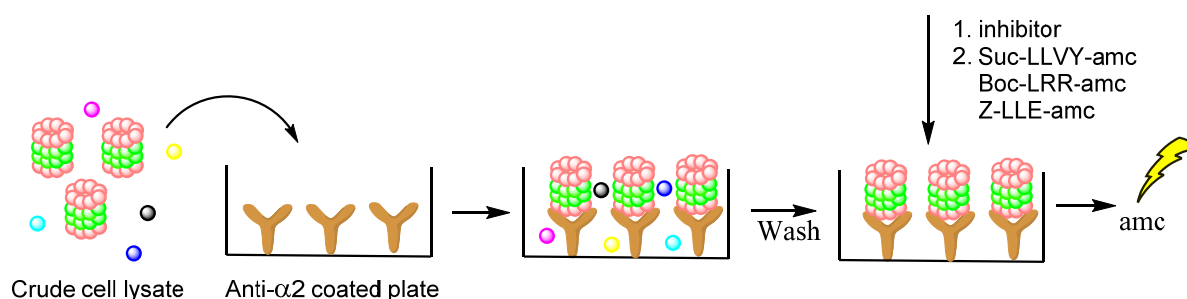


Figure 3. Capture proteasome assay. A crude cell lysate is added to an anti- $\alpha 2$ antibody coated plate. Unbound proteins are removed by washing steps and proteasome activity can be measured using fluorogenic substrates.

Simultaneous, multicolour monitoring of proteasome activities

Since $\beta 5$ subunits determine the rate of protein degradation³⁷, for years, often only proteasomal $\beta 5$ activities were monitored as a measure for total proteasome activity. As well, all proteasome inhibitors that are clinically approved or are in clinical trials have been

designed to primarily inhibit the $\beta 5$ activities.³⁸ However, in the last years it became clear that inhibition of $\beta 1$ or $\beta 2$ does sensitize cancer cells to selective $\beta 5$ inhibition, indicating the importance of these subunits as drug targets.^{39, 40} Furthermore, allosteric cross-talk between the different catalytic subunits, including allosteric up-regulation of one site by another subunit whose active site is occupied by an inhibitor, underscores current thought that the activity of all active subunits should be taken into account.³⁷ For these reasons, there is an increasing interest in the development of methods that allow simultaneous measurement of multiple proteasome activity sites. In a study aimed to deliver such methodology, Lawrence *et al.* developed a substrate for $\beta 5$, equipped with a high wavelength oxazine-based fluorophore ($\lambda_{ex/em}=663/678$), that is quenched internally by a tryptophan residue at P2 (Ac-HWSL-Lys(Fluorophore)).⁴¹ Upon hydrolysis a >20 fold increase in fluorescence was observed, and due to the distinct properties of the oxazine-fluorophore compared to AMC and NA, it can be used simultaneously with Z-LLE-na and Boc-LRR-amc. Simultaneous measurement of various combinations of two of the three activities (chymotrypsin-like activity, the caspase-like activity and the trypsin-like activities) with the appropriate compounds revealed that the rate of hydrolysis of each activity changes when a second substrate is present. This result indicates that the active subunits are indeed allosterically regulated.

In order to simultaneously monitor all three proteasome catalytic activities, Lawrence *et al.* extended their strategy and developed three quenched substrates, each equipped with a different fluorophore (Figure 4).⁴² The Acid-Blue 40 (AB40) fluorescent quencher was coupled to the ϵ -amine of lysine which was installed next to scissile bond of known peptide substrates (the HHSL sequence, which is cleaved at the S-L amide bond, was identified by positional scanning of libraries of tetrapeptide AMC substrates⁴³). The three complementary fluorophores were coupled to the N-terminus of the respective oligopeptides, yielding the conjugates as depicted in Figure 4. Upon proteasome-mediated removal of the quencher moiety in these compounds, a >30-fold increase in fluorescence intensity was observed in each case.

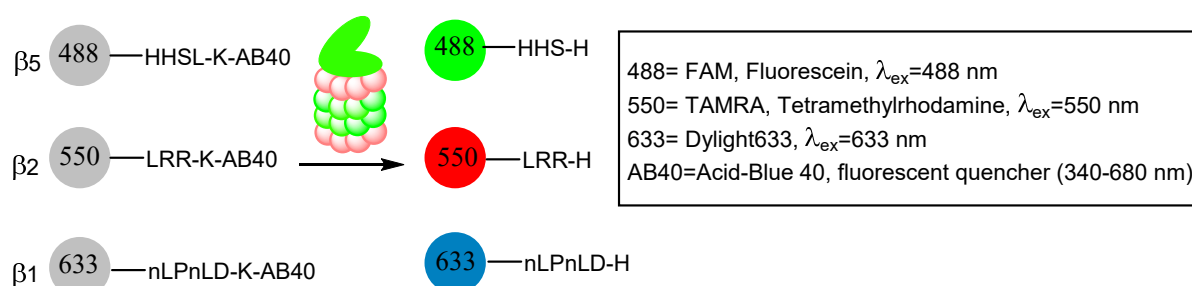


Figure 4. Simultaneous multicolour monitoring of proteasome activity by quenched substrates. Upon hydrolysis of the quenched substrates, the AB40 quencher is cleaved resulting in increased fluorescence. Due to the distinct properties of the fluorophores, the three substrates can be used to simultaneously monitor all three proteasome catalytic activities.

As result of allosteric regulation, the activity of each subunit was substantially lowered in presence of the three substrates. Therefore, low concentrations of substrates are required, which is a caveat because the resulting low hydrolysis rates cause limited sensitivity and long reaction times. Despite these drawbacks, this method was successfully applied to simultaneously measure the three proteasome activities in various samples.

Activity-based proteasome probes

Activity-based protein profiling (ABPP) has been used for decades to detect, identify and/or relatively quantify enzymes in complex samples, including intact cells and cell extracts.¹⁹ In ABPP, activity-based probes (ABPs) are employed to selectively, covalently and irreversibly bind to the active site of an enzyme in order to gain information regarding its activity and (relative) abundance. ABPs generally consist of three components, namely 1) a reactive group, often designated as ‘warhead’, which binds covalently to the active site residue of a protease; 2) a recognition sequence, providing affinity and selectivity for the target enzyme, and 3) a reporter group, such a fluorescent group or affinity tag (biotin), allowing detection of the enzyme by mass spectrometry, SDS-PAGE, fluorescence microscopy or *in situ* imaging (Figure 5). ABPP is complementary to the use of substrate probes. Whereas substrate probes report on (changes in) enzyme activity and turnover rate, ABPs report on the quantity of active enzymes, and not so much on their activity. In the proteasome field, the first ABPs were developed to identify the proteasome as target of natural product electrophiles with, amongst others, cytotoxic activity. More recently, proteasome (subunit-selective) targeting ABPs have been developed as tools to monitor proteasome activity and to identify new proteasome inhibitors.

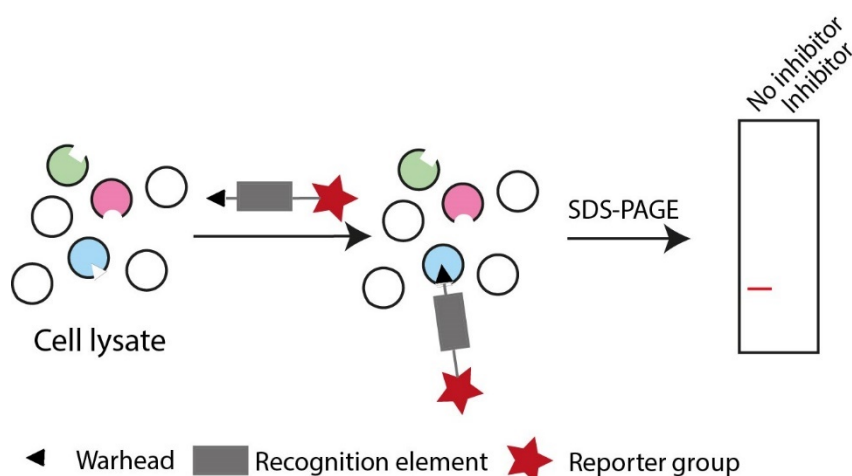


Figure 5. SDS-PAGE based ABPP. A crude cell lysate is treated with an ABP and analysed by SDS-PAGE, showing a band for the ABP-reactive enzyme or enzyme family (comparative ABPP). In the presence of a competitive inhibitor (competitive ABPP), the band disappears.

ABPs for target identification

The first proteasome inhibitors were discovered after grafting a reporting group onto bioactive natural products, suspected (by virtue of electrophilic moieties embedded in these structures) to inactivate their target through covalent and irreversible modification. Lactacystin (Figure 6) was isolated from *Streptomyces* and found to induce neurite outgrowth Neuro-2a-cells and to inhibit cell cycle progression in an osteosarcoma cell line.^{44, 45} Lactacystin in time reacts intramolecular to form *clasto*-lactacystin β -lactone, which was identified as the bioactive species. In order to identify its target, tritiated lactacystin was synthesized (Figure 6). On the basis of its labelling by [³H]-lactacystin, a 700 kDa complex was purified from bovine brain, which was identified to be the 20S proteasome. Lactacystin proved active against all three cCP activities with a preference for β 5c.⁴⁶ 2D-PAGE analysis of proteasome fractions derived from lymphoblasts that were treated with [³H]-lactacystin showed distinct spots for all catalytically active cCP and iCP proteasome subunits, indicating covalent binding of lactacystin to all six catalytic proteasome subunits.⁴⁷ Looking back, [³H]-lactacystin can be considered as the first proteasome targeting ABP.

Originally designed as mechanism-based cysteine protease inhibitors, peptide vinyl sulfones were found to be remarkably effective proteasome inhibitors some two decades ago. Peptide vinyl sulfones act as mechanism-based proteasome inhibitors due to conjugate addition of the N-terminal threonine alcohol to the Michael acceptor. Covalent proteasome modification appears irreversible and peptide vinyl sulfones can therefore serve as a basis for ABP development. Indeed, ¹²⁵I-NIP-L₃VS (Figure 6) was found to irreversibly react with all proteasome subunits, as revealed by SDS-PAGE.⁴⁸ The related ¹²⁵I-NIP-LLN-VS comprises the first ABP employed in screening of compound libraries for the identification of new proteasome inhibitors. Cellular extracts were incubated with a putative inhibitor, followed by labelling of residual proteasome activity by ¹²⁵I-NIP-LLN-VS, SDS-PAGE separation and auto radiographic analysis of the gel slabs. In this competitive ABPP setting, decreased band intensities correlate to inhibition of proteasome activity.⁴⁹ AdaY(¹²⁵I)-Ahx₃-L₃-VS emerged as a pan-reactive proteasome ABP from a study that aimed to demonstrate that N-terminally extended proteasome inhibitors are both more potent and less selective (with respect to proteasome catalytic activities modified) proteasome inhibitors than their tri- or tetrapeptide counterparts.⁵⁰ ABPP was also employed to identify the target of the natural product epoxomicin, for which anti-tumour and anti-inflammatory activities were observed following its discovery.⁵¹ For this purpose, epoxomicin was equipped with a biotin moiety (Figure 6), which can be detected following treatment with with avidin-horseradish peroxidase (HRP).⁵²

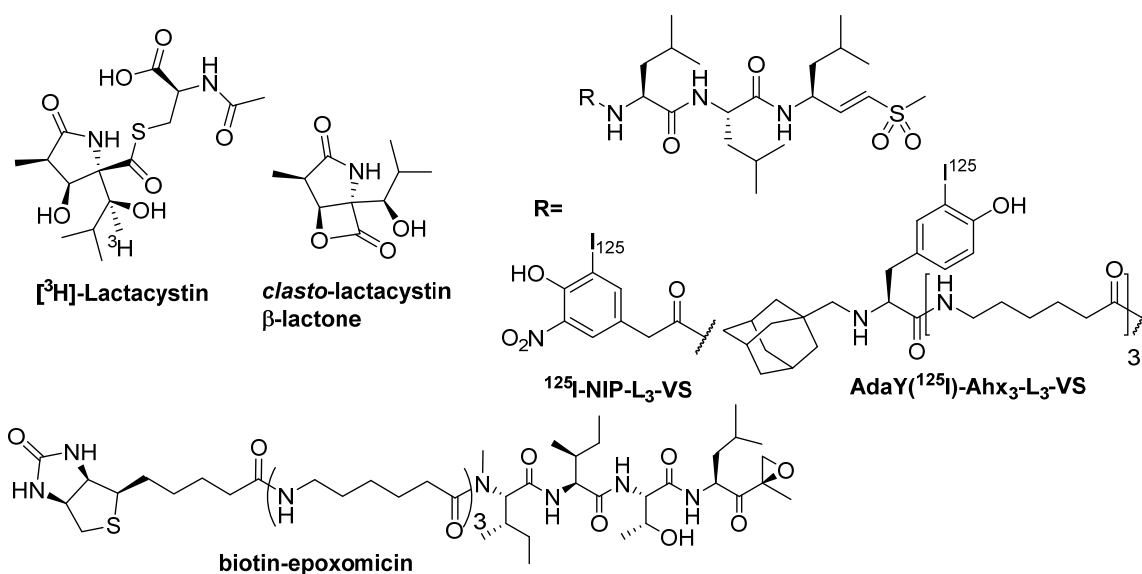


Figure 6. Structures of [³H]-lactacystin, active β-lactone *clasto*-lactacystin, ¹²⁵I-NIP-L₃VS, AdaY(¹²⁵I)-Ahx₃-L₃-VS and biotin-epoxomicin.

Murine EL-4 cells were treated with biotin-epoxomicin, lysed and separated by SDS-PAGE after which biotin detection using avidine-horseradish peroxidase enhanced chemiluminescence revealed multiple bands. Upon trypsin digestion and MALDI-MS analysis of the corresponding bands, β5c, β5i, β2c and β2i were identified as targets of biotin-epoxomicin.⁵²

Pro-CISE assay

In order to quantify the amount of cCP and iCP subunits in cells of different origin, and to determine the inhibitory potency of a putative proteasome inhibitor against all six cCP and iCP active subunits, an enzyme-linked immunosorbent assay (ELISA) was developed (Figure 7).¹⁷ This assay, termed Pro-CISE, makes use of biotin-L₃-epoxyketone (EK), which covalently modifies the active site threonine residues of all six subunits when applied at high concentrations. After incubation of a cell lysate with biotin-L₃-EK, all biotin-containing molecules are captured upon incubation with streptavidin-sepharose beads under denaturing conditions. Subsequently, primary antibodies against each of the six catalytically active subunits are added in individual samples, followed by a secondary horseradish peroxidase (HRP) conjugated antibody. Finally, the wells are developed and luminescence is detected. Using purified iCP and cCP samples, standard curves for each of the six subunits can be obtained, enabling quantification of all six proteasome subunits.

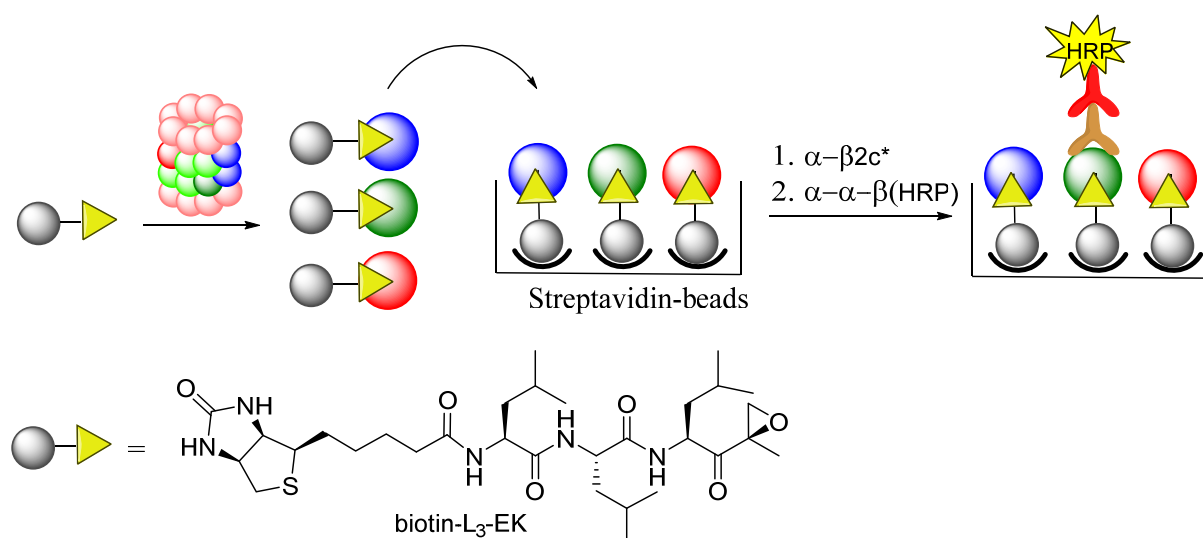


Figure 7. Pro-CISE assay. All active sites are covalently modified with biotin-L₃-EK, which is captured on streptavidin-beads in a 96-well filter-plate. Each of the active subunits can be detected by treatment with subunit-specific antibodies followed by treatment with a secondary HRP-conjugated antibody.

Fluorescent ABPs

In recent years, a number of fluorescent proteasome selective probes were developed that target all active subunits. With these, radioactive probes can be avoided and rapid screening of proteasome activity in multiple samples is feasible. Dansyl-Ahx₃-L₃-VS (Figure 8) comprises the first-in-class fluorescent proteasome ABP and the dansyl moiety can be detected, next to fluorescence read-out of gel slabs (which is a bit hampered by the low quantum yields of the fluorophore), also by dansyl-specific antibodies.⁵³ Using this probe, the subunit binding preferences of bortezomib and MG132 (Z-L₃-aldehyde) were determined. To overcome the weak fluorescent properties of dansyl-Ahx₃-L₃-VS, the BODIPY(TMR) analogue MV151 as well as a number of BODIPY-epoxomicin derivatives were developed (Figure 8).⁵⁴⁻⁵⁷ These ABPs and the vinyl sulfone-based ABP BODIPY(FL)-Ahx₃-L₃-VS⁵⁸ are used in competitive ABPP assays to determine the potency and specificity of putative proteasome inhibitors (Figure 5), in fluorescence microscopy as well as in flow cytometry experiments.

Triple colour ABPP-assay

Due to similar molecular weights of β 1c, β 1i, β 5c and β 5i, the broad-spectrum vinyl sulfone- and epoxyketone-based ABPs are not able to provide full resolution of these subunits on 1D SDS-PAGE. Therefore, these probes cannot be used to determine the potency and subunit selectivity of putative proteasome inhibitors for each individual subunit. To overcome this limitation, ABPs that selectively target a subunit-pair were developed. These APBs were based on the previously developed β 1c/ β 1i-selective and β 5c/ β 5i-selective inhibitors, NC001 and NC005, respectively.³⁹

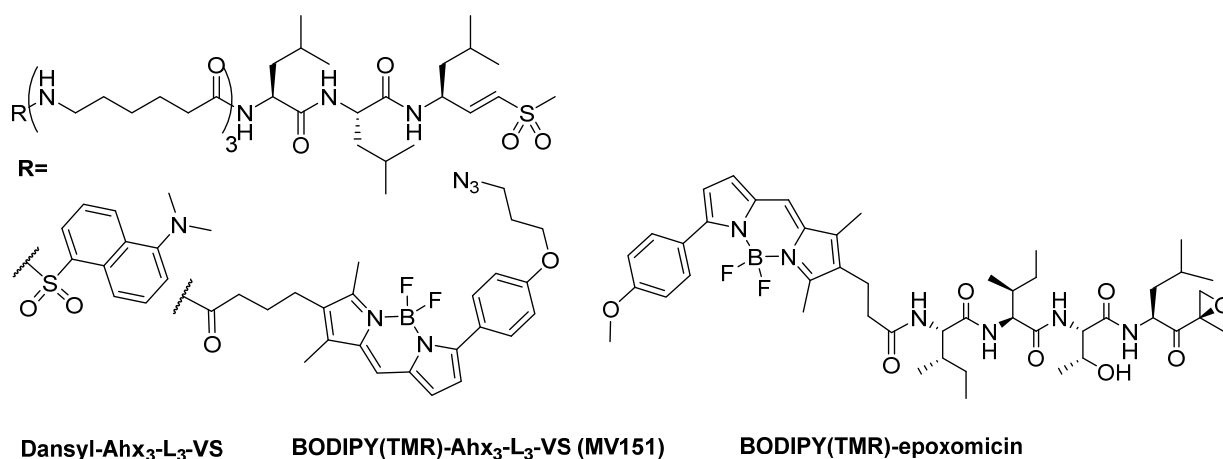


Figure 8. Examples of fluorescent, broad spectrum proteasome ABPs.

β 1c/ β 1i are selectively tagged by BODIPY(FL)-NC001 and β 5c/ β 5i by BODIPY(TMR)-NC005 (Figure 9), resulting in clear resolution of the respective subunits on SDS-PAGE.⁵⁵ In addition, since these APBs are equipped with distinct fluorophores, they can be used to simultaneously resolve β 1c/ β 1i and β 5c/ β 5i on SDS-PAGE.⁵⁹⁻⁶¹ However, a separate analysis using BODIPY-epoxomicin or MV-151 has to be performed to determine β 2c/ β 2i activity. In order to further optimize and simplify the screening of inhibitors using competitive ABPP, a triple colour strategy was developed, making use of three subunit-pair selective ABPs, each equipped with a distinct fluorophore. BODIPY(FL)-LU112 was developed to label β 2c/ β 2i, but was found to also partially modify β 5c/ β 5i.⁶²

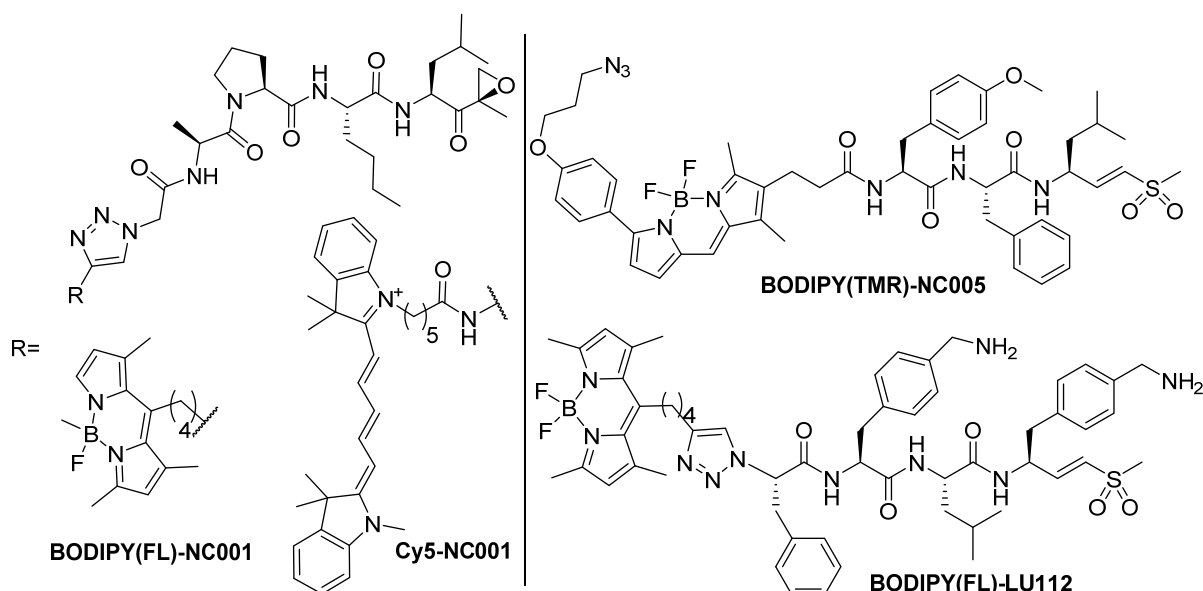


Figure 9. Structures of subunit-pair selective ABPs. The probes selectively target either β 1c/ β 1i (BODIPY(FL)-NC001 and Cy5-NC001), β 5c/ β 5i (BODIPY(TMR)-NC005) or β 2c/ β 2i (BODIPY(FL)-LU112).

However, when applied at optimal concentration, only minimal labelling of $\beta 5c/\beta 5i$ was found. In the end, a cocktail of probes consisting of optimized amounts of BODIPY(FL)-LU112, BODIPY(TMR)-NC005 and Cy5-NC001 was compiled (Figure 9). This probe cocktail labels all six active sites from human cCPs and iCPs simultaneously giving full resolution of the modified subunits on SDS-PAGE (Figure 10).⁶³ The cocktail can be used for rapid and straightforward screening of putative proteasome inhibitors, and was instrumental in the identification of new $\beta 2c$, $\beta 1c$ and $\beta 5c$ -selective inhibitors.

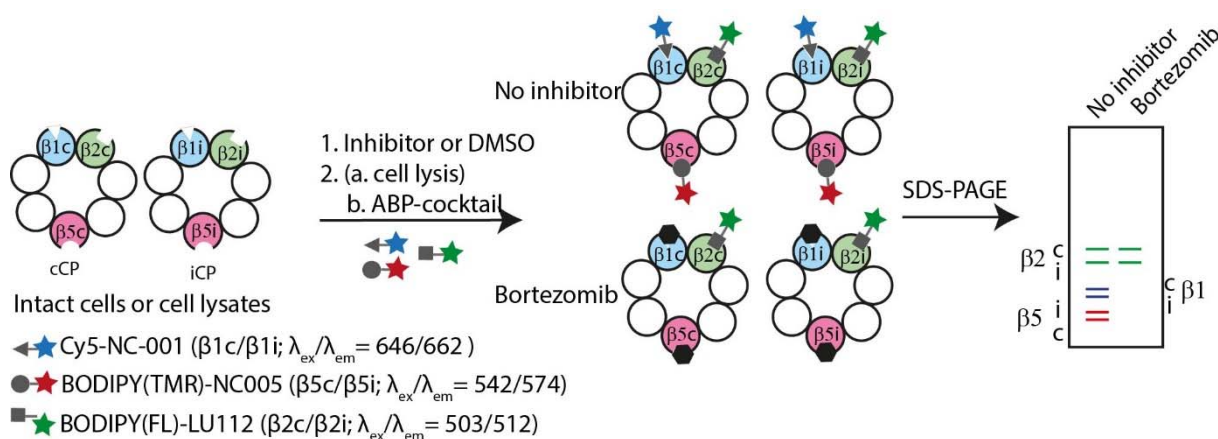


Figure 10. Schematic representation of multi-colour competitive ABPP. Intact cells or cell lysates are treated with inhibitor or DMSO, followed by cell lysis in case of intact cells, and addition of an ABP-cocktail consisting of Cy5-NC001, BODIPY(TMR)-NC005 and BODIPY(FL)-LU112. Subsequent SDS-PAGE analysis reveals full resolution of all six active subunits. Bortezomib inhibits the $\beta 1$ and $\beta 5$ subunits, indicated by disappearance of the corresponding bands.

iCP and cCP subunit selective ABPs

In the past decade, much research has been directed to the discovery of iCP selective inhibitors. In particular $\beta 5i$ -selective inhibitors were sought after, as they have potential as therapeutics against several auto-immune diseases.¹⁴ Based on the $\beta 1i$ selective inhibitor UK101⁶⁴ and the $\beta 5i$ selective inhibitor PR924,⁶⁵ Kim and co-workers developed ABPs selective for either $\beta 1i$ (UK101-Fluor and UK101-B660)⁶⁶ or $\beta 5i$ (LKS01-B650)⁶⁷ (Figure 11). Gel-based competition experiments and Western-blotting revealed that these probes maintain the selectivity of the parent inhibitors. These probes enable the assessment of cellular localization of $\beta 1i$ and $\beta 5i$ using fluorescence microscopy and show substantial co-localization indicating that these probes target fully assembled immunoproteasome complexes. Since $\beta 1i$ might serve as potential tumour biomarker and given the near-infrared properties of UK101-B660 and LKS01-B650, these ABPs might find their application in *in vivo* imaging for cancer screening, disease progression or subcellular localization of the immunoproteasome.⁶⁸ Recently, a $\beta 1i$ selective inhibitor (LU001i) as well as a $\beta 5i$ selective inhibitor (LU035i) with improved selectivity profiles compared to UK101 and PR924 have been developed.⁶⁰

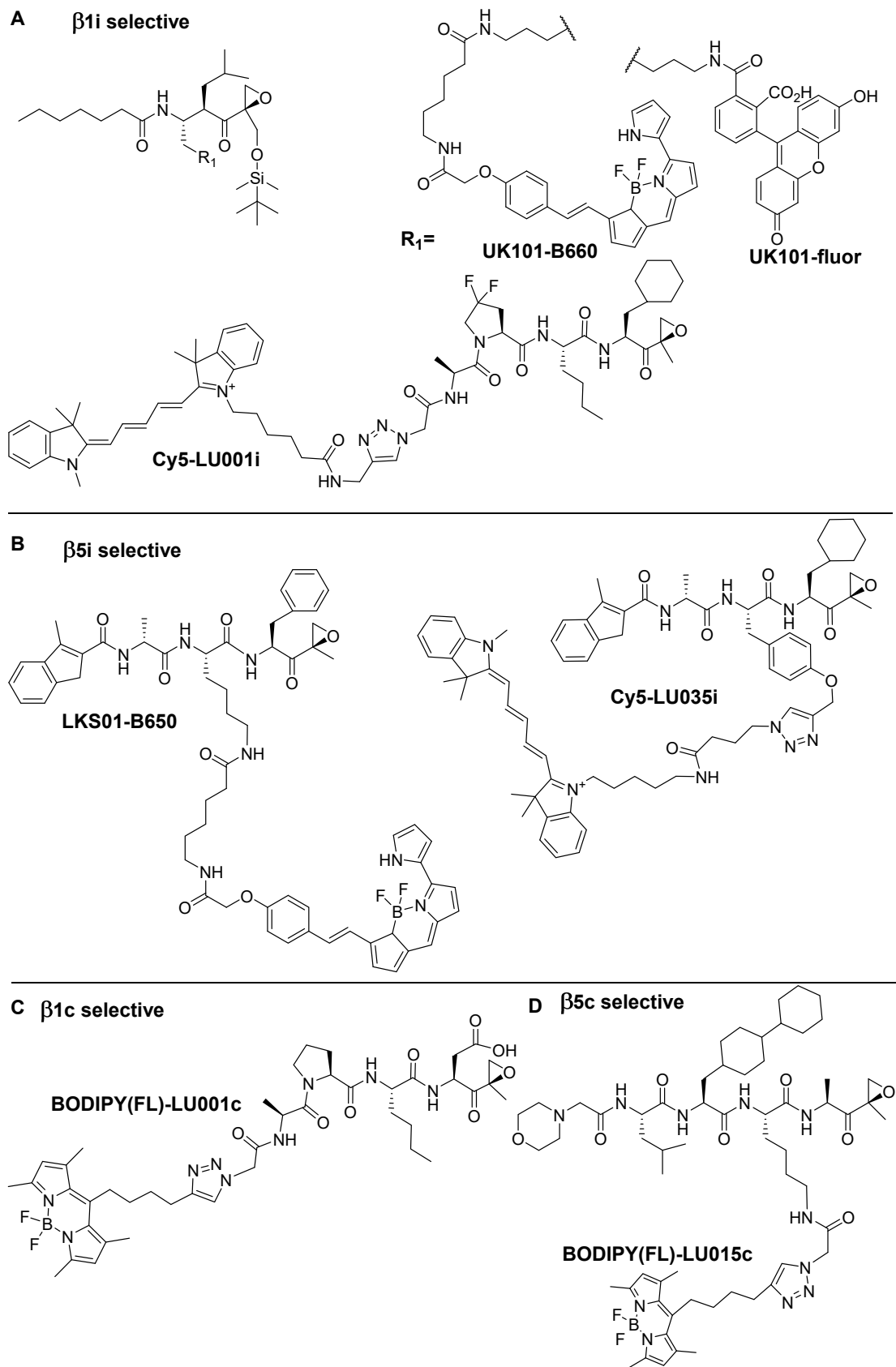


Figure 11. Structures of iCP- (A. $\beta 1i$; B. $\beta 5i$) and cCP (C. $\beta 1c$; D. $\beta 5c$) subunit selective ABPs.

Based on these inhibitors, ABPs Cy5-LU001i and Cy5-LU035i were developed (Figure 11), which exhibit excellent selectivity for their target subunits (see chapter 6). Given the improved selectivity of the parent compounds, it may well be that these ABPs outperform UK101-B660, UK101-Fluor and LKS01-B650 on selective subunit tagging, though a direct comparison has not been made. Using related strategies, the recently discovered β 1c selective and β 5c-selective inhibitors⁶³ were transformed to fluorescent ABPs. BODIPY(FL)-LU001c is completely selective for β 1c, while BODIPY(FL)-LU005c has β 2c/ β 2i as off-target. However, when β 2c/ β 2i are selectively inhibited by a β 2c/ β 2i selective inhibitor, this probe can be used to modify β 5c selectively in presence of β 5i. These four cCP/iCP subunit selective ABPs have been successfully used in the development of a native-PAGE fluorescence resonance energy transfer (FRET) assays for the detection of mixed asymmetric proteasomes (see chapter 10).

Discussion/conclusion

Substrate hydrolysis-based assays and activity-based protein profiling (ABPP) are complementary methods to monitor proteasome activity. Both have been highly optimized and are currently used to screen for proteasome inhibitors and to assess the abundance of individual proteasome subunits and their relative activities. Substrate hydrolysis assays report predominantly on proteasome activity (turn-over rate) and less on abundance of each subunit, while the opposite holds true for ABPP. The applicability of substrate assays to measure proteasome activity has been given a major improvement by the development of cCP and iCP subunit selective substrates, allowing the independent measurement of β 1c, β 1i, β 5c and β 5i activities. In addition, the extensively optimized proteasome-Glo assay allows high throughput analysis of proteasome activity in cell lysates obtained from intact cells, without the need for (partial) proteasome purification. The drawback of substrate hydrolysis assays is the possibility of non-proteasomal hydrolysis, for which extensive controls are required. Another drawback is the lack of β 2c and β 2i selective substrates, making it impossible to measure β 2c and β 2i independently in cells expressing both subunits. Moreover, simultaneous monitoring of multiple proteasome activities using substrates is rather complicated and limited to the simultaneous measurement of caspase (β 1c), trypsin (β 2c/ β 2i) and chymotrypsin activities (β 5c/ β 5i). ABPP was initially used to identify the proteasome as target of certain inhibitors. In the last decade, this technique has evolved and now is often used to assess the activity of individual subunits. The Pro-CISE assay makes use of six subunit selective antibodies, which report on the presence of each active subunit after capture by a broad-spectrum biotinylated ABP. The main disadvantage is the length of the assay (several multiple hour incubations), the use of expensive antibodies, and the requirement of six individual assays to measure each catalytically active subunit. The availability of subunit selective ABPs resulted in the development of an SDS-PAGE based tri-colour ABPP assay that reports on the activity of all

active proteasome subunits in one experiment. This assay requires low amount of cells, is time efficient and does not require extensive controls. Therefore, the tri-colour ABPP assay can be used for screening of putative proteasome inhibitors and rapid assessment of relative abundances of each active proteasome subunit in cell extracts.

References

1. Hershko, A. & Ciechanover, A. The ubiquitin system. *Annu. Rev. Biochem.* **67**, 425-79 (1998).
2. Komander, D. & Rape, M. The ubiquitin code. *Annu. Rev. Biochem.* **81**, 203-229 (2012).
3. Thrower, J.S., Hoffman, L., Rechsteiner, M. & Pickart, C.M. Recognition of the polyubiquitin proteolytic signal. *EMBO J.* **19**, 94-102 (2000).
4. Kisselev, A.F., Akopian, T.N., Woo, K.M. & Goldberg, A.L. The sizes of peptides generated from protein by mammalian 26 and 20S proteasomes: implication for understanding the degradative mechanism and antigen presentation. *J. Biol. Chem.* **274**, 3363-3371 (1999).
5. Sijts, E.J.A.M. & Kloetzel, P.-M. The role of the proteasome in the generation of MHC class I ligands and immune responses. *Cell. Mol. Life. Sci.* **68**, 1491-1502 (2011).
6. Groll, M. et al. Structure of 20S proteasome from yeast at 2.4 Å resolution. *Nature* **386**, 463-71 (1997).
7. Ferrington, D.A. & Gregerson, D.S. Immunoproteasomes: structure, function, and antigen presentation. *Prog. Mol. Biol. Transl. Sci.* **109**, 75-112 (2012).
8. Romero, P., Corradin, G., Luescher, I.F. & Maryanski, J.L. H-2Kd-restricted antigenic peptides share a simple binding motif. *J. Exp. Med.* **174**, 603-12 (1991).
9. Kloetzel, P.M. & Ossendorp, F. Proteasome and peptidase function in MHC-class-I-mediated antigen presentation. *Curr. Opin. Immunol.* **16**, 76-81 (2004).
10. Murata, S. et al. Regulation of CD8+ T cell development by thymus-specific proteasomes. *Science* **316**, 1349-1353 (2007).
11. Florea, B.I. et al. Activity-based profiling reveals reactivity of the murine thymoproteasome-specific subunit $\beta 5t$. *Chem. Biol.* **17**, 795-801 (2010).
12. Huber, Eva M. et al. Immuno- and constitutive proteasome crystal structures reveal differences in substrate and inhibitor specificity. *Cell* **148**, 727-738 (2012).
13. Tomaru, U. et al. Exclusive expression of proteasome subunit $\beta 5t$ in the human thymic cortex. *Blood* **113**, 5186-5191 (2009).
14. Kisselev, A.F. & Groettrup, M. Subunit specific inhibitors of proteasomes and their potential for immunomodulation. *Curr. Opin. Chem. Biol.* **23**, 16-22 (2014).
15. Adams, J. et al. Potent and selective inhibitors of the proteasome: Dipeptidyl boronic acids. *Bioorg. Med. Chem. Lett.* **8**, 333-338 (1998).
16. Gentile, M. et al. Ixazomib for the treatment of multiple myeloma. *Expert Opin. Investig. Drugs* **24**, 1287-98 (2015).
17. Parlati, F. et al. Carfilzomib can induce tumor cell death through selective inhibition of the chymotrypsin-like activity of the proteasome. *Blood* **114**, 3439-3447 (2009).
18. Cenci, S. et al. Pivotal Advance: Protein synthesis modulates responsiveness of differentiating and malignant plasma cells to proteasome inhibitors. *J. Leukoc. Biol.* **92**, 921-931 (2012).
19. Sanman, L.E. & Bogoy, M. Activity-based profiling of proteases. *Annu. Rev. Biochem.* **83**, 249-273 (2014).
20. Wilk, S. & Orłowski, M. Evidence that pituitary cation-sensitive neutral endopeptidase is a multicatalytic protease complex. *J. Neurochem.* **40**, 842-9 (1983).
21. Orłowski, M. The multicatalytic proteinase complex, a major extralysosomal proteolytic system. *Biochemistry* **29**, 10289-97 (1990).
22. Stein, R.L., Melandri, F. & Dick, L. Kinetic characterization of the chymotryptic activity of the 20S proteasome. *Biochemistry* **35**, 3899-3908 (1996).

23. Kisselev, A.F. & Goldberg, A.L. Monitoring activity and inhibition of 26S proteasomes with fluorogenic peptide substrates. *Methods Enzymol.* **398**, 364-78 (2005).
24. Niewerth, D. et al. Interferon-gamma-induced upregulation of immunoproteasome subunit assembly overcomes bortezomib resistance in human hematological cell lines. *J. Hematol. Oncol.* **7**, 7 (2014).
25. Blackburn, C. et al. Characterization of a new series of non-covalent proteasome inhibitors with exquisite potency and selectivity for the 20S beta5-subunit. *Biochem. J.* **430**, 461-76 (2010).
26. Lin, G., Tsu, C., Dick, L., Zhou, X.K. & Nathan, C. Distinct specificities of mycobacterium tuberculosis and mammalian proteasomes for N-acetyl tripeptide substrates. *J. Biol. Chem.* **283**, 34423-34431 (2008).
27. Kisselev, A.F. et al. The caspase-like sites of proteasomes, their substrate specificity, new inhibitors and substrates, and allosteric interactions with the trypsin-like Sites. *J. Biol. Chem.* **278**, 35869-35877 (2003).
28. Orłowski, M., Cardozo, C. & Michaud, C. Evidence for the presence of five distinct proteolytic components in the pituitary multicatalytic proteinase complex. Properties of two components cleaving bonds on the carboxyl side of branched chain and small neutral amino acids. *Biochemistry* **32**, 1563-1572 (1993).
29. Basler, M. et al. Why the structure but not the activity of the immunoproteasome subunit low molecular mass polypeptide 2 rescues antigen presentation. *J. Immunol.* **189**, 1868-1877 (2012).
30. Nazif, T. & Bogyo, M. Global analysis of proteasomal substrate specificity using positional-scanning libraries of covalent inhibitors. *Proc. Natl. Acad. Sci.* **98**, 2967-72 (2001).
31. Lightcap, E.S. et al. Proteasome inhibition measurements: clinical application. *Clin. Chem.* **46**, 673-683 (2000).
32. Crawford, L.J.A. et al. Comparative selectivity and specificity of the proteasome inhibitors BzLLCCHO, PS-341, and MG-132. *Cancer Res.* **66**, 6379-6386 (2006).
33. Moravec, R.A. et al. Cell-based bioluminescent assays for all three proteasome activities in a homogeneous format. *Anal. Biochem.* **387**, 294-302 (2009).
34. Wilkins, O.M. et al. Cell-line-specific high background in the Proteasome-Glo assay of proteasome trypsin-like activity. *Anal. Biochem* **451**, 1-3 (2014).
35. Vigneron, N., Abi Habib, J. & Van den Eynde, B.J. The capture proteasome assay: A method to measure proteasome activity in vitro. *Anal. Biochem* **482**, 7-15 (2015).
36. Guillaume, B. et al. Two abundant proteasome subtypes that uniquely process some antigens presented by HLA class I molecules. *Proc. Natl. Acad. Sci.* **107**, 18599-18604 (2010).
37. Kisselev, A.F., Akopian, T.N., Castillo, V. & Goldberg, A.L. Proteasome active sites allosterically regulate each other, suggesting a cyclical bite-chew mechanism for protein breakdown. *Mol. Cell* **4**, 395-402 (1999).
38. Ping Dou, Q. & A. Zonder, J. Overview of proteasome inhibitor-based anti-cancer therapies: perspective on bortezomib and second generation proteasome inhibitors versus future generation inhibitors of ubiquitin-proteasome System. *Curr. Cancer Drug Targets* **14**, 517-536 (2014).
39. Britton, M. et al. Selective inhibitor of proteasome's caspase-like sites sensitizes cells to specific inhibition of chymotrypsin-like sites. *Chem. Biol.* **16**, 1278-1289 (2009).
40. Kraus, M. et al. The novel β 2-selective proteasome inhibitor LU-102 synergizes with bortezomib and carfilzomib to overcome proteasome inhibitor resistance of myeloma cells. *Haematologica* **100**, 1350-1360 (2015).
41. Wakata, A. et al. Simultaneous fluorescent monitoring of oroteasomal subunit catalysis. *J. Am. Chem. Soc.* **132**, 1578-1582 (2010).
42. Priestman, M.A. et al. Multicolor monitoring of the proteasome's catalytic signature. *ACS Chem. Biol.* **10**, 433-440 (2015).
43. Harris, J.L., Alper, P.B., Li, J., Rechsteiner, M. & Backes, B.J. Substrate specificity of the human proteasome. *Chem. Biol.* **8**, 1131-1141 (2001).
44. Omura, S. et al. Lactacystin, a novel microbial metabolite, induces neurogenesis of neuroblastoma cells. *J. Antibiot. (Tokyo)* **44**, 113-6 (1991).

45. Fenteany, G., Standaert, R.F., Reichard, G.A., Corey, E.J. & Schreiber, S.L. A beta-lactone related to lactacystin induces neurite outgrowth in a neuroblastoma cell line and inhibits cell cycle progression in an osteosarcoma cell line. *Proc. Natl. Acad. Sci.* **91**, 3358-62 (1994).
46. Fenteany, G. et al. Inhibition of proteasome activities and subunit-specific amino-terminal threonine modification by lactacystin. *Science* **268**, 726-731 (1995).
47. Craiu, A. et al. Lactacystin and clasto-lactacystin β -lactone modify multiple proteasome β -subunits and inhibit intracellular protein degradation and major histocompatibility complex class I antigen presentation. *J. Biol. Chem.* **272**, 13437-13445 (1997).
48. Bogyo, M. et al. Covalent modification of the active site threonine of proteasomal β subunits and the Escherichia coli homolog HslV by a new class of inhibitors. *Proc. Natl. Acad. Sci.* **94**, 6629-6634 (1997).
49. Bogyo, M. in *Methods in Enzymology* (ed. Raymond, J.D.) 609-622 (Academic Press, 2005).
50. Kessler, B.M. et al. Extended peptide-based inhibitors efficiently target the proteasome and reveal overlapping specificities of the catalytic β -subunits. *Chem. Biol* **8**, 913-929 (2001).
51. Meng, L. et al. Epoxomicin, a potent and selective proteasome inhibitor, exhibits in vivo antiinflammatory activity. *Proc. Natl. Acad. Sci.* **96**, 10403-10408 (1999).
52. Sin, N. et al. Total synthesis of the potent proteasome inhibitor epoxomicin: a useful tool for understanding proteasome biology. *Bioorg. Med. Chem. Lett.* **9**, 2283-2288 (1999).
53. Berkers, C.R. et al. Activity probe for in vivo profiling of the specificity of proteasome inhibitor bortezomib. *Nat. Methods* **2**, 357-362 (2005).
54. Verdoes, M. et al. Acetylene functionalized BODIPY dyes and their application in the synthesis of activity based proteasome probes. *Bioorg. Med. Chem. Lett.* **17**, 6169-6171 (2007).
55. Verdoes, M. et al. A panel of subunit-selective activity-based proteasome probes. *Org. Biomol. Chem.* **8**, 2719-2727 (2010).
56. Verdoes, M. et al. Chemical proteomics profiling of proteasome activity. *Methods Mol. Biol.* **328**, 51-69 (2006).
57. Verdoes, M. et al. A fluorescent broad-spectrum proteasome inhibitor for labeling proteasomes in vitro and in vivo. *Chem. Biol* **13**, 1217-1226 (2006).
58. Berkers, C.R. et al. Profiling proteasome activity in tissue with fluorescent probes. *Mol. Pharm.* **4**, 739-748 (2007).
59. Li, N. et al. Relative quantification of proteasome activity by activity-based protein profiling and LC-MS/MS. *Nat. Protocols* **8**, 1155-1168 (2013).
60. de Bruin, G. et al. Structure-based design of β 1i or β 5i specific inhibitors of human immunoproteasomes. *J. Med. Chem.* **57**, 6197-6209 (2014).
61. Huber, E.M. et al. Systematic analyses of substrate preferences of 20S proteasomes using peptidic epoxyketone inhibitors. *J. Am. Chem. Soc.* **137**, 7835-7842 (2015).
62. Geurink, P.P. et al. Incorporation of non-natural amino acids improves cell permeability and potency of specific inhibitors of proteasome trypsin-like sites. *J. Med. Chem.* **56**, 1262-1275 (2013).
63. de Bruin, G. et al. A set of activity-based probes to visualize human (immuno)proteasome activities. *Angew. Chem. Int. Ed.* **13**, 4199-4203 (2015).
64. Ho, Y.K., Bargagna-Mohan, P., Wehenkel, M., Mohan, R. & Kim, K.-B. LMP2-specific inhibitors: chemical genetic tools for proteasome biology. *Chem. Biol.* **14**, 419-430 (2007).
65. Singh, A.V. et al. PR-924, a selective inhibitor of the immunoproteasome subunit LMP-7, blocks multiple myeloma cell growth both in vitro and in vivo. *Br. J. of Haematol.* **152**, 155-163 (2011).
66. Carmony, K.C. et al. A bright approach to the immunoproteasome: Development of LMP2/ β 1i-specific imaging probes. *Bioorg. Med. Chem.* **20**, 607-613 (2012).
67. Sharma, L.K. et al. Activity-based near-infrared fluorescent probe for LMP7: A chemical proteomics tool for the immunoproteasome in living cells. *ChemBioChem* **13**, 1899-1903 (2012).
68. Carmony, K.C. & Kim, K.B. Activity-based imaging probes of the proteasome. *Cell Biochem. Biophys.* **67**, 91-101 (2013).

CHAPTER 3

A set of activity-based probes to visualize human (immuno)proteasome activities*

Introduction

Intracellular proteolysis in eukaryotes is mediated predominantly by 26S proteasomes, which consist of a 20S proteolytic core particles (CP) and one or two 19S regulatory complexes. In vertebrates, constitutive 20S proteasome core particles (cCP) are expressed in all tissues.¹ Proteasomes are therapeutic targets for various cancers and autoimmune diseases. Proteasome core particles are C2-symmetrical complexes of four stacked rings of seven subunits each. The outer rings contain seven α -subunits and the inner rings contain seven β -subunits.² Catalytic activity resides in the β -rings, with β 1c cleaving preferentially after acidic residues (caspase-like), β 2c after basic residues (trypsin-like) and β 5c after hydrophobic residues (chymotrypsin-like). Lymphoid tissues express the IFN- γ inducible immunoproteasome core particles (iCP), in which β 1c, β 2c and β 5c are substituted for β 1i (LMP2), β 2i (MECL-1) and β 5i (LMP7) respectively, and substrate preferences of the iCP activities differ from their cCP counterparts.³ For instance, whereas β 1c prefers acidic residues at P1, β 1i cleaves preferentially after hydrophobic residues at this position. As a consequence, iCPs produce oligopeptides with more hydrophobic and basic C-termini, which can bind to MHC-I molecules.^{4,5} The assignment of proteasome catalytic activities can be achieved using synthetic, peptide-based fluorogenic substrates (see chapter 1). However, the majority of fluorogenic proteasome substrates do not distinguish between cCP and iCP activities.⁶ The ELISA-based ProCISE assay is time-consuming and requires antibodies to all six subunits.⁷ Fluorescent, irreversibly binding proteasome probes can be used to assay individual catalytic activities by activity-based protein profiling (ABPP), but β 1c, β 1i, β 5c and β 5i subunits cannot be resolved on SDS-PAGE when labelled with the same probe.⁸⁻¹² This chapter describes the

* de Bruin, G. et al. A set of activity-based probes to visualize human (immuno)proteasome activities. *Angew. Chem. Int. Ed.*, **13**, 4199-4203 (2016).

development of a set of activity-based probes that allows simultaneous detection of all catalytic subunits of human cCP and iCP proteasomes in a rapid SDS-PAGE based assay (Figure 1). This cocktail is used to develop selective inhibitors for $\beta 1c$, $\beta 2c$, $\beta 5c$ and $\beta 2i$, to compare active site specificity of clinical proteasome inhibitors and to demonstrate that many hematologic malignancies predominantly express immunoproteasomes. Furthermore, it is shown that selective and complete inhibition of $\beta 5i$ and $\beta 1i$ is cytotoxic to primary cells from acute lymphocytic leukemia (ALL) patients.

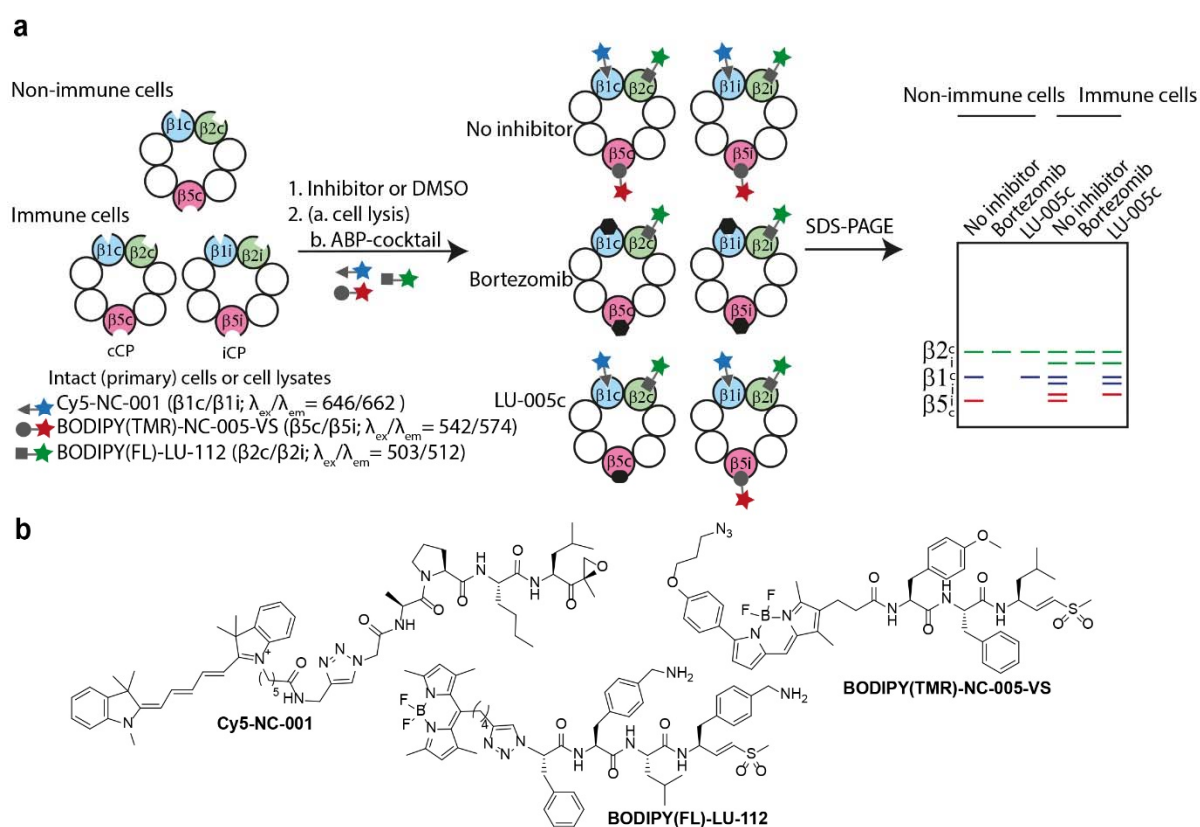


Figure 1. Activity-based probe (ABP) cocktail allows visualisation of the six human active cCP and iCP subunits on SDS-PAGE. A) Schematic representation of competitive activity-based protein profiling (ABPP) using a proteasome ABP cocktail. B) Structures of Cy5-NC-001, BODIPY(FL)-LU-112 and BODIPY(TMR)-NC-005-VS.

Results and discussion

To enable simultaneous resolution of six proteasome subunits, the previously developed site-specific inhibitors NC-001¹³, LU-112¹⁴, and NC-005-VS¹⁵ were equipped with three different fluorophores. This approach yielded $\beta 1c$ and $\beta 1i$ -reactive Cy5-NC-001, $\beta 2c$ and $\beta 2i$ -reactive BODIPY(FL)-LU-112¹⁴ and BODIPY(TMR)-NC-005-VS¹⁶ which modifies the $\beta 5c$ and $\beta 5i$ sites (Figure 1B). Complete and optimal modification of the targeted sites is achieved at 100 nM Cy5-NC-001 and BODIPY(TMR)-NC-005-VS and 30 nM BODIPY(FL)-LU-112 (Figure S1, for

inhibition constants see Figure S2). Treatment of HEK-293 extracts with a cocktail of the three activity based probes (ABPs) followed by SDS-PAGE and in-gel fluorescent detection yielded three clear bands corresponding to the three cCP activities expressed by HEK-293 cells (Figure 2A). Treatment of lysate from Raji cells, a human B-lymphoblastic cell line expressing both cCP and iCP, with the same ABP cocktail resulted in six well-resolved bands, with the two top bands labelled in green corresponding to β 2c and β 2i, the two middle bands in blue to β 1c and β 1i and the two bottom bands in red to β 5c and β 5i (Figure 2A). The specific fluorescence signal can be quantified and is directly proportional to the amount of cells/protein present per sample. The detection limit for all six subunits corresponds to 1×10^3 cells per sample (Figure S3). The time-dependent, IFN- γ -mediated induction of iCP catalytic subunits can be monitored without the need for proteasome subunit specific antibodies (Figure 2B).¹⁷

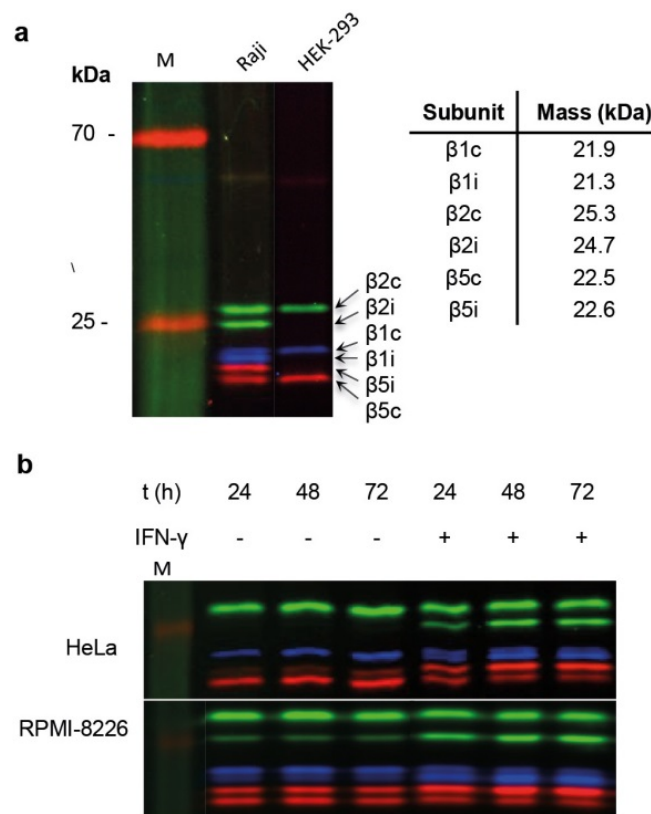


Figure 2. ABP cocktail allows visualisation of the human active cCP and iCP subunits on SDS-PAGE. A) Labelling profiles of Raji and HEK-293 lysates with the ABP probe cocktail. The table shows the molecular weight of the active subunits. B) IFN- γ treated HeLa cells (very low endogenous iCP) and RPMI-8226 (MM cell line permanently expressing both cCP and iCP) show induction of iCP upon treatment with IFN- γ .

Selective inhibitors of individual subunits are much sought after agents to study the role of these subunits in antigen presentation and as drug targets in different diseases.¹⁸ An almost complete set of subunit selective inhibitors has been developed in the past years, which will be partially discussed in the chapters following this one. To complement the previously

reported subunit specific inhibitors LU-001i ($\beta 1i$, chapter 5)¹⁹ and LU-015i ($\beta 5i$, chapter 5)¹⁹ as well as in-class broad-spectrum inhibitors NC-001 ($\beta 1c/\beta 1i$)¹⁵, LU-102 ($\beta 2c/\beta 2i$)¹⁴ and NC-005 ($\beta 5c/\beta 5i$)¹³ the ABP cocktail was used to discover $\beta 1c$, $\beta 2c$, $\beta 2i$, and $\beta 5c$ specific inhibitors (Figure 3).

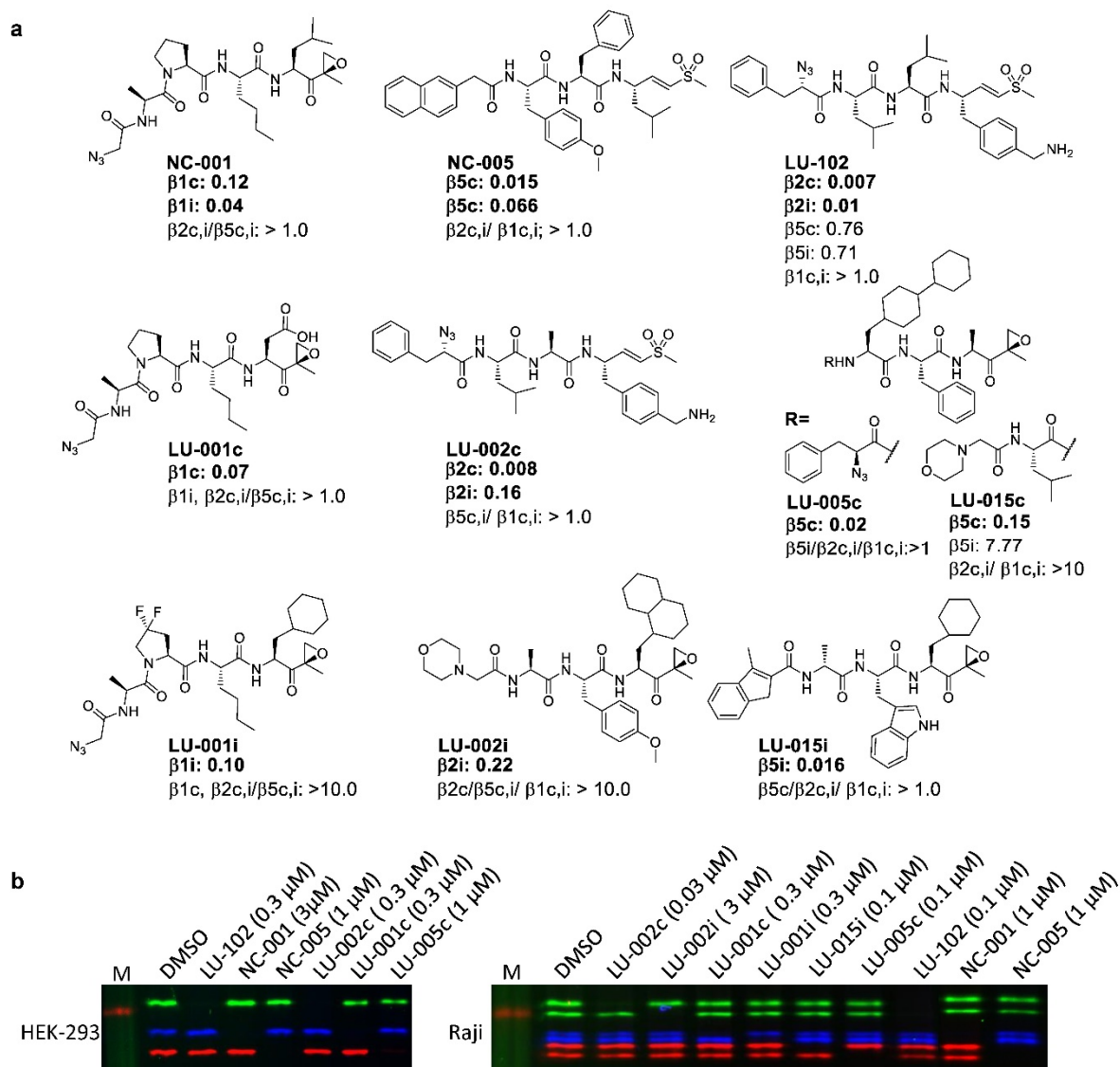


Figure 3. Proteasome subunit specific inhibitors. A) Chemical structures and IC_{50} values (μ M) in Raji lysates of (newly developed) proteasome subunit specific inhibitors. B) Selective inhibition of β -subunits in HEK-293 and Raji lysates by subunit specific proteasome inhibitors assessed by competitive ABPP.

LU-001c (chapter 8) is a β 1c specific inhibitor and LU-005c/LU-015c are β 5c-specific (chapter 7). LU-002c is β 2c-specific, and LU-002i is a specific inhibitor of β 2i.[†] Subunit specificity of all inhibitors was confirmed in Raji and HEK-293 extracts, and in intact RPMI-8226 cells (Figure S4 and Table S1-2 for apparent IC₅₀ values).

Clinical trials of proteasome inhibitors involve pharmacodynamic assessment of proteasome inhibition in blood, where often only combined β 5c and β 5i activity is measured. At the time of bortezomib development, these β 5c and β 5i subunits were considered the exclusive targets of antineoplastic agents.²⁰ Later studies however showed that co-inhibition of other catalytic sites contribute to the antineoplastic activity of bortezomib and carfilzomib.^{9, 21} Therefore, it is important to measure inhibition of all six sites. To demonstrate applicability of the here described ABPP assay for this purpose, a side-by-side comparison of proteasome inhibition in RPMI-8226 cells by the clinical drugs carfilzomib and bortezomib, and the clinical candidates oprozomib²², delanzomib²³ and ixazomib²⁴ was made (Figure 4A-C).^{25, 26} All five compounds proved to be potent β 5c and β 5i inhibitors. As described in the literature bortezomib co-inhibits β 1c/ β 1i²⁷, but β 2c and β 2i are only partially inhibited at micromolar concentrations. Carfilzomib is rather β 5c/ β 5i-specific at lower concentrations, but blocks all 6 sites at higher concentrations. Oprozomib, an orally bioavailable analogue of carfilzomib, is more β 5c/ β 5i-selective. Another boronic acid, delanzomib, matches the activity profile of bortezomib except that delanzomib does not inhibit β 2c/ β 2i even at high concentrations. Ixazomib inhibits four sites, β 5c, β 5i, β 1c and β 1i with about equal potency, but at 10-fold higher concentrations than bortezomib. Comparison of recovery of proteasome activity after 1 h inhibitor treatment, followed by inhibitor washout (Figure 4D,E; Figure S5) confirmed that ixazomib has the fastest off-rate.²⁸ Remarkably, the residence time of the three boronates in β 5c/ β 5i active sites is much shorter than in β 1c/ β 1i active sites.

Information on relative expression of constitutive and immunoproteasomes in primary cells from different hematologic malignancies is limited. Therefore, expression of active immunoproteasomes subunits with their constitutive counterparts in primary cells from ALL, AML, CLL and MM patients were compared by direct quantification based on gel band intensities (Figure 5A). Expression of immunoproteasomes exceeded expression of constitutive proteasomes in all patient samples. In contrast, MM derived cell lines (RPMI-8226 and AMO) show higher expression levels of constitutive subunits (>50% β 5c). Even more striking, in all primary patient samples from lymphoid malignancies (2 x B-ALL, 1 x T-ALL, 2 x CLL) over 90% of β 5 and 75% of β 1 proteasome activity is provided by iCPs. The β 2c/ β 2i ratio was less pronounced, probably reflecting the presence of proteasomes consisting of both

[†] Manuscript regarding β 2c and β 2i inhibitors in preparation by B.T. Xin *et al.*

constitutive and immuno-proteasome subunits, termed hybrid or intermediate proteasomes.^{29, 30} From a drug development perspective, the here presented data strongly indicate that immunoproteasomes should be regarded as a major drug target in MM and lymphoid neoplasmas such as ALL and chronic lymphocytic leukemia (CLL).

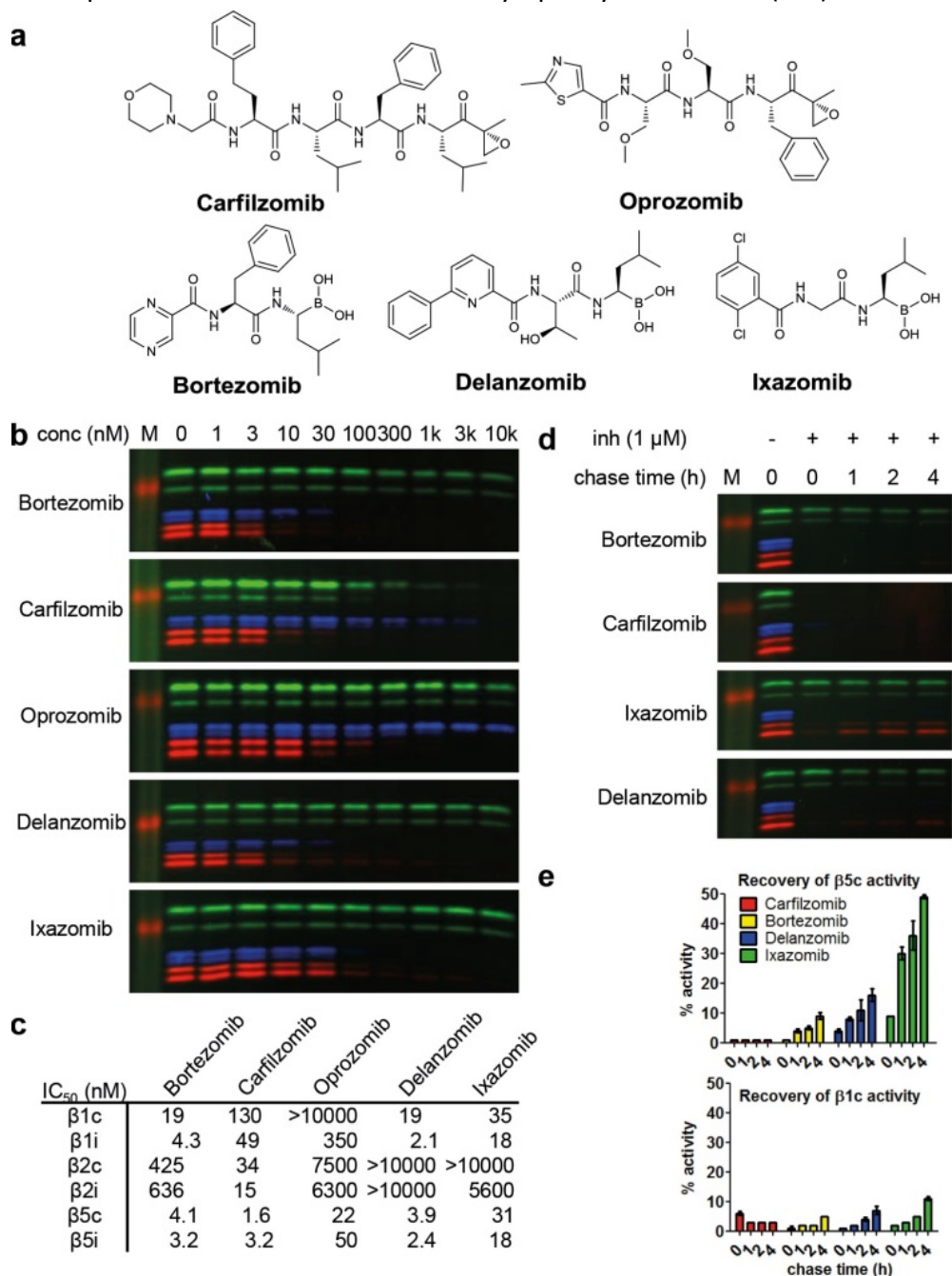


Figure 4. Characterization of proteasome inhibitors used clinically (bortezomib and carfilzomib) and undergoing trials (oprozomib, delanzomib, ixazomib). A) Chemical structures of inhibitors. B,C) Inhibition profiles (B) and apparent IC₅₀ values (C) in living RPMI-8226 cells after 1 hour treatment. D,E) 1 h treatment with inhibitors, followed by washout and chase for 1, 2 or 4 h showed highest recovery of proteasome activity for ixazomib. Recovery of β5c/β5i is much faster than β1c/β1i (E).

In support of this the effect of selective inhibition of $\beta 5i$ activity in primary B- and T-ALL samples was tested. Continuous treatment with LU-015i for 48 h resulted in dose dependent cytotoxicity, which however did not fully correlate with $\beta 5i$ inhibition (Figure S6). Since $\beta 1i$ co-inhibition was observed at higher concentrations, it stands to reason that combined inhibition of $\beta 5i$ and $\beta 1i$ would lead to more efficient cell death.

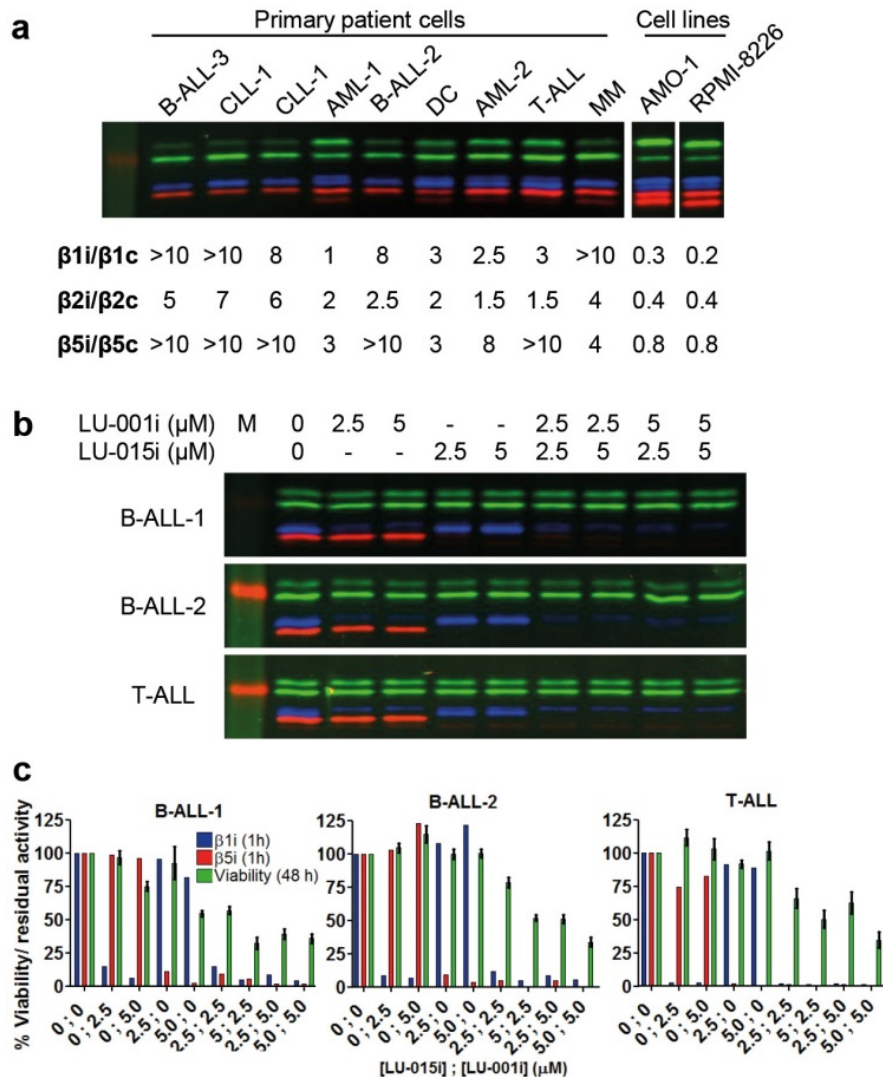


Figure 5. A) Labelling profiles of primary patient cells derived from haematological malignancies, compared to cell lines. Table: ratio between immuno- and constitutive proteasome subunits. B-ALL: B-cell acute lymphoblastic leukemia; T-ALL: T-cell acute lymphoblastic leukemia; CLL: chronic lymphocytic leukemia AML: acute myeloid leukemia; DC: acute leukemia of plasmacytoid dendritic cells MM: multiple myeloma. B) Inhibition profiles of B- and T-ALL cells treated with indicated concentrations of LU-015i or LU-001i. C) Viability of LU-015i and/or LU-001i treated ALL cells after 1 h pulse treatment followed by 48 h chase compared to $\beta 5i$ and $\beta 1i$ inhibition after 1 h.

To test this hypothesis, patient cells were treated for 1 h with a $\beta 5i$ (LU-015i) and/or $\beta 1i$ (LU-001i) inhibitor, washed out unbound inhibitor to ensure specific inhibition (Figure 5B) and assessed cell viability after 48h. It was found that in B-ALL-2 and T-ALL cells, specific $\beta 5i$ or $\beta 1i$ inhibition did not lead to any cytotoxicity, however, combined $\beta 5i$ and $\beta 1i$ inhibition led to up to 70% cell death (Figure 5C). Also in B-ALL-1 cell combined $\beta 5i$ and $\beta 1i$ inhibition resulted in significant higher cytotoxicity than inhibition of only $\beta 5i$ or $\beta 1i$. If these findings are confirmed in additional primary cell samples and animal models, the use of selective inhibitors of the iCP for the treatment of lymphoblastic leukemia and perhaps MM may extend the therapeutic window of proteasome inhibitors, because low iCP expression in the majority of tissues should allow administration of higher doses.

Conclusion

The new ABP probe cocktail presented here provides the first means for rapid, antibody-independent measurement of the six catalytic active cCP and iCP subunits, which can be easily adopted to patients. Furthermore the first comprehensive set of specific inhibitors of all six sites should allow dissection of the contribution of individual proteasome subunits to the generation of antigenic peptides. Finally, the panel of ten subunit specific inhibitors in concert with the activity-based probes provides a good entry point to optimize the therapeutic efficacy of $\beta 5$ -targeted proteasome inhibitors by selective, controlled degrees of co-inhibition of additional active sites of the iCP and/or CP that may be tailored to a given clinical application or disease state.

Supporting figures and tables

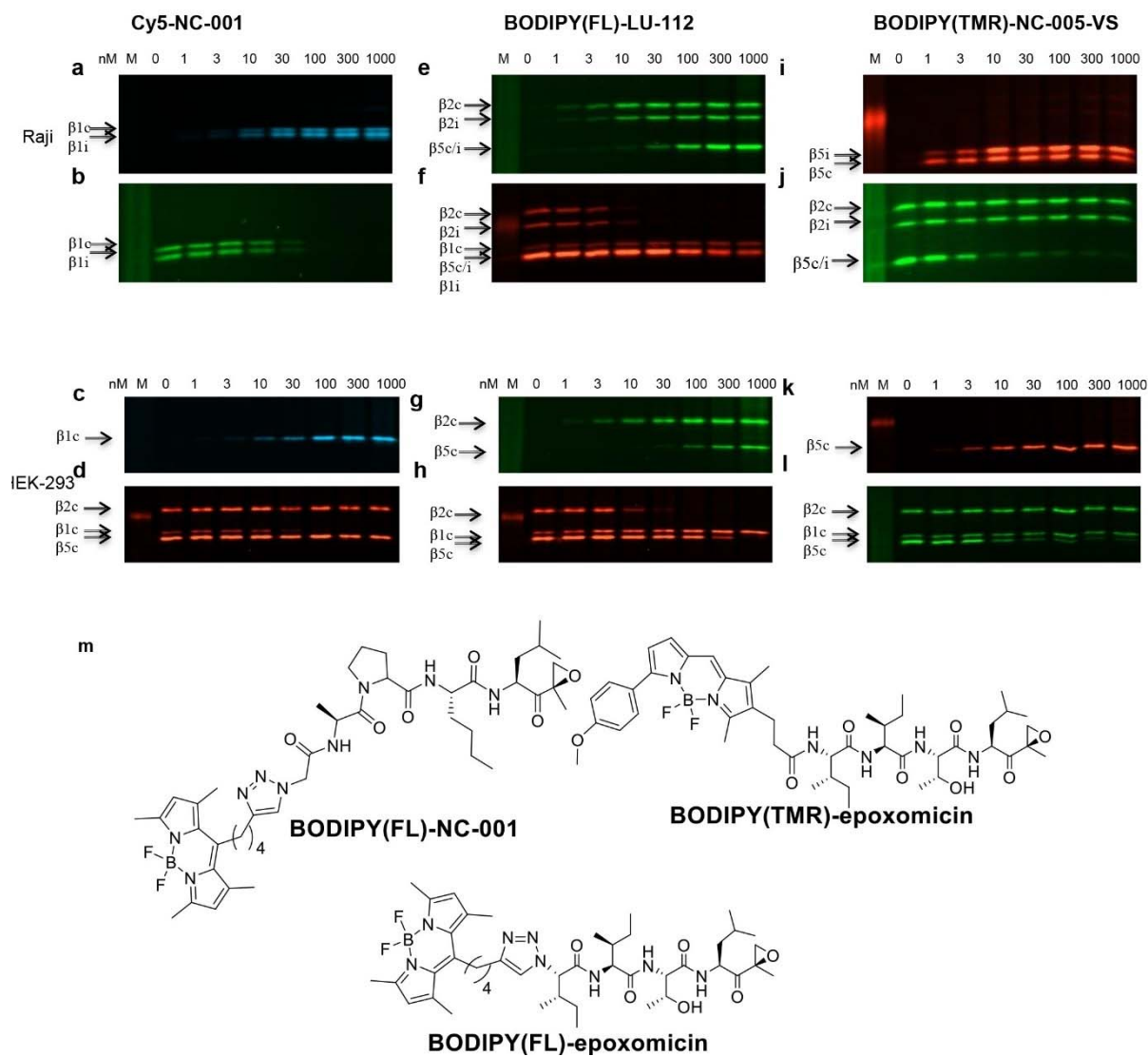


Figure S1. Determination of concentrations of Cy5-NC001 (a-d), BODIPY(FL)-LU-112 (e-h), and BODIPY(TMR)-NC-005-VS (i-l) required for full labelling. Raji/HEK cell lysates were treated with: A-D) Cy5-NC001 for 1 h (A,C), followed by inhibition of β5 by NC005 (5 μM) for 15 min. Residual β1 activity was labelled by BODIPY(FL)-NC-001 (0.5 μM) (B) or BODIPY(TMR)-epoxomicin (0.5 μM) (D); E-H) Extracts were treated with BODIPY(FL)-LU-112 for 1 h (E,H). Residual activity was labelled with BODIPY(TMR)-epoxomicin (0.5 μM) (G,H); I-L) Extracts were treated with BODIPY(TMR)-NC-005-VS for 1 h (I,K), followed by inhibition of β1 by NC-001 (5 μM) for 15 min. Residual activity was labelled by BODIPY(FL)-epoxomicin (J,L). M) Chemical structures of BODIPY(FL)-NC-001, BODIPY-FL-epoxomicin, BODIPY-TMR-epoxomicin.

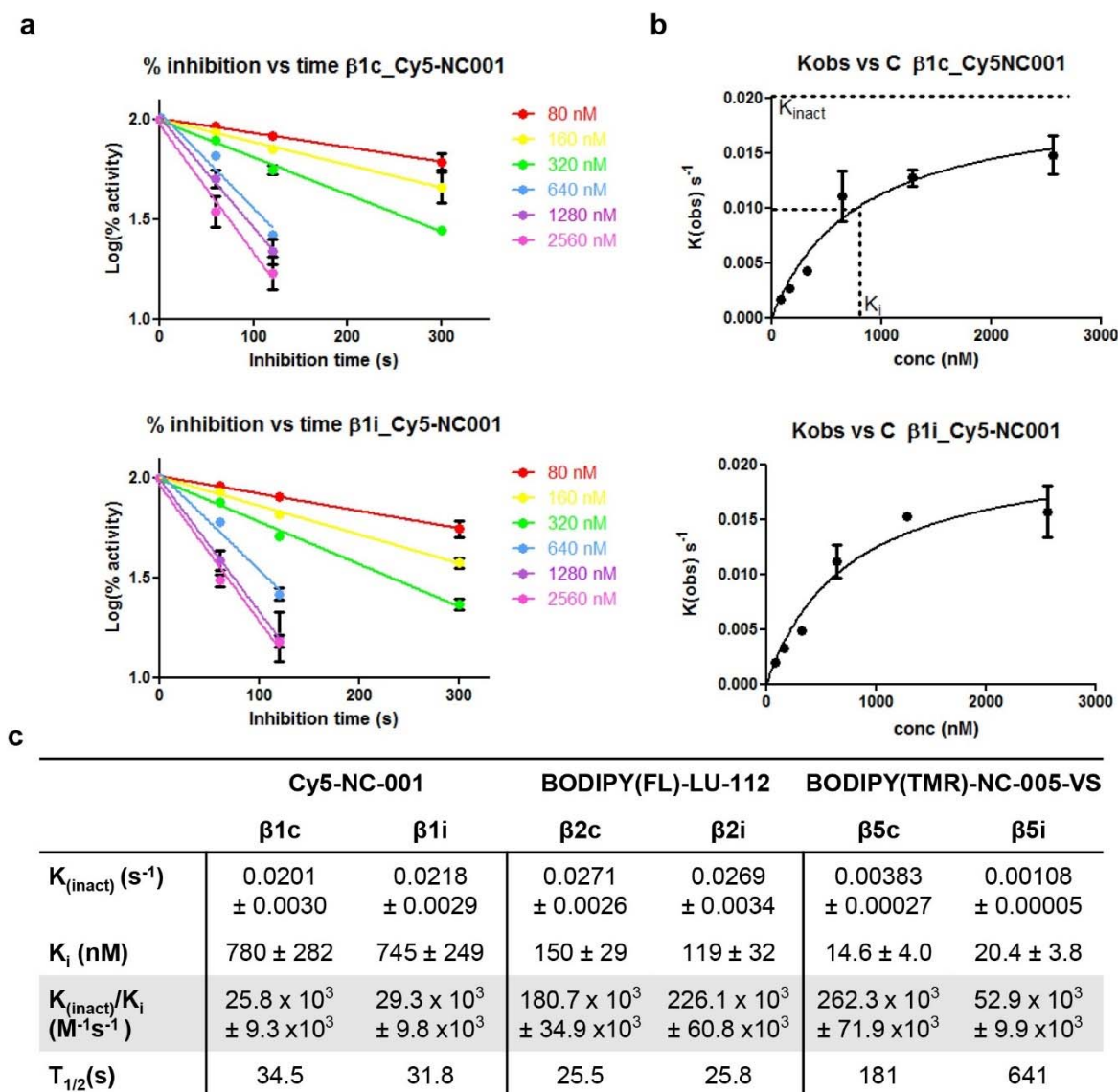


Figure S2. Kinetic constants of Cy5-NC-001, BODIPY(FL)-LU-112, and BODIPY(TMR)-NC-005-VS in Raji lysates. A) Normalized inhibition curves for Cy5-NC001 at various concentrations, providing K_{obs} values (=slope) for each concentration, which are plotted against [probe] in (B). $K_{inact} = \max K_{obs}$, $K_i = [probe]$ at $0.5 K_{inact}$. Similar curves were obtained for BODIPY(FL)-LU-112 and BODIPY(TMR)-NC-005-VS. C) Inhibition constants of the ABP probes.

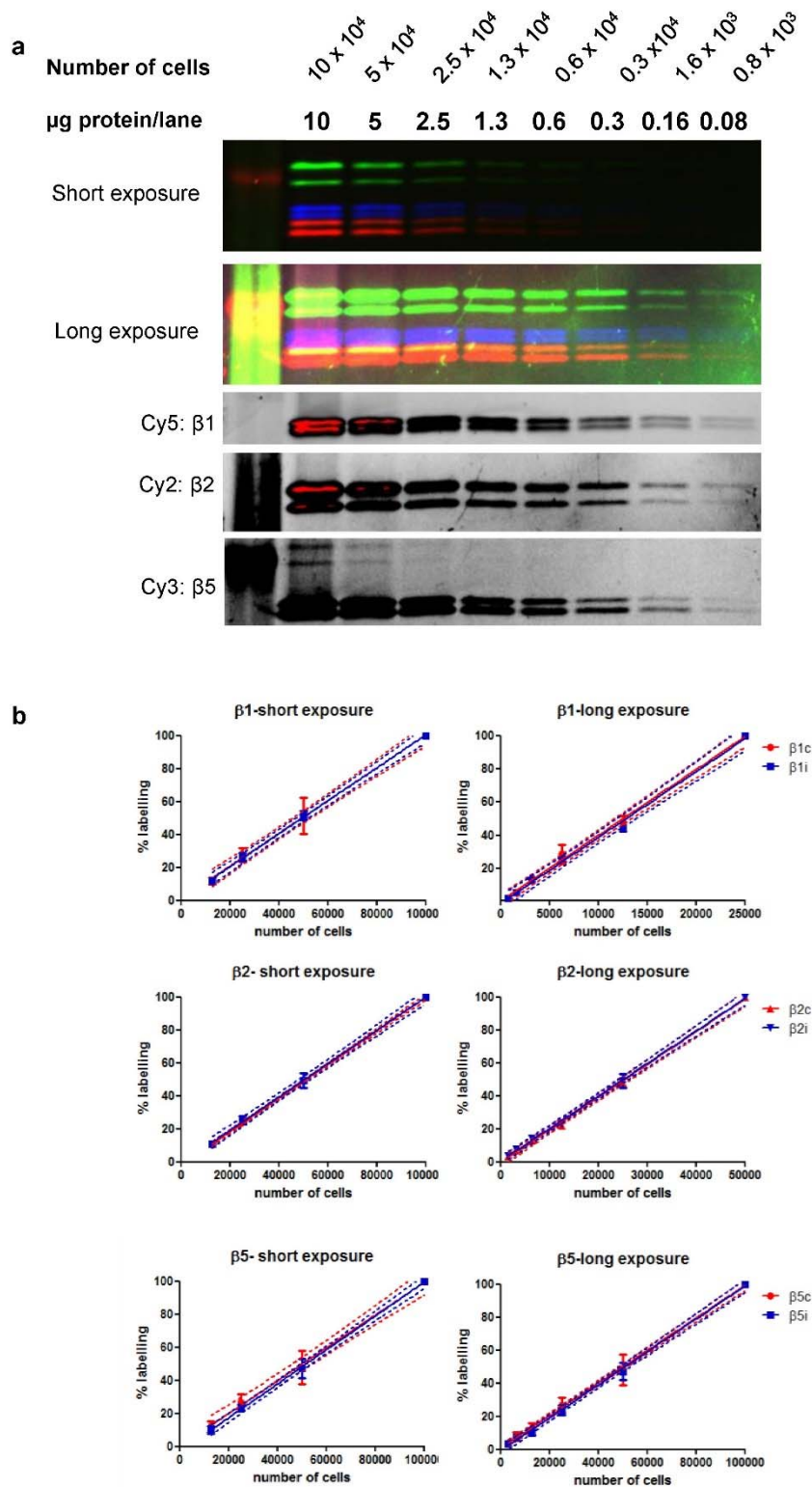


Figure S3. Determination of the linear dynamic range and limit of detection of the ABP cocktail in Raji lysates. A) Labelling profiles of decreasing protein/cell concentrations with ABP cocktail. Gels were exposed for 15/15/5 sec (short) and for 120/120/60 sec (long), respectively for Cy2, Cy3 and Cy5 channels. B) Quantification of gel band intensities shows a linear relation between signal and amount of protein present per lane for each subunit.

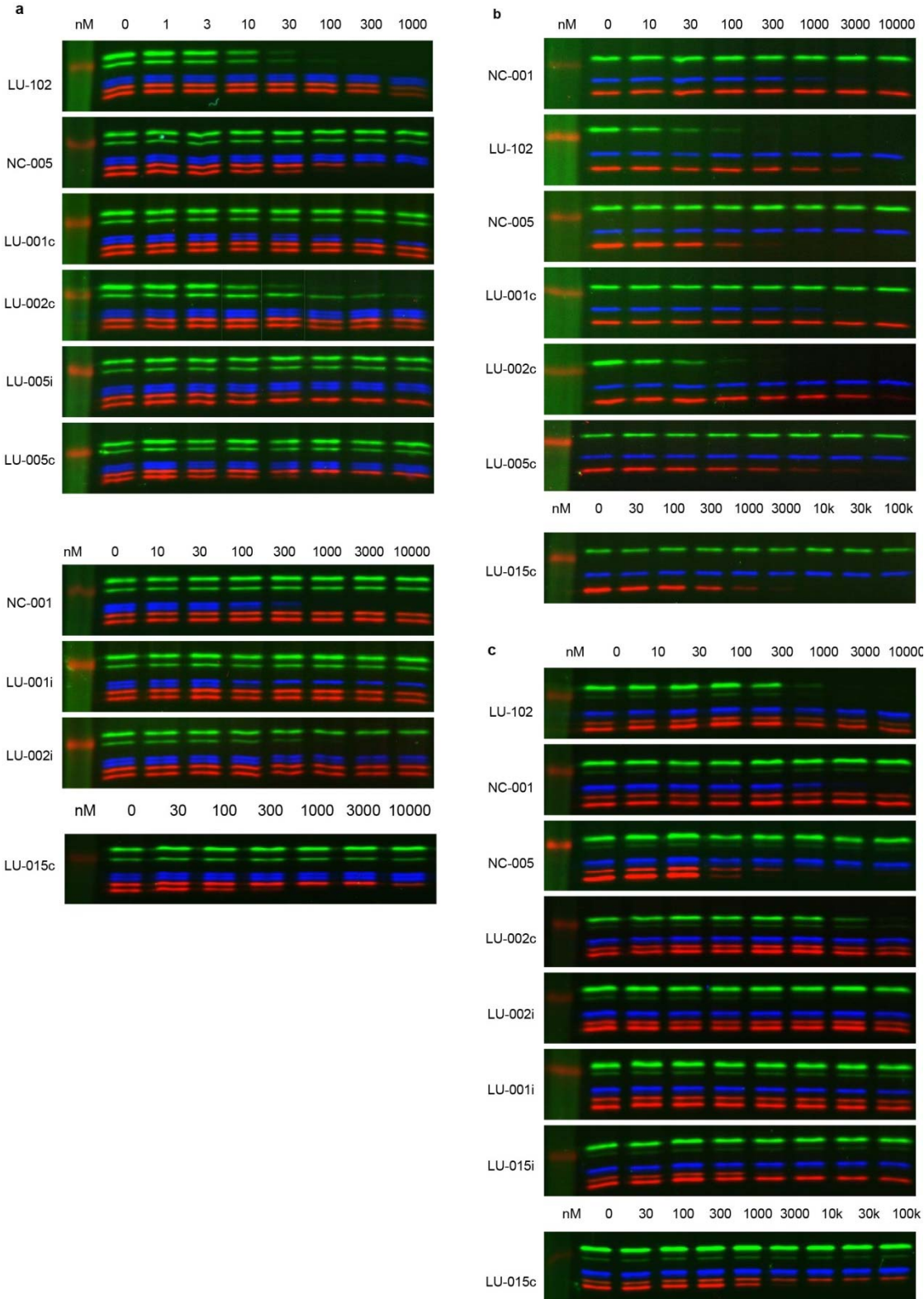


Figure S4. Inhibitory profiles of proteasome subunit selective inhibitors in cell lysates and living cells. A) Raji cell lysates. B) HEK-293 cell lysates. C) Living RPMI-8226 cells.

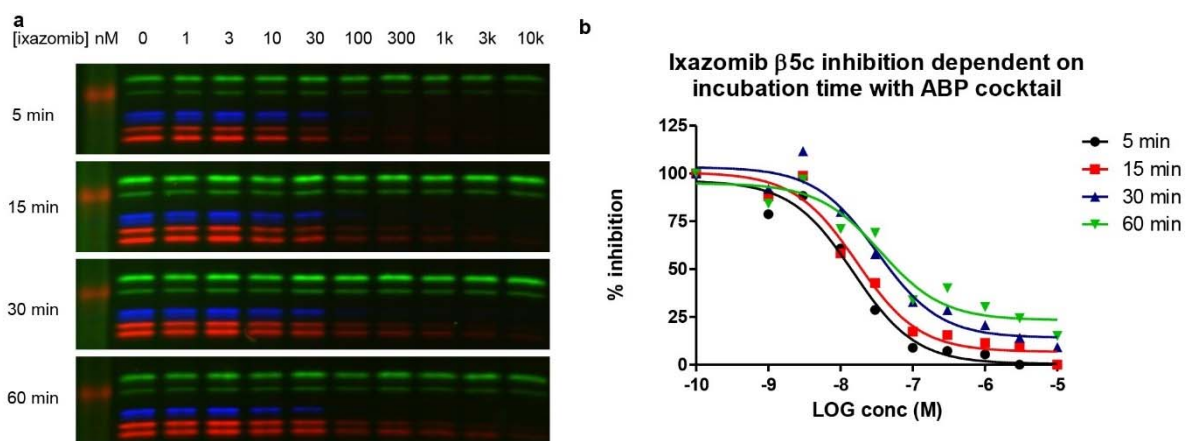


Figure S5. β 5c/ β 5i probe BODIPY(TMR)-NC-005-VS outcompetes ixazomib in time. A) Inhibitory profiles of Raji cell lysates incubated with increasing concentrations of Ixazomib for 1h, followed by 5, 15, 30 or 60 min incubation with probe cocktail. B) Quantification of β 5c inhibition.

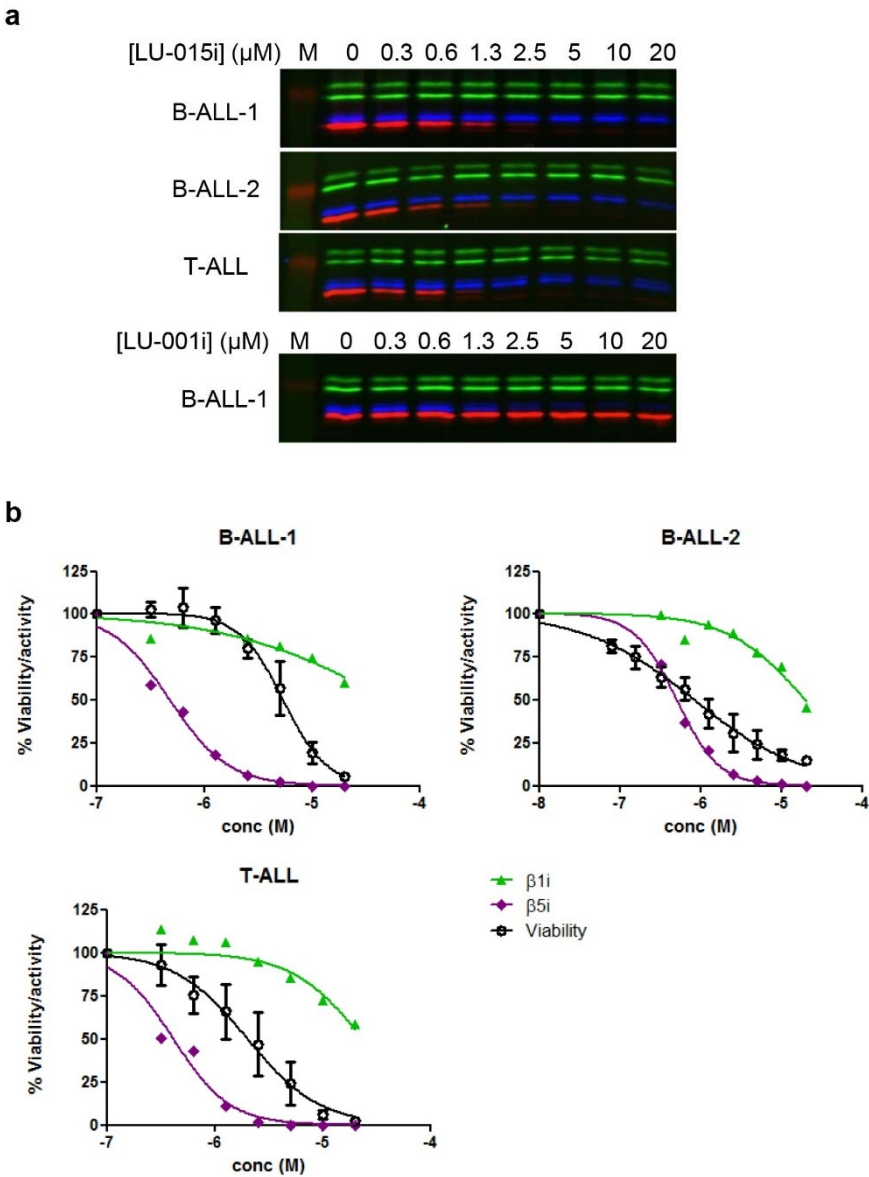


Figure S6. Treatment of ALL cells with LU-015i or LU-001i. A) Inhibition profiles of various primary ALL cells with LU-015i or LU-001i. Cells were treated LU-015i or LU-001i for 1 hour, followed by lysis and labelling with ABP cocktail. B) Viability of LU-015i treated cells after 48 h of continuous exposure compared to $\beta 5i$ and $\beta 1i$ inhibition after 1 h.

A set of activity-based probes to visualize human (immuno)proteasome activities.

Table S1. Apparent IC₅₀ (nM) of subunit specific inhibitors as determined in Raji and HEK-293 cell lysates.

Compound	Raji						HEK-293		
	β1c	β1i	β2c	β2i	β5c	β5i	β1c	β2c	β5c
NC-001	121	44.9	>1000	>1000	>1000	>1000	343	>10000	>10000
LU-102	>1000	>1000	6.98	10.8	766	711	>10000	19.4	837
NC-005	>1000	>1000	>1000	>1000	14.8	65.6	>10000	>10000	59.8
LU-001c	65.5	>1000	>1000	>1000	>1000	>1000	425	>10000	>10000
LU-001i	>10000	98.8	>10000	>10000	>10000	>10000	n.d.	n.d.	n.d.
LU-002c	>1000	>1000	7.90	156	>1000	>1000	>10000	13.9	2838
LU-002i	>10000	>10000	>10000	220	>10000	>10000	n.d.	n.d.	n.d.
LU-005c	>1000	>1000	>1000	>1000	22.9	>1000	>10000	>10000	204
LU-015c	>10000	>10000	>10000	>10000	148	7766	>100000	>100000	255
LU-015i	>1000	>1000	>1000	>10000	>1000	16.0	n.d.	n.d.	n.d.

Table S2. Apparent IC₅₀ (nM) of subunit specific inhibitors as determined in living RPMI-8226 cells

Compound	β1c	β1i	β2c	β2i	β5c	β5i
NC-001	714	461	>10000	>10000	>10000	>10000
LU-102	>10000	>10000	294	407	>10000	>10000
NC-005	>10000	>10000	>10000	>10000	61.4	224
LU-001c	>10000	>10000	>10000	>10000	>10000	>10000
LU-001i	>10000	122	>10000	>10000	>10000	>10000
LU-002c	>10000	>10000	1801	>10000	>10000	>10000
LU-002i	>10000	>10000	>10000	>541	>10000	>10000
LU-015c	>100000	>100000	>100000	>100000	1017	>100000
LU-015i	>10000	>10000	>10000	>10000	>10000	211

Experimental

Biochemical methods

General

Lysates of cells were prepared by treating cell pellets with 4 volumes of lysis buffer containing 50 mM Tris pH 7.5, 2 mM DTT, 5 mM MgCl₂, 10% glycerol, 2 mM ATP, and 0.05% digitonin for 15-60 min. Protein concentration was determined using Qubit[®] protein assay kit (Thermo Fisher). All cell lysate labelling experiments were performed in assay buffer containing 50 mM Tris pH 7.5, 2 mM DTT, 5 mM MgCl₂, 10% glycerol, 2 mM ATP. Cell lysate labelling and competition experiments were performed at 37°C. Prior to fractionation on 12.5% SDS-PAGE (TRIS/glycine), samples were boiled for 3 min in a reducing gel loading buffer. The 7.5x10 cm (L x W) gels were run for 15 min at 80V followed by 120 min at 130V. In-gel detection of (residual) proteasome activity was performed in the wet gel slabs directly on a ChemiDoc™ MP System using Cy2 setting to detect BODIPY(FL)-LU-112, BODIPY(FL)-epoxomicin and BODIPY(FL)-NC-001, Cy3 settings to detect BODIPY(TMR)-NC-005-VS and BODIPY(TMR)-epoxomicin and Cy5 settings to detect Cy5-NC-001. When the probes were used as a mixture the following concentrations were used: 100 nM Cy5-NC-001, 30 nM BODIPY(FL)-LU-112, 100 nM BODIPY(TMR)-NC-005-VS, as premixed 10x concentrated cocktail in DMSO which was incubated with cell lysate for 60 min, unless stated otherwise.

Determination of probe concentration required for full subunit labelling

Cy5-NC001: Raji or HEK-293 cell lysates (10 µg/ 9µL) were treated with increased concentration of Cy5-NC-001 (1 µL from 10x stock in DMSO) for 1 h. Next, for Raji lysates residual β5 activity was blocked (BODIPY(FL)-NC-001 may partially label β5) by NC-005 (5 µM) for 15 min at 37°C followed by labelling of residual β1 activity with BODIPY(FL)-NC001 (0.5 µM) for 1 h. For HEK-293 lysates: residual activity was labelled with BODIPY(FL)-epoxomicin (0.5 µM) for 1 h.

BODIPY(FL)-LU-112: Raji or HEK-293 cell lysates (10 µg/ 9µL) were treated with increased concentration of BODIPY(FL)-LU-112 (1 µL from 10x stock in DMSO) for 1 h. Next, residual proteasome activity was labelled by BODIPY(TMR)-epoxomicin (0.5 µM) for 1 h.

BODIPY(TMR)-NC-005-VS: Raji or HEK-293 cell lysates (10 µg/ 9µL) were treated with increased concentration of BODIPY(TMR)-NC-005-VS (1 µL from 10x stock in DMSO) for 1 h, followed by inhibition of β1 by NC-001 (5 µM) for 15 min. Next, residual proteasome activity was labelled by BODIPY(FL)-epoxomicin (0.5 µM) for 1 h.

Labelling of all six subunits was performed by a mixture of 100 nM Cy5-NC001, 30 nM BODIPY(FL)-LU-112, 100 nM BODIPY(TMR)-NC-005-VS, which were used premixed as 10x concentrated cocktail in DMSO. Chemical structures of BODIPY(FL)-NC-001, BODIPY(FL)-epoxomicin, BODIPY(TMR)-epoxomicin are shown in Figure S1.

Determination of the linear dynamic range and limit of detection of ABP cocktail in Raji lysates.

1 million Raji cells were lysed according to the general method for cell lysis and diluted to the appropriate concentrations followed by labelling with probes according to the general methods, followed by SDS-PAGE. Gels were exposed for 15/15/5 sec (short), and for 120/120/60 sec (long), respectively for the Cy2, Cy3 and Cy5 channels.

Competition experiments in cell lysate

Cell lysates (diluted to 10-15 µg total protein in 9 µL buffer) were exposed to the inhibitors (10x stock in DMSO) at indicated concentrations for 1 h at 37 °C, followed by addition of probe cocktail (10x stock, 1.1 µL) and SDS-PAGE as described in general methods.

Competition experiments in living RPMI-8226 cells

RPMI-8226 were cultured in RPMI-1640 media supplemented with 10% fetal calf serum, GlutaMAX™, penicillin, streptomycin in a 5% CO₂ humidified incubator. $5-8 \times 10^5$ cells/mL were exposed to inhibitors for 1 h at 37 °C. Cells were harvested and washed twice with PBS. Cell pellets were treated with lysis buffer on ice for 15 min, followed by centrifugation at 14000 rpm for 5 min. Proteasome inhibition in the obtained cell lysates was determined using the method described above, with 15 min (in case of bortezomib, MLN2238 and delanzomib, because longer incubation times cause out-competition of boronates, see Figure S4.) or 60 min (all other inhibitors) incubation with ABP cocktail. Intensities of bands were measured by fluorescent densitometry and divided by the intensity of bands in mock-treated extracts. Average values of three independent experiments were plotted against inhibitor concentrations. IC₅₀ (inhibitor concentrations giving 50% inhibition) values were calculated using GraphPad Prism software.

Determination of kinetic constants

Raji cell lysates (10 µg/ 9 µL) were incubated with increasing concentrations of probe for 0, 1, 2 or 5 min. Concentrations used for Cy5-NC001: 80, 160, 320, 640, 1280, 2560 nM; BODIPY(FL)-LU-112 and BODIPY(TMR)-NC-005-VS: 8, 16, 32, 64, 128, 256 nM. The reaction was stopped by snap-freezing in liquid nitrogen and while still frozen, the denaturing sample buffer is added. Next, SDS-PAGE analysis is performed as described in the general methods. Intensities of bands were measured by fluorescent densitometry and normalized to full labelling by either 100 nM Cy5-NC-001, 30 nM BODIPY(FL)-LU-112 or 100 nM BODIPY(TMR)-NC-005-VS for 1 h. When the Log (% activity) is plotted versus time, a straight line is observed, from which the first order rate constants (K_{obs}) can be derived for each concentration. K_{obs} were plotted versus probe concentration, from which inhibition constants K_i and K_{inact} were calculated using Graphpad Prism software.

Inhibitor washout experiments

5×10^5 RPMI-8226 cells were treated with 1 µM of inhibitor (1% DMSO end concentration) at 37°C. After 1 h, the cells were washed with medium (2x) and incubated at 37°C for 0, 1, 2 or 4 hours. The cells were harvested and washed with PBS, lysed in standard lysis buffer for 15 min, followed by centrifugation at 14000 rpm for 5 min. Proteasome inhibition in the obtained cell lysates was determined using the method described above (5 min incubation with probe mixture).

Proteasome labelling in primary patient cells

Primary MM, T-ALL, AML, CLL and DC patient cells were thawed and put in high glucose DMEM medium for 4 hours. Cells were harvested and washed twice with PBS. Cell pellets were treated with lysis buffer on ice for 15 min, followed by centrifugation at 14000 rpm for 10 min. Proteasome inhibition in the obtained cell lysates was determined using the method described above.

Primary ALL cell viability assay

B- and T-ALL primary patient cells (either continuously treated for 48 h with LU-015i at indicated concentrations or pulse treated for 1 h with LU-015i and/or LU-001i at indicated concentrations and washed with medium (2x), followed by a 48 h chase), were assayed for viability by CellTiter Glo-assay (Promega) according to manufacturer's instructions. Luminescence was determined in 96 well microplates in GloMax luminometer (Promega). In parallel, B- and T-ALL cells were treated with indicated concentrations of LU-015i or LU-001i for 1 h and washed with PBS (2x). Cell pellets were treated with lysis buffer on ice for 60 min, followed by centrifugation at 14000 rpm for 10 min. Proteasome inhibition in the obtained cell lysates was determined using the method described above.

Synthetic procedures

General

Acetonitrile (ACN), dichloromethane (DCM), N,N-dimethylformamide (DMF), methanol (MeOH), diisopropylethylamine (DiPEA) and trifluoroacetic acid (TFA) were of peptide synthesis grade, purchased at Biosolve, and used as received. All general chemicals (Fluka, Acros, Merck, Aldrich, Sigma, Iris Biotech) were used as received. Traces of water were removed from reagents used in reactions that require anhydrous conditions by co-evaporation with toluene. Diethylether was stored over 4 Å molecular sieves. Column chromatography was performed on Screening Devices b.v. Silica Gel, with a particle size of 40-63 µm and pore diameter of 60 Å. TLC analysis was conducted on Merck aluminium sheets (Silica gel 60 F254). Compounds were visualized by UV absorption (254 nm), by spraying with a solution of (NH₄)₆Mo₇O₂₄·4H₂O (25 g/L) and (NH₄)₄Ce(SO₄)₄·2H₂O (10 g/L) in 10% sulphuric acid, a solution of KMnO₄ (20 g/L) and K₂CO₃ (10 g/L) in water, or ninhydrin (0.75 g/L) and acetic acid (12.5 mL/L) in ethanol, where appropriate, followed by charring at ca. 150°C. ¹H and ¹³C-NMR spectra were recorded on a Bruker AV-400 (400 MHz) or AV-600 (600 MHz) spectrometer. Chemical shifts are given in ppm (δ) relative to tetramethylsilane, CD₃OD or CDCl₃ as internal standard. High resolution mass spectra were recorded by direct injection (2 µL of a 2 µM solution in water/acetonitrile 50/50 (v/v) and 0.1% formic acid) on a mass spectrometer (Thermo Finnigan LTQ Orbitrap) equipped with an electrospray ion source in positive mode (source voltage 3.5 kV, sheath gas flow 10, capillary temperature 250 °C) with resolution R = 60,000 at m/z 400 (mass range m/z = 150-2,000) and dioctylphthalate (m/z = 391.28428) as a "lock mass". The high resolution mass spectrometer was calibrated prior to measurements with a calibration mixture (Thermo Finnigan). LC-MS analysis was performed on a Finnigan Surveyor HPLC system with a Gemini C18 50 × 4.60 mm column (detection at 200–600 nm) coupled to a Finnigan LCQ Advantage Max mass spectrometer with ESI. The applied buffers were H₂O, MeCN and 1.0% TFA in H₂O (0.1% TFA end concentration). Methods used are: 10→90% MeCN, 13.5 min (0→0.5 min: 10% MeCN; 0.5→8.5 min: gradient time; 8.5→10.5 min: 90% MeCN; 10.5→13.5 min: 90% → 10% MeCN), 0→50% MeCN, 13.5 min (0→0.5 min: 10% MeCN; 0.5→8.5 min: gradient time; 8.5→10.5 min: 90% MeCN; 10.5→13.5 min: 90% → 10% MeCN). HPLC purification was performed on a Gilson HPLC system coupled to a Phenomenex Gemini 5µm 250×10 mm column. All tested compounds are >95% pure on the basis of LC-MS and NMR.

General procedure for azide couplings.

Compounds **5**, **10**, **18**, **25** and **28** were prepared via azide coupling of properly protected peptide hydrazide and properly deprotected epoxyketone amines (Boc-AA-EK were treated with TFA for 30 min, followed by co-evaporation with toluene (2x)). The appropriate hydrazide was dissolved in 1:1 DMF (v/v) and cooled to -30 °C. tBuONO (1.1 equiv.) and HCl (4M solution in 1,4-dioxane, 2.8 equiv.) were added, and the mixture was stirred for 3 h at -30 °C after which TLC analysis (10% MeOH/DCM, v/v) showed complete consumption of the starting material. The epoxyketone as free amine was added to the reaction mixture as a solution in DMF. DiPEA (5 equiv.) was added to the reaction mixture, and this mixture was allowed to warm to RT slowly overnight. The mixture was diluted with EtOAc or DCM and extracted with H₂O (3x). The organic layer was dried over MgSO₄ concentrated and purified by flash column chromatography (1-5% MeOH in DCM) and HPLC-purification (if necessary).

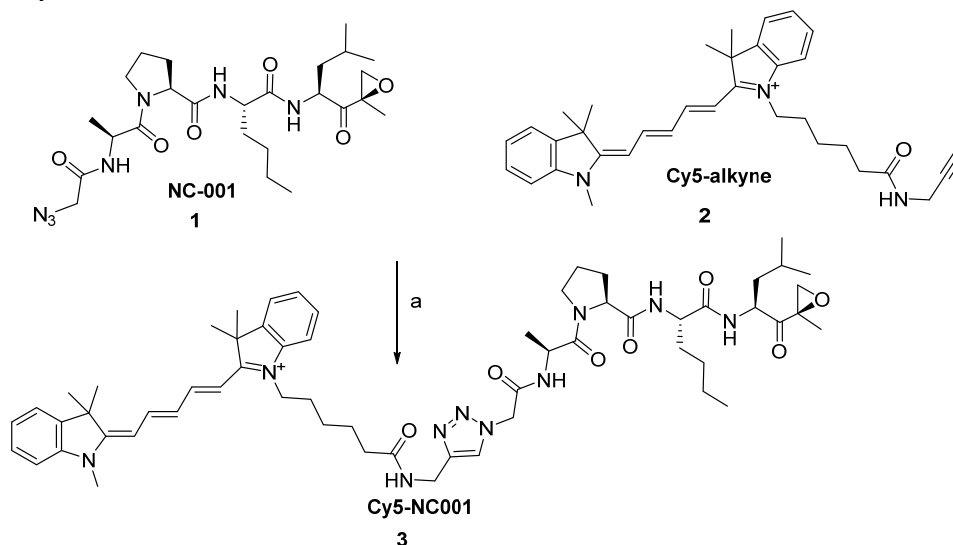
General procedure for Boc removal

Boc protected compounds were treated with TFA (0.1 M) for 30 minutes, followed by co-evaporation with toluene (2x).

General procedure for peptide couplings

Free acid (1.2 equiv.), HCTU (1.2 equiv.) and free amine (1 equiv.) are dissolved in DCM (0.1 M), followed by the addition of DIPEA (3.5 equiv or 4.5 equiv in case of 2-morpholinoacetic acid HCl). After stirring overnight (or alternatively 1-3 hours, until completion), the reaction mixture is concentrated and re-dissolved in EtOAc, washed with 1 N HCl (2x), sat. NaHCO₃ (2x) and brine (in case of morpholino acetic acid coupling, no 1N HCl washings). The organic layer is dried over Na₂SO₄, filtered and concentrated, followed by purification by column chromatography.

Synthesis of Cy5-NC-001

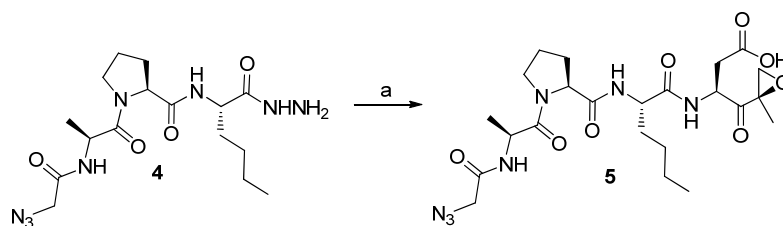


Scheme 1. Synthesis of Cy5-NC001. Reagents and conditions: a. CuSO₄, NaAsc, DMF, H₂O, 54%

Cy5-NC001 (3)

To a degassed solution of NC-001¹³ **1** (7.0 mg, 13 μmol) and Cy5-alkyne **2** (6.0 mg, 12 μmol) in DMF (0.8 mL) under an argon atmosphere was added CuSO₄·5H₂O (0.5 equiv, 6.5 μmol (100 μL from degassed stock solution of 65 μmol/mL)) and NaAsc (0.75 equiv, 9.8 μmol (100 μL from degassed stock solution of 98 μmol/mL)). After stirring overnight, water and EtOAc were added and the layers were separated. The aqueous layer was extracted with DCM (5x). The combined organic layers were evaporated and purified by column chromatography (0-3-5-10-20% MeOH in DCM) providing the product after lyophilisation as a blue powder (7.5 mg, 7 μmol, 54%). ¹H NMR (850 MHz, CDCl₃) δ 7.94 (s, 2H), 7.91 – 7.82 (m, 2H), 7.56 (d, *J* = 39.1 Hz, 2H), 7.40 – 7.36 (m, 2H), 7.37 – 7.33 (m, 2H), 7.23 (dd, *J* = 7.5, 3.7 Hz, 2H), 7.15 – 7.12 (m, 1H), 7.11 (d, *J* = 7.9 Hz, 1H), 6.82 (d, *J* = 12.8 Hz, 2H), 6.43 (d, *J* = 13.5 Hz, 1H), 6.31 (d, *J* = 13.3 Hz, 1H), 5.23 (d, *J* = 14.9 Hz, 1H), 5.14 (d, *J* = 15.8 Hz, 1H), 4.66 – 4.45 (m, 4H), 4.24 (d, *J* = 46.0 Hz, 1H), 4.07 (d, *J* = 7.4 Hz, 2H), 3.65 (d, *J* = 23.0 Hz, 3H), 3.32 (d, *J* = 4.6 Hz, 1H), 2.84 (d, *J* = 5.1 Hz, 1H), 2.42 – 2.29 (m, 2H), 2.05 (d, *J* = 19.8 Hz, 3H), 1.94 (s, 3H), 1.87 – 1.74 (m, 4H), 1.71 (s, 7H), 1.69 – 1.50 (m, 5H), 1.47 (d, *J* = 16.3 Hz, 3H), 1.45 – 1.39 (m, 3H), 1.39 – 1.16 (m, 12H), 0.98 – 0.79 (m, 9H). ¹³C NMR (214 MHz, CDCl₃) δ 208.49, 173.50, 173.11, 172.95, 172.22, 172.08, 171.57, 165.52, 153.30, 152.79, 145.65, 142.90, 142.04, 141.17, 140.86, 129.00, 128.87, 126.42, 125.52, 125.21, 124.44, 122.30, 122.21, 111.09, 110.56, 104.44, 103.99, 60.59, 59.24, 53.83, 52.72, 52.63, 50.38, 49.48, 49.20, 48.61, 47.72, 44.59, 39.90, 36.06, 35.33, 32.07, 31.87, 29.85, 29.52, 28.28, 28.24, 27.96, 27.16, 26.46, 25.44, 25.21, 25.15, 23.55, 22.85, 22.39, 21.41, 17.34, 16.95, 14.29, 14.13. LC-MS (linear gradient 10 → 90% MeCN, 0.1% TFA, 13.0 min): R_t (min): 7.45 (ESI-MS (*m/z*): 1055.53 (M⁺)). HRMS: calculated for C₆₀H₈₃N₁₀O₇ 1055.64407 [M]⁺; found 1055.64425

Synthesis of LU-001c

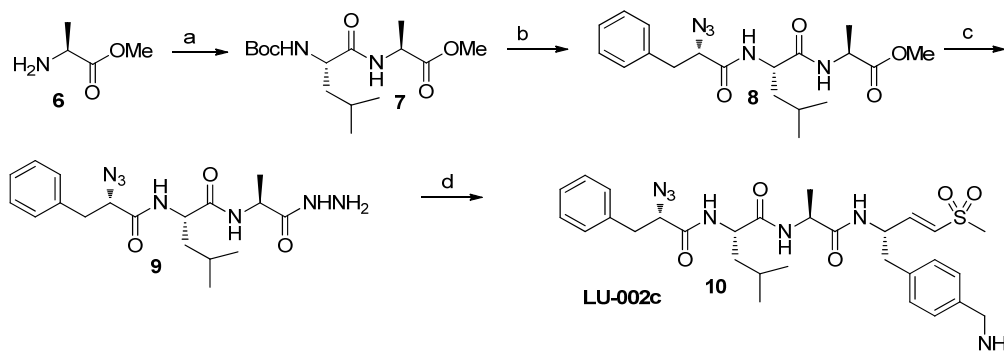


Scheme 2. Synthesis of LU-001c. Reagents and conditions: a. 1. *i*. tBuONO, HCl, DMF, -35°C. ii DiPEA, H₂N-Asp(OtBu)-EK, -35°C-RT. 2. TFA, 1.9 %.

N₃Ac-Ala-Pro-Nle-Asp-EK (LU-001c ,5)

Compound **4** was synthesized as reported before.¹³ This compound was obtained by the general protocol for azide coupling on a 144 μmol scale. Purification by column chromatography (0→3% MeOH in DCM), provided the tert-butyl protected product, which was deprotected by treatment with dry TFA (1 mL) for 10 min, followed by the addition of toluene and concentration. Purification by HPLC (C₁₈, 10-30% MeCN, 0.1% TFA, 15 min gradient), followed by lyophilization provided the product (1.46 mg, 1.9%). Complex NMR due to presence of rotamers, peaks of major rotamer are reported. ¹H NMR (600 MHz, MeOD) δ 4.80 – 4.74 (m, 1H), 4.63 (q, *J* = 7.0 Hz, 1H), 4.46 (dd, *J* = 8.4, 4.5 Hz, 1H), 4.29 – 4.23 (m, 1H), 3.92 – 3.85 (m, 2H), 3.80 (dt, *J* = 9.8, 6.8 Hz, 1H), 3.65 (dt, *J* = 10.1, 6.7 Hz, 1H), 3.23 (d, *J* = 4.7 Hz, 1H), 2.92 (dd, *J* = 12.3, 4.9 Hz, 1H), 2.79 (dd, *J* = 16.5, 4.2 Hz, 1H), 2.70 (dd, *J* = 16.3, 7.6 Hz, 1H), 2.21 (tdd, *J* = 15.0, 9.7, 5.6 Hz, 1H), 2.15 – 2.07 (m, 1H), 2.07 – 1.97 (m, 2H), 1.80 (ddt, *J* = 15.2, 10.8, 5.2 Hz, 1H), 1.71 – 1.57 (m, 1H), 1.40 – 1.30 (m, 7H), 1.22 (s, 3H), 0.97 – 0.88 (m, 3H). ¹³C NMR (151 MHz, MeOD) δ 207.14, 174.28, 174.11, 173.74, 173.24, 169.87, 61.51, 54.67, 53.25, 52.47, 50.51, 49.57, 48.63, 36.13, 32.77, 30.48, 28.93, 26.04, 23.45, 16.82, 14.27. LC-MS (linear gradient 0 → 50% MeCN, 0.1% TFA, 13.5 min): R_t (min): 7.70 (ESI-MS (m/z): 538.07 (M+H)⁺). HRMS: calculated for C₂₃H₃₅N₇O₈ 538.26199 [M+H]⁺; found 538.26202

Synthesis of LU-002c



Scheme 3. Synthesis of LU-002c. Reagents and conditions: a. HCTU, Boc-Leu-OH, DiPEA, DCM, 78%. b. 1. TFA. 2. HCTU, N₃Phe-OH, DiPEA, DCM, 44%. c. Hydrazine hydrate, MeOH, quant. d. 1. *i*. tBuONO, HCl, DMF, -35°C. ii DiPEA, H₂N- Phe(4-CH₂NHBoc)-VS, -35°C-RT. 2. TFA, 25%

Boc-Leu-Ala-OMe (7)

The title compound was prepared by the general procedure for peptide coupling on a 0.5 mmol scale. Column chromatography (10-30% EtOAc/pentane) provided the product (124 mg, 78%). ¹H NMR (400 MHz, CDCl₃) δ 7.07 (d, *J* = 7.3 Hz, 1H), 5.22 (d, *J* = 8.4 Hz, 1H), 4.58-4.51 (m, 1H), 4.24-4.18 (m, 1H), 3.74 (s, 3H), 1.82-1.31 (m, 15H), 0.95-0.88 (m, 6H). ¹³C NMR (101 MHz, CDCl₃) δ 173.25, 172.55, 155.82, 79.93, 52.91, 52.42, 47.96, 41.43, 28.36, 24.68, 23.01, 21.99, 18.03.

N₃Phe-Leu-Ala-OMe (8)

Boc-Leu-Ala-OMe (124 mg, 0.39 mmol) was deprotected using the standard procedure for Boc removal, followed by peptide coupling with N₃Phe-OH using the standard procedure for peptide couplings. Column chromatography (10-30% EtOAc/pentane), provided the product (67 mg, 44%). ¹H NMR (400 MHz, CDCl₃) δ 7.38-7.19 (m, 5H), 6.78 (d, *J* = 7.6 Hz, 2H), 4.59-4.42 (m, 2H), 4.30-4.23 (m, 1H), 3.75 (s, 3H), 3.34-3.29 (m, 1H), 3.09-3.03 (m, 1H), 1.63-1.33 (m, 6H), 0.91-0.86 (m, 6H). ¹³C NMR (101 MHz, CDCl₃) δ 173.20, 171.19, 168.59, 135.94, 129.62, 128.73, 127.35, 65.30, 52.62, 51.56, 48.16, 41.28, 38.38, 24.53, 22.95, 22.15, 18.26.

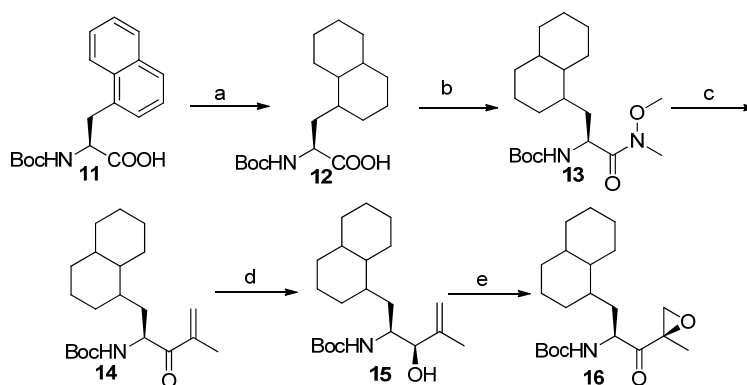
N₃Phe-Leu-Ala-NHNH₂ (9)

N₃Phe-Leu-Ala-OMe (67 mg, 0.17 mmol) was dissolved in MeOH (5 mL), followed by the addition of NH₂NH₂·H₂O (0.25 mL, 5.1 mmol, 30 equiv.). The reaction mixture was stirred overnight and refluxed for 2 h, concentrated and co-evaporated with toluene (2x) thereby providing the product in a quantitative yield. ¹H NMR (400 MHz, MeOD/CDCl₃) δ 7.33-7.14 (m, 5H), 4.40-4.24 (m, 2H), 4.18-4.13 (m, 1H), 3.23-3.18 (m, 1H), 3.02-2.96 (m, 1H), 1.54-1.41 (m, 3H), 1.35-1.33 (m, 3H), 0.88-0.83 (m, 6H). ¹³C NMR (101 MHz, MeOD/CDCl₃) δ 194.90, 173.14, 170.69, 136.81, 131.80, 129.93, 129.11, 127.64, 65.09, 52.40, 41.29, 38.37, 25.11, 23.26, 21.79, 17.99.

N₃Phe-Leu-Ala-Phe(4-CH₂NH₂)-VS TFA salt (LU-002c, 10)

Compound **10** was prepared by the general procedure for azide peptide couplings on a 50 μmol scale (Cbz-Phe(4-CH₂NHBoc)-VS synthesized and deprotected as described before¹⁴). After workup, the crude product was treated with TFA for 30 min, co-evaporation with toluene, subsequent purification by preparative HPLC, followed by lyophilisation, provided the title compound (7.8 mg, 25%). ¹H NMR (600 MHz, MeOD) δ 7.42 – 7.33 (m, 4H), 7.33 – 7.21 (m, 5H), 6.80 (dd, *J* = 15.2, 5.1 Hz, 1H), 6.59 (dd, *J* = 15.2, 1.6 Hz, 1H), 4.85 – 4.79 (m, 1H), 4.34 (dd, *J* = 9.9, 4.7 Hz, 1H), 4.27 – 4.13 (m, 2H), 4.09 (s, 2H), 3.21 (dd, *J* = 14.1, 5.0 Hz, 1H), 3.08 – 2.96 (m, 3H), 2.94 (s, 3H), 1.57 (td, *J* = 6.5, 5.5, 2.5 Hz, 3H), 1.32 (d, *J* = 7.2 Hz, 3H), 0.93 (dd, *J* = 19.8, 6.0 Hz, 6H). ¹³C NMR (150 MHz, MeOD) δ 174.43, 174.21, 171.97, 146.60, 139.64, 137.81, 133.00, 131.81, 131.29, 130.43, 130.21, 129.63, 128.10, 65.43, 53.54, 52.40, 50.78, 44.07, 42.75, 41.48, 40.30, 38.66, 25.80, 23.47, 21.88, 18.04. LC-MS (linear gradient 10 → 90% MeCN/H₂O, 0.1% TFA, 15.0 min):R_t (min): 6.24 (ESI-MS (m/z): 612.13 (M+H⁺)). HRMS calculated for C₃₀H₄₁N₇O₅S 612.29626 [M+H]⁺; found 612.29624.

Synthesis of LU-002i



Scheme S4. Synthesis of Boc-DecAla-EK. Reagents and conditions: a. Rh/Al, H₂, MeOH, quant. b. N,O-Dimethylhydroxylamine, HCTU, DiPEA, DCM, 60%. c. 2-bromopropene, tBuLi, Et₂O, -78°C, 67%. d. CeCl₃·7H₂O, NaBH₄, MeOH, 0°C, quant. e. 1. Vo(acac)₂, tBuOOH, DCM, 0°C. 2. Dess-Martin periodane, DCM, 0°C, 19%.

(2S)-2-((tert-butoxycarbonyl)amino)-3-(decahydronaphthalen-1-yl)propanoic acid (12)

Boc-1-Nal-OH **11** (1.0 g, 3.2 mmol) was dissolved in MeOH (30 mL), followed by the addition of Rh on alumina (5 wt. %, 300 mg). The mixture was placed under H₂ (4 bar, Parr apparatus) for 48h. Subsequent filtration and concentration provided the product in a quantitative yield. ¹H NMR (400 MHz, CDCl₃) δ 11.12 (s, 1H), 6.67-6.20 (m, 0.5H), 5.11-4.86 (m, 0.5H), 4.36-4.13 (m, 1H), 2.11-0.59 (m, 28H). ¹³C NMR (101 MHz, CDCl₃) δ 179.04, 178.68, 178.14, 156.94, 155.91, 155.78, 81.67, 80.13, 52.75, 48.12, 47.61, 43.09, 38.61, 37.86, 37.50, 37.40, 36.95, 36.46, 36.33, 36.22, 35.94, 34.93, 34.70, 34.57, 34.37, 33.35, 32.65, 31.93, 30.80, 30.25, 29.26, 28.40, 27.99, 27.69, 27.01, 26.90, 26.85, 26.76, 26.64, 26.52, 26.48, 26.20, 26.07, 25.95, 25.50, 21.56, 21.40, 21.37, 20.72, 20.39, 20.16, 19.67. HRMS calculated for C₁₈H₃₁NO₄326.23258[M+H]⁺; found 326.23265.

tert-butyl ((2S)-3-(decahydronaphthalen-1-yl)-1-(methoxy(methyl)amino)-1-oxopropan-2-yl)carbamate (13)

The title compound was prepared by the general procedure for peptide coupling on a 2 mmol scale. Column chromatography (10-40% EtOAc/pentane) provided the title compound (427 mg, 60%). ¹H NMR (400 MHz, CDCl₃) δ 5.26-5.06 (m, 1H), 4.70 (s, 1H), 3.78 (d, *J* = 4.9 Hz, 3H), 3.31-3.13 (m, 3H), 2.04-0.56 (m, 28H). ¹³C NMR (101 MHz, CDCl₃) δ 173.95, 155.69, 155.20, 79.20, 77.36, 61.46, 48.63, 48.50, 48.32, 48.28, 48.14, 47.52, 43.01, 41.73, 39.47, 38.47, 37.70, 37.52, 37.22, 36.79, 36.18, 35.99, 35.89, 34.84, 34.72, 34.58, 34.44, 34.39, 34.27, 34.15, 32.48, 32.25, 31.85, 30.63, 30.44, 30.05, 29.99, 29.57, 29.09, 28.55, 28.24, 27.79, 26.87, 26.84, 26.76, 26.73, 26.69, 26.67, 26.53, 26.41, 26.38, 26.32, 26.09, 25.83, 25.71, 25.35, 25.32, 21.58, 21.30, 21.20, 21.14, 20.70, 20.15, 19.31. HRMS calculated for C₂₀H₃₆N₂O₄369.27478[M+H]⁺; found 369.27533.

tert-butyl ((2S)-1-(decahydronaphthalen-1-yl)-4-methyl-3-oxopent-4-en-2-yl)carbamate (14)

To a solution of 2-bromopropene (435 mg, 320 μL, 3.6 mmol, 3 equiv.) in Et₂O at -78°C was added tBuLi (3.20 mL, 4.5 equiv, 1.7 M in pent) in 10 min. After stirring for 15 min. at -78°C, the Weinreb amide **13** (427 mg, 1.2 mmol, 1 equiv.) in Et₂O was added slowly in 10 min. The reaction mixture is stirred for 2 h at -40°C. The reaction was quenched by the addition of sat. NH₄Cl and warmed to RT. The mixture was transferred to a separatory funnel and the water layer was extracted with EtOAc (3X). The combined organic layers were washed with brine, dried over Na₂SO₄, filtered and concentrated. The crude product was purified by column chromatography (1-10% EtOAc/pentane) providing the product (278 mg, 67%). ¹H NMR (400 MHz, CDCl₃) δ 6.21-6.00 (m, 1H), 5.94-5.80 (m, 1H), 5.33-4.89 (m, 2H), 2.18-0.51 (m, 31H). ¹³C NMR (101 MHz, CDCl₃) δ 201.83, 201.61, 155.67, 142.73, 142.20, 126.12, 126.04, 125.87, 125.69, 114.89, 109.66, 79.45, 52.89, 52.29, 47.65, 43.13, 41.81, 38.97, 38.11, 37.64, 37.40, 37.31, 37.21, 36.24, 34.89, 34.79, 34.66, 34.61, 34.53, 34.48, 34.34, 34.18, 32.56, 32.25, 31.65, 31.15, 30.74, 30.37, 30.12, 29.31, 28.33, 27.86, 26.92, 26.83, 26.78, 26.71, 26.62, 26.48, 26.45, 26.40, 26.11, 26.00, 25.91, 25.40, 25.32, 21.61, 21.35, 21.28, 20.66, 20.63, 20.23, 19.97, 17.84.

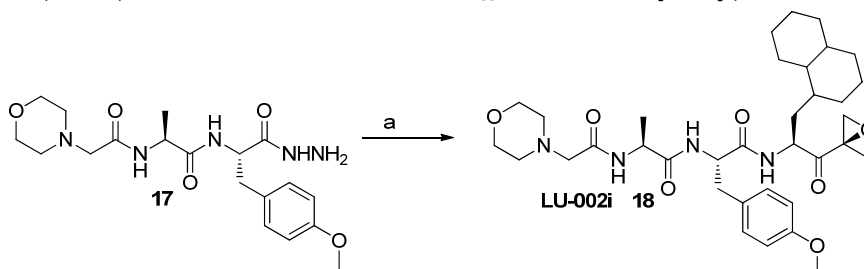
tert-butyl ((2S,3R)-1-(decahydronaphthalen-1-yl)-3-hydroxy-4-methylpent-4-en-2-yl)carbamate (15)

To a solution of alkene **14** (278 mg, 0.8 mg, 1 equiv.) in MeOH was added CeCl₃·7H₂O (477 mg, 1.28 mmol, 1.6 equiv.) and the mixture was stirred until the solution became clear. The mixture is cooled to 0°C and NaBH₄ (39 mg, 1.04 mmol, 1.3 equiv.) is added in portions in 10 min. After 30 min, TLC analysis showed completion of the reaction. The reaction was quenched by the addition of AcOH. The mixture was stirred for 15 min. followed by the addition of toluene and removal of the solvent. The residue was redissolved in a H₂O/ EtOAc mixture, which is then transferred to a separatory funnel. The layers were separated and the aqueous layer was extracted with EtOAc (2X). The combined organic layers were washed with brine, dried over Na₂SO₄, filtered and concentrated. The crude product was purified by column chromatography (10-30% EtOAc/pentane) providing the product in a quantitative yield (283 mg, 0.8 mmol). ¹H NMR (400 MHz, CDCl₃) δ 5.06-5.03 (m, 1H), 4.97-4.71 (m, 2H), 4.16-4.04 (m, 1H), 4.00-3.56 (m, 1H), 3.00 (s, 1H), 2.00-0.53 (m, 31H). ¹³C NMR (101 MHz, CDCl₃) δ 156.24, 156.13, 144.99, 144.55, 111.71, 111.32, 111.21, 111.11, 79.95, 79.34, 79.23, 77.93, 77.80, 77.48, 77.16, 76.84, 50.72, 50.09, 47.69, 43.26, 43.24, 42.32, 40.62, 38.55, 38.44, 38.00, 37.81, 36.18, 35.02, 34.88, 34.81, 34.65, 34.62, 34.55, 34.52, 34.46, 34.35, 34.06, 32.80, 32.66, 32.45, 32.26, 31.36, 30.88, 30.43, 30.30, 29.71, 29.35, 28.43,

28.38, 28.05, 27.03, 26.96, 26.90, 26.88, 26.74, 26.57, 26.52, 26.40, 26.35, 26.05, 25.91, 25.56, 23.37, 21.84, 21.40, 21.33, 20.89, 20.38, 19.51.

tert-butyl ((2S)-3-(decahydronaphthalen-1-yl)-1-((R)-2-methyloxiran-2-yl)-1-oxopropan-2-yl)carbamate (16)

To a solution of alcohol **15** (283 mg, 0.8 mmol) in DCM at 0°C is added VO(acac)₂ (21 mg, 0.08 mmol, 0.1 equiv.) followed by the addition of tBuOOH (5.5 M in decane, 0.44 mL, 2.4 mmol, 3 equiv.). The reaction mixture is stirred at 0°C for 2-3 h after which TLC analysis showed completion of the reaction. The reaction mixture is concentrated, redissolved in EtOAc and washed with 0.5 sat. aq. NaHCO₃ (2x), H₂O and brine. The organic layer is dried over Na₂SO₄, filtered and concentrated. The crude product is added as a solution in DCM to a solution of Dess-Martin-Periodane (679 mg, 1.6 mmol, 2.0 equiv.) in DCM at 0°C. After stirring overnight, the reaction was quenched by the addition of sat. NaHCO₃. The mixture was transferred to a separatory funnel and the layers were separated. The aqueous layer was extracted with DCM (1x) and the combined organics were washed with sat. NaHCO₃ (1x) and brine and dried over Na₂SO₄, filtered and concentrated. The crude product was purified by column chromatography (1-10% EtOAc/pentane) providing the title compound (56.2 mg, 0.15 mmol, 19%). ¹H NMR (400 MHz, CDCl₃) δ 4.97-4.75 (m, 1H), 4.35-4.25 (m, 1H), 3.33-3.27 (m, 1H), 2.90-2.87 (m, 1H), 2.01-0.57 (m, 31H). ¹³C NMR (101 MHz, CDCl₃) δ 210.04, 209.78, 155.86, 79.85, 59.14, 59.07, 52.58, 52.47, 52.39, 52.25, 51.31, 50.82, 47.68, 43.23, 42.15, 37.76, 37.44, 36.50, 36.31, 36.01, 35.41, 35.00, 34.92, 34.73, 34.65, 34.58, 34.55, 34.37, 34.29, 32.66, 32.61, 31.80, 30.90, 30.66, 30.32, 30.22, 29.80, 29.00, 28.42, 28.42, 28.13, 27.52, 27.05, 26.92, 26.89, 26.85, 26.80, 26.62, 26.58, 26.54, 26.50, 26.23, 25.91, 25.80, 25.49, 21.75, 21.45, 21.37, 21.20, 20.85, 20.36, 20.24, 19.34, 16.91, 16.88. HRMS calculated for C₂₁H₃₅NO₄ 366.26389[M+H]⁺; found 366.26401.

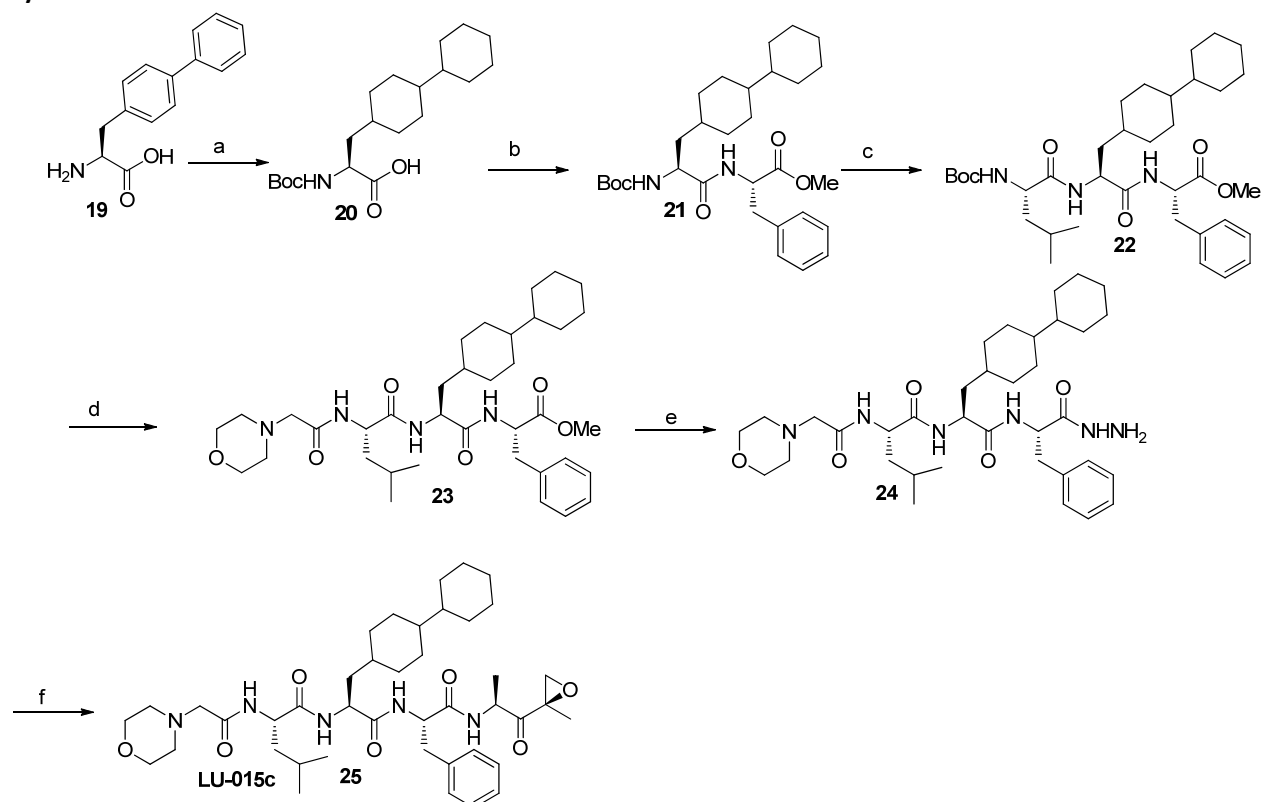


Scheme S5 Synthesis of LU-002i. Reagents and conditions: a. 1. i. tBuONO, HCl, DMF, -35°C. ii DiPEA, H₂N- DecAla-EK, -35°C-RT, 41%.

MorphAc-Ala-Tyr(OMe)-DecAla-EK (LU-002i, 18)

Compound **17** was synthesized as reported before.³¹ Compound **18** was prepared by the general procedure for azide peptide couplings on a 50 μmol scale. Purification by column chromatography (10-30% EtOAc/pent), followed by lyophilisation, provided the title compound (13.2 mg, 20 μmol, 41%). ¹H NMR (600 MHz, MeOD) δ 7.14 (d, *J* = 8.6 Hz, 2H), 6.81 (d, *J* = 8.4 Hz, 2H), 4.67 – 4.49 (m, 2H), 4.42 (p, *J* = 6.9 Hz, 1H), 3.78 (s, 3H), 3.75 – 3.67 (m, 4H), 3.23 (dd, *J* = 23.4, 5.1 Hz, 1H), 3.08 – 3.01 (m, 2H), 2.99 (d, *J* = 4.7 Hz, 1H), 2.94 (tt, *J* = 9.0, 4.5 Hz, 1H), 2.86 – 2.79 (m, 1H), 2.49 (s, 4H), 2.11 – 1.50 (m, 10H), 1.48 (d, *J* = 1.6 Hz, 3H), 1.47 – 1.36 (m, 2H), 1.33 (dd, *J* = 7.1, 1.8 Hz, 3H), 1.31 – 0.60 (m, 7H). ¹³C NMR (151 MHz, MeOD) δ 209.38, 209.07, 173.75, 173.70, 173.02, 172.94, 171.58, 171.53, 159.56, 131.02, 129.64, 129.63, 114.37, 67.48, 62.02, 59.70, 59.53, 59.50, 55.42, 55.38, 55.37, 55.22, 54.32, 52.61, 52.59, 50.62, 50.04, 49.25, 49.17, 44.17, 44.06, 42.69, 41.19, 39.47, 39.03, 38.73, 38.71, 38.68, 38.31, 37.83, 37.78, 37.75, 37.72, 37.15, 37.12, 36.67, 36.17, 36.05, 35.79, 35.67, 35.51, 35.40, 35.30, 35.26, 35.23, 35.11, 35.03, 34.64, 34.58, 34.40, 33.46, 33.36, 32.80, 32.23, 31.51, 30.98, 30.74, 30.24, 29.54, 28.70, 27.76, 27.62, 27.56, 27.52, 27.30, 27.17, 26.88, 26.61, 26.34, 26.25, 26.17, 22.02, 21.95, 21.40, 20.84, 19.84, 18.43, 18.37, 18.32, 16.54, 16.51, 16.43, 16.39. LC-MS (linear gradient 10 → 90% MeCN/H₂O, 0.1% TFA, 13.5 min): R_t (min): 6.71 (ESI-MS (m/z): 641.40 (M+H)⁺). HRMS calculated for C₃₅H₅₂N₄O₇ 641.39088 [M+H]⁺; found 641.39093.

Synthesis of LU-015c



Scheme S6. Synthesis of LU-015c. Reagents and conditions. a. 1. Rh/Al, H₂, MeOH, quant. 2. Boc₂O, THF/H₂O, 85%. b. HCTU, H-Phe-OMe, DiPEA, 80%. c. 1. TFA. 2. HCTU, Boc-Leu-OH, DiPEA, 86%. d. 1. TFA. 2. HCTU, Morpholinoacetic acid HCl, DiPEA, 78%. e. hydrazine hydrate, MeOH, quant. f. 1. i. tBuONO, HCl, DMF, -35°C. ii DiPEA, H₂N-Ala-EK, -35°C-RT, 19.8%.

Boc-BiCha-OH (20)

H-BiPhe-OH **19** (0.5 g, 2.1 mmol) was dissolved in MeOH (20 mL), followed by the addition of Rh on alumina (5 wt. %, 200 mg). The mixture was placed under H₂ (4 bar, Parr apparatus) for 48h. Subsequent filtration and concentration provided the product in a quantitative yield. The crude product was dissolved in 1:1 THF/H₂O (16 mL), followed by the addition of Boc₂O (917 mg, 4.2mmol, 2 eq.) and Et₃N (1.2 mL, 8.4 mmol, 4 equiv.). After stirring overnight, the reaction mixture was concentrated and co-evaporated with toluene. Purification by column chromatography (0-10% MeOH/EtOAc) provided the product (632 mg, 1.79 mmol, 85%). ¹H NMR (400 MHz, CDCl₃) δ 11.79 (s, 1H), 6.58 (s, 0.5H), 5.11 (s, 0.5H), 4.49-3.83 (m, 1H), 2.07-0.54 (m, 32H). ¹³C NMR (101 MHz, CDCl₃) δ 178.23, 177.80, 157.07, 155.72, 114.12, 81.58, 79.94, 77.48, 77.16, 76.84, 53.01, 51.92, 43.28, 41.64, 40.30, 40.17, 36.52, 36.31, 34.28, 33.83, 33.80, 32.71, 31.94, 30.97, 30.55, 30.27, 30.25, 30.15, 29.77, 29.70, 29.67, 29.63, 29.52, 29.37, 29.16, 28.95, 28.63, 28.46, 28.26, 28.22, 28.17, 28.02, 26.86, 26.75, 25.92, 25.59, 25.32, 22.70. HRMS calculated for C₂₀H₃₅NO₄ 354.26389[M+H]⁺; found 354.26399.

Boc-BiCha-Phe-OMe (21)

The title compound was prepared by the general procedure for peptide coupling on a 0.5 mmol scale. Column chromatography (10-30% EtOAc/pentane) provided the product (207 mg, 80%). ¹H NMR (400 MHz, CDCl₃) δ 7.41-7.03 (m, 5H), 6.69 (d, *J* = 7.8 Hz, 1H), 5.03-4.99 (m, 1H), 4.88-4.68 (m, 1H), 4.26-3.99 (m, 1H), 3.69 (s, 3H), 3.20-2.94 (m, 2H), 1.88-0.72 (m, 32H). ¹³C NMR (101 MHz, CDCl₃) δ 172.38, 171.72, 171.71, 155.58, 135.87, 129.33, 128.53, 127.07, 79.94, 77.48, 77.16, 76.84, 53.22, 52.26, 43.28, 41.58, 40.17, 39.92, 37.95, 36.07, 34.33, 33.85, 32.87, 31.02, 30.56, 30.54, 30.25, 29.99, 29.77, 29.62, 28.70, 28.33, 26.86, 26.77, 26.75, 25.61, 25.38.

Boc-Leu-BiCha-Phe-OMe (22)

Boc-BiCha-Phe-OMe **21** (385 mg, 0.75 mmol) was deprotected using the standard procedure for Boc removal, followed by peptide coupling with Boc-Leu-OH using the standard procedure for peptide couplings. Column chromatography (20-40% EtOAc/pentane), provided the product (408 mg, 86%). ¹H NMR (400 MHz, CDCl₃) δ 7.27 (dt, *J* = 14.0, 6.7 Hz, 3H), 7.11 (d, *J* = 6.9 Hz, 2H), 6.75 (d, *J* = 7.5 Hz, 1H), 6.64 (dd, *J* = 14.0, 8.1 Hz, 1H), 5.10 – 5.01 (m, 1H), 4.89 – 4.76 (m, 1H), 4.45 (dq, *J* = 13.7, 7.5, 6.9 Hz, 1H), 4.18 – 4.08 (m, 1H), 3.70 (s, 3H), 3.10 (dd, *J* = 5.8, 3.3 Hz, 2H), 1.92 – 1.48 (m, 12H), 1.45 (s, 9H), 1.41 – 0.98 (m, 11H), 1.03 – 0.77 (m, 9H).

Morph-Leu-BiCha-Phe-OMe (23)

Boc-Leu-BiCha-Phe-OMe **22** (408 mg, 0.65 mmol) was deprotected using the standard procedure for Boc removal, followed by peptide coupling with 2-morpholinoacetic acid HCl using the standard procedure for peptide couplings. Column chromatography (20-40% EtOAc/pentane), provided the product (333 mg, 78%). ¹H NMR (400 MHz, CDCl₃) δ 7.46 (d, *J* = 8.6 Hz, 1H), 7.27 – 7.14 (m, 3H), 7.09 – 6.96 (m, 3H), 6.73 (d, *J* = 7.8 Hz, 1H), 4.84 – 4.69 (m, 1H), 4.55 – 4.41 (m, 1H), 4.41 – 4.29 (m, 1H), 3.73 – 3.65 (m, 4H), 3.63 (s, 3H), 3.04 (dd, *J* = 5.7, 2.4 Hz, 2H), 3.00 – 2.91 (m, 2H), 2.47 (s, 4H), 1.86 – 0.70 (m, 32H). ¹³C NMR (101 MHz, CDCl₃) δ 171.97, 171.86, 171.54, 171.46, 169.93, 135.79, 129.22, 128.48, 127.04, 66.79, 61.72, 53.72, 53.47, 53.24, 52.20, 51.65, 51.27, 51.03, 43.16, 43.11, 41.45, 40.90, 40.05, 39.43, 37.80, 35.55, 34.27, 33.58, 32.89, 30.88, 30.45, 30.16, 29.89, 29.58, 28.59, 26.75, 26.64, 25.50, 25.32, 24.86, 22.93, 22.07.

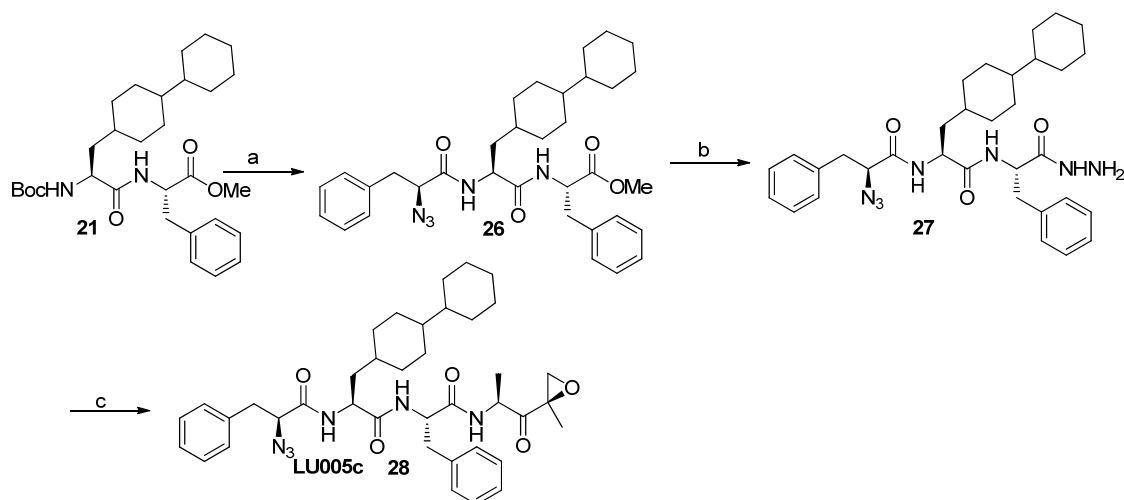
Morph-Leu-BiCha-Phe-NHNH₂ (24)

Morph-Leu-BiCha-Phe-OMe **23** (333 mg, 0.51 mmol) was dissolved in MeOH (7.5 mL), followed by the addition of NH₂NH₂·H₂O (1 mL, 40 equiv.). After stirring for 3 hours, the reaction mixture was concentrated and co-evaporated with toluene (2x) providing the product in a quantitative yield. ¹H NMR (400 MHz, CDCl₃) δ 8.60 (s, 1H), 7.82 (d, *J* = 7.5 Hz, 1H), 7.63 (d, *J* = 7.9 Hz, 1H), 7.22 (ddd, *J* = 28.6, 14.4, 6.7 Hz, 6H), 4.91 (q, *J* = 7.4 Hz, 1H), 4.77 – 4.63 (m, 1H), 4.53 (dt, *J* = 15.4, 8.1 Hz, 1H), 3.80 – 3.67 (m, 4H), 3.17 – 2.94 (m, 4H), 2.54 (s, 4H), 1.80 – 1.44 (m, 12H), 1.45 – 1.23 (m, 7H), 1.11 (dt, *J* = 22.2, 12.4 Hz, 6H), 0.90 (t, *J* = 6.1 Hz, 6H), 0.86 – 0.74 (m, 3H). ¹³C NMR (101 MHz, CDCl₃) δ 171.86, 171.80, 171.69, 170.95, 169.76, 136.14, 128.95, 128.24, 126.68, 66.54, 61.49, 53.52, 52.52, 51.63, 51.16, 50.38, 42.97, 42.91, 41.20, 40.10, 39.78, 38.41, 36.37, 34.21, 33.60, 32.66, 30.92, 30.31, 30.00, 29.73, 29.56, 29.43, 28.61, 26.54, 26.44, 25.44, 25.26, 24.72, 22.68, 22.19.

Morph-Leu-BiCha-Phe-Ala-EK (LU015c, 25)

This compound was obtained by the general protocol for azide coupling on a 100 μmol scale. Purification by column chromatography (0-1-2% MeOH/DCM), followed by lyophilisation provided the product (52.7 mg, 69.2 %). ¹H NMR (400 MHz, CDCl₃) δ 7.55 (s, 1H), 7.37 – 7.14 (m, 7H), 7.03 (s, 1H), 6.81 (s, 1H), 4.74 (q, *J* = 7.1 Hz, 1H), 4.55 – 4.42 (m, 2H), 4.35 (s, 1H), 3.80 (s, 4H), 3.22 (d, *J* = 5.0 Hz, 1H), 3.19 – 2.96 (m, 4H), 2.91 (d, *J* = 5.0 Hz, 1H), 2.60 (d, *J* = 28.7 Hz, 4H), 1.84 – 1.56 (m, 10H), 1.53 (s, 3H), 1.50 – 1.30 (m, 7H), 1.27 (d, *J* = 7.1 Hz, 3H), 1.16 (dt, *J* = 21.8, 12.3 Hz, 5H), 0.94 (dd, *J* = 12.3, 5.9 Hz, 6H), 0.90 – 0.78 (m, 3H). ¹³C NMR (101 MHz, CDCl₃) δ 207.77, 172.15, 172.06, 171.81, 170.40, 136.68, 59.05, 54.09, 52.50, 52.25, 47.94, 41.61, 40.61, 38.09, 34.53, 33.84, 31.14, 30.64, 30.13, 28.62, 26.94, 26.83, 25.67, 25.48, 25.07, 23.09, 22.18, 17.08, 16.93. LC-MS (linear gradient 10 → 90% MeCN, 0.1% TFA, 13 min): *R*_t (min): 7.44 (ESI-MS (*m/z*): 752.20 (M+H)⁺). HRMS: calculated for C₄₂H₆₅N₅O₇ 752.49568 [M+H]⁺; found 752.49561

Synthesis of LU-005c



Scheme S7. Synthesis of LU-005c. Reagents and conditions. a. 1. TFA. 2. HCTU, N₃Phe-OH, DiPEA, 86%. b. Hydrazine hydrate, MeOH, quant. d. 1. i. tBuONO, HCl, DMF, -35°C. ii DiPEA, H₂N- Ala-EK, -35°C-RT, 19.8%.

N₃Phe-BiCha-Phe-OMe (26)

Boc-BiCha-Phe-OMe **21** (207 mg, 0.40 mmol) was deprotected using the standard procedure for Boc removal, followed by peptide coupling with 2-morpholinoacetic acid HCl using the standard procedure for peptide couplings. Column chromatography (10-30% EtOAc/pentane), provided the product (108 mg, 45%). ¹H NMR (400 MHz, CDCl₃) δ 7.37-7.19 (m, 8H), 7.13-6.99 (m, 2H), 6.94-6.88 (m, 1H), 6.72-6.69 (m, 1H), 4.90-4.84 (m, 1H), 4.56-4.46 (m, 1H), 4.05-4.01 (m, 1H), 3.71 (s, 3H), 3.41-2.84 (m, 4H), 1.83-0.71 (m, 23H). ¹³C NMR (101 MHz, CDCl₃) δ 171.66, 171.65, 171.40, 168.55, 136.03, 135.96, 135.83, 129.58, 128.64, 128.60, 127.19, 77.48, 77.16, 76.84, 65.12, 53.25, 52.43, 51.38, 51.01, 43.23, 41.73, 40.50, 39.65, 38.41, 38.34, 37.92, 37.67, 35.55, 34.20, 33.74, 33.03, 30.67, 30.55, 30.29, 29.94, 29.69, 29.62, 28.97, 26.90, 26.80, 25.46, 25.30.

N₃Phe-BiCha-Phe-NHNH₂ (27)

N₃Phe-BiCha-Phe-OMe **26** (108 mg, 0.18 mmol) was dissolved in MeOH (5 mL), followed by the addition of NH₂⁻ NH₂·H₂O (0.26 mL, 30 equiv.). After stirring for overnight followed by 2 hours at reflux temperature, the reaction mixture was concentrated and co-evaporated with toluene (2x) providing the product in a quantitative yield. ¹H NMR (400 MHz, CDCl₃) δ 8.56 (s, 1H), 7.74 (d, *J* = 8.7 Hz, 1H), 7.37-7.07 (m, 10H), 4.82 (q, *J* = 7.7 Hz, 1H), 4.70-4.43 (m, 1H), 4.13-4.10 (m, 2H), 3.32-2.86 (m, 4H), 1.77-0.67 (m, 23H). ¹³C NMR (101 MHz, CDCl₃) δ 172.09, 171.97, 171.41, 169.65, 169.19, 169.16, 136.62, 136.36, 136.16, 136.06, 129.80, 129.37, 129.27, 128.97, 128.65, 128.58, 127.29, 127.01, 64.86, 53.14, 51.80, 51.32, 43.22, 39.72, 38.51, 38.18, 37.66, 35.72, 34.29, 33.90, 32.85, 30.93, 30.55, 30.26, 29.96, 29.75, 29.71, 29.57, 29.41, 28.96, 26.86, 26.74, 25.57, 25.36, 22.76.

N₃Phe-BiCha-Phe-Ala-EK (LU-005c, 28)

This compound was obtained by the general protocol for azide coupling on a 50 μmol scale. Purification by HPLC (C₁₈, 70-90% MeCN, 0.1% TFA, 10 min gradient), followed by lyophilization provided the product (6.77 mg, 19.8 %). ¹H NMR (600 MHz, CDCl₃) δ 7.34 – 7.30 (m, 2H), 7.28 (dt, *J* = 7.0, 2.2 Hz, 3H), 7.22 (ddd, *J* = 9.3, 4.6, 2.0 Hz, 3H), 7.19 (d, *J* = 7.2 Hz, 2H), 6.63 (t, *J* = 6.9 Hz, 1H), 6.49 (t, *J* = 7.5 Hz, 1H), 6.37 (d, *J* = 7.0 Hz, 1H), 4.60 (q, *J* = 7.2 Hz, 1H), 4.47 (td, *J* = 7.1, 2.7 Hz, 1H), 4.36 – 4.29 (m, 0.3H), 4.26 (m, 0.7H), 4.07 (ddd, *J* = 12.2, 7.8, 4.1 Hz, 1H), 3.27 (dt, *J* = 14.1, 3.6 Hz, 1H), 3.18 – 3.15 (m, 1H), 3.07 – 3.03 (m, 2H), 3.03 – 2.97 (m, 1H), 2.89 (d, *J* = 4.9 Hz, 1H), 1.78 – 1.54 (m, 9H), 1.51 (s, 3H), 1.41 – 1.25 (m, 6H), 1.24 (d, *J* = 7.1 Hz, 3H), 1.21 – 0.73 (m, 8H). ¹³C NMR (151 MHz, CDCl₃) δ 207.80, 171.42, 170.11, 168.79, 136.49, 135.84, 129.63, 129.61, 129.40, 128.85, 128.81, 128.73, 127.48, 127.45, 127.16, 65.20, 65.16, 59.02, 54.21, 52.53, 51.67, 51.23, 48.12, 43.37, 43.26, 39.01, 38.42, 38.36,

37.95, 37.91, 34.30, 33.79, 32.96, 30.61, 30.34, 30.01, 29.69, 29.62, 28.88, 26.97, 26.87, 25.48, 25.32, 17.31, 16.92. LC-MS (linear gradient 10 → 90% MeCN, 0.1% TFA, 13.0 min): R_t (min): 10.82 (ESI-MS (m/z): 685.33 (M+H)⁺). HRMS: calculated for C₃₉H₅₂N₆O₅ 685.40720 [M+H]⁺; found 685.40717

References

1. Hershko, A. & Ciechanover, A. The ubiquitin system. *Annu. Rev. Biochem.* **67**, 425-79 (1998).
2. Groll, M. et al. Structure of 20S proteasome from yeast at 2.4Å resolution. *Nature* **386**, 463-471 (1997).
3. Ferrington, D.A. & Gregerson, D.S. Immunoproteasomes: structure, function, and antigen presentation. *Prog. Mol. Biol. Transl. Sci.* **109**, 75-112 (2012).
4. Romero, P., Corradin, G., Luescher, I.F. & Maryanski, J.L. H-2Kd-restricted antigenic peptides share a simple binding motif. *J. Exp. Med.* **174**, 603-12 (1991).
5. Kloetzel, P.M. & Ossendorp, F. Proteasome and peptidase function in MHC-class-I-mediated antigen presentation. *Curr. Opin. Immunol.* **16**, 76-81 (2004).
6. Kisselev, A.F. & Goldberg, A.L. Monitoring activity and inhibition of 26S proteasomes with fluorogenic peptide substrates. *Methods. Enzymol.* **398**, 364-78 (2005).
7. Zhou, H.-J. et al. Design and synthesis of an orally bioavailable and selective peptide epoxyketone proteasome inhibitor (PR-047), *J. Med. Chem.* **52**, 3028-3038 (2009).
8. Verdoes, M. et al. A fluorescent broad-spectrum proteasome inhibitor for labeling proteasomes in vitro and in vivo. *Chem. Biol.* **13**, 1217-1226 (2006).
9. Meng, L. et al. Epoxomicin, a potent and selective proteasome inhibitor, exhibits in vivo antiinflammatory activity. *Proc. Natl. Acad. Sci.* **96**, 10403-10408 (1999).
10. Berkers, C.R. et al. Activity probe for in vivo profiling of the specificity of proteasome inhibitor bortezomib. *Nat. Methods* **2**, 357-62 (2005).
11. Bogyo, M. et al. Covalent modification of the active site threonine of proteasomal β subunits and the Escherichia coli homolog HslV by a new class of inhibitors. *PNAS* **94**, 6629-6634 (1997).
12. Clerc, J. et al. Syringolin A Selectively Labels the 20 S Proteasome in Murine EL4 and Wild-Type and Bortezomib-Adapted Leukaemic Cell Lines. *ChemBioChem* **10**, 2638-2643 (2009).
13. Britton, M. et al. Selective inhibitor of proteasome's caspase-like sites sensitizes cells to specific inhibition of chymotrypsin-like sites. *Chem. Biol.* **16**, 1278-1289 (2009).
14. Geurink, P.P. et al. Incorporation of non-natural amino acids improves cell permeability and potency of specific inhibitors of proteasome trypsin-like sites. *J. Med. Chem.* **56**, 1262-1275 (2013).
15. Screen, M. et al. Nature of pharmacophore influences active site specificity of proteasome inhibitors. *J. Biol. Chem.* **285**, 40125-40134 (2010).
16. Verdoes, M. et al. A panel of subunit-selective activity-based proteasome probes. *Org. Biomol. Chem.* **8**, 2719-2727 (2010).
17. Niewerth, D. et al. Interferon-gamma-induced upregulation of immunoproteasome subunit assembly overcomes bortezomib resistance in human hematological cell lines. *J. Hematol. Oncol.* **7**, 7-22 (2014).
18. Kisselev, A.F. & Groettrup, M. Subunit specific inhibitors of proteasomes and their potential for immunomodulation. *Curr. Opin. Chem. Biol.* **23**, 16-22 (2014).
19. de Bruin, G. et al. Structure-based design of beta1i or beta5i specific inhibitors of human immunoproteasomes. *J. Med. Chem.* **57**, 6197-209 (2014).
20. Adams, J. The development of proteasome inhibitors as anticancer drugs. *Cancer Cell* **5**, 417-421 (2004).
21. Kisselev, A.F., Callard, A. & Goldberg, A.L. Importance of the different proteolytic sites of the proteasome and the efficacy of inhibitors varies with the protein substrate. *J. of Biol. Chem.* **281**, 8582-8590 (2006).

22. Chauhan, D. et al. A novel orally active proteasome inhibitor ONX 0912 triggers in vitro and in vivo cytotoxicity in multiple myeloma. *Blood* **116**, 4906-4915 (2010).
23. Piva, R. et al. CEP-18770: A novel, orally active proteasome inhibitor with a tumor-selective pharmacologic profile competitive with bortezomib. *Blood* **111**, 2765-2775 (2008).
24. Gentile, M. et al. Ixazomib for the treatment of multiple myeloma. *Expert Opin. Investig. Drugs* **24**, 1287-98 (2015).
25. Zhang, J., Wu, P. & Hu, Y. Clinical and marketed proteasome inhibitors for cancer treatment. *Curr. Med. Chem.* **20**, 2537-51 (2013).
26. Dou, Q.P. & Zonder, J.A. Overview of proteasome inhibitor-based anti-cancer therapies: perspective on bortezomib and second generation proteasome inhibitors versus future generation inhibitors of ubiquitin-proteasome system. *Curr. Cancer Drug Targets* **14**, 517-36 (2014).
27. Altun, M. et al. Effects of PS-341 on the activity and composition of proteasomes in multiple myeloma cells. *Cancer Res.* **65**, 7896-901 (2005).
28. Kupperman, E. et al. Evaluation of the proteasome inhibitor MLN9708 in preclinical models of human cancer. *Cancer Res.* **70**, 1970-80 (2010).
29. Vigneron, N. & Van den Eynde, B.J. Proteasome subtypes and regulators in the processing of antigenic peptides presented by class I molecules of the major histocompatibility complex. *Biomolecules* **4**, 994-1025 (2014).
30. Dahlmann, B., Ruppert, T., Kuehn, L., Merforth, S. & Kloetzel, P.M. Different proteasome subtypes in a single tissue exhibit different enzymatic properties. *J. Mol. Biol.* **303**, 643-53 (2000).
31. de Bruin, G. et al. Structure-based design of β 1i or β 5i specific inhibitors of human immunoproteasomes. *J. Med. Chem.* **57**, 6197-6209 (2014).

CHAPTER 4

Systematic analyses of substrate preferences of 20S proteasomes using peptidic epoxyketone inhibitors*

Introduction

The majority of intracellular protein degradation in eukaryotes is mediated by the 20S proteasome core particle (CP). While yeast expresses only one type of proteasome (γ CP), divergent evolution endowed vertebrates with three distinct CPs that differ in their subunit compositions, substrate specificity and biological significance: the constitutive proteasome (cCP, active sites β 1c, β 2c, β 5c), the immunoproteasome (iCP: β 1i, β 2i, β 5i) and the thymoproteasome (tCP: β 1i, β 2i, β 5t).^{1, 2} With their three different proteolytic centers CPs can cleave polypeptides after virtually all amino acids.³ The trypsin-like (T-L) active sites, residing in the β 2 subunits, preferentially cut substrates after positively charged residues. This cleavage specificity is strictly conserved among eukaryotes and between CP types, thus making it highly challenging to design β 2c or β 2i specific inhibitors.⁴ The β 5 active sites exert the most important chymotrypsin-like (ChT-L) activity (processing after hydrophobic residues) by accommodating apolar amino acids in their S1 specificity pocket. In contrast, substrate cleavage preferences between β 1 subunits of γ CP/cCP and iCP significantly differ.^{5, 6} The hydrophilic nature of the $\gamma\beta$ 1 and β 1c active sites promotes the hydrolysis of peptide bonds C-terminally of acidic amino acids (peptidylglutamyl-peptide hydrolyzing (PGPH)⁷ or caspase-like (C-L)⁸ activity), whereas the more hydrophobic lining of the β 1i active site of iCPs is optimized to generate peptides with hydrophobic C-termini for immune surveillance.^{3, 6} These cleavage specificities, which have mostly been investigated by activity assays with natural or synthetic model substrates,^{5, 8-12} served as guidelines for the development of proteasome inhibitors. However, the design of subunit-selective compounds, which represent valuable tools to evaluate the contribution of the individual active sites to antigen processing and to diseases like autoimmune disorders and cancer, requires a more detailed understanding of

* Huber, E.M.; de Bruin, G. *et al.* Systematic analyses of substrate preferences of 20S proteasomes using peptidic epoxyketone inhibitors. *J. Am. Chem. Soc.* **137**, 7835-7842 (2015).

proteasome substrate specificities. This chapter describes the systematic analysis of substrate specificities using 18 synthesized tripeptide α',β' epoxyketone inhibitors (Table 1),¹³ featuring Leu or Pro in P3, Ala or Leu in P2 and distinct side chains in P1. Binding preferences and IC₅₀ values for the human cCP and iCP subunits were determined by competitive activity based protein profiling (ABPP) in Raji cell lysates and for purified γ CPs by fluorogenic substrate assays. A separate series of five inhibitors was used to assess inhibition of β 1 depending on the presence or absence of a P4 site.⁸ X-ray crystallographic analyses of all compounds in complex with the γ CP together with yeast mutagenesis has been performed and will be discussed partly in this chapter to explain the substrate specificities of the synthesized epoxyketone proteasome inhibitors.

Compound	R	P4	P3	P2	P1	Compound	R	P4	P3	P2	P1
Ac-PAD-EK		-				Ac-LAL-EK		-			
Ac-LAD-EK		-				Ac-PAV-EK		-			
Ac-PAE-EK		-				Ac-LAV-EK		-			
Ac-LAE-EK		-				Ac-PAA-EK		-			
Ac-PAF-EK		-				Ac-LAA-EK		-			
Ac-LAF-EK		-				Ac-PLL-EK		-			
Ac-PAY-EK		-				Ac-LLL-EK		-			
Ac-LAY-EK		-				Ac-APLL-EK					
Ac-PAI-EK		-				N ₃ G-APAL-EK					
Ac-LAI-EK		-				N ₃ G-APhLL-EK					
Ac-PAL-EK		-				N ₃ G-A(4,4-F ₂ P)nLL-EK					

Table 1. Chemical structures of synthesized compounds.

Results and Discussion

Choice of employed organisms, proteasome inhibitor types and assay set-up.

The structures of the synthesized peptide epoxyketone inhibitors are shown in Table 1 (for synthetic details: see experimental section). Apparent IC₅₀ values were determined for yeast and human proteasomes in separate experimental setups. Inhibitors were incubated for 1 h with human Raji cell lysate or purified yeast CP. Subsequently, blockage of human CPs was analyzed by determining residual proteasome activity with fluorescently labelled activity based probes^{14, 15} whereas inhibition of the yCP was determined by measuring the residual proteasome activity after the addition of subunit-specific 7-amino-4-methylcoumarin (AMC) substrates (see experimental section).

Compound	Raji lysates (human)						Purified yCP		
	β1c	β1i	β2c	β2i	β5c	β5i	γβ1	γβ2	γβ5
Ac-PAD-EK	1.4	>1000	>1000	>1000	>1000	>1000	22.4	>200	>200
Ac-LAD-EK	1.6	>1000	115	226	21.7	12.3	24.5	>200	~100
Ac-PAE-EK	17.7	>1000	>1000	>1000	>1000	>1000	>200	>200	~200
Ac-LAE-EK	14.8	>1000	3.6	106	>1000	>1000	>200	>200	~200
Ac-PAF-EK	10.8	0.021	540	625	5.5	2.1	>200	>200	10.9
Ac-LAF-EK	61.7	0.23	0.55	0.78	0.02	0.11	>200	10.0	0.23
Ac-PAY-EK	10.3	0.38	69.0	65.1	4.9	1.5	>200	>200	7.9
Ac-LAY-EK	5.3	0.33	0.14	0.14	0.054	0.15	>200	6.0	0.27
Ac-PAI-EK	338	28.9	>1000	>1000	>1000	>1000	>200	>200	>200
Ac-LAI-EK	261	10.8	9.2	8.1	19.7	253	>200	>200	100.4
Ac-PAL-EK	0.11	0.028	326.7	446.6	9.5	10.7	43.3	>200	>200
Ac-LAL-EK	0.95	0.020	0.083	0.074	0.06	1.0	55.5	14.4	0.67
Ac-PAV-EK	>1000	36.0	>1000	>1000	≈1000	>1000	>200	>200	>200
Ac-LAV-EK	>1000	101.5	7.2	15.6	25.9	≈1000	>200	>200	>200
Ac-PAA-EK	>1000	99.5	457	432	248	>1000	>200	>200	>200
Ac-LAA-EK	>100	26.8	1.4	2.8	1.1	>1000	>200	65.8	89.3
Ac-PLL-EK	0.11	0.040	93.2	46.4	10.8	8.8	39.7	>200	~200
Ac-LLL-EK	0.14	0.015	0.041	0.017	0.1	1.0	40.9	10.4	0.72
H-APLL-EK	0.72	0.085	61.5	160	21.9	131	101	>200	>200
Ac-APLL-EK	0.029	0.035	75.1	37.3	26.6	52.4	10.3	>200	~200
N ₃ G-APAL-EK	0.20	0.043	>1000	>1000	43.8	46.2	7.6	>200	>200
N ₃ G-APnLL-EK	0.067	0.026	>100	>100	≈100	≈100	5.3	>200	~200
N ₃ G-A(4,4-F ₂ P)nLL-EK	2.7	0.031	>100	>100	6.2	17.1	11.4	>200	>200
Carfilzomib	0.075	0.017	0.031	0.017	0.00089	0.0013	~200	1.8	0.03
ONX 0914 ¹⁶	>10	0.46	1.1	0.59	0.054	0.0057	>200	5.5	0.42
Bortezomib	0.017	0.0065	0.51	0.57	0.0027	0.0027	1.1	9.3	0.05

Table 2. Apparent IC₅₀ values [μM] of compounds as determined by ABPP with Raji cell lysates or by fluorogenic substrate hydrolysis assays for purified wt yCP

Despite recent progress,^{6, 17} mouse and human CPs are still difficult to crystallize and not suitable for extensive structural analyses with various ligands. Therefore the yCP is used for crystallographic and mutagenesis studies. The conserved fold of proteasome subunits and the identical binding mode of peptidic compounds to yeast and mammalian CPs justify usage of the model system yeast.⁶ Active yCP crystals were soaked with final ligand concentrations of 3.3 mM. At this concentration, even poor inhibitors bind to the active sites of the yCP and thus can be visualized by X-ray crystallography. All synthesized inhibitors share the α',β' epoxyketone (EK/ep) warhead, which afforded us to use carfilzomib and ONX-0914 as reference compounds. Although distinct covalent inhibitor types¹⁸ and natural substrates may slightly vary in their binding mode to the S pockets of the proteasomal active site, the analyses provided here disclose significant tendencies for substrate preferences.

Epoxyketones with P1-valine or -isoleucine are weak proteasome inhibitors

Among the different P1 residues tested (Tables 1 and 2), Val and Ile are the most disfavored ones (IC_{50} for human CP $\geq 7.2 \mu\text{M}$, for yCP $\geq 100 \mu\text{M}$; Tables 2). For example, the compounds Ac-LAI-EK ($\geq 8.1 \mu\text{M}$ for human CP) and Ac-LAV-EK ($\geq 7.2 \mu\text{M}$ for human CP) are significantly less potent than Ac-LAL-EK ($\leq 1 \mu\text{M}$ for human CP). The crystal structures of yCP in complex with the inhibitors showed that the conformation of Val and Ile in the S1 pocket clearly differs from that observed for Leu. Val and Ile are sandwiched in the S1 pocket between the main chain heteroatoms 19O, 45O, 47O and 47N (Figure 1). Based on the interatomic distances, it is expected that also Thr is disfavored at the P1 position, but experimental support for this hypothesis is lacking due to the abortive synthesis of the respective epoxyketones.

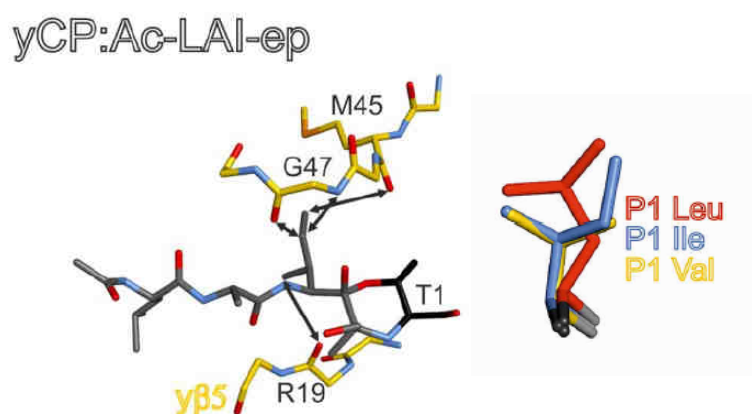


Figure 1. The P1 site: Ile and Val versus Leu. The crystal structure of Ac-LAI-EK at the $y\beta 5$ active site clearly shows that main chain atoms 19O, 45O, 47O and 47N come close to the P1-Val/Ile residues. The overlay of the side chains of P1 Leu, Ile and Val residues show a different conformation for Ile and Val compared to Leu. The main chain atoms of residues 18-20 and 44-48 are shown as sticks. The side chains, except for Met45 forming the bottom of the S1 pocket, are removed for clarity.

Blockage of β 2 subunits

The marginal structural differences between the β 2c and β 2i subunits (Asp53 (β 2c) versus Glu53 ($\gamma\beta$ 2/ β 2i) and Thr48 ($\gamma\beta$ 2/ β 2c) versus Val48 (β 2i)) do not provide an obvious explanation for the biological need of their mutual exchange in mammalian CPs⁶ and complicate the design of β 2c- and β 2i-selective inhibitors.⁴ In order to gain additional insights into the β 2 substrate specificities, all compounds were tested for blockage of the T-L activities. Ligands bearing Pro at P3 poorly inhibit the β 2 active sites of yeast and human CPs, while P3-Leu analogues are much more potent (up to 6000 times). Among the P3-Leu series, inhibitors with Leu, Phe and Tyr at P1 display highest affinities and do not discriminate between the human c- and i-subunits (Table 2). These results confirm that the β 2 subunits accept nonpolar P1 side chains³ besides basic ones such as Arg.⁴ Small P1 residues like Ala, however, are less potent due to the large S1 pockets of β 2 subunits. The acidic amino acids Asp and Glu are also hardly effective towards yeast and human CPs, except for Ac-LAE-EK (IC₅₀: 3.6 μ M; Table 2) which selectively targets the human β 2c subunit. In contrast to β 2i, where Glu53 is oriented towards His35, Asp53O^δ of β 2c may hydrogen-bond to the P1-Glu side chain of the ligand via a solvent molecule, thereby enhancing the affinity of Ac-LAE-EK for β 2c compared to β 2i (IC₅₀: 106 μ M; Table 2) by a factor of 30.^{6, 17}

Inhibition of subunit β 5

Characterization of the β 5 substrate binding channel by numerous natural and synthetic ligands revealed that the S3 pockets of yeast and mammalian β 5 subunits readily accept Leu residues.^{17, 19} Upon testing the impact of Leu versus Pro at the P3 site it was found that the latter is not suitable to target the ChT-L activity (up to 300 times decreased potency compared to P3-Leu inhibitors). Yeast β 5 and mammalian constitutive β 5c subunits lack a defined S2 pocket^{3, 6, 17} (Gly48 vs Cys48 for β 5i) and consequently, exchange of the P2-Ala by Leu does not significantly affect IC₅₀ values. For instance, the compounds Ac-LAL-EK and Ac-LLL-EK as well as Ac-PAL-EK and Ac-PLL-EK are equipotent (Table 2). Nonetheless, potency and subunit selectivity may be affected by larger P2 side chains such as Phe, Tyr or Trp, which provide additional anchorage especially in subunit β 5i by interacting with Cys48.⁶

Proteasomal β 5 subunits select for distinct sizes of apolar P1-residues. In agreement with structural data,⁶ the fluorogenic substrate Ac-WLA-AMC, featuring a P1-Ala side chain can be used to monitor β 5c activity.⁵ We observed that the IC₅₀ value of the P1-Ala compound Ac-LAA-EK for subunit β 5c (1.1 μ M) is reduced up to 55 fold compared to analogues bearing Leu, Phe or Tyr as P1 side chains (IC₅₀: < 0.06 μ M; Tables 2-3). Ac-LAA-EK, however, does not inhibit subunit β 5i and thus it represents a basic scaffold for developing β 5c selective compounds. Crystallographic data disclose that Ala undergoes hydrophobic contacts with Met45 of the

$\gamma\beta 5$ -S1 pocket (Ala C ^{β} to Met45 C ^{γ} /S: 4 Å) without changing its position (Figures S3d and S3g). The $\beta 5i$ -S1 site does not provide this stabilization because the peculiar conformation of Met45 enlarges the S1 pocket. Hence, subunit $\beta 5i$ is not targeted by Ac-LAA-EK (AlaC ^{β} to Met45: 5.7-7.4 Å; Figure 2).⁶

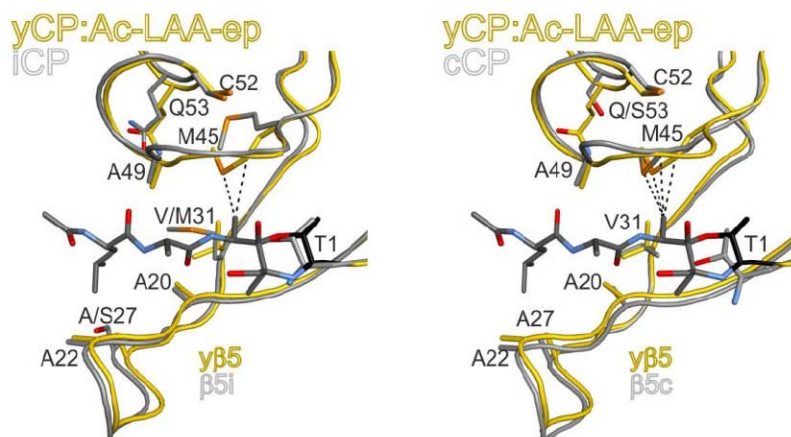


Figure 2. Superposition of $\gamma\beta 5$ in complex with Ac-LAA-EK onto the mouse $m\beta 5$ proteasome subunits. The peculiar conformation of Met45 in $\beta 5i$ (left) cannot stabilize the P1-Ala residue by hydrophobic interactions (black dashed lines; distances 5.7-7.4 Å), whereas the orientations of Met45 in the yeast $\beta 5$ subunit (distances 3.9-4.0 Å) and in $\beta 5c$ of the constitutive proteasome are more favorable (distances 4.2-4.8 Å).

Fluorogenic substrates for $\beta 5c$ and $\beta 5i$ feature either Leu or Tyr as P1 residues (carboxybenzyl-Gly-Gly-Leu-para-nitroanilide (Z-GGL-pNA), N-succinyl-Leu-Leu-Val-Tyr-AMC (Suc-LLVY-AMC)²⁰) and most inhibitors of the $\beta 5$ active site, including the FDA approved drugs bortezomib and carfilzomib, bear Leu in P1. Epoxyketones with Leu, Phe or Tyr in P1 as well as Leu in P3 are very potent inhibitors of both human $\beta 5c$ ($IC_{50} \leq 0.1 \mu M$) and $\beta 5i$ ($IC_{50} \leq 1.0 \mu M$; Table 2) as well as of the yeast counterpart ($IC_{50} \leq 0.72 \mu M$; Table 3). Consistent with previous suggestions,^{6, 21} the P1-Leu residue drives $\beta 5c$ selectivity: Ac-LAL-EK is 17 times more specific for $\beta 5c$ than $\beta 5i$ (Table 2). The tendency of Ac-LAF-EK to favor $\beta 5c$ over $\beta 5i$ (up to 6 times) probably results from the P3 and P2 residues (Table 2). The P3-Leu, which is accepted by both $\beta 5c$ and $\beta 5i$,^{6, 17, 19, 21, 22} and the P2-Ala residue, which fails to interact with Cys48 of $\beta 5i$, do not promote $\beta 5i$ but $\beta 5c$ selectivity. Interestingly, reported $\beta 5i$ inhibitors always have aromatic P2 residues, which interact with Cys48 and small P3 residues which are disfavored by $\beta 5c$.²¹ Altogether, these results imply that the P1 side chain is a major determinant of affinity for $\beta 5$ subunits, but does not act as the sole.

General aspects for targeting β 1

The yeast $\gamma\beta$ 1 and the mammalian constitutive β 1c subunits have been attributed to cleave peptide bonds after negatively charged amino acids.²³ To assay this activity of the proteasome, the fluorogenic substrate Z-Leu-Leu-Glu-AMC is frequently used. However, it has been found^{8,9} that $\gamma\beta$ 1 and β 1c prefer ligands featuring Asp and Leu at P1 over those bearing Glu or any other amino acid in this position (Table 2). For instance, the IC_{50} values of P1-Asp/Leu compounds for β 1c range $\leq 1.6 \mu\text{M}$, whereas those for all other compounds are $\geq 5.3 \mu\text{M}$. In agreement, bortezomib (Leu in P1; $IC_{50} \leq 1 \mu\text{M}$) but not ONX-0914 (Phe in P1; $IC_{50} > 10 \mu\text{M}$) targets the subunits $\gamma\beta$ 1 and β 1c with high affinity (Tables 2). The wild-type $\gamma\text{CP}:\text{Ac-PAE-EK}$ crystal structure revealed that Glu fits well in the $\gamma\beta$ 1 S1 pocket (Figure 3), but lacks any direct interaction with surrounding protein residues. In contrast to Glu, the P1-Asp is hydrogen-bonded to Thr200 γ (2.8 Å) and the P1-Leu undergoes favorable van-der-Waals interactions with the methyl group of Thr20 (3.7 Å). These contacts cause the Asp and Leu side chains to adopt distinct orientations in the S1 pocket. Repulsion of the positively charged Arg45 and the nonpolar P1-Leu side chain is prevented by a negatively charged counter ion (e.g. Cl⁻) that is hydrogen-bonded to Arg45NH1 and Arg45NH2 (Figure 3). The minor stabilization of the Glu side chain compared to Asp and Leu causes its disfavor at the P1 position. In conclusion, the $\gamma\beta$ 1 and β 1c active sites of the proteasome rather exert C-L and ChT-L than PGPH activities, and rather select for a certain size of side chain than for its charge. Regarding potency and selectivity for β 1c, Ac-PAD-EK and Ac-LAD-EK are the most outstanding compounds ($IC_{50} \leq 1.6 \mu\text{M}$; Table 2).

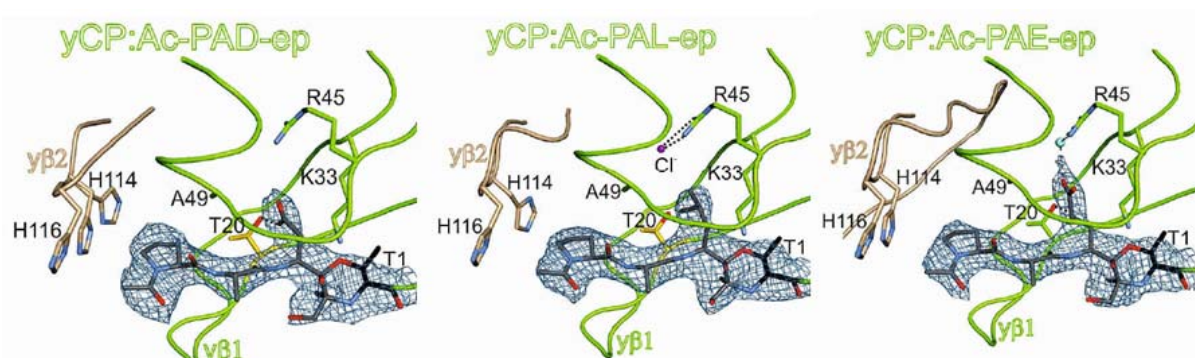


Figure 3. The $\gamma\beta$ 1 active site favors Asp or Leu in its S1 pocket. $2F_o - F_c$ electron density map (blue mesh; contoured at 1σ) for Ac-PAD-EK (left), Ac-PAL-EK (middle) and Ac-PAE-EK (right) bound to the $\gamma\beta$ 1 active site (green) of the wt yeast 20S proteasome (yCP). The active site Thr1 is marked in black, Thr20 in yellow. The chloride ion is depicted as a purple sphere. Hydrogen bonds are indicated by black dashed lines. Important residues of the neighboring subunit $\gamma\beta$ 2 (brown), contributing to the S3 and S4 pockets of the $\gamma\beta$ 1/ $\gamma\beta$ 2 substrate binding channel are illustrated. His114 adopts alternative conformations.

Consistent with structural data^{3, 6} and cleavage pattern analyses¹¹, the β 1i substrate binding channel is targeted by compounds featuring hydrophobic residues (Table 2). The apolar β 1i active site surroundings (e.g. Val20 and Leu45 in β 1i versus Thr20 and Arg45 in β 1c) enhance

the IC₅₀ values of Ac-PAL-EK (IC₅₀: 0.11 μM (β1c)/0.028 μM (β1i)) and Ac-LAL-EK (IC₅₀: 0.95 μM (β1c)/0.020 μM (β1i)) at least four-times compared to β1c by providing favorable van-der-Waals stabilization. Besides Leu, also the aromatic amino acids Phe (IC₅₀: ≥10.8 μM (β1c)/≤0.23 μM (β1i)) and Tyr (IC₅₀: ≥5.3 μM (β1c)/ ≤0.38 μM (β1i)) represent appropriate P1 residues for β1i-ligands. In fact, the respective compounds are up to 500 times more selective for β1i than for β1c (Table 2).¹⁶ Previously it has been suggested that ONX-0914 targets β5i over β1i due to steric hindrance with Phe31 of the β1i S1 pocket.⁶ Nonetheless, Phe containing ligands can be used to block subunit β1i (see also chapter 5).¹⁶

Next, acetyl-capped tetrapeptides and tripeptides were evaluated and it was found that elongation of Ac-PLL-EK by a P4-Ala residue enhances the IC₅₀ value for γβ1 and β1c by a factor of four (Table 2). In addition, Ac-APLL-EK (IC₅₀: 0.029 μM) is 25 times more active for β1c than H-APLL-EK (IC₅₀: 0.72 μM; Table 2). The structural data show that a hydrogen bond between the carbonyl oxygen atom of the acetyl-cap and Thr22O^γ additionally stabilizes these elongated inhibitors in γβ1 (distance ~3 Å; data not shown). Thr22 is conserved in mammalian β1c subunits, but exchanged for Ala in β1i entities. Congruently, the IC₅₀ values of Ac-APLL-EK (IC₅₀: 0.035 μM) and H-APLL-EK (IC₅₀: 0.085 μM) for subunit β1i are almost identical. In summary, capped tetrapeptides may be useful to target β1c.

The S3 pocket – A peculiarity of the β1 active site.

P3-Pro ligands serve as potent inhibitors of C-L^{8, 16} or BrAAP (branched chain amino acid-preferring)^{24, 25} activities and as selective substrates (e.g. Ac-PAL-AMC) to monitor peptide bond hydrolysis by β1i⁵. The structural basis for the β1-preference of the P3-Pro residue, however, remained elusive. The analysis of the subunit selectivity profile of various compounds bearing either Leu or Pro residues at their P3 site for the yeast as well as mammalian CPs revealed that, in contrast to the β1 active sites, the β2 and β5 subunits disfavor inhibitors with Pro at P3 (Table 2). For instance, Ac-LAD-EK is selective for β1c (IC₅₀: 1.6 μM), but is also able to inhibit β5c and β5i quite efficiently (IC₅₀: 21.7 resp. 12.3 μM) and to a lesser extent also the β2 subunits are inhibited. In contrast, Ac-PAD-EK is not able to inhibit the β5 subunits even at 1 mM. Hence, it is the poor affinity of the Pro-ligands for the subunits β2 and β5 that causes their β1 selectivity.

The non-primed substrate binding channels of the proteasome are formed by two adjacent β subunits (β1/2, β2/3 and β5/6), with β2, β3 and β6 contributing to the S3 pockets of the β1, β2 and β5 active sites. For instance, Asp114O^δ of β3 and β6 hydrogen bonds to the amide nitrogen of P3-Leu ligands bound to β2 and β5, respectively (Figure 4c)^{3, 6, 17} and thereby stabilizes the ligand in the substrate binding channel. The backbone nitrogen of P3-Pro compounds, however, is not accessible for this interaction. Furthermore, in β2/3 and β5/6,

the P3-Pro inhibitors are shifted compared to the Leu-counterparts (Figures 4A-B), because Asp114 hinders placing of the Pro side chain in the S3 pocket (distance ≥ 3.0 Å). By contrast, P3-Pro and P3-Leu featuring inhibitors adopt the same conformation in β_1 , suggesting that the structure of the $\beta_1/2$ substrate binding channel tolerates P3-Pro-residues better than the β_2/β_3 and β_5/β_6 active sites. Indeed, the $\beta_1/2$ active site is ideally suited to accommodate P3-Pro ligands. Instead of Asp114, β_2 encodes either His114 (in $\gamma\beta_2/\beta_2i$ subunits) or Tyr114 (in β_2c subunits). According to the mouse cCP and iCP crystal structures, both Tyr114 in β_2c and His114 in β_2i and $\gamma\beta_2$ adopt the same side chain orientation. However, this conformation clearly differs from that observed for Asp114 in β_3 and β_6 and prevents hydrogen-bonding to the P3 nitrogen of ligands (Figures 4D-E). Consequently, at the $\beta_1/2$ active site, P3-Leu ligands are less stabilized and P3-Pro ones do not receive repulsion.

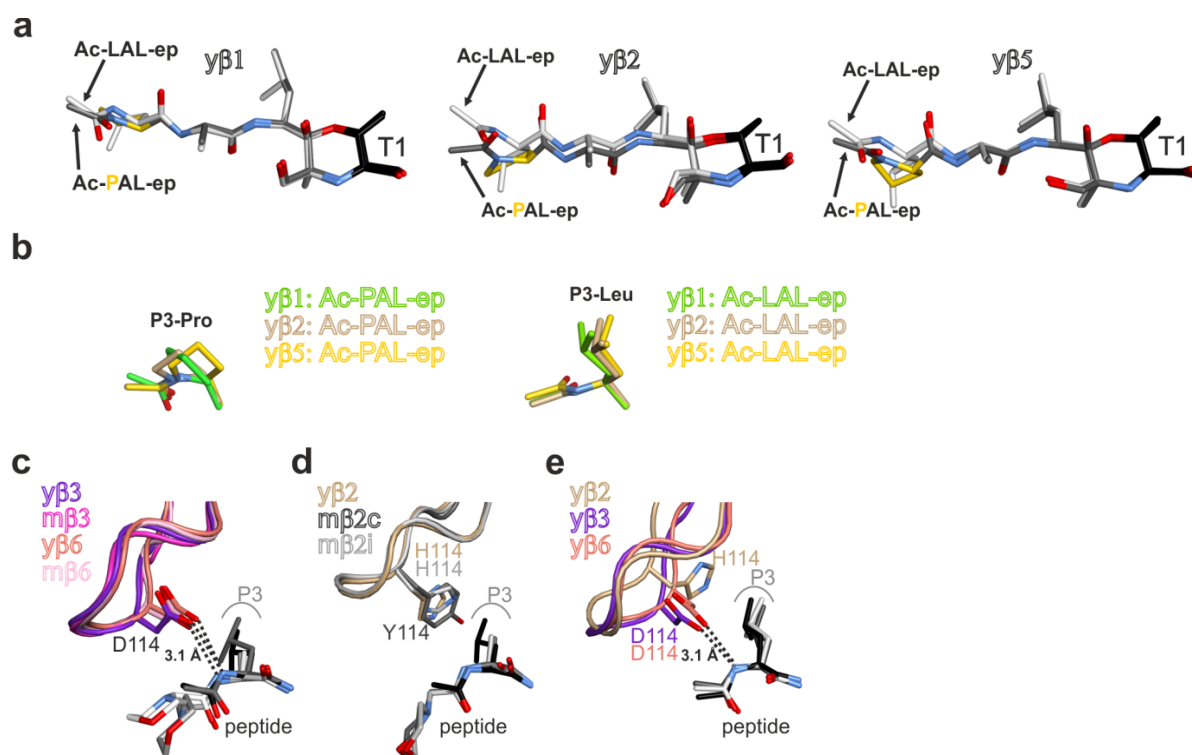


Figure 4. The impact of residue 114 of β_2 , β_3 and β_6 on ligand binding. A) Superposition of the compounds Ac-LAL-EK (light gray) and Ac-PAL-EK (dark gray) bound to the yeast β_1 , β_2 and β_5 subunits highlights differences at the P3 site. P3-Pro and P3-Leu featuring compounds adopt almost identical conformations in the $\gamma\beta_1$ substrate binding channel, while in the $\gamma\beta_2$ and $\gamma\beta_5$ counterpart profound changes are observed. These explain the disfavor of P3-Pro compounds by the latter two active sites. B) Superposition of the Ac-PAL-EK bound to $\gamma\beta_1$ (green), $\gamma\beta_2$ (brown) and $\gamma\beta_5$ (yellow) depicts subunit-specific differences in the orientation of the P3-Pro residue, whereas for the P3-Leu side chain of Ac-LAL-EK no significant alterations are observed. C) Superposition of yeast and mouse β_3 and β_6 subunits visualize that Asp114 occupies the same position in all subunits. Notably, Asp114 is hydrogen-bonded to the P3 amide nitrogen atom of the ligands peptide backbone (Ac-LAF-EK for yeast and ONX 0914 for mouse). The P3 sites of ligands are depicted as sticks. D) Superposition of yeast and mouse β_2 subunits indicates that His114 ($\gamma\beta_2$ and $m\beta_2i$) and Tyr114 ($m\beta_2c$) perfectly overlay and lack any interaction with the ligand's peptide backbone. E) Superposition of the yeast β_2 , β_3 and β_6 subunits depicts that only Asp114 in β_3 and β_6 hydrogen-bonds to the P3 amide nitrogen atom of the ligand. Notably, the position of the C $^\alpha$ atom of His114 in $\gamma\beta_2$ significantly deviates from that observed for Asp114 of $\gamma\beta_3$ and $\gamma\beta_6$.

Conclusion

A series of 23 tri- and tetrapeptide epoxyketone proteasome inhibitors was synthesized. They feature varying P1 residues, including hydrophobic and acidic ones and bear either a P3-Leu or P3-Pro residue. All compounds were examined for their potency and subunit selectivity in human cell lysates and with purified yeast proteasome. The binding modes of all inhibitors were visualized by X-ray crystallography. The obtained data reveal the following key findings: 1) epoxyketones featuring Val or Ile as P1 residues are disfavored by yeast and human proteasomes; 2) two compounds were identified that favor β 2c and β 5c, respectively, over the i-counterparts: Ac-LAE-EK and Ac-LAA-EK; 3) yeast and human constitutive β 1 active sites prefer Asp over Glu at the P1 position and thus exert rather caspase-like activities. Besides Asp, Leu is also well accepted by the $\gamma\beta$ 1/ β 1c S1 pocket; 4) a structural explanation for the β 1-preference of P3-Pro-featuring compounds is provided. Asp114 of β 3 and β 6 impairs binding of P3-Pro ligands to the β 2 and β 5 subunits, while His/Tyr114 of β 2 allows their accommodation in the β 1/2 substrate binding channel due to exceptional backbone and side chain orientations. Together, the structural and biochemical data presented here will support future efforts to improve existing proteasome inhibitors as well as to design proteasome-type selective and subunit-specific inhibitors, as will be described in the next chapters. Such compounds would serve to characterize in more detail the biological roles of the individual proteasomal active sites and might qualify for diverse medical applications including cancer and inflammatory diseases.

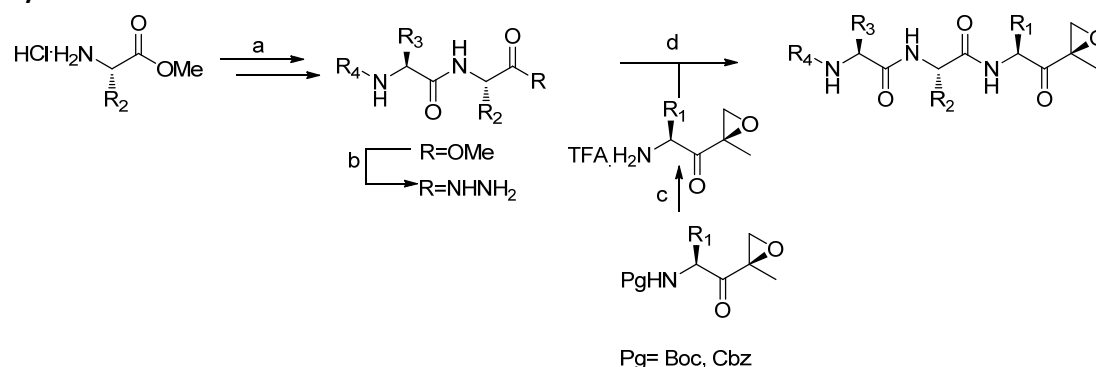
Experimental

Synthetic procedures

General procedures

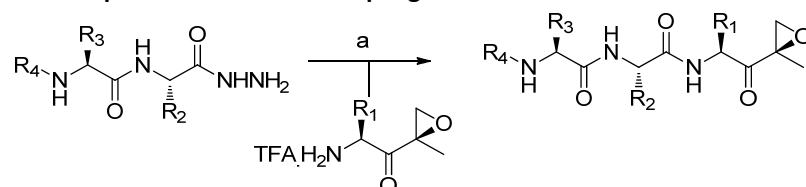
Acetonitrile (ACN), dichloromethane (DCM), N,N-dimethylformamide (DMF), methanol (MeOH), diisopropylethylamine (DiPEA) and trifluoroacetic acid (TFA) were of peptide synthesis grade, purchased at Biosolve, and used as received. All general chemicals (Fluka, Acros, Merck, Aldrich, Sigma, Iris Biotech) were used as received. Traces of water were removed from reagents used in reactions that require anhydrous conditions by co-evaporation with toluene. Diethylether was stored over 4 Å molecular sieves. Column chromatography was performed on Screening Devices b.v. Silica Gel, with a particle size of 40-63 µm and pore diameter of 60 Å. TLC analysis was conducted on Merck aluminium sheets (Silica gel 60 F254). Compounds were visualized by UV absorption (254 nm), by spraying with a solution of (NH₄)₆Mo₇O₂₄·4H₂O (25 g/L) and (NH₄)₄Ce(SO₄)₄·2H₂O (10 g/L) in 10% sulphuric acid, a solution of KMnO₄ (20 g/L) and K₂CO₃ (10 g/L) in water, or ninhydrin (0.75 g/L) and acetic acid (12.5 mL/L) in ethanol, where appropriate, followed by charring at ca. 150°C. ¹H and ¹³C-NMR spectra were recorded on a Bruker AV-400 (400 MHz) or AV-600 (600 MHz) spectrometer. Chemical shifts are given in ppm (δ) relative to tetramethylsilane, CD₃OD or CDCl₃ as internal standard. High resolution mass spectra were recorded by direct injection (2 µL of a 2 µM solution in water/acetonitrile 50/50 (v/v) and 0.1% formic acid) on a mass spectrometer (Thermo Finnigan LTQ Orbitrap) equipped with an electrospray ion source in positive mode (source voltage 3.5 kV, sheath gas flow 10, capillary temperature 250 °C) with resolution R = 60,000 at m/z 400 (mass range m/z = 150-2,000) and dioctylphthalate (m/z = 391.28428) as a "lock mass". The high resolution mass spectrometer was calibrated prior to measurements with a calibration mixture (Thermo Finnigan). Optical rotations were recorded on a Propol automatic polarimeter. LC-MS analysis was performed on a Finnigan Surveyor HPLC system with a Gemini C₁₈ 50 × 4.60 mm column (detection at 200–600 nm) coupled to a Finnigan LCQ Advantage Max mass spectrometer with ESI. The applied buffers were H₂O, MeCN and 1.0% TFA in H₂O (0.1% TFA end concentration). Methods used are: 10→90% MeCN, 13.5 min (0→0.5 min: 10% MeCN; 0.5→8.5 min: gradient time; 8.5→10.5 min: 90% MeCN; 10.5→13.5 min: 90% → 10% MeCN). 0→50% MeCN, 13.5 min (0→0.5 min: 0% MeCN; 0.5→8.5 min: gradient time; 8.5→10.5 min: 90% MeCN; 10.5→13.5 min: 90% → 10 (or 0)% MeCN). HPLC purification was performed on a Gilson HPLC system coupled to a Phenomenex Gemini 5µm 250×10 mm column, or on an Agilent HPLC/MS system coupled to a Phenomenex Gemini 5µm 250×10 mm column or on a Waters autopurifier HPCL/MS system coupled to a Phenomenex Gemini 5µm 150×21.2 mm column. All tested compounds are >95% pure on the basis of LC-MS and NMR, except Ac-PAD-EK, which is >60% pure on the basis of LC-MS and NMR. Boc-Leu-Leu-OMe²⁶, Boc-Leu-EK, Boc-Phe-EK²⁷ were synthesized according to literature procedures. Compound N₃G-A(4,4-F₂P)nLL-EK has been described elsewhere¹⁶.

Synthetic details



Scheme 1. General synthetic route towards peptide-epoxyketones. Reagents and conditions: (a). Sequential peptide coupling/Boc removal. Peptide coupling: HCTU, DiPEA, Boc-AA-OH, DCM. Boc-removal: TFA/DCM. (b) $\text{NH}_2\text{NH}_2 \cdot \text{H}_2\text{O}$, MeOH; (c) TFA or Pd/C, MeOH, TFA, $\text{H}_2(\text{g})$; (d) i) $t\text{BuONO}$, HCl, DMF, DCM, -30°C ; ii) amine (warhead), DiPEA, $-30^\circ\text{C} \rightarrow \text{RT}$.

General procedure for azide couplings.



Scheme 2. Azide coupling towards peptide epoxyketones. Reagents and conditions: (a) i) $t\text{BuONO}$, HCl, DMF, DCM, -30°C ; ii) amine (warhead), DiPEA, $-30^\circ\text{C} \rightarrow \text{RT}$.

All peptide epoxyketones were prepared via azide coupling of properly protected tripeptide hydrazide and properly deprotected epoxyketone amines (see scheme 2). The appropriate hydrazide was dissolved in 1:1 DMF:DCM (v/v) and cooled to -30°C . $t\text{BuONO}$ (1.1 equiv.) and HCl (4M solution in 1,4-dioxane, 2.8 equiv.) were added, and the mixture was stirred for 3h at -30°C after which TLC analysis (10% MeOH/DCM, v/v) showed complete consumption of the starting material. The epoxyketone a free amine was added to the reaction mixture as a solution in DMF. DiPEA (5 equiv.) was added to the reaction mixture, and this mixture was allowed to warm to RT slowly overnight. The mixture was diluted with EtOAc or DCM and extracted with H_2O (3 \times). The organic layer was dried over MgSO_4 concentrated and purified by flash column chromatography (1-5% MeOH in DCM) and HPLC-purification (if necessary).

Ac-PAD(OtBu)-EK

This compound was obtained by the general protocol for azide coupling on a 140 μmol scale. Purification by column chromatography (0 \rightarrow 3% MeOH in DCM) provided the title compound (40 mg, 65%) Complex NMR due to presence of rotamers (8:1) and presence of by-product (reduced epoxide). Peaks of major rotamer of the product are reported. ^1H NMR (400 MHz, CDCl_3) δ 7.40 (d, $J = 6.8$ Hz, 1H), 7.09 (d, $J = 7.4$ Hz, 1H), 4.69 (dt, $J = 7.4$, 5.5 Hz, 1H), 4.53 (dd, $J = 8.0$, 2.1 Hz, 1H), 4.34 (p, $J = 6.8$ Hz, 1H), 3.63 – 3.53 (m, 1H), 3.43 (td, $J = 9.5$, 7.0 Hz, 1H), 3.18 (d, $J = 4.8$ Hz, 1H), 2.87 (d, $J = 4.9$ Hz, 1H), 2.84 – 2.66 (m, 2H), 2.35 (dtd, $J = 14.6$, 8.7, 7.6, 3.3 Hz, 1H), 2.10 (s, 3H), 2.04 – 1.80 (m, 3H), 1.52 (s, 3H), 1.41 (d, $J = 3.7$ Hz, 9H), 1.35 (t, $J = 7.2$ Hz, 3H). ^{13}C NMR (101 MHz, CDCl_3) δ 205.57, 172.08, 171.41, 171.16, 169.51, 81.99, 59.93, 59.79, 59.48, 52.67, 49.55, 49.43, 49.28, 48.47, 37.02, 28.11, 27.78, 25.20, 22.67, 17.79, 17.07. LC-MS (linear gradient 10 \rightarrow 90% MeCN, 0.1% TFA, 12.5 min): R_t (min): 5.37 (ESI-MS (m/z): 440.07 ($\text{M}+\text{H}^+$)). HRMS: calculated for $\text{C}_{21}\text{H}_{33}\text{N}_3\text{O}_7$ 440.23913 [$\text{M}+\text{H}^+$] $^+$; found 440.23914.

Ac-PAD-EK

Ac-PAD(OtBu)-EK (40 mg) was dissolved in dry DCM (1 mL), followed by the addition of dry TFA (1 mL, ampule). After 15 min, 2 mL dry toluene was added and the reaction mixture was concentrated and co-evaporated with toluene. Purification by HPLC (C_{18} , Waters, 5-15% MeCN, 0.1% TFA, 9 min gradient), yielding the product as a white solid after lyophilisation. Analysis revealed partial hydrolysis of the product during HPLC-purification (about 30%). Complex NMR due to mixtures of product with hydrolysed product and rotamers. Peaks reported for product, major rotamer. ^1H NMR (600 MHz, MeOD) δ 4.79 (m, 1H), 4.44 – 4.38 (m, 2H), 3.65 – 3.56 (m, 2H), 3.28 – 3.23 (m, 1H), 2.95 (d, J = 5.0 Hz, 1H), 2.82 (dd, J = 16.6, 4.8 Hz, 1H), 2.73 (dd, J = 16.5, 7.9 Hz, 1H), 2.22 (d, J = 2.4 Hz, 1H), 2.13 – 2.10 (m, 3H), 2.10 – 1.96 (m, 3H), 1.51 (s, 3H), 1.37 (d, J = 7.2 Hz, 3H). ^{13}C NMR (151 MHz, MeOD) δ 207.04, 174.72, 174.49, 173.28, 172.64, 61.37, 53.25, 50.51, 50.11, 49.48, 35.89, 31.04, 25.75, 22.29, 17.64, 17.15. LC-MS (linear gradient 0 \rightarrow 50% MeCN, 0.1% TFA, 12.5 min): R_t (min): 5.40 (ESI-MS (m/z): 384.07 ($\text{M}+\text{H}^+$)); 4.76 (ESI-MS (m/z): 402.07 ($\text{M}+\text{H}^+$) (hydrolysed product)). HRMS: calculated for $\text{C}_{17}\text{H}_{25}\text{N}_3\text{O}_7$ 384.17653 [$\text{M}+\text{H}$] $^+$; found 384.17653.

Ac-LAD(OtBu)-EK

This compound was obtained by the general protocol for azide coupling on a 100 μmol scale. Purification by column chromatography (0 \rightarrow 3% MeOH in DCM) provided the title compound (24.5 mg, 54%) as a white powder after lyophilisation. Complex NMR due to presence of rotamers and presence of by-product (reduced epoxide). Peaks of major rotamer of the product are reported. ^1H NMR (400 MHz, CDCl_3) δ 7.42 (d, J = 7.7 Hz, 1H), 7.12 (d, J = 7.6 Hz, 1H), 6.61 (d, J = 8.5 Hz, 1H), 4.82 – 4.67 (m, 1H), 4.71 – 4.48 (m, 2H), 3.16 (d, J = 4.9 Hz, 1H), 2.88 (d, J = 4.8 Hz, 1H), 2.74 (qt, J = 12.4, 5.7 Hz, 2H), 2.02 (d, J = 3.4 Hz, 3H), 1.70 – 1.46 (m, 6H), 1.40 (d, J = 2.5 Hz, 9H), 1.34 (d, J = 7.0 Hz, 3H), 0.91 (d, J = 6.2 Hz, 6H). ^{13}C NMR (101 MHz, CDCl_3) δ 205.70, 172.26, 172.14, 170.39, 169.43, 82.02, 59.43, 52.58, 51.63, 49.32, 48.82, 41.99, 37.17, 28.12, 24.87, 23.22, 23.06, 22.25, 18.95, 17.03. LC-MS (linear gradient 10 \rightarrow 90% MeCN, 0.1% TFA, 12.5 min): R_t (min): 6.25 (ESI-MS (m/z): 456.07 ($\text{M}+\text{H}^+$)).

Ac-LAD-EK

Ac-LAD(OtBu)-EK (8.7 mg) was dissolved in dry DCM (1 mL), followed by the addition of dry TFA (1 mL, ampule). After 15 min, 2 mL dry toluene was added and the reaction mixture was concentrated and co-evaporated with toluene. Purification by HPLC (C_{18} , Gemini, 21-24% MeCN, 0.1% TFA, 12 min gradient), yielding the product as a white solid after lyophilisation (3.31 mg, 43%). ^1H NMR (600 MHz, MeOD) δ 4.78 – 4.70 (m, 1H), 4.43 – 4.29 (m, 2H), 3.20 (s, 1H), 2.93 – 2.88 (m, 1H), 2.76 (dd, J = 16.4, 4.7 Hz, 1H), 2.68 (dd, J = 16.2, 7.6 Hz, 1H), 1.98 (s, 3H), 1.68 (dt, J = 13.4, 6.7 Hz, 1H), 1.57 (ddt, J = 9.2, 6.0, 3.2 Hz, 2H), 1.49 (s, 3H), 1.34 (d, J = 7.1 Hz, 3H), 0.95 (dd, J = 22.2, 6.6 Hz, 6H). ^{13}C NMR (151 MHz, MeOD) δ 174.75, 174.55, 173.82, 173.56, 68.14, 53.31, 53.15, 50.61, 50.05, 41.76, 36.36, 25.92, 23.46, 22.38, 21.86, 18.05, 17.16. LC-MS (linear gradient 0 \rightarrow 50% MeCN, 0.1% TFA, 12.5 min): R_t (min): 6.59 (ESI-MS (m/z): 400.07 ($\text{M}+\text{H}^+$)). HRMS: calculated for $\text{C}_{18}\text{H}_{29}\text{N}_3\text{O}_7$ 400.20782 [$\text{M}+\text{H}$] $^+$; found 400.20783.

Ac-PAE(OtBu)-EK

This compound was obtained by the general protocol for azide coupling on a 100 μmol scale. Purification by column chromatography (0 \rightarrow 3% MeOH in DCM) provided the title compound (18.06 mg, 41%) as a white powder after lyophilisation. Complex NMR due to presence of rotamers (7:1) and presence of by-product (reduced epoxide). Peaks of major rotamer of the product are reported. ^1H NMR (400 MHz, CDCl_3) δ 7.34 (d, J = 6.9 Hz, 1H), 7.06 (d, J = 7.3 Hz, 1H), 4.56 – 4.42 (m, 2H), 4.38 – 4.27 (m, 1H), 3.63 – 3.53 (m, 1H), 3.50 – 3.38 (m, 1H), 3.30 (d, J = 4.9 Hz, 1H), 2.87 (d, J = 5.0 Hz, 1H), 2.38 – 2.22 (m, 3H), 2.10 (s, 3H), 2.09 – 1.85 (m, 4H), 1.76 (ddd, J = 15.8, 14.4, 7.2 Hz, 1H), 1.50 (d, J = 3.5 Hz, 3H), 1.43 (s, 9H), 1.34 (d, J = 7.1 Hz, 3H). ^{13}C NMR (101 MHz, CDCl_3) δ 207.64, 172.45, 172.34, 171.45, 171.14, 81.03, 59.88, 59.34, 52.59, 51.40, 49.22, 48.48, 31.61, 28.19, 27.97, 25.97, 25.20, 22.67, 17.69, 16.68. LC-MS (linear gradient 10 \rightarrow 90% MeCN, 0.1% TFA, 12.5 min): R_t (min): 5.61 (ESI-MS (m/z): 454.00 ($\text{M}+\text{H}^+$)). HRMS: calculated for $\text{C}_{22}\text{H}_{35}\text{N}_3\text{O}_7$ 454.25478 [$\text{M}+\text{H}$] $^+$; found 454.25461.

Ac-PAE-EK

Ac-PAE(OtBu)-EK (7.5 mg) was dissolved in dry DCM (1 mL), followed by the addition of dry TFA (1 mL, ampule). After 15 min, 2 mL dry toluene was added and the reaction mixture was concentrated and co-evaporated with toluene. Purification by HPLC (C₁₈, Gemini, 13-16% MeCN, 0.1% TFA, 12 min gradient), yielding the product as a white solid after lyophilisation (1.86 mg, 30%). Complex NMR due to presence of rotamers, peaks of major rotamer are reported. ¹H NMR (600 MHz, MeOD) δ 4.50 – 4.41 (m, 1H), 4.41 – 4.35 (m, 1H), 4.32 (q, *J* = 7.2 Hz, 1H), 3.69 – 3.62 (m, 1H), 3.62 – 3.52 (m, 1H), 3.25 (d, *J* = 5.1 Hz, 1H), 2.92 (d, *J* = 5.1 Hz, 1H), 2.44 – 2.27 (m, 3H), 2.26 – 2.18 (m, 1H), 2.09 (s, 3H), 2.08 – 2.00 (m, 2H), 2.00 – 1.92 (m, 2H), 1.82 – 1.72 (m, 1H), 1.48 (s, 3H), 1.35 (t, *J* = 6.5 Hz, 3H). ¹³C NMR (151 MHz, MeOD) δ 208.76, 175.09, 174.80, 174.48, 172.50, 61.21, 53.13, 53.11, 50.23, 49.48, 32.26, 31.03, 27.09, 25.74, 22.29, 17.70, 16.88. LC-MS (linear gradient 0 → 50% MeCN, 0.1% TFA, 12.5 min): R_t (min): 5.77 (ESI-MS (m/z): 398.07 (M+H⁺)). HRMS: calculated for C₁₈H₂₇N₃O₇ 398.19218 [M+H]⁺; found 398.19208.

Ac-LAE(OtBu)-EK

This compound was obtained by the general protocol for azide coupling on a 100 μmol scale. Purification by column chromatography (0→3% MeOH in DCM) provided the title compound (30.0 mg, 64%) as a white powder after lyophilisation. Complex NMR due to presence of rotamers and presence of by-product (reduced epoxide). Peaks of major rotamer of the product are reported. ¹H NMR (400 MHz, CDCl₃) δ 7.39 (d, *J* = 7.4 Hz, 1H), 7.08 (d, *J* = 7.6 Hz, 1H), 6.59 (d, *J* = 8.4 Hz, 1H), 4.67 – 4.43 (m, 3H), 3.28 (d, *J* = 5.0 Hz, 1H), 2.89 (d, *J* = 5.0 Hz, 1H), 2.36 – 2.22 (m, 2H), 2.13 – 1.96 (m, 4H), 1.78 (dd, *J* = 14.4, 7.8 Hz, 1H), 1.51 (s, 6H), 1.42 (s, 10H), 1.33 (d, *J* = 7.0 Hz, 3H), 0.95 – 0.84 (m, 6H). ¹³C NMR (101 MHz, CDCl₃) δ 207.72, 172.43, 172.40, 172.26, 170.39, 81.18, 59.34, 52.49, 51.75, 51.35, 48.79, 41.85, 31.66, 28.18, 26.20, 24.90, 23.21, 23.02, 22.27, 18.81, 16.65. LC-MS (linear gradient 10 → 90% MeCN, 0.1% TFA, 12.5 min): R_t (min): 6.42 (ESI-MS (m/z): 470.00 (M+H⁺)).

Ac-LAE-EK

Ac-LAE(OtBu)-EK (15 mg) was dissolved in dry DCM (1 mL), followed by the addition of dry TFA (1 mL, ampule). After 15 min, 2 mL dry toluene was added and the reaction mixture was concentrated and co-evaporated with toluene. Purification by HPLC (C₁₈, Gemini, 20-23% MeCN, 0.1% TFA, 12 min gradient), yielding the product as a white solid after lyophilisation (6.89 mg, 52%). ¹H NMR (600 MHz, MeOD) δ 4.47 (dd, *J* = 9.2, 4.0 Hz, 1H), 4.43 – 4.27 (m, 2H), 3.25 (d, *J* = 5.1 Hz, 1H), 2.93 (d, *J* = 5.1 Hz, 1H), 2.46 – 2.28 (m, 2H), 2.15 – 2.03 (m, 1H), 1.97 (s, 3H), 1.82 – 1.72 (m, 1H), 1.72 – 1.63 (m, 1H), 1.63 – 1.52 (m, 2H), 1.48 (s, 3H), 1.33 (d, *J* = 7.1 Hz, 3H), 0.95 (dd, *J* = 21.2, 6.6 Hz, 6H). ¹³C NMR (151 MHz, MeOD) δ 208.37, 176.16, 174.52, 174.36, 173.06, 59.80, 52.78, 52.74, 52.50, 49.68, 41.42, 31.11, 30.73, 26.57, 25.52, 23.07, 21.99, 21.50, 17.46, 16.46. LC-MS (linear gradient 0 → 50% MeCN, 0.1% TFA, 12.5 min): R_t (min): 6.85 and 6.61 (ESI-MS (m/z): 414.07 / 414.13 (M+H⁺)) (elutes in two peaks, most likely due to different salt-forms). HRMS: calculated for C₁₉H₃₁N₃O₇ 414.22342 [M+H]⁺; found 414.22348.

Ac-PAF-EK

This compound was obtained by the general protocol for azide coupling on a 100 μmol scale. Purification by column chromatography (0→3% MeOH in DCM) provided the title compound (19.40 mg, 47%) as a white powder after lyophilisation. Complex NMR due to presence of rotamers (8:1). Peaks of major rotamer are reported. ¹H NMR (400 MHz, CDCl₃) δ 7.35 (d, *J* = 7.0 Hz, 1H), 7.30 – 7.24 (m, 2H), 7.23 – 7.20 (m, 1H), 7.18 – 7.12 (m, 2H), 6.86 (d, *J* = 7.4 Hz, 1H), 4.77 (td, *J* = 8.2, 4.9 Hz, 1H), 4.41 (dd, *J* = 8.1, 2.0 Hz, 1H), 4.29 (p, *J* = 7.1 Hz, 1H), 3.54 (td, *J* = 9.1, 8.2, 3.1 Hz, 1H), 3.41 (td, *J* = 9.5, 7.1 Hz, 1H), 3.34 (d, *J* = 4.9 Hz, 1H), 3.11 (dd, *J* = 14.0, 4.9 Hz, 1H), 2.88 (d, *J* = 5.0 Hz, 1H), 2.76 (dd, *J* = 14.0, 8.4 Hz, 1H), 2.36 – 2.21 (m, 1H), 2.09 (s, 3H), 2.07 – 1.75 (m, 3H), 1.47 (s, 3H), 1.23 (d, *J* = 7.1 Hz, 3H). ¹³C NMR (101 MHz, CDCl₃) δ 207.62, 172.05, 171.45, 171.21, 136.01, 129.44, 128.76, 128.57, 127.09, 59.68, 59.40, 52.68, 52.67, 48.93, 48.48, 37.07, 27.61, 25.19, 22.65, 17.09, 16.67. LC-MS (linear gradient 10 → 90% MeCN, 0.1% TFA, 12.5 min): R_t (min): 5.48 (ESI-MS (m/z): 416.13 (M+H⁺)). HRMS: calculated for C₂₂H₂₉N₃O₅ 416.21800 [M+H]⁺; found 416.21783.

Ac-LAF-EK

This compound was obtained by the general protocol for azide coupling on a 100 μ mol scale. Purification by column chromatography (0 \rightarrow 3% MeOH in DCM) provided the title compound (32.69 mg, 76%) as a white powder after lyophilisation. ^1H NMR (400 MHz, CDCl_3 , MeOD) δ 7.33 – 7.15 (m, 5H), 4.79 (dd, J = 8.2, 5.0 Hz, 1H), 4.44 – 4.25 (m, 2H), 3.31 (d, J = 4.9 Hz, 1H), 3.10 (dd, J = 13.9, 4.9 Hz, 1H), 2.92 (d, J = 4.9 Hz, 1H), 2.79 (dd, J = 13.9, 8.3 Hz, 1H), 1.99 (s, 3H), 1.69 – 1.53 (m, 1H), 1.52 – 1.40 (m, 5H), 1.28 (d, J = 7.1 Hz, 3H), 0.92 (dd, J = 11.8, 6.5 Hz, 6H). ^{13}C NMR (101 MHz, CDCl_3 , MeOD) δ 207.72, 172.75, 172.36, 171.32, 135.85, 129.18, 128.40, 126.95, 59.21, 52.79, 52.37, 51.42, 48.58, 40.84, 36.79, 24.59, 22.77, 22.42, 21.52, 17.44, 16.32. LC-MS (linear gradient 10 \rightarrow 90% MeCN, 0.1% TFA, 12.5 min): R_t (min): 6.31 (ESI-MS (m/z): 432.07 ($\text{M}+\text{H}^+$)). HRMS: calculated for $\text{C}_{23}\text{H}_{33}\text{N}_3\text{O}_5$ 432.24930 [$\text{M}+\text{H}^+$] $^+$; found 432.24902.

Ac-PAY-EK

This compound was obtained by the general protocol for azide coupling on a 100 μ mol scale. Purification by column chromatography (0 \rightarrow 5% MeOH in DCM) provided the title compound (13.22 mg, 31%) as a white powder after lyophilisation. Complex NMR due to presence of rotamers (7:1). Peaks of major rotamer are reported. ^1H NMR (400 MHz, CDCl_3) δ 7.30 (d, J = 7.1 Hz, 1H), 6.96 (t, J = 8.5 Hz, 3H), 6.72 (d, J = 8.5 Hz, 2H), 4.74 (td, J = 8.1, 4.5 Hz, 1H), 4.48 – 4.38 (m, 1H), 4.33 (t, J = 7.1 Hz, 1H), 3.63 – 3.48 (m, 1H), 3.43 (q, J = 9.3, 8.9 Hz, 1H), 3.30 (d, J = 4.9 Hz, 1H), 3.08 (dd, J = 14.1, 4.4 Hz, 1H), 2.91 (d, J = 4.9 Hz, 1H), 2.66 (dd, J = 14.1, 8.5 Hz, 1H), 2.23 – 2.13 (m, 1H), 2.08 (s, 4H), 2.08 – 1.84 (m, 5H), 1.51 (s, 3H), 1.21 (d, J = 7.1 Hz, 3H). ^{13}C NMR (101 MHz, CDCl_3) δ 207.70, 172.22, 171.78, 171.34, 155.64, 130.52, 127.20, 115.93, 115.73, 59.93, 59.41, 53.25, 52.73, 49.00, 48.54, 36.15, 28.29, 25.11, 22.56, 17.62, 16.80. LC-MS (linear gradient 10 \rightarrow 90% MeCN, 0.1% TFA, 12.5 min): R_t (min): 4.70 (ESI-MS (m/z): 432.07 ($\text{M}+\text{H}^+$)). HRMS: calculated for $\text{C}_{22}\text{H}_{29}\text{N}_3\text{O}_6$ 432.21291 [$\text{M}+\text{H}^+$] $^+$; found 432.21283.

Ac-LAY-EK

This compound was obtained by the general protocol for azide coupling on a 100 μ mol scale. Purification by column chromatography (0 \rightarrow 5% MeOH in DCM) provided the title compound (22.15 mg, 50.0%) as a white powder after lyophilisation. Complex NMR due to presence of rotamers (7:1). ^1H NMR (400 MHz, CDCl_3) δ 8.11–8.05 (m, 2H), 7.04 (d, J = 8.4 Hz, 1H), 7.04 (d, J = 8.4 Hz, 1H), 6.71–6.68 (m, 2H), 4.87–4.67 (m, 1H), 4.36–4.31 (m, 2H), 3.24 (d, J = 5.2 Hz, 1H), 2.98 (dd, J = 14.0, 4.4 Hz, 1H), 2.91 (d, J = 8.4 Hz, 1H), 1.96 (s, 3H), 1.66–1.63 (m, 1H), 1.53–1.50 (m, 2H), 1.42 (s, 3H), 1.28 (d, J = 7.2 Hz, 3H), 0.92 (dd, J = 16.0, 6.8 Hz, 6H). ^{13}C NMR (101 MHz, MeOD) δ 208.97, 174.71, 174.62, 173.46, 157.36, 131.31, 128.55, 116.22, 60.24, 54.95, 54.86, 53.22, 53.10, 41.81, 36.71, 25.89, 23.46, 22.44, 21.86, 18.11, 16.81. LC-MS (linear gradient 10 \rightarrow 90% MeCN, 0.1% TFA, 12.5 min): R_t (min): 5.36 (ESI-MS (m/z): 448.13 ($\text{M}+\text{H}^+$)). HRMS: calculated for $\text{C}_{23}\text{H}_{33}\text{N}_3\text{O}_6$ 448.24421 [$\text{M}+\text{H}^+$] $^+$; found 448.24411.

Ac-PAI-EK

This compound was obtained by the general protocol for azide coupling on a 100 μ mol scale. Purification by column chromatography (0 \rightarrow 3% MeOH in DCM) provided the title compound (27.50 mg, 72%) as a white powder after lyophilisation. Complex NMR due to presence of rotamers (8:1). Peaks of major rotamer are reported. ^1H NMR (400 MHz, CDCl_3) δ 7.40 (d, J = 6.9 Hz, 1H), 6.79 (d, J = 8.4 Hz, 1H), 4.55 – 4.42 (m, 2H), 4.42 – 4.20 (m, 1H), 3.57 (td, J = 8.9, 8.1, 3.1 Hz, 1H), 3.43 (td, J = 9.4, 7.0 Hz, 1H), 3.30 (d, J = 5.0 Hz, 1H), 2.84 (d, J = 5.0 Hz, 1H), 2.34 – 2.23 (m, 1H), 2.13 – 2.02 (m, 4H), 2.03 – 1.73 (m, 3H), 1.47 (s, 3H), 1.43 – 1.33 (m, 1H), 1.29 (d, J = 7.1 Hz, 3H), 1.15 – 0.99 (m, 1H), 0.92 (dd, J = 6.8, 3.5 Hz, 3H), 0.85 (t, J = 7.4 Hz, 3H). ^{13}C NMR (101 MHz, CDCl_3) δ 209.36, 172.23, 171.66, 171.05, 59.74, 59.58, 55.11, 52.04, 49.24, 48.44, 37.13, 27.92, 25.15, 24.43, 22.60, 17.28, 16.50, 15.95, 11.34. LC-MS (linear gradient 10 \rightarrow 90% MeCN, 0.1% TFA, 12.5 min): R_t (min): 5.17 (ESI-MS (m/z): 382.13 ($\text{M}+\text{H}^+$)). HRMS: calculated for $\text{C}_{19}\text{H}_{31}\text{N}_3\text{O}_5$ 382.23365 [$\text{M}+\text{H}^+$] $^+$; found 382.23367.

Ac-LAI-EK

This compound was obtained by the general protocol for azide coupling on a 100 μmol scale. Purification by column chromatography (0 \rightarrow 3% MeOH in DCM) provided the title compound (27.50 mg, 72%) as a white powder after lyophilisation. ^1H NMR (400 MHz, MeOD) δ 4.46 (d, J = 7.0 Hz, 1H), 4.43 – 4.29 (m, 2H), 3.27 (d, J = 5.1 Hz, 1H), 2.91 (d, J = 5.1 Hz, 1H), 1.97 (s, 3H), 1.83 (dtq, J = 13.8, 6.9, 3.5 Hz, 1H), 1.66 (dq, J = 13.2, 6.6 Hz, 1H), 1.55 (t, J = 7.3 Hz, 2H), 1.52 – 1.39 (m, 4H), 1.29 (d, J = 7.1 Hz, 3H), 1.24 – 1.05 (m, 1H), 1.01 – 0.83 (m, 12H). ^{13}C NMR (101 MHz, MeOD) δ 210.59, 174.72, 174.68, 173.29, 60.42, 56.14, 53.04, 52.40, 50.02, 41.96, 38.19, 25.89, 25.71, 23.46, 22.39, 21.93, 17.82, 16.53, 16.05, 11.37. LC-MS (linear gradient 10 \rightarrow 90% MeCN, 0.1% TFA, 12.5 min): R_t (min): 6.07 (ESI-MS (m/z): 398.20 ($M+H^+$)). HRMS: calculated for $\text{C}_{20}\text{H}_{35}\text{N}_3\text{O}_5$ 398.26495 [$M+H^+$] $^+$; found 398.26486.

Ac-PAL-EK

This compound was obtained by the general protocol for azide coupling on a 100 μmol scale. Purification by column chromatography (0 \rightarrow 3% MeOH in DCM) provided the title compound (14.35 mg, 38%) as a white powder after lyophilisation. Complex NMR due to presence of rotamers (8:1). Peaks of major rotamer are reported. ^1H NMR (400 MHz, CDCl_3) δ 7.34 (d, J = 7.0 Hz, 1H), 6.70 (d, J = 7.0 Hz, 1H), 4.53 (ddd, J = 14.8, 10.0, 5.0 Hz, 2H), 4.35 (t, J = 7.1 Hz, 1H), 3.58 (td, J = 9.1, 8.2, 3.2 Hz, 1H), 3.50 – 3.35 (m, 1H), 3.33 (d, J = 5.0 Hz, 1H), 2.87 (d, J = 5.0 Hz, 1H), 2.36 – 2.24 (m, 1H), 2.10 (s, 4H), 2.05 – 1.74 (m, 3H), 1.62 (dd, J = 6.2, 3.7 Hz, 1H), 1.50 (d, J = 5.1 Hz, 3H), 1.31 (dd, J = 9.9, 5.6 Hz, 4H), 1.32 – 1.21 (m, 3H), 0.92 (d, J = 6.5 Hz, 6H). ^{13}C NMR (101 MHz, CDCl_3) δ 208.55, 172.25, 171.51, 171.14, 59.82, 59.23, 52.60, 50.39, 49.14, 48.48, 40.00, 27.87, 27.85, 25.32, 25.20, 23.48, 22.65, 21.41, 17.36, 16.87. LC-MS (linear gradient 10 \rightarrow 90% MeCN, 0.1% TFA, 12.5 min): R_t (min): 5.21 (ESI-MS (m/z): 382.13 ($M+H^+$)). HRMS: calculated for $\text{C}_{19}\text{H}_{31}\text{N}_3\text{O}_5$ 382.23365 [$M+H^+$] $^+$; found 382.23367.

Ac-LAL-EK

This compound was obtained by the general protocol for azide coupling on a 100 μmol scale. Purification by column chromatography (0 \rightarrow 3% MeOH in DCM) provided the title compound (15.49 mg, 81%) as a white powder after lyophilisation. ^1H NMR (400 MHz, CDCl_3) δ 7.66 (dd, J = 21.3, 8.1 Hz, 2H), 7.14 (d, J = 8.8 Hz, 1H), 4.77 (dp, J = 15.1, 8.1, 7.5 Hz, 2H), 4.69 – 4.53 (m, 1H), 3.29 (d, J = 5.0 Hz, 1H), 2.88 (d, J = 5.0 Hz, 1H), 2.02 (s, 3H), 1.69 – 1.43 (m, 8H), 1.33 (dd, J = 10.2, 4.2 Hz, 1H), 1.29 (d, J = 7.0 Hz, 3H), 0.88 (t, J = 6.4 Hz, 12H). ^{13}C NMR (101 MHz, CDCl_3) δ 208.99, 172.63, 172.44, 170.21, 59.14, 52.40, 51.39, 50.01, 48.51, 42.48, 40.00, 25.20, 24.85, 23.44, 23.14, 22.87, 22.54, 21.40, 18.54, 16.80. LC-MS (linear gradient 10 \rightarrow 90% MeCN, 0.1% TFA, 12.5 min): R_t (min): 6.08 (ESI-MS (m/z): 398.13 ($M+H^+$)). HRMS: calculated for $\text{C}_{20}\text{H}_{35}\text{N}_3\text{O}_5$ 398.26495 [$M+H^+$] $^+$; found 398.26428.

Ac-PAV-EK

This compound was obtained by the general protocol for azide coupling on a 100 μmol scale. Purification by column chromatography (0 \rightarrow 3% MeOH in DCM) provided the title compound (6.95 mg, 19%) as a white powder after lyophilisation. Complex NMR due to presence of rotamers (8:1). Peaks of major rotamer are reported. ^1H NMR (400 MHz, CDCl_3) δ 7.50 (d, J = 6.8 Hz, 1H), 6.77 (d, J = 8.4 Hz, 1H), 4.53 (dd, J = 8.0, 2.4 Hz, 1H), 4.47 (dd, J = 8.5, 5.6 Hz, 1H), 4.32 (p, J = 7.1 Hz, 1H), 3.59 (ddd, J = 11.4, 8.5, 4.4 Hz, 1H), 3.44 (td, J = 9.4, 7.1 Hz, 1H), 3.30 (d, J = 4.9 Hz, 1H), 2.86 (d, J = 5.0 Hz, 1H), 2.37 – 2.29 (m, 1H), 2.16 – 2.04 (m, 4H), 2.03 – 1.82 (m, 3H), 1.49 (s, 3H), 1.34 (d, J = 7.1 Hz, 3H), 0.96 (d, J = 6.8 Hz, 3H), 0.83 (d, J = 6.9 Hz, 3H). ^{13}C NMR (101 MHz, CDCl_3) δ 209.20, 172.33, 171.69, 171.26, 59.82, 59.52, 55.90, 52.17, 49.49, 48.52, 30.43, 27.84, 25.23, 22.69, 19.82, 17.53, 17.18, 16.54. LC-MS (linear gradient 10 \rightarrow 90% MeCN, 0.1% TFA, 12.5 min): R_t (min): 4.72 (ESI-MS (m/z): 368.13 ($M+H^+$)). HRMS: calculated for $\text{C}_{18}\text{H}_{29}\text{N}_3\text{O}_5$ 368.21800 [$M+H^+$] $^+$; found 368.21811.

Ac-LAV-EK

This compound was obtained by the general protocol for azide coupling on a 100 μmol scale. Purification by column chromatography (0 \rightarrow 3% MeOH in DCM) provided the title compound (25.68 mg, 67%) as a white powder after lyophilisation. ^1H NMR (400 MHz, CDCl_3 , MeOD) δ 4.39 (d, J = 5.5 Hz, 1H), 4.37 – 4.23 (m, 2H), 3.19 (d, J =

4.8 Hz, 1H), 2.83 (d, $J = 4.9$ Hz, 1H), 2.14 – 1.97 (m, 1H), 1.92 (s, 3H), 1.61 – 1.35 (m, 6H), 1.24 (d, $J = 7.0$ Hz, 3H), 0.95 – 0.81 (m, 9H), 0.78 (d, $J = 6.8$ Hz, 3H). ^{13}C NMR (101 MHz, CDCl_3 , MeOD) δ 208.81, 172.93, 172.62, 171.39, 59.25, 55.81, 51.74, 51.40, 48.60, 40.89, 30.03, 24.53, 22.56, 22.21, 21.46, 19.27, 17.03, 16.94, 16.08. LC-MS (linear gradient 10 \rightarrow 90% MeCN, 0.1% TFA, 12.5 min): R_t (min): 5.57 (ESI-MS (m/z): 384.13 ($\text{M}+\text{H}^+$)). HRMS: calculated for $\text{C}_{19}\text{H}_{33}\text{N}_3\text{O}_5$ 384.24930 [$\text{M}+\text{H}$] $^+$; found 384.24939.

Ac-PAA-EK

This compound was obtained by the general protocol for azide coupling on a 100 μmol scale. Purification by column chromatography (0 \rightarrow 5% MeOH in DCM) provided the title compound (10.43 mg, 31%) as a white powder after lyophilisation. Complex NMR due to presence of rotamers (9:1). Peaks of major rotamer are reported. ^1H NMR (400 MHz, CDCl_3) δ 7.33 (d, $J = 7.0$ Hz, 1H), 6.81 (d, $J = 6.6$ Hz, 1H), 4.50 (dtd, $J = 14.3, 7.8, 7.2, 2.3$ Hz, 2H), 4.43 – 4.23 (m, 1H), 3.58 (ddd, $J = 11.2, 8.1, 3.2$ Hz, 1H), 3.44 (td, $J = 9.4, 7.0$ Hz, 1H), 3.26 (d, $J = 5.0$ Hz, 1H), 2.87 (d, $J = 5.0$ Hz, 1H), 2.33 (ddd, $J = 12.3, 6.3, 3.0$ Hz, 1H), 2.10 (s, 3H), 2.11 – 1.82 (m, 3H), 1.50 (s, 3H), 1.40 – 1.22 (m, 6H). ^{13}C NMR (101 MHz, CDCl_3) δ 208.37, 171.81, 171.44, 171.15, 59.90, 59.86, 59.13, 52.63, 49.15, 49.09, 49.06, 48.50, 48.05, 47.95, 27.91, 25.20, 22.67, 17.60, 17.56, 17.12, 17.08, 16.94. LC-MS (linear gradient 10 \rightarrow 50% MeCN, 0.1% TFA, 12.5 min): R_t (min): 4.55 (ESI-MS (m/z): 340.07 ($\text{M}+\text{H}^+$)). HRMS: calculated for $\text{C}_{16}\text{H}_{25}\text{N}_3\text{O}_5$ 340.18670 [$\text{M}+\text{H}$] $^+$; found 340.18677.

Ac-LAA-EK

This compound was obtained by the general protocol for azide coupling on a 100 μmol scale. Purification by column chromatography (0 \rightarrow 5% MeOH in DCM) provided the title compound (22.46 mg, 63%) as a white powder after lyophilisation. ^1H NMR (400 MHz, MeOD) δ 4.48 – 4.26 (m, 3H), 3.25 (d, $J = 5.1$ Hz, 1H), 2.93 (d, $J = 5.1$ Hz, 1H), 1.97 (s, 3H), 1.71 – 1.59 (m, 1H), 1.58 – 1.53 (m, 2H), 1.47 (s, 3H), 1.33 (d, $J = 7.1$ Hz, 3H), 1.27 (d, $J = 7.2$ Hz, 3H), 0.94 (dd, $J = 14.3, 6.5$ Hz, 6H). ^{13}C NMR (101 MHz, MeOD) δ 209.49, 174.65, 174.50, 173.39, 60.07, 53.19, 53.16, 49.86, 49.35, 41.83, 25.90, 23.45, 22.40, 21.90, 18.07, 17.05, 16.29. LC-MS (linear gradient 10 \rightarrow 90% MeCN, 0.1% TFA, 12.5 min): R_t (min): 4.77 (ESI-MS (m/z): 356.07 ($\text{M}+\text{H}^+$)). HRMS: calculated for $\text{C}_{17}\text{H}_{29}\text{N}_3\text{O}_5$ 356.21800 [$\text{M}+\text{H}$] $^+$; found 356.21805.

Ac-PLL-EK

This compound was obtained by the general protocol for azide coupling on a 100 μmol scale. Purification by column chromatography (0 \rightarrow 2% MeOH/DCM) provided the title compound (24.4 mg, 58%) as a white powder after lyophilisation. Complex NMR due to presence of rotamers (7:1). Peaks of major rotamer are reported. ^1H NMR (400 MHz, CDCl_3) δ 7.24 (d, $J = 7.6$ Hz, 1H), 6.66 (d, $J = 7.9$ Hz, 1H), 4.54 (ddt, $J = 7.8, 5.4, 3.3$ Hz, 2H), 4.36 – 4.20 (m, 1H), 3.55 (ddd, $J = 11.3, 8.3, 4.1$ Hz, 1H), 3.43 (td, $J = 9.4, 7.1$ Hz, 1H), 3.31 (d, $J = 5.0$ Hz, 1H), 2.85 (d, $J = 5.0$ Hz, 1H), 2.31 (ddd, $J = 12.2, 6.3, 3.1$ Hz, 1H), 2.08 (s, 3H), 2.06 – 1.83 (m, 3H), 1.71 – 1.44 (m, 8H), 1.29 (ddd, $J = 14.0, 10.4, 4.4$ Hz, 1H), 0.94 – 0.82 (m, 12H). ^{13}C NMR (101 MHz, CDCl_3) δ 208.53, 172.09, 171.60, 171.10, 59.78, 59.19, 52.56, 52.19, 50.34, 48.41, 40.33, 40.05, 27.70, 25.29, 25.19, 25.00, 23.46, 23.01, 22.51, 21.99, 21.42, 16.86. LC-MS (linear gradient 10 \rightarrow 90% MeCN, 0.1% TFA, 12.5 min): R_t (min): 6.30 (ESI-MS (m/z): 424.13 ($\text{M}+\text{H}^+$)). HRMS: calculated for $\text{C}_{22}\text{H}_{37}\text{N}_3\text{O}_5$ 424.28060 [$\text{M}+\text{H}$] $^+$; found 424.28040.

Ac-LLL-EK

This compound was obtained by the general protocol for azide coupling on a 100 μmol scale. Purification by column chromatography (0 \rightarrow 2% MeOH/DCM) provided the title compound (28.55 mg, 65%) as a white powder after lyophilisation. ^1H NMR (400 MHz, CDCl_3 , MeOD) δ 4.49 (dd, $J = 10.6, 3.0$ Hz, 1H), 4.35 (dt, $J = 8.7, 6.1$ Hz, 2H), 3.25 (d, $J = 5.0$ Hz, 1H), 2.86 (d, $J = 5.0$ Hz, 1H), 1.93 (s, 3H), 1.68 – 1.35 (m, 11H), 1.34 – 1.14 (m, 1H), 0.97 – 0.76 (m, 18H). ^{13}C NMR (101 MHz, MeOD) δ 208.75, 173.09, 172.53, 171.43, 59.25, 52.52, 51.73, 51.53, 50.51, 41.10, 40.54, 39.62, 25.24, 24.84, 24.70, 23.33, 22.82, 22.76, 22.52, 21.90, 21.12, 16.77. LC-MS (linear gradient

10 → 90% MeCN, 0.1% TFA, 12.5 min): R_t (min): 7.05 (ESI-MS (m/z): 440.20 ($M+H^+$)). HRMS: calculated for $C_{23}H_{41}N_3O_5$ 440.31190 [$M+H$] $^+$; found 440.31171.

Boc-APLL-EK

This compound was obtained by the general protocol for azide coupling on a 100 μ mol scale. Purification by column chromatography (0→2% MeOH/DCM) provided the title compound (yield n.d., all material used in the next step). Complex NMR due to presence of rotamers (3.5:1). 1H NMR (400 MHz, $CDCl_3$) δ 7.62 (d, J = 6.9 Hz, 0.3H), 7.14 (d, J = 7.7 Hz, 0.7H), 6.88 (d, J = 9.2 Hz, 0.3H), 6.59 (d, J = 7.8 Hz, 0.7H), 5.31 (d, J = 7.6 Hz, 0.7H), 5.22 (d, J = 7.4 Hz, 0.3H), 4.70 – 4.09 (m, 4H), 3.70 – 3.60 (m, 1H), 3.57 – 3.46 (m, 1H), 3.30 (d, J = 5.0 Hz, 0.8H), 3.24 (d, J = 4.8 Hz, 0.2H), 2.85 (d, J = 5.1 Hz, 0.8H), 2.83 (d, J = 4.9 Hz, 0.2H), 2.55 (dd, J = 12.3, 6.3 Hz, 0.2), 2.34 – 1.83 (m, 4.8H), 1.74 – 1.44 (m, 8H), 1.41 (s, 8H), 1.37 – 1.22 (m, 4H), 0.96 – 0.79 (m, 12H). ^{13}C NMR (101 MHz, $CDCl_3$) δ 209.43, 208.51, 173.36, 172.64, 172.05, 171.12, 155.31, 80.99, 79.97, 77.48, 77.16, 76.84, 60.87, 60.06, 59.19, 54.87, 52.55, 52.44, 51.87, 50.32, 49.41, 49.24, 48.22, 47.39, 46.76, 40.81, 40.55, 40.10, 39.11, 31.59, 28.45, 27.22, 25.36, 25.26, 24.76, 23.45, 23.35, 23.14, 22.96, 22.13, 21.79, 21.69, 21.41, 18.46, 16.84, 16.71, 16.54. LC-MS (linear gradient 10 → 90% MeCN, 0.1% TFA, 12.5 min): R_t (min): 7.65 (ESI-MS (m/z): 553.13 ($M+H^+$)). HRMS: calculated for $C_{28}H_{48}N_4O_7$ 553.35958 [$M+H$] $^+$; found 553.35925.

TFA-H-APLL-EK

Boc-AlaProLeuLeu-EK was treated with 1:1 TFA/DCM. After stirring for 30 min the reaction mixture was concentrated and co-evaporated with toluene (2x). HPLC-purification (C_{18} 15-50% MeCN, 0.1 % TFA, 10 min gradient) provided the title compound (6.90 mg, 12%) as a white powder after lyophilisation. Complex NMR due to presence of rotamers (7:1). Peaks of major rotamer are reported. 1H NMR (600 MHz, MeOD) δ 4.53 (dd, J = 10.9, 2.9 Hz, 1H), 4.50 (dd, J = 8.6, 4.9 Hz, 1H), 4.37 (dd, J = 9.4, 5.8 Hz, 1H), 4.22 (q, J = 6.9 Hz, 1H), 3.71 – 3.55 (m, 2H), 3.23 (d, J = 5.1 Hz, 1H), 2.94 (d, J = 5.0 Hz, 1H), 2.28 – 2.17 (m, 1H), 2.14 – 2.03 (m, 1H), 2.03 – 1.93 (m, 2H), 1.77 – 1.66 (m, 2H), 1.59 – 1.52 (m, 2H), 1.50 (d, J = 7.0 Hz, 3H), 1.47 (s, 3H), 1.41 – 1.31 (m, 2H), 1.02 – 0.86 (m, 12H). ^{13}C NMR (151 MHz, MeOD) δ 209.58, 174.77, 173.72, 169.51, 61.27, 61.15, 60.11, 53.34, 53.03, 53.01, 52.00, 51.88, 49.43, 49.28, 49.14, 49.00, 48.86, 48.72, 48.57, 42.01, 40.08, 30.46, 26.34, 26.32, 26.03, 25.73, 23.74, 23.45, 22.09, 21.43, 17.04, 16.13. LC-MS (linear gradient 10 → 90% MeCN, 0.1% TFA, 12.5 min): R_t (min): 5.29 (ESI-MS (m/z): 453.20 ($M+H^+$)). HRMS: calculated for $C_{23}H_{40}N_4O_5$ 453.30715 [$M+H$] $^+$; found 453.30704.

Ac-APLL-EK

This compound was obtained by the general protocol for azide coupling on a 100 μ mol scale. Purification by column chromatography (0→2% MeOH/DCM) provided the title compound (32.01 mg, 65%) as a white powder after lyophilisation. Complex NMR due to presence of rotamers (3:1). Peaks of major rotamer are reported for 1H , all peaks are reported for ^{13}C . 1H NMR (400 MHz, $CDCl_3$) δ 7.19 – 7.08 (m, 1H), 6.62 (s, 1H), 6.54 (s, 1H), 4.74 (p, J = 6.9 Hz, 1H), 4.59 – 4.51 (m, 2H), 4.42 – 4.31 (m, 1H), 3.68 (q, J = 8.7, 8.0 Hz, 1H), 3.55 (td, J = 10.1, 9.1, 4.1 Hz, 1H), 3.30 (d, J = 5.0 Hz, 1H), 2.86 (d, J = 5.0 Hz, 1H), 2.25 (d, J = 8.4 Hz, 1H), 2.19 – 2.00 (m, 3H), 1.98 (s, 3H), 1.91 (ddt, J = 12.4, 9.6, 5.9 Hz, 1H), 1.72 – 1.50 (m, 4H), 1.49 (d, J = 4.7 Hz, 3H), 1.43 (s, 1H), 1.34 – 1.29 (m, 2H), 1.29 – 1.21 (m, 1H), 0.96 – 0.81 (m, 12H). ^{13}C NMR (101 MHz, $CDCl_3$) δ 209.55, 208.67, 172.98, 172.50, 172.10, 172.01, 171.03, 170.75, 169.67, 60.99, 59.96, 59.19, 54.68, 52.55, 52.42, 51.83, 50.34, 48.95, 48.86, 47.48, 46.91, 46.79, 40.81, 40.38, 40.23, 40.13, 31.82, 27.39, 25.39, 25.27, 25.24, 25.15, 24.76, 23.46, 23.21, 23.08, 22.85, 22.13, 21.99, 21.83, 21.42, 18.33, 16.83, 16.64, 16.30. LC-MS (linear gradient 10 → 90% MeCN, 0.1% TFA, 12.5 min): R_t (min): 6.01 (ESI-MS (m/z): 495.13 ($M+H^+$)). HRMS: calculated for $C_{25}H_{42}N_4O_6$ 495.31771 [$M+H$] $^+$; found 495.31741.

N₃-GAPAL-EK

This compound was obtained by the general protocol for azide coupling on a 240 μ mol scale. Purification by column chromatography (0→4% MeOH in DCM) provided the title compound (39.0 mg, 76%) as a white powder

after lyophilisation. Complex NMR due to presence of rotamers (4:1). Peaks of major rotamer are reported. ^1H NMR (400 MHz, CDCl_3) δ 7.22 (d, $J = 7.5$ Hz, 1H), 7.12 (d, $J = 7.4$ Hz, 1H), 6.67 (d, $J = 7.8$ Hz, 1H), 4.79 – 4.70 (m, 1H), 4.60 – 4.49 (m, 2H), 4.46 – 4.38 (m, 1H), 3.95 (d, $J = 1.9$ Hz, 2H), 3.73 – 3.52 (m, 2H), 3.29 (d, $J = 5.0$ Hz, 1H), 2.88 (d, $J = 5.0$ Hz, 1H), 2.26 – 1.91 (m, 6H), 1.61 (dd, $J = 6.5, 2.4$ Hz, 1H), 1.49 (s, 3H), 1.38 (d, $J = 6.9$ Hz, 3H), 1.28 (d, $J = 7.0$ Hz, 3H), 0.92 (dd, $J = 6.5, 3.1$ Hz, 6H). ^{13}C NMR (101 MHz, CDCl_3) δ 208.74, 172.15, 172.03, 170.99, 166.31, 60.09, 59.20, 52.57, 52.52, 50.39, 48.83, 47.44, 46.82, 40.08, 27.95, 25.28, 25.20, 23.46, 21.35, 18.25, 18.01, 16.83. LC-MS (linear gradient 10 \rightarrow 90% MeCN, 0.1% TFA, 12.5 min): Rt (min): 5.57 (ESI-18), MS (m/z): 494.13 $[\text{M}+\text{H}]^+$. HRMS: calculated for $\text{C}_{22}\text{H}_{35}\text{N}_7\text{O}_6$ 494.27216 $[\text{M}+\text{H}]^+$; found 494.27191.

Synthesis of warheads

Standard procedures amino acid epoxyketone synthesis

Boc-AA-C(CH₃)=CH₂

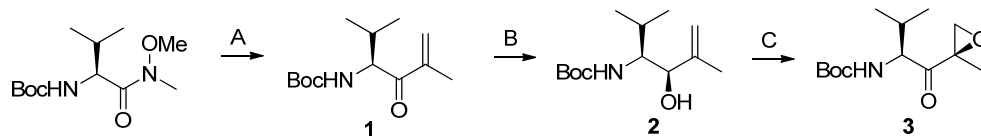
To a solution of 2-bromopropene (3 equiv.) in Et_2O at -78°C is added $t\text{BuLi}$ (4.5 equiv, from 1.7 M in pent) in 10 in. After stirring for 15 min. at -78°C , the Weinreb amide (1 equiv.) in Et_2O is added slowly in 10 min. The reaction mixture is stirred for 2-4 h, while warming up to max. -40°C . After TLC analysis revealed completion of the reaction, the reaction is quenched by the addition of sat. NH_4Cl and warmed to RT. The mixture is transferred to a separatory funnel and the water layer is extracted with EtOAc (3X). The combined organic layers are washed with brine, dried over Na_2SO_4 , filtered and concentrated. The crude product is purified by column chromatography (EtOAc /pent mixtures).

Boc-AA-OH-C(CH₃)=CH₂

To a solution of alkene **A** (1 equiv.) in MeOH is added $\text{CeCl}_3 \cdot 7\text{H}_2\text{O}$ (1.6 equiv.) and the mixture is stirred at RT. After the solution became clear, the mixture is cooled to 0°C and NaBH_4 (1.3 equiv.) is added in portion in 10 min. After TLC analysis showed completion of the reaction (about 30 min), the reaction is quenched by the addition of AcOH. The mixture is stirred for 15 min. followed by the addition of toluene and removal of the solvent. The residue is redissolved in a H_2O / EtOAc mixture, which is then transferred to a separatory funnel. The layers were separated and the aqueous layer was extracted with EtOAc (2X). The combined organic layers are washed with brine, dried over Na_2SO_4 , filtered and concentrated. The crude product was purified (if necessary) by column chromatography (EtOAc /pent mixtures).

Boc-AA-EK

To a solution of alcohol **B** in DCM at 0°C is added $\text{VO}(\text{acac})_2$ (0.1 equiv.) followed by the addition of $t\text{BuOOH}$ (5.5 M in decane, 3 equiv.). The reaction mixture is stirred at 0°C for 2-3 h. after which TLC analysis showed completion of the reaction. The reaction mixture is concentrated, redissolved in EtOAc and washed with 0.5 sat. NaHCO_3 (2x), H_2O and brine. The organic layer is dried over Na_2SO_4 , filtered and concentrated. The crude product is added as a solution in DCM to a solution of Dess-Martin-Periodane (1.5-3 equiv.) in DCM at 0°C . After TLC analysis revealed completion of the reaction, the reaction was quenched by the addition of sat. NaHCO_3 . The mixture was transferred to a separatory funnel and the layers were separated. The aqueous layer was extracted with DCM (1x) and the combined organics were washed with sat. NaHCO_3 (1x) and brine and dried over Na_2SO_4 , filtered and concentrated. The crude product was purified by column chromatography (EtOAc /pent mixtures).

Boc-Val-EK**(S)-tert-butyl (2,5-dimethyl-4-oxohex-5-en-3-yl)carbamate (1)**

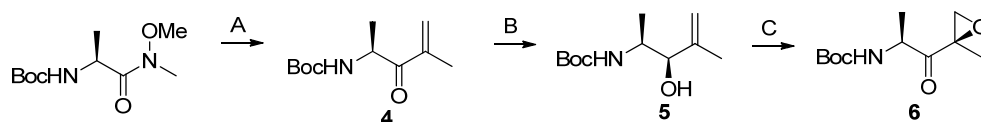
This compound was synthesized according to the general procedure **A** described above on a 10 mmol scale and was isolated after column chromatography (10% EtOAc:pent) (808 mg, 3.33 mmol, 33%). ^1H NMR (400 MHz, CDCl_3) δ 6.04 (s, 1H), 5.96–5.78 (m, 1H), 5.25 (d, J = 8.6 Hz, 1H), 4.90 (dd, J = 9.1, 4.7 Hz, 1H), 2.12–1.94 (m, 1H), 1.87 (s, 3H), 1.40 (s, 9H), 0.94 (d, J = 6.8 Hz, 3H), 0.74 (d, J = 6.8 Hz, 3H). ^{13}C NMR (101 MHz, CDCl_3) δ 201.41, 155.88, 143.05, 79.49, 58.63, 32.07, 28.37, 19.92, 17.76, 16.99.

tert-butyl ((3S,4R)-4-hydroxy-2,5-dimethylhex-5-en-3-yl)carbamate (2)

This compound was synthesized according to the general procedure **B** described above on a 3.33 mmol scale. The crude compound (quantitative yield) was not purified by column chromatography but used crude in procedure **C**. ^1H NMR (400 MHz, CDCl_3) δ 4.96 (s, 1H), 4.91 (s, 1H), 4.49 (d, J = 9.7 Hz, 1H), 4.04 (d, J = 6.7 Hz, 1H), 3.74–3.57 (m, 1H), 2.30–2.10 (m, 1H), 2.10–1.90 (m, 1H), 1.76 (s, 3H), 1.41 (s, 9H), 0.94 (d, J = 6.9 Hz, 3H), 0.86 (d, J = 6.8 Hz, 3H). ^{13}C NMR (101 MHz, CDCl_3) δ 156.37, 145.71, 112.99, 79.22, 77.20, 56.84, 28.39, 27.60, 20.91, 18.17, 16.73.

tert-butyl ((S)-3-methyl-1-((R)-2-methyloxiran-2-yl)-1-oxobutan-2-yl)carbamate (3)

This compound was synthesized according to the general procedure **D** described above on a 4.44 mmol scale and was isolated after column chromatography (5→20% EtOAc:pent) (485 mg, 1.89 mmol, 57%). ^1H NMR (400 MHz, CDCl_3) δ 4.96 (d, J = 9.2 Hz, 1H), 4.17 (dd, J = 9.4, 5.0 Hz, 1H), 3.18 (d, J = 4.9 Hz, 1H), 2.81 (d, J = 5.0 Hz, 1H), 2.01 (dq, J = 13.4, 6.8 Hz, 1H), 1.44 (s, 3H), 1.34 (s, 9H), 0.93 (d, J = 6.8 Hz, 3H), 0.76 (d, J = 6.9 Hz, 3H). ^{13}C NMR (101 MHz, CDCl_3) δ 209.73, 155.75, 79.64, 59.21, 56.99, 51.86, 30.15, 28.32, 19.78, 17.05, 16.47. $[\alpha]_D^{20}$ = 150.6 (C=1, CHCl_3)

Boc-Ala-EK**(S)-tert-butyl (4-methyl-3-oxopent-4-en-2-yl)carbamate (4)**

This compound was synthesized according to the general procedure **A** described above on a 4 mmol scale. The crude product was used in the next step (791 mg, 3.71 mmol, 93%).

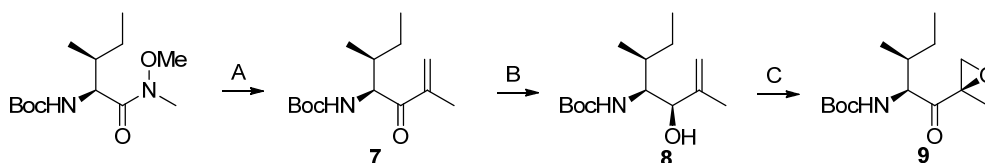
^1H NMR (400 MHz, CDCl_3) δ 6.01 (s, 1H), 5.92–5.78 (m, 1H), 5.45–5.31 (m, 1H), 4.99 (p, J = 7.1 Hz, 1H), 1.87 (s, 3H), 1.40 (s, 9H), 1.27 (d, J = 7.1 Hz, 3H). ^{13}C NMR (101 MHz, CDCl_3) δ 200.89, 155.00, 141.73, 126.08, 79.47, 50.04, 28.27, 20.04, 17.74.

tert-butyl ((2S,3R)-3-hydroxy-4-methylpent-4-en-2-yl)carbamate (5)

This compound was synthesized according to the general procedure **B** described above on a 3.71 mmol scale. The crude compound (quantitative yield) was not purified by column chromatography but used crude in procedure **C**. Equilibrating rotamers in NMR, peaks of major rotamer are reported. ^1H NMR (400 MHz, CDCl_3) δ 5.08–4.81 (m, 3H), 4.10 (s, 1H), 3.84 (d, J = 5.3 Hz, 1H), 1.72 (s, 3H), 1.42 (s, 9H), 1.00 (d, J = 6.8 Hz, 3H). ^{13}C NMR (101 MHz, CDCl_3) δ 156.65, 144.89, 111.17, 48.39, 28.39, 19.35, 13.80.

tert-butyl ((S)-1-((R)-2-methyloxiran-2-yl)-1-oxopropan-2-yl)carbamate (6)

This compound was synthesized according to the general procedure **D** described above on a 3.71 mmol scale and was isolated after column chromatography (5→10% EtOAc:pent) (180 mg, 0.789 mmol, 21%). ¹H NMR (400 MHz, CDCl₃) δ 5.04 (d, *J* = 6.6 Hz, 1H), 4.27 (p, *J* = 7.2 Hz, 1H), 3.20 (d, *J* = 4.7 Hz, 1H), 2.86 (d, *J* = 5.0 Hz, 1H), 1.49 (s, 3H), 1.37 (s, 9H), 1.22 (d, *J* = 7.1 Hz, 3H). ¹³C NMR (101 MHz, CDCl₃) δ 209.20, 155.08, 79.65, 58.84, 52.27, 48.74, 28.24, 17.32, 16.73. [α]_D²⁰ = +111.0 (C=1, CHCl₃).

Boc-Ile-EK**tert-butyl ((4S,5S)-2,5-dimethyl-3-oxohept-1-en-4-yl)carbamate (7)**

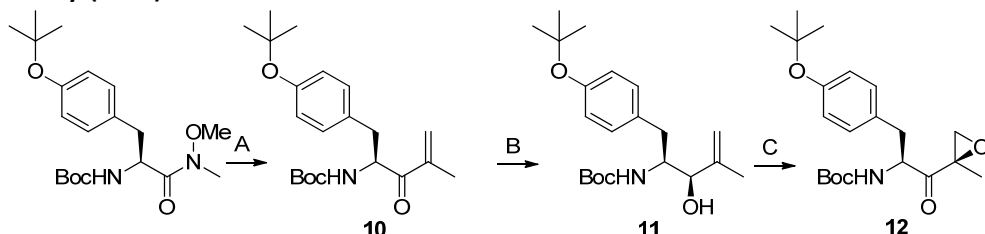
This compound was synthesized according to the general procedure **A** described above on a 9.7 mmol scale and was isolated after column chromatography (0→5% EtOAc:pent) (2.14 g, 8.4 mmol, 84%). ¹H NMR (400 MHz, CDCl₃) δ 6.01 (s, 1H), 5.81 (s, 1H), 5.20 (d, *J* = 8.8 Hz, 1H), 4.87 (dd, *J* = 9.0, 5.2 Hz, 1H), 1.83 (s, 3H), 1.76 – 1.62 (m, 1H), 1.36 (s, 9H), 1.29 – 1.18 (m, 1H), 1.05 – 0.90 (m, 1H), 0.86 (d, *J* = 6.8 Hz, 3H), 0.78 (t, *J* = 7.4 Hz, 3H). ¹³C NMR (101 MHz, CDCl₃) δ 201.76, 155.75, 143.29, 79.45, 58.19, 38.74, 28.34, 24.08, 17.75, 16.14, 11.53.

tert-butyl ((3R,4S,5S)-3-hydroxy-2,5-dimethylhept-1-en-4-yl)carbamate (8)

This compound was synthesized according to the general procedure **B** described above on a 3.71 mmol scale. The crude compound (quantitative yield) was not purified by column chromatography but used crude in procedure **C**. ¹H NMR (300 MHz, CDCl₃) δ 4.91 (d, *J* = 13.3 Hz, 2H), 4.47 (d, *J* = 9.8 Hz, 1H), 4.08 (dd, *J* = 6.8, 2.3 Hz, 1H), 3.66 (dt, *J* = 10.7, 6.3 Hz, 1H), 2.45 (s, 1H), 1.74 (s, 4H), 1.66 – 1.48 (m, 1H), 1.39 (s, 9H), 1.06 – 0.72 (m, 6H). ¹³C NMR (75 MHz, CDCl₃) δ 156.45, 145.78, 79.27, 76.95, 57.26, 34.70, 28.43, 23.65, 18.27, 16.93, 11.82.

tert-butyl ((2S,3S)-3-methyl-1-((R)-2-methyloxiran-2-yl)-1-oxopentan-2-yl)carbamate (9)

This compound was synthesized according to the general procedure **D** described above on a 8.4 mmol scale and was isolated after column chromatography (0→10% EtOAc:pent) (1.20 g, 4.4 mmol, 52%). ¹H NMR (300 MHz, CDCl₃) δ 4.92 (d, *J* = 9.0 Hz, 1H), 4.23 (dd, *J* = 9.4, 5.7 Hz, 1H), 3.24 (d, *J* = 4.8 Hz, 1H), 2.84 (d, *J* = 5.0 Hz, 1H), 1.85 – 1.63 (m, 1H), 1.48 (s, 3H), 1.38 (s, 9H), 1.12 – 0.74 (m, 2H), 0.94 (d, *J* = 6.8 Hz, 3H), 0.85 (t, *J* = 7.3 Hz, 3H). ¹³C NMR (75 MHz, CDCl₃) δ 210.29, 155.69, 79.72, 59.36, 56.41, 51.81, 37.21, 28.36, 24.17, 16.50, 16.01, 11.40. [α]_D²⁰ = 113.8 (C=1, CHCl₃)

Boc-Tyr(OtBu)-EK**(S)-tert-butyl (1-(4-(tert-butoxy)phenyl)-4-methyl-3-oxopent-4-en-2-yl)carbamate compound (10)**

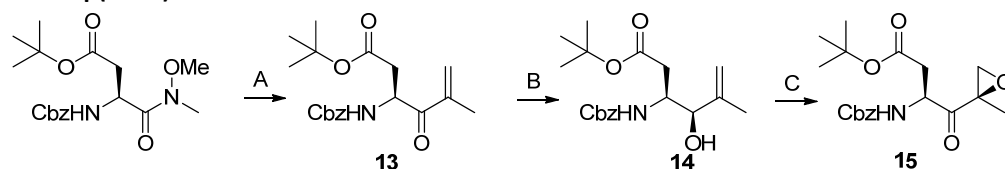
This compound was synthesized according to the general procedure **A** described above on a 10 mmol scale and was isolated after column chromatography (5→10% EtOAc:pent) (2.86 g, 7.9 mmol, 79%). ¹H NMR (400 MHz, CDCl₃) δ 6.96 (d, *J* = 8.3 Hz, 2H), 6.86 (d, *J* = 8.4 Hz, 2H), 5.93 (s, 1H), 5.78 (d, *J* = 1.4 Hz, 1H), 5.24 (dt, *J* = 20.8, 7.8 Hz, 2H), 2.94 (ddd, *J* = 46.6, 13.7, 6.2 Hz, 2H), 1.81 (s, 3H), 1.40 (s, 9H), 1.30 (s, 9H). ¹³C NMR (101 MHz, CDCl₃) δ 200.63, 155.15, 154.30, 142.72, 131.26, 129.91, 126.71, 124.28, 79.77, 78.46, 55.10, 39.61, 28.93, 28.46, 17.77.

***tert*-butyl ((2*S*,3*R*)-1-(4-(*tert*-butoxy)phenyl)-3-hydroxy-4-methylpent-4-en-2-yl)carbamate (11)**

This compound was synthesized according to the general procedure **B** described above on a 7.9 mmol scale and was isolated after column chromatography (10→20% EtOAc:pent) (1.90 g, 5.2 mmol, 66%). The product is formed as 5:1 mixture of diastereomers, but was isolated as 95:5 mixture after column chromatography. ¹H NMR (400 MHz, CDCl₃) δ 7.05 (d, *J* = 8.3 Hz, 2H), 6.87 (d, *J* = 8.3 Hz, 2H), 5.04 (s, 1H), 4.93 (s, 1H), 4.79 (d, *J* = 9.0 Hz, 1H), 4.14 (s, 1H), 3.95 (s, 1H), 3.04 – 2.73 (m, 2H), 2.70 – 2.53 (m, 1H), 1.76 (s, 3H), 1.31 (s, 9H), 1.29 (s, 9H).

***tert*-butyl ((*S*)-3-(4-(*tert*-butoxy)phenyl)-1-((*R*)-2-methyloxiran-2-yl)-1-oxopropan-2-yl)carbamate (12)**

This compound was synthesized according to the general procedure **D** described above on a 5.2 mmol scale and was isolated after column chromatography (5→10% EtOAc:pent) (0.54 g, 1.43 mmol, 27%). ¹H NMR (400 MHz, CDCl₃) δ 7.04 (d, *J* = 8.2 Hz, 2H), 6.90 (d, *J* = 8.4 Hz, 2H), 4.97 (d, *J* = 8.2 Hz, 1H), 4.55 (q, *J* = 8.0 Hz, 1H), 3.26 (d, *J* = 4.8 Hz, 1H), 3.03 (dd, *J* = 13.9, 5.0 Hz, 1H), 2.87 (d, *J* = 4.9 Hz, 1H), 2.67 (dd, *J* = 13.9, 8.0 Hz, 1H), 1.45 (s, 3H), 1.35 (s, 9H), 1.31 (s, 9H). ¹³C NMR (101 MHz, CDCl₃) δ 208.66, 155.24, 154.37, 130.76, 129.86, 124.22, 79.86, 78.45, 59.17, 53.70, 52.37, 37.05, 28.88, 28.31, 16.60. $[\alpha]_D^{20} = 108.2$ (C=1, CHCl₃)

Cbz-Asp(OtBu)-EK**(*S*)-*tert*-butyl 3-(((benzyloxy)carbonyl)amino)-5-methyl-4-oxohex-5-enoate (13)**

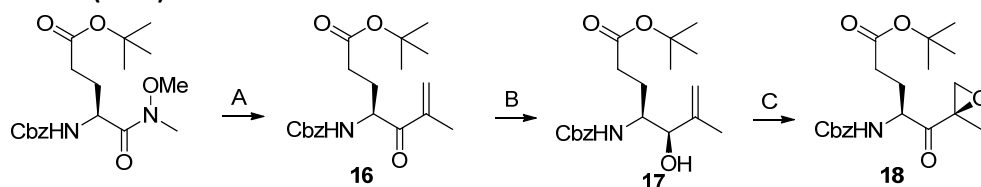
This compound was synthesized according to the general procedure **A** described above on a 8.8 mmol scale and was isolated after column chromatography (5→10% EtOAc:pent) (2.27 g, 5.6 mmol, 64%). ¹H NMR (400 MHz, CDCl₃) δ 7.39 – 7.28 (m, 5H), 6.07 (s, 1H), 5.87 (s, 1H), 5.81 (s, 1H), 5.33 – 5.21 (m, 1H), 5.09 (s, 2H), 2.78 (dd, *J* = 15.7, 5.6 Hz, 1H), 2.59 (dd, *J* = 15.7, 5.7 Hz, 1H), 1.90 (s, 3H), 1.39 (d, *J* = 1.9 Hz, 9H). ¹³C NMR (101 MHz, CDCl₃) δ 198.46, 169.34, 155.46, 141.81, 136.11, 128.38, 128.03, 127.92, 125.97, 81.42, 66.87, 51.47, 38.78, 27.83, 17.86.

(3*S*,4*R*)-*tert*-butyl 3-(((benzyloxy)carbonyl)amino)-4-hydroxy-5-methylhex-5-enoate compound (14)

This compound was synthesized according to the general procedure **B** described above on a 6.5 mmol scale and was isolated after column chromatography (10→30% EtOAc:pent) (quantitative yield). Complex NMR due to presence of rotamers or diastereomers (2:1). ¹H NMR (400 MHz, CDCl₃) δ 7.33 (q, *J* = 5.8, 5.1 Hz, 5H), 5.62 (d, *J* = 8.6 Hz, 0.65H), 5.43 (d, *J* = 8.3 Hz, 0.35H), 5.18 – 5.01 (m, 3H), 4.93 (d, *J* = 15.1 Hz, 1H), 4.20 (s, 0.7H), 4.11 (m, 1.3 H), 3.00 (s, 0.65H), 2.84 (s, 0.35H), 2.67 – 2.35 (m, 2H), 1.76 (s, 3H), 1.42 (s, 3H), 1.40 (s, 6H). ¹³C NMR (101 MHz, CDCl₃) δ 171.97, 156.01, 144.46, 128.55, 128.52, 128.15, 128.12, 128.05, 112.44, 81.32, 76.63, 76.04, 66.79, 50.34, 50.27, 38.28, 34.96, 28.07, 28.01, 19.03.

(*S*)-*tert*-butyl 3-(((benzyloxy)carbonyl)amino)-4-((*R*)-2-methyloxiran-2-yl)-4-oxobutanoate (15)

This compound was synthesized according to the general procedure **D** described above on a 6.5 mmol scale and was isolated after column chromatography (5→10% EtOAc:pent) (0.859 g, 1.43 mmol, 36%) as a single diastereomer. ¹H NMR (400 MHz, CDCl₃) δ 7.45 – 7.24 (m, 5H), 5.77 (d, *J* = 7.8 Hz, 1H), 5.24 – 4.89 (m, 2H), 4.53 (dt, *J* = 7.9, 5.4 Hz, 1H), 3.13 (d, *J* = 4.7 Hz, 1H), 2.88 (d, *J* = 4.7 Hz, 1H), 2.83 – 2.64 (m, 2H), 1.54 (s, 3H), 1.41 (s, 9H). ¹³C NMR (101 MHz, CDCl₃) δ 205.98, 169.32, 155.80, 136.21, 128.57, 128.22, 128.07, 81.95, 67.01, 59.40, 52.49, 51.27, 37.46, 28.03, 17.03. $[\alpha]_D^{20} = 91.6$ (C=1, CHCl₃)

Cbz-Glu(OtBu)-EK**(S)-tert-butyl 4-(((benzyloxy)carbonyl)amino)-6-methyl-5-oxohept-6-enoate (16)**

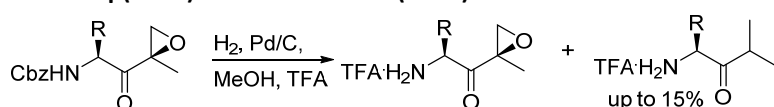
This compound was synthesized according to the general procedure **A** described above on a 10 mmol scale and was isolated after column chromatography (7.5% EtOAc:pent) (1.01 g, 2.8 mmol, 28% (conversion incomplete, but reaction was quenched due to appearance of by-products). ^1H NMR (400 MHz, CDCl_3) δ 7.37 – 7.17 (m, 5H), 6.19 (s, 1H), 5.92 (s, 1H), 5.74 (d, J = 8.2 Hz, 1H), 5.23 – 4.97 (m, 3H), 2.39 – 2.05 (m, 3H), 1.86 (s, 3H), 1.72 – 1.60 (m, 1H), 1.41 (s, 9H). ^{13}C NMR (101 MHz, CDCl_3) δ 199.96, 171.96, 156.00, 141.77, 136.31, 128.44, 128.06, 128.01, 127.21, 80.57, 66.80, 53.77, 30.81, 28.95, 28.02, 17.66.

(4S,5R)-tert-butyl 4-(((benzyloxy)carbonyl)amino)-5-hydroxy-6-methylhept-6-enoate (17)

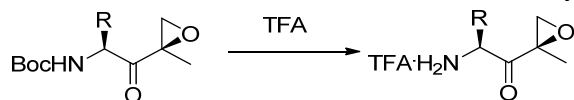
This compound was synthesized according to the general procedure **B** described above on a 2.8 mmol scale and was isolated after column chromatography (10→30% EtOAc:pent) (quantitative yield). Complex NMR due to presence of rotamers or diastereomers (8:1). ^1H NMR (400 MHz, CDCl_3) δ 7.39 – 7.28 (m, 5H), 5.24 (d, J = 9.2 Hz, 1H), 5.14 – 4.88 (m, 4H), 4.18 – 4.04 (m, 1H), 3.90 – 3.71 (m, 1H), 2.48 (bs, 1H), 2.28 (t, J = 7.4 Hz, 2H), 1.89 – 1.70 (m, 4H), 1.69 – 1.54 (m, 1H), 1.43 (s, 1H), 1.41 (s, 8H). ^{13}C NMR (101 MHz, CDCl_3) δ 173.26, 156.55, 144.62, 136.55, 128.60, 128.54, 128.20, 128.16, 111.86, 80.58, 77.27, 66.83, 52.90, 32.15, 28.15, 23.22, 19.35.

(S)-tert-butyl 4-(((benzyloxy)carbonyl)amino)-5-((R)-2-methyloxiran-2-yl)-5-oxopentanoate (18)

This compound was synthesized according to the general procedure **D** described above on a 2.8 mmol scale and was isolated after column chromatography (5→10% EtOAc:pent) (0.480 g, 1.27 mmol, 45%) as a single diastereomer. ^1H NMR (400 MHz, CDCl_3) δ 7.28 (dd, J = 8.9, 2.8 Hz, 5H), 5.63 (d, J = 8.4 Hz, 1H), 5.02 (q, J = 12.3 Hz, 2H), 4.32 (td, J = 8.7, 4.1 Hz, 1H), 3.21 (d, J = 4.9 Hz, 1H), 2.85 (d, J = 4.9 Hz, 1H), 2.29 (t, J = 7.3 Hz, 2H), 2.04 (dtd, J = 14.4, 7.3, 4.3 Hz, 1H), 1.84 – 1.58 (m, 1H), 1.49 (s, 3H), 1.40 (s, 9H). ^{13}C NMR (101 MHz, CDCl_3) δ 208.24, 171.99, 156.07, 136.13, 128.46, 128.10, 127.95, 80.75, 66.83, 59.07, 52.81, 52.15, 31.49, 28.00, 26.31, 16.48. $[\alpha]_D^{20}$ = +82.8 (C=1, CHCl_3)

TFA.H-Asp(OtBu)-EK and TFA.H-Glu(OtBu)-EK

Cbz protected epoxyketones are dissolved in MeOH (20 mg/mL), flushed with argon, followed by the addition of 1.2 equiv. TFA and 10% Pd/C (10 mg/100 mg epoxyketone). The reaction mixture is stirred under a H_2 atmosphere for 15-60 min and is filtered and concentrated upon completion. The product was directly used in the azide couplings to the corresponding hydrazides. Depending on the hydrogenation time, up to 15% reduced epoxide was formed, as was observed by NMR after azide coupling to the corresponding hydrazides. This impurity was removed by HPLC purification of the final compounds.

TFA·H-Leu-EK, TFA·H-Val-EK, TFA·H-Ala-EK, TFA·H-Tyr-EK, TFA·H-Ile-EK

Boc-protected epoxyketones were deprotected by treatment with TFA (neat) for 30 min, followed by concentrations and coevaporation with toluene. The product was directly used in the azide couplings to the corresponding hydrazides.

Synthesis of peptide hydrazides**Boc-Leu-Ala-OMe (19)**

To a solution of HCl-H-Ala-OMe (973 mg, 7 mmol, 1 equiv.) in DCM (70 mL) were added HCTU (3.19 g, 7.7 mmol, 1 equiv.), Boc-Leu-OH (1.78 g, 7.7 mmol, 1.1 equiv.) and DiPEA (4.3 mL, 24.5 mmol, 3.5 equiv.). After stirring overnight, the reaction mixture was concentrated, dissolved in EtOAc and washed with 1N HCl (2x), sat. NaHCO₃ (2x) and brine (1x). The organic layer was dried over NaSO₄, filtered and concentrated. Purification by column chromatography (10%→40% EtOAc/pent) provided the product (2.0 g, 6.3 mmol 90%). ¹H NMR (300 MHz, CDCl₃) δ 7.36 – 7.19 (m, 1H), 5.38 (d, *J* = 8.0 Hz, 1H), 4.41 (q, *J* = 6.9 Hz, 1H), 4.29 – 3.99 (m, 1H), 3.62 (s, 3H), 1.71 – 1.38 (m, 3H), 1.33 (s, 9H), 1.26 (d, *J* = 7.2 Hz, 3H), 0.96 – 0.68 (m, 6H). ¹³C NMR (75 MHz, CDCl₃) δ 173.14, 172.79, 155.84, 79.65, 52.86, 52.21, 47.89, 41.45, 28.31, 24.62, 22.95, 21.90, 17.70.

Ac-Leu-Ala-OMe (20)

Boc-Leu-Ala-OMe (19) (1.80g, 5.7 mmol) was dissolved in 1:1 TFA/DCM (20 mL) and stirred for 1 h, after which the mixture was concentrated and co-evaporated with toluene. TFA-H-Leu-Ala-OMe was dissolved in DCM (60 mL), followed by the addition of DiPEA (3.0 mL, 17 mmol, 3 equiv.) and Ac₂O (652 μL, 6.9 mmol, 1.2 equiv.). After stirring overnight, the reaction mixture was concentrated, dissolved in EtOAc and washed with 1N HCl (2x), sat. NaHCO₃ (2x) and brine (1x). The organic layer was dried over NaSO₄, filtered and concentrated. Purification by column chromatography (0%→2.5% MeOH/DCM) provided the product (1.03 g, 4 mmol, 70%). ¹H NMR (400 MHz, CDCl₃) δ 7.90 (d, *J* = 6.8 Hz, 1H), 7.68 (d, *J* = 8.1 Hz, 1H), 4.53 (q, *J* = 8.4 Hz, 1H), 4.33 (p, *J* = 7.1 Hz, 1H), 3.61 (s, 3H), 1.83 (s, 3H), 1.72 – 1.57 (m, 1H), 1.58 – 1.35 (m, 2H), 1.22 (d, *J* = 7.3 Hz, 3H), 0.80 (dd, *J* = 10.4, 6.6 Hz, 6H). ¹³C NMR (101 MHz, CDCl₃) δ 173.26, 173.04, 170.57, 52.11, 51.68, 48.11, 41.43, 24.59, 22.80, 22.64, 22.00, 17.19.

Ac-Leu-Ala-NHNH₂ (21)

To a solution of Ac-Leu-Ala-OMe (20) (1.03 g, 4 mmol) in MeOH (35 mL) was added hydrazine-hydrate (5.8 mL, 120 mmol, 30 equiv.). After stirring for 3 hours, the reaction was concentrated and co-evaporated with toluene (2x). The product was obtained in a quantitative yield. ¹H NMR (400 MHz, MeOD) δ 4.47 – 4.21 (m, 2H), 1.98 (s, 1H), 1.68 (dp, *J* = 13.8, 6.8 Hz, 1H), 1.62 – 1.46 (m, 2H), 1.34 (d, *J* = 6.9 Hz, 3H), 1.05 – 0.87 (m, 6H).

Boc-Pro-Ala-OMe (22)

To a solution of HCl-H-Ala-OMe (973 mg, 7 mmol, 1 equiv.) in DCM (70 mL) were added HCTU (3.19 g, 7.7 mmol, 1 equiv.), Boc-Pro-OH (1.67 g, 7.7 mmol, 1.1 equiv.) and DiPEA (4.3 mL, 24.5 mmol, 3.5 equiv.). After stirring overnight, the reaction mixture was concentrated, dissolved in EtOAc and washed with 1N HCl (2x), sat. NaHCO₃ (2x) and brine (1x). The organic layer was dried over NaSO₄, filtered and concentrated. Purification by column chromatography (20%→50% EtOAc/pent) provided the product in a quantitative yield. ¹H NMR (300 MHz, MeOD) δ 4.41 (q, *J* = 7.3 Hz, 1H), 4.28 – 4.14 (m, 1H), 3.71 (s, 3H), 3.56 – 3.36 (m, 2H), 2.36 – 2.10 (m, 1H), 2.05 – 1.77 (m, 3H), 1.51 – 1.30 (m, 12H).

Ac-Pro-Ala-OMe (23)

Boc-Pro-Ala-OMe (**22**) (2.0 g, 6.7 mmol) was dissolved in 1:1 TFA/DCM (20 mL) and stirred for 1 h, after which the mixture was concentrated and co-evaporated with toluene. TFA-H-Leu-Ala-OMe was dissolved in DCM (60 mL), followed by the addition of DiPEA (3.5 mL, 20 mmol, 3 equiv.) and Ac₂O (760 μ L, 8.0 mmol, 1.2 equiv.). After stirring overnight, the reaction mixture was concentrated, dissolved in EtOAc and washed with 1N HCl (2x), sat. NaHCO₃ (2x) and brine (1x). The organic layer was dried over NaSO₄, filtered and concentrated. Purification by column chromatography (0%→5% MeOH/DCM) provided the product (0.52 g, 2.14 mmol, 32%). Complex NMR due to presence of rotamers (1:3.5). ¹H NMR (400 MHz, CDCl₃) δ 7.45 (d, *J* = 6.4 Hz, 0.7H), 7.23 (d, 0.3H), 4.54 – 4.42 (m, 1H), 4.34 (p, *J* = 7.1 Hz, 0.75H), 4.23 (dd, *J* = 8.5, 2.5 Hz, 0.25H), 3.62 (s, 3H), 3.58 – 3.41 (m, 1.2H), 3.35 (q, *J* = 9.3 Hz, 0.8H), 2.29 – 1.71 (m, 4H), 1.98 (s, 1H), 2.00 (s, 2H), 1.32 (d, *J* = 7.3 Hz, 0.7H), 1.27 (d, *J* = 7.2 Hz, 2.3H). ¹³C NMR (101 MHz, CDCl₃) δ 173.13, 172.90, 171.81, 170.99, 170.68, 170.55, 61.88, 59.33, 52.26, 52.19, 48.19, 48.10, 47.88, 46.69, 31.98, 27.69, 24.82, 22.80, 22.39, 22.23, 17.67, 17.38.

Ac-Pro-Ala-NHNH₂ (24)

To a solution of Ac-Leu-Ala-OMe (**23**) (0.52 g, 2.14 mmol) in MeOH (20 mL) was added hydrazine-hydrate (3.1 mL, 64 mmol, 30 equiv.). After stirring for 3 h, the reaction was concentrated and co-evaporated with toluene (2x). The product was obtained in a quantitative yield. Complex NMR due to presence of rotamers. ¹H NMR (400 MHz, MeOD) δ 4.56 – 4.30 (m, 2H), 3.74 – 3.46 (m, 2H), 2.30 – 2.17 (m, 1H), 2.13 (s, 3H), 2.08 – 1.88 (m, 3H), 1.38 (d, *J* = 7.2 Hz, 3H). ¹³C NMR (101 MHz, MeOD) δ 174.35, 174.27, 173.97, 173.91, 172.55, 172.37, 62.22, 61.34, 61.30, 49.43, 49.10, 48.96, 47.96, 33.06, 30.92, 25.68, 23.81, 22.39, 22.23, 18.36, 17.98.

Boc-Ala-Pro-Ala-OMe (25)

Boc-L-Ala-OH (1.23 equiv., 0.464 g, 2.45 mmol) was dissolved in DCM (20 mL). HTCU (2 equiv., 0.992 g, 2.4 mmol) and DiPEA (3.53 equiv., 1.2 mL, 7.06 mmol) and TFA-Pro-Ala-OMe (**22b**) (1 equiv., 0.851 g, 2.0 mmol) were added to the mixture. After 1 h the solvent was evaporated and the crude was redissolved in EtOAc. The product was washed with 1M HCl (2x), sat. NaHCO₃ (2x) and brine (1x). The organic layer was dried over MgSO₄, filtered and concentrated. Column chromatography (0→2% MeOH/DCM) provided the product (0.232 g, 0.625 mmol, 31%). Complex NMR due to presence of rotamers. ¹H NMR (300 MHz, CDCl₃) δ 7.34 – 7.13 (m, 1H), 5.47 (d, *J* = 8.1 Hz, 1H), 4.60 – 4.14 (m, 3H), 3.73 – 3.44 (m, 5H), 2.19 – 1.84 (m, 4H), 1.38 – 1.32 (m, 9H), 1.31 – 1.24 (m, 6H). ¹³C NMR (75 MHz, CDCl₃, peaks of major rotamer) δ 173.12, 172.98, 171.01, 155.25, 79.66, 59.73, 52.33, 48.08, 47.75, 47.21, 28.27, 27.85, 24.94, 18.18, 17.78.

N₃Gly-Ala-Pro-Ala-OMe (26)

Boc-Ala-Pro-Ala-OMe (**26**) (140 mg, 0.376 mmol) was dissolved in DCM (2 mL) and TFA (2 mL) and the reaction was stirred for 30 min. After that the solution was evaporated and co-evaporated with toluene (3x), after which it was dissolved in DMF (5 mL), followed by the addition of DiPEA (0.2 mL, 1.1 mmol, 3 eq.) and (ClOAc)₂O (81 mg, 0.45 mmol (1.2 eq.) and stirred till completion (3h). NaN₃ (98 mg, 1.5 mmol, 4 eq.) was added and the reaction was stirred overnight. Reaction mixture was concentrated and redissolved in DCM and washed with 1 M HCl (1x) and brine (1x). Both water layers were back extracted several times with DCM. The organic layer was dried over MgSO₄, filtered and evaporated. Purification by column chromatography (0%→4% MeOH/DCM) yielded the desired compound (84 mg, 0.24 mmol, 63%). Complex NMR due to presence of rotamers. ¹H NMR (400 MHz, CDCl₃) δ 7.28 – 7.23 (m, 1H), 7.03 (d, *J* = 6.5 Hz, 1H), 4.84 – 4.66 (m, 1H), 4.51 (dt, *J* = 14.5, 5.8 Hz, 2H), 3.95 (s, 2H), 3.75 – 3.53 (m, 5H), 2.25 (d, *J* = 9.7 Hz, 1H), 2.20 – 2.05 (m, 1H), 2.05 – 1.90 (m, 2H), 1.45 – 1.29 (m, 6H). ¹³C NMR (101 MHz, CDCl₃, peaks of major rotamer) δ 173.33, 171.96, 170.54, 166.26, 59.99, 52.54, 48.20, 47.39, 46.79, 27.82, 25.14, 18.25.

N₃Gly-Ala-Pro-Ala-NHNH₂ (27)

N₃-Gly-Ala-Pro-Ala-OMe (**26**) (84 mg, 0.24 mmol) was dissolved in MeOH (2.5 mL). Hydrazine hydrate (0.35 mL, 7.1 mmol, 30 eq.) was added and the reaction mixture was stirred overnight. The reaction mixture was concentrated and co-evaporated with toluene (2x). The product was obtained in a quantitative yield. ¹H NMR (400 MHz, MeOD) δ 4.73 – 4.61 (m, 1H), 4.61 – 4.36 (m, 2H), 3.92 (s, 2H), 3.87 – 3.76 (m, 1H), 3.76 – 3.61 (m, 1H), 2.36 – 2.15 (m, 1H), 2.13 – 1.92 (m, 3H), 1.49 – 1.28 (m, 6H). ¹³C NMR (101 MHz, MeOD) δ 172.80, 172.64, 171.95, 171.78, 170.06, 168.46, 60.28, 60.02, 51.06, 47.82, 47.25, 29.17, 29.06, 24.64, 24.60, 16.69, 16.58, 15.49.

Ac-Pro-Leu-OMe (28)

To a solution of HCl-H-Leu-OMe (322 mg, 2 mmol, 1 equiv.) in DCM (20 mL) were added HCTU (913 mg, 2.2 mmol, 1.1 equiv.), Boc-Pro-OH (473 mg, 2.2 mmol, 1.1 equiv.) and DiPEA (1.2 mL, 7 mmol, 3.5 equiv.). After stirring overnight, the reaction mixture was concentrated, dissolved in EtOAc and washed with 1N HCl (2x), sat. NaHCO₃ (2x) and brine (1x). The organic layer was dried over NaSO₄, filtered and concentrated. Purification by column chromatography (20%→50% EtOAc/pent) provided the product (617 mg, 1.80 mmol, 90%) which was dissolved in 1:1 TFA/DCM (10 mL) and stirred for 30 min, after which the mixture was concentrated and co-evaporated with toluene. TFA-H-Pro-Leu-OMe (214 mg, 0.62 mmol) was dissolved in DCM (6 mL), followed by the addition of DiPEA (0.32 mL, 5.4 mmol, 3 equiv.) and Ac₂O (71 μL, 2.2 mmol, 1.2 equiv.). After stirring overnight, the reaction mixture was concentrated. Purification by column chromatography (50%→100% EtOAc/pent followed by 0%→2% MeOH/EtOAc) provided the product (136 mg, 0.47 mmol, 76%). Complex NMR due to presence of rotamers (1:2:3). ¹H NMR (400 MHz, CDCl₃) δ 7.36 (d, *J* = 7.3 Hz, 0.7H), 6.82 (d, *J* = 8.5 Hz, 0.3H), 4.62 – 4.49 (m, 1H), 4.48 – 4.33 (m, 7H), 4.27 (dd, *J* = 8.5, 2.6 Hz, 0.3H), 3.65 (s, 3H), 3.60 – 3.44 (m, 1H), 3.37 (td, *J* = 9.6, 7.1 Hz, 1H), 2.39 – 2.27 (m, 1H), 2.25 – 2.05 (m, 1H), 2.03 (s, 3H), 1.98 – 1.71 (m, 2H), 1.54 (ttd, *J* = 18.4, 8.8, 5.6 Hz, 3H), 0.90 – 0.79 (m, 6H). ¹³C NMR (101 MHz, CDCl₃) δ 173.18, 172.98, 172.07, 171.07, 170.93, 170.78, 62.15, 59.35, 52.28, 52.15, 51.07, 50.66, 48.24, 46.78, 41.06, 40.37, 32.12, 27.30, 25.10, 25.00, 24.91, 22.95, 22.69, 22.39, 22.35, 21.94, 21.36.

Ac-Pro-Leu-NHNH₂ (29)

To a solution of Ac-Pro-Leu-OMe (**28**) (136 mg, 0.47 mmol) in MeOH (5 mL) was added hydrazine-hydrate (0.69 mL, 64 mmol, 30 equiv.). After stirring for 3 hours, the reaction was concentrated and co-evaporated with toluene (2x). The product was obtained in a quantitative yield. Complex NMR due to presence of rotamers. ¹H NMR (400 MHz, MeOD) δ 4.48 – 4.42 (m, 0.4H), 4.42 – 4.36 (m, 1.6H), 3.70 – 3.47 (m, 2H), 2.38 – 2.27 (m, 0.2H), 2.27 – 2.14 (m, 0.8H), 2.10 (s, 2.5H), 2.07 – 1.83 (m, 3.5H), 1.75 – 1.44 (m, 3H), 1.01 – 0.87 (m, 6H). ¹³C NMR (101 MHz, MeOD) δ 174.53, 174.11, 173.65, 173.56, 172.71, 62.30, 61.38, 54.82, 51.79, 51.61, 48.00, 41.97, 41.67, 33.12, 30.94, 25.96, 25.78, 25.72, 23.82, 23.42, 23.32, 22.33, 22.14, 21.93, 21.86.

Ac-Leu-Leu-OMe (30)

A solution of Boc-Leu-Leu-OMe (358 mg, 1 mmol) in 1:1 TFA/DCM (10 mL) was stirred for 30 min, after which the mixture was concentrated and co-evaporated with toluene. TFA-H-Leu-Leu-OMe (214 mg, 0.62 mmol) was dissolved in DCM (6 mL), followed by the addition of DiPEA (0.52 mL, 3 mmol, 3 equiv.) and Ac₂O (113 μL, 1.2 mmol, 1.2 equiv.). After stirring overnight, the reaction mixture was concentrated. Purification by column chromatography (20%→50% EtOAc/pent) provided the product (238 mg, 0.79 mmol, 79%). ¹H NMR (400 MHz, CDCl₃) δ 7.44 (d, *J* = 7.6 Hz, 1H), 7.25 (d, *J* = 8.4 Hz, 1H), 4.57 (td, *J* = 8.5, 6.2 Hz, 1H), 4.43 (td, *J* = 8.5, 5.5 Hz, 1H), 3.64 (s, 3H), 1.88 (s, 3H), 1.76 – 1.39 (m, 6H), 0.83 (dt, *J* = 7.7, 6.1 Hz, 12H). ¹³C NMR (101 MHz, CDCl₃) δ 173.10, 172.98, 170.28, 52.08, 51.59, 50.94, 41.51, 40.78, 24.73, 24.65, 22.82, 22.76, 22.70, 22.39, 21.88.

Ac-Leu-Leu-NHNH₂ (31)

To a solution of Ac-Leu-Leu-OMe (238 mg, 0.79 mmol) in MeOH (8 mL) was added hydrazine-hydrate (1.12 mL, 24 mmol, 30 equiv.). After stirring for 3 hours, the reaction was concentrated and co-evaporated with toluene

(2x). The product was obtained in a quantitative yield. ^1H NMR (400 MHz, MeOD) δ 4.39 (dd, $J = 8.7, 6.1$ Hz, 2H), 1.98 (s, 3H), 1.73 – 1.45 (m, 6H), 0.93 (ddd, $J = 16.3, 6.4, 4.4$ Hz, 12H). ^{13}C NMR (101 MHz, MeOD) δ 174.74, 173.66, 173.39, 53.25, 51.62, 42.00, 41.73, 25.85, 25.76, 23.44, 23.35, 22.42, 22.10, 21.96.

Boc-Ala-Pro-Leu-OMe (32)

To a solution of TFA-H-Pro-Leu-OMe (400 mg, 1.17 mmol) in DCM (12 mL) were added HCTU (580 mg, 1.4 mmol, 1.2 equiv.), Boc-Ala-OH (226 mg, 1.4 mmol, 1.2 equiv.) and DiPEA (0.71 mL, 4.1 mmol, 3.5 equiv.). After stirring overnight, the reaction mixture was concentrated, dissolved in EtOAc and washed with 1N HCl (2x), sat. NaHCO_3 (2x) and brine (1x). The organic layer was dried over NaSO_4 , filtered and concentrated. Purification by column chromatography (50%→100% EtOAc/pent) provided the product (434 mg, 1.1 mmol, 89%). Complex NMR due to presence of rotamers (1:6), peaks of major rotamer reported. ^1H NMR (400 MHz, CDCl_3) δ 7.16 (d, $J = 7.5$ Hz, 1H), 5.36 (d, $J = 8.1$ Hz, 1H), 4.56 (dd, $J = 8.0, 1.9$ Hz, 1H), 4.40 (td, $J = 8.0, 7.2, 4.0$ Hz, 2H), 3.63 (s, 3H), 3.59 (d, $J = 4.4$ Hz, 1H), 3.47 (qd, $J = 9.6, 8.7, 3.6$ Hz, 1H), 2.35 – 2.23 (m, 1H), 2.14 – 1.98 (m, 1H), 1.98 – 1.88 (m, 1H), 1.88 – 1.73 (m, 1H), 1.57 – 1.42 (m, 3H), 1.35 (s, 9H), 1.23 (d, $J = 7.0$ Hz, 3H), 0.81 (dd, $J = 10.3, 5.9$ Hz, 6H). ^{13}C NMR (101 MHz, CDCl_3) δ 173.11, 173.09, 170.66, 155.10, 79.59, 59.52, 52.16, 50.85, 47.66, 47.16, 41.05, 28.31, 26.87, 25.08, 24.70, 22.81, 21.70, 18.48.

Boc-Ala-Pro-Leu-NHNH₂ (33)

To a solution of Boc-Ala-Pro-Leu-OMe (**32**) (215 mg, 0.5 mmol) in MeOH (5 mL) was added hydrazine-hydrate (0.71 mL, 15 mmol, 30 equiv.). After stirring for 3 hours, the reaction was concentrated and co-evaporated with toluene (2x). The product was obtained in a quantitative yield. ^1H NMR (400 MHz, MeOD) δ 4.45 (dd, $J = 8.1, 4.9$ Hz, 1H), 4.41 – 4.32 (m, 2H), 3.85 – 3.74 (m, 1H), 3.70 – 3.59 (m, 1H), 2.27 – 1.86 (m, 4H), 1.63 (dtd, $J = 24.2, 10.4, 9.1, 5.9$ Hz, 3H), 1.43 (s, 9H), 1.30 (d, $J = 7.0$ Hz, 3H), 0.93 (dd, $J = 16.6, 6.4$ Hz, 6H). ^{13}C NMR (101 MHz, MeOD) δ 174.44, 174.16, 173.71, 157.62, 80.46, 61.71, 51.84, 49.66, 41.77, 30.22, 28.79, 28.70, 26.04, 25.73, 23.40, 22.01, 17.13.

Ac-Ala-Pro-Leu-OMe (34)

Boc-Ala-Pro-Leu-OMe (**32**) (215 mg, 0.5 mmol) was treated with TFA (2 mL) for 30 min. The mixture was concentrated and co-evaporated with toluene (2x). To a solution TFA-H-Ala-Pro-Leu-OMe in DCM were added DiPEA (0.26 mL, 1.5 mmol, 3 equiv.) and Ac_2O (60 μL , 0.6 mmol, 1.2 equiv.). After stirring overnight, the reaction mixture was concentrated. Purification by column chromatography (0%→2% MeOH/DCM) provided the product (135 mg, 0.38 mmol, 76%). Complex NMR due to presence of rotamers, peaks of major rotamer reported ^1H NMR (400 MHz, MeOD) δ 4.58 (q, $J = 7.0$ Hz, 1H), 4.47 (dd, $J = 8.6, 4.2$ Hz, 1H), 4.41 (dd, $J = 8.9, 6.1$ Hz, 1H), 3.87 – 3.75 (m, 1H), 3.70 (s, 3H), 3.69 – 3.61 (m, 1H), 2.26 – 2.12 (m, 1H), 2.12 – 1.97 (m, 3H), 1.95 (s, 3H), 1.84 – 1.68 (m, 1H), 1.66 – 1.57 (m, 2H), 1.33 (d, $J = 7.1$ Hz, 3H), 0.94 (dd, $J = 16.7, 6.6$ Hz, 6H). ^{13}C NMR (101 MHz, MeOD) δ 174.58, 174.50, 173.55, 172.88, 61.11, 52.61, 52.23, 49.43, 49.21, 49.00, 48.79, 48.58, 48.46, 48.40, 41.40, 30.36, 25.90, 25.84, 23.31, 22.20, 21.89, 16.76.

Ac-Ala-Pro-Leu-NHNH₂ (35)

To a solution of Ac-Ala-Pro-Leu-OMe (**34**) (215 mg, 0.5 mmol) in MeOH (5 mL) was added hydrazine-hydrate (0.71 mL, 15 mmol, 30 equiv.). After stirring for 3 hours, the reaction was concentrated and co-evaporated with toluene (2x). The product was obtained in a quantitative yield. ^1H NMR (400 MHz, MeOD) δ 4.62 (q, $J = 7.1$ Hz, 1H), 4.46 (dd, $J = 8.2, 4.6$ Hz, 1H), 4.36 (dd, $J = 9.5, 5.6$ Hz, 1H), 3.83 (dt, $J = 10.0, 6.7$ Hz, 1H), 3.74 – 3.61 (m, 1H), 2.29 – 2.15 (m, 1H), 2.15 – 1.92 (m, 6H), 1.79 – 1.52 (m, 3H), 1.36 (d, $J = 7.0$ Hz, 3H), 0.96 (dd, $J = 16.2, 6.4$ Hz, 6H). ^{13}C NMR (101 MHz, MeOD) δ 172.86, 172.51, 172.47, 171.53, 60.25, 50.57, 47.23, 40.57, 28.99, 24.71, 24.44, 22.09, 20.92, 20.75, 15.49.

Biochemical methods

Proteasomes

Wild-type and mutant proteasomes were purified as previously described.²⁸ Purified human constitutive proteasome was bought from Boston Biochem (USA).

Proteasome substrates and inhibitors

AMC-substrates (Bachem) and inhibitors were stored as 50-100 mM solutions in DMSO at -20 °C. Bortezomib was purchased from Selleck Chemicals, carfilzomib from Active Biochemicals, and ONX-0914 from MedKoo Biosciences.

IC₅₀ Determination with purified yCP

Concentrations of purified yCP variants were determined spectrophotometrically at 280 nm. Initial point measurements were carried out with 200 μM of inhibitor. Only compounds that showed significant inhibition at this concentration were further evaluated. Purified yCPs (final concentration: 66 nM in 100 mM Tris-HCl, pH 7.5) were mixed with DMSO as a control or serial dilutions of inhibitor and incubated for 1 h at room temperature. After addition of the peptide substrate Z-LLE-AMC, Boc-LRR-AMC or Suc-LLVY-AMC (final concentration of 200 μM) and incubation for 1 h at room temperature, proteolysis was stopped by diluting the samples 1:10 in 20 mM Tris-HCl, pH 7.5. The AMC-molecules released by residual proteasomal activity were measured in triplicate with a Varian Cary Eclipse Fluorescence Spectrophotometer (Agilent Technologies) at $\lambda_{\text{ex}}=360$ nm and $\lambda_{\text{em}}=460$ nm. Relative fluorescence units were normalized to the DMSO treated control. The calculated residual activities were plotted against the logarithm of the applied inhibitor concentration and fitted with GraphPad Prism 5. IC₅₀ values were deduced from the fitted data. They depend on enzyme concentration and are comparable only within the same experimental settings.

Competition Assays in Raji Cell Lysate.

Lysates of Raji cells were prepared by addition of 4 volumes of lysis buffer containing 50 mM Tris pH 7.5, 2 mM DTT, 5 mM MgCl₂, 10% glycerol, 2 mM ATP, and 0.05% digitonin. Protein concentration was determined by the Bradford assay. Cell lysates (diluted to 10-15 μg total protein in buffer containing 50 mM Tris pH 7.5, 2 mM DTT, 5 mM MgCl₂, 10% glycerol, 2 mM ATP) were exposed to the inhibitors for 1 h at 37 °C prior to incubation with AzidoBODIPY-MeTyr-Phe-Leu-VS (BODIPY(TMR)-NC-005-VS; 0.1 μM; to probe β5), or a mixture of BODIPY(TMR)-EKoxomicin (0.5 μM; to probe all subunits, used for β2-profiling) and BODIPY(FL)-Ala-Pro-Nle-Leu-EK (BODIPY-NC001; 0.25 μM; to probe β1 activity, followed by 3 min boiling with a reducing gel-loading buffer and fractionation on 12.5% SDS-PAGE. In-gel detection of residual proteasome activity was performed in the wet gel slabs directly on a ChemiDoc™ MP System using Cy3 settings to detect BODIPY(TMR)-NC-005 and BODIPY(TMR)-EKoxomicin and Cy2 settings to detect BODIPY-NC-001-VS. Intensities of bands were measured by fluorescent densitometry and normalized to the intensity of bands in mock-treated extracts. Average values of three independent experiments were plotted against inhibitor concentrations. IC₅₀ values were calculated using GraphPad Prism software.

Crystallization and structure determination

The yeast 20S proteasome was crystallized by hanging drop vapour diffusion according to published procedures.²⁸ Inhibitor complex structures were obtained by incubating crystals in 5 μl cryobuffer (20 mM magnesium acetate, 100 mM MES (2-(N-morpholino)ethanesulfonic acid), pH 6.8 and 30% (v/v) MPD (2-methyl-2,4-pentanediol) supplemented with inhibitor at a final concentration of 3.3 mM for at least 12 h prior to vitrification in liquid nitrogen. Diffraction data were collected using synchrotron radiation of $\lambda = 1.0$ Å at the beamline X06SA, Swiss Light Source (SLS), Villigen, Switzerland. Evaluation of reflection intensities and data reduction were performed with the program package XDS. Molecular replacement using the coordinates of the

yCP (PDB entry code: 1RYP13) was carried out by rigid body and anisotropic TLS refinements with REFMAC5; MAIN and COOT served as model building software. The coordinates finally yielded excellent R_{crys}, R_{free}, r.m.s.d. bond and angle values as well as good stereochemistry from the Ramachandran Plot and have been deposited in the RCSB Protein Data Bank (for X-ray data collection and refinement statistics, PDB codes and all structures: see²⁹).

References

1. Groettrup, M., Kirk, C.J. & Basler, M. Proteasomes in immune cells: more than peptide producers? *Nat. Rev. Immunol.* **10**, 73-8 (2010).
2. Murata, S., Takahama, Y. & Tanaka, K. Thymoproteasome: probable role in generating positively selecting peptides. *Curr. Opin. Immunol.* **20**, 192-6 (2008).
3. Groll, M. et al. Structure of 20S proteasome from yeast at 2.4 Å resolution. *Nature* **386**, 463-71 (1997).
4. Mirabella, A.C. et al. Specific cell-permeable inhibitor of proteasome trypsin-like sites selectively sensitizes myeloma cells to bortezomib and carfilzomib. *Chem. Biol.* **18**, 608-18 (2011).
5. Blackburn, C. et al. Characterization of a new series of non-covalent proteasome inhibitors with exquisite potency and selectivity for the 20S beta5-subunit. *Biochem. J.* **430**, 461-76 (2010).
6. Huber, E.M. et al. Immuno- and constitutive proteasome crystal structures reveal differences in substrate and inhibitor specificity. *Cell* **148**, 727-738 (2012).
7. Orłowski, M. The multicatalytic proteinase complex, a major extralysosomal proteolytic system. *Biochemistry* **29**, 10289-97 (1990).
8. Kisselev, A.F. et al. The caspase-like sites of proteasomes, their substrate specificity, new inhibitors and substrates, and allosteric interactions with the trypsin-like sites. *J. Biol. Chem.* **278**, 35869-77 (2003).
9. Nussbaum, A.K. et al. Cleavage motifs of the yeast 20S proteasome beta subunits deduced from digests of enolase 1. *Proc. Natl. Acad. Sci.* **95**, 12504-9 (1998).
10. Harris, J.L., Alper, P.B., Li, J., Rechsteiner, M. & Backes, B.J. Substrate specificity of the human proteasome. *Chem. Biol.* **8**, 1131-41 (2001).
11. Toes, R.E. et al. Discrete cleavage motifs of constitutive and immunoproteasomes revealed by quantitative analysis of cleavage products. *J. Exp. Med.* **194**, 1-12 (2001).
12. Nazif, T. & Bogyo, M. Global analysis of proteasomal substrate specificity using positional-scanning libraries of covalent inhibitors. *Proc. Natl. Acad. Sci.* **98**, 2967-72 (2001).
13. Groll, M., Kim, K.B., Kairies, N., Huber, R. & Crews, C.M. Crystal structure of epoxomicin: 20S proteasome reveals a molecular basis for selectivity of α' , β' -epoxyketone proteasome inhibitors. *J. Am. Chem. Soc.* **122**, 1237-1238 (2000).
14. Verdoes, M. et al. A panel of subunit-selective activity-based proteasome probes. *Org. Biomol. Chem.* **8**, 2719-27 (2010).
15. Li, N. et al. Relative quantification of proteasome activity by activity-based protein profiling and LC-MS/MS. *Nat. Prot.* **8**, 1155-68 (2013).
16. de Bruin, G. et al. Structure-based design of beta1i or beta5i specific inhibitors of human immunoproteasomes. *J. Med. Chem.* **57**, 6197-209 (2014).
17. Harshbarger, W., Miller, C., Diedrich, C. & Sacchettini, J. Crystal Structure of the Human 20S Proteasome in Complex with Carfilzomib. *Structure* **23**, 418-24 (2015).
18. Groll, M., Korotkov, V.S., Huber, E.M., de Meijere, A. & Ludwig, A. A Minimal β -Lactone Fragment for Selective β 5c or β 5i Proteasome Inhibitors. *Angew. Chem. Int. Ed.* **54**, 7810-7814 (2015).
19. Huber, E.M., Heinemeyer, W. & Groll, M. Bortezomib-Resistant Mutant Proteasomes: Structural and Biochemical Evaluation with Carfilzomib and ONX 0914. *Structure* **23**, 407-17 (2015).

20. Heinemeyer, W., Kleinschmidt, J.A., Saidowsky, J., Escher, C. & Wolf, D.H. Proteinase yscE, the yeast proteasome/multicatalytic-multifunctional proteinase: mutants unravel its function in stress induced proteolysis and uncover its necessity for cell survival. *EMBO J.* **10**, 555-62 (1991).
21. Huber, E.M. & Groll, M. Inhibitors for the immuno- and constitutive proteasome: current and future trends in drug development. *Angew. Chem. Int. Ed.* **51**, 8708-20 (2012).
22. Demo, S.D. et al. Antitumor activity of PR-171, a novel irreversible inhibitor of the proteasome. *Cancer Res.* **67**, 6383-91 (2007).
23. Orłowski, M. & Wilk, S. Catalytic activities of the 20 S proteasome, a multicatalytic proteinase complex. *Arch. Biochem. Biophys.* **383**, 1-16 (2000).
24. Cardozo, C., Vinitsky, A., Michaud, C. & Orłowski, M. Evidence that the nature of amino acid residues in the P3 position directs substrates to distinct catalytic sites of the pituitary multicatalytic proteinase complex (proteasome). *Biochemistry* **33**, 6483-9 (1994).
25. Orłowski, M., Cardozo, C. & Michaud, C. Evidence for the presence of five distinct proteolytic components in the pituitary multicatalytic proteinase complex. Properties of two components cleaving bonds on the carboxyl side of branched chain and small neutral amino acids. *Biochemistry* **32**, 1563-72 (1993).
26. Geurink, P.P. et al. Incorporation of non-natural amino acids improves cell permeability and potency of specific inhibitors of proteasome trypsin-like sites. *J. Med. Chem.* **56**, 1262-1275 (2013).
27. Zhou, H.-J. et al. Design and synthesis of an orally bioavailable and selective peptide epoxyketone proteasome inhibitor (PR-047). *J. Med. Chem.* **52**, 3028-3038 (2009).
28. Gallastegui, N. & Groll, M. Analysing properties of proteasome inhibitors using kinetic and X-ray crystallographic studies. *Methods Mol. Biol.* **832**, 373-90 (2012).
29. Huber, E.M. et al. Systematic analyses of substrate preferences of 20S proteasomes using peptidic epoxyketone inhibitors. *J. Am. Chem. Soc.* **137**, 7835-7842 (2015).

Structure-based design of either β 1i or β 5i specific inhibitors of human immunoproteasomes*

Introduction

Proteasomes are large, multi-catalytic complexes that partake in the degradation of cytosolic, nuclear and misfolded ER proteins in most kingdoms of life.¹ The 20S core particles (CP) in which proteolysis takes place are C2-symmetrical barrel-shaped multi-protein complexes composed of four stacked rings of seven subunits each: the two inner rings consisting of seven homologous yet distinct β -subunits (β 1- β 7) are flanked by two outer rings composed of the α -subunits 1-7.² The proteolytic activity resides within three catalytic subunits (one copy in each β -ring), namely β 1c (also referred to as caspase-like, cleaving preferentially after acidic residues), β 2c (trypsin-like, with a preference for basic residues) and β 5c (chymotrypsin-like, preferring neutral, hydrophobic residues at the cleavage site²⁻⁵). Immune-competent cells express next to the constitutive proteasome (cCP) the interferon- γ -inducible subunits β 1i (LMP2), β 2i (MECL-1) and β 5i (LMP7).⁶ Upon cytokine stimulation these subunits replace their constitutive proteasome counterparts (β 1c, β 2c and β 5c, respectively) to form immunoproteasomes (iCPs).

The substrate preference of cCP catalytic subunits considerably overlaps with their iCP analogues, though subtle differences have been observed.⁷ In particular, whereas β 1c prefers acidic residues at P1 (Asp or Glu; the amino acid residue residing at the C-terminus of the scissile peptide bond), β 1i is biased to hydrophobic side chains at this position.⁸ This divergence of substrate preference has been connected to processing and presentation of antigenic peptides from cytosolic/nuclear sources.

Proteasome inhibitors take up a prominent position both in fundamental and applied biomedical research. Based on the structural diversity of natural CP inhibitors, numerous

*de Bruin, G.; Huber, E. *et al.* Structure-based design of β 1i or β 5i specific inhibitors of human immunoproteasomes. *J. Med. Chem.* **57**, 6197-6209 (2014).

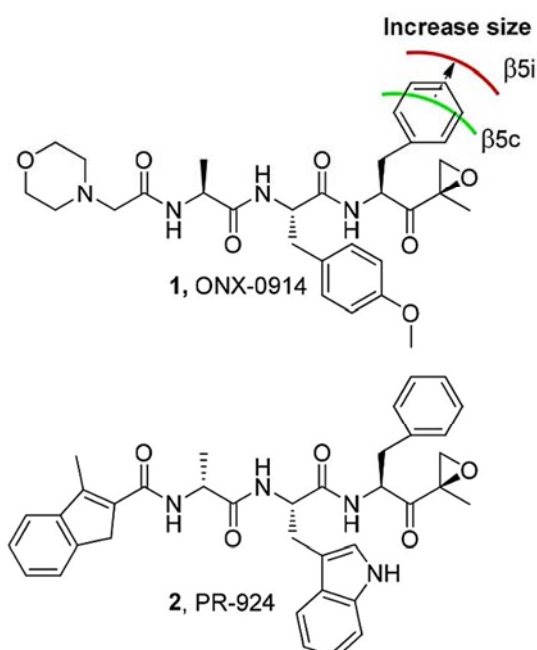
synthetic compounds have been developed. Most of them are peptide-based and feature an electrophile that reacts with the N-terminal nucleophilic threonine hydroxyl group of catalytic proteasome subunits to form a covalent linkage. Depending on the nature of the electrophilic trap the covalent bond is transient (aldehydes, boronic acids), semi-permanent (beta-lactones) or permanent (vinyl sulfones, epoxyketones).^{9, 10} Subunit specificity is largely governed by the nature of the peptide fragment (amino acid sequence) of a given inhibitor, though examples exist in which substitution of the electrophilic head group on an otherwise unaltered compound also impacts the proteasome inhibition profile.^{11, 12} CP inhibitors are broadly used to study the proteolytic system in more detail and to modulate physiological processes, in particular cell proliferation. The finding that proteasomes are valid therapeutic targets in various cancers led to the development of the peptide boronic acid bortezomib (Velcade)¹³⁻¹⁵ as a drug for the treatment of multiple myeloma (MM) and mantle cell lymphoma. This breakthrough was recently followed by the FDA approval of the peptide epoxyketone carfilzomib (Kyprolis)¹⁶⁻¹⁸ as a second-generation CP inhibitor for the treatment of MM. Thus, both reversible and irreversible proteasome inhibitors are relevant candidates for drug development strategies. Currently, several proteasome inhibitors are in clinical trials, including marizomib (salinosporamide A, NPI-0052), delanzomib (CEP-18770)¹⁹, ixazomib (MLN-9708)²⁰, and oprozomib (ONX-0912, PR-047).²¹

Although bortezomib and carfilzomib have been developed to primarily target the chymotrypsin-like active sites $\beta 5c$ and $\beta 5i$, which are the most important ones for the anti-tumor effects, they also co-inhibit the subunits $\beta 1c/\beta 1i$ as well as $\beta 2c/\beta 2i$ at higher concentrations.^{16, 22, 23} More recently, cell permeable ligands specific for one catalytic subunit ($\beta 1^3$, $\beta 2^4$ or $\beta 5^{11, 24}$) of the cCP together with its iCP counterpart have been developed. These compounds demonstrated that cytotoxicity in MM cell lines cannot be reached by exclusive blockage of $\beta 5c/\beta 5i$, but requires co-inhibition of either $\beta 1c/\beta 1i$ or $\beta 2c/\beta 2i$.^{3, 4} Thus, compounds specific for one out of the six catalytic subunits from which cCPs and iCPs are assembled, are highly desirable commodities for research and clinical applications nowadays. This certainly holds true for oncological research, given that in various lymphomas iCPs are the predominant proteasome species, where identification of the ideal target/dosage combination – which catalytic active site should be inhibited, and to what extent – needs to be established. Furthermore, this also applies to the immunological question of which proteolytic center is involved in the generation of a given antigenic peptide.

For many years X-ray diffraction data from yeast proteasomes (yCP) were used to clarify the mode of action and binding specificity of CP inhibitors, including approved drugs and drug candidates.²⁵⁻²⁷ Recently, structure elucidation of the murine cCP and iCP complemented the yeast structures and highlighted the differences between the cCP and iCP.^{28, 29} Perusal of the differences between the two structures and their inhibitor-bound counterparts provide

insight to structural features by which β 1i and β 5i may be targeted independently from β 1c and β 5c, respectively. Specifically, β 5i appears to be able to accommodate a larger amino acid side chain at position P1 than β 5c, while the opposite holds true for the P3 residue. On the other hand, the S1 pocket of β 1i is more hydrophobic when compared to β 1c, while the S3 pocket of β 1i is more restricted in size and more polar compared to its counterpart β 1c. Here the discovery of inhibitors highly specific for either β 5i or β 1i in the presence of all constitutive proteasome and immunoproteasome active site is reported. The design of the β 5i specific inhibitors is based on two compounds previously developed by ONYX Pharmaceuticals, namely ONX-0914^{30, 31} (PR-957, **1**) and PR-924^{30, 32, 33} (**2**) (Figure 1A). Using a structure-based design approach molecules were obtained with considerably improved selectivity for β 5i over β 5c. X-ray crystallographic analysis of the inhibitors in complex with the yCP provided important insights into the molecular basis of β 5i selectivity. For the development of β 1i selective inhibitors the previously reported β 1c/ β 1i specific inhibitor NC-001³ (**3**) (Figure 1B) was used as a starting point. In a first optimization round its key structural element, a proline residue at P3,³⁴ was modified and in a second step structural features at P1 were varied.

A. Towards β 5i selective inhibitors



B. Towards β 1i selective inhibitors

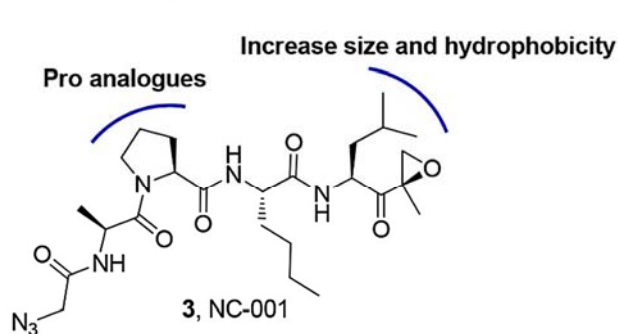


Figure 1. Design principles for immunoproteasome-specific inhibitors. A) Compounds with large hydrophobic P1 side chains display β 5i selectivity. B) Proline analogues in P3 and bulky hydrophobic P1 residues are the prerequisites to design β 1i selective inhibitors.

Altogether, this strategy led to identification of either $\beta 5i$ or $\beta 1i$ selective compounds with high subunit selectivity and potency. All synthesized inhibitors were proven to be cell-permeable and active in mammalian cancer cell lines and hence, provide an excellent tool kit for the systematic evaluation of the distinct proteasomal active sites.

Results

Design, synthesis and evaluation of highly specific $\beta 5i$ inhibitors.

The X-ray structure of **1** covalently bound to the murine cCP and iCP indicates that the phenyl moiety at position P1 induces a major conformational change in the S1 pocket of $\beta 5c$, but only minor alterations in $\beta 5i$.²⁸ This difference in binding likely confers $\beta 5i$ selectivity to inhibitor **1** and it was reasoned that substitution at P1 of phenylalanine epoxyketone for larger hydrophobic P1 residues should lead to compounds with enhanced $\beta 5i$ selectivity (Figure 1A). To determine the optimal P1 residue for this purpose, epoxyketone analogues of **1** featuring an adamantyl- (**4**), biphenyl- (**5**), 2-naphthyl- (**6**), 1-naphthyl- (**7**) or cyclohexyl-alanine (**8**) in the P1 site were synthesized (Table 1). The compounds were evaluated for their potencies against $\beta 5c$ and $\beta 5i$ in Raji-cell lysates (B-cell lymphoma cell line) by competitive activity based protein profiling (ABPP) of the $\beta 5$ -subunits using the $\beta 5c/\beta 5i$ specific probe BODIPY(TMR)-NC-005-VS (Table 1).^{35, 36} In contrast to Muchamuel *et al.* who determined a 30-fold selectivity for $\beta 5i$ over $\beta 5c$ for **1**³¹ using an ELISA-based assay in MOLT-4 cells, a nine-fold selectivity was observed by ABPP. Incorporation of adamantylalanine epoxyketone at P1 of the lead structure (**4**) resulted in complete loss of affinity. Interestingly, the bulky biphenyl side chain in **5** did not show increased selectivity but a two-to-three-fold enhanced potency for $\beta 5c$ and $\beta 5i$. Furthermore, while the 2-naphthyl-side chain in **6** has both high affinity and increased selectivity for $\beta 5i$, the 1-naphthyl derivative **7** is significantly less potent than compound **1**. Different orientations of the 1-naphthyl and 2-naphthyl substituents in the $\beta 5c/\beta 5i$ active sites might explain this observation. The most prominent improvement in selectivity was noticed for **8**, featuring a cyclohexylalanine residue at P1. While the binding strength towards $\beta 5i$ remained similar, the affinity for $\beta 5c$ was significantly impaired compared to the lead structure ONX-0914 (**1**), hereby enhancing $\beta 5i$ selectivity almost five times. For further optimization three side chains were pursued: cyclohexyl (highest selectivity), biphenyl (highest potency) and phenyl (for comparison). Cyclohexyl (**9**) and biphenyl (**10**) analogues of the phenyl-bearing compound PR-924 (**2**) – another $\beta 5i$ selective inhibitor with 100-fold preference for $\beta 5i$ – were synthesized.^{33, 37} **9** turned out to be 500-fold selective for $\beta 5i$ over $\beta 5c$ yet with threefold lower potency compared to **2**. Compound **10** appeared less selective than **2**, indicating that a biphenyl substituent at P1 is not suitable for optimal $\beta 5i$ selectivity.

Structure-based design of either β 1i or β 5i specific inhibitors of human immunoproteasomes

Table 1. Optimization of β 5i Selective Inhibitors Based on 1 (ONX-0914) and 2 (PR-924). IC₅₀ values were determined using ABPP in Raji cell lysates. >[conc] indicates less than 50% inhibition at indicated concentration.

Compound	R	P3	P2	P1	Apparent IC ₅₀ (nM)		Ratio
					β 5i	β 5c	
1 ONX-0914					5.7	54	9
4					>50x10 ³	>50x10 ³	-
5					2.0	20	10
6					3.1	97	32
7					244	1.8 x 10 ³	7
8 LU-005i					6.6	287	43
2 PR-924					2.5	227	91
9 LU-015i					8.3	4.6x10 ³	553
10					5.0	79	16
11 LU-025i					36	1.9 x 10 ³	52
12					3.0	14.5	5
13 LU-035i					11	5.5 x 10 ³	500
14					5.0	6.0	1
15 LU-045i					32	827	26
16					13	104	8
17					14	116	8

Compound					Apparent IC ₅₀ (nM)		Ratio
	R	P3	P2	P1	β _{5i}	β _{5c}	β _{5c} / β _{5i}
18					3	157	52
19					1.4	12.6	9
20					2.1	14	6
21					1.2	9.9	8
22					3.3	43	13
23 Vinyl Sulfone					392	14 x 10 ³	37
24 Vinyl Sulfone					5700	>100 x 10 ³	>18
25, LU-055i Vinyl Sulfone					53	25 x 10 ³	464
26 Vinyl Sulfone					632	62 x 10 ³	98

Next, hybrid compounds featuring elements from both **1** and **2** with various P1 amino acid derivatives were evaluated (**11-22**, Table 1). From this focused set of compounds, several β_{5c}/β_{5i} inhibition and selectivity patterns emerge. First, differences in potency and selectivity between P2 residues such as 4-methyltyrosine (4MeTyr)- and tryptophan-derived epoxyketones are marginal. Second, the chirality (D/L) of the alanine in P3 can have significant influence on β_{5i} selectivity and -potency. For example, the *N*-acylmorpholine capped compounds **8** and **11** show a similar selectivity profile, however **11** (featuring D-Ala in P3) is fivefold less active towards β_{5i} and β_{5c} compared to **8** (bearing L-Ala in P3). In contrast, the 3-methyl-1*H*-indene capped inhibitor **12** with L-Ala in P3 displays a significant decrease in selectivity but an increase in potency versus its D-Ala featuring analogue **13**. It can be concluded that L-Ala at P3 combines better with an *N*-acylmorpholine cap, whereas D-Ala at P3 requires a 3-methyl-1*H*-indene *N*-cap for optimal β_{5i} selectivity. Compounds **9** and **13** show the highest β_{5i} selectivity, indicating that D-Ala/3-methyl-1*H*-indene is preferred over L-Ala/*N*-acylmorpholine for β_{5i} selectivity.

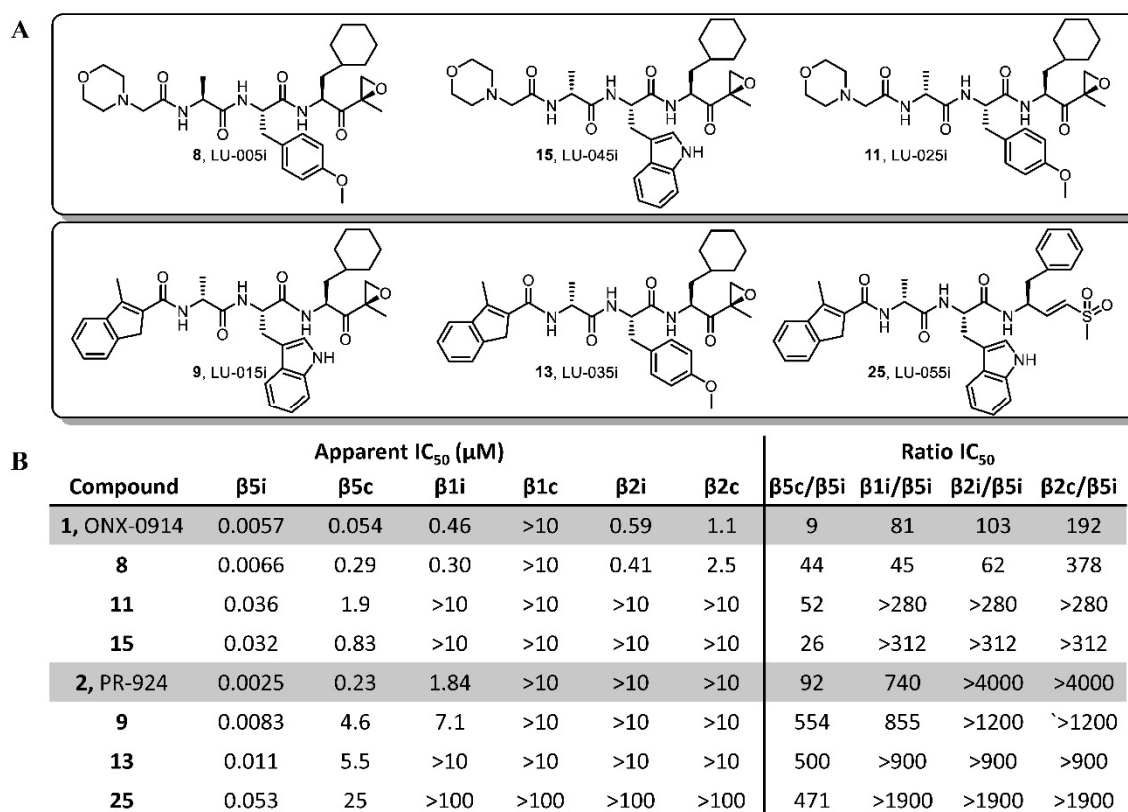


Figure 2. A) Chemical structures of the β 5i inhibitors which show the largest improvement in β 5i selectivity compared to **1** and **2**. B) Apparent IC₅₀ values of compounds in Raji cell lysates as determined by ABPP.

As previously reported, subunit selectivity of proteasome inhibitors can be influenced by the electrophilic trap.^{11, 12} For example, exchanging the epoxyketone warhead by a vinyl sulfone in β 5-selective inhibitors improves β 5-selectivity.¹¹ Based on these results, epoxyketones **1**, **2**, **8** and **9** were compared with their vinyl sulfone counterparts **23**, **24**, **25** and **26** (Table 1). All tested peptide epoxyketones outperform their peptide vinyl sulfone analogues where it comes to β 5i inhibition potency. Of the peptide vinyl sulfone series only **25** is a moderately potent β 5i inhibitor, however with four times higher selectivity for β 5i compared to **2**.

The six most specific and potent epoxyketone compounds, namely **8**, **9**, **11**, **13**, **15** and the vinyl sulfone **25** were evaluated for selectivity over the other subunits, i.e. β 1c/ β 1i and β 2c/ β 2i using ABPP in Raji cell lysates with β 1c/ β 1i selective probe BODIPY(FL)-NC001 and pan-reactive probe BODIPY(TMR)-epoxomicin (Figure 2).³⁵ The obtained results disclose that **8** targets β 1i and β 2i with slightly more potency than **1**, while β 1c is completely unaffected. Compound **2** and to a lesser extent **9** also co-inhibit β 1i in the low micromolar range, whereas compounds **11**, **13**, **15** and **25** are highly specific for β 5c/ β 5i and do not inhibit β 1c/ β 1i and β 2c/ β 2i at concentrations up to 10 μ M.

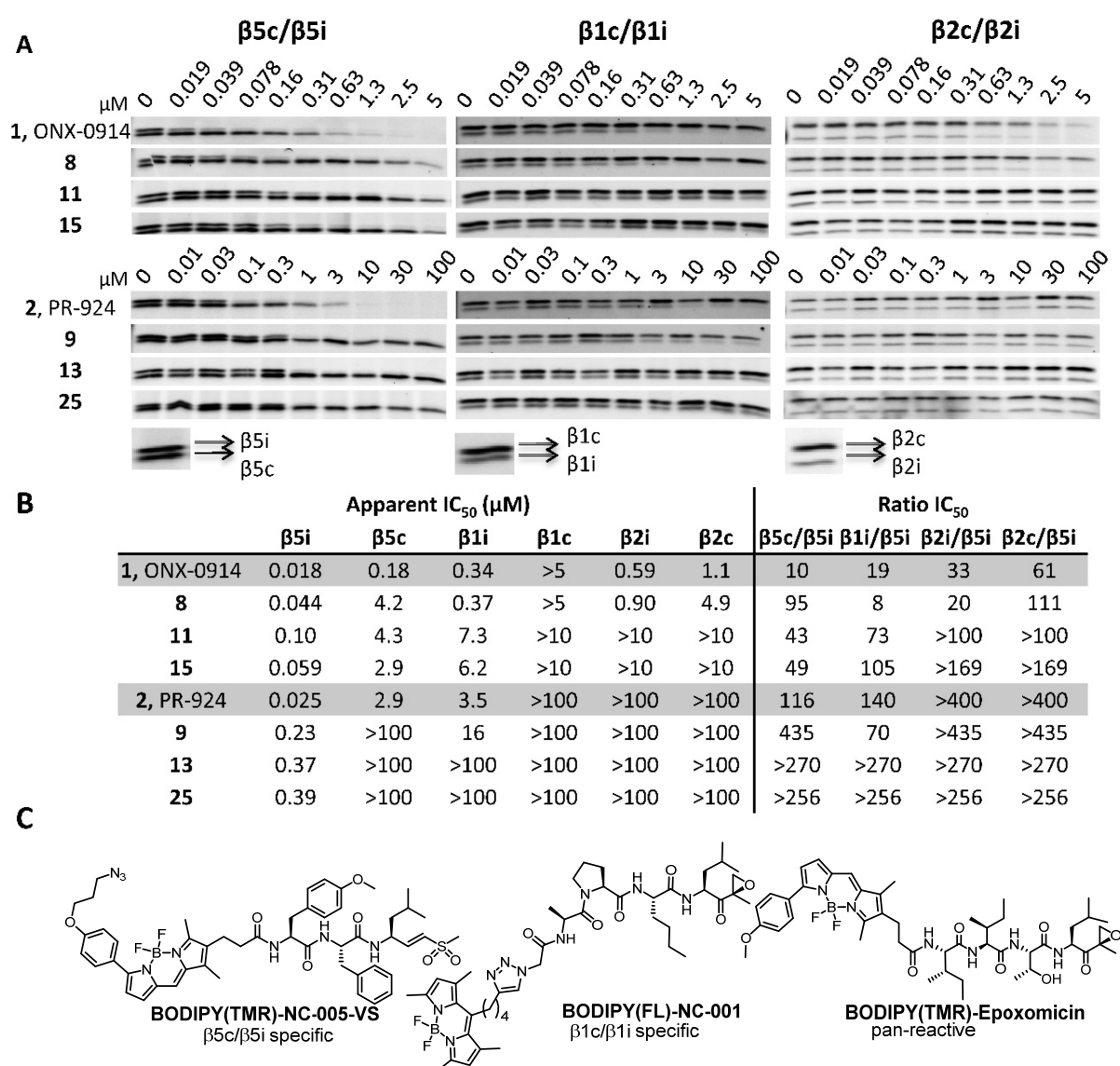


Figure 3. Evaluation of selected β5i inhibitors in RPMI-8226 cells. Inhibition profiles of β5i inhibitors (A), which are used to determine apparent IC₅₀ values (B). Cells were treated with the distinct compounds at indicated concentrations for 1 h, lysed and the occupancy of the remaining active sites was probed with BODIPY(TMR)-NC-005-VS (β5), BODIPY(TMR)-Epoxomicin (pan-reactive, used for β2) or BODIPY(FL)-NC-001 (β1) (C).

Next, the cellular potency and selectivity of **8**, **9**, **11**, **13**, **15** and **25** in RPMI-8226 (MM-cell line) was tested (Figure 3). All inhibitors proved to be cell-permeable and selectivity trends resemble those observed in Raji lysates. Compound **8** exhibits an increased selectivity for β5i over β5c compared to **1**. Notably, it also favours β1i and β2i over β5c, making it a broad-spectrum immunoproteasome inhibitor, when applied at a concentration of 1 μM. As far as known, this is the first proteasome inhibitor able to selectively inhibit all three iCP subunits over their constitutive counterparts. Although the potency of the D-alanine containing compounds **11** and **15** towards β5i is decreased by a factor of 3-5, they are 4 times more selective for β5i than **1**. Moreover, the analogues **9**, **13** and **25** are >10 times less reactive

towards β 5i compared to **2**. However, in case of **13** and **25** all other subunits remain fully active up to 100 μ M (Figure 3). In conclusion, compounds **9**, **13** and **25** are the most selective β 5i inhibitors known to date.

X-ray structures of β 5i specific inhibitors in complex with the yeast CP

The compounds **2**, **8**, **9**, **11** and **17** complexed with γ CP were further analyzed by X-ray crystallography. Despite the high concentrations used for crystal soakings the D-Ala-featuring inhibitors **2**, **9**, **11** and **17** solely target subunit $\gamma\beta$ 5. In contrast, **1** (P3-L-Ala) was shown to inhibit all three active sites of the γ CP²⁸ and its cyclohexyl analogue **8** (L-Ala) occupies at least the subunits $\gamma\beta$ 5 and $\gamma\beta$ 2. The P3-D-Ala residue hence confers selectivity for the chymotrypsin-like active sites, which is consistent with the ABPP results in Raji cell lysate and RPMI-8226 cell assays (Figures 2 and 3). Structural modelling by superposition with the murine substrate binding channels, which are built up of the two neighbouring subunits β 1/2, β 2/3 and β 5/6, respectively, provide explanations for this subunit preference (Sequence numbering according to Huber *et al.*²⁸).

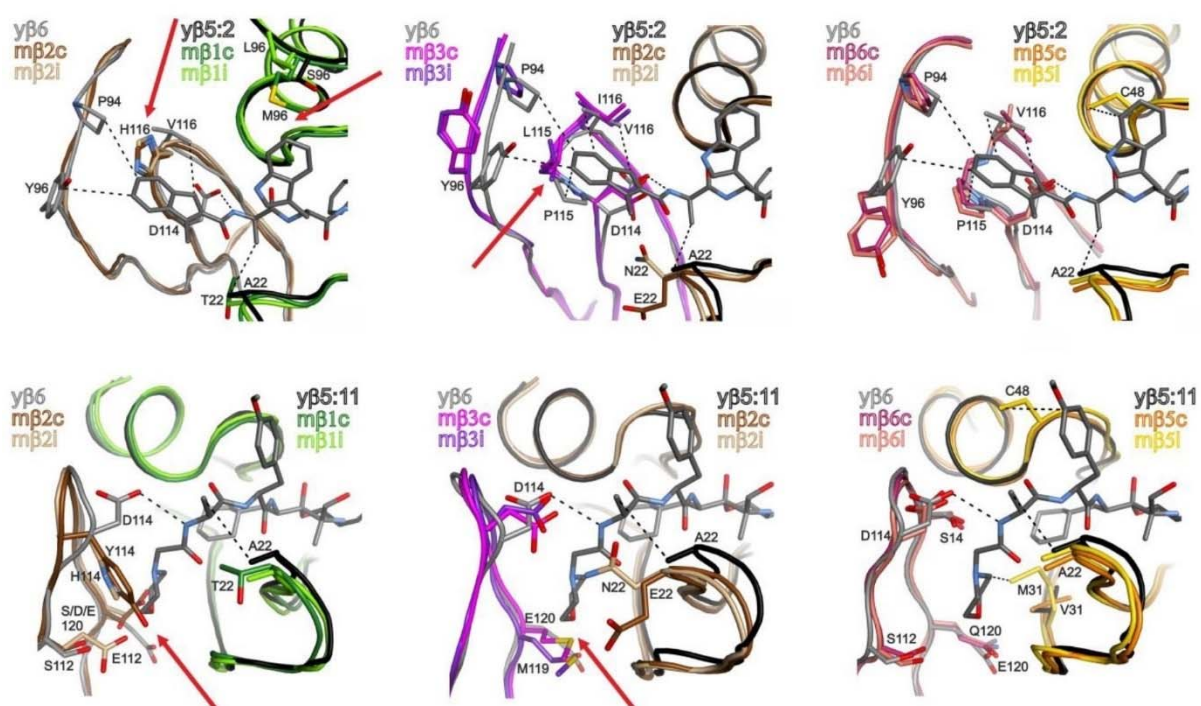


Figure 4. Superposition of $\gamma\beta$ 5:ligand complexes onto murine β 1 and β 2 subunits. Superposition's of the $\gamma\beta$ 5/6 substrate binding channel in complex with **2** and **11** onto the $m\beta$ 1/2 (left panel), $m\beta$ 2/3 (middle) and $m\beta$ 5/6 (right) active sites of the murine cCP and iCP provide structural insights into the β 5i selectivity of **2** and **11** (as well as **9** and **17**). Steric clashes with surrounding amino acids (red arrows) prevent/impair binding to the $m\beta$ 1 and $m\beta$ 2 subunits. Hydrophobic interactions and hydrogen bonds are marked by black dotted lines.

The compounds **11** and **17** do not properly fit into the $\beta 1/\beta 2$ substrate binding channels due to clashes of their N-caps with Glu112 ($\beta 2i$; 1.8 Å), His114/Tyr114 ($\beta 2i/c$; 2.7-3.1 Å) and Asp120 ($\beta 2c$; direct contact) (Figure 4). Inhibition of the more polar caspase-like $\gamma\beta 1/\beta 1c$ active sites is further disfavoured by the hydrophobicity of the ligand. In addition, modelling **11** into the $\beta 2/3$ substrate binding channel depicts that the *N*-acylmorpholine cap clashes with Met119 ($\beta 3$) (distance 1.3-2.3 Å), thereby preventing its binding.

Compound **2** and its derivative **9** preferentially bind to the subunits $\gamma\beta 5$, $\beta 5c/i$ and $\beta 1i$, a fact that is mostly due to the favourable interactions between their hydrophobic P1 sites and the respective protein S1 pockets. Compared to $\beta 5$ subunits, the affinity for $\beta 1$ active sites is reduced by a clash with His116.

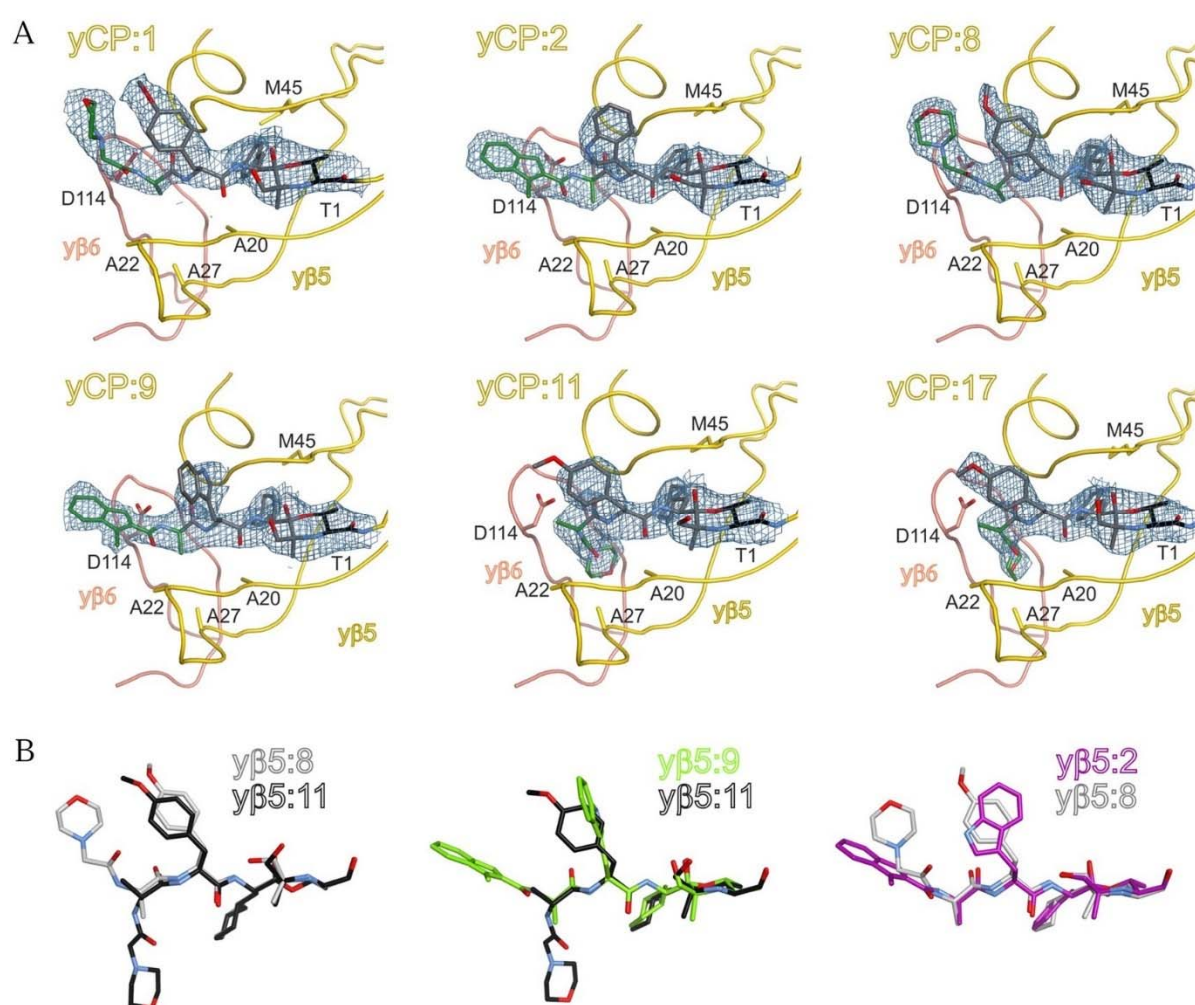


Figure 5. Crystallographic analysis of yCP:ligand complexes. A) Illustration of the yeast $\gamma\beta 5/6$ substrate binding channel in complex with the indicated compounds. All inhibitors are covalently bound to Thr1 (black) of subunit $\gamma\beta 5$ (yellow). Depending on the compound, the P3 site and the N-cap (marked in green) adopt different conformations. The $2F_o - F_c$ electron density map for the ligand (blue) is contoured at 1σ . The inhibitor and Thr1 have been omitted prior to phasing. B) Inversion of the P3-chirality from L to D results in a flip of the *N*-acylmorpholine cap. While *N*-acylmorpholine capped compounds adopt a bended conformation, 3-methyl-1*H*-indene *N*-capped inhibitors bind in an extended form due to their restricted flexibility.

Polarity reasons and steric hindrance with Met96 (2.3 Å) further impair binding to the $\gamma\beta$ 1/ β 1c active sites. A clash of the 3-methyl-1*H*-indene cap with Leu115 (β 3; 2.0-2.3 Å) as well as Asn22 (β 2i; 2.6 Å) leads to reduced affinity also for the β 2/3 substrate binding channel (Figure 4).

In agreement with the β 5-selectivity of the investigated compounds, no clashes with residues from the β 5/6 substrate binding channels in cCP or iCP were identified. Inspection of the 2F_O-F_C electron density maps, however, revealed pronounced differences in the binding mode of **1** and **8** compared to **11** and **17** as well as **2** and **9**. Compound **8** adopts a conformation, which is identical to **1**²⁸, whereas this does not apply to **11** and **17**, the P3-D-Ala analogues of **1** and **8** (Figure 5). The inverted chirality induces a sharp (almost 90°) turn in the peptide backbone of **11** and **17** and forces their P3 site as well as their *N*-acylmorpholine cap to undergo unique interactions. By contrast, binding of **2** and its analogue **9**, both featuring a D-Ala at P3 in combination with a 3-methyl-1*H*-indene cap is comparable to that of **1** and **8** (Figure 5).

Development of β 1i specific inhibitors

The crystal structures of the murine cCP and iCP depict differences between the substrate binding channels of β 1c and β 1i to exist predominantly in the S1 and S3 pockets.²⁸ As a result of the substitutions T20V, T31F, R45L and T52A in β 1i (relative to β 1c), the cleavage preference for acidic residues at P1 is largely abolished, while processing after hydrophobic amino acids is enhanced.⁵ Furthermore, the S1 and S3 pockets appear diminished in size when compared to β 1c and the S3 pocket is more polar than in β 1c.

For the development of β 1i specific inhibitors, az-NC001¹⁵ (**3**), a potent β 1c/ β 1i -specific ligand was chosen as starting point (Figure 1B). Since the β 1c/ β 1i selectivity of **3** appears to be governed by the turn-inducing P3-proline residue (see chapter 4), seven analogues of **3** (**27-33**) in which Pro was substituted for proline isosters were evaluated (Figure 6A). With the aim to increase the polarity of the P3 residue, hydroxyproline (Hyp) (**27**) and thioproline (Thz) (**28**) were selected. The optimal ring size was determined by comparing L-azetidine-2-carboxylic acid (Aze, 4-membered ring) (**29**) and L-pipecolic acid (Pip, 6-membered ring) (**30**). Fluorinated proline analogues **31**, **32** and **33** were included to probe the effect of altering *cis/trans* ratios around the peptide bonds.^{38, 39}

The analogues **27-33** were evaluated by ABPP for blockage of β 1c and β 1i in Raji lysates (Figure 6B). As anticipated, **32** (P3 = *R*-4FPro) was found to be about tenfold more potent than **31** (P3 = *S*-4FPro), however, the affinity was not increased compared to **3**. Interestingly, **33** (P3 = 4,4-F₂Pro) showed a clear preference for β 1i versus β 1c, without loss of potency.

To further enhance $\beta 1i$ selectivity the P1 side chain was modified. During the evaluation of the $\beta 5i$ specific inhibitors, it was observed that compounds bearing a phenyl or cyclohexyl residue at P1 inhibit $\beta 1i$ much stronger than $\beta 1c$ (Figure 2B), confirming that the S1 pocket of $\beta 1i$ is more apolar than that of $\beta 1c$.²⁸ In addition, neither $\beta 1c$ nor $\beta 1i$ is inhibited by compounds featuring a biphenyl substituent at P1 (data not shown), a finding that supports structural data showing that $\beta 1c/i$ have a smaller S1 pocket than $\beta 5c/i$.²⁸ Hence, a series of analogues of **3** with phenyl or cyclohexylalanine in P1 and Pro or 4,4-F₂Pro in P3 were synthesized (Figure 7A). Compound **34** (P1 = Phe) binds to $\beta 1i$ without loss of potency compared to **3**, indicating that bulky residues in P1 are tolerated by $\beta 1i$ (Figure 7C). Substitution of the phenylalanine moiety for cyclohexylalanine (as in **35**) further increases the selectivity by a factor of four. Combining bulky residues in P1 with 4,4-F₂Pro in P3 resulted in the compounds **36** and **37**, of which the latter showed 250-fold selectivity for $\beta 1i$ over $\beta 1c$. In RPMI-8226 cells as well as Raji lysate, **37** is selective for $\beta 1i$ and as potent as **3** (Figure 7D). Finally, **37** was compared to the epoxyketone UK-101 (**38**)^{40, 41}, the so far only $\beta 1i$ specific irreversible inhibitor (ML-604440⁴² is the only other $\beta 1i$ inhibitor reported, which is equipped with the reversible boronic acid warhead) (Figure 7B). In Raji lysate, the potency of UK-101 (**38**) for $\beta 1i$ is comparable to **37**, however, it is about two-fold less specific for $\beta 1i$ and also targets $\beta 5c/\beta 5i$ before $\beta 1c$ (Figure 7C). In conclusion, **37** is the most specific and cell-permeable non-reversible $\beta 1i$ inhibitor known to date.

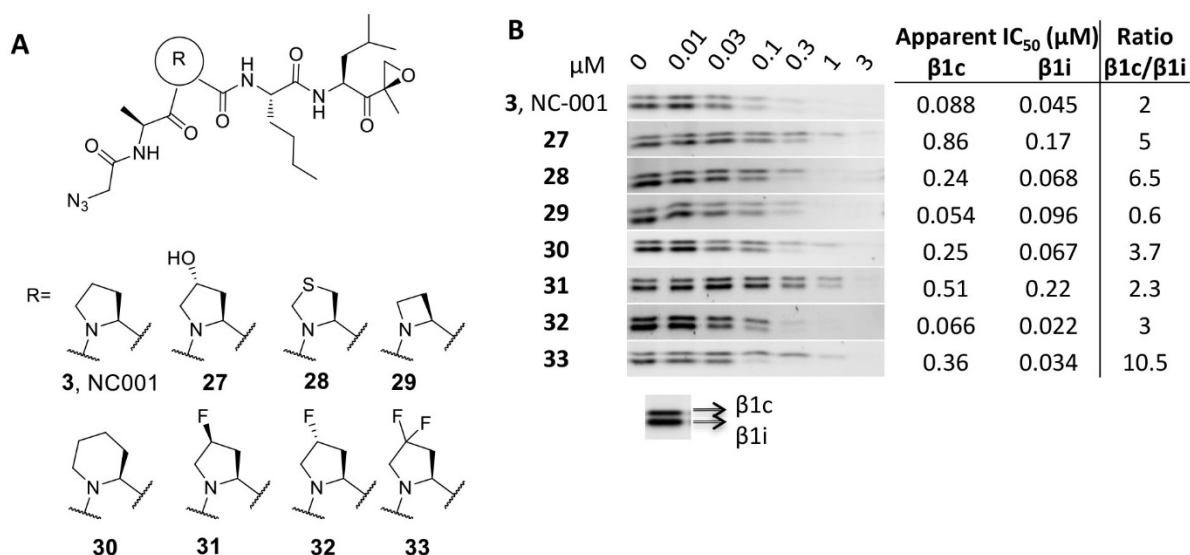


Figure 6. Inhibition profiles of P3 proline analogues of **3 in Raji lysates.** A) Chemical structures of compounds 27-33. B) After incubation of compounds with Raji lysates for 1h, $\beta 5$ activity was blocked by NC-005 for an additional hour. Subsequently, the remaining $\beta 1$ activity was probed by BOPIPY(FL)-NC-001.

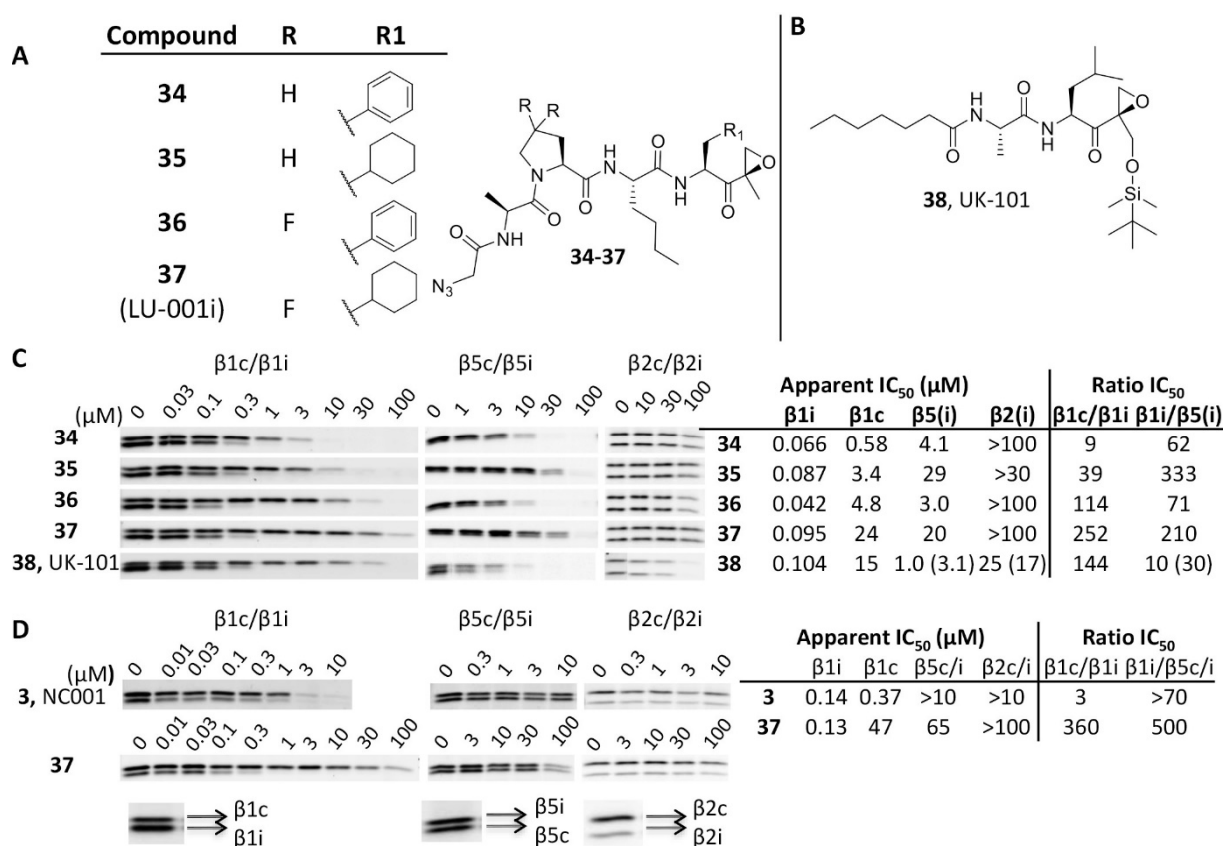


Figure 7. Optimization of β 1i selective inhibitors. A) Chemical structures of compounds 34-37. B) Chemical structure of 38 (UK101). C) Raji lysates were incubated with the compounds for 1h, followed by cell lysis. Lysates were probed with BODIPY-NC005 (β 5), BODIPY-NC001 (β 1) or BODIPY-epoxomicin (pan-reactive, used for β 2). D) Assay of the most selective β 1i inhibitor 37, compared to 3 in RPMI-8226-cells.

Discussion/conclusion

This chapter describes the development of improved β 5i inhibitors as well as a new class of β 1i inhibitors, using design parameters derived from previously determined crystal structures.^{2-5, 43} The co-crystallization of the β 5i inhibitor ONX-0914 (**1**) with the murine cCP and iCP showed that the subunit-selectivity of **1** is mainly caused by the P1 phenyl ring.²⁸ This feature causes major structural rearrangements in the backbone and the S1 pocket of the β 5c subunit, whereas β 5i is able to accommodate the aromatic ring without pronounced conformational changes. Hence, it was hypothesized that larger P1 residues would further disfavor binding to β 5c and enhance potency as well as selectivity for β 5i. Indeed, large residues such as biphenyl (**5**) and 2-naphthyl (**6**) in P1 yielded more potent β 5i inhibitors. Yet, the 1-naphthyl derivative (**7**) resulted in a 40-fold drop in activity and the adamantyl analogue (**4**) was not active at all. Interestingly, β 5i selectivity is enhanced by the 2-naphthyl (**6**; three-fold) and cyclohexyl (**8**; four-fold) P1 side chains. Notably, this is due to the reduced affinity for subunit β 5c. These observations indicate that only certain bulky P1 residues improve β 5i

selectivity and that the difference in the S1 pockets between β 5c and β 5i are not in their linear depth but in their bottom. This is in agreement with the X-ray structures of the murine cCP in complex with ONX-0914 (**1**), which showed that Met45 forming the bottom of the S1 pocket is displaced upon ligand docking. From a structural point of view binding of both cyclohexyl and phenyl moieties to the S1 pocket of the $\gamma\beta$ 5 subunit is identical, yet, further analysis essentially requires crystal structures of the human cCP and iCP (in complex with the investigated compounds). Removing the aromatic system tends to increase the IC₅₀ values in both the β 5c and β 5i active sites, indicating that the π -system might interact with the sulphur of Met45 and that the strength of this contact depends on its orientation. Inverting the chirality of the P3 residue can also significantly impact β 5-affinity and selectivity. Furthermore, the γ CP complex structures provide detailed explanation for the β 5-selectivity of the D-Ala/3-methyl-1*H*-indene compounds.

Based on the observation that the β 5i inhibitors preferentially target β 1i over β 1c at higher concentrations, the P1 leucine epoxyketone of the β 1c/ β 1i specific inhibitor NC-001 was substituted for either phenylalanine or cyclohexylalanine epoxyketone. The resulting compounds were indeed more specific for subunit β 1i. Since the mouse cCP and iCP crystal structures show subtle differences between the S3 pockets of β 1c and β 1i, a P3 Pro analogue scan using **3** as a template was performed. This analysis revealed that the 4,4F₂-Pro (**33**) induces β 1i selectivity without loss of activity. Combination of the cyclohexylalanine and the 4,4F₂-Pro ultimately led to compound **37**, which has a >300 fold binding preference for β 1i over all other subunits in RPMI-8226 cells.

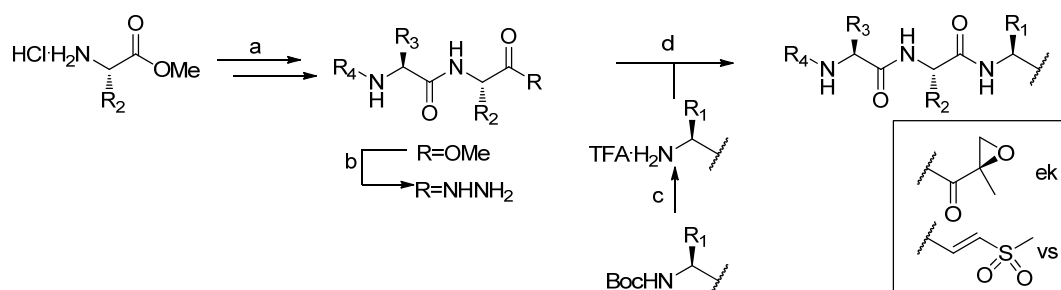
The set of improved subunit-specific and cell-permeable β 5i and β 1i inhibitors represent a useful tool to investigate the cytotoxic effect of subunit-specific proteasome inhibition in MM cells and disease models, for which controversial data exist.^{33,37}

Experimental

Synthetic procedures

General procedures

Acetonitrile (ACN), dichloromethane (DCM), N,N-dimethylformamide (DMF), methanol (MeOH), diisopropylethylamine (DiPEA) and trifluoroacetic acid (TFA) were of peptide synthesis grade, purchased at Biosolve, and used as received. All general chemicals (Fluka, Acros, Merck, Aldrich, Sigma, Iris Biotech) were used as received. Traces of water were removed from reagents used in reactions that require anhydrous conditions by co-evaporation with toluene. Solvents that were used in reactions were stored over 4 Å molecular sieves, except methanol and acetonitrile which were stored over 3 Å molecular sieves. Column chromatography was performed on Screening Devices b.v. Silica Gel, with a particle size of 40-63 μ m and pore diameter of 60 Å. The eluents toluene, ethyl acetate and petroleum ether (40-60 °C boiling range) were distilled prior to use. TLC analysis was conducted on Merck aluminium sheets (Silica gel 60 F254). Compounds were visualized by UV absorption (254 nm), by spraying with a solution of $(\text{NH}_4)_6\text{Mo}_7\text{O}_{24}\cdot 4\text{H}_2\text{O}$ (25 g/L) and $(\text{NH}_4)_4\text{Ce}(\text{SO}_4)_4\cdot 2\text{H}_2\text{O}$ (10 g/L) in 10% sulphuric acid, a solution of KMnO_4 (20 g/L) and K_2CO_3 (10 g/L) in water, or ninhydrin (0.75 g/L) and acetic acid (12.5 mL/L) in ethanol, where appropriate, followed by charring at ca. 150 °C. ^1H and ^{13}C NMR spectra were recorded on a Bruker AV-400 (400 MHz) or AV-600 (600 MHz) spectrometer. Chemical shifts are given in ppm (δ) relative to tetramethylsilane, CD_3OD or CDCl_3 as internal standard. High resolution mass spectra were recorded by direct injection (2 μ L of a 2 μ M solution in water/acetonitrile 50/50 (v/v) and 0.1% formic acid) on a mass spectrometer (Thermo Finnigan LTQ Orbitrap) equipped with an electrospray ion source in positive mode (source voltage 3.5 kV, sheath gas flow 10, capillary temperature 250 °C) with resolution $R = 60,000$ at m/z 400 (mass range $m/z = 150$ -2,000) and dioctylphthalate ($m/z = 391.28428$) as a "lock mass". The high resolution mass spectrometer was calibrated prior to measurements with a calibration mixture (Thermo Finnigan). Optical rotations were recorded on a Propol automatic polarimeter. LCMS analysis was performed on a Finnigan Surveyor HPLC system with a Gemini C18 50 \times 4.60 mm column (detection at 200-600 nm), coupled to a Finnigan LCQ Advantage Max mass spectrometer with ESI. The applied buffers were H_2O , MeCN and 1.0% TFA in H_2O (0.1% TFA end concentration). Methods used are: 15 min (0 \rightarrow 0.5 min: 10% MeCN; 0.5 \rightarrow 10.5 min: 10% \rightarrow 90% MeCN; 10.5 \rightarrow 12.5 min: 90% MeCN; 12.5 \rightarrow 15 min: 90% \rightarrow 10% MeCN) or 12.5 min (0 \rightarrow 0.5 min: 10% MeCN; 0.5 \rightarrow 8.5 min: 10% \rightarrow 90% MeCN; 8.5 \rightarrow 10.5 min: 90% MeCN; 10.5 \rightarrow 12.5 min: 90% \rightarrow 10% MeCN). HPLC purification was performed on a Gilson HPLC system coupled to a Phenomenex Gemini 5 μ m 250 \times 10 mm column and a GX281 fraction collector. Boc-Adamantyl-Ala-OH⁴⁴, Boc-Leu-EK, Boc-Phe-EK and Boc-Phe-VS^{21, 30, 45} were synthesized according to literature procedures. All tested compounds are >95% pure on the basis of LC-MS and NMR.



Scheme S1. General synthetic route towards peptide-epoxyketones and peptide vinylsulfones. Reagent and conditions: (a). Sequential peptide coupling/Boc or Fmoc removal. Peptide coupling: HCTU, DiPEA, Boc-AA-OH/Fmoc-AA-OH, DCM. Boc-removal: TFA/DCM. Fmoc-removal: THF, DBU, EtSH; (b) $\text{NH}_2\text{NH}_2\cdot\text{H}_2\text{O}$, MeOH; (c) TFA; (d) i) $t\text{BuONO}$, HCl, DMF, DCM, -30°C; ii) amine (warhead), DiPEA, -30°C \rightarrow RT.

General procedure for azide couplings.

Compounds **4-37** were prepared via azide coupling of properly protected tripeptide hydrazide and properly deprotected vinyl sulfone amines and epoxyketone amines. The appropriate hydrazide was dissolved in 1:1 DMF:DCM (v/v) and cooled to -30 °C. *t*BuONO (1.1 equiv.) and HCl (4M solution in 1,4-dioxane, 2.8 equiv.) were added, and the mixture was stirred for 3h at -30 °C after which TLC analysis (10% MeOH/DCM, v/v) showed complete consumption of the starting material. The epoxyketone or vinyl sulfone as a free amine was added to the reaction mixture as a solution in DMF. DiPEA (5 equiv.) was added to the reaction mixture, and this mixture was allowed to warm to RT slowly overnight. The mixture was diluted with EtOAc and extracted with H₂O (3×). The organic layer was dried over MgSO₄ and purified by flash column chromatography (1-5% MeOH in DCM) and HPLC-purification (if necessary).

General procedure for peptide couplings

Free acid (1.2 equiv.), HCTU (1.2 equiv.) and free amine (1 equiv.) are dissolved in DCM (0.1 M), followed by the addition of DiPEA (3.5 equiv or 4.5 equiv in case of 2-morpholinoacetic acid HCl). After stirring overnight (or alternatively 1-3 hours, until completion), the reaction mixture is concentrated and re-dissolved in EtOAc, washed with 1 N HCl (2x), sat. NaHCO₃ (2x) and brine (in case of morpholino acetic acid coupling, no 1N HCl washings). The organic layer is dried over Na₂SO₄, filtered and concentrated, followed by purification by column chromatography.

General procedure for Boc removal

Boc protected compounds were treated with TFA (0.1 M) for 30 minutes, followed by co-evaporation with toluene (2x).

Standard procedures amino acid epoxyketone synthesis

A. Boc-AA-N(OMe)Me

To a solution of Boc-AA-OH (1 equiv.) in DCM are added HCTU (1.2 equiv.), N,O,-dimethylhydroxylamine (2 equiv.) and DiPEA (3.5 equiv.). After completion of the reaction (1 h to overnight), the solvent is removed. The residue is dissolved in EtOAc and washed with 1M HCl (2x), sat aq NaHCO₃ (2x), brine and dried over Na₂SO₄, filtered and concentrated. The crude product is purified by column chromatography (EtOAc /pent).

B. Boc-AA-C(CH₃)=CH₂

To a solution of 2-bromopropene (3 equiv.) in Et₂O at -78°C is added *t*BuLi (4.5 equiv, from 1.7 M in pent) in 10 min. After stirring for 15 min. at -78°C, the Weinreb amide (1 equiv.) in Et₂O is added slowly in 10 min. The reaction mixture is stirred for 2-4 h, while warming up to max. -40°C. After TLC analysis revealed completion of the reaction, the reaction is quenched by the addition of sat. NH₄Cl and warmed to RT. The mixture is transferred to a separatory funnel and the water layer is extracted with EtOAc (3X). The combined organic layers are washed with brine, dried over Na₂SO₄, filtered and concentrated. The crude product is purified by column chromatography (EtOAc /pent mixtures).

C. Boc-AA-OH-C(CH₃)=CH₂

To a solution of alkene **B** (1 equiv.) in MeOH is added CeCl₃·7H₂O (1.6 equiv.) and the mixture is stirred at RT. After the solution became clear, the mixture is cooled to 0°C and NaBH₄ (1.3 equiv.) is added in portion in 10 min. After TLC analysis showed completion of the reaction (about 30 min), the reaction is quenched by the addition of AcOH. The mixture is stirred for 15 min. followed by the addition of toluene and removal of the solvent. The residue is redissolved in a H₂O/ EtOAc mixture, which is then transferred to a separatory funnel. The layers were separated and the aqueous layer was extracted with EtOAc (2X). The combined organic layers are washed with brine, dried over Na₂SO₄, filtered and concentrated. The crude product was purified (if necessary) by column chromatography (EtOAc /pent mixtures) .

D. Boc-AA-EK

To a solution of alcohol **C** in DCM at 0°C is added VO(acac)₂ (0.1 equiv.) followed by the addition of tBuOOH (5.5 M in decane, 3 equiv.). The reaction mixture is stirred at 0°C for 2-3 h. after which TLC analysis showed completion of the reaction. The reaction mixture is concentrated, redissolved in EtOAc and washed with 0.5 sat. NaHCO₃ (2x), H₂O and brine. The organic layer is dried over Na₂SO₄, filtered and concentrated. The crude product is added as a solution in DCM to a solution of Dess-Martin-Periodane (1.5-3 equiv.) in DCM at 0°C. After TLC analysis revealed completion of the reaction, the reaction was quenched by the addition of sat. NaHCO₃. The mixture was transferred to a separatory funnel and the layers were separated. The aqueous layer was extracted with DCM (1x) and the combined organics were washed with sat. NaHCO₃ (1x) and brine and dried over Na₂SO₄, filtered and concentrated. The crude product was purified by column chromatography (EtOAc /pent mixtures).

MorphAc-Ala-Tyr(OMe)-Ala(Ada)-EK (4)

This compound was obtained by the general protocol for azide coupling on a 50 μ mol scale. Purification by column chromatography (2 \rightarrow 4% MeOH in DCM) provided the title compound (21.62 mg, 68%) as a white powder after lyophilisation. ¹H NMR (400 MHz, CDCl₃) δ 7.43 (d, *J* = 7.6 Hz, 1H), 7.14 (d, *J* = 8.6 Hz, 2H), 6.92 – 6.66 (m, 3H), 6.14 (d, *J* = 7.5 Hz, 1H), 4.58 – 4.47 (m, 2H), 4.41 (p, *J* = 7.3 Hz, 1H), 3.76 (s, 3H), 3.68 (t, *J* = 4.6 Hz, 4H), 3.32 (d, *J* = 5.0 Hz, 1H), 3.00 – 2.91 (m, 3H), 2.89 – 2.83 (m, 2H), 2.44 (q, *J* = 4.2 Hz, 4H), 1.91 (s, 3H), 1.70 – 1.53 (m, 6H), 1.50 (s, 3H), 1.44 – 1.40 (m, 5H), 1.39 – 1.28 (m, 5H), 1.01 – 0.93 (m, 1H). ¹³C NMR (101 MHz, CDCl₃) δ 207.78, 172.02, 170.31, 170.23, 158.67, 130.54, 128.54, 114.08, 67.03, 61.72, 59.06, 55.33, 54.29, 53.86, 52.54, 48.32, 47.92, 44.66, 42.44, 36.83, 36.62, 32.91, 28.62, 17.66, 17.07. LC-MS (linear gradient 10 \rightarrow 90% MeCN, 0.1% TFA, 15 min): R_t (min): 6.52 (ESI-MS (m/z): 639.6 (M+H⁺)) HRMS: calculated for C₃₅H₅₀N₄O₇ 639.37523 [M+2H]²⁺; found 639.37524

MorphAc-Ala-Tyr(OMe)-BiPhe-EK (5)

This compound was obtained by the general protocol for azide coupling on a 50 μ mol scale. Purification by column chromatography (2 \rightarrow 4% MeOH in DCM) provided the title compound (21.18 mg, 64.5%) as a white powder after lyophilisation. ¹H NMR (400 MHz, CDCl₃) δ 7.59 – 7.51 (m, 2H), 7.51 – 7.38 (m, 5H), 7.34 (d, *J* = 7.3 Hz, 1H), 7.09 (dd, *J* = 8.4, 3.2 Hz, 4H), 6.77 (d, *J* = 8.6 Hz, 2H), 6.68 (d, *J* = 7.5 Hz, 1H), 6.36 (d, *J* = 7.3 Hz, 1H), 4.77 (td, *J* = 7.9, 4.7 Hz, 1H), 4.50 (t, *J* = 7.1 Hz, 1H), 4.34 (t, *J* = 7.2 Hz, 1H), 3.73 (s, 3H), 3.67 (t, *J* = 4.5 Hz, 4H), 3.29 (d, *J* = 4.9 Hz, 1H), 3.12 (dd, *J* = 14.1, 4.6 Hz, 1H), 2.98 – 2.78 (m, 5H), 2.73 (dd, *J* = 14.1, 8.3 Hz, 1H), 2.44 – 2.38 (m, 4H), 1.51 (s, 3H), 1.26 (d, *J* = 7.0 Hz, 3H). ¹³C NMR (101 MHz, CDCl₃) δ 207.02, 171.96, 170.52, 170.30, 158.69, 140.66, 140.05, 134.76, 130.52, 129.76, 128.89, 128.33, 127.44, 127.32, 127.09, 114.11, 67.02, 61.68, 59.36, 55.30, 54.32, 53.82, 52.75, 52.65, 48.39, 36.79, 36.65, 17.69, 16.69. LC-MS (linear gradient 10 \rightarrow 90% MeCN, 0.1% TFA, 15 min): R_t (min): 7.05 (ESI-MS (m/z): 657.13 (M+H⁺)). HRMS: calculated for C₃₇H₄₄N₄O₇ 657.32828 [M+H]⁺; found 657.32831

MorphAc-Ala-Tyr(OMe)-2-Nal-EK (6)

This compound was obtained by the general protocol for azide coupling on a 50 μ mol scale. Purification by column chromatography (2 \rightarrow 4% MeOH in DCM) followed by purification by HPLC (20-70% MeCN, 0.1 % TFA, 10 min gradient) provided the title compound (13.75 mg, 43.5%) as a white powder after lyophilisation. ¹H NMR (400 MHz, CDCl₃) δ 7.82 – 7.70 (m, 3H), 7.49 – 7.34 (m, 4H), 7.18 (dd, *J* = 8.4, 1.6 Hz, 1H), 7.06 (d, *J* = 8.6 Hz, 2H), 6.75 (d, *J* = 8.6 Hz, 2H), 6.61 (d, *J* = 7.5 Hz, 1H), 6.33 (d, *J* = 7.2 Hz, 1H), 4.88 – 4.78 (m, 1H), 4.46 (q, *J* = 7.0 Hz, 1H), 4.31 – 4.22 (m, 1H), 3.74 (s, 3H), 3.67 (t, *J* = 4.5 Hz, 4H), 3.34 – 3.20 (m, 2H), 2.96 – 2.75 (m, 6H), 2.45 – 2.37 (m, 4H), 1.50 (s, 3H), 1.15 (d, *J* = 7.1 Hz, 3H). ¹³C NMR (101 MHz, CDCl₃) δ 207.03, 171.89, 170.48, 170.25, 158.68, 133.43, 133.21, 132.53, 130.53, 128.39, 128.34, 128.01, 127.80, 127.63, 127.25, 126.36, 125.95, 114.10, 67.01, 61.67, 59.42, 55.33, 54.31, 53.81, 52.74, 52.67, 48.38, 37.26, 36.82, 17.59, 16.69. LC-MS (linear gradient 10 \rightarrow 90% MeCN, 0.1% TFA, 15 min): R_t (min): 6.60 (ESI-MS (m/z): 631.20 (M+H⁺)). HRMS: calculated for C₃₅H₄₂N₄O₇ 631.31263 [M+H]⁺; found 631.31262

MorphAc-Ala-Tyr(OMe)-1-Nal-EK (7)

This compound was obtained by the general protocol for azide coupling on a 50 μmol scale. Purification by column chromatography (2 \rightarrow 4% MeOH in DCM) followed by purification by HPLC (20-70% MeCN, 0.1% TFA, 10 min gradient) provided the title compound (9.51 mg, 30.1%) as a white powder after lyophilisation. ^1H NMR (400 MHz, CDCl_3) δ 8.17 (d, J = 8.3 Hz, 1H), 7.85 (d, J = 7.5 Hz, 1H), 7.74 (d, J = 8.3 Hz, 1H), 7.60 – 7.46 (m, 2H), 7.40 (d, J = 7.5 Hz, 1H), 7.30 (dd, J = 8.1, 7.1 Hz, 2H), 7.12 (d, J = 8.6 Hz, 2H), 6.97 (d, J = 6.7 Hz, 1H), 6.82 (d, J = 8.6 Hz, 2H), 6.54 (d, J = 7.3 Hz, 1H), 6.09 (d, J = 6.6 Hz, 1H), 4.83 (ddd, J = 9.8, 6.6, 4.7 Hz, 1H), 4.42 – 4.26 (m, 2H), 3.79 (s, 3H), 3.72 – 3.57 (m, 5H), 3.33 (d, J = 4.9 Hz, 1H), 2.97 – 2.78 (m, 6H), 2.43 (s, 4H), 1.51 (s, 3H), 1.24 (d, J = 7.1 Hz, 3H). ^{13}C NMR (101 MHz, CDCl_3) δ 207.37, 171.79, 170.29, 158.76, 134.01, 132.02, 131.85, 130.64, 129.03, 128.53, 128.32, 127.53, 126.71, 126.10, 125.25, 123.65, 114.14, 67.04, 61.71, 59.54, 55.39, 54.36, 53.84, 52.79, 52.08, 48.33, 37.10, 34.63, 17.80, 16.61. LC-MS (linear gradient 10 \rightarrow 90% MeCN, 0.1% TFA, 15 min): R_t (min): 6.56 (ESI-MS (m/z): 631.13 ($\text{M}+\text{H}^+$)). HRMS: calculated for $\text{C}_{35}\text{H}_{42}\text{N}_4\text{O}_7$ 631.31263 [$\text{M}+\text{H}^+$] $^+$; found 631.31262

MorphAc-Ala-Tyr(OMe)-Cha-EK (8)

This compound was obtained by the general protocol for azide coupling on a 50 μmol scale. Purification by column chromatography (2 \rightarrow 4% MeOH in DCM) provided the title compound (21.88 mg, 74.5%) as a white powder after lyophilization. ^1H NMR (400 MHz, CDCl_3) δ 7.45 (d, J = 7.5 Hz, 1H), 7.10 (d, J = 8.6 Hz, 2H), 6.85 – 6.69 (m, 3H), 6.27 (d, J = 7.7 Hz, 1H), 4.62 – 4.49 (m, 2H), 4.49 – 4.34 (m, 1H), 3.76 (s, 3H), 3.69 (t, J = 4.5 Hz, 4H), 3.25 (d, J = 5.0 Hz, 1H), 3.03 – 2.91 (m, 3H), 2.90 – 2.81 (m, 2H), 2.49 – 2.38 (m, 4H), 1.85 – 1.51 (m, 6H), 1.49 (s, 3H), 1.35 (d, J = 7.0 Hz, 3H), 1.25 – 1.06 (m, 5H), 0.88 (dd, J = 15.7, 7.9 Hz, 2H). ^{13}C NMR (101 MHz, CDCl_3) δ 208.24, 171.99, 170.71, 170.30, 158.66, 130.50, 128.35, 114.07, 67.03, 61.72, 59.15, 55.31, 54.39, 53.86, 52.51, 49.74, 48.43, 38.63, 36.81, 34.42, 34.02, 31.98, 26.42, 26.33, 26.05, 17.84, 16.83. LC-MS (linear gradient 10 \rightarrow 90% MeCN, 0.1% TFA, 15 min): R_t (min): 6.62 (ESI-MS (m/z): 587.13 ($\text{M}+\text{H}^+$)). HRMS: calculated for $\text{C}_{31}\text{H}_{46}\text{N}_4\text{O}_7$ 587.34393 [$\text{M}+\text{H}^+$] $^+$; found 587.34393.

3MeIndAc-D-Ala-Trp-Cha-EK (9)

This compound was obtained by the general protocol for azide coupling on a 50 μmol scale. Purification by column chromatography (1 \rightarrow 2% MeOH in DCM) provided the title compound (23.45 mg, 75%) as a white powder after lyophilization. ^1H NMR (400 MHz, CDCl_3) δ 8.53 – 8.48 (m, 1H), 7.66 (d, J = 7.8 Hz, 1H), 7.43 (t, J = 7.2 Hz, 2H), 7.38 – 7.28 (m, 3H), 7.17 – 7.02 (m, 4H), 6.61 (d, J = 6.9 Hz, 1H), 6.53 (d, J = 7.7 Hz, 1H), 4.77 (q, J = 7.0 Hz, 1H), 4.55 – 4.45 (m, 2H), 3.54 (s, 2H), 3.29 (dd, J = 14.7, 6.5 Hz, 1H), 3.24 – 3.11 (m, 2H), 2.80 (d, J = 5.0 Hz, 1H), 2.48 (s, 3H), 1.72 – 1.38 (m, 9H), 1.33 (d, J = 7.0 Hz, 3H), 1.20 – 0.97 (m, 5H), 0.80 (d, J = 11.4 Hz, 2H). ^{13}C NMR (101 MHz, CDCl_3) δ 208.40, 172.66, 171.31, 166.10, 148.10, 145.58, 142.28, 136.31, 131.61, 127.48, 127.39, 126.84, 123.91, 123.74, 122.22, 120.90, 119.75, 118.79, 111.38, 110.35, 59.15, 53.85, 52.53, 49.92, 49.27, 38.33, 34.31, 33.90, 31.99, 27.80, 26.38, 26.19, 25.98, 18.46, 16.83, 12.48. LC-MS (linear gradient 10 \rightarrow 90% MeCN, 0.1% TFA, 15 min): R_t (min): 10.36 (ESI-MS (m/z): 625.13 ($\text{M}+\text{H}^+$)). HRMS: calculated for $\text{C}_{37}\text{H}_{44}\text{N}_4\text{O}_5$ 625.33845 [$\text{M}+\text{H}^+$] $^+$; found 625.33844.

3MeIndAc-D-Ala-Trp-BiPhe-EK (10)

This compound was obtained by the general protocol for azide coupling on a 50 μmol scale. Purification by column chromatography (1 \rightarrow 2% MeOH in DCM) provided the title compound (33.13 mg, 95.3%) as a white powder after lyophilisation. ^1H NMR (400 MHz, CDCl_3) δ 8.11 (s, 1H), 7.61 (d, J = 7.8 Hz, 1H), 7.57 – 7.51 (m, 2H), 7.46 – 7.28 (m, 9H), 7.20 (d, J = 8.0 Hz, 1H), 7.13 (t, J = 7.0 Hz, 1H), 7.10 – 6.99 (m, 3H), 6.89 (d, J = 2.2 Hz, 1H), 6.82 (d, J = 7.8 Hz, 1H), 6.72 (d, J = 7.5 Hz, 1H), 6.46 (d, J = 6.5 Hz, 1H), 4.80 – 4.67 (m, 2H), 4.42 (p, J = 6.9 Hz, 1H), 3.52 (dd, J = 7.3, 2.1 Hz, 2H), 3.35 – 3.22 (m, 2H), 3.13 – 2.98 (m, 2H), 2.84 (d, J = 4.9 Hz, 1H), 2.67 (dd, J = 13.8, 8.9 Hz, 1H), 2.48 (t, J = 2.1 Hz, 3H), 1.43 (s, 3H), 1.34 (d, J = 7.0 Hz, 3H). ^{13}C NMR (101 MHz, CDCl_3) δ 207.18, 172.58, 171.09, 166.32, 148.29, 145.55, 142.29, 140.51, 139.56, 136.11, 135.39, 131.49, 129.87, 129.03, 127.54, 127.48, 127.44, 127.11, 126.96, 126.86, 123.93, 123.56, 122.28, 120.95, 119.81, 118.72, 111.34, 110.02, 59.36,

53.56, 53.24, 52.64, 49.58, 38.33, 36.38, 27.47, 18.10, 16.65, 12.51. LC-MS (linear gradient 10 \rightarrow 90% MeCN, 0.1% TFA, 15 min): R_t (min): 10.61 (ESI-MS (m/z): 695.07 (M+H⁺)). HRMS: calculated for C₄₃H₄₂N₄O₅ 695.32280 [M+H]⁺; found 695.32275

MorphAc-D-Ala-Tyr(OMe)-Cha-EK (11)

This compound was obtained by the general protocol for azide coupling on a 50 μ mol scale. Purification by column chromatography (1 \rightarrow 3% MeOH in DCM) provided the title compound (23.19 mg, 79.0%) as a white powder after lyophilisation. ¹H NMR (400 MHz, CDCl₃) δ 7.56 (d, J = 6.9 Hz, 1H), 7.11 (d, J = 8.5 Hz, 2H), 6.81 (d, J = 8.5 Hz, 2H), 6.58 (d, J = 8.1 Hz, 1H), 6.36 (d, J = 7.8 Hz, 1H), 4.65 – 4.48 (m, 2H), 4.34 (t, J = 7.1 Hz, 1H), 3.77 (s, 3H), 3.72 (t, J = 4.5 Hz, 4H), 3.27 (d, J = 5.0 Hz, 1H), 3.10 – 2.91 (m, 4H), 2.86 (d, J = 5.0 Hz, 1H), 2.60 – 2.46 (m, 4H), 1.65 (td, J = 38.0, 37.2, 13.3 Hz, 6H), 1.48 (s, 3H), 1.31 (d, J = 7.0 Hz, 3H), 1.27 – 1.10 (m, 5H), 0.93 – 0.83 (m, 2H). ¹³C NMR (101 MHz, CDCl₃) δ 208.29, 171.77, 170.65, 158.79, 130.54, 128.18, 114.17, 67.06, 61.76, 59.15, 55.34, 54.18, 53.89, 52.46, 49.63, 48.86, 38.48, 37.10, 34.31, 34.02, 32.00, 26.44, 26.28, 26.01, 17.87, 16.81. LC-MS (linear gradient 10 \rightarrow 90% MeCN, 0.1% TFA, 15 min): R_t (min): 6.80 (ESI-MS (m/z): 587.27 (M+H⁺)) HRMS: calculated for C₃₁H₄₆N₄O₇ 587.34393 [M+H]⁺; found 587.34393.

3MeIndAc-Ala-Tyr(OMe)-Cha-EK (12)

This compound was obtained by the general protocol for azide coupling on a 50 μ mol scale. Purification by column chromatography (1 \rightarrow 2% MeOH in DCM) provided the title compound (21.22 mg, 68.9%) as a white powder after lyophilisation. ¹H NMR (400 MHz, CDCl₃) δ 7.53 – 7.43 (m, 2H), 7.42 – 7.31 (m, 2H), 7.06 (d, J = 8.6 Hz, 2H), 6.91 (d, J = 7.8 Hz, 1H), 6.62 (d, J = 8.6 Hz, 2H), 6.44 (d, J = 7.9 Hz, 1H), 6.12 (d, J = 7.0 Hz, 1H), 4.68 – 4.53 (m, 3H), 3.56 – 3.48 (m, 2H), 3.47 (s, 3H), 3.28 (d, J = 5.0 Hz, 1H), 3.00 (d, J = 6.8 Hz, 2H), 2.88 (d, J = 5.0 Hz, 1H), 2.52 (t, J = 2.2 Hz, 3H), 1.84 – 1.53 (m, 5H), 1.50 (s, 3H), 1.43 (d, J = 7.0 Hz, 3H), 1.30 – 1.03 (m, 6H), 0.97 – 0.77 (m, 2H). ¹³C NMR (101 MHz, CDCl₃) δ 208.32, 172.43, 170.89, 166.11, 158.63, 148.85, 145.56, 142.10, 131.03, 130.34, 128.32, 127.64, 127.03, 123.97, 121.04, 113.93, 59.18, 54.97, 54.38, 52.53, 49.72, 48.74, 38.68, 38.21, 36.74, 34.46, 34.02, 32.05, 26.45, 26.33, 26.08, 17.84, 16.85, 12.50. LC-MS (linear gradient 10 \rightarrow 90% MeCN, 0.1% TFA, 15 min): R_t (min): 10.34 (ESI-MS (m/z): 616.13 (M+H⁺)). HRMS: calculated for C₃₆H₄₅N₃O₆ 616.32811 [M+H]⁺; found 616.32813

3MeIndAc-D-Ala-Tyr(OMe)-Cha-EK (13)

This compound was obtained by the general protocol for azide coupling on a 50 μ mol scale. Purification by column chromatography (1 \rightarrow 2% MeOH in DCM) provided the title compound (23.50 mg, 76.3%) as a white powder after lyophilization. ¹H NMR (400 MHz, CDCl₃) δ 7.45 (t, J = 5.7 Hz, 2H), 7.38 – 7.29 (m, 2H), 7.12 (d, J = 8.5 Hz, 2H), 6.94 (d, J = 8.0 Hz, 1H), 6.78 (d, J = 8.5 Hz, 2H), 6.49 (dd, J = 7.4, 2.7 Hz, 2H), 4.70 – 4.47 (m, 3H), 3.70 (s, 3H), 3.58 (s, 2H), 3.24 (d, J = 5.0 Hz, 1H), 3.01 (ddt, J = 22.1, 14.4, 7.6 Hz, 2H), 2.83 (d, J = 5.0 Hz, 1H), 2.51 (s, 3H), 1.78 – 1.45 (m, 5H), 1.43 (s, 3H), 1.38 (d, J = 7.0 Hz, 3H), 1.31 – 0.94 (m, 6H), 0.91 – 0.77 (m, 2H). ¹³C NMR (101 MHz, CDCl₃) δ 208.31, 172.53, 170.87, 166.10, 158.74, 148.39, 145.57, 142.22, 131.44, 130.54, 128.30, 127.48, 126.89, 123.91, 120.94, 114.09, 59.14, 55.25, 54.38, 52.47, 49.74, 49.10, 38.55, 38.32, 37.00, 34.34, 33.97, 31.99, 26.39, 26.24, 25.98, 18.49, 16.79, 12.50. LC-MS (linear gradient 10 \rightarrow 90% MeCN, 0.1% TFA, 15 min): R_t (min): 10.44 (ESI-MS (m/z): 616.13 (M+H⁺)) HRMS: calculated for C₃₆H₄₅N₃O₆ 616.33811 [M+H]⁺; found 616.33813.

3MeIndAc-Ala-Tyr(OMe)-Phe-EK (14)

This compound was obtained by the general protocol for azide coupling on a 50 μ mol scale. Purification by column chromatography (1 \rightarrow 2% MeOH in DCM) provided the title compound (15.31 mg, 50.2%) as a white powder after lyophilisation. ¹H NMR (400 MHz, CDCl₃) δ 7.53 – 7.42 (m, 2H), 7.42 – 7.30 (m, 2H), 7.24 (d, J = 7.3 Hz, 3H), 7.08 – 6.99 (m, 4H), 6.82 (d, J = 7.7 Hz, 1H), 6.62 (d, J = 8.6 Hz, 2H), 6.45 (d, J = 7.5 Hz, 1H), 6.08 (d, J = 7.1 Hz, 1H), 4.84 – 4.74 (m, 1H), 4.59 – 4.47 (m, 2H), 3.53 – 3.45 (m, 5H), 3.29 (d, J = 4.9 Hz, 1H), 3.09 (dd, J = 14.0,

5.0 Hz, 1H), 2.91 (dd, $J = 13.0, 5.9$ Hz, 3H), 2.71 (dd, $J = 13.9, 8.2$ Hz, 1H), 2.53 (t, $J = 2.2$ Hz, 3H), 1.48 (s, 3H), 1.36 (d, $J = 7.0$ Hz, 3H). ^{13}C NMR (101 MHz, CDCl_3) δ 207.21, 172.44, 170.60, 166.09, 158.64, 148.82, 145.58, 142.12, 135.77, 131.08, 130.34, 129.39, 128.65, 128.34, 128.06, 127.63, 127.22, 127.02, 123.97, 121.04, 120.46, 113.97, 59.34, 55.02, 54.34, 52.68, 52.60, 48.63, 38.21, 37.27, 36.75, 17.78, 16.63, 12.50. LC-MS (linear gradient 10 \rightarrow 90% MeCN, 0.1% TFA, 15 min): R_t (min): 9.57 (ESI-MS (m/z): 610.13 ($\text{M}+\text{H}^+$)). HRMS: calculated for $\text{C}_{36}\text{H}_{39}\text{N}_3\text{O}_6$ 610.29116 [$\text{M}+\text{H}$] $^+$; found 610.29114

MorphAc-D-Ala-Trp-Cha-EK (15)

This compound was obtained by the general protocol for azide coupling on a 50 μmol scale. Purification by column chromatography (1 \rightarrow 3% MeOH in DCM) provided the title compound (23.27 mg, 78.1%) as a white powder after lyophilisation. ^1H NMR (400 MHz, CDCl_3) δ 8.35 (s, 1H), 7.67 (d, $J = 7.8$ Hz, 1H), 7.56 (d, $J = 6.9$ Hz, 1H), 7.36 (d, $J = 8.1$ Hz, 1H), 7.23 – 7.07 (m, 3H), 6.77 (d, $J = 7.7$ Hz, 1H), 6.28 (d, $J = 7.7$ Hz, 1H), 4.69 (q, $J = 7.3$ Hz, 1H), 4.53 – 4.43 (m, 1H), 4.36 (p, $J = 7.1$ Hz, 1H), 3.81 – 3.62 (m, 4H), 3.32 (dd, $J = 14.6, 5.7$ Hz, 1H), 3.23 – 3.07 (m, 2H), 2.95 (s, 2H), 2.82 (d, $J = 5.0$ Hz, 1H), 2.50 (tt, $J = 11.7, 7.2$ Hz, 4H), 1.73 – 1.57 (m, 4H), 1.45 (s, 5H), 1.31 (d, $J = 7.0$ Hz, 3H), 1.21 – 1.00 (m, 5H), 0.90 – 0.79 (m, 2H). ^{13}C NMR (101 MHz, CDCl_3) δ 208.33, 171.87, 171.00, 136.31, 127.49, 123.61, 122.40, 119.91, 118.87, 111.42, 110.35, 67.02, 61.74, 59.09, 53.85, 53.80, 52.52, 49.74, 48.85, 38.51, 34.23, 33.94, 31.99, 27.96, 26.41, 26.23, 26.01, 18.02, 16.81. LC-MS (linear gradient 10 \rightarrow 90% MeCN, 0.1% TFA, 15 min): R_t (min): 6.85 (ESI-MS (m/z): 596.20 ($\text{M}+\text{H}^+$)) HRMS: calculated for $\text{C}_{32}\text{H}_{45}\text{N}_5\text{O}_6$ 596.34426 [$\text{M}+\text{H}$] $^+$; found 596.34418.

MorphAc-D-Ala-Trp-Phe-EK (16)

This compound was obtained by the general protocol for azide coupling on a 50 μmol scale. Purification by column chromatography (1 \rightarrow 3% MeOH in DCM) provided the title compound (19.43 mg, 65.9%) as a white powder after lyophilisation. ^1H NMR (400 MHz, CDCl_3) δ 8.15 (s, 1H), 7.64 (d, $J = 7.9$ Hz, 1H), 7.55 (d, $J = 6.2$ Hz, 1H), 7.35 (d, $J = 8.1$ Hz, 1H), 7.23 – 7.05 (m, 5H), 6.92 (d, $J = 2.2$ Hz, 1H), 6.88 (d, $J = 6.4$ Hz, 2H), 6.68 (d, $J = 7.8$ Hz, 1H), 6.42 (d, $J = 7.5$ Hz, 1H), 4.66 (p, $J = 7.6$ Hz, 2H), 4.30 (p, $J = 7.0$ Hz, 1H), 3.78 – 3.60 (m, 4H), 3.30 (dd, $J = 14.7, 5.2$ Hz, 1H), 3.22 (d, $J = 4.9$ Hz, 1H), 3.05 (dd, $J = 14.6, 7.3$ Hz, 1H), 2.97 – 2.89 (m, 3H), 2.84 (d, $J = 4.9$ Hz, 1H), 2.61 (dd, $J = 13.8, 8.4$ Hz, 1H), 2.56 – 2.38 (m, 4H), 1.42 (s, 3H), 1.31 (d, $J = 7.0$ Hz, 3H). ^{13}C NMR (101 MHz, CDCl_3) δ 207.22, 171.83, 170.77, 136.18, 136.12, 129.43, 128.60, 127.46, 126.93, 123.57, 122.43, 119.94, 118.86, 111.41, 110.03, 67.03, 61.67, 59.25, 53.82, 53.66, 52.93, 52.59, 48.87, 36.97, 27.70, 17.63, 16.57. LC-MS (linear gradient 10 \rightarrow 90% MeCN, 0.1% TFA, 15 min): R_t (min): 6.25 (ESI-MS (m/z): 590.13 ($\text{M}+\text{H}^+$)). HRMS: calculated for $\text{C}_{32}\text{H}_{39}\text{N}_5\text{O}_6$ 590.29731 [$\text{M}+\text{H}$] $^+$; found 590.29730

MorphAc-D-Ala-Tyr(OMe)-Phe-EK (17)

This compound was obtained by the general protocol for azide coupling on a 50 μmol scale. Purification by column chromatography (1 \rightarrow 3% MeOH in DCM) provided the title compound (21.60 mg, 74.4%) as a white powder after lyophilisation. ^1H NMR (400 MHz, CDCl_3) δ 7.55 (d, $J = 6.2$ Hz, 1H), 7.23 (d, $J = 6.8$ Hz, 3H), 7.07 (d, $J = 8.6$ Hz, 2H), 7.01 (dd, $J = 7.3, 1.8$ Hz, 2H), 6.79 (d, $J = 8.6$ Hz, 2H), 6.61 (d, $J = 8.0$ Hz, 1H), 6.43 (d, $J = 7.5$ Hz, 1H), 4.72 (td, $J = 7.9, 4.9$ Hz, 1H), 4.52 (q, $J = 6.7$ Hz, 1H), 4.33 (p, $J = 7.0$ Hz, 1H), 3.77 (s, 3H), 3.74 – 3.67 (m, 4H), 3.27 (d, $J = 5.0$ Hz, 1H), 3.03 (dd, $J = 13.9, 4.8$ Hz, 1H), 2.97 (s, 2H), 2.93 (dd, $J = 6.4, 4.7$ Hz, 2H), 2.89 (d, $J = 5.0$ Hz, 1H), 2.71 (dd, $J = 13.9, 8.2$ Hz, 1H), 2.59 – 2.40 (m, 4H), 1.44 (s, 3H), 1.28 (d, $J = 7.0$ Hz, 3H). ^{13}C NMR (101 MHz, CDCl_3) δ 207.24, 171.83, 170.41, 158.78, 135.91, 130.50, 129.41, 128.65, 128.21, 127.17, 114.19, 67.05, 61.69, 59.28, 55.37, 54.28, 53.85, 52.83, 52.54, 48.74, 37.14, 37.04, 17.66, 16.56. LC-MS (linear gradient 10 \rightarrow 90% MeCN, 0.1% TFA, 15 min): R_t (min): 6.17 (ESI-MS (m/z): 581.20 ($\text{M}+\text{H}^+$)) HRMS: calculated for $\text{C}_{31}\text{H}_{40}\text{N}_4\text{O}_7$ 581.29698 [$\text{M}+\text{H}$] $^+$; found 581.29694

3MeIndAc-D-Ala-Tyr(OMe)-Phe-EK (18)

This compound was obtained by the general protocol for azide coupling on a 50 μ mol scale. Purification by column chromatography (1 \rightarrow 2% MeOH in DCM) provided the title compound (23.89 mg, 78.3%) as a white powder after lyophilisation. ^1H NMR (400 MHz, CDCl_3) δ 7.46 (t, J = 6.3 Hz, 2H), 7.40 – 7.27 (m, 2H), 7.12 (dt, J = 26.3, 7.8 Hz, 5H), 6.99 (d, J = 6.9 Hz, 2H), 6.89 (d, J = 7.9 Hz, 1H), 6.75 (d, J = 8.6 Hz, 2H), 6.60 (d, J = 7.5 Hz, 1H), 6.43 (d, J = 6.9 Hz, 1H), 4.72 (td, J = 8.0, 5.0 Hz, 1H), 4.62 – 4.48 (m, 2H), 3.70 (s, 3H), 3.60 – 3.54 (m, 2H), 3.24 (d, J = 4.9 Hz, 1H), 3.04 – 2.93 (m, 3H), 2.85 (d, J = 4.9 Hz, 1H), 2.68 (dd, J = 13.8, 8.3 Hz, 1H), 2.53 (t, J = 2.1 Hz, 3H), 1.40 (s, 3H), 1.32 (d, J = 7.0 Hz, 3H). ^{13}C NMR (101 MHz, CDCl_3) δ 207.31, 172.54, 170.61, 166.15, 158.72, 148.43, 145.59, 142.27, 135.82, 131.45, 130.50, 129.34, 128.52, 128.31, 127.49, 127.09, 126.91, 123.94, 120.97, 114.10, 59.30, 55.27, 54.37, 52.86, 52.53, 49.05, 38.31, 37.19, 36.87, 18.33, 16.53, 12.52. LC-MS (linear gradient 10 \rightarrow 90% MeCN, 0.1% TFA, 15 min): R_t (min): 9.62 (ESI-MS (m/z): 610.07 ($\text{M}+\text{H}^+$)). HRMS: calculated for $\text{C}_{36}\text{H}_{39}\text{N}_3\text{O}_6$ 610.29116 [$\text{M}+\text{H}$] $^+$; found 610.29114

3MeIndAc-Ala-Tyr(OMe)-BiPhe-EK (19)

This compound was obtained by the general protocol for azide coupling on a 50 μ mol scale. Purification by column chromatography (1 \rightarrow 2% MeOH in DCM) provided the title compound (18.21 mg, 53.1%) as a white powder after lyophilisation. ^1H NMR (400 MHz, CDCl_3) δ 7.58 – 7.28 (m, 11H), 7.12 (d, J = 8.2 Hz, 2H), 7.02 (d, J = 8.6 Hz, 2H), 6.85 (d, J = 7.8 Hz, 1H), 6.61 (d, J = 8.6 Hz, 2H), 6.55 (d, J = 7.5 Hz, 1H), 6.08 (d, J = 7.0 Hz, 1H), 4.81 (td, J = 8.1, 4.8 Hz, 1H), 4.60 – 4.49 (m, 2H), 3.55 – 3.37 (m, 5H), 3.32 (d, J = 4.9 Hz, 1H), 3.14 (dd, J = 14.0, 4.7 Hz, 1H), 2.95 (d, J = 6.9 Hz, 2H), 2.92 (d, J = 4.9 Hz, 1H), 2.76 (dd, J = 14.0, 8.4 Hz, 1H), 2.51 (t, J = 2.2 Hz, 3H), 1.51 (s, 3H), 1.34 (d, J = 7.0 Hz, 3H). ^{13}C NMR (101 MHz, CDCl_3) δ 207.01, 172.33, 170.61, 165.99, 158.52, 148.66, 145.44, 141.99, 140.57, 139.90, 134.77, 130.96, 130.22, 129.67, 128.75, 128.19, 127.93, 127.49, 127.27, 127.18, 126.97, 126.89, 123.84, 120.91, 120.34, 113.85, 59.25, 54.86, 54.18, 52.61, 52.52, 48.57, 38.08, 36.65, 36.59, 17.65, 16.56, 12.37. LC-MS (linear gradient 10 \rightarrow 90% MeCN, 0.1% TFA, 15 min): R_t (min): 10.56 (ESI-MS (m/z): 686.13 ($\text{M}+\text{H}^+$)). HRMS: calculated for $\text{C}_{42}\text{H}_{43}\text{N}_3\text{O}_6$ 686.32246 [$\text{M}+\text{H}$] $^+$; found 686.32245

MorphAc-D-Ala-Trp-BiPhe-EK (20)

This compound was obtained by the general protocol for azide coupling on a 50 μ mol scale. Purification by column chromatography (1 \rightarrow 3% MeOH in DCM) provided the title compound (21.86 mg, 63.7%) as a white powder after lyophilisation. ^1H NMR (400 MHz, CDCl_3) δ 7.97 (s, 1H), 7.67 – 7.32 (m, 9H), 7.22 (d, J = 8.0 Hz, 1H), 7.16 (t, J = 7.3 Hz, 1H), 7.10 (t, J = 7.1 Hz, 1H), 6.97 (d, J = 8.0 Hz, 2H), 6.83 (d, J = 1.7 Hz, 1H), 6.64 (d, J = 7.9 Hz, 1H), 6.55 (d, J = 7.6 Hz, 1H), 4.79 – 4.63 (m, 2H), 4.28 (p, J = 7.0 Hz, 1H), 3.78 – 3.62 (m, 4H), 3.35 (dd, J = 14.7, 4.7 Hz, 1H), 3.29 (d, J = 4.9 Hz, 1H), 3.08 – 2.95 (m, 2H), 2.92 (s, 2H), 2.88 (d, J = 4.9 Hz, 1H), 2.68 (dd, J = 13.8, 8.7 Hz, 1H), 2.56 – 2.39 (m, 4H), 1.46 (s, 3H), 1.32 (d, J = 7.0 Hz, 3H). ^{13}C NMR (101 MHz, CDCl_3) δ 207.14, 174.77, 171.84, 170.82, 140.51, 139.50, 136.07, 135.40, 129.90, 129.10, 127.62, 127.51, 127.15, 126.99, 123.48, 122.39, 119.91, 118.82, 111.33, 109.86, 67.03, 61.61, 59.29, 53.79, 53.55, 52.99, 52.64, 49.01, 36.41, 27.48, 17.38, 16.63. LC-MS (linear gradient 10 \rightarrow 90% MeCN, 0.1% TFA, 15 min): R_t (min): 7.33 (ESI-MS (m/z): 666.20 ($\text{M}+\text{H}^+$)). HRMS: calculated for $\text{C}_{42}\text{H}_{43}\text{N}_3\text{O}_6$ 666.32861 [$\text{M}+\text{H}$] $^+$; found 666.32861

MorphAc-D-Ala-Tyr(OMe)-BiPhe-EK (21)

This compound was obtained by the general protocol for azide coupling on a 50 μ mol scale. Purification by column chromatography (1 \rightarrow 3% MeOH in DCM) provided the title compound (25.08 mg, 746.3.4%) as a white powder after lyophilisation. ^1H NMR (400 MHz, CDCl_3) δ 7.60 – 7.38 (m, 7H), 7.34 (d, J = 7.4 Hz, 1H), 7.08 (d, J = 8.1 Hz, 4H), 6.78 (d, J = 8.6 Hz, 2H), 6.66 (d, J = 8.1 Hz, 1H), 6.51 (d, J = 7.5 Hz, 1H), 4.77 (td, J = 7.9, 4.6 Hz, 1H), 4.56 (q, J = 6.6 Hz, 1H), 4.33 (p, J = 7.0 Hz, 1H), 3.71 (s, 3H), 3.68 (d, J = 4.7 Hz, 4H), 3.29 (d, J = 4.9 Hz, 1H), 3.07 (dd, J = 13.9, 4.5 Hz, 1H), 3.03 – 2.86 (m, 5H), 2.78 (dd, J = 13.9, 8.2 Hz, 1H), 2.53 – 2.36 (m, 4H), 1.47 (s, 3H), 1.28 (d, J = 7.0 Hz, 3H). ^{13}C NMR (101 MHz, CDCl_3) δ 207.13, 171.85, 170.48, 158.80, 140.65, 139.93, 135.00, 130.53, 129.83, 128.92, 128.18, 127.45, 127.30, 127.09, 114.19, 67.03, 61.61, 59.30, 55.30, 54.24, 53.79, 52.87, 52.59,

48.76, 37.02, 36.65, 17.53, 16.61. LC-MS (linear gradient 10 → 90% MeCN, 0.1% TFA, 15 min): R_t (min): 7.26 (ESI-MS (m/z): 657.27 (M+H⁺)). HRMS: calculated for C₃₇H₄₄N₄O₇ 657.32828 [M+H]⁺; found 657.32831

3MeIndAc-D-Ala-Tyr(OMe)-BiPhe-EK (22)

This compound was obtained by the general protocol for azide coupling on a 50 μmol scale. Purification by column chromatography (1→3% MeOH in DCM) provided the title compound (26.38 mg, 79.2%) as a white powder after lyophilisation. ¹H NMR (400 MHz, CDCl₃) δ 7.54 – 7.49 (m, 2H), 7.47 – 7.27 (m, 9H), 7.08 (dd, *J* = 8.2, 5.8 Hz, 4H), 6.83 (d, *J* = 7.9 Hz, 1H), 6.73 (d, *J* = 8.6 Hz, 2H), 6.62 (d, *J* = 7.5 Hz, 1H), 6.36 (d, *J* = 6.9 Hz, 1H), 4.76 (td, *J* = 8.1, 4.7 Hz, 1H), 4.66 – 4.45 (m, 2H), 3.64 (s, 3H), 3.56 – 3.49 (m, 2H), 3.28 (d, *J* = 4.9 Hz, 1H), 3.10 – 2.90 (m, 3H), 2.90 – 2.86 (m, 1H), 2.72 (dd, *J* = 13.9, 8.5 Hz, 1H), 2.50 (t, *J* = 2.1 Hz, 3H), 1.43 (s, 3H), 1.33 (d, *J* = 7.0 Hz, 3H). ¹³C NMR (101 MHz, CDCl₃) δ 207.17, 172.52, 170.72, 166.19, 158.74, 148.56, 145.55, 142.22, 140.61, 139.89, 134.99, 131.34, 130.51, 129.82, 128.88, 128.28, 127.50, 127.40, 127.22, 127.03, 126.90, 123.94, 120.99, 114.10, 59.34, 55.21, 54.30, 52.93, 52.58, 49.17, 38.27, 36.85, 36.66, 18.29, 16.60, 12.51. LC-MS (linear gradient 10 → 90% MeCN, 0.1% TFA, 15 min): R_t (min): 10.67 (ESI-MS (m/z): 686.13 (M+H⁺)). HRMS: calculated for C₄₂H₄₃N₃O₆ 686.32246 [M+H]⁺; found 686.32251

MorphAc-Ala-Tyr(OMe)-Phe-VS (23)

This compound was obtained by the general protocol for azide coupling on a 50 μmol scale. Purification by column chromatography (1→3% MeOH in DCM) provided the title compound (13.08 mg, 43.5%) as a white powder after lyophilisation. Isolated with 19% *cis* isomer. Peaks reported correspond to *trans* isomer. ¹H NMR (400 MHz, CDCl₃) δ 7.47 (s, 1H), 7.35 – 7.20 (m, 5H), 7.16 – 7.10 (m, 2H), 7.01 (d, *J* = 8.6 Hz, 2H), 6.85 – 6.75 (m, 2H), 6.57 (dd, *J* = 24.5, 6.5 Hz, 1H), 6.18 (dd, *J* = 15.1, 1.7 Hz, 1H), 4.98 (p, *J* = 7.1 Hz, 1H), 4.56 – 4.41 (m, 1H), 4.27 – 4.11 (m, 1H), 3.77 (s, 3H), 3.72 (t, *J* = 4.5 Hz, 4H), 3.08 – 2.75 (m, 9H), 2.47 (d, *J* = 32.6 Hz, 4H), 1.31 (d, *J* = 7.1 Hz, 3H). ¹³C NMR (101 MHz, CDCl₃) δ 172.09, 170.45, 158.72, 146.23, 136.09, 130.37, 130.11, 129.48, 129.34, 128.82, 128.76, 128.07, 127.25, 114.35, 114.22, 66.88, 61.50, 55.36, 54.82, 53.86, 50.45, 49.44, 42.75, 39.81, 36.34, 17.27. LC-MS (linear gradient 10 → 90% MeCN, 0.1% TFA, 12.5 min): R_t (min): 4.98 (ESI-MS (m/z): 601.27 (M+H⁺)). HRMS: calculated for C₃₀H₄₆N₄O₇S 601.26905 [M+H]⁺; found 601.26904

MorphAc-Ala-Tyr(OMe)-Cha-VS (24)

This compound was obtained by the general protocol for azide coupling on a 50 μmol scale. Purification by column chromatography (1→3% MeOH in DCM) provided the title compound (15.27 mg, 50.3%) as a white powder after lyophilisation. Isolated with 13% *cis* isomer. Peaks reported correspond to *trans* isomer. ¹H NMR (400 MHz, CDCl₃) δ 7.48 (d, *J* = 6.2 Hz, 1H), 7.11 (d, *J* = 8.6 Hz, 2H), 6.84 (d, *J* = 8.6 Hz, 2H), 6.72 (dd, *J* = 15.1, 4.5 Hz, 1H), 6.63 (d, *J* = 7.5 Hz, 1H), 6.45 (d, *J* = 8.3 Hz, 1H), 6.18 (dd, *J* = 15.1, 1.7 Hz, 1H), 4.72 (p, *J* = 7.4 Hz, 1H), 4.55 (q, *J* = 7.4 Hz, 1H), 4.28 (p, *J* = 7.0 Hz, 1H), 3.79 (s, 3H), 3.72 (t, *J* = 4.5 Hz, 4H), 3.15 (dd, *J* = 14.0, 6.1 Hz, 1H), 3.04 – 2.94 (m, 2H), 2.89 (s, 3H), 2.83 (d, *J* = 16.7 Hz, 1H), 2.48 (dq, *J* = 11.7, 7.1 Hz, 4H), 1.83 – 1.51 (m, 5H), 1.45 – 1.33 (m, 5H), 1.29 – 1.04 (m, 4H), 1.04 – 0.76 (m, 2H). ¹³C NMR (101 MHz, CDCl₃) δ 172.14, 170.45, 158.78, 147.69, 130.48, 129.15, 128.14, 114.39, 66.95, 61.56, 55.35, 54.87, 53.89, 49.47, 47.41, 42.80, 41.30, 36.33, 34.05, 33.63, 32.46, 26.46, 26.31, 26.15, 17.45. LC-MS (linear gradient 10 → 90% MeCN, 0.1% TFA, 12.5 min): R_t (min): 5.44 (ESI-MS (m/z): 607.33 (M+H⁺)). HRMS: calculated for C₃₀H₄₆N₄O₇S 607.31600 [M+H]⁺; found 607.31604

3MeIndAc-Ala-Tyr(OMe)-Phe-VS (25)

This compound was obtained by the general protocol for azide coupling on a 50 μmol scale. Purification by column chromatography (1→3% MeOH in DCM) provided the title compound (15.11 mg, 47.3%) as a white powder after lyophilization. Isolated with 16% *cis* isomer. Peaks reported correspond to *trans* isomer. ¹H NMR (400 MHz, CDCl₃) δ 8.24 (s, 1H), 7.61 (d, *J* = 7.6 Hz, 1H), 7.45 (dd, *J* = 6.3, 2.3 Hz, 2H), 7.38 – 7.30 (m, 3H), 7.24 – 7.09 (m, 5H), 7.06 (dd, *J* = 7.3, 1.9 Hz, 2H), 6.95 (d, *J* = 8.6 Hz, 1H), 6.76 (d, *J* = 2.2 Hz, 1H), 6.68 (dd, *J* = 15.0, 4.4 Hz, 2H), 6.32 (d, *J* = 5.7 Hz, 1H), 6.15 (dd, *J* = 15.1, 1.7 Hz, 1H), 4.92 (dt, *J* = 12.1, 6.0 Hz, 1H), 4.81 – 4.68 (m, 1H),

4.23 (q, $J = 6.7$ Hz, 1H), 3.63 – 3.43 (m, 2H), 3.35 (dd, $J = 14.6, 5.1$ Hz, 1H), 3.22 – 3.09 (m, 1H), 2.76 (d, $J = 7.6$ Hz, 2H), 2.70 (s, 3H), 2.54 – 2.44 (m, 3H), 1.42 (d, $J = 7.0$ Hz, 3H). ^{13}C NMR (101 MHz, CDCl_3) δ 173.04, 171.06, 166.84, 148.99, 146.31, 145.34, 142.25, 136.68, 136.17, 130.83, 129.98, 129.79, 129.36, 128.75, 128.62, 127.76, 127.54, 126.99, 126.94, 124.03, 123.48, 122.50, 121.09, 119.97, 118.47, 111.70, 109.63, 54.34, 50.90, 50.30, 43.75, 42.65, 39.50, 38.36, 26.96, 17.43, 12.71. LC-MS (linear gradient 10 \rightarrow 90% MeCN, 0.1% TFA, 12.5 min): R_t (min): 7.78 (ESI-MS (m/z): 639.13 ($\text{M}+\text{H}^+$)). HRMS: calculated for $\text{C}_{36}\text{H}_{38}\text{N}_4\text{O}_5\text{S}$ 639.26357 [$\text{M}+\text{H}^+$] $^+$; found 639.26355.

3MeIndAc-Ala-Tyr(OMe)-Phe-VS (26)

This compound was obtained by the general protocol for azide coupling on a 50 μmol scale. Purification by column chromatography (1 \rightarrow 3% MeOH in DCM) provided the title compound (9.98 mg, 30.9%) as a white powder after lyophilisation. ^1H NMR (400 MHz, CDCl_3) δ 8.52 (s, 1H), 7.66 (d, $J = 7.7$ Hz, 1H), 7.49 – 7.41 (m, 2H), 7.40 – 7.28 (m, 3H), 7.22 – 7.03 (m, 3H), 6.96 (d, $J = 7.8$ Hz, 1H), 6.63 – 6.59 (m, 1H), 6.57 (d, $J = 4.6$ Hz, 1H), 6.41 (d, $J = 6.1$ Hz, 1H), 6.05 (dd, $J = 15.1, 1.4$ Hz, 1H), 4.79 (tt, $J = 10.1, 5.1$ Hz, 1H), 4.68 (p, $J = 7.0$ Hz, 1H), 4.35 (q, $J = 6.7$ Hz, 1H), 3.58 – 3.34 (m, 3H), 3.24 (dd, $J = 14.4, 7.7$ Hz, 1H), 2.72 (s, 3H), 2.44 (t, $J = 2.1$ Hz, 3H), 1.67 – 1.50 (m, 5H), 1.46 (d, $J = 7.0$ Hz, 3H), 1.33 – 1.23 (m, 3H), 1.21 – 1.04 (m, 3H), 0.95 – 0.68 (m, 2H). ^{13}C NMR (101 MHz, CDCl_3) δ 173.02, 171.07, 166.62, 148.87, 147.57, 145.39, 142.22, 136.36, 130.91, 129.07, 127.68, 127.42, 126.96, 123.97, 123.69, 122.53, 121.04, 120.06, 118.58, 111.81, 109.99, 54.48, 50.03, 47.37, 42.68, 40.96, 38.33, 33.99, 33.35, 32.65, 27.51, 26.41, 26.17, 26.10, 17.80, 12.60. LC-MS (linear gradient 10 \rightarrow 90% MeCN, 0.1% TFA, 12.5 min): R_t (min): 8.34 (ESI-MS (m/z): 645.20 ($\text{M}+\text{H}^+$)). HRMS: calculated for $\text{C}_{36}\text{H}_{44}\text{N}_4\text{O}_5\text{S}$ 645.31052 [$\text{M}+\text{H}^+$] $^+$; found 645.31055

N₃Gly-Ala-Hyp-Nle-Leu-EK (27)

This compound was obtained by the general protocol for azide coupling on a 64 μmol scale. Purification by column chromatography (0 \rightarrow 1.5% MeOH in DCM) provided the product (7.6 mg, 12.5 μmol , 20%), which was next deprotected in 1:1 DCM:TFA (2 mL). After stirring for 30 min, the mixture was evaporated and co-evaporated with toluene (3x). Purification by HPLC (C18, linear gradient 20 \rightarrow 70% MeCN: MeOH, 0.1% TFA) yielded the title compound (2.55 mg, 4.63 μmol , 7%). Complex NMR due to a 9:1 ratio of rotamers. Peaks of major rotamer are reported. ^1H NMR (600 MHz, CDCl_3) δ 7.13 (dd, $J = 18.5, 7.3$ Hz, 2H), 6.40 (d, $J = 8.0$ Hz, 1H), 4.73 – 4.69 (m, 1H), 4.66 (t, $J = 7.8$ Hz, 1H), 4.59 (dt, $J = 9.9, 5.5$ Hz, 2H), 4.28 (q, $J = 7.8$ Hz, 1H), 3.99 (s, 2H), 3.85 (d, $J = 11.1$ Hz, 1H), 3.63 (dd, $J = 11.1, 4.0$ Hz, 1H), 3.29 (d, $J = 5.0$ Hz, 1H), 2.89 (d, $J = 5.0$ Hz, 1H), 2.44 – 2.36 (m, 1H), 2.18 – 2.10 (m, 1H), 1.86 – 1.76 (m, 1H), 1.66 – 1.60 (m, 1H), 1.54 (ddd, $J = 13.2, 9.7, 3.2$ Hz, 1H), 1.51 (s, 3H), 1.38 (d, $J = 6.9$ Hz, 3H), 1.35 – 1.22 (m, 7H), 0.93 (dd, $J = 6.5, 4.5$ Hz, 6H), 0.88 (t, $J = 7.1$ Hz, 3H). ^{13}C NMR (151 MHz, CDCl_3) δ 208.56, 172.29, 171.71, 170.78, 166.79, 70.46, 59.21, 58.89, 55.47, 53.77, 52.59, 52.55, 50.50, 47.06, 40.21, 36.41, 31.79, 27.66, 25.34, 23.49, 22.47, 21.42, 17.97, 16.88, 14.03. LC-MS (linear gradient 10 \rightarrow 90% MeCN, 0.1% TFA, 12.5 min): R_t (min): 6.10 (ESI-MS (m/z): 552.20 ($\text{M}+\text{H}^+$)). HRMS: calculated for $\text{C}_{25}\text{H}_{41}\text{N}_7\text{O}_7$ 552.31402 [$\text{M}+\text{H}^+$] $^+$; found 552.31403

N₃Gly-Ala-Thz-Nle-Leu-EK (28)

This compound was obtained by the general protocol for azide coupling on a 50 μmol scale. Purification by column chromatography (0 \rightarrow 2% MeOH in DCM) provided the title compound (10.4 mg, 18.7 μmol , 37) as a white powder after lyophilisation. Complex NMR due to a 2:1 ratio of rotamers. ^1H NMR (600 MHz, CDCl_3) δ 7.38 (m, 0.3H) 7.09 (d, $J = 13.0$ Hz, 0.7H), 7.01 – 6.70 (m, 1.4H), 6.27 (d, $J = 6.8$ Hz, 0.6H), 5.07 – 4.12 (m, 7H), 4.07 – 3.87 (m, 2H), 3.75 – 2.70 (m, 3H), 2.09 – 1.03 (m, 15H), 1.00 – 0.66 (m, 9H). ^{13}C NMR (151 MHz, CDCl_3) δ 209.62, 208.41, 171.90, 171.61, 171.52, 171.40, 171.27, 168.95, 168.65, 168.54, 166.34, 68.33, 63.48, 63.08, 62.63, 59.20, 56.06, 53.55, 52.68, 52.56, 52.36, 50.62, 49.93, 49.61, 49.44, 49.11, 47.10, 40.75, 40.28, 35.09, 32.22, 31.34, 29.83, 27.45, 25.35, 23.49, 22.47, 22.22, 21.47, 18.54, 16.87, 13.99.

LC-MS (linear gradient 10 \rightarrow 90% MeCN, 0.1% TFA, 12.5 min): R_t (min): 7.12 (ESI-MS (m/z): 554.13 ($\text{M}+\text{H}^+$)). HRMS: calculated for $\text{C}_{24}\text{H}_{39}\text{N}_7\text{O}_6\text{S}$ 554.27553 [$\text{M}+\text{H}^+$] $^+$; found 554.27545

N₃Gly-Ala-Aze-Nle-Leu-EK (29)

This compound was obtained by the general protocol for azide coupling on a 50 μ mol scale. Purification by column chromatography (1 \rightarrow 2% MeOH in DCM) provided the title compound (14.4 mg, 55%) as a white powder after lyophilisation. Complex NMR due to a 5:1 ratio of rotamers. Peaks of major rotamer are reported. ¹H NMR (400 MHz, CDCl₃) δ 7.83 (d, *J* = 7.7 Hz, 1H), 6.99 (d, *J* = 6.8 Hz, 1H), 6.42 (d, *J* = 8.0 Hz, 1H), 4.91 (dd, *J* = 9.3, 6.4 Hz, 1H), 4.62 – 4.48 (m, 2H), 4.32 (ddd, *J* = 12.6, 5.0, 2.8 Hz, 2H), 4.16 – 4.07 (m, 1H), 3.98 (d, *J* = 3.2 Hz, 2H), 3.31 (d, *J* = 5.0 Hz, 1H), 2.87 (d, *J* = 5.0 Hz, 1H), 2.80 – 2.66 (m, 1H), 2.57 – 2.40 (m, 1H), 1.93 – 1.71 (m, 1H), 1.68 – 1.50 (m, 3H), 1.49 (s, 3H), 1.39 – 1.17 (m, 8H), 0.92 (dd, *J* = 6.4, 3.5 Hz, 6H), 0.86 (t, *J* = 7.1 Hz, 3H). ¹³C NMR (101 MHz, CDCl₃) δ 208.61, 174.09, 171.51, 170.25, 166.41, 62.12, 59.20, 53.58, 52.58, 50.43, 49.15, 44.70, 40.21, 31.67, 27.66, 25.36, 23.46, 22.44, 21.46, 18.68, 18.28, 16.86, 14.05. LC-MS (linear gradient 10 \rightarrow 90% MeCN, 0.1% TFA, 12.5 min): R_t (min): 6.64 (ESI-MS (*m/z*): 522.20 (M+H⁺)). HRMS: calculated for C₂₆H₄₃N₇O₆ 522.30346 [M+H]⁺; found 522.30341

N₃Gly-Ala-Pip-Nle-Leu-EK (30)

This compound was obtained by the general protocol for azide coupling on a 50 μ mol scale. Purification by column chromatography (1 \rightarrow 2% MeOH in DCM) provided the title compound (18.6 mg, 67%) as a white powder after lyophilisation. Complex NMR due to a 1.5:1 ratio of rotamers. ¹H NMR (400 MHz, CDCl₃) δ 7.44 (d, *J* = 8.2 Hz, 0.4H), 7.38 (d, *J* = 7.3 Hz, 0.6H), 7.06 (d, *J* = 6.0 Hz, 0.4H), 6.84 (d, *J* = 8.7 Hz, 0.4H), 6.45 (d, *J* = 7.7 Hz, 0.6H), 6.28 (d, *J* = 7.9 Hz, 0.6H), 5.18 (d, *J* = 4.3 Hz, 0.6H), 4.96 (p, *J* = 6.9 Hz, 0.6H), 4.83 (p, *J* = 6.9 Hz, 0.4H), 4.67 – 4.48 (m, 2H), 4.38 – 4.25 (m, 1H), 3.98 (d, *J* = 5.4 Hz, 1.2H), 3.95 – 3.91 (m, 0.8H), 3.78 (d, *J* = 13.5 Hz, 0.6H), 3.28 (d, *J* = 5.0 Hz, 1H), 3.25 – 3.16 (m, 0.6H), 2.88 (d, *J* = 5.0 Hz, 0.6H), 2.85 (d, *J* = 4.9 Hz, 0.4H), 2.62 – 2.55 (m, 0.4H), 2.50 (dd, m, 0.4H), 2.22 – 2.14 (m, 0.6H), 1.86 – 1.06 (m, 20H), 0.95 – 0.83 (m, 9H). ¹³C NMR (101 MHz, CDCl₃) δ 208.71, 208.68, 172.48, 172.40, 171.74, 171.59, 170.62, 169.25, 168.65, 166.25, 59.46, 59.26, 57.11, 55.76, 53.37, 52.99, 52.83, 52.69, 52.44, 50.84, 49.97, 46.44, 45.87, 44.06, 40.82, 40.56, 40.41, 32.51, 31.66, 28.60, 27.86, 26.85, 25.98, 25.66, 25.59, 25.51, 25.14, 23.79, 23.72, 22.73, 22.53, 21.64, 21.06, 20.53, 18.74, 17.29, 17.13, 17.04, 14.26. LC-MS (linear gradient 10 \rightarrow 90% MeCN, 0.1% TFA, 12.5 min): R_t (min): 7.34 (ESI-MS (*m/z*): 550.07 (M+H⁺)). HRMS: calculated for C₂₆H₄₃N₇O₆ 550.33476 [M+H]⁺; found 550.33472

N₃Gly-Ala-(4S)-FPro-Nle-Leu-EK (31)

This compound was obtained by the general protocol for azide coupling on a 50 μ mol scale. Purification by column chromatography (2 \rightarrow 3% MeOH in DCM) followed by purification by HPLC (30-70% MeCN, 0.1 % TFA, 10 min gradient) provided the title compound (2.51 mg, 9%) as a white powder after lyophilisation. Complex NMR due to a 3:2 ratio of rotamers. ¹H NMR (600 MHz, CDCl₃) δ 7.36 (d, *J* = 7.0 Hz, 0.4H), 7.05 (d, *J* = 7.2 Hz, 0.6H), 6.85 (d, *J* = 9.0 Hz, 0.4 H), 6.81 (d, *J* = 5.5 Hz, 0.4H), 6.73 (d, *J* = 7.7 Hz, 0.6H), 6.29 (d, *J* = 7.9 Hz, 0.6H), 5.43 – 5.24 (m, 1H), 4.79 – 4.64 (m, 1.6H), 4.60 – 4.54 (m, 1H), 4.48 (d, *J* = 9.4 Hz, 0.4H), 4.39 – 4.30 (m, 0.6H), 4.20 (m, 0.4H), 4.04 – 3.80 (m, 4H), 3.30 (d, *J* = 5.0 Hz, 0.6H), 3.27 (d, *J* = 4.9 Hz, 0.4H), 2.94 (t, *J* = 15.5 Hz, 0.4H), 2.88 (d, *J* = 5.0 Hz, 0.6H), 2.85 (d, *J* = 4.9 Hz, 0.4H), 2.83 – 2.74 (m, 0.6H), 2.40 – 2.16 (m, 1H), 1.90 – 1.16 (m, 15H), 1.10 (ddd, *J* = 14.0, 10.3, 4.5 Hz, 0.4H), 0.99 – 0.89 (m, 6H), 0.86 (t, *J* = 7.1 Hz, 3H). ¹³C NMR (151 MHz, CDCl₃) δ 209.58, 208.31, 172.97, 172.12, 171.95, 171.54, 170.09, 169.60, 168.52, 166.44, 92.20 (d, *J* = 179.4 Hz), 90.36 (d, *J* = 176.2 Hz), 59.61, 59.49, 59.26, 58.89, 55.87, 54.38 (d, *J* = 24.0 Hz), 54.19 (d, *J* = 24.1 Hz), 53.21, 52.61, 52.57, 52.48, 52.36, 50.49, 49.26, 48.68, 46.93, 40.84, 40.14, 38.80 (d, *J* = 21.3 Hz), 34.60 (d, *J* = 21.4 Hz), 32.05, 31.23, 30.47, 27.99, 27.26, 25.32, 25.25, 23.59, 23.51, 22.46, 22.17, 21.57, 21.43, 18.40, 16.90, 16.70, 16.61, 14.00, 13.95. LC-MS (linear gradient 10 \rightarrow 90% MeCN, 0.1% TFA, 15 min): R_t (min): 7.78 (ESI-MS (*m/z*): 554.20 (M+H⁺)). HRMS: calculated for C₂₅H₄₁N₇O₆ [M+H]⁺; 554.30969, found 554.30969.

N₃Gly-Ala-(4R)-FPro-Nle-Leu-EK (32)

This compound was obtained by the general protocol for azide coupling on a 50 μ mol scale. Purification by column chromatography (1 \rightarrow 2% MeOH in DCM) followed by purification by HPLC (30-70% MeCN, 0.1 % TFA, 10

min gradient) provided the title compound (2.95 mg, 11%) as a white powder after lyophilisation. Complex NMR due to a 95:5 ratio of rotamers. Peaks of major rotamer are reported. ^1H NMR (600 MHz, CDCl_3) δ 7.21 (d, $J = 6.9$ Hz, 1H), 6.98 (d, $J = 7.6$ Hz, 1H), 6.23 (d, $J = 8.0$ Hz, 1H), 5.32 (d, $J = 52.5$ Hz, 1H), 4.76 (p, $J = 6.9$ Hz, 1H), 4.70 (t, $J = 8.0$ Hz, 1H), 4.62 – 4.56 (m, 1H), 4.30 (q, $J = 7.7$ Hz, 1H), 4.09 – 3.93 (m, 3H), 3.65 (ddd, $J = 34.0, 12.3, 3.1$ Hz, 1H), 3.29 (d, $J = 4.9$ Hz, 1H), 2.90 (d, $J = 5.0$ Hz, 1H), 2.65 – 2.49 (m, 1H), 2.43 (ddd, $J = 22.6, 14.8, 8.2$ Hz, 1H), 1.81 (dq, $J = 13.3, 7.3, 6.6$ Hz, 1H), 1.67 – 1.59 (m, 2H), 1.55 (ddd, $J = 13.0, 9.7, 3.1$ Hz, 1H), 1.51 (s, 3H), 1.48 – 1.42 (m, 1H), 1.36 (d, $J = 6.9$ Hz, 3H), 1.34 – 1.21 (m, 4H), 0.94 (t, $J = 6.7$ Hz, 6H), 0.89 (t, $J = 7.1$ Hz, 3H). ^{13}C NMR (151 MHz, CDCl_3) δ 208.52, 171.99, 171.42, 169.92, 166.11, 91.74 (d, $J = 180.5$), 59.21, 58.63, 53.80, 53.69 (d, $J = 16$ Hz), 52.70, 52.59, 50.51, 47.05, 40.31, 34.25 (d, $J = 21.7$ Hz), 31.97, 27.61, 25.37, 23.50, 22.48, 21.45, 18.33, 16.88, 14.04. LC-MS (linear gradient 10 \rightarrow 90% MeCN, 0.1% TFA, 15 min): R_t (min): 7.65 (ESI-MS (m/z): 554.20 (M+H⁺)). HRMS: calculated for $\text{C}_{25}\text{H}_{41}\text{FN}_7\text{O}_6$ [M+H]⁺; 554.30969, found 554.30969.

N₃Gly-Ala-4,4-F₂Pro-Nle-Leu-EK (33)

This compound was obtained by the general protocol for azide coupling on a 69 μmol scale. Purification by column chromatography (0 \rightarrow 1.5% MeOH in DCM) provided the title compound (16.9 mg, 18.7 μmol , 24%) as a white powder after lyophilisation. Complex NMR due to a 3:1 ratio of rotamers. ^1H NMR (600 MHz, CDCl_3) δ 7.56 (d, $J = 7.2$ Hz, 0.3H), 7.12 (d, $J = 7.2$ Hz, 0.7H), 7.03 (d, $J = 7.7$ Hz, 0.7H), 7.00 – 6.95 (m, 0.3H), 6.76 (d, $J = 8.8$ Hz, 0.3H), 6.36 (d, $J = 8.0$ Hz, 0.7H), 4.77 (dd, $J = 9.2, 5.7$ Hz, 0.8H), 4.72 – 4.63 (m, 1H), 4.59 (ddd, $J = 10.8, 8.2, 3.0$ Hz, 0.7H), 4.35 (q, $J = 7.7$ Hz, 1.5H), 4.29 – 4.05 (m, 1H), 4.00 (d, $J = 4.9$ Hz, 1.4H), 3.98 – 3.81 (m, 1.3H), 3.76 (m, 0.3H), 3.29 (d, $J = 5.0$ Hz, 0.7H), 3.26 (d, $J = 4.4$ Hz, 0.3H), 2.90 (d, $J = 5.0$ Hz, 0.7H), 2.88 – 2.77 (m, 1H), 2.71 (m, 0.3H), 2.58 (m, 1H), 1.92 – 1.16 (m, 15H), 0.97 – 0.82 (m, 9H). ^{13}C NMR (151 MHz, CDCl_3 , peaks of major rotamer) δ ^{13}C NMR (151 MHz, CDCl_3) δ 208.55, 172.20, 171.37, 168.73, 166.41, 126.20 (t, $J = 249.2$ Hz), 59.21, 58.10, 53.76 (t, $J = 23.0$ Hz), 53.60, 52.55, 50.56, 46.84, 40.17, 39.73, 39.56, 35.77 (t, $J = 24.2$ Hz) 32.22, 27.42, 25.32, 23.46, 22.45, 21.38, 18.03, 16.86, 14.00. LC-MS (linear gradient 10 \rightarrow 90% MeCN, 0.1% TFA, 12.5 min): R_t (min): 7.25 (ESI-MS (m/z): 572.20 (M+H⁺)). HRMS: calculated for $\text{C}_{25}\text{H}_{39}\text{F}_2\text{N}_7\text{O}_6$ 572.30326 [M+H]⁺; found 572.30323

N₃Gly-Ala-Pro-Nle-Phe-EK (34)

This compound was obtained by the general protocol for azide coupling on a 50 μmol scale. Purification by column chromatography (0 \rightarrow 2% MeOH in DCM) provided the title compound (12.14 mg, 43%) as a white powder after lyophilisation. Complex NMR due to a 5:1 ratio of rotamers. Peaks of major rotamer are reported. ^1H NMR (400 MHz, CDCl_3) δ 7.32 – 7.20 (m, 3H), 7.17 – 7.12 (m, 3H), 7.02 (d, $J = 7.6$ Hz, 1H), 6.52 (d, $J = 7.5$ Hz, 1H), 4.81 (td, $J = 7.9, 5.1$ Hz, 1H), 4.74 (p, $J = 7.0$ Hz, 1H), 4.49 (dd, $J = 8.1, 2.8$ Hz, 1H), 4.23 (td, $J = 7.9, 5.6$ Hz, 1H), 3.97 (d, $J = 4.7$ Hz, 2H), 3.70 – 3.49 (m, 2H), 3.31 (d, $J = 4.9$ Hz, 1H), 3.13 (dd, $J = 14.0, 5.0$ Hz, 1H), 2.90 (d, $J = 4.9$ Hz, 1H), 2.79 (dd, $J = 14.0, 8.1$ Hz, 1H), 2.26 (ddd, $J = 12.8, 6.6, 3.3$ Hz, 1H), 2.17 – 2.06 (m, 1H), 2.01 (ddq, $J = 16.4, 7.2, 4.4, 3.9$ Hz, 1H), 1.89 (ddd, $J = 18.2, 12.4, 7.8$ Hz, 1H), 1.73 (dq, $J = 13.4, 7.3$ Hz, 2H), 1.48 (s, 3H), 1.36 (d, $J = 6.9$ Hz, 3H), 1.32 – 1.11 (m, 6H), 0.92 – 0.77 (m, 3H). ^{13}C NMR (101 MHz, CDCl_3) δ 207.56, 171.32 171.40, 170.81, 166.18, 135.79, 129.85, 129.45, 128.69, 128.54, 127.23, 60.01, 59.39, 53.34, 52.67, 52.65, 47.47, 46.80, 37.20, 31.58, 27.56, 27.26, 25.29, 22.44, 18.39, 16.68, 13.99. LC-MS (linear gradient 10 \rightarrow 90% MeCN, 0.1% TFA, 12.5 min): R_t (min): 6.76 (ESI-MS (m/z): 570.13 (M+H⁺)). HRMS: calculated for $\text{C}_{28}\text{H}_{39}\text{N}_7\text{O}_6$ 570.30346 [M+H]⁺; found 570.30347

N₃Gly-Ala-Pro-Nle-Cha-EK (35)

This compound was obtained by the general protocol for azide coupling on a 50 μmol scale. Purification by column chromatography (0 \rightarrow 2% MeOH in DCM) provided the title compound (11.35 mg, 39%) as a white powder after lyophilisation. Complex NMR due to a 5:1 ratio of rotamers. Peaks of major rotamer are reported. ^1H NMR (400 MHz, CDCl_3) δ 7.16 (d, $J = 7.5$ Hz, 1H), 7.08 (d, $J = 7.7$ Hz, 1H), 6.35 (d, $J = 7.9$ Hz, 1H), 4.76 (p, $J = 7.0$ Hz, 1H), 4.57 (dd, $J = 8.1, 2.4$ Hz, 2H), 4.29 (td, $J = 7.8, 5.8$ Hz, 1H), 3.97 (d, $J = 5.0$ Hz, 2H), 3.69 – 3.51 (m, 2H), 3.30 (d, $J = 5.0$ Hz, 1H), 2.87 (d, $J = 5.0$ Hz, 1H), 2.32 (ddd, $J = 12.5, 6.7, 3.3$ Hz, 1H), 2.18 – 1.87 (m, 3H), 1.84 – 1.53 (m, 10H),

1.50 (s, 3H), 1.38 (d, $J = 6.9$ Hz, 3H), 1.34 – 1.07 (m, 9H), 0.87 (t, $J = 7.1$ Hz, 3H). ^{13}C NMR (101 MHz, CDCl_3 , all peaks reported) δ 208.63, 172.28, 171.59, 170.83, 166.18, 60.08, 59.23, 53.43, 52.67, 52.61, 49.82, 47.48, 46.82, 38.64, 34.54, 34.11, 32.04, 31.81, 27.60, 27.40, 26.47, 26.36, 26.08, 25.31, 22.50, 18.42, 16.89, 14.04. LC-MS (linear gradient 10 \rightarrow 90% MeCN, 0.1% TFA, 12.5 min): R_t (min): 7.50 (ESI-MS (m/z): 576.27 ($\text{M}+\text{H}^+$)). HRMS: calculated for $\text{C}_{28}\text{H}_{45}\text{N}_7\text{O}_6$ 576.35041 [$\text{M}+\text{H}^+$] $^+$; found 576.35040

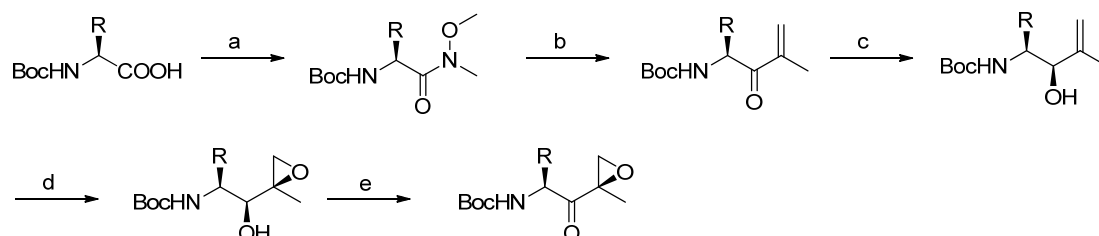
N₃Gly-Ala-4,4-F₂Pro-Nle-Phe-EK (36)

This compound was obtained by the general protocol for azide coupling on a 50 μmol scale. Purification by column chromatography (0 \rightarrow 2% MeOH in DCM) provided the title compound (15.20 mg, 50%) as a white powder after lyophilisation. Complex NMR due to a 2:1 ratio of rotamers. Peaks of major rotamer are reported. ^1H NMR (400 MHz, CDCl_3) δ 7.33 – 7.20 (m, 3H), 7.16 – 7.11 (m, 3H), 6.89 (d, $J = 7.7$ Hz, 1H), 6.36 (d, $J = 7.4$ Hz, 1H), 4.81 (td, $J = 7.8, 5.0$ Hz, 1H), 4.72 – 4.62 (m, 2H), 4.28 – 4.21 (m, 1H), 4.14 (td, $J = 12.3, 7.7$ Hz, 1H), 3.99 (d, $J = 3.7$ Hz, 2H), 3.93 – 3.75 (m, 1H), 3.30 (d, $J = 4.9$ Hz, 1H), 3.14 (dd, $J = 14.1, 5.0$ Hz, 1H), 2.91 (d, $J = 4.9$ Hz, 1H), 2.78 (dt, $J = 14.0, 7.0$ Hz, 2H), 2.53 – 2.44 (m, 1H), 1.85 – 1.66 (m, 2H), 1.50 (s, 3H), 1.36 (d, $J = 6.9$ Hz, 3H), 1.23 (ddt, $J = 26.4, 15.1, 5.0$ Hz, 4H), 0.85 (td, $J = 7.0, 3.8$ Hz, 3H). ^{13}C NMR (101 MHz, CDCl_3) δ 207.45, 172.27, 171.05, 168.58, 166.35, 135.61, 129.92, 129.42, 128.76, 128.59, 127.34, 127.08, 126.18, 59.43, 58.00, 56.06, 53.70 (t, $J = 31$ Hz), 53.51, 52.79, 52.57, 52.14, 46.81, 37.10, 35.46 (t, $J = 23$ Hz), 31.87, 27.37, 22.43, 18.06, 16.71, 13.99.

LC-MS (linear gradient 10 \rightarrow 90% MeCN, 0.1% TFA, 12.5 min): R_t (min): 7.24 (ESI-MS (m/z): 606.20 ($\text{M}+\text{H}^+$)). HRMS: calculated for $\text{C}_{28}\text{H}_{37}\text{F}_2\text{N}_7\text{O}_6$ 606.28461 [$\text{M}+\text{H}^+$] $^+$; found 606.28467

N₃Gly-Ala-4,4-F₂Pro-Nle-Cha-EK (37)

Compound **37** was obtained by the general protocol for azide coupling on a 50 μmol scale. Purification by column chromatography (0 \rightarrow 2% MeOH in DCM) provided the title compound (14.01 mg, 46%) as a white powder after lyophilization. Complex NMR due to a 2.5:1 ratio of rotamers. ^1H NMR (400 MHz, CDCl_3 , peaks of major rotamer) δ 7.08 (d, $J = 7.3$ Hz, 1H), 6.95 (d, $J = 7.7$ Hz, 1H), 6.13 (d, $J = 7.9$ Hz, 1H), 4.78 (dd, $J = 9.3, 5.5$ Hz, 1H), 4.67 (t, $J = 7.1$ Hz, 1H), 4.63 – 4.53 (m, 1H), 4.32 (td, $J = 7.7, 5.6$ Hz, 1H), 4.26 – 4.07 (m, 1H), 4.00 (d, $J = 4.2$ Hz, 2H), 3.91 – 3.79 (m, 1H), 3.28 (d, $J = 5.0$ Hz, 1H), 3.04 – 2.91 (m, 1H), 2.89 (d, $J = 5.0$ Hz, 1H), 2.65 – 2.48 (m, 1H), 1.87 – 1.54 (m, 10H), 1.51 (s, 3H), 1.39 (d, $J = 6.9$ Hz, 3H), 1.35 – 1.07 (m, 9H), 0.88 (t, $J = 7.0$ Hz, 3H). ^{13}C NMR (151 MHz, CDCl_3 , all peaks reported) δ 209.85, 208.58, 172.22, 171.73, 171.56, 171.28, 168.78, 168.67, 168.58, 166.34, 126.18 (t, $J = 241.6$ Hz), 59.24, 59.07, 59.03, 58.91, 58.06, 56.08, 53.73, 53.57, 52.59, 52.54, 52.50, 52.17, 49.95, 48.70, 47.79, 46.82, 38.58, 35.62 (t, $J = 25.7$ Hz), 34.48, 34.23, 34.09, 32.21, 32.02, 31.97, 31.32, 28.05, 27.37, 26.45, 26.42, 26.31, 26.03, 22.47, 22.23, 18.08, 16.89, 16.69, 16.65, 14.03, 13.97. LC-MS (linear gradient 10 \rightarrow 90% MeCN, 0.1% TFA, 12.5 min): R_t (min): 7.91 (ESI-MS (m/z): 612.27 ($\text{M}+\text{H}^+$)). HRMS: calculated for $\text{C}_{28}\text{H}_{43}\text{F}_2\text{N}_7\text{O}_6$ 612.33157 [$\text{M}+\text{H}^+$] $^+$; found 612.33154.



Scheme S2. Epoxyketone warhead synthesis. Reagents and conditions: (a) $\text{NH}(\text{Me})\text{OMe}\cdot\text{HCl}$, HCTU, DiPEA, DCM; (b) 2-bromopropene, $t\text{BuLi}$, Et_2O , -78 $^\circ\text{C}$; (c) NaBH_4 , $\text{CeCl}_3\cdot 7\text{H}_2\text{O}$, MeOH, 0 $^\circ\text{C}$; (d) $t\text{BuOOH}$, $\text{VO}(\text{Acac})_2$, DCM, 0 $^\circ\text{C}$; (e) Dess-Martin periodinane, DCM. R = cyclohexyl (compounds **38-41**), adamantyl (compounds **42-45**), 2-naphthyl (compounds **46-49**), 1-naphthyl (compounds **50-53**), biphenyl (compounds **54-57**)

(S)-tert-butyl(3-cyclohexyl-1-(methoxy(methyl)amino)-1-oxopropan-2-yl)carbamate (39)

This compound was synthesized according to the general procedure **A** described above on a 3.7 mmol scale and was isolated after column chromatography (10 \rightarrow 30% EtOAc:pent) in a quantitative yield. ^1H NMR (400 MHz, CDCl_3) δ 5.03 (d, J = 9.3 Hz, 1H), 4.75 – 4.59 (m, 1H), 3.70 (s, 3H), 3.11 (s, 3H), 1.83 (d, J = 12.6 Hz, 1H), 1.71 – 1.47 (m, 4H), 1.46 – 1.24 (m, 12H), 1.23 – 0.96 (m, 3H), 0.85 (dt, J = 30.7, 11.6 Hz, 2H). ^{13}C NMR (101 MHz, CDCl_3) δ 173.93, 155.63, 79.35, 61.55, 48.27, 40.43, 34.01, 33.93, 32.15, 32.08, 28.31, 26.45, 26.24, 26.02. LC-MS (linear gradient 10 \rightarrow 90% MeCN, 0.1% TFA, 15 min): R_t (min): 9.13 (ESI-MS (m/z): 314.80 ($M+H^+$)). HRMS: calculated for $\text{C}_{16}\text{H}_{30}\text{N}_2\text{O}_4$ 315.22783 [$M+2H$] $^{2+}$; found 315.22781. $[\alpha]_D^{20}$ = -20 (C=1, CHCl_3)

(S)-tert-butyl (1-cyclohexyl-4-methyl-3-oxopent-4-en-2-yl)carbamate (40)

This compound was synthesized according to the general procedure **B** described above on a 3.7 mmol scale and was isolated after column chromatography (10 \rightarrow 30% EtOAc:pent) (842 mg, 2.85 mmol, 77%). ^1H NMR (400 MHz, CDCl_3) δ 6.00 (s, 1H), 5.79 (s, 1H), 5.15 (d, J = 8.6 Hz, 1H), 5.02 (dd, J = 12.4, 6.1 Hz, 1H), 1.91 (d, J = 12.0 Hz, 1H), 1.81 (s, 3H), 1.70 – 1.40 (m, 5H), 1.35 (s, 9H), 1.26 – 0.96 (m, 5H), 0.95 – 0.65 (m, 2H). ^{13}C NMR (101 MHz, CDCl_3) δ 201.59, 155.53, 142.21, 126.01, 79.43, 51.91, 41.62, 34.21, 34.06, 32.36, 28.30, 26.40, 26.26, 26.06, 17.84.

tert-butyl((S)-3-cyclohexyl-1-((R)-2-methyloxiran-2-yl)-1-oxopropan-2-yl)carbamate (41)

This compound was synthesized according to the general procedure **C** described above on a 11.5 mmol scale and the crude (quant) was used directly in used in procedure **D** and was isolated after column chromatography (10 \rightarrow 30% EtOAc:pent) (210 mg, 0.68 mmol, 49%). ^1H NMR (400 MHz, CDCl_3) δ 4.83 (d, J = 8.6 Hz, 1H), 4.38 – 4.22 (m, 1H), 3.26 (d, J = 4.9 Hz, 1H), 2.86 (d, J = 5.0 Hz, 1H), 1.84 (d, J = 12.7 Hz, 1H), 1.74 – 1.52 (m, 5H), 1.49 (s, 3H), 1.39 (s, 9H), 1.27 – 1.03 (m, 5H), 1.03 – 0.80 (m, 2H). ^{13}C NMR (101 MHz, CDCl_3) δ 209.76, 155.73, 79.81, 59.12, 52.47, 50.86, 38.92, 34.36, 34.19, 32.01, 28.40, 26.48, 26.36, 26.04, 16.90. LC-MS (linear gradient 10 \rightarrow 90% MeCN, 0.1% TFA, 15 min): R_t (min): 10.06 (ESI-MS (m/z): 311.60 ($M+H^+$)). HRMS: calculated for $\text{C}_{17}\text{H}_{29}\text{NO}_4$ 312.21693 [$M+H$] $^+$; found 312.21689. $[\alpha]_D^{20}$ = 113.2 (C=0.5, CHCl_3)

tert-butyl((R)-3-((3R,5R,7R)-adamantan-1-yl)-1-(methoxy(methyl)amino)-1-oxopropan-2-yl)carbamate (42)

This compound was synthesized according to the general procedure **A** described above on a 1.55 mmol scale and was isolated after column chromatography (0 \rightarrow 20% EtOAc:pent) (552 mg, 97%). ^1H NMR (400 MHz, CDCl_3) δ 4.96 (d, J = 9.5 Hz, 1H), 4.77 (t, J = 8.4 Hz, 1H), 3.76 (s, 3H), 3.15 (s, 3H), 1.97 – 1.86 (m, 3H), 1.71 – 1.56 (m, 6H), 1.56 – 1.46 (m, 6H), 1.39 (s, 9H), 1.29 – 1.18 (m, 2H). ^{13}C NMR (101 MHz, CDCl_3) δ 174.56, 155.25, 79.48, 61.64, 47.04, 46.74, 42.57, 42.48, 37.02, 36.97, 32.69, 32.34, 28.75, 28.71, 28.47.

tert-butyl((R)-1-((3R,5R,7R)-adamantan-1-yl)-4-methyl-3-oxopent-4-en-2-yl)carbamate (43)

This compound was synthesized according to the general procedure **B** described above on a 1 mmol scale and was isolated after column chromatography (0 \rightarrow 20% EtOAc:pent) (239 mg, 69%). ^1H NMR (400 MHz, CDCl_3) δ 6.06 (s, 1H), 5.81 (s, 1H), 5.11 (t, J = 8.5 Hz, 1H), 4.99 (d, J = 9.1 Hz, 1H), 1.91 (s, 3H), 1.85 (s, 3H), 1.69 – 1.46 (m, 13H), 1.38 (s, 9H), 1.10 (dd, J = 14.7, 9.6 Hz, 1H). ^{13}C NMR (101 MHz, CDCl_3) δ 201.68, 154.96, 142.05, 125.76, 79.42, 49.88, 47.12, 42.46, 36.75, 32.94, 28.52, 28.27, 17.90.

tert-butyl((2R,3S)-1-((3R,5R,7R)-adamantan-1-yl)-3-hydroxy-4-methylpent-4-en-2-yl)carbamate (44)

This compound was synthesized according to the general procedure **C** described above on a 0.69 mmol scale and the crude (quant) was used directly in the next step. ^1H NMR (400 MHz, CDCl_3) δ 5.02 (s, 1H), 4.93 (s, 1H), 4.71 (d, J = 8.4 Hz, 1H), 4.09 (s, 1H), 3.85 (dd, J = 17.4, 8.6 Hz, 1H), 2.43 (bs, 1H), 1.91 (s, 3H), 1.74 (s, 3H), 1.71 – 1.56 (m, 6H), 1.55 – 1.36 (m, 14H), 1.30 – 1.20 (m, 2H), 0.98 (dd, J = 14.7, 10.2 Hz, 1H). ^{13}C NMR (101 MHz, CDCl_3) δ 155.61, 145.07, 111.36, 79.43, 79.04, 48.50, 42.77, 42.68, 42.49, 37.09, 31.90, 28.77, 28.60, 28.50, 19.67.

tert-butyl((R)-3-((3R,5R,7R)-adamantan-1-yl)-1-((R)-2-methyloxiran-2-yl)-1-oxopropan-2-yl)carbamate (45)

This compound was synthesized according to the general procedure **D** described above on a 0.69 mmol scale and was isolated after column chromatography (0→20% EtOAc:pent) (88 mg, 0.24 mmol, 33%). ¹H NMR (400 MHz, CDCl₃) δ 4.75 (d, *J* = 8.6 Hz, 1H), 4.37 (t, *J* = 8.4 Hz, 1H), 3.31 (d, *J* = 5.0 Hz, 1H), 2.87 (d, *J* = 5.0 Hz, 1H), 1.95 (s, 3H), 1.73 – 1.53 (m, 12H), 1.51 (s, 3H), 1.40 (s, 9H), 1.35 (d, *J* = 1.9 Hz, 1H), 0.96 (dd, *J* = 14.5, 9.7 Hz, 1H). ¹³C NMR (101 MHz, CDCl₃) δ 209.42, 155.35, 79.85, 58.96, 52.49, 49.02, 45.18, 42.68, 36.98, 33.03, 28.78, 28.50, 17.12. LC-MS (linear gradient 10 → 90% MeCN, 0.1% TFA, 15 min): R_t (min): 11.03 (ESI-MS (m/z): 363.80 HRMS: calculated for C₂₁H₃₃NO₄ 364.24824 [M+H]⁺; found 364.24832. [α]_D²⁰ = 99.2 (C=0.5, CHCl₃)

tert-butyl(R)-1-(methoxy(methyl)amino)-3-(naphthalen-2-yl)-1-oxopropan-2-yl)carbamate (46)

This compound was synthesized according to the general procedure **A** described above on a 1.0 mmol scale and was isolated after column chromatography (10→50% EtOAc:pent) in a quantitative yield. ¹H NMR (400 MHz, CDCl₃) δ 7.79-7.77 (m, 3H), 7.61 (s, 1H), 7.46-7.39 (m, 2H), 7.32 (d, *J* = 8.0 Hz, 1H), 5.27(d, *J* = 8.0 Hz, 1H), 5.05 (m, 1H), 3.64 (s, 3H), 3.25-3.20 (m, 1H), 3.15 (s, 3H), 3.06-3.00 (m, 1H), 1.35 (s, 9H). ¹³C NMR (101 MHz, CDCl₃) δ 172.33, 155.26, 134.18, 133.47, 132.40, 128.10, 127.99, 127.67, 127.61, 126.00, 125.55, 79.63, 61.62, 51.50, 38.99, 32.12, 28.32. LC-MS (linear gradient 10 → 90% MeCN, 0.1% TFA, 15 min): R_t (min): 8.79 (ESI-MS (m/z): 358.73 (M+H⁺)). HRMS: cald. for C₂₀H₂₆N₂O₄, 359.19666 [M+H]⁺; found 359.19653. [α]_D²⁰ = + 19.8 (C=1, CHCl₃)

tert-butyl(R)-1-(4-methyl-1-(naphthalen-2-yl)-3-oxopent-4-en-2-yl)carbamate (47)

This compound was synthesized according to the general procedure **B** described above on a 1.0 mmol scale and was isolated after column chromatography (10→30% EtOAc:pent) (251 mg, 0.74 mmol, 74%). ¹H NMR (400 MHz, CDCl₃) δ 7.73-7.71 (m, 3H), 7.50 (s, 1H), 7.44-7.39 (m, 2H), 7.21 (d, *J* = 8.4 Hz, 1H), 6.02 (s, 1H), 5.79 (s, 1H), 5.37-5.35 (m, 2H), 3.28-3.24 (m, 1H), 3.08-3.04 (m, 1H), 1.83 (s, 3H), 1.38 (s, 9H). ¹³C NMR (101 MHz, CDCl₃) δ 200.12, 155.12, 142.45, 133.74, 133.39, 132.38, 128.14, 128.04, 127.65, 126.69, 126.06, 125.62, 79.69, 54.95, 39.91, 29.73, 28.33, 17.76.

tert-butyl((2R,3S)-3-hydroxy-4-methyl-1-(naphthalen-2-yl)pent-4-en-2-yl)carbamate (48)

This compound was synthesized according to the general procedure **C** described above on a 0.74 mmol scale and was isolated after column chromatography (1→10% EtOAc:pent) (126 mg, 0.37 mmol, 50%). ¹H NMR (400 MHz, CDCl₃) δ 7.78-7.76 (m, 3H), 7.60 (s, 1H), 7.44-7.39 (m, 2H), 7.32 (d, *J* = 1.2 Hz, 1H), 5.10 (s, 1H), 4.90 (s, 1H), 4.86 (d, *J* = 8.4 Hz, 1H), 4.21 (s, 1H), 4.10 (d, *J* = 7.2 Hz, 1H), 3.08-3.01 (m, 2H), 2.89 (t, *J* = 10 Hz, *J* = 13.2 Hz, 1H), 1.82 (s, 3H), 1.35 (s, 9H). ¹³C NMR (101 MHz, CDCl₃) δ 155.90, 144.85, 136.13, 133.54, 132.20, 127.89, 127.62, 127.53, 125.91, 125.31, 112.36, 79.47, 53.75, 34.55, 28.26, 19.16.

tert-butyl((R)-1-((R)-2-methyloxiran-2-yl)-3-(naphthalen-2-yl)-1-oxopropan-2-yl)carbamate (49)

This compound was synthesized according to the general procedure **D** described above on a 0.37 mmol scale and was isolated after column chromatography (10→30% EtOAc:pent) (75 mg, 0.21 mmol, 57%). ¹H NMR (400 MHz, CDCl₃) δ 7.82-7.76 (m, 3H), 7.58 (s, 1H), 7.47-7.40 (m, 2H), 7.30 (d, *J* = 1.6 Hz, 1H), 5.03 (d, *J* = 8.0 Hz, 1H), 4.69 (m, 1H), 3.32-3.29 (m, 1H), 3.27 (d, *J* = 4.8 Hz, 1H), 2.90 (d, *J* = 4.8 Hz, 1H), 2.88-2.82 (m, 1H), 1.50 (s, 3H), 1.33 (s, 9H). ¹³C NMR (101 MHz, CDCl₃) δ 208.43, 155.33, 133.59, 133.45, 132.50, 128.31, 128.11, 127.76, 127.62, 127.49, 126.22, 125.78, 79.94, 59.35, 53.78, 52.55, 37.62, 28.30, 16.72. LC-MS (linear gradient 10 → 90% MeCN, 0.1% TFA, 15 min): R_t (min): 9.70 (ESI-MS (m/z): 355.67 (M+H⁺)). HRMS: calculated for C₂₁H₂₅NO₄, 356.18557 [M+H]⁺; found 356.18563. [α]_D²⁰ = 146.4 (C=1, CHCl₃)

tert-butyl(R)-(1-(methoxy(methyl)amino)-3-(naphthalen-1-yl)-1-oxopropan-2-yl)carbamate (50)

This compound was synthesized according to the general procedure **A** described above on a 1.0 mmol scale and was isolated after column chromatography (10 \rightarrow 50% EtOAc:pent) in a quantitative yield. ^1H NMR (400 MHz, CDCl_3) δ 8.20 (d, J = 8.0 Hz, 1H), 7.79 (d, J = 8.0 Hz, 1H), 7.69 (d, J = 8.0 Hz, 1H), 7.52-7.29 (m, 4H), 5.58 (d, J = 9.0 Hz, 2H), 5.15-5.10 (m, 1H), 3.59-3.34 (m, 5H), 3.03 (s, 3H), 1.35 (s, 9H). ^{13}C NMR (101 MHz, CDCl_3) δ 172.09, 154.95, 133.48, 132.68, 132.14, 128.60, 128.45, 128.18, 127.44, 127.30, 125.80, 125.25, 124.99, 123.33, 123.04, 79.02, 77.36, 61.02, 50.77, 35.75, 31.66, 28.05. LC-MS (linear gradient 10 \rightarrow 90% MeCN, 0.1% TFA, 15 min): R_t (min): 8.56 (ESI-MS (m/z): 360.1 (M+H $^+$)). HRMS: calculated for $\text{C}_{20}\text{H}_{26}\text{N}_2\text{O}_4$, 359.19663 [M] $^+$; found 359.19653. $[\alpha]_D^{20}$ = 8.4 (C=1, CHCl_3)

tert-butyl (R)-(4-methyl-1-(naphthalen-1-yl)-3-oxopent-4-en-2-yl)carbamate (51)

This compound was synthesized according to the general procedure **B** described above on a 1.0 mmol scale and was isolated after column chromatography (10 \rightarrow 30% EtOAc:pent) (200 mg, 0.59 mmol, 59%). ^1H NMR (400 MHz, CDCl_3) δ 8.12 (d, J = 8.4 Hz, 1H), 7.81 (d, J = 8.0 Hz, 1H), 7.70 (d, J = 8.4 Hz, 1H), 7.54-7.50 (m, 1H), 7.46 (t, J = 7.2 Hz, 1H), 7.32 (t, J = 7.6 Hz, 1H), 7.17 (d, J = 7.2 Hz, 1H), 5.64 (s, 1H), 5.48-5.43 (m, 3H), 3.54 (m, 1H), 3.38-3.33 (m, 1H), 1.68 (s, 3H), 1.4 (s, 9H). ^{13}C NMR (101 MHz, CDCl_3): δ ppm 200.92, 155.09, 142.78, 133.83, 132.66, 132.23, 129.05, 128.78, 128.15, 127.70, 126.55, 126.37, 125.66, 125.21, 123.69, 123.18, 79.66, 53.95, 37.42, 28.36, 17.41.

tert-butyl((2R,3S)-3-hydroxy-4-methyl-1-(naphthalen-1-yl)pent-4-en-2-yl)carbamate (52)

This compound was synthesized according to the general procedure **C** described above on a 0.59 mmol scale and was isolated after column chromatography (1 \rightarrow 10% EtOAc:pent) (119 mg, 0.35 mmol, 60%). ^1H NMR (400 MHz, CDCl_3) δ 8.01 (d, J = 8.0 Hz, 1H), 7.85 (d, J = 7.6 Hz, 1H), 7.34 (d, J = 8.0 Hz, 1H), 7.52-7.44 (m, 2H), 7.40 (t, J = 7.2 Hz, 1H), 7.33 (d, J = 6.8 Hz, 1H), 5.21 (s, 1H), 5.08 (s, 1H), 4.76 (d, J = 8.8 Hz, 1H), 4.34 (s, 1H), 4.04-4.02 (m, 1H), 3.44 (d, J = 14.0 Hz, 1H), 3.17 (t, J = 10.8 Hz, 1H), 2.94 (s, 1H), 1.87 (s, 3H), 1.28 (s, 9H). ^{13}C NMR (101 MHz, CDCl_3) δ 155.92, 144.97, 134.94, 133.97, 132.51, 128.87, 128.09, 127.34, 127.13, 125.99, 125.51, 123.64, 112.94, 112.47, 79.45, 77.66, 53.92, 30.92, 29.80, 28.31, 27.55, 19.47.

tert-butyl((2R)-1-hydroxy-1-((R)-2-methyloxiran-2-yl)-3-(naphthalen-1-yl)propan-2-yl)carbamate (53)

This compound was synthesized according to the general procedure **D** described above on a 1.38 mmol scale and was isolated after column chromatography (10 \rightarrow 30% EtOAc:pent) (117 mg, 0.33 mmol, 93%). ^1H NMR (400 MHz, CDCl_3) δ 8.28 (d, J = 8.4 Hz, 1H), 7.86 (d, J = 8 Hz, 1H), 7.78 (d, J = 8.4 Hz, 1H), 7.60-7.56 (m, 1H), 7.52-7.48 (m, 1H), 7.41 (t, J = 7.2 Hz, 1H), 7.27 (d, J = 7.6 Hz, 1H), 4.98 (d, J = 7.6 Hz, 1H), 4.74-4.69 (m, 1H), 3.66 (dd, J = 4.8 Hz, 1H), 3.34 (d, J = 4.8 Hz, 1H), 3.03-2.97 (m, 1H), 2.91 (d, J = 4.8 Hz, 1H), 1.48 (s, 3H), 1.30 (s, 9H). ^{13}C NMR (101 MHz, CDCl_3): δ ppm 208.95, 208.90, 155.24, 133.99, 132.27, 128.91, 128.83, 128.53, 128.11, 127.80, 127.69, 126.56, 125.93, 125.58, 125.31, 125.15, 123.87, 123.74, 123.62, 79.91, 59.44, 53.91, 52.98, 52.62, 52.37, 51.59, 37.19, 35.17, 29.81, 28.44, 28.32, 27.66, 16.61. LC-MS (linear gradient 10 \rightarrow 90% MeCN, 0.1% TFA, 15 min): R_t (min): 9.71 (ESI-MS (m/z): 355.53 (M $^+$)). HRMS: calculated for $\text{C}_{21}\text{H}_{25}\text{NO}_4$ 356.18563 [M+H] $^+$; found 356.18556.

tert-butyl(R)-(3-([1,1'-biphenyl]-4-yl)-1-(methoxy(methyl)amino)-1-oxopropan-2-yl)carbamate (54)

This compound was synthesized according to the general procedure **A** described above on a 2 mmol scale and was isolated after column chromatography (10 \rightarrow 50% EtOAc:pent) in a quantitative yield. ^1H NMR (400 MHz, CDCl_3) δ ppm 7.56 (t, J = 7.2 Hz, 2H), 7.54 (d, J = 8.4 Hz, 2H), 7.49 (t, J = 7.6 Hz, 2H), 7.31-7.23 (m, 3), 5.36 (d, J = 8.8 Hz, 1H), 5.00-4.98 (m, 1H), 3.65 (s, 3H), 3.16 (s, 3H), 3.13-3.08 (d, J = 5.6 Hz, 2H), 2.93-2.88 (m, 1H), 1.39 (s, 9H). ^{13}C NMR (101 MHz, CDCl_3) δ 172.14, 155.15, 140.76, 139.45, 135.67, 129.82, 128.65, 127.07, 126.91, 126.87, 79.42, 61.45, 51.43, 38.23, 31.96, 28.23. LC-MS (linear gradient 10 \rightarrow 90% MeCN, 0.1% TFA, 15 min): R_t (min): 9.37 (ESI-MS (m/z): 385.73 (M+H $^+$)). HRMS: calculated for $\text{C}_{22}\text{H}_{28}\text{N}_2\text{O}_4$ 358.21218 [M+H] $^+$; found 385.21255. $[\alpha]_D^{20}$ = +10 (C=1, CHCl_3)

***tert*-butyl (R)-1-([1,1'-biphenyl]-4-yl)-4-methyl-3-oxopent-4-en-2-yl)carbamate (55)**

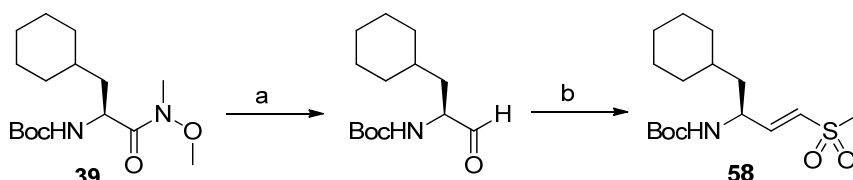
This compound was synthesized according to the general procedure **B** described above on a 2.0 mmol scale and was isolated after column chromatography (10→30% EtOAc:pent) (679 mg, 1.86 mmol, 93%). ¹H NMR (400 MHz, CDCl₃) δ 7.56-7.54 (m, 2H), 7.49 (d, *J* = 8.0 Hz, 2H), 7.42 (t, *J* = 7.2 Hz, 2H), 7.32 (t, *J* = 7.2 Hz, 1H), 7.14 (d, *J* = 8.0 Hz, 2H), 6.05 (s, 1H), 5.86 (s, 1H), 5.38-5.30 (m, 2H), 3.18-3.13 (m, 1H), 2.97-2.92 (m, 1H), 1.87 (s, 3H), 1.41 (s, 9H). ¹³C NMR (101 MHz, CDCl₃): δ ppm 200.02, 155.11, 142.41, 140.78, 139.70, 135.25, 130.10, 129.93, 129.90, 128.76, 127.22, 127.07, 126.99, 126.68, 79.70, 54.96, 39.39, 29.74, 28.36, 17.80.

***tert*-butyl((2R,3S)-1-([1,1'-biphenyl]-4-yl)-3-hydroxy-4-methylpent-4-en-2-yl)carbamate (56)**

This compound was synthesized according to the general procedure **C** described above on a 1.86 mmol scale and was isolated after column chromatography (1→10% EtOAc:pent) (444 mg, 1.21 mmol, 65%). ¹H NMR (400 MHz, CDCl₃) δ 7.57-7.55 (m, 2H), 7.51 (d, *J* = 8.0 Hz, 2H), 7.44-7.40 (m, 2H), 7.34-7.32 (m, 1H), 7.27-7.24 (m, 2H), 5.10 (s, 1H), 5.00 (s, 1H), 4.78 (d, *J* = 8.8 Hz, 1H), 4.21 (s, 1H), 4.04 (s, 1H), 2.95 (dd, *J* = 4.0, 3.6 Hz, 1H), 2.77-2.71 (m, 1H), 2.66 (s, 1H), 1.83 (s, 3H), 1.34 (s, 9H). ¹³C NMR (101 MHz, CDCl₃) δ 144.89, 141.15, 139.24, 137.71, 129.96, 128.84, 127.17, 127.15, 127.09, 112.41, 79.59, 77.26, 53.86, 34.13, 28.39, 19.21.

***tert*-butyl((R)-3-([1,1'-biphenyl]-4-yl)-1-((R)-2-methyloxiran-2-yl)-1-oxopropan-2-yl)carbamate (57)**

This compound was synthesized according to the general procedure **D** described above on a 1.21 mmol scale and was isolated after column chromatography (10→30% EtOAc:pent) (194 mg, 0.51 mmol, 42%). ¹H NMR (400 MHz, CDCl₃) δ 7.59-7.52 (m, 5H), 7.45-7.41 (m, 2H), 7.35-7.31 (m, 1H), 7.24 (d, *J* = 8.0 Hz, 1H), 5.00 (d, *J* = 8 Hz, 1H), 4.64-4.59 (m, 1H), 3.31 (d, *J* = 4.8 Hz, 1H), 3.18 (d, *J* = 4.4 Hz, 1H), 2.93 (d, *J* = 6.2 Hz, 1H), 2.79-2.74 (m, 1H), 1.53 (s, 3H), 1.37 (s, 9H). ¹³C NMR (101 MHz, CDCl₃) δ 208.41, 155.36, 140.85, 139.98, 135.06, 129.95, 128.87, 127.36, 127.34, 127.13, 80.02, 59.32, 53.78, 52.06, 37.14, 28.38, 16.77. LC-MS (linear gradient 10 → 90% MeCN, 0.1% TFA, 15 min): *R*_t (min): 10.22 (ESI-MS (*m/z*): 381.40 (M⁺)). HRMS: calculated for C₂₃H₂₇NO₄ 382.20125 [M+H]⁺; found 382.20128. [α]_D²⁰ = +115.6 (C=1, CHCl₃)



Scheme S3. Synthesis of Boc-Cha-VS (58). Reagents and conditions: (a) LiAlH₄, Et₂O; (b) Diethyl((methylsulfonyl)methyl) phosphonate, NaH, THF, 0°C, 72% (over two steps).

(S,E)-*tert*-butyl (1-cyclohexyl-4-(methylsulfonyl)but-3-en-2-yl)carbamate (58)

Weinreb amide **38** (0.80 g, 2.60 mmol) was dissolved in Et₂O (25 mL), put under an argon atmosphere and cooled to 0 °C. LiAlH₄ (1.5 equiv, 3.9 mmol, 3.9 mL of a 1 M solution in THF) was added slowly and the mixture was stirred at 0 °C for 0.5 h after which TLC analysis indicated complete conversion of the starting compound. 1 M aq. HCl was slowly added and the layers were separated. The organic layer was extracted with 1 M HCl and brine, dried over Na₂SO₄ and concentrated. Diethyl((methylsulfonyl)methyl) phosphonate (1.5 equiv, 3.90 mmol, 0.90 g) was dissolved in THF (25 mL) and cooled to 0 °C under an argon atmosphere. NaH (1.5 equiv, 3.90 mmol, 156 mg, 60% w/w in mineral oil) was slowly added and the mixture was stirred at 0 °C for 30 min. Next, the freshly obtained aldehyde (in THF (5 mL)) was slowly added and the mixture was stirred for 1.5 h while slowly warming it to RT. After this time TLC analysis indicated complete conversion of the aldehyde. EtOAc was added and the mixture was extracted with 1 M aq. HCl (2×) and brine, dried over Na₂SO₄ and concentrated. Column chromatography (10→30% EA:pent) yielded the title compound (617 mg, 1.86 mmol, 72%, contains 16% *Z*-isomer, based on NMR). ¹H NMR (Peaks reported for *E*-isomer) (400 MHz, CDCl₃) δ 6.78 (dd, *J* = 15.1, 5.0 Hz, 1H),

6.45 (dd, $J = 15.1, 1.5$ Hz, 1H), 4.68 (d, $J = 7.7$ Hz, 1H), 4.40 (s, 1H), 2.89 (s, 3H), 1.75 (d, $J = 12.8$ Hz, 1H), 1.71 – 1.50 (m, 4H), 1.39 (m, 11H), 1.15 (m, 4H), 1.02 – 0.71 (m, 2H). ^{13}C NMR (101 MHz, CDCl_3) δ 155.13, 149.30, 148.83, 128.93, 80.01, 48.80, 43.79, 42.92, 41.97, 34.07, 33.96, 33.87, 33.52, 32.61, 28.43, 28.38, 28.35, 26.40, 26.36, 26.27, 26.17, 26.02. LC-MS (linear gradient 10 \rightarrow 90% MeCN, 0.1% TFA, 15 min): R_t (min): 7.94 (ESI-MS (m/z): 331.80 (M+H⁺)). HRMS: calculated for $\text{C}_{16}\text{H}_{29}\text{NO}_4\text{S}$ 332.18901 [M+H]⁺; found 332.18912. $[\alpha]_D^{20} = -9.2$ (C=1, CHCl_3)

Synthesis of peptide hydrazides

MorphAc-Ala-Tyr(OMe)-OMe (60b)

Boc-Ala-Tyr(OMe)-OMe was prepared by the general procedure for peptide coupling on a 1 mmol scale. Column chromatography provided (10 \rightarrow 40% EtOAc:pent) the product (365 mg, 0.96 mmol, 96%). Boc-Ala-Tyr(OMe)-OMe (365 mg, 0.54 mmol, 1 equiv.) was deprotected using the standard procedure for Boc removal. MorphAc-Ala-Tyr(OMe)-OMe (60b) was prepared by the general procedure for peptide coupling on a 0.96 mmol scale. Column chromatography provided (1 \rightarrow 3% MeOH:DCM) the product in a quantitative yield. ^1H NMR (400 MHz, CDCl_3) δ 7.53 (d, $J = 7.9$ Hz, 1H), 7.00 (d, $J = 8.6$ Hz, 2H), 6.77 (d, $J = 8.6$ Hz, 2H), 6.71 (d, $J = 7.7$ Hz, 1H), 4.74 (q, $J = 6.8$ Hz, 1H), 4.49 (p, $J = 7.1$ Hz, 1H), 3.74 (s, 3H), 3.70 (s, 3H), 3.69 – 3.64 (m, 4H), 3.12 – 2.87 (m, 4H), 2.52 – 2.40 (m, 4H), 1.34 (d, $J = 7.0$ Hz, 3H). ^{13}C NMR (101 MHz, CDCl_3) δ 171.89, 171.85, 169.91, 158.68, 130.29, 127.73, 114.01, 66.96, 61.77, 55.23, 53.80, 53.53, 52.46, 48.16, 36.89, 18.27.

MorphAc-Ala-Tyr(OMe)-NHNH₂ (61)

Methyl ester **60b** (390 mg, 0.96 mmol, 1 equiv.) was dissolved in MeOH (10 mL). Hydrazine hydrate (1500 μL , 29 mmol, 30 equiv.) was added and the mixture was stirred for 3 h before being co-evaporated with toluene (3x). The residue was used without further purification. ^1H NMR (400 MHz, MeOD) δ 7.07 (d, $J = 8.5$ Hz, 2H), 6.77 (d, $J = 8.6$ Hz, 2H), 4.46 (t, $J = 7.3$ Hz, 1H), 4.39 (d, $J = 7.0$ Hz, 1H), 3.73 (s, 3H), 3.71 – 3.65 (m, 4H), 3.06 – 2.77 (m, 4H), 2.50 – 2.42 (m, 4H), 1.29 (d, $J = 7.0$ Hz, 3H). ^{13}C NMR (101 MHz, MeOD) δ 173.82, 172.46, 171.73, 159.73, 131.41, 129.71, 115.00, 68.02, 62.55, 56.16, 54.85, 54.77, 38.43, 19.26.

Fmoc-D-Ala-Trp(Boc)-OMe (62)

The title compound was prepared by the general procedure for peptide coupling on a 1.53 mmol scale. Column chromatography (20 \rightarrow 80% EtOAc:pent) provided the product in a quantitative yield.

^1H NMR (400 MHz, CDCl_3) δ 8.10 (s, 1H), 7.74 (d, $J = 7.5$ Hz, 2H), 7.56 (d, $J = 6.9$ Hz, 2H), 7.48 (d, $J = 7.6$ Hz, 1H), 7.44 – 7.34 (m, 3H), 7.31 – 7.25 (m, 3H), 7.22 (t, $J = 7.4$ Hz, 1H), 7.00 (d, $J = 7.2$ Hz, 1H), 5.68 (d, $J = 7.4$ Hz, 1H), 4.99 – 4.89 (m, 1H), 4.41 – 4.28 (m, 3H), 4.21 – 4.14 (m, 1H), 3.65 (s, 3H), 3.32 – 3.09 (m, 2H), 1.65 (s, 9H), 1.36 (d, $J = 6.7$ Hz, 3H). ^{13}C NMR (101 MHz, CDCl_3) δ 172.16, 171.86, 155.90, 149.50, 143.87, 143.74, 141.27, 141.25, 135.27, 130.33, 127.70, 127.05, 125.11, 124.60, 124.23, 122.61, 119.96, 118.72, 115.32, 114.79, 83.71, 67.08, 60.44, 52.51, 52.46, 50.38, 47.04, 28.18, 27.39, 19.02, 14.23.

H-D-Ala-Trp(Boc)-OMe (63)

To a solution of Fmoc-D-Ala-Trp(Boc)-OMe **62** (1.19 g, 1.53 mmol, 1 equiv.) in THF (15 mL) were added DBU (67 μL , 0.46 mmol, 0.3 equiv.) and ethanethiol (11 mL, 15.3 mmol, 10 equiv.). After 45 min. the reaction mixture was concentrated and co-evaporated with toluene. Column chromatography (50 \rightarrow 100% EtOAc:pent \rightarrow 10% MeOH in EtOAc) yielded the title compound (575 mg, 1.38 mmol, 90%) ^1H NMR (400 MHz, CDCl_3) δ 8.10 (s, 1H), 7.53 (d, $J = 9.1$ Hz, 1H), 7.43 (s, 1H), 7.32 (t, $J = 7.3$ Hz, 1H), 7.25 (t, $J = 6.6$ Hz, 1H), 4.84 (s, 1H), 3.73 (s, 3H), 3.49 – 3.13 (m, 3H), 1.68 (s, 9H), 1.24 (d, $J = 5.2$ Hz, 3H). ^{13}C NMR (101 MHz, CDCl_3) δ 176.17, 171.94, 130.07, 124.33, 123.68, 122.32, 118.41, 115.09, 114.93, 83.68, 55.14, 52.08, 52.05, 49.80, 49.55, 27.65, 26.78, 20.26. LC-MS (linear gradient 10 \rightarrow 90% MeCN, 0.1% TFA, 15 min): R_t (min): 6.58 (ESI-MS (m/z): 389.93 (M+H⁺)).

3MeIndAc-D-Ala-Trp-OMe (64)

The title compound was prepared by the general procedure for peptide coupling on a 0.4 mmol scale. Column chromatography (20→60% EtOAc:pent) provided the product (198 mg, 0.36 mmol, 90%). ¹H NMR (400 MHz, CDCl₃) δ 8.16 – 8.03 (m, 1H), 7.51 (d, *J* = 7.7 Hz, 1H), 7.46 – 7.37 (m, 3H), 7.37 – 7.23 (m, 4H), 7.20 (t, *J* = 7.4 Hz, 1H), 6.60 (d, *J* = 7.3 Hz, 1H), 4.93 (q, *J* = 6.5 Hz, 1H), 4.75 (p, *J* = 6.9 Hz, 1H), 3.66 (s, 3H), 3.54 (s, 2H), 3.36 – 3.16 (m, 2H), 2.47 (s, 3H), 1.64 (s, 9H), 1.42 (d, *J* = 6.9 Hz, 3H). ¹³C NMR (101 MHz, CDCl₃) δ 172.53, 171.86, 165.75, 147.51, 145.53, 142.22, 131.84, 130.34, 127.25, 126.74, 124.62, 124.27, 123.85, 122.64, 120.79, 118.75, 115.34, 114.97, 83.72, 52.63, 52.57, 48.63, 38.32, 28.23, 27.33, 18.97, 12.31. LC-MS (linear gradient 10 → 90% MeCN, 0.1% TFA, 15 min): R_t (min): 10.51 (ESI-MS (m/z): 545.93 (M+H⁺)).

3MeIndAc-D-Ala-Trp(Boc)-NHNH₂ (65)

Methyl ester **64** (165 mg, 0.30 mmol, 1 equiv.) was dissolved in MeOH (4 mL). Hydrazine hydrate (523 μL, 10.5 mmol, 35 equiv.) was added and the mixture was stirred for 3 h before being co-evaporated with toluene (3x). The residue was used without further purification (isolated as mixture of + and - Boc). ¹H NMR (400 MHz, MeOD) δ 7.61 – 7.49 (m, 1H), 7.49 – 7.38 (m, 3H), 7.28 (dq, *J* = 26.3, 11.2, 9.3 Hz, 3H), 7.07 – 6.92 (m, 2H), 4.73 – 4.59 (m, 1H), 4.59 – 4.48 (m, 1H), 4.45 – 4.33 (m, 1H), 3.65 – 3.41 (m, 1H), 3.27 – 3.14 (m, 1H), 2.45 (d, *J* = 7.5 Hz, 2H), 1.42 (s, 6H (partially -Boc)), 1.30 – 1.15 (m, 3H). LC-MS (linear gradient 10 → 90% MeCN, 0.1% TFA, 15 min): R_t (min): 6.16 (ESI-MS (m/z): 445.93 (M+H⁺-Boc) and 7.76 (ESI-MS (m/z): 546.00 (M+H⁺+Boc)).

Boc-D-Ala-Tyr(OMe)-OMe (66)

The title compound was prepared by the general procedure for peptide coupling on a 1 mmol scale. Column chromatography (20→60% EtOAc:pent) provided the product (349 mg, 0.92 mmol, 92%). ¹H NMR (400 MHz, CDCl₃) δ 6.99 (d, *J* = 8.6 Hz, 2H), 6.87 – 6.71 (m, 3H), 5.17 (d, *J* = 7.5 Hz, 1H), 4.85 – 4.70 (m, 1H), 4.29 – 4.11 (m, 1H), 3.73 (s, 3H), 3.67 (s, 3H), 3.01 (qd, *J* = 14.0, 5.9 Hz, 2H), 1.40 (s, 9H), 1.26 (d, *J* = 7.1 Hz, 3H). ¹³C NMR (101 MHz, CDCl₃) δ 172.42, 171.97, 158.66, 155.45, 130.29, 127.74, 113.98, 79.98, 55.18, 53.27, 52.33, 49.94, 37.04, 28.34, 18.56.

MorphAc-D-Ala-Tyr(OMe)-OMe (67)

Boc-D-Ala-Tyr(OMe)-OMe (365 mg, 0.54 mmol, 1 equiv.) was deprotected using the standard procedure for Boc removal. The title compound was prepared by the general procedure for peptide coupling on a 0.54 mmol scale. Column chromatography (1→3% MeOH:DCM) provided the product (160 mg, 0.39 mmol, 79%). ¹H NMR (400 MHz, CDCl₃) δ 7.61 (d, *J* = 8.0 Hz, 1H), 7.01 (dd, *J* = 14.1, 8.4 Hz, 3H), 6.76 (d, *J* = 8.6 Hz, 2H), 4.73 (q, *J* = 7.3 Hz, 1H), 4.53 (p, *J* = 7.0 Hz, 1H), 3.71 (s, 3H), 3.65 (d, *J* = 4.8 Hz, 7H), 3.09 – 2.85 (m, 4H), 2.51 – 2.36 (m, *J* = 4.3 Hz, 4H), 1.24 (d, *J* = 7.0 Hz, 3H). ¹³C NMR (101 MHz, CDCl₃) δ 171.82, 171.80, 169.78, 158.58, 130.25, 127.79, 113.85, 66.86, 61.74, 55.15, 53.69, 53.25, 52.28, 48.00, 36.92, 18.65.

MorphAc-D-Ala-Tyr(OMe)-NHNH₂ (68)

Methyl ester **67** (160 mg, 0.39 mmol, 1 equiv.) was dissolved in MeOH (4 mL). Hydrazine hydrate (567 μL, 11.7 mmol, 30 equiv.) was added and the mixture was stirred for 3 h before being co-evaporated with toluene (3x). The residue was used without further purification. ¹H NMR (400 MHz, MeOD) δ 7.10 (d, *J* = 8.6 Hz, 2H), 6.80 (d, *J* = 8.7 Hz, 2H), 4.54 (dd, *J* = 9.4, 5.5 Hz, 1H), 4.30 (q, *J* = 7.0 Hz, 1H), 3.74 (s, 3H), 3.70 (t, *J* = 4.6 Hz, 4H), 3.12 (dd, *J* = 14.0, 5.5 Hz, 1H), 2.98 (d, *J* = 3.6 Hz, 2H), 2.79 (dd, *J* = 14.0, 9.4 Hz, 1H), 2.56 – 2.39 (m, *J* = 4.3 Hz, 4H), 1.13 (d, *J* = 7.1 Hz, 3H). ¹³C NMR (101 MHz, MeOD) δ 173.59, 171.81, 171.34, 159.17, 130.68, 129.29, 114.37, 67.38, 61.89, 55.51, 54.14, 53.98, 37.50, 18.50. LC-MS (linear gradient 10 → 90% MeCN, 0.1% TFA, 15 min): R_t (min): 3.14 (ESI-MS (m/z): 408.13 (M+H⁺)).

3MeIndAc-D-Ala-Tyr(OMe)-OMe (69)

Boc-D-Ala-Tyr(OMe)-OMe (365 mg, 0.50 mmol, 1 equiv.) was deprotected using the standard procedure for Boc removal. The title compound was prepared by the general procedure for peptide coupling on a 0.5 mmol scale. Column chromatography (10 \rightarrow 80% EtOAc:pent) provided the product (159 mg, 0.36 mmol, 73%). ^1H NMR (400 MHz, CDCl_3) δ 7.39 (d, J = 7.2 Hz, 2H), 7.31 (q, J = 7.1 Hz, 2H), 7.17 (d, J = 8.0 Hz, 1H), 7.06 (d, J = 8.5 Hz, 2H), 6.76 (d, J = 8.5 Hz, 2H), 6.66 (d, J = 7.0 Hz, 1H), 4.81 (q, J = 7.6 Hz, 1H), 4.67 (p, J = 6.9 Hz, 1H), 3.68 (s, 3H), 3.67 (s, 3H), 3.51 (s, 2H), 3.13 (dd, J = 14.0, 5.3 Hz, 1H), 3.00 (dd, J = 14.0, 7.5 Hz, 1H), 2.42 (s, 3H), 1.35 (d, J = 7.0 Hz, 3H). ^{13}C NMR (101 MHz, CDCl_3) δ 172.75, 172.32, 165.93, 158.66, 147.94, 145.41, 142.22, 131.49, 130.27, 127.85, 127.30, 126.72, 123.81, 120.77, 113.93, 55.11, 53.49, 52.48, 48.85, 38.17, 36.79, 18.57, 12.23.

3MeIndAc-D-Ala-Tyr(OMe)-NHNH₂ (70)

Methyl ester **69** (159 mg, 0.36 mmol, 1 equiv.) was dissolved in MeOH (4 mL). Hydrazine hydrate (523 μl , 10.8 mmol, 30 equiv.) was added and the mixture was stirred for 3 h before being co-evaporated with tol (3x). The residue was used without further purification. ^1H NMR (400 MHz, MeOD) δ 7.47 – 7.25 (m, 4H), 7.08 (d, J = 8.6 Hz, 2H), 6.72 (d, J = 8.6 Hz, 2H), 4.61 – 4.52 (m, 1H), 4.41 (q, J = 7.1 Hz, 1H), 3.60 (d, J = 14.3 Hz, 5H), 3.11 (dd, J = 14.0, 5.4 Hz, 1H), 2.86 (dd, J = 14.0, 8.9 Hz, 1H), 2.46 (s, 3H), 1.25 (d, J = 7.1 Hz, 3H). ^{13}C NMR (101 MHz, MeOD) δ 174.39, 171.92, 167.55, 159.10, 149.04, 145.83, 142.99, 131.82, 130.62, 129.01, 127.89, 127.22, 124.29, 121.26, 114.31, 55.36, 53.85, 49.98, 38.48, 37.28, 17.86, 12.45. LC-MS (linear gradient 10 \rightarrow 90% MeCN, 0.1% TFA, 15 min): R_t (min): 5.88 (ESI-MS (m/z): 437.00 ($\text{M}+\text{H}^+$)).

MorphAc-D-Ala-Trp(Boc)-OMe (71)

The title compound was prepared by the general procedure for peptide coupling on a 0.43 mmol scale. Column chromatography (1 \rightarrow 3% MeOH:DCM) provided the product (349 mg, 0.92 mmol, 92%). ^1H NMR (400 MHz, CDCl_3) δ 8.08 (d, J = 6.9 Hz, 1H), 7.60 (d, J = 8.0 Hz, 1H), 7.45 (d, J = 7.7 Hz, 1H), 7.38 (s, 1H), 7.27 (t, J = 7.0 Hz, 1H), 7.20 (t, J = 7.5 Hz, 1H), 7.05 (d, J = 7.8 Hz, 1H), 4.85 (q, J = 6.0 Hz, 1H), 4.54 (p, J = 7.0 Hz, 1H), 3.72 – 3.62 (m, 7H), 3.20 (qd, J = 14.8, 5.9 Hz, 2H), 2.98 – 2.85 (m, 2H), 2.49 – 2.37 (m, J = 4.5 Hz, 4H), 1.63 (s, 9H), 1.29 (d, J = 7.0 Hz, 3H). ^{13}C NMR (101 MHz, CDCl_3) δ 171.92, 171.80, 169.86, 149.51, 130.30, 124.61, 124.26, 122.62, 118.76, 115.31, 114.84, 83.73, 66.93, 61.74, 53.73, 53.37, 52.51, 52.34, 48.11, 28.22, 27.32, 18.52. LC-MS (linear gradient 10 \rightarrow 90% MeCN, 0.1% TFA, 15 min): R_t (min): 6.68 (ESI-MS (m/z): 517.07 ($\text{M}+\text{H}^+$)).

MorphAc-D-Ala-Trp(Boc)-NHNH₂ (72)

Methyl ester **71** (234 mg, 0.43 mmol, 1 equiv.) was dissolved in MeOH (6 mL). Hydrazine hydrate (640 μl , 12.9 mmol, 30 equiv.) was added and the mixture was stirred for 3 h before being co-evaporated with tol (3x). The residue was used without further purification (isolated as mixture of + and - Boc). ^1H NMR (400 MHz, MeOD) δ 7.55 (d, J = 8.7 Hz, 1H), 7.32 (d, J = 8.1 Hz, 1H), 7.09 (t, J = 7.1 Hz, 1H), 7.07 – 6.97 (m, 2H), 4.67 – 4.55 (m, 2H), 4.31 (q, J = 7.0 Hz, 1H), 3.67 (hept, J = 6.9, 5.9 Hz, 4H), 3.26 (dd, J = 14.7, 6.1 Hz, 1H), 3.13 (dd, J = 14.7, 7.6 Hz, 1H), 2.91 (d, J = 4.6 Hz, 2H), 2.51 – 2.34 (m, 4H), 1.42 (s, 5H (Boc, partially removed)), 1.15 (d, J = 7.1 Hz, 3H). ^{13}C NMR (101 MHz, MeOD) δ 173.36, 172.21, 171.28, 137.02, 127.87, 123.96, 122.07, 119.47, 118.62, 111.90, 109.76, 67.27, 61.81, 54.16, 54.03, 53.31, 49.14, 28.53, 28.29, 18.26. LC-MS (linear gradient 10 \rightarrow 90% MeCN, 0.1% TFA, 15 min): R_t (min): 3.56 (ESI-MS (m/z): 417.07 ($\text{M}+\text{H}^+$)).

3MeIndAc-Ala-Tyr(OMe)-OMe (73)

The title compound was prepared by the general procedure for peptide coupling on a 0.21 mmol scale. Column chromatography (10 \rightarrow 50% EtOAc:pent) provided the product (66 mg, 0.15 mmol, 75%). ^1H NMR (400 MHz, CDCl_3) δ 7.45 (t, J = 7.9 Hz, 2H), 7.34 (p, J = 7.0 Hz, 2H), 7.01 (d, J = 8.5 Hz, 2H), 6.87 (d, J = 7.9 Hz, 1H), 6.68 (d, J = 8.5 Hz, 2H), 6.36 (d, J = 7.4 Hz, 1H), 4.81 (q, J = 7.1 Hz, 1H), 4.69 (p, J = 7.0 Hz, 1H), 3.73 (s, 3H), 3.57 (s, 3H), 3.54 (s, 2H), 3.11 (dd, J = 14.1, 5.4 Hz, 1H), 2.99 (dd, J = 14.1, 7.0 Hz, 1H), 2.52 (s, 3H), 1.43 (d, J = 7.0 Hz, 3H). ^{13}C NMR (101 MHz, CDCl_3) δ 172.28, 171.92, 165.81, 158.69, 148.13, 145.59, 142.17, 131.53, 130.25, 127.74, 127.42,

126.88, 123.91, 120.89, 113.96, 55.05, 53.57, 52.47, 48.49, 38.27, 37.02, 18.27, 12.39. LC-MS (linear gradient 10 → 90% MeCN, 0.1% TFA, 15 min): R_t (min): 8.42 (ESI-MS (m/z): 437.00 (M+H⁺)).

3MeIndAc-Ala-Tyr(OMe)-NHNH₂ (74)

Methyl ester **73** (66 mg, 0.15 mmol, 1 equiv.) was dissolved in MeOH (1.5 mL) and CHCl₃ (0.5 mL). Hydrazine hydrate (218 μL, 4.5 mmol, 30 equiv.) was added and the mixture was stirred for 3 h before being co-evaporated with toluene (3x). The residue was used without further purification. No NMR-analysis was performed due to poor solubility of the product in MeOD and CDCl₃ and mixtures thereof. LC-MS (linear gradient 10 → 90% MeCN, 0.1% TFA, 15 min): R_t (min): 6.14 (ESI-MS (m/z): 437.00 (M+H⁺)).

Fmoc-Hyp(tBu)-Nle-OMe (75)

The title compound was prepared by the general procedure for peptide coupling on a 3 mmol scale. Column chromatography (30→60% EtOAc:pent) provided the product (1.75 g, 3.00 mmol, 100%). Complex NMR due to a presence of rotamers. ¹H NMR (400 MHz, CDCl₃) δ 7.72 (d, *J* = 7.4 Hz, 2H), 7.63 – 7.48 (m, 2H), 7.36 (t, *J* = 7.3 Hz, 2H), 7.32 – 7.22 (m, 2H), 7.17 (d, *J* = 7.5 Hz, 0.7H), 6.46 (d, *J* = 7.7 Hz, 0.3H), 4.62 – 4.08 (m, 6H), 3.69 (s, 3H), 3.54 (s, 1H), 3.44 – 3.20 (m, 1H), 2.48 – 2.34 (m, 0.8H), 2.19 (s, 0.8H), 2.06 – 1.88 (m, 1H), 1.86 – 1.72 (m, 0.8H), 1.65 (dd, *J* = 14.3, 7.2 Hz, 0.6H), 1.33 – 1.07 (m, 13H), 0.79 (q, *J* = 9.2, 7.8 Hz, 3H). ¹³C NMR (101 MHz, CDCl₃) δ 172.64, 171.83, 171.18, 155.81, 154.77, 144.00, 143.76, 143.67, 141.16, 127.61, 126.92, 73.94, 69.56, 68.43, 67.79, 60.25, 59.45, 58.88, 54.03, 53.04, 52.36, 52.11, 51.76, 47.00, 39.02, 36.09, 32.02, 31.70, 28.20, 27.30, 22.11, 13.75.

H-Hyp(tBu)-Nle-OMe (76)

Fmoc-Hyp(tBu)-Nle-OMe **75** (1745 mg, 3.00 mmol, 1 equiv.) was dissolved in THF (30 mL). After addition of ethanethiol (2.22 mL, 30 mmol, 10 equiv.) and DBU (45 μL, 0.3 mmol, 0.1 equiv.), the reaction mixture was stirred for 1 h. The reaction mixture was then concentrated and co-evaporated with toluene (3x). Purification by column chromatography (10→100% EtOAc: Pent) yielded the title compound (540 mg, 1.72 mmol, 57%, not completely pure). The product was used without further purification.

Fmoc-Ala-Hyp(tBu)-Nle-OMe (77)

The title compound was prepared by the general procedure for peptide coupling on a 3 mmol scale. Column chromatography (30→60% EtOAc:pent) yielded the product (211 mg, 0.348 mmol, 48%, not completely pure) which was used without further purification.

H-Ala-Hyp(tBu)-Nle-OMe (78)

Fmoc-Ala-Hyp(tBu)-Nle-OMe **77** (639 mg, 1.05 mmol, 1 equiv.) was dissolved in THF (11 mL). After addition of ethanethiol (0.78 mL, 10.5 mmol, 10 equiv.) and DBU (32 μL, 0.21 mmol, 0.2 equiv.) the reaction mixture was stirred for 1h. the reaction mixture was concentrated and co-evaporated with toluene (3x). Purification by column chromatography (4:6:0→9:0:1 EtOAc: Pent: MeOH) yielded the title compound (247 mg, 0.64 mmol, 61%), which was directly used in the next step.

N₃Gly-Ala-Hyp(tBu)-Nle-OMe (79)

Ala-Hyp(tBu)-Nle-OMe (247 mg, 0.64 mmol, 1 equiv.) was dissolved in DMF (7 mL) before adding (ClAc)₂O (131 mg, 0.77 mmol, 1.2 equiv.) and DiPEA (0.45 mL, 2.56 mmol, 4 equiv.). The reaction mixture was stirred for 1h before NaN₃ (166 mg, 2.56 mmol, 4 equiv.) was added. The reaction mixture was then stirred overnight followed by addition of EtOAc (50 mL). The mixture was washed with 1M HCl (2x), sat. aq. NaHCO₃ (2x) and brine (1x). The organic layer was dried over Na₂SO₄, filtered and concentrated. Purification by column chromatography (0→3% MeOH: DCM) yielded the title compound (114 mg, 0.29, 46%). ¹H NMR (400 MHz, CDCl₃) δ 7.29 (d, *J* = 3.7 Hz, 1H), 7.14 (d, *J* = 7.8 Hz, 1H), 4.65 – 4.51 (m, 2H), 4.51 – 4.22 (m, 2H), 3.91 (s, 2H), 3.73 – 3.51 (m, 4H), 3.49 –

3.22 (m, 1H), 2.48 – 2.18 (m, 1H), 1.87 (m, 1H), 1.80 – 1.65 (m, 1H), 1.65 – 1.47 (m, 1H), 1.36 – 0.94 (m, 16H), 0.81 (t, $J = 6.9$ Hz, 3H). ^{13}C NMR (101 MHz, CDCl_3) δ 172.70, 171.68, 170.48, 166.06, 74.14, 69.82, 58.56, 53.53, 52.28, 52.25, 52.20, 46.51, 35.49, 31.74, 28.13, 27.28, 22.11, 18.01, 13.77. LC-MS (linear gradient 10 \rightarrow 90% MeCN, 0.1% TFA, 12.5 min): R_t (min): 6.62 (ESI-MS (m/z): 469.07 ($\text{M}+\text{H}^+$)).

$\text{N}_3\text{Gly-Ala-Hyp(tBu)-Nle-NHNH}_2$ (80)

Azido-Ac-Ala-Hyp(tBu)-Nle-OMe **79** was dissolved in MeOH (3 mL). After addition of hydrazine (0.42 mL, 8.7 mmol, 30 equiv.) the reaction mixture was stirred for approximately 2 hours at room temperature. The reaction mixture was concentrated before being co-evaporated with MeOH (2x). This yielded the title compound in a quantitative yield. ^1H NMR (400 MHz, MeOD) δ 4.66 (q, $J = 6.9$ Hz, 1H), 4.56 (t, $J = 7.1$ Hz, 1H), 4.52 – 4.41 (m, 1H), 4.24 (dd, $J = 8.4, 5.9$ Hz, 1H), 3.90 (d, $J = 9.7$ Hz, 2H), 3.82 (dd, $J = 10.3, 5.6$ Hz, 1H), 3.70 – 3.19 (m, 2H), 2.21 – 2.00 (m, 2H), 1.86 – 1.57 (m, 2H), 1.51 – 1.06 (m, 16H), 0.93 (t, $J = 6.6$ Hz, 3H). ^{13}C NMR (101 MHz, MeOD) δ 173.99, 173.45, 173.22, 169.59, 75.42, 71.34, 71.14, 69.27, 60.39, 55.46, 54.95, 53.59, 52.51, 49.66, 49.45, 49.23, 49.02, 48.81, 48.60, 48.42, 48.38, 48.12, 38.29, 32.82, 28.99, 28.55, 23.37, 17.09, 14.30. LC-MS (linear gradient 10 \rightarrow 90% MeCN, 0.1% TFA, 12.5 min): R_t (min): 4.77 (ESI-MS (m/z): 469.13 ($\text{M}+\text{H}^+$)).

Boc-Thz-Nle-OMe (81)

The title compound was prepared by the general procedure for peptide coupling on a 3 mmol scale. Column chromatography (10 \rightarrow 50% EtOAc:pent) provided the product (989 mg, 2.74 mmol, 91%). ^1H NMR (400 MHz, CDCl_3) δ 7.11 (bs, 1H), 6.62 (bs, 1H), 4.92 – 4.46 (m, 3H), 4.46 – 4.15 (m, 1H), 3.71 (s, 3H), 3.54 – 2.95 (m, 2H), 1.96 – 1.73 (m, 1H), 1.73 – 1.55 (m, 1H), 1.47 (s, 9H), 1.36 – 1.09 (m, 4H), 0.99 – 0.69 (m, 3H). ^{13}C NMR (101 MHz, CDCl_3) δ 172.63, 169.94, 80.04, 52.43, 52.41, 52.23, 32.28, 28.30, 28.25, 27.31, 27.27, 22.34, 22.31, 13.97, 13.95.

Boc-Ala-Thz-Nle-OMe (82)

Boc-Thz-Nle-OMe **81** (989 mg, 2.74 mmol) was deprotected using the standard procedure for Boc removal. The title compound was prepared by the general procedure for peptide coupling on a 2.74 mmol scale. Column chromatography (40 \rightarrow 60% EtOAc:pent) provided the product (747 mg, 1.73 mmol, 63%). ^1H NMR (400 MHz, CDCl_3) δ 8.03 (d, $J = 6.3$ Hz, 0.3H), 7.50 (d, $J = 7.9$ Hz, 0.2H), 6.97 (d, $J = 5.9$ Hz, 0.5H), 5.36 (d, $J = 6.6$ Hz, 0.6H), 5.16 (m, 0.4H), 5.01 (m, 0.5H), 4.81 (d, $J = 9.3$ Hz, 0.6H), 4.74 – 4.62 (m, 0.4H), 4.61 – 4.35 (m, 2.5H), 4.35 – 4.20 (m, 0.6H), 4.16 (dd, $J = 7.4, 4.2$ Hz, 0.3H), 3.94 (d, $J = 9.9$ Hz, 0.2H), 3.78 – 3.57 (m, 3H), 3.52 – 3.29 (m, 1H), 3.21 – 2.98 (m, 1H), 2.02 – 1.70 (m, 1H), 1.70 – 1.50 (m, 1H), 1.50 – 1.04 (m, 16H), 0.84 (d, $J = 5.5$ Hz, 3H). ^{13}C NMR (101 MHz, CDCl_3) δ 172.70, 170.67, 168.89, 80.04, 66.01, 62.89, 62.21, 53.65, 53.24, 52.50, 52.44, 52.40, 52.22, 52.06, 49.38, 49.19, 48.05, 35.37, 34.55, 32.16, 31.95, 31.81, 30.28, 28.39, 28.17, 27.48, 27.21, 22.27, 18.82, 16.54, 13.93.

$\text{N}_3\text{Gly-Ala-Thz-Nle-OMe}$ (3) (83)

Boc-Ala-Thz-Nle-OMe **82** (349 mg, 0.81 mmol) was deprotected using the standard procedure for Boc removal. The crude TFA salt was dissolved in DMF (8 mL) before adding $(\text{ClAc})_2\text{O}$ (164 mg, 0.97 mmol, 1.2 equiv.) and DiPEA (0.56 mL, 3.24 mmol, 4 equiv.). The reaction mixture was stirred for 1 h before NaN_3 (210 mg, 3.24 mmol, 4 equiv.) was added. After stirring overnight, EtOAc (50 mL) was added to the reaction mixture before being washed with 1M HCl (2x), sat. aq. NaHCO_3 (2x) and brine (1x). The organic layer was dried over Na_2SO_4 , filtered and concentrated. Purification by column chromatography (80 \rightarrow 100% EtOAc:Tol) yielded the title compound (213 mg, 0.51 mmol, 64%). Complex NMR due to a presence of rotamers. ^1H NMR (400 MHz, CDCl_3) δ 7.85 (d, $J = 7.4$ Hz, 0.2H), 7.30 (d, $J = 9.1$ Hz, 0.8H), 7.14 (d, 0.3H), 7.00 (d, $J = 7.6$ Hz, 0.7H), 4.97 – 4.30 (m, 5H), 3.91+3.84 (2xs, 2H), 3.68+3.62 (2xs, 3H), 3.37 (dd, $J = 11.7, 4.1$ Hz, 1H), 3.18 (dd, $J = 11.6, 7.3$ Hz, 1H), 1.92 – 1.71 (m, 1H), 1.71 – 1.51 (m, 1H), 1.48 – 1.04 (m, 7H), 0.84 (t, $J = 6.8$ Hz, 3H). ^{13}C NMR (101 MHz, CDCl_3) δ 172.73, 171.27, 168.83, 166.44, 62.83, 62.29, 53.14, 52.43, 52.37, 52.29, 52.21, 51.73, 49.51, 49.31, 48.61, 46.89, 34.79, 32.19, 31.85, 30.47, 29.62, 28.03, 27.17, 22.19, 21.99, 18.27, 16.62, 13.83.

N₃Gly-Ala-Thz-Nle-NHNH₂ (84)

Azido-Ac-Ala-Thz-Nle-OMe **83** (213 mg, 0.51 mmol) was dissolved in MeOH (5 mL). After addition of hydrazine hydrate (0.75 mL, 15.4 mmol, 30 equiv.) the reaction mixture was stirred for 2 h. The reaction mixture was then concentrated before being co-evaporated with MeOH (3x). This yielded the title compound in a quantitative yield. Complex NMR due to a presence of rotamers. ¹H NMR (400 MHz, CDCl₃) δ 7.72 – 7.44 (m, 2H), 7.37 (d, *J* = 8.1 Hz, 1H), 5.15 – 4.22 (m, 5H), 3.92 (s, 2H), 3.84 – 3.40 (m, 3H), 3.40 – 3.05 (m, 2H), 1.84 – 1.47 (m, 2H), 1.47 – 1.05 (m, 7H), 0.82 (t, *J* = 6.5 Hz, 3H). ¹³C NMR (101 MHz, CDCl₃) δ 172.02, 171.48, 169.47, 169.21, 166.87, 62.93, 62.72, 53.22, 52.19, 52.12, 51.80, 49.71, 49.16, 48.17, 47.08, 34.96, 32.66, 32.40, 31.46, 30.31, 29.66, 27.93, 27.58, 22.30, 21.18, 17.98, 17.37, 13.93. LC-MS (linear gradient 10 → 90% MeCN, 0.1% TFA, 12.5 min): R_t (min): 4.11 (ESI-MS (m/z): 415.00 (M+H⁺)).

Boc-Aze-Nle-OMe (85)

The title compound was prepared by the general procedure for peptide coupling on a 1.0 mmol scale. Column chromatography (30→60% EtOAc:pent) provided the product (270 mg, 0.82 mmol, 82%).

¹H NMR (300 MHz, CDCl₃) δ 4.75-4.48 (m, 2H), 3.95-3.75 (m, 2H), 3.75 (s, 3H, OCH₃), 2.52-2.35 (m, 2H), 1.88-1.70 (m, 2H), 1.65-1.22 (m, 4H), 1.48 (s, 9H), 0.91 (m, 3H). ¹³C NMR (300 MHz, CDCl₃) δ 172.46, 171.28, 80.87, 62.01, 52.12, 51.94, 47.01, 31.93, 29.59, 28.12, 27.29, 22.20, 13.20.

Boc-Ala-Aze-Nle-OMe (86)

Boc-Aze-Nle-OMe **85** (270 mg, 0.82 mmol, 1 equiv.) was deprotected using the standard procedure for Boc removal. The title compound was prepared by the general procedure for peptide coupling on a 2.74 mmol scale. Column chromatography (50→100% EtOAc:pent) provided the product (280 mg, 0.7 mmol, 85%). Complex NMR due to a 7:1 ratio of rotamers. Peaks of major rotamer are reported. ¹H NMR (300 MHz, CDCl₃) δ 8.00 (d, *J* = 7.5 Hz, 1H), 5.24 (d, 7.5 Hz), 4.94 (q, *J* = 6.3 Hz, 1H), 4.48 (q, *J* = 7.5 Hz, 1H), 4.26 (m, 2H), 4.08 (m, 1H), 3.71 (s, 3H), 2.76-2.69 (m, 1H), 2.51-2.42 (m, 1H), 1.82-1.61 (m, 2H), 1.41 (s, 9H), 1.24 (m, 7H), 0.87 (t, *J* = 7.2 Hz, 3H). ¹³C NMR (300 MHz, CDCl₃) δ 174.89, 172.44, 170.10, 155.10, 79.77, 61.79, 52.34, 52.22, 48.82, 45.50, 31.60, 28.27, 27.29, 22.14, 18.41, 18.34, 13.84.

N₃Gly-Ala-Aze-Nle-OMe (87)

Boc-Ala-Aze-Nle-OMe **86** (256 mg, 0.64 mmol, 1 equiv.) was deprotected using the standard procedure for Boc removal. The obtained TFA-salt was dissolved in DMF (6 mL) and (ClOAc)₂O (348 mg, 2.0 mmol, 1.2 equiv.) and DiPEA (1.18 mL, 6.8 mmol, 4 equiv.) were added. After 1.5 h, NaN₃ (0.27 g, 4.1 mmol) was added and the resulting mixture was stirred overnight. The reaction mixture was diluted with EtOAc, washed with 1M HCl, sat. aq. NaHCO₃ and brine, dried over MgSO₄ and concentrated. Purification by column chromatography (1→3% MeOH:DCM) yielded the title compound (144 mg, 0.38 mmol, 59%). Complex NMR due to a 7.5:1 ratio of rotamers. Peaks of major rotamer are reported. ¹H NMR (400 MHz, CDCl₃) δ 7.91 (d, *J* = 7.7 Hz, 1H), 7.26 (d, *J* = 7.3 Hz, 1H), 4.95 (dd, *J* = 9.3, 6.3 Hz, 1H), 4.58 – 4.49 (m, 2H), 4.35 (q, *J* = 8.8 Hz, 1H), 4.19 – 4.08 (m, 1H), 3.98 (s, 2H), 3.74 (s, 3H), 2.80 – 2.69 (m, 1H), 2.57 – 2.43 (m, 1H), 1.83 (dq, *J* = 14.2, 5.5, 4.8 Hz, 1H), 1.76 – 1.59 (m, 1H), 1.41 – 1.19 (m, 7H), 0.89 (q, *J* = 7.2 Hz, 3H). ¹³C NMR (101 MHz, CDCl₃) δ 173.83, 172.45, 169.77, 166.48, 61.80, 52.29, 52.25, 52.18, 49.00, 44.39, 31.63, 27.24, 22.12, 18.46, 17.99, 13.82. LC-MS (linear gradient 10 → 90% MeCN, 0.1% TFA, 12.5 min): R_t (min): 5.44 (ESI-MS (m/z): 383.07 (M+H⁺)).

N₃Gly-Ala-Aze-Nle-NHNH₂ (88)

Methyl ester **87** (144 mg, 0.38 mmol, 1 equiv.) was dissolved in MeOH (4 mL) before adding hydrazine hydrate (582 μL, 11.4 mmol, 30 equiv.). After stirring for 4 h at RT, TLC analysis showed complete conversion. The reaction mixture was concentrated and co-evaporated with toluene to give the title compound in a quantitative yield. No NMR-analysis was performed due to poor solubility of the product in MeOD and CDCl₃ and mixtures thereof. LC-MS (linear gradient 10 → 90% MeCN, 0.1% TFA, 12.5 min): R_t (min): 3.67 (ESI-MS (m/z): 383.07 (M+H⁺)).

Boc-Ala-Pip-Nle-OMe (89)

Boc-Pip-Nle-OMe was prepared by the general procedure for peptide coupling on a 3 mmol scale. Column chromatography (50→80% EtOAc:pent) provided the product (1.09 g, 2.79 mmol, 93%). Boc-Pip-Nle-OMe was deprotected using the standard procedure for Boc removal. The title compound was prepared by the general procedure for peptide coupling on a 3 mmol scale. Column chromatography (50→80% EtOAc:pent) provided the product in a quantitative yield. Complex NMR due to a 2:1 ratio of rotamers. ^1H NMR (400 MHz, CDCl_3) δ 7.88 (d, $J = 7.5$ Hz, 0.3H), 6.47 (d, $J = 7.5$ Hz, 0.7H), 5.55 (d, $J = 7.8$ Hz, 0.7H), 5.26 (d, $J = 6.2$ Hz, 0.4H), 5.17 (d, $J = 4.8$ Hz, 0.7H), 4.65 (q, $J = 6.9$ Hz, 0.6H), 4.55 (d, $J = 13.5$ Hz, 0.4H), 4.51 – 4.39 (m, 1.4H), 4.34 (ddd, $J = 9.3, 7.7, 5.5$ Hz, 0.4H), 3.75 (d, $J = 12.8$ Hz, 0.6H), 3.67 (s, 2H), 3.63 (s, 1H), 3.13 (t, $J = 12.2$ Hz, 0.6H), 2.44 (q, $J = 12.9$ Hz, 0.8H), 2.16 (d, $J = 13.6$ Hz, 0.6H), 1.88 – 1.40 (m, 6H), 1.38 (s, 6H), 1.33 (s, 3H), 1.28 – 1.12 (m, 7H), 0.85 – 0.77 (m, 3H). ^{13}C NMR (101 MHz, CDCl_3) δ 172.93, 172.74, 172.15, 170.37, 169.83, 156.28, 155.03, 80.19, 79.58, 52.13, 46.50, 43.65, 39.92, 31.96, 30.44, 27.40, 26.36, 25.59, 25.33, 24.82, 22.21, 22.11, 20.67, 20.21.

 $\text{N}_3\text{Gly-Ala-Pip-Nle-OMe}$ (90)

1:1 DCM/TFA (10 mL) was added to **89** (726 mg, 1.7 mmol, 1 equiv.) and after 30 min, the reaction mixture was concentrated and co-evaporated with toluene to give the deprotected peptide, which was dissolved in DMF (14 mL). $(\text{ClAc})_2\text{O}$ (348 mg, 2.0 mmol, 1.2 equiv.) and DiPEA (1.18 mL, 6.8 mmol, 4 equiv.) were added. After 1.5 h, NaN_3 (0.27 g, 4.1 mmol) was added and the resulting mixture was stirred overnight. The reaction mixture was diluted with EtOAc, washed with 1M HCl, sat. aq. NaHCO_3 and brine, dried over MgSO_4 and concentrated. Purification by column chromatography (1→3% MeOH:DCM) yielded the title compound (631 mg, 1.53 mmol, 90%). Complex NMR due to a 3.5:1 ratio of rotamers. ^1H NMR (400 MHz, CDCl_3) δ 7.57 (d, $J = 7.6$ Hz, 0.2H), 7.40 (d, $J = 7.3$ Hz, 0.8H), 7.04 (d, $J = 5.8$ Hz, 0.2H), 6.42 (d, $J = 7.6$ Hz, 0.8H), 5.21 (d, $J = 4.7$ Hz, 0.7H), 4.96 (p, $J = 6.9$ Hz, 0.7H), 4.70 (p, $J = 6.7$ Hz, 0.7H), 4.57 (d, $J = 13.4$ Hz, 0.7H), 4.50 (m, 1H), 4.47 – 4.36 (m, 0.3H), 3.96 (d, $J = 5.2$ Hz, 1.3H), 3.77 (d, $J = 13.2$ Hz, 0.8H), 3.72 (s, 2.3 H), 3.69 (s, 0.7H), 3.28 – 3.18 (m, 0.8H), 2.54 (t, $J = 13.3$ Hz, 0.5H), 2.21 (d, $J = 13.7$ Hz, 0.8H), 1.88 – 1.40 (m, 8H), 1.35 (d, $J = 6.9$ Hz, 3H), 1.33 – 1.14 (m, 4H), 0.85 (t, $J = 7.1$ Hz, 3H). ^{13}C NMR (101 MHz, CDCl_3) δ 172.87, 172.07, 170.16, 169.49, 165.96, 52.69, 52.30, 52.14, 43.78, 40.26, 32.12, 30.77, 28.26, 27.48, 26.64, 25.83, 25.38, 24.87, 22.32, 22.17, 20.72, 20.22. LC-MS (linear gradient 10 → 90% MeCN, 0.1% TFA, 12.5 min): R_t (min): 6.36 (ESI-MS (m/z): 410.93 ($\text{M}+\text{H}^+$)).

 $\text{N}_3\text{Gly-Ala-Pip-Nle-NHNH}_2$ (91)

Methyl ester **90** (631 mg, 1.53 mmol, 1 equiv.) was dissolved in MeOH (15 mL) before adding hydrazine hydrate (2.2 mL, 45.9 mmol, 30 equiv.). After stirring for 4 h at RT, TLC analysis showed complete conversion. The reaction mixture was concentrated and co-evaporated with toluene to give the title compound in a quantitative yield. No NMR-analysis was performed due to poor solubility of the product in MeOD and CDCl_3 and mixtures thereof. LC-MS (linear gradient 10 → 90% MeCN, 0.1% TFA, 12.5 min): R_t (min): 4.35 (ESI-MS (m/z): 411.00 ($\text{M}+\text{H}^+$)).

Boc-(4S)FPro-Nle-OMe (92)

The title compound was prepared by the general procedure for peptide coupling on a 1 mmol scale. Column chromatography (50% EtOAc:pent) provided the product in a quantitative yield. ^1H NMR (400 MHz, CDCl_3): δ 6.17 (s, 1H), 4.83 (d, $J = 48.2$ Hz, 1H), 4.26 (s, 1H), 4.08 (s, 1H), 3.68 – 3.23 (m, 5H), 2.69 – 1.96 (m, 2H), 1.68 (s, 1H), 1.52 (s, 1H), 1.38 (s, 9H), 1.17 (m, 4H), 0.80 (t, $J = 6.0$ Hz, 3H). ^{13}C NMR (101 MHz, CDCl_3): δ 172.47, 92.45, 90.73, 81.37, 59.89, 53.94, 52.11, 37.47, 32.15, 28.07, 26.80, 22.15, 13.71; LC-MS (linear gradient 10 → 90% MeCN, 0.1% TFA, 15 min): R_t (min): 7.60 (ESI-MS (m/z): 360.93 ($\text{M}+\text{H}^+$)).

Boc-Ala-(4S)-FPro-Nle-OMe (93)

Boc-Pip-Nle-OMe was deprotected using the standard procedure for Boc removal. The title compound was prepared by the general procedure for peptide coupling on a 1.9 mmol scale. Column chromatography (40:20 EtOAc:pent) provided the product (755 mg, 1.8 mmol, 93%). Complex NMR due to rotamers. ^1H NMR (400 MHz,

CDCl₃) δ 8.10 (d, J = 8.0 Hz, 0.4 H), 7.01 (d, J = 7.5 Hz, 0.6 H), 5.53 – 5.03 (m, 2H), 4.80 (d, J = 9.8 Hz, 0.6 H), 4.63 – 4.21 (m, 2.4 H), 4.06 – 3.76 (m, 2H), 3.72 (s, 2H), 3.66 (s, 1H), 3.04 – 2.82 (m, 1H), 2.41 – 2.07 (m, 1H), 1.98 – 1.71 (m, 1H), 1.71 – 1.52 (m, 1H), 1.52 – 1.33 (m, 10H), 1.34 – 1.08 (m, 6H), 0.85 (q, J = 6.9 Hz, 3H). ¹³C NMR (101 MHz, CDCl₃) δ 173.97, 172.82, 172.74, 172.64, 170.58, 169.52, 155.94, 155.26, 93.15, 91.37, 91.19, 89.44, 80.24, 79.93, 59.30, 59.15, 54.12, 53.88, 52.61, 52.32, 52.22, 52.08, 48.66, 47.83, 38.61, 38.35, 38.14, 34.32, 34.11, 31.94, 30.14, 29.68, 28.37, 28.32, 28.22, 27.77, 26.81, 22.24, 22.00, 18.57, 16.58, 13.83. LC-MS (linear gradient 10 \rightarrow 90% MeCN, 0.1% TFA, 15 min): R_t (min): 7.28 (ESI-MS (m/z): 431.93 (M+H⁺)).

N₃Gly-Ala-(4S)-FPro-Nle-OMe (94)

TFA (6 mL) was added to **93** (1.75 mmol, 1 equiv.). After 30 min, the reaction mixture was concentrated and co-evaporated with toluene to give the deprotected peptide, which was dissolved in DMF (18 mL). (ClOAc)₂O (0.36 g, 2.1 mmol) and DiPEA (0.9 mL, 5.3 mmol) were added and the reaction mixture turned deep red. After 1.5 h NaN₃ (0.34 g, 5.2 mmol) was added and the resulting mixture was stirred overnight. The reaction mixture was diluted with EtOAc, washed with 1M HCl, sat. aq. NaHCO₃ and brine, dried over MgSO₄ and concentrated. Purification by column chromatography (9:1 EA:pent \rightarrow 1:9 MeOH:EA) yielded the title compound (425 mg, 1.0 mmol, 59%). Complex NMR due to rotamers. ¹H NMR (400 MHz, CDCl₃) δ 7.77 (d, J = 7.9 Hz, 0.3 H), 7.14 (d, J = 6.9 Hz, 0.7 H), 6.93 (d, J = 7.4 Hz, 0.7 H), 6.73 (d, J = 4.6 Hz, 0.3 H), 5.32 (m, 1H), 4.86 – 4.65 (m, 1H), 4.67 – 4.33 (m, 2H), 4.15 – 3.85 (m, 4H), 3.76 (s, 2H), 3.71 (s, 1H), 2.93 – 2.75 (m, 1H), 2.42 – 2.04 (m, 1H), 1.95 – 1.60 (m, 2H), 1.55 (d, J = 6.9 Hz, 2H), 1.42 (d, J = 6.9 Hz, 1H), 1.37 – 1.07 (m, 4H), 0.88 (t, J = 7.0 Hz, 3H).

N₃Gly-Ala-(4S)-FPro-Nle-NHNH₂ (95)

Methyl ester **94** (1.0 mmol, 1 equiv.) was dissolved in MeOH (10 mL) before adding hydrazine hydrate (1.0 mL, 21 mmol, 21 equiv.). After stirring for 4 h at rt TLC analysis showed incomplete conversion and the reaction mixture was refluxed for 45 min to achieve full consumption of the starting material. The reaction mixture was concentrated and co-evaporated with toluene to give the title compound in a quantitative yield. No NMR-analysis was performed due to poor solubility of the product in MeOD and CDCl₃ and mixtures thereof. LC-MS (linear gradient 10 \rightarrow 90% MeCN, 0.1% TFA, 15 min): R_t (min): 4.49 (ESI-MS (m/z): 415.07 (M+H⁺)).

Boc-(4R)-FPro-Nle-OMe (96)

The title compound was prepared by the general procedure for peptide coupling on a 1 mmol scale. Column chromatography (50% EtOAc:pent) provided the product (288 mg, 0.80 mmol, 80%). Complex NMR due to rotamers. ¹H NMR (400 MHz, CDCl₃) δ 7.33 (d, J = 6.3 Hz, 0.6H), 6.50 (s, 0.4H), 5.16 (d, J = 53.0 Hz, 1H), 4.57 – 4.20 (m, 2H), 4.15 – 3.74 (m, 1H), 3.69 (s, 3H), 3.56 – 3.26 (m, 1H), 2.72 – 2.18 (m, 2H), 1.85 – 1.72 (m, 1H), 1.72 – 1.53 (m, 1H), 1.43 (s, 9H), 1.23 (d, J = 17.3 Hz, 4H), 0.83 (t, J = 5.5 Hz, 3H). ¹³C NMR (101 MHz, CDCl₃) δ 172.72, 170.71, 92.88, 91.13, 80.99, 59.42, 58.06, 53.54, 53.31, 52.50, 52.31, 52.05, 37.81, 34.68, 34.47, 32.38, 31.96, 29.73, 28.31, 27.35, 22.31, 13.87.

Boc-Ala-(4R)-FPro-Nle-OMe (97)

Boc-(4R)FPro-Nle-OMe (**96**) was deprotected using the standard procedure for Boc removal. The title compound was prepared by the general procedure for peptide coupling on a 1.43 mmol scale. Column chromatography (50 \rightarrow 60% EA:pent) provided the product (592 mg, 1.40 mmol, 98%). ¹H NMR (400 MHz, CDCl₃): δ 7.23 (s, 1H), 5.53 (d, J = 6.8 Hz, 1H), 5.33 (d, J = 52.6 Hz, 1H), 4.77 (t, J = 7.8 Hz, 1H), 4.51 (m, 2H), 4.21 – 4.03 (m, 1H), 3.74 (s, 3H), 3.71 – 3.54 (m, 1H), 2.46 (m, 2H), 1.90 – 1.56 (m, 2H), 1.44 (s, 9H), 1.31 (m, 7H), 0.88 (t, J = 5.6 Hz, 3H). ¹³C NMR (101 MHz, CDCl₃): δ 172.76, 169.94, 155.06, 92.68, 90.89, 79.82, 58.25, 53.60, 53.37, 52.55, 52.39, 47.93, 34.22, 33.99, 31.90, 28.39, 27.36, 22.26, 18.68, 13.91; LC-MS (linear gradient 10 \rightarrow 90% MeCN, 0.1% TFA, 15 min): R_t (min): 7.15 (ESI-MS (m/z): 431.93 (M+H⁺)).

N₃Gly-Ala-(4R)-FPro-Nle-OMe (98)

TFA (4.6 mL) was added to **97** (592 mg, 1.40 mmol, 1 equiv.) and after 30 min, the reaction mixture was concentrated and co-evaporated with toluene to give the deprotected peptide, which was dissolved in DMF (14 mL). (ClOAc)₂O (0.28 g, 1.60 mmol, 1.1 equiv.) and DiPEA (0.9 mL, 5.3 mmol, 3.8 equiv.) were added and the reaction mixture turned deep red. After 1.5 h NaN₃ (0.27 g, 4.1 mmol) was added and the resulting mixture was stirred overnight. The reaction mixture was diluted with EtOAc, washed with 1M HCl, sat. aq. NaHCO₃ and brine, dried over MgSO₄ and concentrated. Purification by column chromatography (1:1 EA:pent) yielded the title compound (383 mg, 0.92 mmol, 67%). ¹H NMR (400 MHz, CDCl₃): δ 7.34 (d, *J* = 7.2 Hz, 1H), 7.18 (d, *J* = 7.7 Hz, 1H), 5.33 (d, *J* = 52.6 Hz, 1H), 4.76 (dt, *J* = 12.3, 7.5 Hz, 2H), 4.57 – 4.46 (m, 1H), 4.17 – 3.59 (m, 7H), 2.53 (ddt, *J* = 46.6, 17.0, 6.2 Hz, 2H), 1.84 (ddd, *J* = 13.5, 10.2, 6.1 Hz, 1H), 1.70 (ddd, *J* = 13.6, 8.7, 4.7 Hz, 1H), 1.39 – 1.25 (m, 7H), 0.89 (t, *J* = 6.7 Hz, 3H). ¹³C NMR (101 MHz, CDCl₃): δ 172.76, 171.65, 169.87, 166.13, 92.70, 90.91, 58.36, 53.73, 53.50, 52.55, 52.47, 52.39, 46.90, 34.54, 34.32, 31.88, 27.38, 22.26, 18.14, 13.90; LC-MS (linear gradient 10 \rightarrow 90% MeCN, 0.1% TFA, 15 min): R_t (min): 5.82 (ESI-MS (m/z): 415.00 (M+H⁺)).

N₃Gly-Ala-(4R)-FPro-Nle-NHNH₂ (99)

Methyl ester **98** (383 mg, 0.92 mmol, 1 equiv.) was dissolved in MeOH (9.2 mL) before adding hydrazine hydrate (0.9 mL, 18.4 mmol, 20 equiv.). After stirring for 4 h at RT, TLC analysis showed incomplete conversion and the reaction mixture was refluxed for 45 min to achieve full consumption of the starting material. The reaction mixture was concentrated and co-evaporated with toluene to give the title compound in a quantitative yield. No NMR-analysis was performed due to poor solubility of the product in MeOD and CDCl₃ and mixtures thereof. LC-MS (linear gradient 10 \rightarrow 90% MeCN, 0.1% TFA, 15 min): R_t (min): 4.20 (ESI-MS (m/z): 415.07 (M+H⁺)).

Boc-4,4-F₂Pro-Nle-OMe (100)

The title compound was prepared by the general procedure for peptide coupling on a 1 mmol scale. Column chromatography (10 \rightarrow 30% EtOAc:pent) provided the product (352 mg, 0.93 mmol, 93%). ¹H NMR (400 MHz, CDCl₃) δ 4.57 (bs, 2H), 4.03 – 3.57 (m, 2H), 3.75 (s, 3H), 3.04 – 2.45 (m, 2H), 1.85 (m, 1H), 1.68 (m, 1H), 1.49 (s, 9H), 1.29 (m, 4H), 0.89 (t, *J* = 7.0 Hz, 3H). ¹³C NMR (101 MHz, CDCl₃) δ 172.64, 53.59, 52.42, 32.11, 28.25, 27.23, 22.34, 13.89.

Boc-Ala-4,4-F₂Pro-Nle-OMe (101)

Boc-4,4-F₂Pro-Nle-OMe (**100**) (302 mg, 0.80 mmol, 1 equiv.) was deprotected using the standard procedure for Boc removal. The title compound was prepared by the general procedure for peptide coupling on a 0.93 mmol scale. Column chromatography (30 \rightarrow 50% EA:pent) provided the product (167 mg, 0.37 mmol, 46%). Complex NMR due to a presence of rotamers. ¹H NMR (400 MHz, CDCl₃) δ 8.21 (d, *J* = 8.1 Hz, 0.3H), 7.13 (d, *J* = 7.3 Hz, 0.7H), 5.38 (d, *J* = 7.6 Hz, 0.7H), 5.21 (bs, 0.3H), 4.79 (dd, *J* = 9.2, 5.3 Hz, 0.7H), 4.60 – 3.72 (m, 3.3H), 3.65 (2xs, 3H), 3.36 – 2.11 (m, 2H), 1.98 – 1.50 (m, 2H), 1.43 – 1.13 (m, 16H), 0.82 (t, *J* = 6.8 Hz, 3H).

N₃Gly-Ala-4,4-F₂Pro-Nle-OMe (102)

Boc-Ala-4,4-F₂Pro-Nle-OMe (167 mg, 0.37 mmol, 1 equiv.) **101** was dissolved in 1:1 TFA: DCM (10 mL). After 30 min the reaction mixture was concentrated before being co-evaporated with toluene (3x). The crude TFA salt was dissolved in DMF (4 mL) before adding (ClAc)O₂ (76 mg, 0.45 mmol, 1.2 equiv.) and DiPEA (0.26 mL, 1.49 mmol, 4 equiv.). The reaction mixture was stirred for one hour at room temperature and under argon atmosphere before NaN₃ (97 mg, 1.49 mmol, 4 equiv.) was added. The reaction mixture was then stirred overnight at room temperature and under argon atmosphere. EtOAc (50 mL) was then added to the reaction mixture before being washed with 1M HCl (2x), sat. aq. NaHCO₃ (2x) and brine (1x). The organic layer was dried over Na₂SO₄, filtered and concentrated. Purification by column chromatography (0 \rightarrow 3% MeOH:DCM) yielded the title compound (117 mg, 0.27 mmol, 73%). Complex NMR due to a presence of rotamers. ¹H NMR (400 MHz, CDCl₃) δ 8.01 (d, *J* = 8.0 Hz, 0.2H), 7.18 (d, *J* = 7.1 Hz, 0.8H), 7.06 (d, *J* = 7.4 Hz, 0.8H), 6.97 (s, 0.2H), 4.76 (dd, *J* =

9.1, 5.7 Hz, 1H), 4.64 (p, $J = 6.9$ Hz, 1H), 4.58 – 4.37 (m, 1H), 4.15 (td, $J = 12.1, 7.1$ Hz, 1H), 3.94 (s, 2H), 3.91 – 3.75 (m, 1H), 3.67 (d, $J = 22.4$ Hz, 3H), 3.01 – 2.43 (m, 2H), 1.79 (m, 1H), 1.63 (m, 1H), 1.34 (d, $J = 6.8$ Hz, 3H), 1.24 (dd, $J = 18.0, 6.8$ Hz, 4H), 0.83 (t, $J = 6.8$ Hz, 3H). ^{13}C NMR (101 MHz, CDCl_3) δ 172.83, 172.70, 172.10, 171.42, 169.35, 168.64, 167.67, 166.45, 128.72, 126.24, 123.75, 59.02, 57.86, 53.99, 53.68, 53.34, 53.00, 52.55, 52.44, 52.37, 52.26, 51.79, 47.37, 46.70, 35.99, 35.74, 35.49, 31.88, 30.38, 27.97, 27.21, 22.22, 21.96, 17.87, 16.76, 13.84.

Azido-Ac-Ala-4,4- F_2 Pro-Nle-NHNH $_2$ (103)

Azido-Ac-Ala-4,4- F_2 -Nle-OMe (117 mg, 0.27 mmol) **102** was dissolved in MeOH (3 mL). After addition of hydrazine hydrate (0.41 mL, 8.31 mmol, 30 equiv.) the reaction mixture was stirred for 2 h. The reaction mixture was then concentrated before being co-evaporated with MeOH (3x). This yielded the title compound in a quantitative yield. Complex NMR due to a presence of rotamers. ^1H NMR (400 MHz, MeOD) δ 4.69-4.63 (m, 1H), 4.54 (q, $J = 7.0$ Hz, 1H), 4.42 – 4.14 (m, 2H), 4.14 – 3.92 (m, 1H), 3.88-3.82 (m, 2H), 2.89 – 2.57 (m, 1H), 2.56 – 2.26 (m, 1H), 1.85 – 1.49 (m, 2H), 1.30 (m, 7H), 0.87 (t, $J = 6.9$ Hz, 3H). ^{13}C NMR (101 MHz, MeOD) δ 173.60, 173.24, 171.93, 169.90, 130.30, 127.83, 125.37, 60.02, 59.22, 54.99, 54.66, 54.34, 53.57, 52.42, 52.12, 48.36, 48.06, 38.18, 37.94, 37.69, 32.97, 32.37, 29.12, 28.84, 23.33, 23.20, 17.23, 16.75, 14.23. LC-MS (linear gradient 10 \rightarrow 90% MeCN, 0.1% TFA, 12.5 min): R_t (min): 4.24 (ESI-MS (m/z): 433.00 (M+H $^+$)).

Biochemical methods

Competition Assays in Cell Lysate.

Lysates of Raji cells were prepared by sonication in 3 volumes of lysis buffer containing 50 mM Tris pH 7.5, 1 mM DTT, 5 mM MgCl_2 , 250 mM sucrose, 2 mM ATP, and 0.025% digitonin. Protein concentration was determined by the Bradford assay. Cell lysates (diluted to 10-15 μg total protein in buffer containing 50 mM Tris pH 7.5, 2 mM DTT, 5 mM MgCl_2 , 10% glycerol, 2 mM ATP) were exposed to the inhibitors for 1 h at 37 $^\circ\text{C}$ prior to incubation with AzidoBODIPY-MeTyr-Phe-Leu-VS (BODIPY-NC005; 0.1-0.5 μM ; to probe β_5), BODIPY-epoxomicin (0.5 μM ; to probe all subunits, used for β_2 -profiling) or BODIPY-FL-Ala-Pro-Nle-Leu-EK (BODIPY-NC001; 1 μM ; to probe β_1 activity). This probe does bind slightly to β_5 , so lysates were treated for 1 h with NC005VS 11 (5 μM), prior to probe incubation for an additional 1 h at 37 $^\circ\text{C}$, followed by 3 min boiling with a reducing gel-loading buffer and fractionation on 12.5% SDS-PAGE. In-gel detection of residual proteasome activity was performed in the wet gel slabs directly on a ChemiDoc $^{\text{TM}}$ MP System using Cy3 settings to detect BODIPY-NC005 and BODIPY-epoxomicin and Cy2 settings to detect BODIPY-NC001. Intensities of bands were measured by fluorescent densitometry and normalized to the intensity of bands in mock-treated extracts. Average values of at least two or three independent experiments were plotted against inhibitor concentrations. IC_{50} (inhibitor concentrations giving 50% inhibition) values were calculated using GraphPad Prism software.

Competition Assays in living RPMI-8226 cells.

RPMI-8226 were cultured in RPMI-1640 media supplemented with 10% fetal calfs serum, GlutaMAX $^{\text{TM}}$, penicillin, streptomycin in a 5% CO_2 humidified incubator. $5\text{-}8 \times 10^5$ cells/mL were exposed to inhibitors for 1 h at 37 $^\circ\text{C}$. Cells were harvested and washed with twice with PBS. Cell pellets were treated with lysis buffer (50 μL : 50 mM Tris pH 7.5, 2 mM DTT, 5 mM MgCl_2 , 10% glycerol, 2 mM ATP, 0.05% digitonin) on ice for 1.5 h, followed by centrifugation at 14000 rpm for 15 min. Proteasome inhibition in the obtained cell lysates was determined using the method described above. Intensities of bands were measured by fluorescent densitometry and divided by the intensity of bands in mock-treated extracts. Gels were stained by Coomassie Brilliant Blue, which was used to correct for gel loading differences. Average values of two or three independent experiments were plotted against inhibitor concentrations. IC_{50} (inhibitor concentrations giving 50% inhibition) values were calculated using GraphPad Prism software.

Crystallographic analysis.

γ CP crystals were grown by hanging drop vapour diffusion as previously described.⁴⁶ Crystal drops were incubated for 12 h with 5 μ l of cryo protectant and 0.5 μ l of inhibitor (concentration: 50 mM in DMSO). Diffraction datasets were collected using synchrotron radiation of $\lambda=1.0$ Å at the beamline X06SA, Swiss Light Source (SLS), Villigen, Switzerland. Structure determination was performed as previously reported.⁴⁶ For model building the programs SYBYL, MAIN⁴⁷ and COOT⁴⁸ were used. Refinement with REFMAC5⁴⁹ yielded excellent R factors as well as r.m.s.d. bond and angle values. Coordinates were confirmed to fulfill the Ramachandran plot. Figures were prepared with PyMOL. (For X-ray data collection and refinement statistics, PDB codes and all structures: see⁵⁰).

References

1. Hershko, A. & Ciechanover, A. The ubiquitin system. *Annu. Rev. Biochem.* **67**, 425-79 (1998).
2. Lowe, J. et al. Crystal structure of the 20S proteasome from the archaeon *T. acidophilum* at 3.4 Å resolution. *Science* **268**, 533-539 (1995).
3. Britton, M. et al. Selective inhibitor of proteasome's caspase-like sites sensitizes cells to specific inhibition of chymotrypsin-like sites. *Chem. Biol.* **16**, 1278-1289 (2009).
4. Geurink, P.P. et al. Incorporation of non-natural amino acids improves cell permeability and potency of specific inhibitors of proteasome trypsin-like sites. *J. Med. Chem.* **56**, 1262-1275 (2013).
5. Groll, M. et al. Structure of 20S proteasome from yeast at 2.4Å resolution. *Nature* **386**, 463-471 (1997).
6. Tanaka, K. Role of proteasomes modified by interferon-gamma in antigen processing. *J. Leukoc. Biol.* **56**, 571-5 (1994).
7. Strehl, B. et al. Antitopes define preferential proteasomal cleavage site usage. *J. Biol. Chem.* **283**, 17891-17897 (2008).
8. Orłowski, M., Cardozo, C. & Michaud, C. Evidence for the presence of five distinct proteolytic components in the pituitary multicatalytic proteinase complex. Properties of two components cleaving bonds on the carboxyl side of branched chain and small neutral amino acids. *Biochemistry* **32**, 1563-1572 (1993).
9. Kisselev, Alexei F., van der Linden, W.A. & Overkleeft, Herman S. Proteasome inhibitors: an expanding army attacking a unique target. *Chem. Biol.* **19**, 99-115 (2012).
10. Beck, P., Dubiella, C. & Groll, M. Covalent and non-covalent reversible proteasome inhibition. *Biol. Chem.* **393**, 1101 (2012).
11. Screen, M. et al. Nature of pharmacophore influences active site specificity of proteasome inhibitors. *J. Biol. Chem.* **285**, 40125-40134 (2010).
12. Stein, M.L. et al. Systematic comparison of peptidic proteasome inhibitors highlights the α -ketoamide electrophile as an auspicious reversible lead motif. *Angew. Chem. Int. Ed.* **53**, 1679-1683 (2014).
13. Adams, J. et al. Potent and selective inhibitors of the proteasome: Dipeptidyl boronic acids. *Bioorg. Med. Chem. Lett.* **8**, 333-338 (1998).
14. Adams, J. et al. Proteasome inhibitors: a novel class of potent and effective antitumor agents. *Cancer Res.* **59**, 2615-2622 (1999).
15. Adams, J. The proteasome: a suitable antineoplastic target. *Nat. Rev. Cancer* **4**, 349-60 (2004).
16. Demo, S.D. et al. Antitumor Activity of PR-171, a Novel Irreversible Inhibitor of the Proteasome. *Cancer Res.* **67**, 6383-6391 (2007).
17. Eloffsson, M., Splittgerber, U., Myung, J., Mohan, R. & Crews, C.M. Towards subunit-specific proteasome inhibitors: synthesis and evaluation of peptide α' , β' -epoxyketones. *Chem. Biol.* **6**, 811-822 (1999).
18. O'Connor, O.A. et al. A phase 1 dose escalation study of the safety and pharmacokinetics of the novel proteasome inhibitor carfilzomib (PR-171) in patients with hematologic malignancies. *Clin. Canc. Res.* **15**, 7085-7091 (2009).

19. Dorsey, B.D. et al. Discovery of a potent, selective, and orally active proteasome inhibitor for the treatment of cancer. *J. Med. Chem.* **51**, 1068-1072 (2008).
20. Kupperman, E. et al. Evaluation of the proteasome inhibitor MLN9708 in preclinical models of human cancer. *Cancer Res.* **70**, 1970-1980 (2010).
21. Zhou, H.-J. et al. Design and synthesis of an orally bioavailable and selective peptide epoxyketone proteasome inhibitor (PR-047). *J. Med. Chem.* **52**, 3028-3038 (2009).
22. Kuhn, D.J. et al. Potent activity of carfilzomib, a novel, irreversible inhibitor of the ubiquitin-proteasome pathway, against preclinical models of multiple myeloma. *Blood* **110**, 3281-3290 (2007).
23. Kisselev, A.F., Callard, A. & Goldberg, A.L. Importance of the different proteolytic sites of the proteasome and the efficacy of inhibitors varies with the protein substrate. *J. Biol. Chem.* **281**, 8582-8590 (2006).
24. Geurink, P.P. et al. Incorporation of fluorinated phenylalanine generates highly specific inhibitor of proteasome's chymotrypsin-like sites. *J. Med. Chem.* **53**, 2319-2323 (2010).
25. Borissenko, L. & Groll, M. 20S Proteasome and its Inhibitors: crystallographic knowledge for drug development. *Chem. Rev.* **107**, 687-717 (2007).
26. Groll, M., Kim, K.B., Kairies, N., Huber, R. & Crews, C.M. Crystal structure of epoxomicin:20S proteasome reveals a molecular basis for selectivity of α' , β' -epoxyketone proteasome inhibitors. *J. Am. Chem. Soc.* **122**, 1237-1238 (2000).
27. Groll, M., Huber, R. & Potts, B.C.M. Crystal structures of salinosporamide A (NPI-0052) and B (NPI-0047) in complex with the 20S proteasome reveal important consequences of β -lactone ring opening and a mechanism for irreversible binding. *J. Am. Chem. Soc.* **128**, 5136-5141 (2006).
28. Huber, Eva M. et al. Immuno- and constitutive proteasome crystal structures reveal differences in substrate and inhibitor specificity. *Cell* **148**, 727-738 (2012).
29. Huber, E.M. & Groll, M. Inhibitors for the immuno- and constitutive proteasome: current and future trends in drug development. *Angew. Chem. Int. Ed.* **51**, 8708-8720 (2012).
30. Shenk, K.D.P., F.; Zhou, H.-J.; Sylvain, C.; Smyth, M.S.; Bennet, M.K.; Laidig, G. J., *US/20070293465*, (2007).
31. Muchamuel, T. et al. A selective inhibitor of the immunoproteasome subunit LMP7 blocks cytokine production and attenuates progression of experimental arthritis. *Nat. Med.* **15**, 781-787 (2009).
32. Kuhn, D. J. et al. Targeted inhibition of the immunoproteasome is a potent strategy against models of multiple myeloma that overcomes resistance to conventional drugs and nonspecific proteasome inhibitors. *Blood* **113**, 4667-4676 (2009).
33. Parlati, F. et al. Carfilzomib can induce tumor cell death through selective inhibition of the chymotrypsin-like activity of the proteasome. *Blood* **114**, 3439-3447 (2009).
34. Myung, J., Kim, K.B., Lindsten, K., Dantuma, N.P. & Crews, C.M. Lack of proteasome active site allostery as revealed by subunit-specific inhibitors. *Mol. Cell* **7**, 411-420 (2001).
35. Verdoes, M. et al. A panel of subunit-selective activity-based proteasome probes. *Org. Biomol. Chem.* **8**, 2719-2727 (2010).
36. Li, N. et al. Relative quantification of proteasome activity by activity-based protein profiling and LC-MS/MS. *Nat. Protocols* **8**, 1155-1168 (2013).
37. Singh, A.V. et al. PR-924, a selective inhibitor of the immunoproteasome subunit LMP-7, blocks multiple myeloma cell growth both in vitro and in vivo. *Br. J. Haematol.* **152**, 155-163 (2011).
38. Renner, C. et al. Fluoroprolines as tools for protein design and engineering. *Ang. Chem. Int. Ed.* **40**, 923-925 (2001).
39. Staas, D.D. et al. Discovery of potent, selective 4-fluoroproline-based thrombin inhibitors with improved metabolic stability. *Bioorg. Med. Chem.* **14**, 6900-6916 (2006).
40. Ho, Y.K., Bargagna-Mohan, P., Wehenkel, M., Mohan, R. & Kim, K.-B. LMP2-specific inhibitors: chemical genetic tools for proteasome biology. *Chem. Biol.* **14**, 419-430 (2007).
41. Wehenkel, M. et al. A selective inhibitor of the immunoproteasome subunit LMP2 induces apoptosis in PC-3 cells and suppresses tumour growth in nude mice. *Br. J. Cancer* **107**, 53-62 (2012).

42. Basler, M. et al. Why the structure but not the activity of the immunoproteasome subunit low molecular mass polypeptide 2 rescues antigen presentation. *J. Immunol.* **189**, 1868-1877 (2012).
43. Unno, M. et al. Structure determination of the constitutive 20S proteasome from bovine liver at 2.75 Å resolution. *J. Biochem.* **131**, 171-3 (2002).
44. Augeri, D. J. et al. Discovery and preclinical profile of saxagliptin (BMS-477118): a highly potent, long-acting, orally active dipeptidyl peptidase IV inhibitor for the treatment of type 2 diabetes. *J. Med. Chem.* **48**, 5025-5037 (2005).
45. Thompson, S.A., Andrews, P.R. & Hanzlik, R.P. Carboxyl-modified amino acids and peptides as protease inhibitors. *J. Med. Chem* **29**, 104-111 (1986).
46. Groll, M. & Huber, R. in *Methods in Enzymology* (ed. Raymond, J.D.) 329-336 (Academic Press, 2005).
47. Turk, D. Improvement of a Programme for Molecular Graphics and Manipulation of Electron Densities and Its Application for Protein Structure Determination. *PhD thesis, Technische Univ. München* (1992).
48. Emsley, P., Lohkamp, B., Scott, W.G. & Cowtan, K. Features and development of Coot. *Acta crystallographica. Section D, Biological crystallography* **66**, 486-501 (2010).
49. Vagin, A.A. et al. REFMAC5 dictionary: organization of prior chemical knowledge and guidelines for its use. *Acta Crystallographica Section D* **60**, 2184-2195 (2004).
50. de Bruin, G. et al. Structure-based design of β 1i or β 5i specific inhibitors of human immunoproteasomes. *J. Med. Chem.* **57**, 6197-209 (2014).

CHAPTER 6

Development of β 1i and β 5i selective activity-based probes

Introduction

The ubiquitin proteasome system is responsible for the degradation of the majority of proteins inside living cells and is an important target in both cancer and immune diseases.¹ Ubiquitinated proteins are recognized by the 19S regulatory particles of the proteasome, where the ubiquitin chain is removed and the protein is unfolded and translocated to the 20S core particle (CP). The 20S CP is a cylindrical protein complex, consisting out of two outer α -rings and two inner β -rings in which the catalytic activity resides. Proteins are cleaved into 3-12 amino acid peptides, which can be further degraded by aminopeptidases or presented to the immune system on the outside of the cell by MHC-I complexes. The 20S CP exist in two major forms, namely the constitutive proteasome (cCP) and the immunoproteasome (iCP). In the cCP the catalytic active subunits are β 1c (caspase-like), β 2c (trypsin-like) and β 5c (chymotrypsin like). In immune cells and in tissues exposed to inflammatory cytokines (for instance interferon- γ) the iCP is expressed in which β 1c, β 2c and β 5c are (partly) replaced by β 1i (chymotrypsin-like), β 2i (trypsin-like) and β 5i (chymotrypsin-like). The changed substrate specificities of the iCP results in the generation of peptides with higher affinity for MHC-I complexes and as such the iCP plays a major role in the immune system.² Proteasome inhibitors have been widely used to study the proteolytic system and proteasome inhibition was found to induce cytotoxicity in certain cancers, leading to the development of bortezomib³ (Velcade, approved for the treatment of multiple myeloma (MM) and mantle cell lymphoma) and carfilzomib⁴ (Kyprolis, FDA approved for the treatment of MM). Bortezomib and carfilzomib target both cCPs and iCPs, however, many haematological malignancies predominantly express iCPs. The last years, much research has been directed to the development of selective immunoproteasome inhibitors and selective β 5i inhibition has already been shown suppress autoimmunity in various preclinical mouse models.⁵ In addition,

it was found that selective inhibition of $\beta 5i$ and $\beta 1i$ is cytotoxic to acute lymphocytic leukemia (ALL) cells.⁶

Fluorescently labelled activity-based probes (ABPs) have been widely used to monitor proteasome activities *in vitro* and *in vivo* and are used for inhibitor screening and functional studies (see chapter 2). Most proteasome ABPs are either broad spectrum (for instance BODIPY-epoxomicin⁷ and MV-151⁸) or are in-class selective, targeting subunit pairs, such as Cy5-NC-001⁶, BODIPY(FL)-LU-112⁹, BODIPY(TMR)-NC-005-VS⁷ (see chapter 3). However, given the fact that the iCP is gaining attention and that the iCP subunits are considered to be important drug targets, it would be desirable to have access to iCP subunit selective ABPs. Such probes could facilitate research aiming to unravel the role and functions of iCP subunits. Based on the first generation of $\beta 5i$ (PR-924) and $\beta 1i$ (UK-101) inhibitors (see chapter 5), Kim and co-workers developed ABPs selective for either $\beta 5i$ (LKS01-B650)¹⁰ or $\beta 1i$ (UK101-B660 and UK101-Fluor)¹¹ (Figure 1). However, given the selectivity windows of PR-924 and especially UK101, which is only 10x selective for $\beta 1i$ over $\beta 5c/\beta 5i$, the selectivity of these probes is questionable. As described in the previous chapter, a new generation of $\beta 5i$ and $\beta 1i$ inhibitors with improved selectivity profiles has been developed.¹² In this chapter, these optimized iCP subunit selective inhibitors are taken as starting point for the development of fluorescent ABPs that are selective for either $\beta 5i$ or $\beta 1i$.

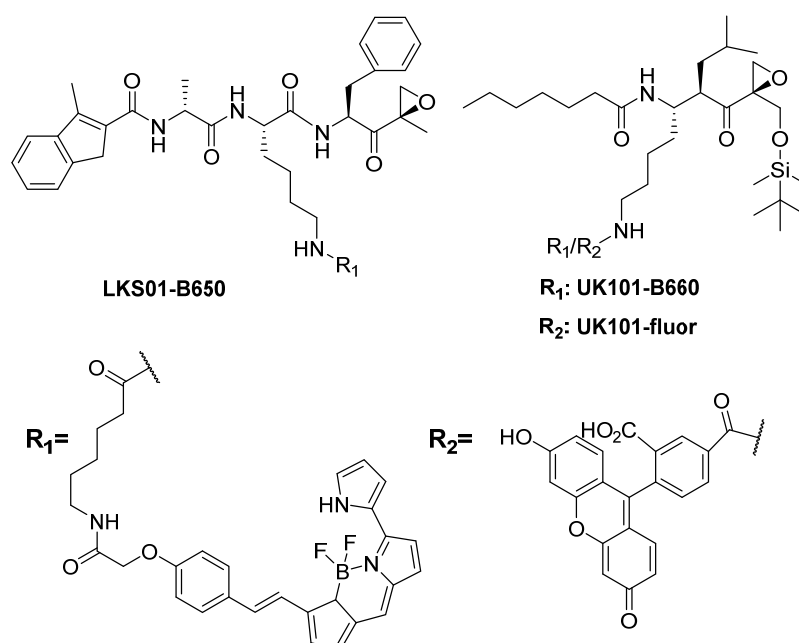


Figure 1. Structures of activity-based probes selective for $\beta 5i$ (LKS01-B650) or $\beta 1i$ (UK101-B660/Fluor).

Results and discussion

β 5i selective probes

Substitution of the P1 Phe residue of PR-924 for cyclohexylalanine (Cha) in LU-015i (Figure 2) led to a 4-fold increase in β 5i selectivity, making this compound the most selective β 5i inhibitor known to date (see chapter 5). Therefore, LU-015i was taken as a lead compound for the development of a β 5i selective probe. Many proteasome ABPs bear a fluorescent group at the N-terminus, however, LU-015i does not have a N-terminal group that allows straightforward functionalization with a fluorophore. Therefore, ABP **1** and **2** (Figure 2) were designed in which the 3-methylindene N-cap of LU-015i is replaced by azido-Phe to which BODIPY(FL)-alkyne¹³ or Cy5-alkyne can be attached via a copper(I)-catalysed azide-alkyne cycloaddition (CuAAC, or 'click') reaction.

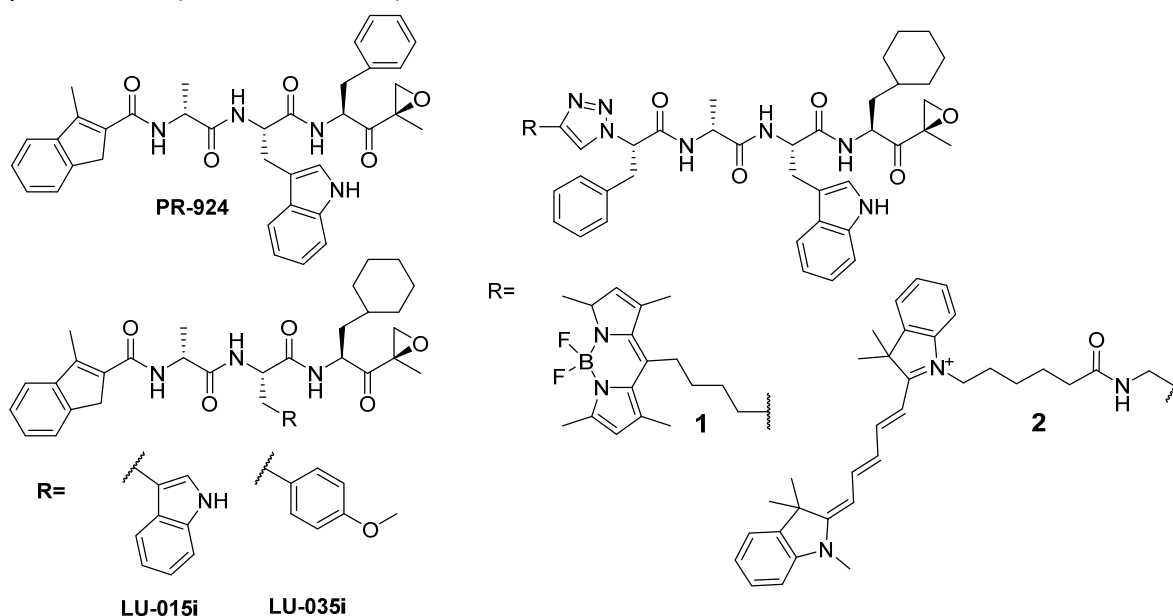
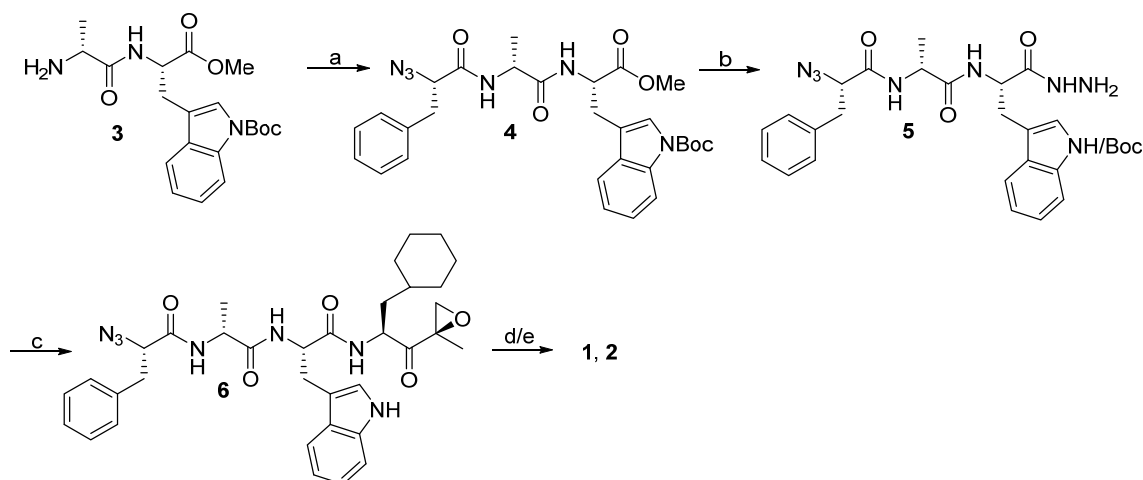


Figure 2. Chemical structures of PR-924, LU-015i, LU-035i and ABPs 1 and 2.

The synthesis of ABPs **1** and **2** commenced with a peptide coupling between dipeptide **3** (chapter 5) and azido-Phe giving tripeptide **4**, which was converted to hydrazide **5** by hydrazinolysis of the methyl ester (Scheme 1). Azide coupling with deprotected Cha epoxyketone provided compound **5**, which was reacted to either BODIPY(FL)-alkyne or Cy5-alkyne yielding ABPs **1** and **2**. Both probes were evaluated for β 5i selectivity in Raji cell lysate. Because most proteasome probes do not resolve β 5c and β 5i on SDS-PAGE, the samples were treated with BODIPY(TMR)-NC-005⁷ (chemical structure: see chapter 3) after incubation with ABP **1** or **2** to verify the amount of inhibition for β 5c and β 5i (Figure 3). Although both probes show some selectivity for β 5i, complete labelling of β 5i without concomitant modification of β 5c could not be achieved.



Scheme 1. Synthesis of ABP 1. Reagents and conditions: a. $\text{N}_3\text{Phe-OH}$, HCTU, DiPEA, DCM, 81%; b. $\text{NH}_2\text{NH}_2\cdot\text{H}_2\text{O}$, MeOH, 100%; c. 1. tBuONO , HCl, DMF. 2. H-Cha-EK, DiPEA, 37%; d. BODIPY(FL)-alkyne, CuSO_4 , NaAsc, DMF/ H_2O , 100%; e. Cy5-alkyne, CuSO_4 , NaAsc, DMF/ H_2O , 20%.

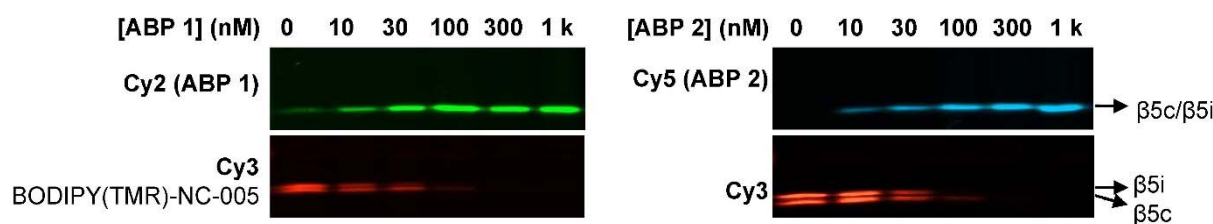
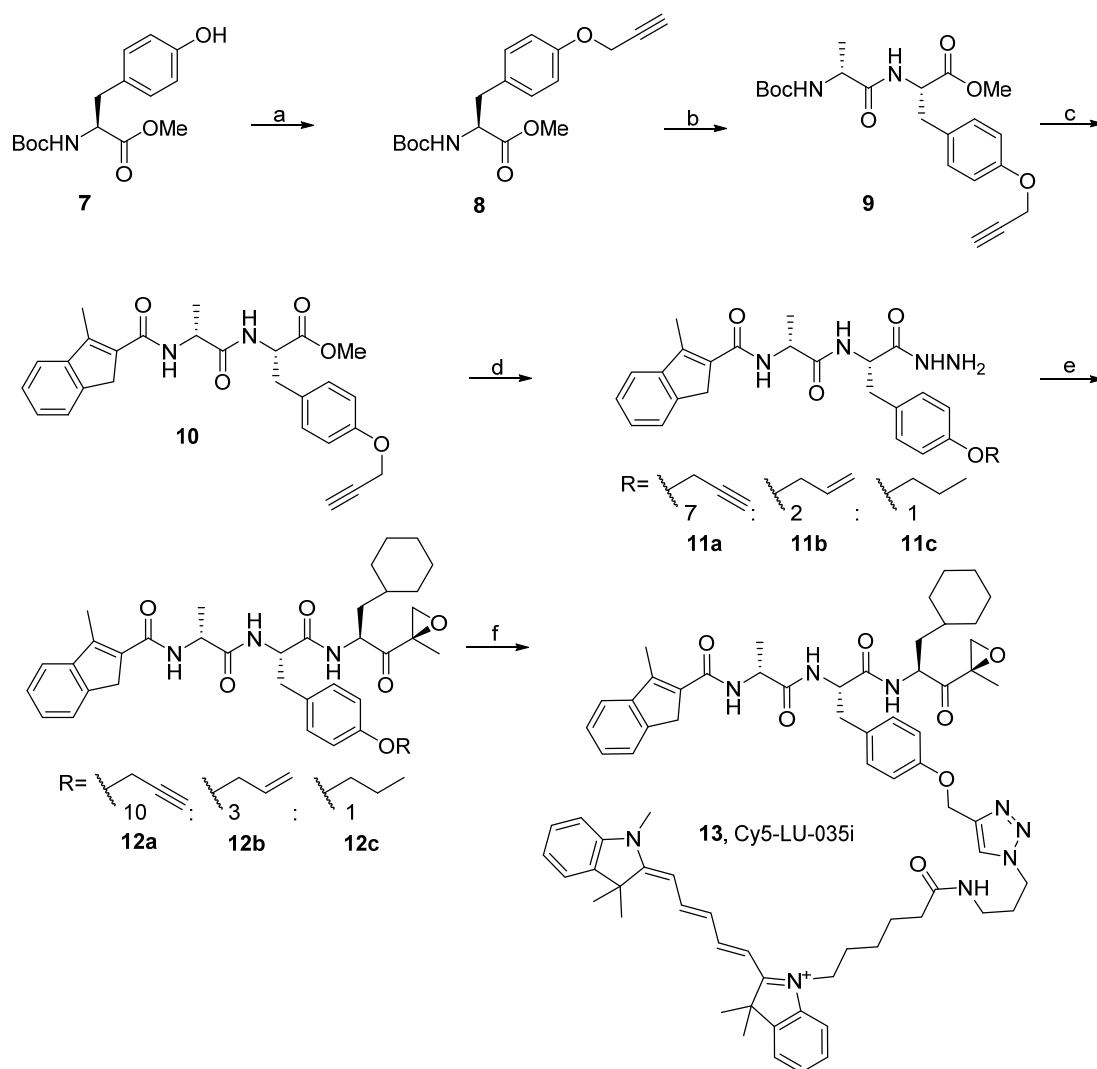


Figure 3. Evaluation of ABPs **1** and **2** in Raji lysate. Lysates were treated with indication concentrations of probe **1** or **2** for 1 h, followed by the addition of 100 nM BODIPY(TMR)-NC-005 (end concentration) for 1 h.

Clearly, the nature of the N-cap of $\beta 5i$ inhibitors is highly important to maintain selectivity (see also chapter 5). Although ABPs **1** and **2** are not selective for $\beta 5i$ over $\beta 5c$, both probes do not target $\beta 1c/\beta 1i$ and $\beta 2c/\beta 2i$ and can therefore be used as $\beta 5c/\beta 5i$ selective probes, complementary to BODIPY(TMR)-NC-005.

Since attachment of a fluorophore at the P4 position proved to be detrimental for $\beta 5i$ selectivity, a new probe was designed with a fluorophore at the P2 position, similarly to ABP LKS01-B650 (Figure 1). The S2 pockets of all proteasome active β -subunits are solvent exposed and therefore fit large residues.^{10, 11, 14} Due to a mutation of Gly48 in $\beta 5c$ to Cys48 in $\beta 5i$, the S2 pocket of $\beta 5i$ is more shallow than $\beta 5c$.¹⁴ Residues that can interact with Cys48 are favoured and required for $\beta 5i$ selectivity^{15, 16}, consequently, all currently known $\beta 5i$ selective inhibitors have aromatic residues at P2 (either O-methyl-Tyr or Trp^{12, 17}). Therefore, LU-035i (Figure 2) was chosen as starting point, as it was envisioned that an alkyne functionality could be easily introduced at the 4-OH position of Tyr. This strategy resulted in the design of ABP **13** (Cy5-LU-035i, Scheme 2). The synthesis commenced with the alkylation of Boc-Tyr-OMe **7** with propargyl bromide to provide alkyne **8**. Boc removal followed by a peptide coupling with Boc-

D-Ala-OH provided dipeptide **9**. Boc removal and peptide coupling with 3-methylindene-2-carboxylic acid provided compound **10**, which was converted to hydrazide **11**. During hydrazinolysis, partial reduction of the alkyne functionality resulted in a 7:2:1 mixture of products **11a:11b:11c**. The synthesis was continued with the mixture and standard azide coupling of hydrazide **11a/b/c** with deprotected Cha epoxyketone yielded compounds **12a/b/c**. Since only alkyne **12a** would react in a CuAAC reaction, it was decided to perform the 'click' reaction with the mixture of compounds. For future studies a β 5i probe with near infrared properties was desired, therefore Cy5-azide was chosen as fluorophore (see chapter 10) and was reacted to **12a/b/c** affording pure ABP **13** after HPLC purification.



Scheme 2. Synthesis of ABP 13. Reagents and conditions: a. K_2CO_3 , propargylbromide, DMF, 72%; b. 1. TFA; 2. Boc-D-Ala-OH, HCTU, DiPEA, DCM, 100%; c. 1. TFA; 2. 3-methylindene-2-carboxylic acid, HCTU, DiPEA, DCM, 93%; d. $NH_2NH_2 \cdot H_2O$, MeOH, 100%; e. 1. tBuONO, HCl, DMF. 2. H-Cha-EK, DiPEA, 50%; f. Cy5-azide, $CuSO_4$, NaAsc, DMF/ H_2O , 28%.

As before, ABP **13** was tested in Raji lysates for $\beta 5i$ selectivity (Figure 4). In contrast to ABPs **1** and **2**, ABP **13** shows both good selectivity for $\beta 5i$ over $\beta 5c$. At 100 nM, complete labelling of $\beta 5i$ is found and $\beta 5c$ remains untouched up to 300 nM. In addition, at concentrations up to 300 nM no labelling of the $\beta 1$ or $\beta 2$ subunits is visible. However, at higher concentrations at which $\beta 5i$ and $\beta 5c$ both are completely labelled by ABP **13** the band in the Cy5 channel shows higher intensities at increasing concentration of **13**, indicating partial labelling of the $\beta 1$ subunits (compare 10000 and 30000 nM). The selectivity of ABP **13** becomes also apparent from the kinetic constants (Figure 4B). ABP **13** has a ten-fold higher K_{inact} for $\beta 5i$ compared to $\beta 5c$, meaning that the covalent bond formation of **13** with $\beta 5i$ is 10x faster than with $\beta 5c$. In addition, the K_i (concentration of inhibitor at 0.5 K_{inact}) of **13** is also 3 times lower for $\beta 5i$ compared to $\beta 5c$, indicating a higher affinity for $\beta 5i$. The selectivity of a covalent inhibitor for its target can best be determined by comparing the second order rate constants (K_{inact}/K_i) for the different targets.¹⁸ The K_{inact}/K_i value of ABP **13** is >30x higher for $\beta 5i$ compared to $\beta 5c$, confirming the good selectivity for $\beta 5i$.

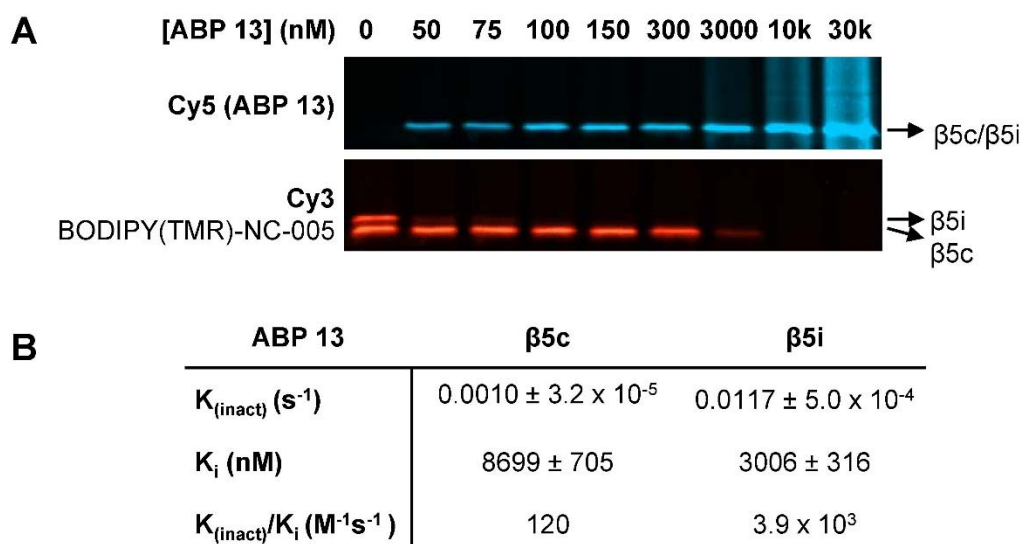
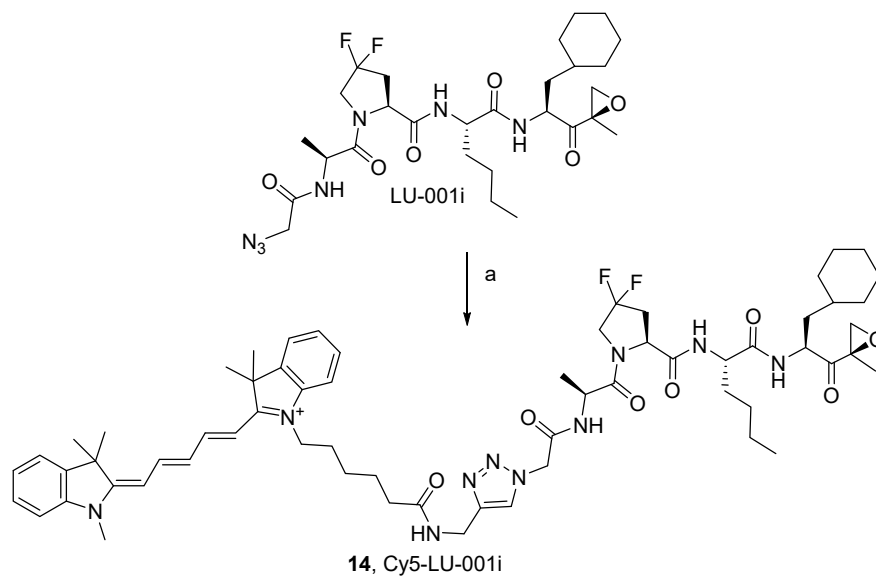


Figure 4. Evaluation of ABP 13 in Raji lysate. A) Lysates were treated with indicate concentrations of ABP **13** for 1 h, followed by the addition of 100 nM BODIPY(TMR)-NC-005 (end concentration) for 1 h. B) Kinetic constants of ABP **13** as determined in Raji lysates. Log (% activity) for various concentrations is plotted versus time, from which the first order rate constants (K_{obs}) are derived. K_{obs} were plotted versus probe concentration, yielding $K_{inact} = \max K_{obs}$ and $K_i = [\text{probe}]$ at 0.5 K_{inact} . K_{inact}/K_i = second order rate constant.

β 1i selective probe

As described in chapter 5, the substitution of P1 Leu for Cha and P3 Pro for 4,4-F₂-Pro in NC-001¹⁹ resulted in the highly selective β 1i inhibitor LU-001i.¹² Since LU-001i is already equipped with a N-terminal azido-Gly residue, it could straightforwardly be converted to a fluorescent ABP by CuAAC with Cy5 alkyne, providing ABP **14** (Cy5-LU-001i, Scheme 3). Again, for future studies also a β 1i probe with near infrared properties was desired.



Scheme 3. Synthesis of ABP 14. Reagents and conditions: a. Cy5-alkyne, CuSO₄, NaAsc, DMF/H₂O, 75%.

The potency and selectivity of ABP **14** was also evaluated in Raji lysates. After incubation of lysates with increasing concentrations of ABP **14** for 1 h, the residual activity of β 1c and β 1i was labelled by β 1 selective probe BODIPY(FL)-NC-001 (Figure 5A).⁷ At 100 nM β 1i is inhibited completely, while very minor labelling of β 1c is visible at 1 μ M. The inhibition of β 5c and β 5i by ABP **14** was also examined in more detail (Figure 5B). Because of overlapping bands for the β 1 and β 5 subunits on SDS-PAGE, β 1c and β 1i were completely blocked by β 1 selective inhibitor NC-001¹⁹, before incubation with ABP **14**. Residual activity of β 5c and β 5i was labelled by β 5 selective probe BODIPY(TMR)-NC-005. At concentrations of >2 μ M β 5i is significantly inhibited, while β 5c is barely inhibited even at concentration up to 30 μ M. In addition, inhibition of β 1c by ABP **14** was investigated in more detail (Figure 5C). In order to do so, β 1i and β 5c/ β 5i were inhibited by LU-001i and NC-005, prior to incubation with ABP **14**. Residual activity of β 1c was labelled by β 1c selective ABP BODIPY(FL)-LU-001c (see chapter 8). Labelling of β 1c by ABP **14** is already visible at 470 nM, however, complete labelling is only visible at 15 μ M. The kinetic constants also prove the high β 1i selectivity of ABP **14** (Figure 5D). Compared to β 1c and β 5i, the K_{inact} is about 10 x larger and the K_i about 10x smaller for β 1i. This results in a 100x larger second order rate constant (K_{inact}/K_i) for β 1i compared to β 1c and β 5i, indicating that ABP **14** has excellent selectivity for β 1i.

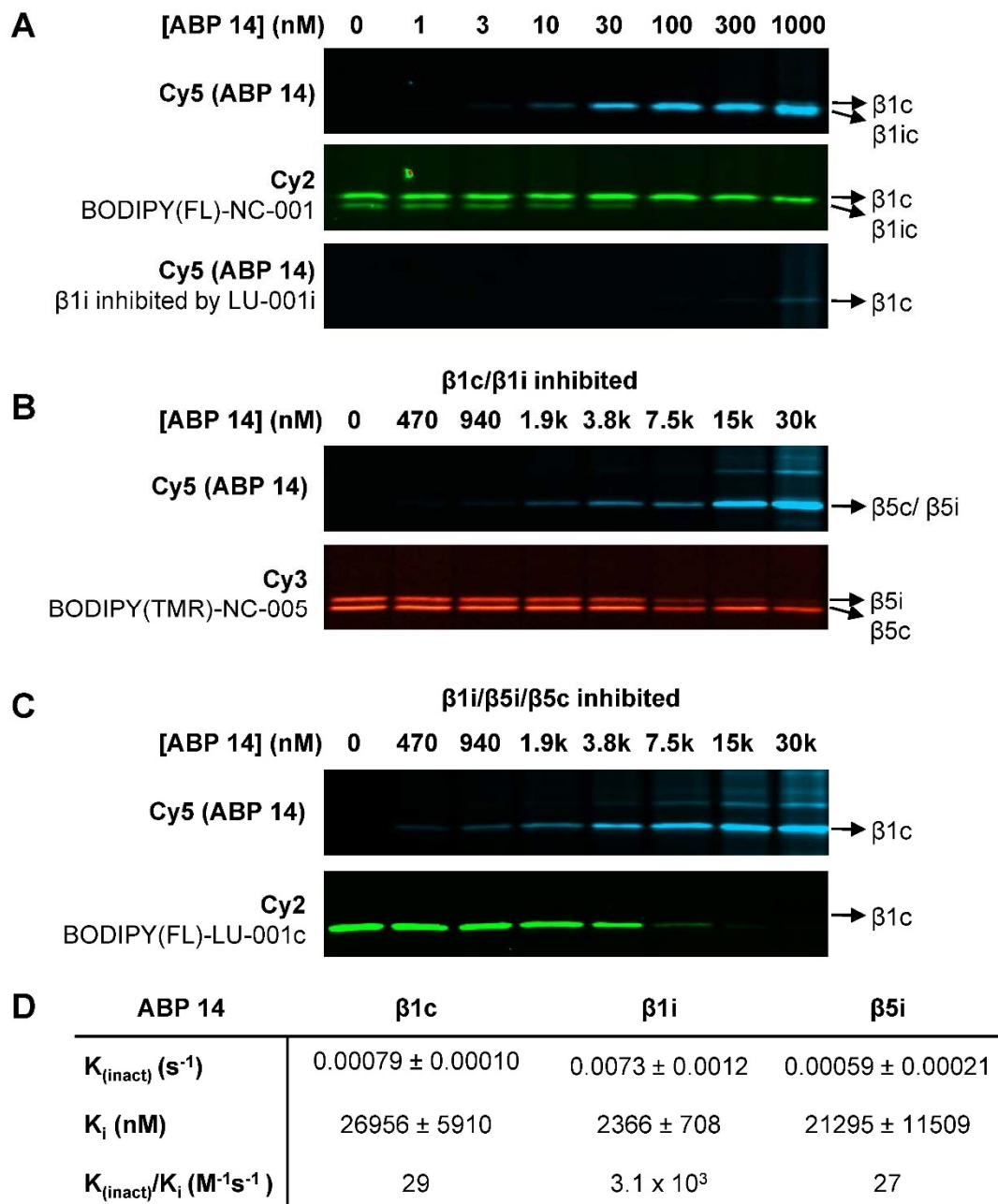


Figure 5. Evaluation of ABP 14 in Raji lysate. A) Lysates were treated with indication concentrations of ABP 13 for 1 h, followed by the addition of BODIPY(FL)-NC-001 (100 nM end concentration) for 1 h. B) Raji lysates were treated with NC-001 (5 μ M) for 1 h to inhibit β 1c and β 1i, followed by incubation with ABP 14 at indicated concentrations for 1h. Subsequently, the samples were treated with BODIPY(TMR)-NC-005 (100 nM end concentration) to label residual β 5c or β 5i activity. C) Raji lysates were treated with LU-001i (1 μ M) and NC-005 (2.5 μ M) for 1 h to inhibit β 1i, β 5c and β 5i, followed by incubation with ABP 14 at indicated concentrations for 1h. Subsequently, the samples were treated with BODIPY(FL)-LU-001c (100 nM end concentration) to label residual β 1c activity. D) Kinetic constants of ABP 14 as determined in Raji lysates. Log (% activity) for various concentrations is plotted versus time, from which the first order rate constants (K_{obs}) are derived. K_{obs} were plotted versus probe concentration, yielding $K_{inact} = \max k_{obs}$ and $K_i = [probe]$ at $0.5 K_{inact}$. $K_{inact}/K_i =$ second order rate constant.

Conclusion

Based on inhibitors selective for β 5i or β 1i, activity-based probes selective for either β 5i (ABP **13**) or β 1i (ABP **14**) were developed. Straightforward N-terminal attachment of a Cy5 fluorophore to β 1i inhibitor LU-001i provided a potent and selective probe for β 1i. In contrast, it proved to be impossible to obtain a selective β 5i probe by N-terminal attachment of a Cy5 fluorophore to a β 5i selective inhibitor. However, when the fluorophore was positioned at the P2 position a potent and selective β 5i probe was obtained. In cell lysate both probes have a good selectivity window in which only β 5i (ABP **13**) or β 1i (ABP **14**). The probes have not been verified in intact cells, however, the positive charge of the Cy5 dye could cause poor membrane permeability. Therefore, when a selective β 5i or β 1i probe is desired it might be necessary to replace Cy5 by an uncharged fluorophore, such as a BODIPY dye. Although both probes were not directly compared to the probes published Kim *et al.* (LKS01-B650 and UK-101-B660/Fluor, Figure 1) it is expected that, based on the selectivity of the parent compounds, these new probes are more selective for their respective targets.

Experimental

Synthetic procedures

General procedures

Acetonitrile (ACN), dichloromethane (DCM), N,N-dimethylformamide (DMF), methanol (MeOH), diisopropylethylamine (DiPEA) and trifluoroacetic acid (TFA) were of peptide synthesis grade, purchased at Biosolve, and used as received. All general chemicals (Fluka, Acros, Merck, Aldrich, Sigma, Iris Biotech) were used as received. Column chromatography was performed on Screening Devices b.v. Silica Gel, with a particle size of 40-63 μm and pore diameter of 60 \AA . TLC analysis was conducted on Merck aluminium sheets (Silica gel 60 F254). Compounds were visualized by UV absorption (254 nm), by spraying with a solution of $(\text{NH}_4)_6\text{Mo}_7\text{O}_{24}\cdot 4\text{H}_2\text{O}$ (25 g/L) and $(\text{NH}_4)_4\text{Ce}(\text{SO}_4)_4\cdot 2\text{H}_2\text{O}$ (10 g/L) in 10% sulphuric acid, a solution of KMnO_4 (20 g/L) and K_2CO_3 (10 g/L) in water, or ninhydrin (0.75 g/L) and acetic acid (12.5 mL/L) in ethanol, where appropriate, followed by charring at ca. 150 $^\circ\text{C}$. ^1H and ^{13}C NMR spectra were recorded on a Bruker AV-300 (MHz), AV-400 (400 MHz), AV-600 (600 MHz) spectrometer. Chemical shifts are given in ppm (δ) relative to tetramethylsilane, CD_3OD or CDCl_3 as internal standard. High resolution mass spectra were recorded by direct injection (2 μL of a 2 μM solution in water/acetonitrile 50/50 (v/v) and 0.1% formic acid) on a mass spectrometer (Thermo Finnigan LTQ Orbitrap) equipped with an electrospray ion source in positive mode (source voltage 3.5 kV, sheath gas flow 10, capillary temperature 250 $^\circ\text{C}$) with resolution $R = 60,000$ at m/z 400 (mass range $m/z = 150$ -2,000) and dioctylphthalate ($m/z = 391.28428$) as a "lock mass". The high resolution mass spectrometer was calibrated prior to measurements with a calibration mixture (Thermo Finnigan). LC-MS analysis was performed on a Finnigan Surveyor HPLC system with a Gemini C_{18} 50 \times 4.60 mm column (detection at 200-600 nm), coupled to a Finnigan LCQ Advantage Max mass spectrometer with ESI. The applied buffers were H_2O , ACN and 1.0% aq. TFA. Method: xx \rightarrow xx% MeCN, 13.0 min (0 \rightarrow 0.5 min: 10% MeCN; 0.5 \rightarrow 8.5 min: gradient time; 8.5 \rightarrow 10.5 min: 90% MeCN; 10.5 \rightarrow 13.0 min: 10% MeCN), 15 min (0 \rightarrow 0.5 min: 10% MeCN; 0.5 \rightarrow 10.5 min: gradient time; 10.5 \rightarrow 12.5 min: 90% MeCN; 12.5 \rightarrow 15 min: 90% \rightarrow 10% MeCN). HPLC purification was performed on a Gilson HPLC system coupled to a Phenomenex Gemini 5 μm 250 \times 10 mm column and a GX281 fraction collector. H-D-Ala-H-Trp(Boc)-OMe, Boc-Cha-EK and LU-001i were synthesized as described in chapter 5.

N₃Phe-D-Ala-Trp-OMe (4)

H-D-Ala-H-Trp(Boc)-OMe **3** (149 mg, 0.38 mmol, 1 equiv.) was dissolved in DCM. HCTU (198 mg, 0.48 mmol, 1.3 equiv.), N₃Phe-OH (92 mg, 0.48 mmol, 1.3 equiv.) and DiPEA (0.24 mL, 1.4 mmol, 3.7 equiv.) were added and the mixture was stirred overnight before being concentrated. The residue was dissolved in EtOAc and washed with 1M HCl (2x), sat aq NaHCO_3 (2x), brine and dried over Na_2SO_4 , filtered and concentrated. Column chromatography (20 \rightarrow 40% EtOAc:pent) yielded the title compound (175 mg, 0.31 mmol, 82%). ^1H NMR (400 MHz, CDCl_3) δ 8.10 (d, $J = 6.3$ Hz, 1H), 7.49 (d, $J = 7.7$ Hz, 1H), 7.42 (s, 1H), 7.34 – 7.14 (m, 7H), 7.10 (d, $J = 7.7$ Hz, 1H), 6.99 (d, $J = 7.5$ Hz, 1H), 4.89 (q, $J = 6.1$ Hz, 1H), 4.54 (p, $J = 7.0$ Hz, 1H), 4.01 (dd, $J = 9.1, 4.6$ Hz, 1H), 3.67 (s, 3H), 3.34 – 3.11 (m, 3H), 2.86 (dd, $J = 13.9, 9.2$ Hz, 1H), 1.64 (s, 9H), 1.27 (d, $J = 7.0$ Hz, 3H). ^{13}C NMR (101 MHz, CDCl_3) δ 171.73, 171.43, 168.68, 149.53, 136.30, 130.34, 129.35, 128.72, 127.21, 124.64, 124.28, 122.60, 118.77, 115.34, 114.82, 83.78, 65.27, 53.54, 52.59, 52.45, 48.71, 38.74, 28.19, 27.36, 18.55. LC-MS (linear gradient 10 \rightarrow 90% MeCN, 0.1% TFA, 15 min): R_t (min): 10.45 (ESI-MS (m/z): 562.87 (M+H⁺)).

N₃Phe-D-Ala-Trp(Boc)-NHNH₂ (5)

Methyl ester **4** (175 mg, 0.31 mmol, 1 equiv.) was dissolved in MeOH (4 mL). Hydrazine hydrate (425 μL , 9.0 mmol, 30 equiv.) was added and the mixture was stirred for 3 h before being co-evaporated with tol (3x). The residue was used without further purification (isolated as mixture of compounds with or without Boc). ^1H NMR (400 MHz,

MeOD) δ 7.55 (dd, J = 7.6, 4.2 Hz, 1H), 7.35 – 7.14 (m, 7H), 7.06 (dt, J = 27.1, 7.6 Hz, 2H), 4.69 – 4.59 (m, 1H), 4.22 (p, J = 7.0 Hz, 1H), 3.95 (ddd, J = 10.3, 8.5, 6.1 Hz, 1H), 3.26 (dt, J = 14.6, 5.2 Hz, 1H), 3.13 (dq, J = 14.6, 8.1, 7.5 Hz, 2H), 3.04 – 2.82 (m, 1H), 1.43 (s, 5H (partially –Boc)), 1.05 (dd, J = 10.5, 7.1 Hz, 3H). ^{13}C NMR (101 MHz, MeOD) δ 173.16, 172.16, 170.54, 136.98, 136.64, 129.69, 129.06, 127.79, 127.57, 125.02, 124.41, 123.89, 123.12, 122.05, 119.43, 119.27, 118.57, 116.35, 115.61, 111.88, 109.77, 64.65, 53.35, 52.43, 49.65, 38.65, 28.51, 28.34, 28.21, 27.75, 17.78, 17.64. LC-MS (linear gradient 10 \rightarrow 90% MeCN, 0.1% TFA, 15 min): R_t (min): 6.24 (ESI-MS (m/z): 462.93 (M+H⁺-Boc) and 7.83 (ESI-MS (m/z): 562.93 (M+H⁺+Boc).

N₃Phe-D-Ala-Trp-Cha-EK (6)

Hydrazide **5** (28 mg, 0.05 mmol, 1 equiv.) was dissolved in DMF (1 mL) and cooled to -30 °C. *t*BuONO (8 μ L, 1.1 equiv.) and HCl (35 μ L, 4M solution in 1,4-dioxane, 2.8 equiv.) were added, and the mixture was stirred for 3h at -30 °C after which TLC analysis (10% MeOH/DCM, v/v) showed complete consumption of the starting material. TFA-H-Cha-EK (1.1 equiv.) was added to the reaction mixture as a solution in DMF (1 mL). DiPEA (5 equiv.) was added to the reaction mixture, and this mixture was allowed to warm to RT slowly overnight. The mixture was diluted with EtOAc and extracted with H₂O (3 \times). Purification by column chromatography (1 \rightarrow 2% MeOH in DCM) provided the title compound (12.01 mg, 37.4%) as a white powder after lyophilisation. ^1H NMR (400 MHz, CDCl₃) δ 8.26 (s, 1H), 7.72 (d, J = 7.8 Hz, 1H), 7.41 – 7.05 (m, 9H), 6.86 (d, J = 7.0 Hz, 1H), 6.71 (d, J = 7.4 Hz, 1H), 6.14 (d, J = 7.7 Hz, 1H), 4.69 (td, J = 7.7, 5.8 Hz, 1H), 4.53 – 4.43 (m, 1H), 4.33 (p, J = 7.0 Hz, 1H), 4.04 (dd, J = 9.0, 4.6 Hz, 1H), 3.31 (dd, J = 14.1, 4.9 Hz, 2H), 3.19 (d, J = 5.0 Hz, 1H), 3.11 (dd, J = 14.5, 7.9 Hz, 1H), 2.97 – 2.85 (m, 1H), 2.81 (d, J = 5.0 Hz, 1H), 1.78 – 1.38 (m, 10H), 1.25 (d, J = 6.9 Hz, 3H), 1.20 – 0.97 (m, 4H), 0.94 – 0.68 (m, 2H). ^{13}C NMR (101 MHz, CDCl₃) δ 208.24, 171.42, 170.92, 168.99, 136.40, 136.37, 129.49, 128.89, 128.07, 127.44, 127.40, 123.73, 122.48, 120.47, 120.00, 118.97, 111.43, 110.48, 65.44, 59.13, 53.83, 52.57, 50.00, 49.35, 38.89, 38.56, 34.30, 33.99, 32.01, 28.25, 26.42, 26.22, 26.00, 18.25, 16.85. LC-MS (linear gradient 10 \rightarrow 90% MeCN, 0.1% TFA, 15 min): R_t (min): 10.16 (ESI-MS (m/z): 642.20 (M+H⁺)). HRMS: calculated for C₃₅H₄₃N₇O₅ 642.33984 [M+H]⁺; found 642.33984

BODIPY(FL)-Phe-D-Ala-Trp-EK (1)

To a degassed solution of azide **6** (4.3 mg, 6.7 μ mol, 1 equiv.) and BODIPY(FL)-alkyne (3.3 mg, 10.1 μ mol, 1.5 equiv.) in DMF (0.8 mL) under an argon atmosphere was added CuSO₄·5H₂O (0.5 equiv, 3.4 μ mol (100 μ L from degassed stock solution of 34 μ mol/mL)) and NaAsc (0.75 equiv, 5.0 μ mol (100 μ L from degassed stock solution of 50 μ mol/mL)). After stirring overnight, the reaction solution was diluted with EtOAc and washed with H₂O (1 \times) and brine (1 \times). The organic layer was dried over Na₂SO₄, filtered and concentrated. Purification by column chromatography (0 \rightarrow 3% MeOH:DCM) provided the title compound in a quantitative yield. ^1H NMR (600 MHz, CDCl₃) δ 8.20 (s, 1H), 7.66 (d, J = 7.9 Hz, 1H), 7.46 (s, 1H), 7.35 (d, J = 8.1 Hz, 1H), 7.18 (dd, J = 6.1, 2.4 Hz, 4H), 7.13 – 7.06 (m, 2H), 7.03 (d, J = 3.3 Hz, 2H), 6.89 (s, 1H), 6.52 (d, J = 7.2 Hz, 1H), 6.21 – 6.12 (m, 1H), 6.03 (s, 2H), 5.27 (s, 1H), 4.65 (q, J = 7.4 Hz, 1H), 4.48 (dd, J = 12.3, 5.3 Hz, 1H), 4.27 – 4.17 (m, 1H), 3.49 (dd, J = 13.4, 7.4 Hz, 1H), 3.32 (ddd, J = 19.4, 14.1, 6.8 Hz, 2H), 3.19 (d, J = 4.9 Hz, 1H), 3.07 (dd, J = 14.6, 7.7 Hz, 1H), 2.99 – 2.91 (m, 2H), 2.81 (d, J = 5.0 Hz, 1H), 2.74 (t, J = 7.3 Hz, 2H), 2.51 (s, 6H), 2.37 (s, 6H), 1.92 – 1.83 (m, 2H), 1.75 – 1.51 (m, 10H), 1.45 (m, 4H), 1.11 (m, 5H), 0.86 – 0.77 (m, 2H). ^{13}C NMR (151 MHz, CDCl₃) δ 208.54, 171.00, 167.33, 154.06, 146.07, 140.45, 136.34, 135.18, 131.54, 129.05, 128.95, 127.64, 127.47, 125.67, 123.62, 122.50, 121.81, 119.98, 118.88, 111.49, 110.28, 67.25, 65.93, 59.14, 53.72, 52.57, 49.94, 39.59, 38.52, 34.29, 33.99, 32.01, 31.45, 30.48, 29.63, 28.23, 26.42, 26.20, 26.00, 16.85, 16.59, 14.60. LC-MS (linear gradient 10 \rightarrow 90% MeCN, 0.1% TFA, 15 min): R_t (min): 11.45 (ESI-MS (m/z): 970.20 (M+H⁺)). HRMS: calculated for C₅₄H₈₆BF₂N₉O₅ 970.53298 [M+H]⁺; found 970.53345

Cy5-Phe-D-Ala-Trp-EK (2)

To a degassed solution of azide **6** (1.82 mg, 2.8 μ mol) and Cy5-alkyne (3.2 mg, 5.6 μ mol, 2 equiv.) in DMF (1 mL) under an argon atmosphere was added CuSO₄·5H₂O (0.5 equiv, 1.4 μ mol (100 μ L from degassed stock solution of

14 $\mu\text{mol/mL}$) and NaAsc (0.75 equiv, 2.1 μmol (100 μL from degassed stock solution of 21 $\mu\text{mol/mL}$)). After stirring overnight, the reaction mixture immediately purified by HPLC (C_{18} , 50-80% MeCN, 0.1% TFA, 10 min gradient) provided the product as a blue powder after lyophilisation (0.66 mg, 0.56 μmol , 20%). ^1H NMR (850 MHz, MeOD) δ 8.22 (td, $J = 13.1, 5.5$ Hz, 2H), 8.04 (s, 1H), 7.53 (d, $J = 7.9$ Hz, 1H), 7.48 (d, $J = 7.0$ Hz, 2H), 7.44 – 7.35 (m, 2H), 7.30 (d, $J = 8.1$ Hz, 1H), 7.28 – 7.18 (m, 7H), 7.16 (d, $J = 7.0$ Hz, 2H), 7.06 – 7.02 (m, 1H), 7.00 (s, 1H), 6.98 – 6.94 (m, 1H), 6.58 (t, $J = 12.4$ Hz, 1H), 6.27 (d, $J = 13.6$ Hz, 1H), 6.22 (d, $J = 13.7$ Hz, 1H), 5.51 (t, $J = 8.0$ Hz, 1H), 4.60 (dd, $J = 9.3, 4.9$ Hz, 1H), 4.50 (dd, $J = 10.5, 3.1$ Hz, 1H), 4.47 (d, $J = 15.2$ Hz, 1H), 4.39 (d, $J = 15.3$ Hz, 1H), 4.10 (q, $J = 7.1$ Hz, 1H), 4.05 (t, $J = 8.0$ Hz, 2H), 3.57 (s, 3H), 3.42 (dd, $J = 13.6, 8.3$ Hz, 1H), 3.40 – 3.38 (m, 1H), 3.36 – 3.33 (m, 1H), 3.23 – 3.22 (m, 1H), 3.22 (d, $J = 5.2$ Hz, 1H), 2.98 (dd, $J = 14.9, 9.2$ Hz, 1H), 2.85 (d, $J = 5.1$ Hz, 1H), 2.25 – 2.19 (m, 2H), 1.71 (d, $J = 2.5$ Hz, 6H), 1.71 – 1.70 (m, 6H), 1.40 (s, 3H), 0.96 (d, $J = 7.1$ Hz, 3H), 1.84 – 0.81 (m, 19H). ^{13}C NMR (214 MHz, MeOD) δ 209.76, 175.59, 174.28, 173.82, 169.21, 155.39, 146.01, 144.25, 143.51, 142.64, 142.50, 138.02, 136.81, 130.25, 129.79, 129.71, 129.63, 128.70, 128.29, 126.65, 126.25, 126.11, 124.49, 123.84, 123.38, 123.25, 122.42, 119.79, 119.35, 112.30, 112.09, 111.80, 111.03, 104.36, 65.80, 60.14, 57.48, 55.00, 53.13, 51.27, 51.15, 50.55, 50.47, 49.48, 49.38, 44.78, 39.93, 38.48, 36.55, 35.71, 35.51, 35.16, 32.94, 31.49, 30.90, 28.41, 28.12, 27.95, 27.82, 27.55, 27.32, 27.06, 26.36, 17.11, 17.08. HRMS: calculated for $C_{70}H_{85}N_{10}O_6$ 1161.66481 $[\text{M}]^+$; found 1161.66479 LC-MS (linear gradient 10 \rightarrow 90% MeCN/ H_2O , 0.1% TFA, 13.0 min): R_t (min): 8.48 (ESI-MS (m/z): 1161.73 (M^+)).

Boc-Tyr(OCH₂CCH)-OMe (8)

To a solution of Boc-Tyr-OMe **7** (380 mg, 1.28 mmol, 1 equiv.) in DMF (10 mL) were added K_2CO_3 (353 mg, 2.56 mmol, 2 equiv.) and propargylbromide (193 μL , 2.56 mmol, 2 equiv.). After stirring overnight at rt, the reaction mixture was diluted with EtOAc and washed with 1N HCl (2x) and brine (1x). The organic layer was dried over Na_2SO_4 , filtered and concentrated. Purification by column chromatography (10 \rightarrow 20% EtOAc/pent) provided the title compound (309 mg, 0.93 mmol, 72%). ^1H NMR (300 MHz, CDCl_3) δ 7.04 (d, $J = 8.4$ Hz, 2H), 6.88 (d, $J = 8.6$ Hz, 2H), 4.99 (d, $J = 7.9$ Hz, 1H), 4.64 (d, $J = 2.3$ Hz, 2H), 4.52 (q, $J = 6.0$ Hz, 1H), 3.69 (s, 3H), 3.12 – 2.84 (m, 2H), 2.51 (t, $J = 2.3$ Hz, 1H), 1.40 (s, 9H). ^{13}C NMR (75 MHz, CDCl_3) δ 172.43, 156.68, 130.36, 129.03, 114.99, 79.93, 78.63, 75.62, 55.83, 54.54, 52.26, 37.50, 28.35.

Boc-D-Ala-Tyr(OCH₂CCH)-OMe (9)

Boc-Tyr(OCH₂CCH)-OMe **8** (309 mg, 0.93 mmol) was treated with 1:1 TFA/DCM for 30 min, followed by co-evaporation with toluene (2x). The resulting product TFA-H-Tyr(OCH₂CCH)-OMe was dissolved in DCM and Boc-D-Ala-OH (211 mg, 0.11 mmol, 1.2 equiv.), HCTU (461 mg, 0.11 mmol, 1.2 equiv.) and DiPEA (566 μL , 3.26 mmol, 3.5 equiv.) were added. After stirring overnight, the reaction mixture was concentrated and redissolved in EtOAc and washed with 1N HCl (2x), sat. NaHCO_3 (2x) and brine (1x). The organic layer was dried over NaSO_4 , filtered, concentrated providing the title compound in a quantitative yield. ^1H NMR (400 MHz, CDCl_3) δ 7.02 (d, $J = 8.7$ Hz, 2H), 6.85 (d, $J = 8.7$ Hz, 2H), 6.81 (d, $J = 7.4$ Hz, 1H), 5.16 (d, $J = 7.5$ Hz, 1H), 4.85 – 4.73 (m, 1H), 4.62 (d, $J = 2.4$ Hz, 2H), 4.23 – 4.10 (m, 1H), 3.67 (s, 3H), 3.10 – 2.93 (m, 2H), 2.50 (t, $J = 2.4$ Hz, 1H), 1.40 (s, 9H), 1.25 (d, $J = 7.1$ Hz, 3H). ^{13}C NMR (101 MHz, CDCl_3) δ 172.47, 171.97, 156.68, 155.49, 130.32, 128.80, 114.98, 80.04, 78.55, 75.64, 55.79, 53.23, 52.38, 49.96, 37.04, 28.35, 18.54.

3MeIndAc-D-Ala-Tyr(OCH₂CCH)-OMe (10)

Boc-D-Ala-Tyr(OCH₂CCH)-Me **9** (430 mg, 0.93 mmol) was treated with 1:1 TFA/DCM for 30 min, followed by co-evaporation with toluene (2x). The resulting product TFA-D-Ala-Tyr(OCH₂CCH)-OMe was dissolved in DCM and 3-Methylindene-2-carboxylic acid (194 mg, 0.11 mmol, 1.2 equiv.), HCTU (461 mg, 0.11 mmol, 1.2 equiv.) and DiPEA (566 μL , 3.26 mmol, 3.5 equiv.) were added. After stirring overnight, the reaction mixture was concentrated and redissolved in EtOAc and washed with 1N HCl (2x), sat. NaHCO_3 (2x) and brine (1x). The organic layer was dried over NaSO_4 , filtered and concentrated. Purification by column chromatography (20 \rightarrow 75% EtOAc/pent) provided the title compound (396 mg, 0.86 mmol, 93%). ^1H NMR (400 MHz, CDCl_3) δ 7.46 – 7.39 (m, 2H), 7.32

(dtd, $J = 15.9, 7.3, 1.2$ Hz, 2H), 7.19 (d, $J = 8.1$ Hz, 1H), 7.07 (d, $J = 8.6$ Hz, 2H), 6.83 (d, $J = 8.7$ Hz, 2H), 6.63 (d, $J = 7.3$ Hz, 1H), 4.90 – 4.78 (m, 1H), 4.72 (p, $J = 7.0$ Hz, 1H), 4.53 (d, $J = 2.4$ Hz, 2H), 3.67 (s, 3H), 3.61 – 3.53 (m, 2H), 3.20 – 2.94 (m, 2H), 2.48 (t, $J = 2.1$ Hz, 4H), 1.37 (d, $J = 7.0$ Hz, 3H). ^{13}C NMR (101 MHz, CDCl_3) δ 172.44, 171.92, 165.73, 156.64, 147.62, 145.50, 142.17, 131.78, 130.36, 128.86, 127.29, 126.77, 123.85, 120.80, 114.91, 78.52, 75.61, 55.68, 53.32, 52.42, 48.69, 38.30, 36.98, 18.91, 12.32.

3MeIndAc-D-Ala-Tyr(OCH₂CCH)-NHNH₂ (11)

To a solution of 3MeIndAc-D-Ala-Tyr(OCH₂CCH)-OMe **10** (396 mg, 0.86 mmol) in MeOH (10 mL) was added hydrazine-hydrate (2.5 mL, 50 mmol, 60 equiv.). After stirring for 3 hours, the reaction mixture was concentrated and co-evaporated with toluene (3x) providing the product in a quantitative yield. Partial reduction of the alkyne functionality resulted in a 7:2:1 mixture of triple:double:single bond, as determined by HPLC/MS analysis (See Figure 6). ^1H NMR (400 MHz, $\text{CDCl}_3/\text{MeOD}$) (peaks reported for desired product). δ 7.51 – 7.44 (m, 2H), 7.39 – 7.30 (m, 2H), 7.13 (d, $J = 8.6$ Hz, 2H), 6.83 (d, $J = 8.6$ Hz, 2H), 4.64 – 4.58 (m, 1H), 4.54 (d, $J = 2.4$ Hz, 2H), 4.48 – 4.39 (m, 1H), 3.65 – 3.56 (m, 2H), 3.16 (dt, $J = 13.4, 6.7$ Hz, 1H), 2.88 (dd, $J = 14.0, 9.0$ Hz, 1H), 2.68 (t, $J = 2.4$ Hz, 1H), 2.50 (t, $J = 2.1$ Hz, 3H), 1.26 (d, $J = 7.2$ Hz, 3H). ^{13}C NMR (101 MHz, MeOD) (all peaks reported) δ 174.37, 171.79, 167.57, 157.13, 149.07, 145.85, 142.98, 133.78, 131.83, 130.64, 130.01, 129.21, 127.92, 127.25, 124.29, 121.30, 117.64, 115.35, 115.17, 114.94, 100.61, 78.95, 76.12, 69.15, 56.10, 53.74, 38.49, 37.31, 17.93, 12.46.

RT: 0.00 - 13.20

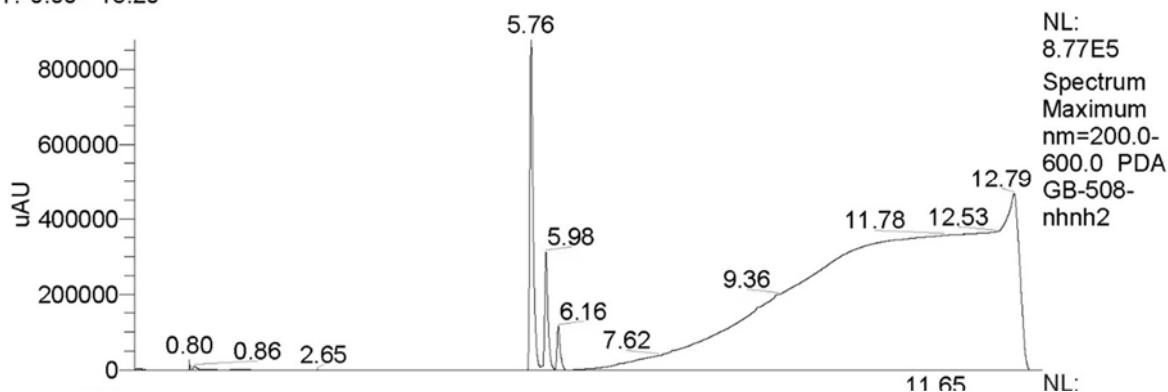


Figure 6. HPLC trace of compound **11**. Retention time (min)/(m/z): 5.76/461.07 (alkyne); 5.98/463.07 (alkene); 6.16/465.00 (alkane).

3MeIndAc-D-Ala-Tyr(OCH₂CCH)-Cha-EK (12)

Hydrazide **12** (47 mg, 0.1 mmol, 1 equiv.) was dissolved in DMF (2 mL) and cooled to -30 °C. *t*BuONO (16 μL , 1.1 equiv.) and HCl (70 μL , 4M solution in 1,4-dioxane, 2.8 equiv.) were added, and the mixture was stirred for 3h at -30 °C after which TLC analysis (10% MeOH/DCM, v/v) showed complete consumption of the starting material. TFA-H-Cha-EK was added to the reaction mixture as a solution in DMF (1 mL). DiPEA (5 equiv.) was added to the reaction mixture, and this mixture was allowed to warm to RT slowly overnight. The mixture was diluted with EtOAc and extracted with H₂O (3x). The organic layer was dried over MgSO_4 , concentrated and purified by column chromatography (0-2% MeOH in DCM) providing the product as 7:2:1 mixture of triple:double:single bond (32 mg, 0.05 mmol, 50%). ^1H NMR (400 MHz, CDCl_3) (peaks reported for desired product) δ 7.50 – 7.42 (m, 2H), 7.40 – 7.28 (m, 2H), 7.14 (d, $J = 8.7$ Hz, 2H), 6.95 (t, $J = 8.7$ Hz, 1H), 6.85 (d, $J = 8.7$ Hz, 2H), 6.53 – 6.46 (m, 2H), 4.71 – 4.47 (m, 5H), 3.58 (s, 2H), 3.23 (d, $J = 5.0$ Hz, 1H), 3.04 (d, $J = 6.8$ Hz, 2H), 2.83 (d, $J = 5.0$ Hz, 1H), 2.51 (t, $J = 2.2$ Hz, 3H), 2.48 (t, $J = 2.4$ Hz, 1H), 1.92 (s, 1H), 1.80 – 1.44 (m, 5H), 1.43 (s, 3H), 1.36 (d, $J = 7.0$ Hz, 3H), 1.28 – 1.05 (m, 5H), 0.83 (m, 2H). ^{13}C NMR (101 MHz, CDCl_3) (all peaks reported) δ 208.31, 172.56, 170.83, 166.09, 156.76, 148.36, 145.57, 142.23, 133.34, 131.48, 130.57, 130.53, 129.41, 128.53, 127.49, 126.91, 123.92, 120.95, 117.71, 115.09, 114.93, 114.70, 76.84, 75.61, 68.81, 59.15, 55.85, 54.35, 52.47, 49.79, 49.10, 38.56, 38.34, 37.02, 34.38, 33.98, 32.02, 26.40, 26.24, 25.98, 18.53, 16.81, 12.50.

Cy5-LU-035i (13)

To a degassed solution of **12** (mix alkyne, alkene and alkane) (10 mg, 16 μmol) and Cy5-alkyne (13 mg, 24 μmol , 1.5 equiv.) in DMF (1 mL) under an argon atmosphere was added $\text{CuSO}_4 \cdot 5\text{H}_2\text{O}$ (0.5 equiv, 8 μmol (100 μL from degassed stock solution of 8 $\mu\text{mol}/\text{mL}$)) and NaAsc (0.75 equiv, 12 μmol (100 μL from degassed stock solution of 120 $\mu\text{mol}/\text{mL}$)). After stirring overnight, the reaction mixture immediately purified by HPLC (C_{18} , 55-65% MeCN, 0.1% TFA, 10 min gradient) provided the product as a blue powder after lyophilisation (5.91 mg, 4.5 μmol , 28%). ^1H NMR (600 MHz, CDCl_3) δ 8.05 (s, 1H), 7.86 (s, 1H), 7.76 (td, $J = 13.0, 8.2$ Hz, 2H), 7.54 (d, $J = 7.9$ Hz, 1H), 7.45 (d, $J = 7.5$ Hz, 2H), 7.38 (t, $J = 7.7$ Hz, 2H), 7.34 (d, $J = 7.6$ Hz, 3H), 7.32 – 7.28 (m, 2H), 7.26 – 7.21 (m, 2H), 7.18 (d, $J = 6.7$ Hz, 1H), 7.12 (d, $J = 8.0$ Hz, 1H), 7.07 (d, $J = 8.3$ Hz, 3H), 7.02 – 6.97 (m, 1H), 6.74 (d, $J = 8.5$ Hz, 2H), 6.62 (t, $J = 12.5$ Hz, 1H), 6.28 (d, $J = 13.7$ Hz, 1H), 6.17 (d, $J = 13.5$ Hz, 1H), 5.13 – 5.03 (m, 2H), 4.62 – 4.49 (m, 3H), 4.42 (t, $J = 6.9$ Hz, 2H), 4.00 (t, $J = 7.5$ Hz, 2H), 3.77 – 3.62 (m, 2H), 3.55 (s, 3H), 3.25 (d, $J = 5.1$ Hz, 1H), 3.22 (d, $J = 9.4$ Hz, 2H), 3.04 (q, $J = 6.3, 4.0$ Hz, 2H), 2.81 (d, $J = 5.1$ Hz, 1H), 2.49 (t, $J = 2.0$ Hz, 3H), 2.28 (t, $J = 7.6$ Hz, 2H), 2.14 – 2.04 (m, 2H), 1.85 – 1.04 (m, 33H), 0.93 – 0.78 (m, 3H). ^{13}C NMR (151 MHz, CDCl_3) δ 208.35, 173.32, 172.92, 171.47, 166.20, 157.05, 153.15, 152.55, 148.29, 145.65, 142.82, 142.55, 141.94, 141.05, 140.74, 131.81, 130.45, 129.69, 129.08, 128.91, 127.40, 126.78, 126.00, 125.71, 125.29, 124.22, 124.02, 122.26, 122.19, 120.85, 115.69, 111.16, 110.49, 104.24, 103.54, 67.23, 62.24, 59.19, 55.26, 52.51, 49.97, 49.81, 49.50, 49.15, 48.08, 44.50, 38.39, 38.25, 36.95, 36.32, 36.00, 34.38, 34.30, 33.92, 32.04, 31.26, 30.46, 30.26, 29.83, 29.79, 29.74, 29.59, 29.39, 29.28, 28.17, 27.15, 26.51, 26.48, 26.25, 26.05, 25.31, 25.06, 18.27, 16.95, 12.52. HRMS: calculated for $\text{C}_{73}\text{H}_{90}\text{N}_9\text{O}_7$ 1204.69577 $[\text{M}]^+$; found 1204.69580 LC-MS (linear gradient 10 \rightarrow 90% MeCN/ H_2O , 0.1% TFA, 13.0 min): R_t (min): 8.46 (ESI-MS (m/z): 1204.47 (M^+)).

Cy5-LU-001i (14)

To a degassed solution of LU-001i (6.0 mg, 9.8 μmol) and Cy5-alkyne (5.0 mg) in DMF (0.8 mL) under an argon atmosphere was added $\text{CuSO}_4 \cdot 5\text{H}_2\text{O}$ (0.5 equiv, 4.9 μmol (100 μL from degassed stock solution of 49 $\mu\text{mol}/\text{mL}$)) and NaAsc (0.75 equiv, 7.4 μmol (100 μL from degassed stock solution of 74 $\mu\text{mol}/\text{mL}$)). After stirring overnight, the reaction mixture was concentrated and purified by column chromatography (0-3-6-10% MeOH in DCM) providing the product after lyophilisation as a blue powder (8.3 mg, 7.3 μmol , 75%). ^1H NMR (850 MHz, CDCl_3) δ 7.88 (s, 2H), 7.78 (q, $J = 12.5$ Hz, 2H), 7.31 (ddd, $J = 10.1, 6.2, 2.8$ Hz, 3H), 7.29 (dd, $J = 7.1, 2.6$ Hz, 2H), 7.16 (q, $J = 7.2$ Hz, 2H), 7.10 – 7.06 (m, 1H), 7.04 (d, $J = 7.9$ Hz, 1H), 6.74 (s, 1H), 6.55 (s, 1H), 6.30 (d, $J = 13.4$ Hz, 1H), 6.22 (d, $J = 13.5$ Hz, 1H), 5.14 (s, 2H), 4.76 (s, 1H), 4.50 (td, $J = 16.8, 13.7, 8.5$ Hz, 3H), 4.24 – 4.18 (m, 1H), 4.18 – 4.07 (m, 2H), 3.98 (s, 2H), 3.80 (s, 1H), 3.56 (d, $J = 11.7$ Hz, 3H), 3.23 (d, $J = 5.0$ Hz, 1H), 2.78 (d, $J = 5.0$ Hz, 1H), 2.60 (s, 2H), 2.30 – 2.20 (m, 2H), 1.87 – 0.93 (m, 40H), 0.95 – 0.69 (m, 7H). ^{13}C NMR (214 MHz, CDCl_3) δ 208.60, 173.03, 172.99, 172.24, 171.87, 169.56, 153.23, 152.76, 142.86, 142.01, 141.16, 140.88, 129.00, 128.83, 126.45, 126.28, 125.51, 125.21, 125.13, 122.29, 122.21, 111.13, 110.57, 105.98, 104.29, 103.96, 92.00, 66.91, 59.23, 58.32, 54.05, 52.61, 49.73, 49.47, 49.21, 48.07, 44.58, 38.83, 38.35, 34.36, 34.04, 32.06, 31.94, 31.67, 29.83, 29.79, 29.50, 28.30, 28.25, 27.65, 27.29, 26.55, 26.48, 26.32, 26.02, 25.24, 22.83, 22.41, 17.16, 16.92, 14.27, 14.09. HRMS: calculated for $\text{C}_{63}\text{H}_{85}\text{F}_2\text{N}_{10}\text{O}_7$ 1131.65653 $[\text{M}]^+$; found 1131.65649. LC-MS (linear gradient 10 \rightarrow 90% MeCN/ H_2O , 0.1% TFA, 13.0 min): R_t (min): 7.96 (ESI-MS (m/z): 1131.67 (M^+)).

Biochemical experiments**General**

Lysates of cells were prepared by treating cell pellets with 4 volumes of lysis buffer containing 50 mM Tris pH 7.5, 2 mM DTT, 5 mM MgCl_2 , 10% glycerol, 2 mM ATP, and 0.05% digitonin for 60 min. Protein concentration was determined using Qubit[®] protein assay kit (ThermoFisher). All cell lysate labelling experiments were performed in assay buffer containing 50 mM Tris pH 7.5, 2 mM DTT, 5 mM MgCl_2 , 10% glycerol, 2 mM ATP. Cell lysate labelling and competition experiments were performed at 37°C. Prior to fractionation on 12.5% SDS-PAGE

(TRIS/glycine), samples were boiled for 3 min in a reducing gel loading buffer. The 7.5x10 cm (L x W) gels were run for 15 min at 80V followed by 120 min at 130V. In-gel detection of (residual) proteasome activity was performed in the wet gel slabs directly on a ChemiDoc™ MP System using Cy2 setting to detect BODIPY(FL), Cy3 settings to detect BODIPY(TMR) and Cy5 settings to detect Cy5.

Competition experiments in cell lysate

Cell lysates (diluted to 10-15 μ g total protein in 9 μ L buffer) were exposed to the inhibitors (10 or 20x stock in DMSO) or ABPs (10 or 20x stock in DMSO) at indicated concentrations for 1 h at 37 °C. In case of multiple inhibition/labelling steps, max 20% DMSO is used and incubation conditions are always 1 h at 37 °C. SDS-PAGE analysis is performed as described above.

Determination of kinetic constants

General

All incubations are performed at 37 °C. Raji cell lysates (10 μ g/ 9 μ L) were incubated with appropriate inhibitor(s) (1 μ L from 10x stock in DMSO) followed by incubation with increasing concentrations of ABP for different lengths of time. The reaction was stopped by snap-freezing in liquid nitrogen and while still frozen, the denaturing sample buffer is added. Next, SDS-PAGE analysis is performed as described in the general methods. Intensities of bands were measured by fluorescent densitometry and normalized to full labelling. When the Log (% activity) is plotted versus time, a straight line is observed, from which the first order rate constants (K_{obs}) can be derived for each concentration. K_{obs} were plotted versus probe concentration, from which inhibition constants K_i and K_{inact} were calculated using Graphpad Prism software. See chapter 3, supporting figure S3 for example.

ABP 13

β 5c: Raji cell lysates (10 μ g/ 9 μ L) were incubated LU-035i (1 μ M, 1 μ L from 10x stock, to inhibit β 5i) and NC-001 2.5 μ M, 1 μ L from 10x stock, to inhibit β 1c/ β 1i) for 1 h, followed by incubation with increasing concentrations of probe for 0, 15, 30 or 60 min. Concentrations used: 0.1, 0.3, 1.0, 3.0, 10, 30 μ M; Full labelling of β 5c is achieved by incubation with 30 μ M of probe for 1 h.

β 5i: Raji cell lysates (10 μ g/ 9 μ L) were incubated LU-005c (1 μ M, 1 μ L from 10x stock, to inhibit β 5c) and NC-001 2.5 μ M, 1 μ L from 10x stock, to inhibit β 1c/ β 1i) for 1 h, followed by incubation with increasing concentrations of probe for 0, 1, 2 or 5 min. Concentrations used: 80, 160, 320, 640, 1280, 2560, 5120, 10240 nM; Full labelling of β 5i is achieved by incubation with 100 nM of probe for 1 h.

ABP 14

β 1c: Raji cell lysates (10 μ g/ 9 μ L) were incubated LU-001i (1 μ M, 1 μ L from 10x stock, to inhibit β 1i) and NC-005 5.0 μ M, 1 μ L from 10x stock, to inhibit β 5c/ β 5i) for 1 h, followed by incubation with increasing concentrations of probe for 0, 15, 30 or 60 min. Concentrations used: 0.94, 1.89, 3.75, 7.5, 15, 30 μ M; Full labelling of β 1c is not achieved by incubation with 30 μ M of probe for 1 h, however, higher concentrations did show too much background. Therefore the labelling with 30 μ M of probe for 1 h was used as a reference and was determined to be 94%.

β 1i: Raji cell lysates (10 μ g/ 9 μ L) were incubated LU-001c (10 μ M, 1 μ L from 10x stock, to inhibit β 1c) and NC-005 5.0 μ M, 1 μ L from 10x stock, to inhibit β 5c/ β 5i) for 1 h, followed by incubation with increasing concentrations of probe for 0, 1, 2 or 5 min. Concentrations used: 100, 200, 400, 800, 1600, 3200 nM; Full labelling of β 1i is achieved by incubation with 300 nM of probe for 1 h.

β5i: Raji cell lysates (10 μg/ 9 μL) were incubated NC-001 (2.5 μM, 1μL from 10x stock, to inhibit β1c/β1i) for 1 h, followed by incubation with increasing concentrations of probe for 0, 1, 2 or 5 min. Concentrations used: 100, 200, 400, 800, 1600, 3200 nM; Full labelling of β5i is achieved by incubation with 30 μM of probe for 1 h.

References

1. Hershko, A. & Ciechanover, A. The ubiquitin system. *Annu. Rev. Biochem.* **67**, 425-79 (1998).
2. Ferrington, D.A. & Gregerson, D.S. Immunoproteasomes: structure, function, and antigen presentation. *Prog. Mol. Biol. Transl. Sci.* **109**, 75-112 (2012).
3. Adams, J. et al. Proteasome inhibitors: A novel class of potent and effective antitumor agents. *Cancer Res.* **59**, 2615-2622 (1999).
4. Demo, S.D. et al. Antitumor Activity of PR-171, a novel irreversible inhibitor of the proteasome. *Cancer Res.* **67**, 6383-6391 (2007).
5. Kisselev, A.F. & Groettrup, M. Subunit specific inhibitors of proteasomes and their potential for immunomodulation. *Curr. Opin. Chem. Biol.* **23**, 16-22 (2014).
6. de Bruin, G. et al. A set of activity-based probes to visualize human (immuno)proteasome activities. *Ang. Chem. Int. Ed.* **13**, 4199-4203 (2015).
7. Verdoes, M. et al. A panel of subunit-selective activity-based proteasome probes. *Org. Biomol. Chem.* **8**, 2719-2727 (2010).
8. Verdoes, M. et al. A fluorescent broad-spectrum proteasome inhibitor for labeling proteasomes in vitro and in vivo. *Chem. Biol.* **13**, 1217-1226 (2006).
9. Geurink, P.P. et al. Incorporation of non-natural amino acids improves cell permeability and potency of specific inhibitors of proteasome trypsin-like sites. *J. Med. Chem.* **56**, 1262-1275 (2013).
10. Sharma, L.K. et al. Activity-based near-infrared fluorescent probe for LMP7: a chemical proteomics tool for the immunoproteasome in living cells. *ChemBioChem* **13**, 1899-1903 (2012).
11. Carmony, K.C. et al. A bright approach to the immunoproteasome: development of LMP2/β1i-specific imaging probes. *Bioorg. Med. Chem. Lett.* **20**, 607-613 (2012).
12. de Bruin, G. et al. Structure-based design of β1i or β5i specific inhibitors of human immunoproteasomes. *J. Med. Chem.* **57**, 6197-6209 (2014).
13. Verdoes, M. et al. Acetylene functionalized BODIPY dyes and their application in the synthesis of activity based proteasome probes. *Bioorg. Med. Chem. Lett.* **17**, 6169-71 (2007).
14. Huber, Eva M. et al. Immuno- and constitutive proteasome crystal structures reveal differences in substrate and inhibitor specificity. *Cell* **148**, 727-738 (2012).
15. Huber, E.M. et al. Systematic analyses of substrate preferences of 20S proteasomes using peptidic epoxyketone inhibitors. *J. Am. Chem. Soc.* **137**, 7835-7842 (2015).
16. Shenk, K.D. et al. *US/20070293465*, (2007).
17. Muchamuel, T. et al. A selective inhibitor of the immunoproteasome subunit LMP7 blocks cytokine production and attenuates progression of experimental arthritis. *Nat Med* **15**, 781-787 (2009).
18. Singh, J., Petter, R.C., Baillie, T.A. & Whitty, A. The resurgence of covalent drugs. *Nat. Rev. Drug. Discov.* **10**, 307-317 (2011).
19. Britton, M. et al. Selective inhibitor of proteasome's caspase-like sites sensitizes cells to specific inhibition of chymotrypsin-like sites. *Chem. Biol.* **16**, 1278-1289 (2009).

CHAPTER 7

Development of an inhibitor and activity-based probe selective for $\beta 5c$

Introduction

The chymotryptic sites of mammalian proteasomes are often considered as the major proteolytic activities and are the predominant targets in proteasome-directed drug discovery programs. Indeed, the clinical drug bortezomib, while targeting also caspase-like proteasome activities, was initially developed to exclusively disable proteasome chymotryptic sites, and also the second-in-class clinical drug/proteasome inhibitor carfilzomib, has as its major target these activities. Despite the large body of evidence pointing towards the importance of the tryptic-like and caspase-like proteasome activities in protein turnover and (especially) in MHC class I directed antigen presentation, most studies reporting on the discovery of proteasome inhibitors present data on inhibition of chymotryptic activities only.

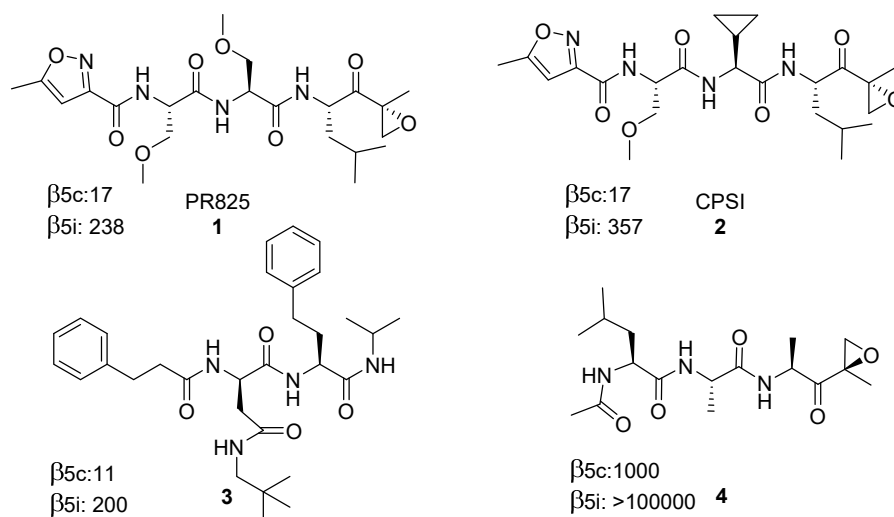


Figure 1. Structures and IC_{50} values (nM) of $\beta 5c$ selective inhibitors. IC_{50} values have been determined using different assays. 1/2: PROCISE assay (1. intact cells; 2. purified 20S), 3: fluorogenic substrates (purified 20S), 4: ABPP (cell lysate).

Given the predominant focus in proteasome inhibitor research on chymotryptic sites, it is perhaps surprising that only a few studies report on inhibitors able to discriminate between the respective chymotryptic activities of human constitutive proteasomes and immunoproteasomes, β 5c and β 5i. Of these studies, the majority focus on β 5i selective inhibitors (see also chapter 5), and those few inhibitors reported as selective for β 5c have only small selectivity windows. Currently known β 5c selective inhibitors are shown in Figure 1. Both **1** and **2** have been identified in a medicinal chemistry effort aiming to develop orally available β 5c/ β 5i selective proteasome inhibitors.¹ Inhibitors **1** and **2** differ at the P2 position only, and arguably these residues have limited interaction with the large and solvent exposed S2 pockets of both β 5c and β 5i active sites.² When the P1 Leu residue of **1** is replaced by Phe, β 5c selectivity is completely abolished, resulting in equal activity against β 5c and β 5i, which can be explained by the preference of β 5i for large P1 residues.¹ While β 5i prefers small residues at P3, β 5c favours large P3 residues, as can be deduced from mouse 20S (immuno)proteasome crystal structures.^{2, 3} β 5i selective inhibitors require a P3 Ala residue,³ therefore, most likely, the relatively large P3 Ser(OMe) side chain is disfavoured by the β 5i subunit, leading to β 5c selectivity. As well, capped dipeptide **3** features a large P3 substituent, which is responsible for its β 5c selectivity.⁴ As is described in chapter 4, β 5c has a smaller S1 pocket than β 5i and this difference is caused by a different conformation adopted by Met45 in the respective active site pockets. For this reason, compound **4** (P1 Ala) displays high β 5c selectivity, however, the potency of β 5c inhibition is relatively low and the β 2 subunits are also targeted.⁵ Currently, there is no evidence that selective β 5c inhibition could form the basis for the development of therapies against human diseases. However, from a more fundamental perspective, it is desirable to be able to selectively inhibit each individual proteasome subunit in order to determine the exact role of each proteasome subunit in protein turnover and antigen processing. Selective β 5c inhibition by epoxyketone **2** has already shown that, unlike carfilzomib which inhibits both β 5c and β 5i, inhibition of β 5c in haematological derived cancer cell lines without inhibition of β 5i did not result in significant cytotoxicity.¹ Given the poor selectivity profiles of existing β 5c selective inhibitors (compounds **1**, **2** and **3** are only 20-fold selective), it would be beneficial to have access to more selective β 5c inhibitors. In this chapter the development of β 5c inhibitors with both good potency and much higher selectivity windows compared to existing β 5c inhibitors are described. In addition, these optimized β 5c inhibitors form the basis for the development of an activity-based probe (ABP) that is selective for β 5c over β 5i.

Results and discussion

As stated above, β 5c has a larger S3 pocket than β 5i. Therefore, a series of compounds was designed varying in their (bulky, hydrophobic) P3 substituent: 1-naphthylalanine (1-Nap), 2-naphthylalanine (2-Nap), biphenylalanine (BiPhe), cyclohexylalanine (Cha), tryptophan (Trp), adamantylalanine (Ala(Ada)), tert-butylalanine (Ala(tBu)), tert-butyl-O-Ser (Ser(OtBu)), and tert-butyl-O-Thr (Thr(OtBu)), see Figure 2. These amino acids were incorporated in the otherwise identical N₃Phe-XXX-Phe-Leu-epoxyketone (except for compound **10**, which contains a P2 Leu residue) scaffold using standard solution phase Boc/Fmoc chemistry and standard azide coupling of the peptide hydrazides and deprotected warheads, as described in the experimental part and in previous chapters. All inhibitors were evaluated for their inhibition activities against all six subunits at four different concentrations in Raji-lysates using the ABPP-assay described in chapter 3 (Figure 2). The compounds with aromatic substituents at the P3 sites (**5**, **6**, **7**, **9**) do not show any selectivity for β 5c. Interestingly, compounds **5** (1-Nap), **6** (2-Nap) and **9** (Trp) do also inhibit β 2 at higher concentrations whereas compound **7** (BiPhe) does not target β 2, even not at 10 μ M, making **7** a highly potent and selective β 5c/ β 5i inhibitor. Compound **8** (Cha) shows almost complete inhibition of β 5c at 10 nM, and some 10-fold selectivity for β 5c over β 5i. Incorporation of an adamantyl side chain (**10**) results in loss of potency and similar selectivity as **8**.

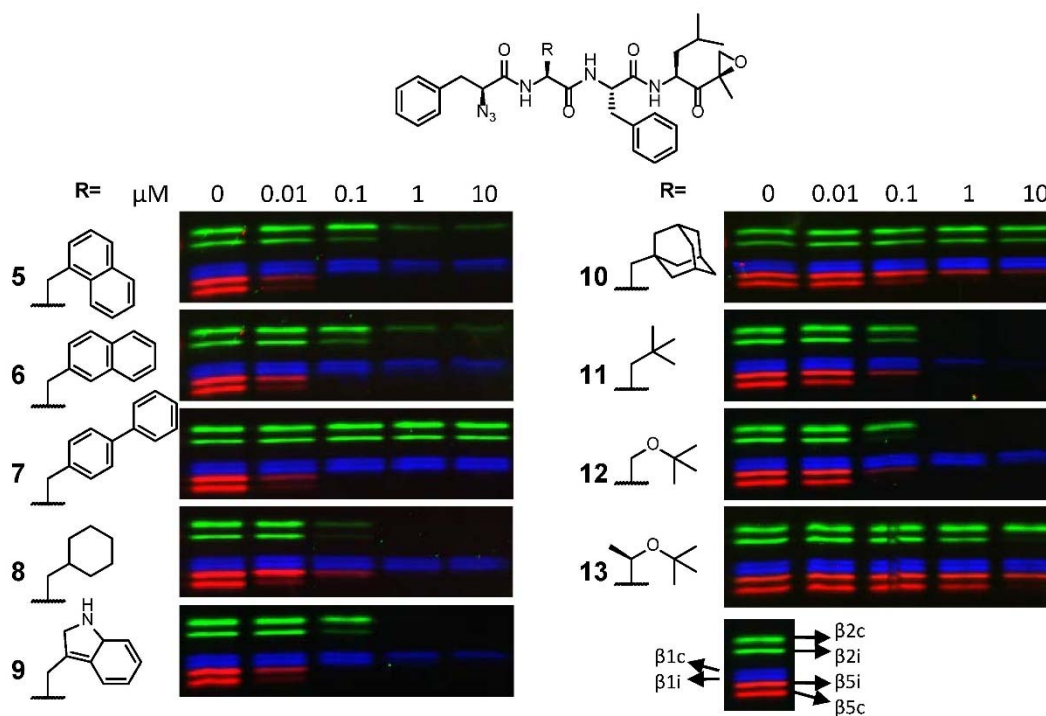


Figure 2. Structure and inhibition profiles in Raji lysates of a small library of compounds with different bulky hydrophobic P3 substituents. *P2=Leu

Compounds **11** (Ala(tBu)) and **12** (Ser(OtBu)) do not show selectivity for $\beta 5c$, while compound **13** (Thr(OtBu)) is selective for $\beta 5c$, however, only at high concentrations.

To further improve the selectivity towards $\beta 5c$, a series of compounds was synthesized equipped with Ala at P1 and at P3 either one of the $\beta 5c$ -selectivity inducing amino acids Cha, Ala(Ada), Thr(OtBu) (compounds **14**, **15** and **16**) or BiPhe (compound **17**) (Figure 3). A very high selectivity for $\beta 5c$ over $\beta 5i$ was observed for compound **14**, which however also targets $\beta 2c/\beta 2i$. In contrast, while still being selective for $\beta 5c$, Ala(Ada) (**15**) and Thr(OtBu) (**16**) at P3 in combination with Ala at P1 result in severe loss of potency. Compound **17** shows the highest potency for $\beta 5c$ and also a good selectivity over all other subunits. These results indicate the importance of both the P3 and P1 substituents for gaining $\beta 5c$ selectivity. Since compound **14** (P3 Cha) shows the highest selectivity for $\beta 5c$ over $\beta 5i$, but no selectivity for $\beta 5c$ over $\beta 2c/\beta 2i$, bicyclohexylalanine (BiCha, as a 1:3 mixture of isomers, synthesized by reduction of BiPhe) was incorporated at P3. The resulting compound **18** shows similar selectivity for $\beta 5c$ over $\beta 5i$ as compound **14**, but does, due to the extra cyclohexyl group, no longer inhibit the $\beta 2$ subunits.

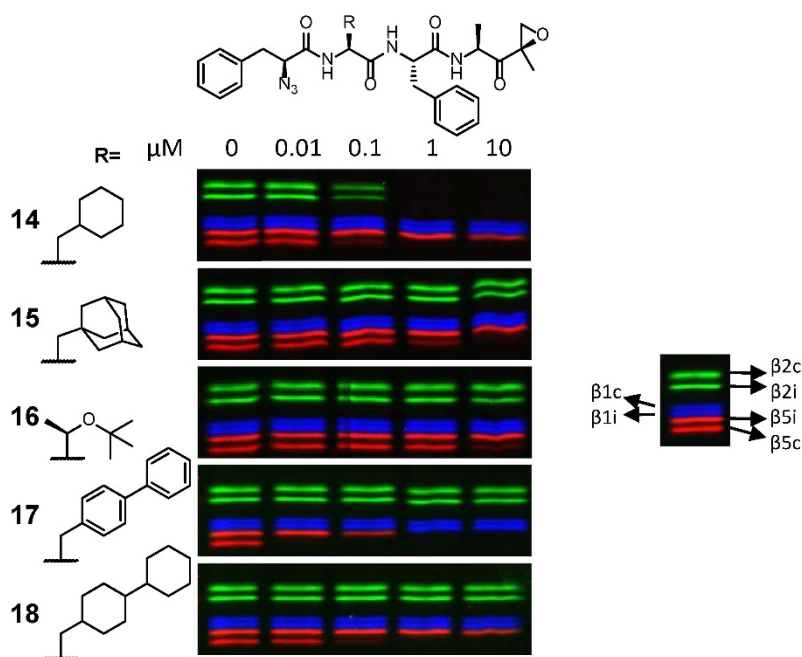


Figure 3. Structure and inhibition profiles of $\beta 5c$ selective compounds with P1 Ala and different P3 substituents. *P2=Leu

In order to verify whether compound **18** also can be used to selectively inhibit $\beta 5c$ in intact cells, the IC_{50} value of **18** for all subunits was determined in intact RPMI-8226 cells (a multiple myeloma cell line). Unfortunately, no inhibition could be observed, presumably due to the poor solubility since in living cells a lower amount of DMSO was used (1% vs. 10% in lysates) (Figure 4). In order to increase the solubility, the azido-Phe P4 residue of **18** was substituted for 2-morpholino acetate, providing compound **19**. 2-Morpholino acetate has also been used

to increase the solubility of YU-101⁶, resulting in the FDA approved drug carfilzomib.⁷ Interestingly, compound **19** shows decreased potency and almost no selectivity for $\beta 5c$ (Figure 4). It was reasoned that the incorporation of an extra amino acid could recover both the potency and selectivity, since carfilzomib also contains an extra amino acid. Both Leu (as in carfilzomib) and Phe (similar to P4 azido-Phe) were incorporated at P4 and both compounds **20** and **21** were evaluated for proteasome inhibition. Clearly, compound **20** is more selective for $\beta 5c$ than **21**, which also targets $\beta 2c/\beta 2i$ at higher concentrations (Figure 4). More importantly, while being less potent than compound **18** in Raji lysates, compound **20** shows good activity and selectivity for $\beta 5c$ in living RPMI-8226 cells. Together, compounds **18** and **20** represent the most selective $\beta 5c$ inhibitors known to date.

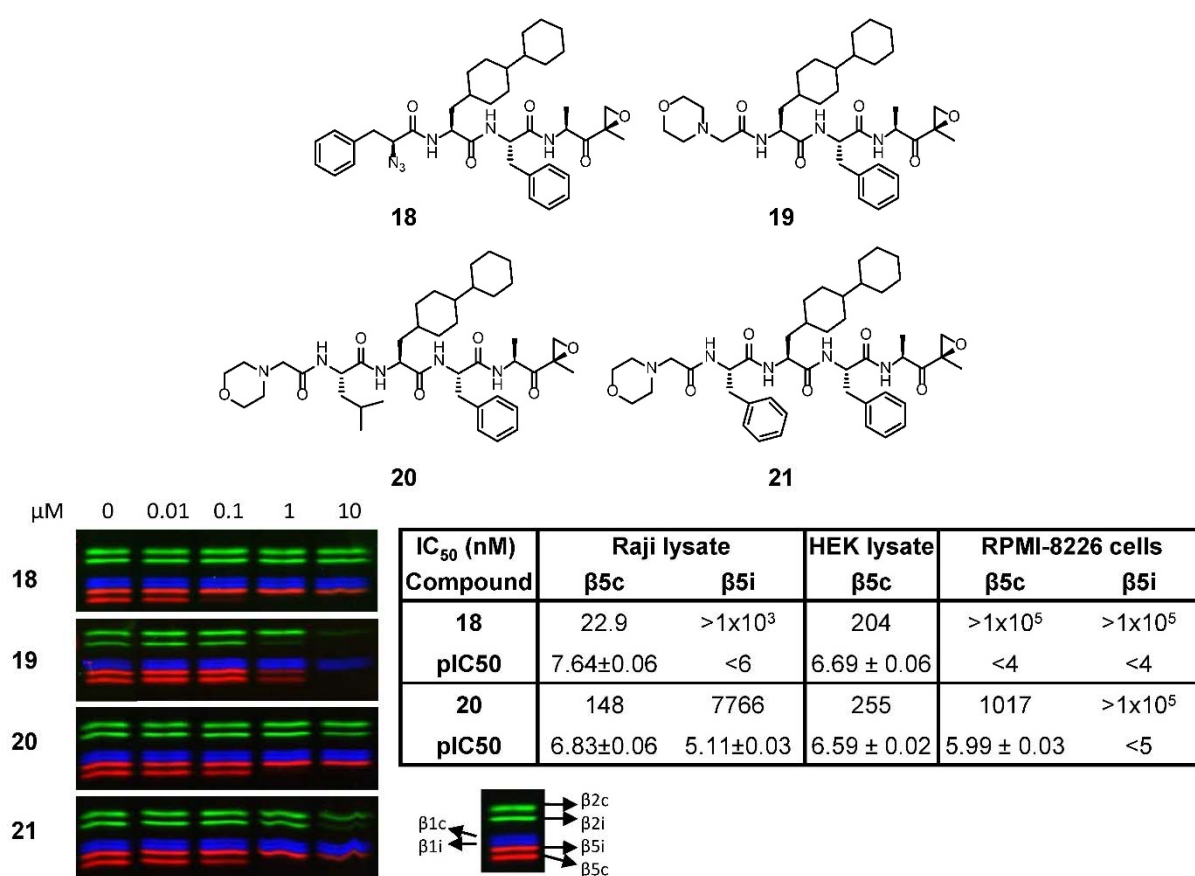
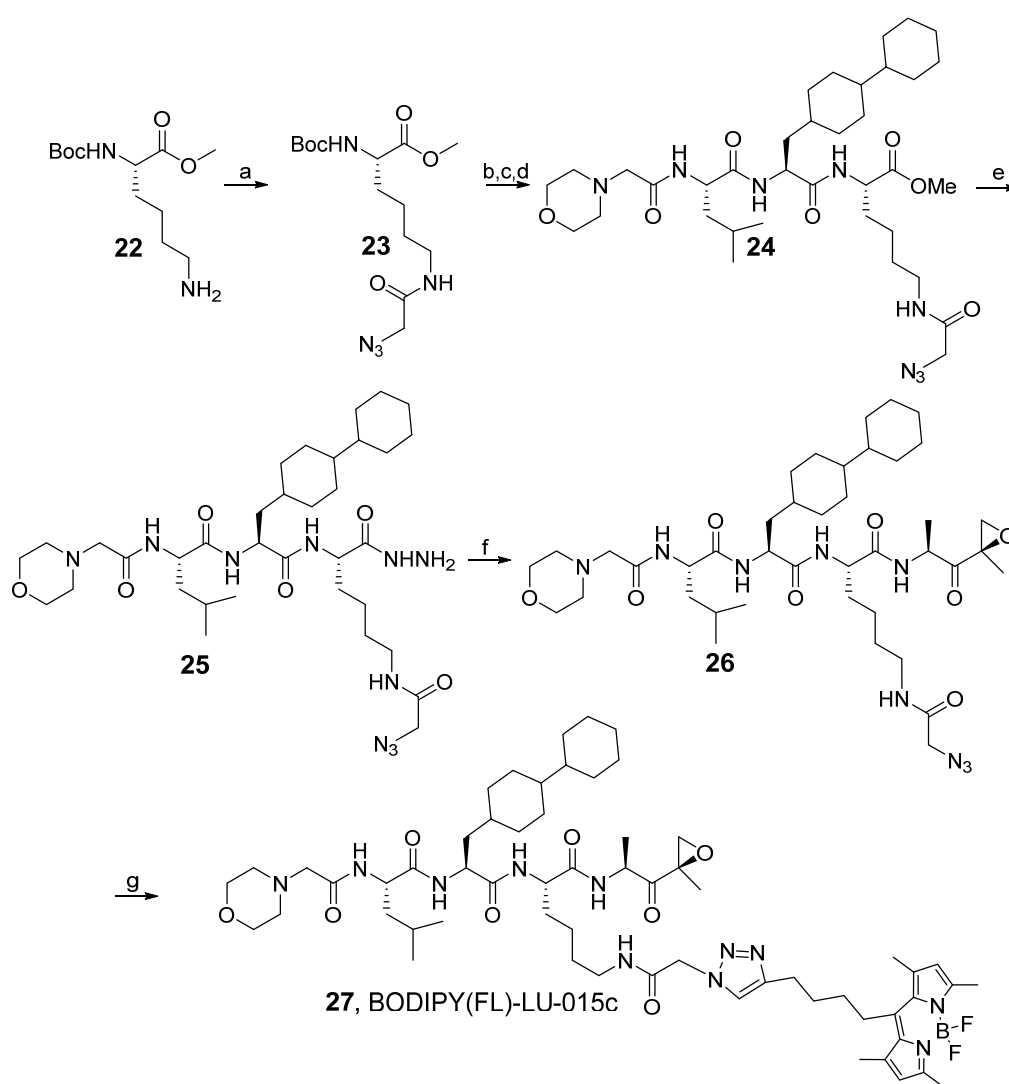


Figure 4. Structures and inhibition profiles of compound **18-20** in Raji lysates and apparent IC₅₀ values of the optimized inhibitors **18** and **20**. Only the IC₅₀ values for the $\beta 5$ subunits are reported; no inhibition of other subunits was observed at concentrations up to 10 μ M (in lysates) or 100 μ M (in intact cells).

Currently, no selective ABPs for $\beta 5c$ are known. Therefore, the optimized $\beta 5c$ inhibitors were used to design $\beta 5c$ -probe **27** (Scheme 1). Given the fact that the P4 residue of $\beta 5c$ inhibitors appeared to be important for the selectivity and solubility of the inhibitors, it was decided to install the fluorophore at the P2 position, since the S2 pockets are solvent exposed.⁵ It has already been shown that extension of the P2 side chain is a viable strategy towards subunit

selective proteasome ABPs.^{8,9} To ensure good solubility, it was decided to use compound **21** as starting point. Since for future studies a β 5c probe equipped with a BODIPY(FL) fluorophore was desired (see chapter 10) and because BODIPY(FL)-alkyne¹⁰ was readily available, a Lys residue elongated with 2-azidoacetic acid was chosen as P2 residue. This enables straightforward attachment of the fluorophore using copper(I)-catalysed azide-alkyne cycloaddition (CuAAC). Starting from Boc-Lys-OMe, the azide tag was installed through peptide coupling with 2-azidoacetic acid, providing compound **23**. Standard solution phase Boc chemistry yielded capped tripeptide **24**. Hydrazinolysis of the methyl ester followed by a standard azide coupling with deprotected Ala epoxyketone provided compound **26**, which was converted to probe **27** by CuAAC with BODIPY(FL)-Alkyne.



Scheme 1. Synthesis of β 5c selective ABP **27.** Reagents and conditions: a. N_3AcOSu , DiPEA, DCM, 35%; b. 1. TFA; 2. Boc-BiCha-OH, HCTU, DiPEA, DCM, 70%; c. 1. TFA; 2. Boc-Leu-OH, HCTU, DiPEA, DCM, 80%; d. 1. TFA; 2. 2-morpholinoacetic acid, HCTU, DiPEA, DCM, 92%; e. $\text{NH}_2\text{NH}_2\cdot\text{H}_2\text{O}$, MeOH, 100%; f. 1. tBuONO, HCl, DMF. H-Ala-EK, DiPEA, 55%; g. BODIPY(FL)-alkyne, CuSO_4 , NaAsc, DMF/ H_2O , 28%.

The potency and selectivity of ABP **27** was evaluated in Raji lysate. Because most probes do not show separate bands for $\beta 5c$ and $\beta 5i$ on SDS-PAGE, the samples were treated with BODIPY(TMR)-NC-005 (chemical structure: see chapter 3) after incubation with ABP **27** to verify the amount of inhibition for $\beta 5c$ and $\beta 5i$ (Figure 5). Labelling of $\beta 5c$ is already visible at 30 nM and complete labelling is achieved at 1 μM , while $\beta 5i$ remains untouched, however, significant labelling of both $\beta 2c$ and $\beta 2i$ is visible.

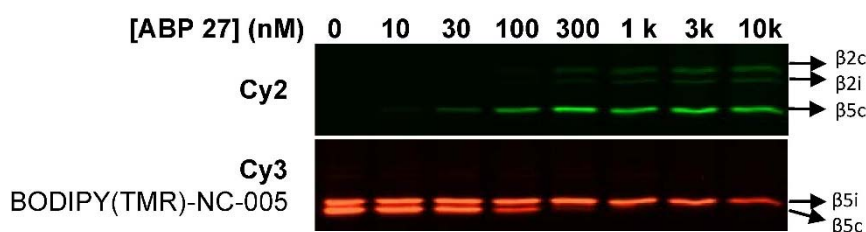


Figure 5. Evaluation of ABP **27** in Raji lysate. Lysates were treated with indicated concentrations of probe **27** for 1 h, followed by the addition of 100 nM BODIPY(TMR)-NC-005 (end concentration) for 1 h.

Conclusion

This chapter describes the design, synthesis and evaluation of new and improved $\beta 5c$ selective inhibitors. The nature of both P1 and P3 residues appears highly important to achieve good selectivity. A small P1 substituent (CH_3) in combination with a large, bulky P3 substituent (bicyclohexyl) proved to be optimal for selective and potent $\beta 5c$ inhibition. Compound **18** represents the most selective $\beta 5c$ inhibitor known to date and is the compound of choice when a high concentration of DMSO (at least 10%) can be used. In case lower DMSO concentrations are required, for instance, when $\beta 5c$ inhibition in living cells is desired, compound **21** can be used, which is more soluble due to the 2-morpholinoacetate *N*-cap. In addition, probe **27** was synthesized which allows selective labelling of $\beta 5c$ over $\beta 5i$, however, significant labelling of the $\beta 2$ subunits is observed. In case only $\beta 5c$ labelling is desired, a $\beta 2$ selective inhibitor (for instance, LU-102¹¹) can be used to block the $\beta 2$ subunits. Since the BiCha building block used for these $\beta 5c$ inhibitors exist in an inseparable 1:3 mixture of isomers, further research is directed towards the synthesis of the pure isoforms which might lead to $\beta 5c$ inhibitors with improved activity and selectivity profiles. Together, these new $\beta 5c$ selective inhibitors and the ABP represent a valuable toolset which can be used to study the role of the $\beta 5c$ subunit in various biological processes and diseases, such as antigen presentation, auto-immune diseases and cancer.

Experimental

Synthetic procedures

General procedures

Acetonitrile (ACN), dichloromethane (DCM), N,N-dimethylformamide (DMF), methanol (MeOH), diisopropylethylamine (DIPEA) and trifluoroacetic acid (TFA) were of peptide synthesis grade, purchased at Biosolve, and used as received. All general chemicals (Fluka, Acros, Merck, Aldrich, Sigma, Iris Biotech) were used as received. Column chromatography was performed on Screening Devices b.v. Silica Gel, with a particle size of 40-63 μm and pore diameter of 60 \AA . TLC analysis was conducted on Merck aluminium sheets (Silica gel 60 F254). Compounds were visualized by UV absorption (254 nm), by spraying with a solution of $(\text{NH}_4)_6\text{Mo}_7\text{O}_{24}\cdot 4\text{H}_2\text{O}$ (25 g/L) and $(\text{NH}_4)_4\text{Ce}(\text{SO}_4)_4\cdot 2\text{H}_2\text{O}$ (10 g/L) in 10% sulphuric acid, a solution of KMnO_4 (20 g/L) and K_2CO_3 (10 g/L) in water, or ninhydrin (0.75 g/L) and acetic acid (12.5 mL/L) in ethanol, where appropriate, followed by charring at ca. 150 $^\circ\text{C}$. ^1H - and ^{13}C -NMR spectra were recorded on a Bruker AV-400 (400 MHz), AV-600 (600 MHz) or AV-850 (850 MHz) spectrometer. Chemical shifts are given in ppm (δ) relative to tetramethylsilane, CD_3OD or CDCl_3 as internal standard. High resolution mass spectra were recorded by direct injection (2 μL of a 2 μM solution in water/acetonitrile 50/50 (v/v) and 0.1% formic acid) on a mass spectrometer (Thermo Finnigan LTQ Orbitrap) equipped with an electrospray ion source in positive mode (source voltage 3.5 kV, sheath gas flow 10, capillary temperature 250 $^\circ\text{C}$) with resolution $R = 60,000$ at m/z 400 (mass range $m/z = 150$ -2,000) and dioctylphthalate ($m/z = 391.28428$) as a "lock mass". The high resolution mass spectrometer was calibrated prior to measurements with a calibration mixture (Thermo Finnigan). LC-MS analysis was performed on a Finnigan Surveyor HPLC system with a Gemini C_{18} 50 \times 4.60 mm column (detection at 200-600 nm), coupled to a Finnigan LCQ Advantage Max mass spectrometer with ESI. The applied buffers were H_2O , ACN and 1.0% aq. TFA. Methods used are: xx \rightarrow xx% MeCN, 15 min (0 \rightarrow 0.5 min: 10% MeCN; 0.5 \rightarrow 10.5 min: gradient time; 10.5 \rightarrow 12.5 min: 90% MeCN; 12.5 \rightarrow 15.0 min: 10% MeCN); xx \rightarrow xx% MeCN, 13.0 min (0 \rightarrow 0.5 min: 10% MeCN; 0.5 \rightarrow 8.5 min: gradient time; 8.5 \rightarrow 10.5 min: 90% MeCN; 10.5 \rightarrow 13.0 min: 10% MeCN). HPLC purification was performed on a Gilson HPLC system coupled to a Phenomenex Gemini 5 μm 250 \times 10 mm column and a GX281 fraction collector. Boc-Ala(Ada)-OH was synthesized as described in chapter 11, Boc-Leu-EK and Boc-Ala-EK as described in chapter 4. H-BiCha-Phe-OMe, compounds **10** and **20** were synthesized as described in chapter 3.

General procedure for azide couplings.

Compounds **5-21** were prepared via azide coupling of peptide hydrazides and properly deprotected epoxyketone amines. The appropriate hydrazide was dissolved in DMF or 1:1 DMF:DCM (v/v) or and cooled to -30 $^\circ\text{C}$. *t*BuONO (1.1 equiv.) and HCl (4M solution in 1,4-dioxane, 2.8 equiv, 3.8 equiv in case of morpholino N-cap)) were added, and the mixture was stirred for 3 h at -30 $^\circ\text{C}$ after which TLC analysis (10% MeOH/DCM, v/v) showed complete consumption of the starting material. The epoxyketone as a free amine was added to the reaction mixture as a solution in DMF. DIPEA (5 equiv.) was added to the reaction mixture, and this mixture was allowed to warm to RT slowly overnight. The mixture was diluted with EtOAc and extracted with H_2O (3 \times). The organic layer was dried over MgSO_4 and purified by flash column chromatography (1 \rightarrow 5% MeOH in DCM) and HPLC-purification (if necessary).

General procedure for peptide couplings

Free acid (1.2 equiv.), HCTU (1.2 equiv.) and free amine (1 equiv.) are dissolved in DCM (0.1 M), followed by the addition of DIPEA (3.5 equiv or 4.5 equiv in case of 2-morpholinoacetic acid HCl). After stirring overnight (or alternatively 1-3 hours, until completion), the reaction mixture is concentrated and re-dissolved in EtOAc, washed with 1 N HCl (2 \times), sat. NaHCO_3 (2 \times) and brine (in case of 2-morpholino acetic acid coupling, no 1N HCl

washings). The organic layer is dried over Na_2SO_4 , filtered and concentrated, followed by purification by column chromatography.

General procedure for Boc removal

Boc protected compounds were treated with TFA (0.1 M) for 30 minutes, followed by co-evaporation with toluene (2x).

N₃Phe-1-Nal-Phe-Leu-EK (5)

This compound was obtained by the general protocol for azide coupling on a 50 μmol scale. Purification by column chromatography (10 \rightarrow 40% EtOAc/pent) provided the title compound (22.9 mg, 66%) as a white powder after lyophilisation. ^1H NMR (400 MHz, CDCl_3) δ 8.13 – 8.06 (m, 1H), 7.88 (dd, J = 8.0, 1.4 Hz, 1H), 7.78 (d, J = 8.2 Hz, 1H), 7.63 – 7.48 (m, 2H), 7.37 (dd, J = 8.3, 7.0 Hz, 1H), 7.31 – 7.18 (m, 4H), 7.19 – 7.10 (m, 5H), 6.93 – 6.85 (m, 2H), 6.84 (d, J = 6.9 Hz, 1H), 6.12 (d, J = 7.9 Hz, 1H), 6.01 (d, J = 7.4 Hz, 1H), 4.64 (d, J = 7.0 Hz, 1H), 4.55 – 4.35 (m, 1H), 3.94 (dd, J = 8.3, 4.0 Hz, 1H), 3.46 (d, J = 6.7 Hz, 1H), 3.35 (d, J = 7.2 Hz, 1H), 3.23 (d, J = 5.0 Hz, 1H), 3.12 (dd, J = 14.1, 4.0 Hz, 1H), 2.93 (d, J = 6.2 Hz, 1H), 2.87 (d, J = 4.9 Hz, 1H), 2.75 (dd, J = 14.1, 8.0 Hz, 2H), 1.50 (s, 3H), 1.48 – 1.39 (m, 2H), 1.23 (d, J = 21.5 Hz, 1H), 0.91 (dd, J = 13.1, 5.9 Hz, 6H). ^{13}C NMR (101 MHz, CDCl_3) δ 207.93, 170.03, 169.97, 168.87, 136.08, 135.81, 134.10, 132.19, 131.96, 129.51, 129.35, 129.09, 128.78, 128.67, 128.36, 127.89, 127.48, 127.10, 126.85, 126.19, 125.45, 123.67, 65.21, 59.15, 54.17, 54.14, 52.45, 50.23, 40.01, 38.45, 37.62, 34.81, 25.17, 23.50, 21.42, 16.81. LC-MS (linear gradient 10 \rightarrow 90% MeCN, 0.1% TFA, 15.0 min): R_t (min): 10.91 (ESI-MS (m/z): 689.07 [$\text{M}+\text{H}$] $^+$). HRMS: calculated for $\text{C}_{40}\text{H}_{44}\text{N}_6\text{O}_5$ 689.34460 [$\text{M}+\text{H}$] $^+$; found 689.34479

N₃Phe-2-Nal-Phe-Leu-EK (6)

This compound was obtained by the general protocol for azide coupling on a 50 μmol scale. Purification by column chromatography (10 \rightarrow 40% EtOAc/pent) provided the title compound (16.8 mg, 49%) as a white powder after lyophilisation. ^1H NMR (400 MHz, CDCl_3) δ 7.83 – 7.78 (m, 1H), 7.78 – 7.72 (m, 2H), 7.52 – 7.43 (m, 3H), 7.32 – 7.06 (m, 9H), 6.99 – 6.90 (m, 2H), 6.72 (d, J = 7.6 Hz, 1H), 6.27 (d, J = 7.5 Hz, 1H), 6.05 (d, J = 7.9 Hz, 1H), 4.64 (q, J = 6.7 Hz, 1H), 4.55 (q, J = 6.8 Hz, 1H), 4.50 – 4.38 (m, 1H), 4.00 (dd, J = 8.0, 4.1 Hz, 1H), 3.22 – 3.12 (m, 3H), 3.03 (ddd, J = 13.9, 6.4, 3.3 Hz, 2H), 2.87 – 2.78 (m, 3H), 1.49 (s, 3H), 1.47 – 1.37 (m, 2H), 1.16 – 1.06 (m, 1H), 0.87 (dd, J = 15.6, 6.0 Hz, 6H). ^{13}C NMR (101 MHz, CDCl_3) δ 207.93, 170.16, 169.87, 168.77, 136.05, 135.75, 133.56, 133.37, 132.64, 129.57, 129.37, 128.81, 128.71, 128.66, 128.18, 127.82, 127.69, 127.51, 127.27, 127.14, 126.49, 126.09, 65.15, 59.16, 54.22, 54.04, 52.47, 50.35, 39.96, 38.42, 37.77, 37.69, 25.21, 23.44, 21.41, 16.82. LC-MS (linear gradient 10 \rightarrow 90% MeCN, 0.1% TFA, 15.0 min): R_t (min): 10.86 (ESI-MS (m/z): 689.13 [$\text{M}+\text{H}$] $^+$). HRMS: calculated for $\text{C}_{40}\text{H}_{44}\text{N}_6\text{O}_5$ 689.34460 [$\text{M}+\text{H}$] $^+$; found 689.34473

N₃Phe-BiPhe-Phe-Leu-EK (7)

This compound was obtained by the general protocol for azide coupling on a 50 μmol scale. Purification by column chromatography (10 \rightarrow 40% EtOAc/pent) provided the title compound (23.7 mg, 66%) as a white powder after lyophilisation. ^1H NMR (400 MHz, CDCl_3) δ 7.57 – 7.53 (m, 2H), 7.50 (d, J = 8.1 Hz, 2H), 7.42 (t, J = 7.5 Hz, 2H), 7.37 – 7.27 (m, 4H), 7.20 (q, J = 5.6 Hz, 5H), 7.10 (d, J = 8.1 Hz, 2H), 7.07 – 7.02 (m, 2H), 6.74 (d, J = 7.5 Hz, 1H), 6.41 (d, J = 7.6 Hz, 1H), 6.16 (d, J = 7.9 Hz, 1H), 4.61 (qd, J = 6.8, 3.0 Hz, 2H), 4.56 – 4.40 (m, 1H), 4.03 (dd, J = 8.0, 4.0 Hz, 1H), 3.22 (dt, J = 9.4, 4.2 Hz, 2H), 3.05 (td, J = 13.8, 6.3 Hz, 2H), 2.98 – 2.81 (m, 4H), 1.49 (s, 3H), 1.48 – 1.42 (m, 2H), 1.18 (t, J = 9.8 Hz, 1H), 0.87 (dd, J = 12.0, 5.9 Hz, 6H). ^{13}C NMR (101 MHz, CDCl_3) δ 207.99, 170.23, 169.88, 168.77, 140.60, 140.25, 136.13, 135.80, 134.88, 129.79, 129.62, 129.44, 128.93, 128.82, 128.71, 127.62, 127.54, 127.18, 127.08, 65.16, 59.14, 54.19, 54.05, 52.43, 50.31, 40.03, 38.43, 37.93, 37.18, 25.21, 23.43, 21.39, 16.80. LC-MS (linear gradient 10 \rightarrow 90% MeCN, 0.1% TFA, 15.0 min): R_t (min): 11.10 (ESI-MS (m/z): 715.13 [$\text{M}+\text{H}$] $^+$). HRMS: calculated for $\text{C}_{42}\text{H}_{47}\text{N}_6\text{O}_5$ 715.36025 [$\text{M}+\text{H}$] $^+$; found 715.36047

N₃Phe-Cha-Phe-Leu-EK (8)

This compound was obtained by the general protocol for azide coupling on a 50 μ mol scale. Purification by column chromatography (10 \rightarrow 40% EtOAc in pent) provided the title compound (3.9 mg, 12%) as a white powder after lyophilisation. ¹H NMR (400 MHz, CDCl₃) δ 7.37 – 7.13 (m, 10H), 6.70 (d, J = 7.8 Hz, 1H), 6.58 (d, J = 7.7 Hz, 1H), 6.35 (d, J = 8.0 Hz, 1H), 4.64 (q, J = 7.0 Hz, 1H), 4.53 (td, J = 10.1, 9.1, 2.8 Hz, 1H), 4.42 – 4.31 (m, 1H), 4.03 (dd, J = 7.9, 4.1 Hz, 1H), 3.27 (dd, J = 14.1, 4.0 Hz, 1H), 3.23 (d, J = 4.9 Hz, 1H), 3.10 – 2.95 (m, 3H), 2.87 (d, J = 4.9 Hz, 1H), 1.70 – 1.51 (m, 6H), 1.49 (s, 3H), 1.47 – 1.02 (m, 8H), 0.89 (dd, J = 11.6, 6.2 Hz, 6H), 0.86 – 0.73 (m, 2H). ¹³C NMR (101 MHz, CDCl₃) δ 208.01, 171.39, 170.53, 168.79, 136.40, 135.91, 129.58, 129.43, 128.82, 128.69, 127.45, 127.12, 65.14, 59.09, 54.08, 52.42, 51.11, 50.18, 40.20, 39.14, 38.37, 37.88, 33.95, 33.56, 32.60, 26.38, 26.11, 26.02, 25.19, 23.47, 21.42, 16.78. LC-MS (linear gradient 10 \rightarrow 90% MeCN, 0.1% TFA, 15.0 min): R_t (min): 11.02 (ESI-MS (m/z): 645.07 [M+H]⁺). HRMS: calculated for C₃₆H₄₉N₆O₅ 645.37590 [M+H]⁺; found 645.37598

N₃Phe-Trp-Phe-Leu-EK (9)

This compound was obtained by the general protocol for azide coupling on a 50 μ mol scale. Purification by HPLC (C₁₈, 50 \rightarrow 90% MeCN/H₂O, 0.1% TFA, 10 min gradient) provided the title compound (1.0 mg, 3%) as a white powder after lyophilisation. ¹H NMR (600 MHz, CDCl₃) δ 8.10 (s, 1H), 7.59 (d, J = 7.9 Hz, 1H), 7.40 (d, J = 8.1 Hz, 1H), 7.38 – 7.09 (m, 10H), 6.90 (d, J = 2.2 Hz, 1H), 6.84 (d, J = 7.0 Hz, 2H), 6.81 (d, J = 6.9 Hz, 1H), 6.13 (d, J = 8.0 Hz, 1H), 5.98 (d, J = 7.8 Hz, 1H), 4.60 – 4.49 (m, 3H), 3.98 (dd, J = 7.7, 4.1 Hz, 1H), 3.32 – 3.28 (m, 2H), 3.24 (dd, J = 14.2, 4.1 Hz, 1H), 3.05 – 2.93 (m, 3H), 2.91 (d, J = 5.0 Hz, 1H), 2.69 (dd, J = 13.9, 6.7 Hz, 1H), 1.54 (s, 3H), 1.49 – 1.38 (m, 2H), 1.24 – 1.17 (m, 1H), 0.91 (dd, J = 28.0, 6.3 Hz, 6H). ¹³C NMR (151 MHz, CDCl₃) δ 207.89, 170.17, 168.67, 136.23, 135.91, 135.68, 129.54, 129.26, 128.69, 128.53, 127.39, 127.12, 126.92, 125.52, 123.13, 122.68, 120.01, 118.91, 111.31, 110.03, 65.00, 59.04, 53.89, 53.65, 52.32, 50.07, 39.83, 38.18, 37.18, 30.32, 27.26, 25.03, 23.33, 21.26, 16.69. LC-MS (linear gradient 10 \rightarrow 90% MeCN, 0.1% TFA, 15.0 min): R_t (min): 9.94 (ESI-MS (m/z): 678.13 [M+H]⁺). HRMS: calculated for C₃₈H₄₄N₇O₅ 678.33984 [M+H]⁺; found 678.33984

N₃Phe-Ala(Ada)-Leu-Leu-EK (10)

This compound was obtained by the general protocol for azide coupling on a 50 μ mol scale. Purification by column chromatography (1 \rightarrow 2% MeOH/DCM) provided the title compound (20.2 mg, 61%) as a white powder after lyophilisation. ¹H NMR (400 MHz, CDCl₃) δ 7.39 – 7.25 (m, 5H), 6.68 (d, J = 7.9 Hz, 1H), 6.50 (dd, J = 10.7, 8.2 Hz, 2H), 4.59 (ddd, J = 10.8, 8.0, 3.1 Hz, 1H), 4.53 – 4.34 (m, 2H), 4.23 (dd, J = 8.3, 4.0 Hz, 1H), 3.38 – 3.30 (m, 2H), 3.03 (dd, J = 14.1, 8.3 Hz, 1H), 2.91 (d, J = 5.0 Hz, 1H), 1.95 (s, 3H), 1.87 – 1.16 (m, 23H), 0.99 – 0.89 (m, 12H). ¹³C NMR (101 MHz, CDCl₃) δ 208.47, 172.01, 171.66, 168.46, 135.98, 129.65, 128.82, 127.48, 65.40, 59.24, 52.58, 51.84, 50.43, 49.47, 45.96, 42.47, 40.79, 40.15, 38.35, 36.83, 32.34, 29.84, 28.57, 25.30, 24.85, 23.57, 22.95, 22.26, 21.43, 16.89. LC-MS (linear gradient 50 \rightarrow 90% MeCN, 0.1% TFA, 15.0 min): R_t (min): 9.29 (ESI-MS (m/z): 663.27 [M+H]⁺). HRMS: calculated for C₃₇H₅₅N₆O₅ 663.42285 [M+H]⁺; found 663.42291

N₃Phe-Ala(tBu)-Phe-Leu-EK (11)

This compound was obtained by the general protocol for azide coupling on a 50 μ mol scale. Purification by column chromatography (0 \rightarrow 1% MeOH/DCM) followed by HPLC (C₁₈, 70 \rightarrow 90% MeCN/H₂O, 0.1% TFA, 10 min gradient) provided the title compound (14.4 mg, 47%) as a white powder after lyophilisation. ¹H NMR (600 MHz, CDCl₃) δ 7.37 – 7.28 (m, 5H), 7.28 – 7.19 (m, 5H), 6.68 (d, J = 7.7 Hz, 1H), 6.50 (d, J = 7.6 Hz, 1H), 6.34 (d, J = 7.9 Hz, 1H), 4.64 (q, J = 7.2 Hz, 1H), 4.56 (ddd, J = 10.4, 8.1, 2.8 Hz, 1H), 4.28 (td, J = 8.0, 4.3 Hz, 1H), 3.97 (dd, J = 8.1, 3.9 Hz, 1H), 3.34 – 3.26 (m, 2H), 3.16 – 3.02 (m, 2H), 2.97 (dd, J = 14.1, 8.1 Hz, 1H), 2.91 (d, J = 5.0 Hz, 1H), 1.86 (dd, J = 14.6, 4.2 Hz, 1H), 1.53 (s, 3H), 1.52 – 1.45 (m, 2H), 1.33 – 1.22 (m, 2H), 0.93 (dd, J = 17.1, 6.2 Hz, 6H), 0.84 (s, 9H). ¹³C NMR (151 MHz, CDCl₃) δ 208.01, 171.56, 170.62, 168.55, 136.52, 135.82, 129.66, 129.43, 128.89, 128.71, 127.51, 127.10, 65.09, 59.16, 53.96, 52.49, 51.08, 50.29, 44.39, 40.09, 38.25, 37.49, 30.36, 29.67, 25.19, 23.51, 21.38, 16.83. LC-MS (linear gradient 10 \rightarrow 90% MeCN, 0.1% TFA, 13.0 min): R_t (min): 9.28 (ESI-MS (m/z): 619.20 [M+H]⁺). HRMS: calculated for C₃₄H₄₇N₆O₅ 619.36025 [M+H]⁺; found 619.36023

N₃Phe-Ser(OtBu)-Phe-Leu-EK (12)

This compound was obtained by the general protocol for azide coupling on a 50 μmol scale. Purification by column chromatography (0 \rightarrow 1% MeOH/DCM) followed by (C₁₈, 70 \rightarrow 90% MeCN/H₂O, 0.1% TFA, 10 min gradient) provided the title compound (9.6 mg, 30%) as a white powder after lyophilisation. ¹H NMR (600 MHz, CDCl₃) δ 7.37 – 7.24 (m, 8H), 7.20 (d, *J* = 6.9 Hz, 2H), 7.08 (d, *J* = 6.4 Hz, 1H), 6.95 (d, *J* = 8.1 Hz, 1H), 6.24 (d, *J* = 8.3 Hz, 1H), 4.70 – 4.64 (m, 1H), 4.60 (td, *J* = 10.3, 9.3, 2.5 Hz, 1H), 4.31 (ddd, *J* = 8.3, 6.5, 4.2 Hz, 1H), 4.17 (dd, *J* = 8.0, 4.0 Hz, 1H), 3.67 (dd, *J* = 9.1, 4.1 Hz, 1H), 3.32 (dd, *J* = 14.1, 4.0 Hz, 1H), 3.26 (d, *J* = 4.9 Hz, 1H), 3.21 (dd, *J* = 13.9, 5.8 Hz, 1H), 3.16 (t, *J* = 8.7 Hz, 1H), 3.06 (dd, *J* = 14.1, 8.0 Hz, 1H), 2.96 (dd, *J* = 13.9, 6.8 Hz, 1H), 2.91 (d, *J* = 4.9 Hz, 1H), 1.52 (s, 3H), 1.51 – 1.43 (m, 2H), 1.18 (dd, *J* = 19.8, 9.6 Hz, 1H), 1.14 (s, 9H), 0.95 (d, *J* = 6.0 Hz, 3H), 0.89 (d, *J* = 6.2 Hz, 3H). ¹³C NMR (151 MHz, CDCl₃) δ 208.09, 170.36, 169.54, 168.68, 136.21, 135.90, 129.67, 129.53, 128.86, 128.77, 127.45, 127.32, 74.79, 65.32, 60.90, 59.04, 54.23, 53.12, 52.44, 50.06, 40.32, 38.59, 37.78, 27.42, 25.05, 23.45, 21.32, 16.78. LC-MS (linear gradient 10 \rightarrow 90% MeCN, 0.1% TFA, 13.0 min): R_t (min): 9.25 (ESI-MS (m/z): 635.20 [M+H]⁺). HRMS: calculated for C₃₄H₄₇N₆O₆ 635.35516 [M+H]⁺; found 635.35504

N₃Phe-Thr(OtBu)-Phe-Leu-EK (13)

This compound was obtained by the general protocol for azide coupling on a 50 μmol scale. Purification by column chromatography (0 \rightarrow 1% MeOH/DCM) followed by HPLC (C₁₈, 70 \rightarrow 90% MeCN/H₂O, 0.1% TFA, 10 min gradient) provided the title compound (5.9 mg, 18%) as a white powder after lyophilisation. ¹H NMR (600 MHz, CDCl₃) δ 7.34 – 7.22 (m, 9H), 7.15 (d, *J* = 6.9 Hz, 2H), 6.93 (d, *J* = 9.0 Hz, 1H), 6.26 (d, *J* = 8.3 Hz, 1H), 4.75 (dt, *J* = 9.0, 5.9 Hz, 1H), 4.61 (td, *J* = 9.4, 8.5, 2.6 Hz, 1H), 4.29 – 4.16 (m, 2H), 3.88 (dd, *J* = 6.5, 4.3 Hz, 1H), 3.32 (d, *J* = 5.0 Hz, 1H), 3.29 – 3.27 (m, 1H), 3.26 (d, *J* = 4.3 Hz, 1H), 3.12 (dd, *J* = 14.1, 7.2 Hz, 1H), 2.91 (d, *J* = 6.3 Hz, 1H), 2.90 – 2.87 (m, 1H), 1.48 (s, 3H), 1.45 – 1.38 (m, 2H), 1.13 – 1.10 (m, 10H), 0.92 (d, *J* = 5.9 Hz, 3H), 0.85 (d, *J* = 6.1 Hz, 3H), 0.73 (d, *J* = 6.5 Hz, 3H). ¹³C NMR (151 MHz, CDCl₃) δ 208.09, 170.60, 168.52, 168.20, 136.12, 135.69, 129.78, 129.57, 128.93, 128.71, 127.46, 127.43, 75.92, 66.07, 65.11, 59.12, 57.35, 53.67, 52.45, 49.93, 40.26, 38.30, 37.56, 28.01, 24.84, 23.39, 21.25, 16.84, 16.77. LC-MS (linear gradient 10 \rightarrow 90% MeCN, 0.1% TFA, 13.0 min): R_t (min): 9.67 (ESI-MS (m/z): 649.13 [M+H]⁺). HRMS: calculated for C₃₅H₄₉N₆O₆ 649.37081 [M+H]⁺; found 649.37079

N₃Phe-Cha-Phe-Ala-EK (14)

This compound was obtained by the general protocol for azide coupling on a 50 μmol scale. Purification by HPLC (C₁₈, 70 \rightarrow 80% MeCN/H₂O, 0.1% TFA, 10 min gradient) provided the title compound (5.70 mg, 19%) as a white powder after lyophilisation. ¹H NMR (600 MHz, CDCl₃) δ 7.36 – 7.15 (m, 10H), 6.69 (d, *J* = 7.7 Hz, 1H), 6.55 (d, *J* = 7.8 Hz, 1H), 6.42 (d, *J* = 7.0 Hz, 1H), 4.62 (q, *J* = 7.2 Hz, 1H), 4.47 (p, *J* = 7.1 Hz, 1H), 4.35 (td, *J* = 8.3, 6.1 Hz, 1H), 4.07 (dd, *J* = 8.0, 4.1 Hz, 1H), 3.28 (dd, *J* = 14.1, 4.1 Hz, 1H), 3.17 (d, *J* = 4.9 Hz, 1H), 3.05 (d, *J* = 7.1 Hz, 2H), 3.00 (dd, *J* = 14.1, 8.0 Hz, 1H), 2.89 (d, *J* = 4.9 Hz, 1H), 1.70 – 1.54 (m, 6H), 1.51 (s, 3H), 1.35 (ddd, *J* = 14.3, 8.8, 6.0 Hz, 1H), 1.24 (d, *J* = 7.1 Hz, 3H), 1.21 – 1.06 (m, 4H), 0.84 (s, 2H). ¹³C NMR (151 MHz, CDCl₃) δ 207.79, 171.47, 170.16, 168.80, 136.47, 135.95, 129.59, 129.40, 128.84, 128.72, 127.47, 127.15, 65.19, 59.00, 54.20, 52.52, 51.10, 48.09, 39.06, 38.43, 38.02, 33.99, 33.55, 32.65, 26.40, 26.16, 26.06, 17.32, 16.91. LC-MS (linear gradient 10 \rightarrow 90% MeCN, 0.1% TFA, 13.0 min): R_t (min): 9.08 (ESI-MS (m/z): 603.27 [M+H]⁺). HRMS: calculated for C₃₃H₄₃N₆O₅ 603.32894 [M+H]⁺; found 603.32874

N₃Phe-Ala(Ada)-Leu-Ala-EK (15)

This compound was obtained by the general protocol for azide coupling on a 50 μmol scale. Purification by column chromatography (1 \rightarrow 2% MeOH/DCM) provided the title compound (23.9 mg, 77%) as a white powder after lyophilisation. ¹H NMR (400 MHz, CDCl₃) δ 7.37 – 7.20 (m, 5H), 6.80 (dd, *J* = 7.2, 5.2 Hz, 2H), 6.68 (d, *J* = 8.2 Hz, 1H), 4.54 – 4.37 (m, 3H), 4.18 (dd, *J* = 8.4, 3.9 Hz, 1H), 3.33 – 3.27 (m, 1H), 3.23 (d, *J* = 4.9 Hz, 1H), 3.05 – 2.93 (m, 1H), 2.88 (d, *J* = 4.9 Hz, 1H), 1.91 (s, 3H), 1.72 – 1.54 (m, 9H), 1.51 (s, 3H), 1.50 – 1.37 (m, 6H), 1.27 (d, *J* = 7.1 Hz, 3H), 1.26 – 1.20 (m, 2H), 0.89 (dd, *J* = 13.1, 6.2 Hz, 6H). ¹³C NMR (101 MHz, CDCl₃) δ 208.24, 172.09, 171.43,

168.45, 136.08, 129.60, 128.79, 127.43, 65.31, 59.13, 52.60, 51.68, 49.45, 48.06, 46.10, 42.45, 41.02, 38.32, 36.83, 32.37, 28.58, 24.82, 22.92, 22.27, 17.07, 16.93. LC-MS (linear gradient 50 → 90% MeCN, 0.1% TFA, 15.0 min): R_t (min): 7.35 (ESI-MS (m/z): 621.20 [M+H]⁺). HRMS: calculated for C₃₄H₄₉N₆O₅ 621.37690 [M+H]⁺; found 621.37592

N₃Phe-Thr(OtBu)-Phe-Ala-EK (16)

This compound was obtained by the general protocol for azide coupling on a 50 μmol scale. Purification by HPLC (C₁₈, 60→90% MeCN/H₂O, 0.1% TFA, 10 min gradient) provided the title compound (1.79 mg, 6%) as a white powder after lyophilisation. ¹H NMR (850 MHz, CDCl₃) δ 7.32 – 7.28 (m, 3H), 7.27 – 7.23 (m, 6H), 7.15 (d, *J* = 7.1 Hz, 2H), 6.81 (d, *J* = 9.1 Hz, 1H), 6.55 (d, *J* = 7.1 Hz, 1H), 4.75 (dt, *J* = 9.1, 5.8 Hz, 1H), 4.54 (p, *J* = 7.1 Hz, 1H), 4.23 (ddd, *J* = 11.3, 6.6, 4.3 Hz, 2H), 3.91 – 3.84 (m, 1H), 3.30 – 3.25 (m, 3H), 3.13 (dd, *J* = 14.2, 7.3 Hz, 1H), 2.93 – 2.90 (m, 1H), 2.90 (d, *J* = 5.0 Hz, 1H), 1.50 (s, 3H), 1.17 (d, *J* = 7.1 Hz, 3H), 1.10 (s, 9H), 0.73 (d, *J* = 6.5 Hz, 3H). ¹³C NMR (214 MHz, CDCl₃) δ 207.74, 170.42, 168.31, 168.20, 136.03, 135.71, 129.79, 129.57, 128.96, 128.71, 127.48, 127.47, 76.06, 66.19, 65.12, 59.12, 57.23, 53.45, 52.58, 47.92, 38.32, 37.69, 27.99, 17.24, 16.88, 16.68. LC-MS (linear gradient 10 → 90% MeCN, 0.1% TFA, 13.0 min): R_t (min): 8.87 (ESI-MS (m/z): 607.13 [M+H]⁺). HRMS: calculated for C₃₂H₄₃N₆O₆ 607.32386 [M+H]⁺; found 607.32385

N₃Phe-BiPhe-Phe-Ala-EK (17)

This compound was obtained by the general protocol for azide coupling on a 50 μmol scale. Purification by HPLC (C₁₈, 60→80% MeCN/H₂O, 0.1% TFA, 10 min gradient) provided the title compound (9.02 mg, 27%) as a white powder after lyophilisation. ¹H NMR (600 MHz, CDCl₃) δ 7.57 – 7.52 (m, 2H), 7.48 (d, *J* = 8.2 Hz, 2H), 7.42 (t, *J* = 7.7 Hz, 2H), 7.37 – 7.28 (m, 3H), 7.29 – 7.24 (m, 1H), 7.24 – 7.15 (m, 5H), 7.12 – 7.04 (m, 4H), 6.75 (d, *J* = 7.8 Hz, 1H), 6.44 (d, *J* = 7.6 Hz, 1H), 6.25 (d, *J* = 7.0 Hz, 1H), 4.62 (q, *J* = 7.0 Hz, 1H), 4.56 (q, *J* = 7.0 Hz, 1H), 4.46 – 4.35 (m, 1H), 4.09 (dd, *J* = 8.0, 4.1 Hz, 1H), 3.23 (dd, *J* = 14.1, 4.1 Hz, 1H), 3.11 (d, *J* = 4.9 Hz, 1H), 3.04 – 2.96 (m, 2H), 2.96 – 2.87 (m, 3H), 2.85 (d, *J* = 4.9 Hz, 1H), 1.49 (s, 3H), 1.16 (d, *J* = 7.1 Hz, 3H). ¹³C NMR (151 MHz, CDCl₃) δ 207.78, 170.01, 169.81, 168.71, 140.62, 140.18, 136.21, 135.87, 134.93, 129.81, 129.65, 129.38, 128.94, 128.83, 128.80, 128.71, 127.52, 127.50, 127.18, 127.06, 65.19, 58.98, 54.26, 54.14, 52.48, 48.09, 38.48, 38.12, 37.36, 17.19, 16.88. LC-MS (linear gradient 10 → 90% MeCN, 0.1% TFA, 13.0 min): R_t (min): 9.16 (ESI-MS (m/z): 673.27 [M+H]⁺). HRMS: calculated for C₃₉H₄₁N₆O₅ 673.31329 [M+H]⁺; found 673.31329

N₃Phe-BiCha-Phe-Ala-EK (18)

This compound was obtained by the general protocol for azide coupling on a 50 μmol scale. Purification by HPLC (C₁₈, 70→90% MeCN/H₂O, 0.1% TFA, 10 min gradient) provided the title compound (6.77 mg, 20%) as a white powder after lyophilisation. ¹H NMR (600 MHz, CDCl₃) δ 7.35 – 7.16 (m, 10H), 6.63 (t, *J* = 6.9 Hz, 1H), 6.49 (t, *J* = 7.5 Hz, 1H), 6.37 (d, *J* = 7.0 Hz, 1H), 4.60 (q, *J* = 7.2 Hz, 1H), 4.52 – 4.44 (m, 1H), 4.35 – 4.29 (m, 0.33H), 4.26 (td, *J* = 8.3, 6.1 Hz, 0.67H), 4.08 (dd, *J* = 7.7, 4.2 Hz, 0.67H), 4.07 – 4.04 (m, 0.33H), 3.27 (dt, *J* = 14.1, 3.6 Hz, 1H), 3.18 – 3.15 (m, 1H), 3.07 – 3.04 (m, 2H), 3.04 – 2.96 (m, 1H), 2.89 (d, *J* = 4.9 Hz, 1H), 1.77 – 1.53 (m, 8H), 1.51 (s, 3H), 1.42 – 1.25 (m, 7H), 1.24 (d, *J* = 7.1 Hz, 3H), 1.23 – 0.74 (m, 8H). ¹³C NMR (151 MHz, CDCl₃) δ 207.80, 207.76, 171.42, 170.12, 170.11, 168.79, 136.49, 135.84, 129.63, 129.61, 129.40, 128.85, 128.81, 128.73, 127.48, 127.45, 127.16, 65.20, 65.16, 59.02, 54.21, 52.53, 51.67, 51.23, 48.12, 43.37, 43.26, 39.01, 38.42, 38.36, 37.95, 37.91, 34.30, 33.79, 32.96, 30.61, 30.34, 30.01, 29.70, 29.62, 28.88, 26.97, 26.87, 25.48, 25.32, 17.32, 16.92. LC-MS (linear gradient 10 → 90% MeCN, 0.1% TFA, 13.0 min): R_t (min): 10.82 (ESI-MS (m/z): 685.33 [M+H]⁺). HRMS: calculated for C₃₉H₅₃N₆O₅ 685.40720 [M+H]⁺; found 685.40729

Morph-BiCha-Phe-Ala-EK (19)

This compound was obtained by the general protocol for azide coupling on a 100 μmol scale. Purification by column chromatography (1→2% MeOH/DCM) provided the title compound (36.0 mg, 56%) as a white powder after lyophilisation. ¹H NMR (400 MHz, CDCl₃) δ 7.37 – 7.12 (m, 6H), 6.82 (d, *J* = 6.3 Hz, 1H), 6.52 (d, *J* = 6.0 Hz,

1H), 4.58 (q, $J = 7.2$ Hz, 1H), 4.46 (q, $J = 7.1$ Hz, 1H), 4.34 (tt, $J = 14.2, 7.3$ Hz, 1H), 3.68 (s, 4H), 3.17 (d, $J = 4.9$ Hz, 1H), 3.08 – 2.82 (m, 5H), 2.45 (h, $J = 7.5$ Hz, 4H), 1.91 – 1.56 (m, 8H), 1.50 (s, 3H), 1.31 (ddd, $J = 20.7, 8.1, 4.2$ Hz, 7H), 1.22 (d, $J = 7.1$ Hz, 3H), 1.20 – 0.72 (m, 8H). ^{13}C NMR (101 MHz, CDCl_3) δ 207.84, 171.94, 170.57, 170.24, 136.63, 129.42, 128.64, 127.02, 66.98, 66.25, 61.76, 58.98, 54.36, 53.90, 52.49, 51.45, 50.92, 48.03, 43.32, 43.22, 41.57, 40.25, 37.80, 35.07, 34.75, 33.96, 32.80, 31.45, 30.62, 30.30, 30.12, 29.71, 28.79, 26.91, 26.82, 25.68, 25.48, 17.25, 16.88. HRMS: calculated for $\text{C}_{36}\text{H}_{54}\text{N}_4\text{O}_5$ 639.41161 $[\text{M}+\text{H}]^+$; found 639.41162

Morph-Leu-BiCha-Phe-Ala-EK (20)

This compound was obtained by the general protocol for azide coupling on a 100 μmol scale. Purification by column chromatography (0 \rightarrow 2% MeOH/DCM), followed by lyophilisation provided the product (52.7 mg, 69.2 %). ^1H NMR (400 MHz, CDCl_3) δ 7.55 (s, 1H), 7.37 – 7.14 (m, 7H), 7.03 (s, 1H), 6.81 (s, 1H), 4.74 (q, $J = 7.1$ Hz, 1H), 4.55 – 4.42 (m, 2H), 4.35 (s, 1H), 3.80 (s, 4H), 3.22 (d, $J = 5.0$ Hz, 1H), 3.19 – 2.96 (m, 4H), 2.91 (d, $J = 5.0$ Hz, 1H), 2.60 (d, $J = 28.7$ Hz, 4H), 1.84 – 1.56 (m, 10H), 1.53 (s, 3H), 1.50 – 1.30 (m, 7H), 1.27 (d, $J = 7.1$ Hz, 3H), 1.16 (dt, $J = 21.8, 12.3$ Hz, 5H), 0.94 (dd, $J = 12.3, 5.9$ Hz, 6H), 0.90 – 0.78 (m, 3H). ^{13}C NMR (101 MHz, CDCl_3) δ 207.77, 172.15, 172.06, 171.81, 170.40, 136.68, 59.05, 54.09, 52.50, 52.25, 47.94, 41.61, 40.61, 38.09, 34.53, 33.84, 31.14, 30.64, 30.13, 28.62, 26.94, 26.83, 25.67, 25.48, 25.07, 23.09, 22.18, 17.08, 16.93. LC-MS (linear gradient 10 \rightarrow 90% MeCN, 0.1% TFA, 13 min): R_t (min): 7.44 (ESI-MS (m/z): 752.20 (M+H) $^+$). HRMS: calculated for $\text{C}_{42}\text{H}_{65}\text{N}_5\text{O}_7$ 752.49568 $[\text{M}+\text{H}]^+$; found 752.49561

Morph-Phe-BiCha-Phe-Ala-EK (21)

This compound was obtained by the general protocol for azide coupling on a 100 μmol scale. Purification by column chromatography (1 \rightarrow 2% MeOH/DCM) provided the title compound (63.1 mg, 80%) as a white powder after lyophilisation. ^1H NMR (400 MHz, CDCl_3) δ 7.39 – 7.13 (m, 12H), 6.84 (s, 2H), 4.74 (q, $J = 7.3$ Hz, 2H), 4.51 (td, $J = 7.0, 2.4$ Hz, 1H), 4.35 (s, 1H), 3.60 (s, 4H), 3.24 (d, $J = 4.9$ Hz, 1H), 3.21 – 2.96 (m, 6H), 2.91 (d, $J = 5.0$ Hz, 1H), 2.33 (d, $J = 28.3$ Hz, 4H), 1.88 – 1.60 (m, 7H), 1.54 (s, 4H), 1.49 – 1.30 (m, 7H), 1.28 (d, $J = 7.1$ Hz, 3H), 1.15 (dt, $J = 21.9, 12.2$ Hz, 5H), 0.97 – 0.78 (m, 3H). ^{13}C NMR (101 MHz, CDCl_3) δ 207.66, 177.52, 171.56, 171.22, 170.30, 136.68, 136.24, 129.31, 129.10, 128.82, 128.50, 127.19, 126.91, 58.93, 53.92, 52.39, 52.27, 47.79, 43.23, 37.79, 34.42, 31.01, 30.50, 30.20, 29.99, 26.80, 26.70, 25.52, 25.33, 17.01, 16.80. LC-MS (linear gradient 10 \rightarrow 90% MeCN, 0.1% TFA, 13.0 min): R_t (min): 7.47 (ESI-MS (m/z): 786.20 $[\text{M}+\text{H}]^+$). HRMS: calculated for $\text{C}_{45}\text{H}_{64}\text{N}_5\text{O}_7$ 786.48003 $[\text{M}+\text{H}]^+$; found 786.48022

Boc-Lys(N-N₃Ac)-OMe (23)

To a mixture of Boc-Lys-OMe-TFA **22** (373 mg, 1 mmol), N_3AcOSu (198 mg, 1 mmol, 1 equiv.) in DCM (10 mL) was added DiPEA (200 μl , 1.15 mmol, 1.15 equiv.). After stirring overnight, the reaction mixture was concentrated and dissolved in EtOAc and washed with 1N HCl (2x), sat. NaHCO_3 (2x) and brine (1x). The organic layer was dried over NaSO_4 , filtered, concentrated and purified by column chromatography (50 \rightarrow 80% EtOAc/pent) providing the title compound (120 mg, 0.35 mmol, 35%). ^1H NMR (400 MHz, CDCl_3) δ 6.51 (s, 1H), 5.15 (d, $J = 8.0$ Hz, 1H), 4.33 – 4.18 (m, 1H), 3.95 (s, 2H), 3.72 (s, 3H), 3.26 (q, $J = 6.8$ Hz, 2H), 1.78 (dt, $J = 11.3, 5.8$ Hz, 1H), 1.69 – 1.59 (m, 1H), 1.54 (m, 2H), 1.42 (s, 9H), 1.40 – 1.30 (m, 2H). ^{13}C NMR (101 MHz, CDCl_3) δ 173.23, 166.74, 155.51, 79.93, 53.19, 52.65, 52.33, 39.09, 32.35, 28.90, 28.32, 22.62.

Boc-BiCha-Lys(N-N₃Ac)-OMe (24a)

Boc-Lys(N-N₃Ac)-OMe **23** (120 mg, 0.35 mmol) was treated with TFA for 15 min, followed by co-evaporation with toluene (2x). The resulting product TFA-Lys(N-N₃Ac)-OMe was dissolved in DCM and Boc-BiCha-OH (148 mg, 0.42 mmol, 1.2 equiv.), HCTU (167 mg, 0.42 mmol, 1.2 equiv.) and DiPEA (206 μl , 1.23 mmol, 3.5 equiv.) were added. After stirring overnight, the reaction mixture was concentrated and redissolved in EtOAc and washed with 1N HCl (2x), sat. NaHCO_3 (2x) and brine (1x). The organic layer was dried over NaSO_4 , filtered, concentrated and purified by column chromatography (50 \rightarrow 70% EtOAc/pent) providing the title compound (143 mg, 0.25 mmol,

70%). ^1H NMR (400 MHz, CDCl_3) δ 7.10 (d, J = 7.3 Hz, 1H), 6.96 (d, J = 14.5 Hz, 1H), 5.24 (d, J = 8.3 Hz, 1H), 4.57 – 4.36 (m, 1H), 4.35 – 4.15 (m, 1H), 4.06 – 3.87 (m, 2H), 3.71 (s, 3H), 3.43 – 3.08 (m, 2H), 1.42 (s, 9H), 1.90 – 0.74 (m, 29H). ^{13}C NMR (101 MHz, CDCl_3) δ 173.35, 172.48, 167.26, 155.92, 80.11, 52.81, 52.57, 52.39, 52.22, 43.29, 41.34, 39.73, 38.88, 36.53, 34.44, 33.97, 32.73, 31.54, 31.38, 30.60, 30.26, 29.95, 29.82, 29.70, 28.78, 28.49, 28.37, 26.87, 26.75, 25.80, 25.62, 22.69.

Boc-Leu-BiCha-Lys(*N*- N_3Ac)-OMe (24b)

Boc-BiCha-Lys(*N*- N_3Ac)-OMe **24a** (72 mg, 0.13 mmol) was treated with TFA for 15 min, followed by co-evaporation with toluene (2x). The resulting product TFA·BiCha-Lys(*N*- N_3Ac)-OMe was dissolved in DCM and Boc-Leu-OH (35 mg, 0.15 mmol, 1.2 equiv.), HCTU (62 mg, 0.15 mmol, 1.2 equiv.) and DiPEA (76 μL , 0.44 mmol, 3.5 equiv.) were added. After stirring overnight, the reaction mixture was concentrated and redissolved in EtOAc and washed with 1N HCl (2x), sat. NaHCO_3 (2x) and brine (1x). The organic layer was dried over NaSO_4 , filtered, concentrated and purified by column chromatography (40 \rightarrow 80% EtOAc/pent) providing the title compound (69 mg, 0.1 mmol, 80%). ^1H NMR (400 MHz, CDCl_3) δ 6.94 (d, J = 7.8 Hz, 1H), 6.88 – 6.73 (m, 2H), 5.09 (d, J = 5.9 Hz, 1H), 4.56 – 4.34 (m, 2H), 4.12 (d, J = 6.9 Hz, 1H), 4.07 – 3.92 (m, 2H), 3.73 (s, 3H), 3.44 – 3.30 (m, 1H), 3.23 – 3.11 (m, 1H), 1.85 (dt, J = 14.5, 8.7 Hz, 2H), 1.77 – 1.46 (m, 13H), 1.44 (s, 9H), 1.42 – 1.06 (m, 15H), 1.03 – 0.81 (m, 8H). ^{13}C NMR (101 MHz, CDCl_3) δ 173.04, 172.43, 171.99, 167.40, 155.81, 80.32, 53.40, 52.66, 52.45, 52.05, 51.67, 51.24, 43.34, 43.30, 41.66, 41.17, 40.24, 38.72, 34.34, 31.28, 30.99, 30.61, 30.30, 30.00, 29.77, 28.74, 28.37, 26.91, 26.80, 25.63, 25.45, 24.83, 23.04, 22.28, 21.99.

Morph-Leu-BiCha-Lys(*N*- N_3Ac)-OMe (24c)

Boc-Leu-BiCha-Lys(*N*- N_3Ac)-OMe **24b** (69 mg, 0.1 mmol) was treated with TFA for 15 min, followed by co-evaporation with toluene (2x). The resulting product TFA·Leu-BiCha-Lys(*N*- N_3Ac)-OMe was dissolved in DCM and morpholino acetic acid·HCl (22 mg, 0.12 mmol, 1.2 equiv.), HCTU (50 mg, 0.12 mmol, 1.2 equiv.) and DiPEA (78 μL , 0.45 mmol, 4.5 equiv.) were added. After stirring for 1 hour, the reaction mixture was concentrated and redissolved in EtOAc and washed with sat. NaHCO_3 (2x) and brine (1x). The organic layer was dried over NaSO_4 , filtered, concentrated and purified by column chromatography (0 \rightarrow 20% MeOH/DCM) providing the title compound (66 mg, 0.92 mmol, 92%). ^1H NMR (400 MHz, CDCl_3) δ 7.47 (d, J = 6.9 Hz, 1H), 6.90 (d, J = 7.9 Hz, 1H), 6.85 (d, J = 7.9 Hz, 1H), 6.80 – 6.71 (m, 1H), 4.52 – 4.31 (m, 3H), 4.05 – 3.88 (m, 2H), 3.83 – 3.60 (m, 7H), 3.43 – 3.26 (m, 1H), 3.23 – 3.10 (m, 1H), 3.02 (s, 2H), 2.52 (s, 4H), 1.82 (dt, J = 14.7, 8.2 Hz, 2H), 1.77 – 1.00 (m, 28H), 0.90 (dd, J = 12.9, 6.1 Hz, 6H), 0.87 – 0.74 (m, 2H). ^{13}C NMR (101 MHz, CDCl_3) δ 172.46, 172.11, 171.94, 167.34, 66.84, 61.82, 53.86, 52.66, 52.46, 51.98, 51.76, 51.59, 51.37, 43.30, 41.53, 40.80, 40.09, 39.48, 38.68, 38.63, 35.73, 34.43, 33.83, 32.87, 31.33, 31.14, 30.60, 30.29, 30.03, 29.75, 28.74, 28.64, 26.87, 26.77, 25.70, 25.51, 25.03, 23.02, 22.25, 22.04.

Morph-Leu-BiCha-Lys(*N*- N_3Ac)-NHNH₂ (25)

To a solution of Morph-Leu-BiCha-Lys(*N*- N_3Ac)-OMe **24c** (66 mg, 0.92 mmol) in MeOH (1 mL) was added hydrazine-hydrate (135 μL , 2.7 mmol, 30 equiv.). After stirring for 3 h, the reaction mixture was concentrated and co-evaporated with toluene (3x) providing the product in a quantitative yield. ^1H NMR (400 MHz, MeOD/Chloroform-*d*) δ 4.48 (t, J = 7.0 Hz, 1H), 4.45 – 4.33 (m, 1H), 4.33 – 4.25 (m, 1H), 3.90 (s, 2H), 3.81 – 3.69 (m, 4H), 3.23 (tt, J = 13.4, 6.6 Hz, 2H), 3.07 (s, 2H), 2.56 (s, 4H), 1.87 – 1.05 (m, 30H), 0.96 (dd, J = 11.6, 5.4 Hz, 6H), 0.91 – 0.79 (m, 2H). ^{13}C NMR (101 MHz, MeOD, CDCl_3) δ 173.79, 173.59, 172.56, 171.60, 169.09, 67.41, 62.12, 54.25, 52.66, 52.51, 52.45, 52.18, 43.97, 42.22, 41.70, 40.78, 39.53, 38.84, 35.93, 35.01, 33.02, 32.11, 31.75, 31.16, 30.87, 30.64, 30.24, 29.25, 28.86, 27.39, 27.30, 26.29, 26.01, 25.54, 23.33, 23.30, 22.04.

Morph-Leu-BiCha-Lys(*N*-N₃Ac)-Ala-EK (26)

To a solution of Morph-Leu-BiCha-Lys(*N*-N₃Ac)-NHNH₂ **25** (72 mg, 0.1 mmol) in DMF at -35°C was added HCl (4N in dioxane, 95 μ L, 3.8 equiv.) and *tert*-butyl nitrite (16 μ L, 0.11 mmol, 1.1 equiv.). After stirring for 3 hours, TFA-Ala-EK (0.12 mmol, 1.2 equiv, obtained by treatment of Boc-Ala-EK with TFA for 30 min) and DiPEA (120 μ L, 7 equiv.) were added and the reaction mixture was stirred overnight while warming up to room temperature. The reaction mixture was concentrated and purified by column chromatography (0 \rightarrow 2% MeOH/DCM) providing the title compound as a white powder after lyophilization (35.4 mg, 0.42 mmol, 42%). ¹H NMR (400 MHz, CDCl₃) δ 7.71 – 7.50 (m, 2H), 7.37 (d, *J* = 6.0 Hz, 1H), 6.85 (d, *J* = 6.4 Hz, 1H), 6.71 (t, *J* = 5.6 Hz, 1H), 4.73 – 4.58 (m, 1H), 4.53 (q, *J* = 7.5 Hz, 1H), 4.49 – 4.38 (m, 2H), 4.00 (q, *J* = 16.2 Hz, 2H), 3.82 – 3.67 (m, 4H), 3.39 (dq, *J* = 13.6, 6.8 Hz, 1H), 3.29 (d, *J* = 5.1 Hz, 1H), 3.18 (dq, *J* = 11.8, 5.8 Hz, 1H), 3.06 (dd, *J* = 13.6, 9.4 Hz, 2H), 2.91 – 2.84 (m, 1H), 2.55 (bs, 4H), 1.84 – 1.52 (m, 15H), 1.50 (s, 3H), 1.37 (dd, *J* = 19.6, 9.7 Hz, 10H), 1.27 (d, *J* = 7.1 Hz, 3H), 1.13 (dt, *J* = 22.4, 12.7 Hz, 5H), 0.90 (dd, *J* = 10.8, 5.9 Hz, 6H), 0.83 (d, *J* = 10.0 Hz, 2H). HRMS (*m/z*): calculated for C₄₁H₆₉N₉O₈ [M+H]⁺ 816.53419, found 816.53406.

Morph-Leu-BiCha-Lys(*N*-Ac-BODIPY(FL))-Ala-EK (27)

To a degassed solution of epoxyketone **26** (7.2 mg, 8.8 μ mol) and BODIPY(FL)-alkyne (4.4 mg, 24 μ mol, 1.5 equiv.) in DMF (1 mL) under an argon atmosphere was added CuSO₄·5H₂O (0.5 equiv, 4.4 μ mol (100 μ L from degassed stock solution of 44 μ mol/mL)) and NaAsc (0.75 equiv, 6.6 μ mol (100 μ L from degassed stock solution of 66 μ mol/mL)). After stirring overnight, the reaction mixture immediately purified by HPLC (C₁₈, 55-65% MeCN, 0.1% TFA, 10 min gradient) provided the product as a blue powder after lyophilisation (2.81 mg, 2.5 μ mol, 28%). ¹H NMR (850 MHz, CDCl₃) δ 7.59 (s, 1H), 7.31 (s, 1H), 7.07 (s, 1H), 6.96 (s, 1H), 6.79 (s, 1H), 6.05 (s, 2H), 5.08 (s, 2H), 4.51 – 4.46 (m, 1H), 4.42 – 4.30 (m, 3H), 3.82 (s, 4H), 3.70 (s, 2H), 3.36 (dt, *J* = 13.2, 6.6 Hz, 1H), 3.24 (d, *J* = 5.0 Hz, 1H), 3.15 (dd, *J* = 13.5, 5.5 Hz, 1H), 3.02 – 2.97 (m, 2H), 2.90 (dd, *J* = 4.9, 2.1 Hz, 1H), 2.86 (bs, 4H), 2.82 – 2.76 (m, 2H), 2.51 (s, 6H), 2.39 (s, 6H), 2.00 – 1.07 (m, 37H), 1.52 (s, 3H), 1.30 (d, *J* = 7.1 Hz, 3H), 0.94 – 0.90 (m, 3H), 0.87 (t, *J* = 5.5 Hz, 3H). ¹³C NMR (214 MHz, CDCl₃) δ 208.61, 172.85, 172.78, 171.22, 165.91, 154.08, 147.98, 146.04, 140.40, 131.51, 125.67, 123.11, 121.82, 67.23, 59.21, 53.52, 52.95, 52.70, 52.68, 52.11, 51.71, 48.35, 43.38, 43.31, 40.65, 38.96, 34.55, 33.82, 32.74, 31.64, 30.98, 30.66, 30.46, 30.36, 30.34, 30.00, 29.83, 29.73, 28.51, 28.23, 28.14, 26.96, 26.86, 25.68, 25.59, 25.49, 25.09, 23.01, 22.96, 21.96, 21.93, 21.86, 16.98, 16.94, 16.91, 16.59, 14.61. LC-MS (linear gradient 10 \rightarrow 90% MeCN/H₂O, 0.1% TFA, 13.0 min):R_t (min): 8.30 (ESI-MS (*m/z*): 1144.27 [M+H]⁺). HRMS (*m/z*): calculated for C₆₀H₉₂BF₂N₁₁O₈ [M+H]⁺ 1144.72741, found 1144.72742.

Boc-1-Nap-Phe-OMe (28)

The title compound was prepared by the general procedure for peptide coupling on a 1 mmol scale. Column chromatography provided the product (423 mg, 89%). ¹H NMR (400 MHz, CDCl₃) δ 8.13 (d, *J* = 8.0 Hz, 1H), 7.85 (d, *J* = 8.0 Hz, 1H), 7.75 (d, *J* = 8.2 Hz, 1H), 7.59 – 7.52 (m, 1H), 7.52 – 7.45 (m, 1H), 7.41 – 7.28 (m, 2H), 7.23 – 7.14 (m, 3H), 6.98 – 6.88 (m, 2H), 6.09 – 5.93 (m, 1H), 5.20 – 5.07 (m, 1H), 4.80 – 4.57 (m, 1H), 4.54 – 4.38 (m, 1H), 3.58 (s, 3H), 3.55 – 3.42 (m, 2H), 3.14 – 2.87 (m, 2H), 1.48 – 1.15 (m, 9H). ¹³C NMR (101 MHz, CDCl₃) δ 171.06, 170.87, 135.66, 134.03, 132.81, 132.06, 129.30, 128.90, 128.59, 127.92, 127.18, 126.62, 125.92, 125.50, 123.71, 55.58, 53.45, 52.32, 38.05, 35.86, 28.36.

N₃Phe-1-Nap-Phe-OMe (29)

Boc-1-Nap-Phe-OMe **28** (143 mg, 0.3 mmol) was deprotected using the standard procedure for Boc removal, followed by peptide coupling with N₃Phe-OH using the standard procedure for peptide couplings. Column chromatography provided the product in a quantitative yield. ¹H NMR (400 MHz, CDCl₃) δ 8.12 (d, *J* = 8.4 Hz, 1H), 7.84 – 7.78 (m, 1H), 7.71 (d, *J* = 8.2 Hz, 1H), 7.55 – 7.42 (m, 2H), 7.34 – 7.11 (m, 10H), 7.08 (d, *J* = 8.1 Hz, 1H), 6.86 (dd, *J* = 6.6, 2.9 Hz, 2H), 6.36 (d, *J* = 7.4 Hz, 1H), 4.90 (q, *J* = 8.1 Hz, 1H), 4.61 (q, *J* = 6.0 Hz, 1H), 3.89 (dd, *J* = 8.8, 3.9 Hz, 1H), 3.55 (s, 3H), 3.40 (dd, *J* = 13.9, 6.5 Hz, 1H), 3.28 (dd, *J* = 13.9, 8.3 Hz, 1H), 3.13 (dd, *J* = 14.0, 3.9 Hz, 1H), 2.96 (dd, *J* = 13.8, 5.7 Hz, 1H), 2.87 (dd, *J* = 13.8, 6.1 Hz, 1H), 2.70 (dd, *J* = 14.0, 8.8 Hz, 1H). ¹³C NMR (101

MHz, CDCl₃) δ 170.78, 170.06, 168.38, 136.15, 135.54, 133.90, 132.27, 132.00, 129.54, 129.19, 128.84, 128.65, 128.46, 128.24, 127.96, 127.28, 127.12, 126.48, 125.81, 125.36, 123.71, 65.14, 53.65, 53.49, 52.22, 38.54, 37.95, 35.83.

N₃Phe-1-Nap-Phe-NHNH₂ (30)

N₃Phe-1-Nap-Phe-OMe **29** (0.3 mmol) was dissolved in 1:1 DCM/MeOH (6 mL), followed by the addition of NH₂NH₂·H₂O (872 μ L, 18 mmol, 60 equiv.). The reaction mixture was stirred for 4 h, concentrated and co-evaporated with toluene (2x) thereby providing the product in a quantitative yield. Due to poor solubility of the product in MeOD, CDCl₃ and mixtures thereof, only a ¹H NMR could be measured. ¹H NMR (400 MHz, MeOD/CDCl₃) δ 8.07 (d, *J* = 8.4 Hz, 1H), 7.85 (d, *J* = 7.6 Hz, 1H), 7.76 (d, *J* = 8.2 Hz, 1H), 7.64 – 7.44 (m, 3H), 7.44 – 7.32 (m, 1H), 7.32 – 7.04 (m, 10H), 4.68 (t, *J* = 6.8 Hz, 1H), 4.52 – 4.40 (m, 1H), 4.02 (dd, *J* = 8.8, 4.3 Hz, 1H), 3.41 – 3.25 (m, 2H), 2.99 (t, *J* = 13.6 Hz, 2H), 2.81 (dd, *J* = 13.6, 7.9 Hz, 1H), 2.65 (dd, *J* = 14.0, 8.9 Hz, 1H).

Boc-2-Nap-Phe-OMe (31)

The title compound was prepared by the general procedure for peptide coupling on a 1 mmol scale. Column chromatography provided the product (465 mg, 97%). ¹H NMR (400 MHz, CDCl₃) δ 7.83 – 7.74 (m, 3H), 7.64 (s, 1H), 7.50 – 7.41 (m, 2H), 7.35 (d, *J* = 8.2 Hz, 1H), 7.20 – 7.11 (m, 3H), 6.95 – 6.88 (m, 2H), 6.33 (d, *J* = 6.8 Hz, 1H), 5.18 – 5.07 (m, 1H), 4.83 – 4.72 (m, 1H), 4.52 – 4.39 (m, 1H), 3.54 (s, 3H), 3.20 (d, *J* = 6.5 Hz, 2H), 3.02 (qd, *J* = 13.8, 6.0 Hz, 2H), 1.39 (s, 9H). ¹³C NMR (101 MHz, CDCl₃) δ 171.31, 170.85, 155.38, 135.61, 134.14, 133.53, 132.52, 129.22, 128.53, 128.46, 128.14, 127.71, 127.65, 127.48, 127.13, 126.23, 125.79, 80.26, 55.76, 53.37, 52.25, 38.59, 37.99, 28.30.

N₃Phe-2-Nap-Phe-OMe (32)

Boc-2-Nap-Phe-OMe **31** (143 mg, 0.3 mmol) was deprotected using the standard procedure for Boc removal, followed by peptide coupling with N₃Phe-OH using the standard procedure for peptide couplings. Column chromatography provided the product in a quantitative yield. ¹H NMR (400 MHz, MeOD) δ 7.83 (d, *J* = 8.9 Hz, 1H), 7.79 – 7.67 (m, 3H), 7.39 (tdd, *J* = 10.5, 9.2, 8.0, 3.6 Hz, 2H), 7.30 – 7.06 (m, 11H), 4.74 (t, *J* = 7.1 Hz, 1H), 4.63 (dd, *J* = 7.9, 6.0 Hz, 1H), 3.99 (dd, *J* = 8.8, 4.7 Hz, 1H), 3.48 (s, 3H), 3.16 (dd, *J* = 13.7, 6.3 Hz, 1H), 3.12 – 2.88 (m, 4H), 2.70 (dd, *J* = 14.0, 8.9 Hz, 1H). ¹³C NMR (101 MHz, MeOD) δ 172.89, 172.43, 170.96, 137.55, 137.49, 135.04, 134.74, 133.79, 130.32, 130.25, 129.59, 129.51, 129.17, 129.11, 128.67, 128.63, 128.51, 128.08, 127.95, 127.60, 127.06, 126.67, 120.82, 110.60, 65.61, 55.20, 55.11, 52.88, 49.95, 49.74, 49.52, 49.31, 49.10, 48.88, 48.67, 39.29, 39.08, 38.57.

N₃Phe-2-Nap-Phe-NHNH₂ (33)

N₃Phe-2-Nap-Phe-OMe **32** (0.3 mmol) was dissolved in 1:1 DCM/MeOH (6 mL), followed by the addition of NH₂·NH₂·H₂O (872 μ L, 18 mmol, 60 equiv.). The reaction mixture was refluxed for 2 h, concentrated and co-evaporated with toluene (2x) thereby providing the product in a quantitative yield. Due to poor solubility of the product in MeOD, CDCl₃ and mixtures thereof, only a ¹H NMR could be measured.

Boc-BiPhe-Phe-OMe (34)

The title compound was prepared by the general procedure for peptide coupling on a 1 mmol scale. Column chromatography provided the product (497 mg, 99%). ¹H NMR (400 MHz, CDCl₃) δ 7.51 (dd, *J* = 17.6, 7.7 Hz, 4H), 7.39 (t, *J* = 7.5 Hz, 2H), 7.34 – 7.13 (m, 6H), 7.01 (d, *J* = 6.5 Hz, 2H), 6.58 (d, *J* = 7.6 Hz, 1H), 5.19 (d, *J* = 7.9 Hz, 1H), 4.86 – 4.75 (m, 1H), 4.51 – 4.38 (m, 1H), 3.60 (s, 3H), 3.18 – 2.97 (m, 4H), 1.40 (s, 9H). ¹³C NMR (101 MHz, CDCl₃) δ 171.26, 170.76, 155.18, 140.53, 139.58, 135.51, 129.65, 129.05, 128.58, 128.35, 127.06, 126.91, 126.78, 79.91, 55.43, 53.17, 52.08, 37.78, 28.10.

N₃Phe-BiPhe-Phe-OMe (35)

Boc-BiPhe-Phe-OMe **34** (143 mg, 0.28 mmol) was deprotected using the standard procedure for Boc removal, followed by peptide coupling with N₃Phe-OH using the standard procedure for peptide couplings. Column chromatography provided the product (155 mg, 90%). ¹H NMR (400 MHz, CDCl₃) δ 7.54 – 7.42 (m, 4H), 7.37 (t, *J* = 7.4 Hz, 2H), 7.34 – 7.14 (m, 9H), 7.11 (d, *J* = 8.1 Hz, 2H), 7.03 – 6.93 (m, 3H), 6.78 (d, *J* = 7.7 Hz, 1H), 4.90 (q, *J* = 6.9 Hz, 1H), 4.86 – 4.73 (m, 1H), 3.95 (dd, *J* = 8.3, 4.0 Hz, 1H), 3.61 (s, 3H), 3.23 (dd, *J* = 14.1, 4.0 Hz, 1H), 3.01 (dt, *J* = 13.8, 6.8 Hz, 3H), 2.91 (dt, *J* = 14.1, 7.8 Hz, 2H). ¹³C NMR (101 MHz, CDCl₃) δ 171.22, 170.01, 168.45, 140.66, 139.98, 136.02, 135.62, 135.07, 129.94, 129.87, 129.62, 129.41, 129.27, 128.79, 128.68, 128.64, 128.54, 127.39, 127.35, 127.30, 127.27, 127.20, 127.01, 65.07, 53.74, 53.35, 52.35, 38.47, 38.16, 37.97.

N₃Phe-BiPhe-Phe-NHNH₂ (36)

N₃Phe-BiPhe-Phe-OMe **35** (0.25 mmol) was dissolved in 1:1 DCM/MeOH (6 mL), followed by the addition of NH₂NH₂·H₂O (726 μ L, 15 mmol, 60 equiv.). The reaction mixture was stirred at rt for 4 h, concentrated and co-evaporated with toluene (2x) thereby providing the product in a quantitative yield. Due to poor solubility of the product in MeOD, CDCl₃ and mixtures thereof, only a ¹H NMR could be measured. ¹H NMR (400 MHz, MeOD / CDCl₃) δ 7.60 (d, *J* = 6.1 Hz, 1H), 7.59 – 7.53 (m, 2H), 7.49 (d, *J* = 8.1 Hz, 2H), 7.41 (t, *J* = 7.6 Hz, 2H), 7.35 – 7.11 (m, 12H), 4.69 – 4.59 (m, 1H), 4.52 (t, *J* = 7.4 Hz, 1H), 4.08 (dd, *J* = 8.7, 4.6 Hz, 1H), 3.19 – 2.97 (m, 3H), 2.97 – 2.80 (m, 3H).

Boc-Cha-Phe-OMe (37)

The title compound was prepared by the general procedure for peptide coupling on a 1 mmol scale. Column chromatography provided the product (424 mg, 98%). ¹H NMR (400 MHz, CDCl₃) δ 7.30 – 7.19 (m, 3H), 7.11 (d, *J* = 6.8 Hz, 2H), 6.66 (d, *J* = 7.2 Hz, 1H), 4.99 (d, *J* = 7.7 Hz, 1H), 4.84 (q, *J* = 6.1 Hz, 1H), 4.22 – 4.09 (m, 1H), 3.69 (s, 3H), 3.10 (qd, *J* = 13.8, 5.9 Hz, 2H), 1.85 – 1.53 (m, 8H), 1.44 (s, 9H), 1.33 – 1.04 (m, 5H), 1.04 – 0.77 (m, 2H). ¹³C NMR (101 MHz, CDCl₃) δ 172.20, 171.56, 155.40, 135.67, 129.17, 128.38, 126.93, 79.79, 53.04, 52.26, 52.13, 39.79, 37.78, 33.86, 33.45, 32.44, 28.16, 26.25, 26.06, 25.90.

N₃Phe-Cha-Phe-OMe (38)

Boc-Cha-Phe-OMe **37** (130 mg, 0.3 mmol) was deprotected using the standard procedure for Boc removal, followed by peptide coupling with N₃Phe-OH using the standard procedure for peptide couplings. Column chromatography provided the product (143 mg, 94%). ¹H NMR (400 MHz, CDCl₃) δ 7.35 – 7.20 (m, 8H), 7.12 – 7.08 (m, 2H), 6.97 (d, *J* = 7.9 Hz, 1H), 6.70 (d, *J* = 8.5 Hz, 1H), 4.88 (dt, *J* = 7.7, 6.0 Hz, 1H), 4.59 (td, *J* = 8.5, 6.5 Hz, 1H), 3.97 (dd, *J* = 8.2, 4.0 Hz, 1H), 3.71 (s, 3H), 3.29 (dd, *J* = 14.1, 4.0 Hz, 1H), 3.19 – 3.04 (m, 2H), 2.98 (dd, *J* = 14.1, 8.2 Hz, 1H), 1.73 – 1.52 (m, 6H), 1.45 – 1.32 (m, 1H), 1.24 – 1.05 (m, 4H), 1.00 – 0.73 (m, 2H). ¹³C NMR (101 MHz, CDCl₃) δ 171.64, 171.38, 168.43, 136.08, 135.83, 129.56, 129.37, 128.71, 128.59, 127.31, 127.20, 65.16, 53.21, 52.41, 50.76, 39.77, 38.43, 37.97, 33.86, 33.44, 32.77, 26.37, 26.11, 26.04.

N₃Phe-Cha-Phe-NHNH₂ (39)

N₃Phe-Cha-Phe-OMe **38** (0.3 mmol) was dissolved in 1:1 DCM/MeOH (6 mL), followed by the addition of NH₂NH₂·H₂O (872 μ L, 18 mmol, 60 equiv.). The reaction mixture was stirred at rt for 4 h, concentrated and co-evaporated with toluene (2x) thereby providing the product in a quantitative yield. Due to poor solubility of the product in MeOD, CDCl₃ and mixtures thereof, NMR analysis could not be performed.

Fmoc-Trp(Boc)-Phe-OMe (40)

The title compound was prepared by the general procedure for peptide coupling on a 2 mmol scale. Column chromatography (10→30% EtOAc/pent) provided the product (726 mg, 52%), which was directly used in the next step.

H-Trp(Boc)-Phe-OMe (41)

A solution of Fmoc-Trp(Boc)-Phe-OMe **40** (726 mg, 1.04 mmol) in 1:1 DCM/diethylamine (10 mL) was stirred for 1 h. After evaporation of the solvent, the residue does is washed with MeCN and DCM (product does not dissolve, Fmoc residues do) and evaporated to dryness providing the product with impurities left (293 mg, 0.63 mmol). LC-MS (linear gradient 10 → 90% MeCN/H₂O, 0.1% TFA, 13.0 min):R_t (min): 7.89 (ESI-MS (m/z): 433.8 [M+ Na - tBu]⁺).

N₃Phe-Trp(Boc)-Phe-OMe (42)

The title compound was prepared by the general procedure for peptide coupling on a 0.63 mmol scale. Column chromatography provided the product (60 mg, 15%). LC-MS (linear gradient 10 → 90% MeCN/H₂O, 0.1% TFA, 13.0 min):R_t (min): 10.82 (ESI-MS (m/z): 639.00 [M+H]⁺)

N₃Phe-Trp(+Boc)-Phe-NHNH₂ (43)

N₃Phe-Trp(Boc)-Phe-OMe (**42**) (60 mg, 0.1 mmol) was dissolved in MeOH (1 mL), followed by the addition of NH₂NH₂·H₂O (145 μL, 3 mmol, 30 equiv.). The reaction mixture was stirred for 3 h at rt, concentrated and co-evaporated with toluene (2x) thereby providing the product as a mixture of compounds (+ and – Boc). LC-MS (linear gradient 10 → 90% MeCN/H₂O, 0.1% TFA, 13.0 min):R_t (min): 7.06 (ESI-MS (m/z): 539.00 [M+H]⁺, -Boc), 8.45. (ESI-MS (m/z): 639.07 [M+H]⁺, +Boc)

Boc-Ala(Ada)-Leu-OMe (44)

The title compound was prepared by the general procedure for peptide coupling on a 0.31 mmol scale. Column chromatography (5-20% EtOAc/pent) provided the product (125 mg, 92%). ¹H NMR (400 MHz, CDCl₃) δ 6.54 (d, *J* = 8.0 Hz, 1H), 4.83 (d, *J* = 8.3 Hz, 1H), 4.57 (td, *J* = 8.7, 4.8 Hz, 1H), 4.20 – 4.07 (m, 1H), 3.69 (s, 3H), 1.93 (s, 3H), 1.79 – 1.48 (m, 16H), 1.42 (s, 9H), 1.23 (dd, *J* = 14.5, 8.0 Hz, 1H), 0.90 (d, *J* = 6.0 Hz, 6H). ¹³C NMR (101 MHz, CDCl₃) δ 173.20, 172.80, 155.52, 80.16, 52.30, 50.76, 50.63, 46.01, 42.53, 41.61, 36.96, 32.28, 28.67, 28.41, 24.78, 22.95, 21.92.

N₃Phe-Ala(Ada)-Leu-OMe (45)

Boc-Ala(Ada)-Leu-OMe **44** (124 mg, 0.39 mmol) was deprotected using the standard procedure for Boc removal, followed by peptide coupling with N₃Phe-OH using the standard procedure for peptide couplings. Column chromatography (10→20% EtOAc/pent), provided the product (149 mg, 100%). ¹H NMR (400 MHz, CDCl₃) δ 7.26 (p, *J* = 7.2 Hz, 5H), 6.76 (d, *J* = 8.2 Hz, 1H), 6.62 (d, *J* = 8.1 Hz, 1H), 4.53 (td, *J* = 8.4, 5.4 Hz, 1H), 4.45 (td, *J* = 7.9, 4.8 Hz, 1H), 4.16 (dd, *J* = 8.4, 3.9 Hz, 1H), 3.70 (s, 3H), 3.29 (dd, *J* = 14.1, 3.9 Hz, 1H), 2.98 (dd, *J* = 14.1, 8.5 Hz, 1H), 1.91 (s, 3H), 1.76 – 1.48 (m, 10H), 1.44 (s, 6H), 1.32 – 1.18 (m, 1H), 0.90 (t, *J* = 5.9 Hz, 6H). ¹³C NMR (101 MHz, CDCl₃) δ 173.00, 171.70, 168.22, 135.98, 129.49, 128.66, 127.29, 65.24, 52.26, 50.86, 49.22, 45.95, 42.30, 41.34, 38.24, 36.74, 32.23, 28.48, 24.87, 22.73, 21.99.

N₃Phe-Ala(Ada)-Leu-NHNH₂ (46)

N₃Phe-Ala(Ada)-Leu-OMe **45** (149 mg, 0.29 mmol) was dissolved in MeOH (2 mL), followed by the addition of NH₂NH₂·H₂O (350 μL, 8.6 mmol, 30 equiv.). The reaction mixture was stirred for 2 h at rt, followed by refluxing for 2 h, concentrated and co-evaporated with toluene (2x) thereby providing the product in a quantitative yield. ¹H NMR (400 MHz, MeOD/CDCl₃) δ 7.35 – 7.21 (m, 5H), 4.54 – 4.28 (m, 2H), 4.16 (dd, *J* = 8.6, 4.6 Hz, 1H), 3.22 (dd, *J* = 14.1, 4.6 Hz, 1H), 3.00 (dd, *J* = 14.0, 8.6 Hz, 1H), 1.95 (d, *J* = 10.7 Hz, 3H), 1.77 – 1.33 (m, 17H), 0.93 (dd, *J* = 15.5, 6.1 Hz, 6H). ¹³C NMR (101 MHz, MeOD/CDCl₃) δ 173.69, 172.90, 170.14, 136.92, 129.94, 129.15, 127.69, 65.17, 50.99, 50.39, 46.63, 42.88, 41.42, 38.32, 37.35, 32.95, 29.26, 25.28, 23.09, 22.15.

Boc-Ala(tBu)-Phe-OMe (47)

The title compound was prepared by the general procedure for peptide coupling on a 1 mmol scale. Column chromatography (10 \rightarrow 20% EtOAc/pent) provided the product (400 mg, 100%). ^1H NMR (400 MHz, CDCl_3) δ 7.35 – 7.20 (m, 3H), 7.11 (d, J = 6.8 Hz, 2H), 6.71 (d, J = 7.5 Hz, 1H), 4.94 (d, J = 7.9 Hz, 1H), 4.82 (q, J = 6.0 Hz, 1H), 4.20 – 4.09 (m, 1H), 3.69 (s, 3H), 3.10 (qd, J = 13.8, 6.0 Hz, 2H), 1.81 (d, J = 14.4 Hz, 1H), 1.43 (s, 9H), 1.37 (dd, J = 14.5, 8.8 Hz, 1H), 0.93 (s, 9H). ^{13}C NMR (101 MHz, CDCl_3) δ 172.66, 171.69, 155.33, 135.87, 129.35, 128.54, 127.09, 80.02, 53.30, 52.26, 45.60, 37.95, 30.42, 29.67, 28.38.

 $\text{N}_3\text{Phe-Ala(tBu)-Phe-OMe (48)$

Boc-Ala(tBu)-Cha-Phe-OMe **47** (130 mg, 0.3 mmol) was deprotected using the standard procedure for Boc removal, followed by peptide coupling with $\text{N}_3\text{Phe-OH}$ using the standard procedure for peptide couplings. Column chromatography provided the product (445 mg, 93%). ^1H NMR (300 MHz, CDCl_3) δ 7.36 – 7.24 (m, 8H), 7.24 – 7.12 (m, 3H), 6.79 (d, J = 8.6 Hz, 1H), 4.91 (q, J = 6.2 Hz, 1H), 4.64 (td, J = 8.2, 4.7 Hz, 1H), 3.96 (dd, J = 8.6, 3.8 Hz, 1H), 3.73 (s, 3H), 3.34 (dd, J = 14.0, 3.7 Hz, 1H), 3.14 (qd, J = 14.0, 6.1 Hz, 2H), 2.97 (dd, J = 14.0, 8.7 Hz, 1H), 1.85 (dd, J = 14.5, 4.6 Hz, 1H), 1.40 (dd, J = 14.5, 7.9 Hz, 1H), 0.89 (s, 9H). ^{13}C NMR (75 MHz, CDCl_3) δ 171.69, 171.62, 168.10, 136.08, 135.89, 129.55, 129.32, 128.66, 128.49, 127.24, 127.10, 65.05, 53.20, 52.27, 50.49, 45.23, 38.23, 37.93, 30.34, 29.59.

 $\text{N}_3\text{Phe-Ala(tBu)-Phe-NHNH}_2$ (49)

$\text{N}_3\text{Phe-Ala(tBu)-Cha-Phe-OMe}$ **48** (445 mg, 0.93 mmol) was dissolved in MeOH (10 mL), followed by the addition of $\text{NH}_2\text{NH}_2\cdot\text{H}_2\text{O}$ (1.36 mL, 28 mmol, 30 equiv.). The reaction mixture was stirred at rt for 4 h, concentrated and co-evaporated with toluene (2x) thereby providing the product in a quantitative yield. ^1H NMR (400 MHz, MeOD) δ 7.37 – 7.10 (m, 10H), 4.60 (t, J = 7.4 Hz, 1H), 4.46 (dd, J = 8.5, 4.1 Hz, 1H), 4.08 (dd, J = 8.8, 4.4 Hz, 1H), 3.16 (dd, J = 14.1, 4.4 Hz, 1H), 3.09 (dd, J = 13.7, 6.8 Hz, 1H), 3.00 – 2.87 (m, 2H), 1.60 (dd, J = 14.5, 4.2 Hz, 1H), 1.43 (dd, J = 14.5, 8.6 Hz, 1H), 0.87 (s, 9H). ^{13}C NMR (101 MHz, MeOD) δ 173.36, 171.69, 170.11, 137.23, 136.97, 129.94, 129.82, 129.19, 129.00, 127.67, 127.38, 65.11, 53.94, 53.85, 51.81, 51.71, 45.70, 38.64, 38.38, 30.86, 29.82.

Fmoc-Ser(OtBu)-Phe-OMe (50)

The title compound was prepared by the general procedure for peptide coupling on a 2 mmol scale. Column chromatography (10 \rightarrow 50% EtOAc/pent) provided the product (960 mg, 88%). ^1H NMR (300 MHz, CDCl_3) δ 7.78 (d, J = 7.5 Hz, 2H), 7.62 (d, J = 7.3 Hz, 2H), 7.42 (t, J = 7.4 Hz, 8H), 7.15 (d, J = 6.5 Hz, 2H), 5.80 (s, 1H), 4.93 (q, J = 5.8 Hz, 1H), 4.41 (d, J = 6.9 Hz, 2H), 4.25 (t, J = 7.0 Hz, 2H), 3.84 (dd, J = 8.1, 3.4 Hz, 1H), 3.72 (s, 3H), 3.41 (t, J = 8.4 Hz, 1H), 3.15 (t, J = 5.0 Hz, 2H), 1.20 (s, 9H). ^{13}C NMR (75 MHz, CDCl_3) δ 171.48, 170.01, 143.93, 143.77, 141.32, 135.82, 129.31, 128.62, 127.76, 127.19, 127.11, 125.18, 120.03, 74.38, 67.22, 61.71, 54.23, 53.43, 52.28, 47.17, 38.08, 27.35.

H-Ser(OtBu)-Phe-OMe (51)

Fmoc-Ser(OtBu)-Phe-OMe **50** (547 mg, 1 mmol) was dissolved in THF (10 mL), followed by the addition of EtSH (0.72 mL, 10 mmol, 10 equiv.) and DBU (15 μL , 0.1 mmol, 0.1 equiv.). After stirring for 90 min, the reaction mixture was concentrated and purified by column chromatography (10 \rightarrow 100% EtOAc/pent) yielding the product (260 mg, 81%). ^1H NMR (300 MHz, MeOD) δ 7.34 – 7.05 (m, 5H), 4.78 (t, J = 6.2 Hz, 1H), 3.69 (s, 3H), 3.49 – 3.34 (m, 3H), 3.08 (qd, J = 13.8, 6.2 Hz, 2H), 1.13 (s, 9H).

 $\text{N}_3\text{Phe-Ser(OtBu)-Phe-OMe (52)$

The title compound was prepared by the general procedure for peptide coupling on a 0.81 mmol scale. Column chromatography (10 \rightarrow 50% EtOAc/pent) provided the product (230 mg, 58%). ^1H NMR (300 MHz, CDCl_3) δ 7.37 – 7.18 (m, 9H), 7.16 – 7.03 (m, 3H), 4.87 (q, J = 6.0 Hz, 1H), 4.45 – 4.32 (m, 1H), 4.31 – 4.21 (m, 1H), 3.71 (s, 3H), 3.63 (dd, J = 8.4, 3.9 Hz, 1H), 3.31 (dd, J = 14.0, 3.9 Hz, 1H), 3.20 – 3.01 (m, 4H), 1.14 (s, 9H). ^{13}C NMR (75 MHz,

CDCl₃) δ 171.40, 169.54, 168.41, 135.89, 135.70, 129.57, 129.23, 128.56, 127.21, 127.14, 74.40, 65.19, 60.86, 53.32, 52.43, 52.23, 38.40, 37.95, 27.24.

N₃Phe-Ser(OtBu)-Phe-NHNH₂ (53)

N₃Phe-Ser(OtBu)-Phe-OMe **52** (445 mg, 0.93 mmol) was dissolved in MeOH (5 mL), followed by the addition of NH₂NH₂·H₂O (670 μ L, 14 mmol, 30 equiv.). The reaction mixture was stirred for 30 min at rt, concentrated and co-evaporated with toluene (2x) thereby providing the product in a quantitative yield. ¹H NMR (300 MHz, CDCl₃) δ 7.37 – 7.11 (m, 10H), 7.07 (d, *J* = 6.9 Hz, 1H), 6.79 (d, *J* = 8.5 Hz, 1H), 4.71 (dt, *J* = 8.3, 6.4 Hz, 1H), 4.32 (td, *J* = 7.9, 4.4 Hz, 1H), 4.19 (dd, *J* = 7.7, 4.1 Hz, 1H), 3.56 (dd, *J* = 9.0, 4.4 Hz, 1H), 3.28 (dd, *J* = 14.1, 4.1 Hz, 1H), 3.19 (dd, *J* = 13.8, 6.2 Hz, 1H), 3.14 – 2.97 (m, 3H), 1.12 (s, 9H). ¹³C NMR (75 MHz, CDCl₃) δ 170.84, 169.52, 168.70, 135.90, 135.71, 129.53, 129.19, 128.81, 128.59, 127.28, 74.81, 65.00, 61.06, 53.04, 53.01, 38.31, 37.59, 27.18.

Fmoc-Thr(OtBu)-Phe-OMe (54)

The title compound was prepared by the general procedure for peptide coupling on a 2 mmol scale. Column chromatography (10→50% EtOAc/pent) provided the product (420 mg, 38%). ¹H NMR (300 MHz, CDCl₃) δ 7.76 (d, *J* = 7.5 Hz, 2H), 7.71 (d, *J* = 7.6 Hz, 1H), 7.61 (d, *J* = 7.4 Hz, 2H), 7.40 (t, *J* = 7.4 Hz, 2H), 7.35 – 7.19 (m, 5H), 7.13 (d, *J* = 6.4 Hz, 2H), 6.00 (d, *J* = 4.2 Hz, 1H), 4.88 (q, *J* = 6.3 Hz, 1H), 4.38 (d, *J* = 7.1 Hz, 2H), 4.23 (t, *J* = 7.2 Hz, 1H), 4.19 – 4.04 (m, 2H), 3.73 (s, 3H), 3.13 (qd, *J* = 14.0, 6.1 Hz, 2H), 1.21 (s, 9H), 1.08 (d, *J* = 6.4 Hz, 3H). ¹³C NMR (75 MHz, CDCl₃) δ 171.65, 169.22, 156.11, 143.79, 141.38, 135.98, 129.22, 128.71, 127.80, 127.26, 127.14, 125.25, 120.08, 75.63, 67.07, 66.75, 58.43, 53.53, 52.32, 47.26, 38.05, 28.14, 16.44.

H-Thr(OtBu)-Phe-OMe (55)

Fmoc-Thr(OtBu)-Phe-OMe **54** (370 mg, 0.66 mmol) was dissolved in 20% piperidine/DMF. After stirring for 90 min, the reaction mixture was concentrated and purified by column chromatography (0→20% MeOH/EtOAc) yielding the product (185 mg, 83%). ¹H NMR (300 MHz, CDCl₃) δ 7.95 (d, *J* = 7.8 Hz, 1H), 7.33 – 7.10 (m, 5H), 4.83 (q, *J* = 6.4 Hz, 1H), 4.01 (qd, *J* = 6.2, 3.3 Hz, 1H), 3.69 (s, 3H), 3.14 (d, *J* = 3.3 Hz, 1H), 3.08 (t, *J* = 6.6 Hz, 2H), 1.96 (bs, 2H), 1.14 – 1.05 (m, 12H). ¹³C NMR (75 MHz, CDCl₃) δ 173.39, 172.05, 136.28, 129.43, 129.25, 128.55, 127.05, 74.11, 67.91, 59.75, 53.11, 52.18, 38.19, 29.72, 28.90, 28.51, 19.47.

N₃Phe-Thr(OtBu)-Phe-OMe (56)

The title compound was prepared by the general procedure for peptide coupling on a 0.55 mmol scale. Column chromatography (5→20% EtOAc/pent) provided the product (126 mg, 45%). ¹H NMR (300 MHz, CDCl₃) δ 7.62 (d, *J* = 7.5 Hz, 1H), 7.39 – 7.18 (m, 9H), 7.09 (d, *J* = 6.6 Hz, 2H), 4.81 (q, *J* = 6.5 Hz, 1H), 4.23 (dt, *J* = 7.6, 3.9 Hz, 2H), 3.91 (dd, *J* = 6.3, 4.3 Hz, 1H), 3.71 (s, 3H), 3.28 (dd, *J* = 14.0, 4.0 Hz, 1H), 3.08 (ddt, *J* = 20.2, 14.0, 6.4 Hz, 3H), 1.20 (s, 9H), 0.76 (d, *J* = 6.4 Hz, 3H). ¹³C NMR (75 MHz, CDCl₃) δ 171.59, 168.93, 168.23, 135.94, 135.83, 129.72, 129.20, 128.72, 128.66, 127.36, 127.27, 75.70, 66.08, 65.23, 57.20, 53.50, 52.32, 38.36, 37.96, 28.11, 16.33.

N₃Phe-Thr(OtBu)-Phe-NHNH₂ (57)

N₃Phe-Thr(OtBu)-Phe-OMe **56** (126 mg, 0.25 mmol) was dissolved in MeOH (2.5 mL), followed by the addition of NH₂NH₂·H₂O (362 μ L, 7.4 mmol, 30 equiv.). The reaction mixture was stirred for 2.5 h at rt, concentrated and co-evaporated with toluene (2x) thereby providing the product in a quantitative yield. ¹H NMR (300 MHz, CDCl₃) δ 7.36 – 7.17 (m, 10H), 7.18 – 7.11 (m, 2H), 6.59 (d, *J* = 9.2 Hz, 1H), 4.77 (dt, *J* = 9.2, 5.9 Hz, 1H), 4.31 – 4.18 (m, 2H), 3.85 (dt, *J* = 10.9, 5.5 Hz, 1H), 3.36 – 3.20 (m, 2H), 3.11 (dd, *J* = 14.1, 7.1 Hz, 1H), 2.95 (dd, *J* = 13.7, 6.3 Hz, 1H), 1.96 (s, 2H), 1.10 (s, 9H), 0.68 (d, *J* = 6.4 Hz, 3H). ¹³C NMR (75 MHz, CDCl₃) δ 171.41, 168.65, 136.16, 136.04, 130.13, 129.77, 129.42, 129.07, 127.93, 127.83, 76.56, 66.64, 65.38, 57.69, 53.15, 38.62, 38.01, 28.28, 21.40, 17.08.

Morph-BiCha-Phe-OMe (58)

The title compound was prepared by the general procedure for peptide coupling on a 0.5 mmol scale. Column chromatography (20 \rightarrow 100% EtOAc/pent; followed by 5% MeOH/DCM) provided the product (209 mg, 77%). ^1H NMR (300 MHz, CDCl_3) δ 7.40 (d, J = 8.1 Hz, 1H), 7.34 – 7.20 (m, 3H), 7.13 (d, J = 6.8 Hz, 2H), 6.79 – 6.69 (m, 1H), 4.82 (q, J = 6.7 Hz, 1H), 4.53 – 4.36 (m, 1H), 3.73 (s, 3H), 3.72 – 3.66 (m, 4H), 3.17 (dd, J = 13.9, 5.5 Hz, 1H), 3.05 (dd, J = 14.2, 6.5 Hz, 1H), 2.97 (d, J = 3.9 Hz, 2H), 2.53 – 2.44 (m, 4H), 1.93 – 0.76 (m, 23H). ^{13}C NMR (75 MHz, CDCl_3) δ 171.35, 171.26, 169.78, 135.51, 128.88, 128.14, 126.66, 66.49, 61.34, 53.41, 52.89, 51.98, 50.71, 50.23, 42.84, 41.10, 39.76, 38.66, 37.36, 35.04, 34.20, 33.49, 32.40, 30.92, 30.15, 29.83, 29.62, 29.26, 28.39, 26.44, 26.34, 25.23, 25.03.

Morph-BiCha-Phe-NHNH₂ (59)

Morph-BiCha-Phe-NHNH₂ **58** (209 mg, 0.41 mmol) was dissolved in MeOH (5 mL), followed by the addition of $\text{NH}_2\text{NH}_2\cdot\text{H}_2\text{O}$ (550 μL , 12 mmol, 30 equiv.). The reaction mixture was stirred for 3 h at rt, concentrated and co-evaporated with toluene (2x) thereby providing the product in a quantitative yield. ^1H NMR (400 MHz, MeOD) δ 7.35 – 7.11 (m, 5H), 4.57 (ddt, J = 8.7, 6.4, 3.3 Hz, 1H), 4.50 – 4.34 (m, 1H), 3.74 – 3.63 (m, 4H), 3.08 (dd, J = 13.7, 6.3 Hz, 1H), 3.00 (s, 2H), 2.97 – 2.87 (m, 1H), 2.47 (d, J = 4.4 Hz, 4H), 1.86 – 0.75 (m, 23H). ^{13}C NMR (101 MHz, MeOD) δ 172.87, 172.82, 171.00, 136.90, 129.07, 128.11, 126.45, 66.51, 61.16, 53.43, 53.27, 51.29, 50.83, 43.33, 41.67, 40.27, 39.36, 37.79, 35.61, 34.43, 33.73, 32.29, 31.16, 30.38, 30.07, 29.89, 29.71, 29.50, 28.15, 26.61, 26.53, 25.44, 25.15.

Boc-Phe-BiCha-Phe-OMe (60)

The title compound was prepared by the general procedure for peptide coupling on a 0.75 mmol scale. Column chromatography (20 \rightarrow 40% EtOAc/pent) provided the product (473 mg, 95%). ^1H NMR (400 MHz, CDCl_3) δ 7.35 – 7.17 (m, 9H), 7.14 (d, J = 7.1 Hz, 2H), 6.96 (d, J = 7.3 Hz, 1H), 6.84 – 6.74 (m, 1H), 4.84 (q, J = 6.3 Hz, 1H), 4.50 (dt, J = 13.7, 7.7 Hz, 2H), 3.70 (s, 3H), 3.20 – 2.95 (m, 4H), 1.41 (s, 9H), 1.87 – 0.73 (m, 23H). ^{13}C NMR (101 MHz, CDCl_3) δ 171.65, 171.48, 171.43, 171.40, 155.49, 136.66, 135.89, 129.38, 129.29, 128.56, 127.08, 126.84, 80.05, 55.46, 53.50, 53.42, 52.26, 51.64, 51.23, 43.23, 43.17, 41.61, 40.26, 37.90, 35.83, 34.13, 33.61, 30.71, 30.49, 30.19, 29.79, 29.62, 29.54, 28.91, 28.27, 26.83, 26.72, 25.44, 25.29.

Morph-Phe-BiCha-Phe-OMe (61)

Boc-Phe-BiCha-Phe-OMe **60** (473 mg, 0.7 mmol) was deprotected using the standard procedure for Boc removal, followed by peptide coupling with 2-morpholinoacetic acid using the standard procedure for peptide couplings. Column chromatography (2% MeOH/DCM), provided the product (503 mg, 100%). ^1H NMR (400 MHz, CDCl_3) δ 7.51 (d, J = 7.8 Hz, 1H), 7.33 – 7.15 (m, 9H), 7.15 – 7.10 (m, 2H), 7.00 (d, J = 7.8 Hz, 1H), 6.75 (d, J = 7.8 Hz, 1H), 4.82 (q, J = 6.2 Hz, 1H), 4.73 (td, J = 8.5, 5.7 Hz, 1H), 4.48 – 4.32 (m, 1H), 3.70 (s, 3H), 3.55 (t, J = 4.2 Hz, 4H), 3.23 – 2.95 (m, 5H), 2.38 – 2.27 (m, 2H), 2.27 – 2.17 (m, 2H), 1.88 – 0.71 (m, 23H). ^{13}C NMR (101 MHz, CDCl_3) δ 171.67, 171.41, 171.08, 170.99, 170.34, 136.43, 135.86, 129.28, 129.12, 128.67, 128.53, 127.08, 127.01, 66.81, 61.58, 53.52, 53.33, 53.23, 52.30, 51.82, 51.40, 43.20, 43.11, 41.47, 40.06, 39.31, 38.61, 37.74, 37.09, 37.00, 35.51, 34.33, 33.63, 32.84, 30.96, 30.49, 30.20, 29.92, 29.64, 28.62, 26.78, 26.68, 25.54, 25.36.

Morph-Phe-BiCha-Phe-NHNH₂ (62)

Morph-Phe-BiCha-Phe-NHNH₂ **58** (203 mg, 0.7 mmol) was dissolved in MeOH (7.5 mL), followed by the addition of NH₂NH₂·H₂O (1 mL, 21 mmol, 30 equiv.). The reaction mixture was stirred for 3 h at rt, concentrated and co-evaporated with toluene (2x) thereby providing the product in a quantitative yield. ¹H NMR (400 MHz, CDCl₃, Methanol-*d*) δ 7.36 – 7.14 (m, 10H), 4.72 – 4.68 (m, 1H), 4.57 (t, *J* = 7.4 Hz, 1H), 4.40 – 4.27 (m, 1H), 3.65 – 3.54 (m, 4H), 3.20 – 3.07 (m, 2H), 3.08 – 2.82 (m, 4H), 2.36 (dd, *J* = 10.8, 6.4 Hz, 2H), 2.25 (dt, *J* = 11.1, 4.3 Hz, 2H), 1.87 – 0.70 (m, 23H). ¹³C NMR (101 MHz, CDCl₃, MeOD) δ 173.52, 173.03, 171.82, 171.67, 137.43, 137.23, 129.84, 129.25, 129.10, 127.65, 127.48, 67.43, 61.99, 54.31, 54.12, 54.06, 52.93, 52.50, 49.64, 49.43, 49.21, 49.00, 48.79, 48.57, 48.36, 44.06, 42.42, 41.08, 39.86, 38.41, 38.24, 35.97, 34.95, 33.20, 31.57, 31.21, 30.95, 30.68, 29.00, 27.46, 27.38, 26.22, 25.94.

Biochemical experiments**General**

Lysates of cells were prepared by treating cell pellets with 4 volumes of lysis buffer containing 50 mM Tris pH 7.5, 2 mM DTT, 5 mM MgCl₂, 10% glycerol, 2 mM ATP, and 0.05% digitonin for 60 min. Protein concentration was determined using Qubit[®] protein assay kit (ThermoFisher). All cell lysate labelling experiments were performed in assay buffer containing 50 mM Tris pH 7.5, 2 mM DTT, 5 mM MgCl₂, 10% glycerol, 2 mM ATP. Cell lysate labelling and competition experiments were performed at 37°C. Probe cocktail consist of: 100 nM Cy5-NC-001, 30 nM BODIPY(FL)-LU-112, 100 nM BODIPY(TMR)-NC-005-VS, used as premixed 10x concentrated cocktail in DMSO which is incubated with cell lysate for 60 min. Prior to fractionation on 12.5% SDS-PAGE (TRIS/glycine), samples were boiled for 3 min in a reducing gel loading buffer. The 7.5x10 cm (L x W) gels were run for 15 min at 80V followed by 120 min at 130V. In-gel detection of (residual) proteasome activity was performed in the wet gel slabs directly on a ChemiDoc[™] MP System using Cy2 setting to detect BODIPY(FL)-LU-112, BODIPY(FL)-epoxomicin and BODIPY(FL)-NC-001, Cy3 settings to detect BODIPY(TMR)-NC-005-VS and BODIPY(TMR)-epoxomicin and Cy5 settings to detect Cy5-NC-001.

Competition experiments in cell lysate

Cell lysates (diluted to 10-15 µg total protein in 9 µL buffer) were exposed to the inhibitors (10x stock in DMSO) at indicated concentrations for 1 h at 37 °C, followed by addition of probe cocktail (10x stock, 1.1 µL) and SDS-PAGE as described above. For IC₅₀ determinations, intensities of bands were measured by fluorescent densitometry and divided by the intensity of bands in mock-treated lysates. Average values of three independent experiments were plotted against inhibitor concentrations. IC₅₀ values were calculated using GraphPad Prism software.

Competition experiments in living RPMI-8226 cells

RPMI-8226 were cultured in RPMI-1640 media supplemented with 10% fetal calf serum, GlutaMAX[™], penicillin, streptomycin in a 5% CO₂ humidified incubator. 5-8 × 10⁵ cells/mL were exposed to inhibitors for 1 h at 37 °C. Cells were harvested and washed twice with PBS. Cell pellets were treated with lysis buffer on ice for 15 min, followed by centrifugation at 14000 rpm for 5 min. Proteasome inhibition in the obtained cell lysates was determined using the method described above. Intensities of bands were measured by fluorescent densitometry and divided by the intensity of bands in mock-treated cells. Average values of three independent experiments were plotted against inhibitor concentrations. IC₅₀ values were calculated using GraphPad Prism software.

References

1. Zhou, H.-J. et al. Design and synthesis of an orally bioavailable and selective peptide epoxyketone proteasome inhibitor (PR-047). *J. Med. Chem.* **52**, 3028-3038 (2009).
2. Huber, Eva M. et al. Immuno- and constitutive proteasome crystal structures reveal differences in substrate and inhibitor specificity. *Cell* **148**, 727-738 (2012).
3. de Bruin, G. et al. Structure-based design of $\beta 1i$ or $\beta 5i$ specific inhibitors of human immunoproteasomes. *J. Med. Chem.* **57**, 6197-6209 (2014).
4. Blackburn, C. et al. Characterization of a new series of non-covalent proteasome inhibitors with exquisite potency and selectivity for the 20S $\beta 5$ -subunit. *Biochem. J.* **430**, 461-476 (2010).
5. Huber, E.M. et al. Systematic analyses of substrate preferences of 20S proteasomes using peptidic epoxyketone inhibitors. *J. Am. Chem. Soc.* **137**, 7835-7842 (2015).
6. Elofsson, M., Splittgerber, U., Myung, J., Mohan, R. & Crews, C.M. Towards subunit-specific proteasome inhibitors: synthesis and evaluation of peptide α' , β' -epoxyketones. *Chem. Biol.* **6**, 811-22 (1999).
7. Demo, S.D. et al. Antitumor activity of PR-171, a novel irreversible inhibitor of the proteasome. *Cancer Res.* **67**, 6383-6391 (2007).
8. Sharma, L.K. et al. Activity-based near-infrared fluorescent probe for LMP7: a chemical proteomics tool for the immunoproteasome in living cells. *Chembiochem* **13**, 1899-903 (2012).
9. Carmony, K.C. et al. A bright approach to the immunoproteasome: development of LMP2/ $\beta 1i$ -specific imaging probes. *Bioorg. Med. Chem.* **20**, 607-13 (2012).
10. Verdoes, M. et al. Acetylene functionalized BODIPY dyes and their application in the synthesis of activity based proteasome probes. *Bioorg. Med. Chem. Lett.* **17**, 6169-71 (2007).
11. Geurink, P.P. et al. Incorporation of non-natural amino acids improves cell permeability and potency of specific inhibitors of proteasome trypsin-like sites. *J. Med. Chem.* **56**, 1262-1275 (2013).

CHAPTER 8

Development of an inhibitor and activity-based probe selective for β 1c

Introduction

Proteasome inhibitors in clinical use and evaluated as clinical candidates for the treatment of haematological cancers do not distinguish between constitutive (cCPs) and immunoproteasomes (iCPs) (see chapter 3). The reason for this may be historical: initially cCPs, and in particular the β 5c subunits, were thought to be the essential targets in treating haematological cancers with proteasome inhibitors. From later studies it became apparent that the two clinical drugs that target proteasomes and that were developed as β 5c inhibitors (bortezomib and carfilzomib) inhibit next to β 5c also β 5i as well as a number of other cCP and iCP subunits. In order to establish which cCP/iCP subunits are ideally targeted for the treatment of various tumours, but also to discriminate their individual role in antigen processing and presentation, it would be advantageous to have available a set of inhibitors and activity-based probes uniquely modulating one of each of the six cCP/iCP subunits. In the previous chapters a number of such inhibitors and probes is described. For instance, chapter 7 reports on the development of selective β 5c selective inhibitors and a β 5c-selective activity based probe (ABP). This chapter describes the development of an inhibitor and ABP with high selectivity for β 1c.

The nature of the S1 pocket of β 1c promotes hydrolysis of peptide bonds C-terminally of acidic amino acids and as such, the catalytic activity of β 1c is designated as peptidylglutamyl-peptide hydrolyzing (PGPH)¹ or cysteine-aspartic-acid-protease (caspase)-like.² To assess the activity of β 1c, Z-Leu-Leu-Glu-AMC is often used as fluorogenic substrate, even though the hydrolysis rate of this substrate is rather low.² To overcome this limitation, Ac-Nle-Pro-Nle-Asp-AMC was developed which showed a much higher cleavage rate, indicating that β 1c prefers Asp over Glu at P1. Indeed, direct comparison of Ac-Gly-Pro-Leu-Asp-AMC with Ac-Gly-Pro-Leu-Glu-AMC showed a two-fold slower conversion of the latter substrate.² This finding was confirmed

by a systematic study in which substrate preferences of all proteasome subunits were analysed using tripeptide epoxyketones (EK) with different P1 amino acids.³ It was found that Ac-PAD-EK and Ac-LAD-EK showed ten-fold lower IC_{50} values than Ac-PAE-EK and Ac-LAE-EK (see chapter 4). The preference of $\beta 1c$ for substrates and inhibitors with acidic residues on P1 can be explained by the increased hydrophobicity of the S1 pocket of $\beta 1i$ caused by mutations (Val20 and Leu45 in $\beta 1i$ versus Thr20 and Arg45 in $\beta 1c$, see chapter 4).

Although Ac-PAD-EK shows complete selectivity for $\beta 1c$ over all subunits, the IC_{50} for $\beta 1c$ is rather high (1.4 μM , Figure 1). In addition, Ac-PAD-EK lacks an azide or alkyne functionality for direct attachment of a fluorophore in order to obtain a $\beta 1c$ selective ABP. In this chapter a more potent $\beta 1c$ inhibitor based on Ac-PAD-EK and $\beta 1c/\beta 1i$ specific inhibitor NC-001⁴ is described (Figure 1). This inhibitor is equipped with an azide group, which allowed direct functionalization with a fluorophore and yielded the first ABP selective for $\beta 1c$.

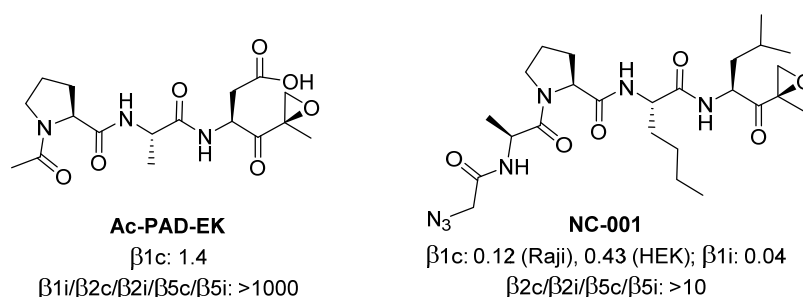
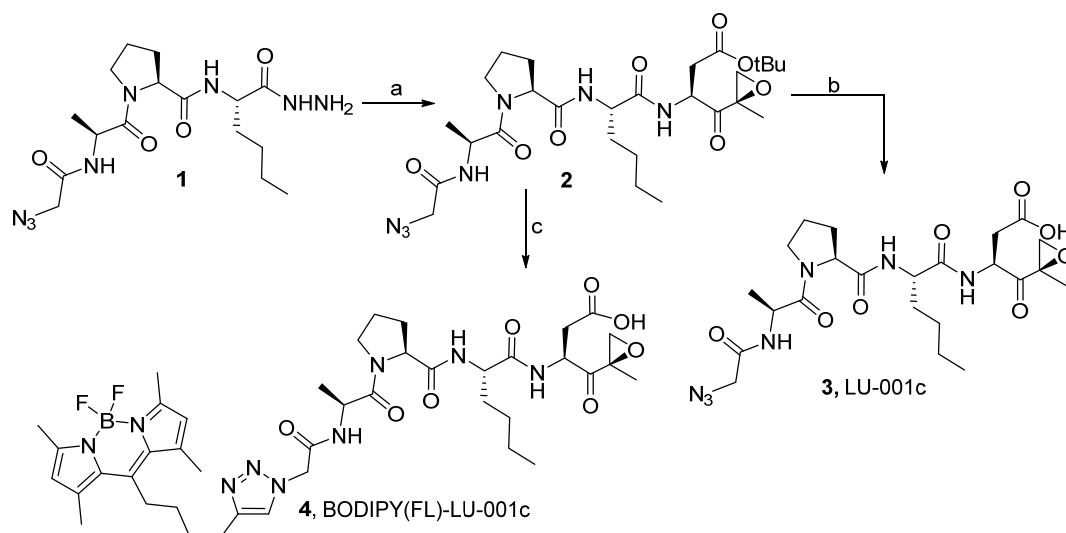


Figure 1. Structures and IC_{50} values (μM) of NC-001 ($\beta 1c/\beta 1i$ selective) and Ac-PAD-EK ($\beta 1c$ selective). IC_{50} values have been determined by ABPP in Raji or HEK cell lysate.

Results and discussion

NC-001 is 10-fold more potent for $\beta 1c$ than Ac-PAD-EK, but also targets $\beta 1i$ (Figure 1). In addition, elongation of tripeptide Ac-PLL-EK with a P4 Ala residue resulted in a four-fold lower IC_{50} value for $\beta 1c$ (see chapter 4). Therefore it was hypothesized that substitution of the P1 Leu residue of NC-001 for Asp (compound **3**, LU-001c) would result in more a potent $\beta 1c$ inhibitor. For the synthesis of compound **3**, first an azide coupling between hydrazide **1**⁵ and TFA-H-Asp(OtBu)-EK (synthesized as described in chapter 4) was performed providing compound **2** (Scheme 1). Treatment of **2** with dry TFA yielded compound **3**. Significant amounts of side products were formed due to partial reduction of the epoxide during the hydrogenation of Cbz-Asp(OtBu)-EK and significant hydrolysis of the epoxyketone moiety during the final deprotection (see also chapter 4). Therefore, HPLC purification was necessary and compound **3** could be isolated in excellent purity but only in a low yield. Evaluation of LU-001c **3** in Raji lysate showed a 20-fold improved potency for $\beta 1c$ compared to Ac-PAD-EK (Figure 2A). Both in Raji and HEK lysate, the IC_{50} values of LU-001c **3** for $\beta 1c$ are comparable

to NC-001 (Figure 1 and 2). In addition, up to concentrations of 100 μ M no inhibition of other proteasome subunits was observed. On the contrary, in intact RPMI-8226 cells, no inhibition of β 1c could be observed at concentration up to 100 μ M, most likely due to poor cell permeability caused by the negatively charged carboxylic acid moiety.



Scheme 1. Synthesis of LU-001c (2). Reagents and conditions: a) 1. i. tBuONO , HCl , DMF , -35°C . ii. DiPEA , $\text{TFA}\cdot\text{H}\cdot\text{Asp}(\text{OtBu})\cdot\text{EK}$, $-35^\circ\text{C}\text{-RT}$; b) TFA , 1.9% (total yield over a and b); c) 1. TFA . 2. BODIPY(FL)-alkyne , CuSO_4 , NaAsc , $\text{DMF}/\text{H}_2\text{O}$, 31%.

Since LU-001c **3** has been equipped with an azide functionality, a fluorophore can be attached straightforwardly by copper(I)-catalysed azide-alkyne cycloaddition (CuAAC). For further studies aimed at establishing the composition of 20S proteasome core particles (see chapter 10) a β 1c probe equipped with a BODIPY(FL) fluorophore was desired. Therefore, compound **2** was treated with TFA and directly used (without purification) in the CuAAC reaction with BODIPY(FL)-alkyne⁶. ABP **4** (BODIPY(FL)-LU-001c) was isolated in a reasonable yield and excellent purity after purification by HPLC. Assessment of ABP **4** in Raji lysate showed good selectivity and potency for β 1c (Figure 2B). Labelling of the other proteasome subunits was not observed and therefore the kinetic constants could only be determined for β 1c (Figure 2C).

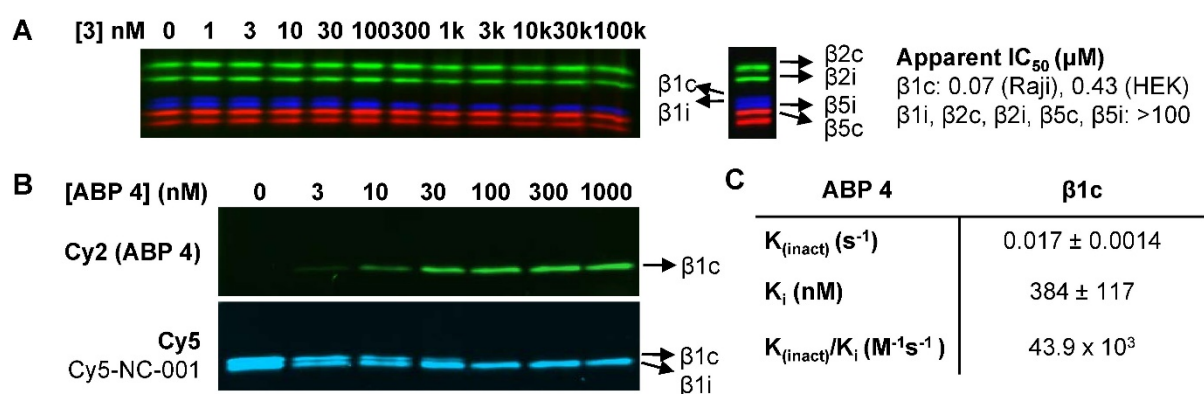


Figure 2. Evaluation of LU-001c (3) and ABP 4 in Raji lysate. A) Inhibition profile (Raji lysate) and apparent IC_{50} values of LU-001c (3) as determined in Raji and HEK lysates. B) Evaluation of ABP 4. Raji lysates were treated with indicated concentrations of ABP 4 for 1 h, followed by the addition of Cy5-NC-001 (100 nM end concentration, labels $\beta 1c/\beta 1i$, see chapter 3) for 1 h. C) Kinetic constants of ABP 4 as determined in Raji lysates. Log (% activity) for various concentrations is plotted versus time, from which the first order rate constants (K_{obs}) are derived. K_{obs} were plotted versus probe concentration, yielding $K_{inact} = \max K_{obs}$ and $K_i = [probe]$ at $0.5 K_{inact}$. $K_{inact}/K_i =$ second order rate constant.

Conclusion

Based on the $\beta 1c$ selective inhibitor Ac-PAD-EK and $\beta 1c/\beta 1i$ selective inhibitor NC-001, LU-001c (3) was synthesized, which showed increased inhibitory potency for $\beta 1c$. LU-001c (3) can therefore be considered as the most selective and potent $\beta 1c$ selective inhibitor known to date. Due to poor cell permeability, this inhibitor can only be used to block $\beta 1c$ in cell lysates. In addition, LU-001c (3) was used to synthesize the first ABP able to selectively label $\beta 1c$ (BODIPY(FL)-LU-001c, ABP 4) in lysates. Although this probe has not been evaluated in intact cells, it is envisioned that this probe also suffers from poor cell permeability. It might be possible to overcome the poor cell permeability of LU-001c (3) and ABP 4 by converting the carboxylic acid moiety to an ester (for instance a methyl- or ethyl ester), which can be hydrolysed by esterases once the compound has entered the cell.

Experimental

Synthetic procedures

General procedures

Acetonitrile (ACN), dichloromethane (DCM), N,N-dimethylformamide (DMF), methanol (MeOH), diisopropylethylamine (DiPEA) and trifluoroacetic acid (TFA) were of peptide synthesis grade, purchased at Biosolve, and used as received. All general chemicals (Fluka, Acros, Merck, Aldrich, Sigma, Iris Biotech) were used as received. Column chromatography was performed on Screening Devices b.v. Silica Gel, with a particle size of 40-63 μm and pore diameter of 60 \AA . TLC analysis was conducted on Merck aluminium sheets (Silica gel 60 F254). Compounds were visualized by UV absorption (254 nm), by spraying with a solution of $(\text{NH}_4)_6\text{Mo}_7\text{O}_{24}\cdot 4\text{H}_2\text{O}$ (25 g/L) and $(\text{NH}_4)_4\text{Ce}(\text{SO}_4)_4\cdot 2\text{H}_2\text{O}$ (10 g/L) in 10% sulphuric acid, a solution of KMnO_4 (20 g/L) and K_2CO_3 (10 g/L) in water, or ninhydrin (0.75 g/L) and acetic acid (12.5 mL/L) in ethanol, where appropriate, followed by charring at ca. 150 $^\circ\text{C}$. ^1H and ^{13}C NMR spectra were recorded on a Bruker AV-300 (300 MHz), AV-400 (400 MHz), AV-600 (600 MHz) spectrometer. Chemical shifts are given in ppm (δ) relative to tetramethylsilane, CD_3OD or CDCl_3 as internal standard. High resolution mass spectra were recorded by direct injection (2 μL of a 2 μM solution in water/acetonitrile 50/50 (v/v) and 0.1% formic acid) on a mass spectrometer (Thermo Finnigan LTQ Orbitrap) equipped with an electrospray ion source in positive mode (source voltage 3.5 kV, sheath gas flow 10, capillary temperature 250 $^\circ\text{C}$) with resolution $R = 60,000$ at m/z 400 (mass range $m/z = 150\text{--}2,000$) and dioctylphthalate ($m/z = 391.28428$) as a "lock mass". The high resolution mass spectrometer was calibrated prior to measurements with a calibration mixture (Thermo Finnigan). LC-MS analysis was performed on a Finnigan Surveyor HPLC system with a Gemini C_{18} 50 \times 4.60 mm column (detection at 200-600 nm), coupled to a Finnigan LCQ Advantage Max mass spectrometer with ESI. The applied buffers were H_2O , ACN and 1.0% aq. TFA. Method: xx \rightarrow xx% MeCN, 13.0 min (0 \rightarrow 0.5 min: 10% MeCN; 0.5 \rightarrow 8.5 min: gradient time; 8.5 \rightarrow 10.5 min: 90% MeCN; 10.5 \rightarrow 13.0 min: 10% MeCN). HPLC purification was performed on a Gilson HPLC system coupled to a Phenomenex Gemini 5 μm 250 \times 10 mm column and a GX281 fraction collector. H-Asp(OtBu)-EK was synthesized as described in chapter 4.

$\text{N}_3\text{Ac-Ala-Pro-Nle-Asp-EK}$ (LU-001c,3)

Compound **4** was synthesized as reported before.⁵ The title compound was prepared via azide coupling of hydrazide **4** and TFA·H-Asp(OtBu) epoxyketone. Hydrazide **4** (57 mg, 144 μmol , 1 equiv.) was dissolved in DMF and cooled to -30 $^\circ\text{C}$. tBuONO (23 μL , 1.1 equiv.) and HCl (100 μL , 4M solution in 1,4-dioxane, 2.8 equiv.) were added, and the mixture was stirred for 3h at -30 $^\circ\text{C}$ after which TLC analysis (10% MeOH/DCM, v/v) showed complete consumption of the starting material. The epoxyketone as free amine was added to the reaction mixture as a solution in DMF. DiPEA (144 μL , 5 equiv.) was added to the reaction mixture, and this mixture was allowed to warm to RT slowly overnight. The mixture was diluted with EtOAc or DCM and extracted with H_2O (3 \times). The organic layer was dried over MgSO_4 concentrated and purified by flash column chromatography (0-3% MeOH in DCM), provided tert-butyl protected product **2**, which was deprotected by treatment with dry TFA (1 mL) for 10 min, followed by the addition of toluene and concentration. Purification by HPLC (C_{18} , 10-30% MeCN, 0.1% TFA, 15 min gradient), followed by lyophilization provided the product (1.46 mg, 1.9%). Complex NMR due to presence of rotamers, peaks of major rotamer are reported. ^1H NMR (600 MHz, MeOD) δ 4.80 – 4.74 (m, 1H), 4.63 (q, $J = 7.0$ Hz, 1H), 4.46 (dd, $J = 8.4, 4.5$ Hz, 1H), 4.29 – 4.23 (m, 1H), 3.92 – 3.85 (m, 2H), 3.80 (dt, $J = 9.8, 6.8$ Hz, 1H), 3.65 (dt, $J = 10.1, 6.7$ Hz, 1H), 3.23 (d, $J = 4.7$ Hz, 1H), 2.92 (dd, $J = 12.3, 4.9$ Hz, 1H), 2.79 (dd, $J = 16.5, 4.2$ Hz, 1H), 2.70 (dd, $J = 16.3, 7.6$ Hz, 1H), 2.21 (tdd, $J = 15.0, 9.7, 5.6$ Hz, 1H), 2.15 – 2.07 (m, 1H), 2.07 – 1.97 (m, 2H), 1.80 (ddt, $J = 15.2, 10.8, 5.2$ Hz, 1H), 1.71 – 1.57 (m, 1H), 1.40 – 1.30 (m, 7H), 1.22 (s, 3H), 0.97 – 0.88 (m, 3H). ^{13}C NMR (151 MHz, MeOD) δ 207.14, 174.28, 174.11, 173.74, 173.24, 169.87, 61.51, 54.67, 53.25, 52.47,

50.51, 49.57, 48.63, 36.13, 32.77, 30.48, 28.93, 26.04, 23.45, 16.82, 14.27. LC-MS (linear gradient 0 → 50% MeCN, 0.1% TFA, 13.5 min): R_t (min): 7.70 (ESI-MS (m/z): 538.07 (M+H)⁺). HRMS: calculated for C₂₃H₃₅N₇O₈ 538.26199 [M+H]⁺; found 538.26202

BODIPY(FL)-LU-001c (4)

Tert-butyl protected LU-001c **2** (10 mg, 17 μmol) was treated with dry TFA (1 mL) for 15 min, followed by co-evaporation with dry toluene to afford crude LU-001c, which was directly used in the next step. To a degassed solution of LU-001c (crude, 17 μmol) and BODIPY(FL)-alkyne (8.3 mg, 25 μmol, 1.5 equiv.) in DMF (1 mL) under an argon atmosphere was added CuSO₄·5H₂O (0.5 equiv, 8.5 μmol (100 μL from degassed stock solution of 85 μmol/mL)) and NaAsc (0.75 equiv, 12.8 μmol (100 μL from degassed stock solution of 128 μmol/mL)). After stirring overnight, the reaction mixture was immediately purified by HPLC (C₁₈, 40-70% MeCN, 0.1% TFA, 10 min gradient), providing the product as a yellow powder after lyophilisation (4.62 mg, 5.3 μmol, 31%). ¹H NMR (600 MHz, MeOD) δ 7.77 (s, 1H), 6.14 (s, 2H), 5.20 – 5.12 (m, 2H), 4.80 (dd, *J* = 7.5, 4.9 Hz, 1H), 4.63 (q, *J* = 7.0 Hz, 1H), 4.45 (dd, *J* = 8.3, 4.6 Hz, 1H), 4.28 (dd, *J* = 8.7, 5.3 Hz, 1H), 3.77 (dt, *J* = 9.4, 6.8 Hz, 1H), 3.65 (dt, *J* = 9.6, 6.3 Hz, 1H), 3.24 (d, *J* = 5.0 Hz, 1H), 3.06 (dd, *J* = 10.3, 6.8 Hz, 2H), 2.94 (d, *J* = 5.0 Hz, 1H), 2.84 – 2.79 (m, 3H), 2.73 (dd, *J* = 16.5, 7.6 Hz, 1H), 2.46 (s, 6H), 2.43 (d, *J* = 6.1 Hz, 6H), 2.26 – 2.17 (m, 1H), 2.16 – 1.90 (m, 5H), 1.88 – 1.77 (m, 1H), 1.77 – 1.68 (m, 2H), 1.68 – 1.59 (m, 1H), 1.51 (s, 3H), 1.46 – 1.33 (m, 7H), 1.00 – 0.90 (m, 3H). ¹³C NMR (151 MHz, MeOD) δ 206.71, 173.80, 173.66, 172.81, 167.13, 154.52, 148.16, 147.52, 141.87, 132.21, 124.54, 122.19, 67.75, 61.11, 59.93, 54.24, 52.87, 52.32, 35.74, 32.39, 31.97, 30.36, 30.03, 28.70, 28.50, 25.62, 25.57, 23.03, 16.77, 16.38, 16.13, 14.02, 13.87. LC-MS (linear gradient 10 → 90% MeCN/H₂O, 0.1% TFA, 13.0 min): R_t (min): 7.35, (ESI-MS (m/z): 846.07 (M-F)⁺). HRMS: calculated for C₄₂H₅₈BF₂N₉O₈ 866.45422 [M+H]⁺; found 866.45426.

Biochemical experiments

General

Lysates of cells were prepared by treating cell pellets with 4 volumes of lysis buffer containing 50 mM Tris pH 7.5, 2 mM DTT, 5 mM MgCl₂, 10% glycerol, 2 mM ATP, and 0.05% digitonin for 60 min. Protein concentration was determined using Qubit[®] protein assay kit (ThermoFisher). All cell lysate labelling experiments were performed in assay buffer containing 50 mM Tris pH 7.5, 2 mM DTT, 5 mM MgCl₂, 10% glycerol, 2 mM ATP. Cell lysate labelling and competition experiments were performed at 37°C. Probe cocktail consist of: 100 nM Cy5-NC-001, 30 nM BODIPY(FL)-LU-112, 100 nM BODIPY(TMR)-NC-005-VS, used as premixed 10x concentrated cocktail in DMSO which is incubated with cell lysate for 60 min. Prior to fractionation on 12.5% SDS-PAGE (TRIS/glycine), samples were boiled for 3 min in a reducing gel loading buffer. The 7.5x10 cm (L x W) gels were run for 15 min at 80V followed by 120 min at 130V. In-gel detection of (residual) proteasome activity was performed in the wet gel slabs directly on a ChemiDoc™ MP System using Cy2 setting to detect BODIPY(FL), Cy3 settings to detect BODIPY(TMR) and Cy5 settings to detect Cy5.

Competition experiments in cell lysate

Cell lysates (diluted to 10-15 μg total protein in 9 μL buffer) were exposed to the inhibitor (10x stock in DMSO) at indicated concentrations for 1 h at 37 °C, followed by addition of probe cocktail (10x stock, 1.1 μL) and SDS-PAGE as described above. For IC₅₀ determinations, intensities of bands were measured by fluorescent densitometry and divided by the intensity of bands in mock-treated extracts. Average values of three independent experiments were plotted against inhibitor concentrations. IC₅₀ values were calculated using GraphPad Prism software.

Evaluation of ABP 4

Cell lysates (diluted to 10-15 μ g total protein in 9 μ L buffer) were exposed to ABP 4 (10x stock in DMSO) at indicated concentrations for 1 h at 37 °C. Residual β 1c/ β 1i activity is labelled by Cy5-NC-001 (100 nM end concentration). SDS-PAGE analysis is performed as described above.

Determination of kinetic constants

Raji cell lysates (10 μ g/ 9 μ L) were incubated with increasing concentrations of ABP 3 (160, 320, 640, 1280, 2560, 5120 nM) for different lengths of time (0, 1, 2, 5 min). The reaction was stopped by snap-freezing in liquid nitrogen and while still frozen, the denaturing sample buffer is added. Next, SDS-PAGE analysis is performed as described in the general methods. Intensities of bands were measured by fluorescent densitometry and normalized to full labelling. When the Log (% activity) is plotted versus time, a straight line is observed, from which the first order rate constants (K_{obs}) can be derived for each concentration. K_{obs} were plotted versus probe concentration, from which inhibition constants K_i and K_{inact} were calculated using Graphpad Prism software. See chapter 2, supporting figure S2 for example.

References

1. Orłowski, M. The multicatalytic proteinase complex, a major extralysosomal proteolytic system. *Biochemistry* **29**, 10289-97 (1990).
2. Kisselev, A.F. et al. The caspase-like sites of proteasomes, their substrate specificity, new inhibitors and substrates, and allosteric interactions with the trypsin-like sites. *J. Biol. Chem.* **278**, 35869-77 (2003).
3. Huber, E.M. et al. Systematic analyses of substrate preferences of 20S proteasomes using peptidic epoxyketone inhibitors. *J. Am. Chem. Soc.* **137**, 7835-7842 (2015).
4. Britton, M. et al. Selective inhibitor of proteasome's caspase-like sites sensitizes cells to specific inhibition of chymotrypsin-like sites. *Chem. Biol.* **16**, 1278-1289 (2009).
5. Verdoes, M. et al. A panel of subunit-selective activity-based proteasome probes. *Org. Biomol. Chem.* **8**, 2719-2727 (2010).
6. Verdoes, M. et al. Acetylene functionalized BODIPY dyes and their application in the synthesis of activity based proteasome probes. *Bioorg. Med. Chem. Lett.* **17**, 6169-71 (2007).

Towards β 2 selective inhibitors with reduced basicity

Introduction

Proteasomes are large proteolytic machineries responsible for the degradation of the majority of proteins in eukaryotic cells. Inhibition of protein degradation through blockage of the proteolytic sites of the proteasome is cytotoxic for certain cancers. Bortezomib and carfilzomib are approved drugs for the treatment of multiple myeloma (MM) and mantle cell lymphoma, while various proteasome inhibitors are currently being evaluated in clinical trials for a variety of cancers. Constitutive proteasomes, which are expressed in every cell, have three different proteolytic activities, namely caspase-like (β 1c), trypsin-like (β 2c) and chymotrypsin-like (β 5c). Immune cells and cells exposed to inflammatory cytokines, express an additional proteasome-type, termed immunoproteasome, in which β 1i, β 2i and β 5i replace β 1c, β 2c and β 5c as catalytic activities. These subunits have slightly changed substrate specificities compared to their constitutive counterparts. The chymotryptic activities of the proteasome (β 5c and β 5i) have long been considered to be the only suitable subunits to target for drug development and bortezomib, carfilzomib and various clinical candidates were developed to target the β 5 subunits.¹ However, bortezomib efficiently inhibits β 1c and β 1i with similar potency as the β 5 active sites,² while carfilzomib inhibits both β 1 and β 2 activities at higher concentrations (see also chapter 3). It has been demonstrated that selective β 5 inhibition is not cytotoxic to most MM cell lines, but that partial co-inhibition of either β 1 or β 2 is necessary for cytotoxicity.³ In order to be able to investigate the effect of β 2 inhibition on MM cells, selective β 2 inhibitors have been developed. The first in-class β 2 selective inhibitors bears an arginine residue at P1 and/or P3 (NC-002 and NC-022, Figure 1). While NC-022 was more potent than NC-002 against purified proteasomes, it suffered from poor cell permeability caused by two positively charge Arg residues. Using NC-002 it was shown for the first time that selective β 2 inhibition sensitizes MM cells to bortezomib and carfilzomib.⁴ However, to overcome the lability of the arginine epoxyketone moiety (intramolecular attack of the guanidine group to the epoxyketone moiety), low yielding synthesis and poor cell

permeability in solid tumours, a second generation $\beta 2$ inhibitor was developed (LU-102, Figure 1).⁵ LU-102 bears a (4)-aminomethyl-phenylalanine (4-CH₂NH₂)Phe vinyl sulfone at P1, which can be straightforwardly synthesized on large scale and shows greater stability than the Arg epoxyketone of NC-002. Introduction of a P3 4-(CH₂NH₂)Phe in LU-112 further increased the potency and selectivity in lysate compared to LU-102, but dramatically impaired cell permeability (Figure 1).

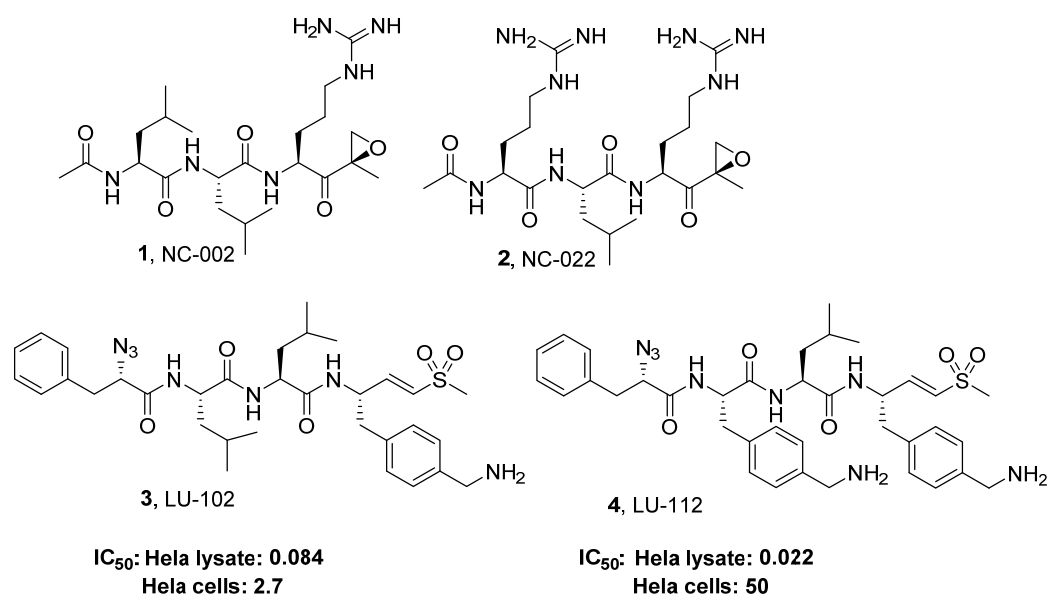
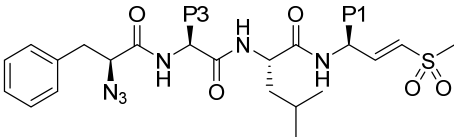


Figure 1. Structures of $\beta 2$ selective inhibitors. IC₅₀ values (μ M) have been determined in HeLa cell lysates (1 h treatment) or intact HeLa cells (4 h treatment).⁵

With LU-102 it has been shown that selective $\beta 2$ inhibition does not only sensitize MM cells to bortezomib and carfilzomib⁵, but also overcomes resistance to bortezomib and carfilzomib, a major problem which arises during treatment of patients with proteasome inhibitors.⁶ While LU-102 shows nanomolar potency in cell lysates, much higher IC₅₀ values are found in living cells.^{6, 7} Therefore, high concentrations of LU-102 are necessary to achieve efficient $\beta 2$ inhibition. In order to increase the cell permeability, one possibility is to lower the charge of the molecule at physiological pH. For this, basic amino acids with pK_a closer to physiological pH could be incorporated. In this chapter, amine-containing amino acids with various pK_a values are explored. In table 1 the structures of compounds and associated pK_a values described in this chapter are shown. The electron withdrawing properties of the double (Lys(4-ene)), triple (Lys(4-yn)) or amide bond (diaminopropionic acid-Gly, Dap(Gly)) in the Lys analogues cause significantly lower pK_a values of the ϵ -amine compared to Lys.⁸



Compound	P1	P3	Compound	P1	P3
3, (LU-102)			10		
5			11		
6			12		
7			13		
8			14		
9					
$pK_a =$					
	9.3	9.7	8.9	8.1	6.5

Table 1. Structures of compounds synthesized in this study. pK_a values of conjugated acids are shown.⁸

Synthesis

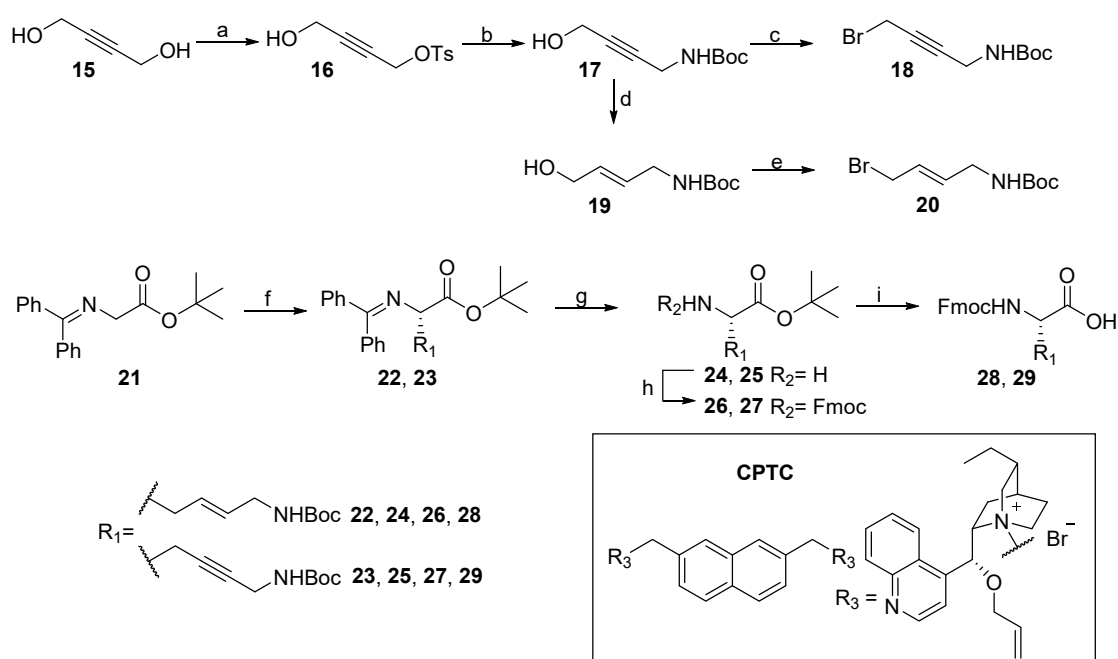
This section describes the synthesis of compounds 5-14. Since no syntheses of asymmetric L-Lys(4-ene) or L-Lys(4-yn) exist, an enantioselective synthesis for both amino acids was developed, with as key step the catalytic enantioselective phase-transfer alkylation of a glycine derivative. Also the synthesis of the amide bond containing analogue of Lys is described (Dap(Gly)), which is made by peptide coupling between the β -amine of L-diaminopropionic acid (Dap) and Gly. The appropriate building blocks of the Lys analogues and

His could be converted to their corresponding vinyl sulfones and were incorporated at the P1, P3 or at P1 and P3 of tetrapeptide vinyl sulfones.

Synthesis of L-Lys(4-ene) or L-Lys(4-yn) containing inhibitors

The synthesis of α -amino acids by catalytic enantioselective phase transfer alkylation of a glycine derivative has been highly optimized by Park *et al.*⁹ They developed a dimeric cinchona-derived chiral phase transfer catalyst (CPTC, Scheme 1) and applied this in the synthesis of a wide range of α -amino acids, including allyl-Gly and propargyl-Gly. Based on these results, it was envisioned that this method could also be applied to the enantioselective synthesis of L-Lys(4-ene) and L-Lys(4-yn). In order to do so, first the appropriate bromides **18** and **20** were synthesized, which could be used in the chiral phase transfer alkylation of glycine derivative **21** (Scheme 1). Subsequent protection group manipulations provided the required building blocks **28** and **29**, which could be used for further synthesis of the desired inhibitors (Scheme 2).

The synthesis of bromides **18** and **20** commenced with the mono-tosylation of diol **15**. Next, the O-Ts moiety of compound **16** was substituted by ammonia¹⁰ followed by Boc protection of the amine providing compound **17**. In order to obtain the *E*-alkene, propargyl alcohol **17** could be selectively reduced by LiAlH₄ to give allyl alcohol **19**.^{11, 12}



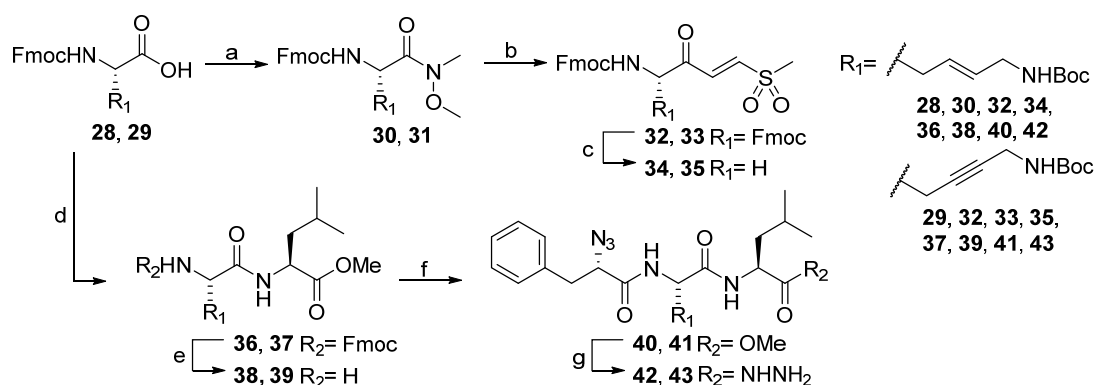
Scheme 1. Synthesis of lysine(4-ene) and lysine(4-yn) building blocks. Reagents and conditions: a. TsCl, pyridine, DCM, 63%; b. 1. 25% aq. NH₃; 2. Boc₂O, Et₃N, THF, DCM, 42%; c. PPh₃, CBr₄, DCM, 0°C 68%; d. LiAlH₄, THF, Δ , 38%; e. PPh₃, CBr₄, DCM, 0°C, 58%; f. **19** or **20**, CPTC, Tol/CHCl₃, 50% aq. KOH **22**: 84%, 79% ee; **23**: 84%, 80% ee; g. 15% aq. citric acid, THF, 0°C-rt; h. FmocOSu, DiPEA, DCM, **26**: 83%, **27**: 89% (over steps g/h); i. 1. TFA; 2. Boc₂O, DiPEA, MeCN, **28**: 82%, **29**: 63%

The low yielding reduction of alkyne **17** to alkene **19** is possibly caused by the harsh conditions (strong reducing agent and elevated temperature), which could result in partial Boc removal. Alcohol **17** and **19** were reacted in an Appel reaction providing bromides **18** and **20**. Although several steps towards the bromides were rather low-yielding, the reactions could be easily performed on large scale and sufficient quantities of both bromides were obtained.

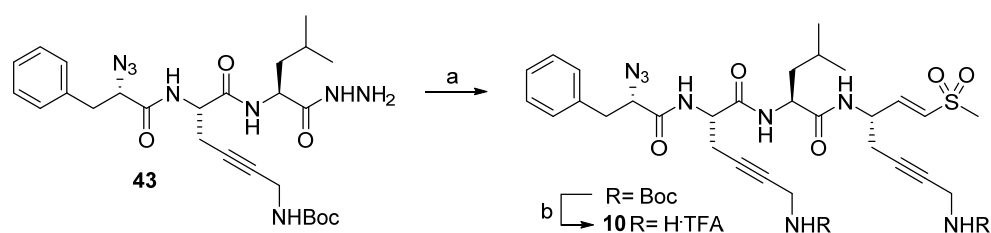
Both bromides were used in the chiral phase transfer alkylation of Gly-derivative **21**, providing compounds **22** and **23** in high yields and good enantiomeric excess (*ee*, 79% for **22** vs. 80% for **23**), as determined by chiral HPLC analysis.⁹ Mildly acidic hydrolysis of the imine provided amines **24** and **25**, which were Fmoc protected yielding compounds **26** and **27**. Subsequent Boc and t-Bu ester removal by treatment with TFA and Boc protection of the ϵ -amine, yielded building blocks **28** and **29** in good yields.

For the synthesis of the corresponding vinyl sulfones, **28** and **29** were converted to Weinreb amides **30** and **31** (Scheme 2). Using standard procedures for the synthesis of vinyl sulfones⁵, the Weinreb amides were reduced to the aldehydes directly followed by a Horner-Wadsworth-Emmons reaction to provide Fmoc protected vinyl sulfones **32** and **33**. The Fmoc group could be removed by treatment with diethylamine, providing free amines **34** and **35**.

For the incorporation of L-Lys(4-ene) or L-Lys(4-yn) at the P3 site, building blocks **28** and **29** were coupled to H-Leu-OMe by a standard peptide coupling yielding dipeptides **36** and **37** (Scheme 2). Subsequent Fmoc removal, peptide coupling to N₃Phe-OH and hydrazinolysis of the methylester provided hydrazides **42** and **43**. Standard azide couplings (see Scheme 3 for an example) between hydrazides **42**, **43**, or N₃Phe-Leu-Leu-NHNH₂⁵ and vinyl sulfones **34**, **35**, or H-Leu-VS followed by Boc removal provided the desired final compounds.



Scheme 2. Synthesis of Lys(4-ene) and Lys(4-yn) vinyl sulfones and peptide hydrazides. Reagents and conditions: a. HCTU, N,O-dimethyl hydroxylamine, **30**: 100%, **31**: 85%; b. 1. LiAlH₄, THF. 2. diethyl((methylsulfonyl)-methyl)-phosphonate, NaH, THF, **32**: 40%, **33**: 70%; c. Et₂NH, MeCN, **34**: 70%, **35**: 47%; d. H-Leu-OMe, HCTU, DiPEA, DCM, **36**: 96%, **37**: 76%; e. Piperidine, DMF, **38**: 94%, **39**: 100%; f. N₃Phe-OH, HCTU, DiPEA, DCM, **40**: 60%, **41**: 91%; g. hydrazine monohydrate, MeOH, 100%.

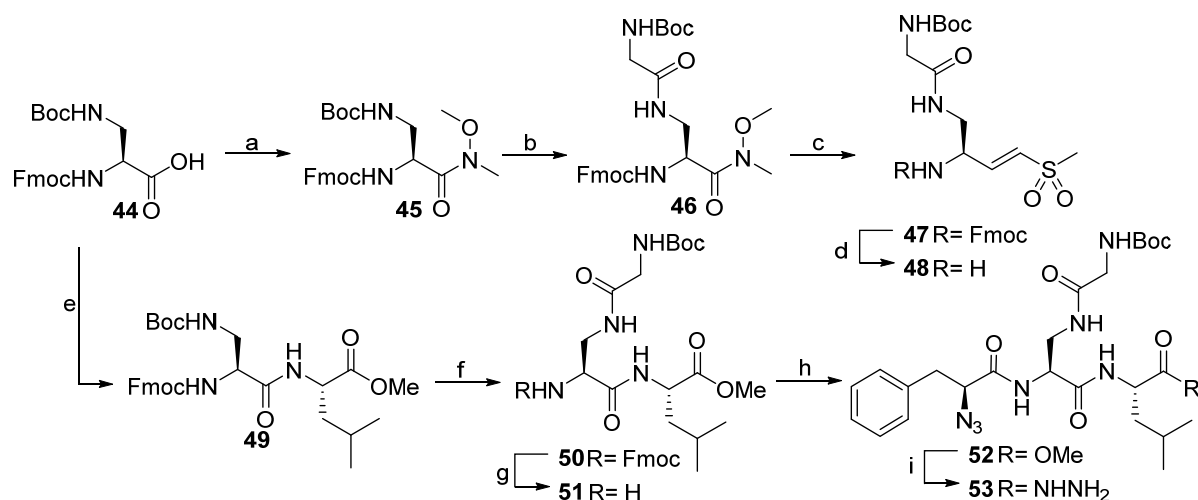


Scheme 3. Synthesis of compound 10 as example of an azide coupling followed by Boc removal. Reagents and conditions: a. 1. $t\text{BuONO}$, HCl, DMF. 2. H-Lys(4-yn)-VS, DiPEA; b. TFA, 79% over 2 steps

Synthesis of Dap(Gly) containing inhibitors

The synthesis of Dap(Gly) vinyl sulfone and peptide hydrazide for the synthesis of P3 Dap(Gly) compounds is shown in Scheme 4. The synthesis of the vinyl sulfone commenced with the conversion of commercially available Fmoc-Dap(Boc)-OH **44** to Weinreb amide **45**. Subsequent Boc removal and peptide coupling with Boc-Gly-OH provided compound **46**, followed by conversion of the Weinreb amide to the vinyl sulfone using similar procedures as described above, eventually yielding vinyl sulfone free amine **48**.

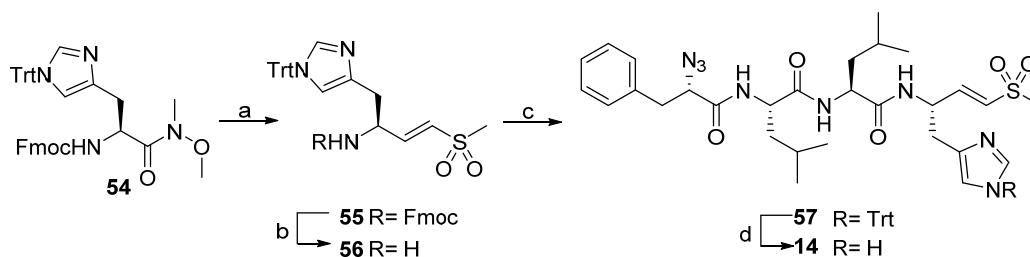
For the synthesis of the peptide hydrazide, Fmoc-Dap(Boc)-OH **44** was first coupled to H-Leu-OMe, followed by Boc removal and coupling of Boc-Gly-OH, providing dipeptide **50**. Fmoc removal, peptide coupling to N₃Phe-OH and hydrazinolysis of the methylester resulted in peptide hydrazide **53**. The desired inhibitors with Dap(Gly) at P1 and/or P3 were obtained by standard azide couplings between the appropriate hydrazides and vinyl sulfones, and Boc removal (in the same way as shown in Scheme 3).



Scheme 4. Synthesis of Dap(Gly) vinyl sulfone and peptide hydrazide. Reagents and conditions: a. HCTU, N,O-dimethyl hydroxylamine, 96%; b. HCTU, Boc-Gly-OH, DiPEA, DCM, 100%. c. 1. LiAlH_4 , THF. 2. diethyl((methylsulfonyl)-methyl)-phosphonate, NaH, THF, 43%; d. Et_2NH , MeCN, 100%; e. HCTU, H-Leu-OMe, DiPEA, DCM, 94%; f. 1. TFA; 2. HCTU, Boc-Gly-OH, DiPEA, DCM, 100% g. Piperidine, DMF, 100%; h. N₃Phe, HCTU, DiPEA, DCM, 68%; i. hydrazine monohydrate, MeOH, 100%.

Synthesis of His containing inhibitor **14**

The synthesis of P1 His compound **14** is depicted in Scheme 5. The properly protected His Weinreb amide¹³ **54** was converted to the vinyl sulfone, using similar procedures as described above. Vinyl sulfone free amine **56** was reacted in an azide coupling reaction with N₃Phe-Leu-Leu-NHNH₂ to provide tetrapeptide vinyl sulfone **57**. Subsequent trityl removal by TFA with the help of TIPS as cation scavenger yielded compound **14**.



Scheme 5. Synthesis of compound 14. Reagents and conditions: a. 1. LiAlH₄, THF. 2. diethyl((methylsulfonyl)-methyl)-phosphonate, NaH, THF, 65%; b. Et₂NH, MeCN, 64%; c. 1. N₃Phe-Leu-Leu-NHNH₂, tBuONO, HCl, DMF. 2. **56**, DiPEA, 53%; d. TFA, TIPS, DCM, 38%.

Biological evaluation

All newly synthesized compounds were evaluated for proteasome inhibition in Raji cell lysates (a human B-cell lymphoma cell line expressing constitutive and immunoproteasomes) and compared to LU-102 **3** by activity-based protein profiling (ABPP) (Figure 2). Cell lysates were incubated with inhibitors at four different concentrations (0.1, 1, 10 and 100 μM) for 1 h, followed by labelling of residual proteasome activity by the activity-based probe cocktail as described in chapter 3.⁷ For all compounds, a dramatic loss of potency against the $\beta 2$ subunits is found. Compounds **5** (P1: Lys(4-ene)) and compounds **8** (P1: Lys(4-yn)) both show some $\beta 2$ selectivity, although a more than 10 fold decrease in potency was observed. Incorporation of Lys(4-ene) or Lys(4-yn) at P3 or at P1 and P3 resulted in compounds with even lower potency (compounds **6**, **7**, **9**, **10**). The compounds with Dap(Gly) at P1 and/or P3 (**11**, **12**, **13**) were all very weak inhibitors, with almost no selectivity for $\beta 2$ over $\beta 5$. Finally, compounds **14** (P1: His) inhibited $\beta 2$ with similar potency as compounds **5** and **8** (complete inhibition at 10 μM), however, with poor selectivity over the $\beta 5$ subunits. Since all compounds showed much lower activity than LU-102 (**3**), it was anticipated that these compounds would also show poor activity in living cells. Indeed, compounds **8**, **9**, and **10** did not display any inhibitory activity in living Hela cells up to 100 μM (data not shown).

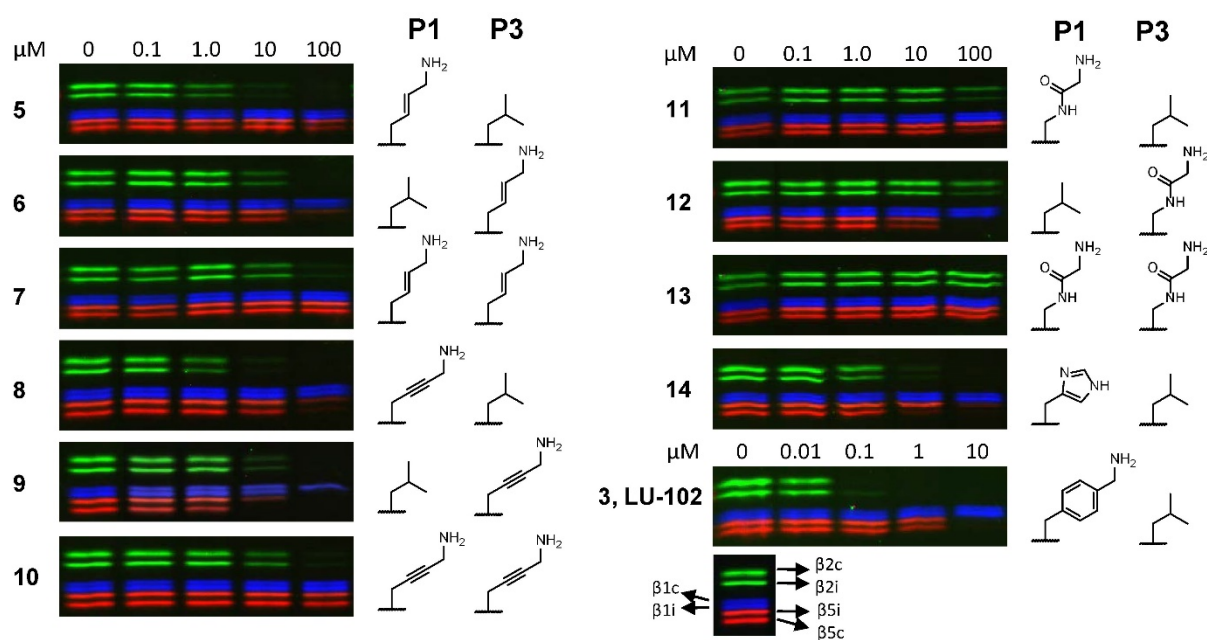


Figure 2. Inhibition profiles of compounds 5-14, compared to 3 (LU-102) in Raji lysates.

Discussion

All synthesized tetrapeptide vinyl sulfones showed reduced activity against $\beta 2$ compared to LU-102 (**3**). The low activity of these inhibitors could originate from several factors, such as lower basicity of the amine, lack of interactions due to loss of the aromatic ring or a lack of interactions between the side chain amine and the $\beta 2$ subunit due to a shorter side chain of the Lys analogues compared to the benzylamine side chain in LU-102.

The crystal structure of LU-102 in complex with yeast proteasome and superposition on mammalian constitutive proteasomes (murine and bovine) showed that the amino-group interacts with Asp53 in the S1 pocket of the $\beta 2$ subunit via hydrogen bonding.⁵ Due to absence of an acidic residue in the S1 pockets of $\beta 1$ and $\beta 5$, these interactions are the driving force for the $\beta 2$ selectivity of compounds equipped with P1 basic residues. So in order to maintain $\beta 2$ selectivity, compounds should have a strong interaction with Asp53. Compounds **5** (P1: Lys(4-ene) and **8** (P1: Lys(4-yn) show similar potency, indicating that the lower pK_a value of Lys(4-yn) compared to Lys(4-ene) does not result in additional loss of activity suggesting that both residues are able to interact with Asp53. In contrast, compound **6** shows a much lower activity, which might indicate that lower basicity of the amine (pK_a 8) is too low in order to establish a strong interaction with Asp53. However, the loss of activity of compound **6** could also be caused by unfavourable interactions between the side chain amide bond and the $\beta 2$ subunit or by a changed orientation of the side chain caused by the amide.

The S1 pocket of $\beta 2$ is spacious and therefore able to accommodate the P1 aromatic residue of LU-102. Absence of interactions between the much less sterically demanding Lys analogues

and the protein could be a reason for the lower potency of compounds **5** and **8**. Another important factor is the length of the side chains, which is one carbon atom shorter in case of the Lys analogues compared to the 4-aminomethyl-Phe residue of LU-102. This most likely results in a larger distance between Asp53 and the P1 amine of the inhibitors, causing a weaker interaction and thus lower potency of the compounds. In fact, in a previous study, Lys at P1 also showed a ten-fold lower potency compared to LU-102⁵, indicating that the low potency of compounds **5** and **8** is not a result of the lower basicity of the amine.

In case of His at P1 (compound **14**) the distance between Asp53 and the basic residue is even larger, most likely resulting in the absence of an interaction between the imidazole moiety and Asp53. However, compound **14** is still moderately active indicating that His at P1 might be stabilized by other interactions, similarly to the phenyl group of LU-102. Interestingly, compound **14** shows a 10-fold preference for β 5c over β 5i. This was unexpected, since β 5i prefers large (see chapter 5)¹⁴ and β 5c small (see chapter 7) residues at P1.¹⁵ This selectivity probably originates from a combination of Leu at P3 and His at P1. Leu at P3 is disfavoured by β 5i, see also chapter 4 in which all compounds with hydrophobic P1 residues and Leu at P3 showed selectivity for β 5c over β 5i.¹⁶ His at P1 might, due to its relatively small size, suffer less from unfavourable interactions with the relatively small S1 pocket of β 5c compared to the Lys analogues and 4-aminomethyl-Phe of LU-102.

The superposition of the crystal structure of LU-112 in complex with yeast proteasome on mammalian proteasome (murine and bovine) showed that the P3 amine group did not interact with an acidic residue of the proteasome. However, the P3 amine group is stabilized by several surrounding polar residues. These interactions can probably not be established with the shorter P3 residues of compound **6**, **7**, **9**, **10**, **12** and **13**. In addition, similarly to the S1 pocket, the S3 pocket is also spacious and the P3 phenyl moiety of LU-112 is stabilized by several van der Waals interactions.⁵ However, the P3 Leu moiety of LU-102 does not show any favourable interaction with the protein. Likely, compounds with Lys analogues at P3 do also not benefit from van der Waals interactions with the protein and do therefore not show increased potency.

Conclusion

In order to obtain β 2 selective inhibitors that are less charged at physiological pH, several Lys analogues with lower pK_a values were explored as basic residues in potential β 2 targeting inhibitors. A straightforward enantioselective synthesis of Lys(4-ene) and Lys(4-yn) was developed, which gives access to amino acid building blocks suitable for standard Fmoc chemistry. In addition, these amino acids could be converted to their corresponding vinyl sulfones and were incorporated as P1 and/or P3 residues in tetrapeptide vinyl sulfones.

Moreover, a Lys analogue equipped a peptide bond in the side chain (Dap(Gly)) was incorporated as P1 and/or P3 residues in potential proteasome inhibitors. Finally, His was explored as basic residue at P1. Evaluation by ABPP revealed that all compounds targeted β 2 with much lower potency than LU-102. The low activity of compounds with Lys(4-ene) and Lys(4-ene) at P1 and/or P3 is most likely not caused by the lower pK_a value of the amine group, but by the suboptimal distance between the side chain amine and Asp53 of β 2 and by the lack of van der Waals interactions.

Experimental

Synthetic procedures

General procedures

Acetonitrile (ACN), dichloromethane (DCM), N,N-dimethylformamide (DMF), methanol (MeOH), diisopropylethylamine (DiPEA) and trifluoroacetic acid (TFA) were of peptide synthesis grade, purchased at Biosolve, and used as received. All general chemicals (Fluka, Acros, Merck, Aldrich, Sigma, Iris Biotech) were used as received. Column chromatography was performed on Screening Devices b.v. Silica Gel, with a particle size of 40-63 μ m and pore diameter of 60 Å. TLC analysis was conducted on Merck aluminium sheets (Silica gel 60 F254). Compounds were visualized by UV absorption (254 nm), by spraying with a solution of $(\text{NH}_4)_6\text{Mo}_7\text{O}_{24}\cdot 4\text{H}_2\text{O}$ (25 g/L) and $(\text{NH}_4)_4\text{Ce}(\text{SO}_4)_4\cdot 2\text{H}_2\text{O}$ (10 g/L) in 10% sulphuric acid, a solution of KMnO_4 (20 g/L) and K_2CO_3 (10 g/L) in water, or ninhydrin (0.75 g/L) and acetic acid (12.5 mL/L) in ethanol, where appropriate, followed by charring at ca. 150 °C. ^1H and ^{13}C NMR spectra were recorded on a Bruker AV-300 (MHz), AV-400 (400 MHz) or AV-600 (600 MHz) spectrometer. Chemical shifts are given in ppm (δ) relative to tetramethylsilane, CD_3OD or CDCl_3 as internal standard. High resolution mass spectra were recorded by direct injection (2 μ L of a 2 μ M solution in water/acetonitrile 50/50 (v/v) and 0.1% formic acid) on a mass spectrometer (Thermo Finnigan LTQ Orbitrap) equipped with an electrospray ion source in positive mode (source voltage 3.5 kV, sheath gas flow 10, capillary temperature 250 °C) with resolution $R = 60,000$ at m/z 400 (mass range $m/z = 150$ -2,000) and dioctylphthalate ($m/z = 391.28428$) as a "lock mass". The high resolution mass spectrometer was calibrated prior to measurements with a calibration mixture (Thermo Finnigan). LC-MS analysis was performed on a Finnigan Surveyor HPLC system with a Gemini C_{18} 50 \times 4.60 mm column (detection at 200-600 nm), coupled to a Finnigan LCQ Advantage Max mass spectrometer with ESI. The applied buffers were H_2O , ACN and 1.0% aq. TFA. Method: xx \rightarrow xx% MeCN, 13.0 min (0 \rightarrow 0.5 min: 10% MeCN; 0.5 \rightarrow 8.5 min: gradient time; 8.5 \rightarrow 10.5 min: 90% MeCN; 10.5 \rightarrow 13.0 min: 10% MeCN). HPLC purification was performed on a Gilson HPLC system coupled to a Phenomenex Gemini 5 μ m 250 \times 10 mm column and a GX281 fraction collector. Enantiomeric excess (*ee*) was determined using chiral HPLC analysis (Daicell Chiralcel OD column (250 \times 5.4 mm), hexane/isopropanol (99/1), flowrate: 1 mL/min, detection: UV254). All tested compounds are >95% pure on the basis of LC-MS and NMR.

General procedure for azide couplings.

Compounds **5-14** were prepared via azide coupling of peptide hydrazides and properly deprotected vinyl sulfone amines. The appropriate hydrazide was dissolved in DMF or 1:1 DMF:DCM (v/v) and cooled to -30°C. *t*BuONO (1.1 equiv.) and HCl (4M solution in 1,4-dioxane, 2.8 equiv.) were added, and the mixture was stirred for 3h at -30 °C after which TLC analysis (10% MeOH/DCM, v/v) showed complete consumption of the starting material. The vinyl sulfone as a free amine was added to the reaction mixture as a solution in DMF. DiPEA (5 equiv.) was added to the reaction mixture, and this mixture was allowed to warm to RT slowly overnight. The mixture was diluted with EtOAc and extracted with H_2O (3 \times). The organic layer was dried over MgSO_4 and purified by flash column chromatography (1-5% MeOH in DCM) and HPLC purification (if necessary).

General procedure for peptide couplings

Free acid (1.2 equiv.), HCTU (1.2 equiv.) and free amine (1 equiv.) are dissolved in DCM (0.1 M), followed by the addition of DiPEA (3.5 equiv or 4.5 equiv in case of 2-morpholinoacetic acid HCl). After stirring overnight (or alternatively 1-3 h, until completion), the reaction mixture is concentrated and re-dissolved in EtOAc, washed with 1 N HCl (2x), sat. NaHCO_3 (2x) and brine (in case of morpholino acetic acid coupling, no 1N HCl washings). The organic layer is dried over Na_2SO_4 , filtered and concentrated, followed by purification by column chromatography.

General procedure for Boc removal

Boc protected compounds are treated with TFA (0.1 M) for 30 minutes, followed by co-evaporation with toluene (2x).

General procedure for Fmoc removal

Fmoc protected compounds are treated dissolved in 20% piperidine in DMF and stirred until completion of the reactions (about 30 minutes), followed by concentration of the reaction mixture and purification by column chromatography.

N₃Phe-Leu-Leu-Lys(-4-ene)-VS (5)

This compound was obtained by the general protocol for azide coupling on a 60 μmol scale. Purification by column chromatography (0→2% MeOH/DCM) provided the Boc protected compound, which was deprotected using the standard procedure for Boc removal, providing the title compound after purification by HPLC followed by lyophilization (6.1 mg, 8.5 μmol, 14%). ¹H NMR (600 MHz, MeOD) δ 7.39 – 7.24 (m, 5H), 6.89 – 6.85 (m, 1H), 6.84 – 6.67 (m, 1H), 5.97 – 5.82 (m, 1H), 5.82 – 5.63 (m, 1H), 4.73 (dtd, *J* = 9.1, 5.2, 1.6 Hz, 1H), 4.42 – 4.30 (m, 2H), 4.30 – 4.20 (m, 1H), 3.60 – 3.55 (m, 2H), 3.27 (dd, *J* = 14.0, 4.9 Hz, 1H), 3.05 (dd, *J* = 14.1, 8.6 Hz, 1H), 3.03 (s, 3H), 2.58 (dddd, *J* = 10.7, 9.5, 5.4, 2.7 Hz, 1H), 2.51 – 2.37 (m, 1H), 1.79 – 1.53 (m, 6H), 1.08 – 0.89 (m, 12H). ¹³C NMR (151 MHz, MeOD) δ 174.89, 174.81, 174.48, 171.83, 146.86, 146.65, 137.83, 134.27, 134.14, 131.84, 131.67, 130.49, 130.44, 129.64, 129.60, 128.10, 128.07, 126.50, 126.33, 65.45, 53.97, 53.94, 53.45, 50.37, 42.75, 42.69, 42.18, 42.11, 41.55, 41.50, 38.64, 37.45, 25.98, 25.81, 23.45, 23.35, 22.00, 21.79. LC-MS (linear gradient 10→90% MeCN, 0.1% TFA, 13.0 min Rt (min): 6.15 (ESI-MS (*m/z*): 604.06 (M+H⁺)). HRMS: calculated for C₂₉H₄₆N₇O₅S 604.32756 [M+H⁺]; found 604.32751.

N₃Phe-Lys(-4-ene)-Leu-Leu-VS (6)

This compound was obtained by the general protocol for azide coupling on a 50 μmol scale. Purification by column chromatography (0→2% MeOH/DCM) provided the Boc protected compound, which was deprotected using the standard procedure for Boc removal, providing the title compound after purification by HPLC followed by lyophilization (7.04 mg, 9.7 μmol, 20%). Isolated with 15% *cis* isomer. Peaks reported correspond to *trans* isomer. ¹H NMR (600 MHz, MeOD) δ 7.35 – 7.19 (m, 5H), 6.80 (dd, *J* = 15.2, 5.3 Hz, 1H), 6.60 (dd, *J* = 15.2, 1.6 Hz, 1H), 5.83 – 5.72 (m, 1H), 5.72 – 5.54 (m, 1H), 4.61 (dtd, *J* = 10.3, 5.1, 1.6 Hz, 1H), 4.41 (t, *J* = 7.1 Hz, 1H), 4.34 (dd, *J* = 10.0, 5.2 Hz, 1H), 4.14 (dd, *J* = 8.6, 5.2 Hz, 1H), 3.49 (d, *J* = 6.5 Hz, 2H), 3.20 (dd, *J* = 13.9, 5.3 Hz, 1H), 3.02 – 2.95 (m, 1H), 2.98 (s, 3H), 2.52 (dd, *J* = 13.8, 7.4 Hz, 1H), 2.44 (q, *J* = 6.8 Hz, 1H), 1.77 – 1.41 (m, 6H), 1.04 – 0.86 (m, 12H). ¹³C NMR (151 MHz, MeOD) δ 174.51, 172.69, 171.62, 148.43, 137.79, 133.81, 130.85, 130.42, 129.63, 128.11, 126.17, 65.35, 54.12, 53.58, 53.54, 43.08, 42.75, 42.13, 41.80, 38.73, 36.06, 25.95, 25.82, 23.40, 23.38, 21.98, 21.91. LC-MS (linear gradient 10→90% MeCN, 0.1% TFA, 13.0 min Rt (min): 6.12 (ESI-MS (*m/z*): 604.13 (M+H⁺)). HRMS: calculated for C₂₉H₄₆N₇O₅S 604.32756 [M+H⁺]; found 604.32758.

N₃Phe-Lys-4-ene-Leu-Lys(-4-ene)-VS (7)

This compound was obtained by the general protocol for azide coupling on a 50 μmol scale. Purification by column chromatography (0→2% MeOH/DCM) provided the Boc protected compound, which was deprotected using the standard procedure for Boc removal, providing the title compound after purification by HPLC followed by lyophilization (8.6 mg, 10.2 μmol, 20%). ¹H NMR (600 MHz, MeOD) δ 7.39 – 7.33 (m, 2H), 7.33 – 7.24 (m, 3H), 6.87 (dd, *J* = 15.2, 5.1 Hz, 1H), 6.70 (dd, *J* = 15.2, 1.7 Hz, 1H), 5.97 – 5.79 (m, 2H), 5.77 – 5.64 (m, 2H), 4.71 (dtd, *J* = 9.0, 5.6, 1.7 Hz, 1H), 4.42 (dd, *J* = 8.0, 6.6 Hz, 1H), 4.37 – 4.30 (m, 1H), 4.23 – 4.15 (m, 1H), 3.56 (dd, *J* = 19.1, 6.6 Hz, 4H), 3.25 (dd, *J* = 14.0, 5.2 Hz, 1H), 3.04 (s, 3H), 3.07 – 3.01 (m, 1H), 2.63 – 2.54 (m, 2H), 2.54 – 2.42 (m, 2H), 1.81 – 1.67 (m, 2H), 1.58 (ddd, *J* = 13.8, 8.9, 4.6 Hz, 1H), 1.04 (d, *J* = 6.5 Hz, 3H), 0.99 (d, *J* = 6.5 Hz, 3H). ¹³C NMR (151 MHz, MeOD) δ 174.57, 173.21, 171.82, 146.79, 137.80, 134.17, 133.77, 131.73, 130.46, 130.42, 129.64, 128.12, 126.45, 126.27, 65.30, 54.53, 53.67, 50.53, 42.70, 42.18, 42.12, 41.59, 40.40, 38.73, 37.29, 35.81,

25.95, 23.46, 21.72. LC-MS (linear gradient 10 \rightarrow 90% MeCN, 0.1% TFA, 13.0 min Rt (min): 4.77/4.84 different salt-forms (ESI-MS (m/z): 617.07 (M+H⁺)). HRMS: calculated for C₂₉H₄₅N₈O₅S 617.32281 [M+H⁺]; found 617.32275.

N₃Phe-Leu-Leu-Lys(-4-yl)-VS (8)

This compound was obtained by the general protocol for azide coupling on a 100 μ mol scale. Purification by column chromatography (0 \rightarrow 1.5% MeOH/DCM) provided the Boc protected compound, which was deprotected using the standard procedure for Boc removal, providing the title compound (20.4 mg, 28.5 μ mol, 92 %) as a white powder after lyophilisation. ¹H NMR (400 MHz, MeOD) δ 7.35 – 7.20 (m, 5H), 6.87 (dd, *J* = 15.3, 5.0 Hz, 1H), 6.73 (dd, *J* = 15.2, 1.5 Hz, 1H), 4.81 – 4.71 (m, 1H), 4.35 (dd, *J* = 10.1, 4.5 Hz, 2H), 4.19 (tt, *J* = 8.6, 4.9 Hz, 1H), 3.22 (dd, *J* = 14.1, 4.8 Hz, 1H), 3.04 – 2.93 (m, 4H), 2.77 – 2.56 (m, 2H), 1.81 – 1.47 (m, 6H), 1.03 – 0.80 (m, 12H). ¹³C NMR (101 MHz, MeOD) δ 174.81, 174.49, 171.86, 145.39, 137.79, 132.53, 130.43, 129.61, 128.07, 84.22, 75.48, 65.47, 53.80, 53.47, 49.96, 42.66, 41.53, 41.41, 38.62, 30.37, 25.95, 25.79, 24.39, 23.47, 23.35, 21.95, 21.73. LC-MS (linear gradient 10 \rightarrow 90% MeCN, 0.1% TFA, 13.0 min Rt (min): 6.84 (ESI-MS (m/z): 602.7 (M+H⁺)). HRMS: calculated for C₂₉H₄₄N₇O₅S, 602.31191 [M+H⁺]; found 602.31195.

N₃Phe-Lys-4(-yl)-Leu-Leu-VS (9)

This compound was obtained by the general protocol for azide coupling on a 90 μ mol scale. Purification by column chromatography (0 \rightarrow 1.5% MeOH/DCM) provided the Boc protected compound, which was deprotected using the standard procedure for Boc removal, providing title compound (34.2 mg, 48 μ mol, 53%) as a white powder after lyophilisation. Isolated with 10% *cis* isomer. Peaks reported correspond to *trans* isomer. ¹H NMR (400 MHz, MeOD) δ 7.40 – 7.15 (m, 5H), 6.79 (dd, *J* = 15.2, 5.2 Hz, 1H), 6.60 (dd, *J* = 15.2, 1.4 Hz, 1H), 4.68 – 4.58 (m, 1H), 4.52 (t, *J* = 7.1 Hz, 1H), 4.38 (dd, *J* = 9.6, 5.3 Hz, 1H), 4.15 (dd, *J* = 8.6, 5.2 Hz, 1H), 3.74 (s, 2H), 3.20 (dd, *J* = 13.9, 5.3 Hz, 1H), 3.03 – 2.91 (m, 4H), 2.74 – 2.46 (m, 2H), 1.81 – 1.42 (m, 6H), 1.06 – 0.85 (m, 12H). ¹³C NMR (101 MHz, MeOD) δ 174.39, 171.70, 148.37, 137.72, 130.84, 130.38, 129.61, 128.09, 83.97, 75.47, 65.28, 53.40, 43.06, 42.76, 41.82, 38.78, 30.49, 25.90, 23.35, 22.86, 21.95. LC-MS (linear gradient 10 \rightarrow 90% MeCN, 0.1% TFA, 13.0 min Rt (min): 6.78 (ESI-MS (m/z): 602.7 (M+H⁺)). HRMS: calculated for C₂₉H₄₄N₇O₅S, 602.31191 [M+H⁺]; found 602.31171.

N₃Phe-Lys(-4-yl)-Leu-Lys(-4-yl)-VS (10)

This compound was obtained by the general protocol for azide coupling on a 90 μ mol scale. Purification by column chromatography (0 \rightarrow 1.5% MeOH/DCM) provided the Boc protected compound, which was deprotected using the standard procedure for Boc removal, providing the title compound (29.2 mg, 34.7 μ mol, 79%) as a white powder after lyophilisation. Isolated with 10% *cis* isomer. Peaks reported correspond to *trans* isomer. ¹H NMR (400 MHz, MeOD) δ 7.36 – 7.20 (m, 5H), 6.88 (dd, *J* = 15.2, 5.1 Hz, 1H), 6.74 (dd, *J* = 15.2, 1.5 Hz, 1H), 4.82 – 4.70 (m, 1H), 4.53 (t, *J* = 7.2 Hz, 1H), 4.37 (dd, *J* = 10.3, 4.9 Hz, 1H), 4.16 (dd, *J* = 8.6, 5.3 Hz, 1H), 3.81 – 3.69 (m, 4H), 3.21 (dd, *J* = 13.9, 5.2 Hz, 1H), 3.05 – 2.94 (m, 4H), 2.79 – 2.56 (m, 2H), 1.81 – 1.63 (m, 2H), 1.63 – 1.51 (m, 1H), 1.02 – 0.88 (m, 6H). ¹³C NMR (101 MHz, MeOD) δ 174.59, 172.11, 145.33, 137.74, 132.57, 130.40, 129.63, 128.11, 84.21, 75.55, 65.28, 53.68, 53.61, 50.09, 49.64, 42.66, 41.64, 38.79, 30.35, 25.90, 24.30, 23.47, 22.64, 21.70. LC-MS (linear gradient 10 \rightarrow 90% MeCN, 0.1% TFA, 13.0 min Rt (min): 5.51 (ESI-MS (m/z): 613.7 (M+H⁺)). HRMS: calculated for C₂₉H₄₁N₈O₅S 614.29934 [M+H⁺]; found 614.29935.

N₃Phe-Leu-Leu-Dap(Gly)-VS (11)

This compound was obtained by the general protocol for azide coupling on a 50 μ mol scale. Purification by column chromatography (0 \rightarrow 4% MeOH/DCM) provided the Boc-protected product, which was deprotected using the standard procedure for Boc removal. Purification by HPLC (30-50% MeCN, 0.1 % TFA, 10 min gradient) provided the title compound (3.16 mg, 8.6%) as a white powder after lyophilisation. ¹H NMR (600 MHz, MeOD) δ 7.34 – 7.22 (m, 5H), 6.83 (dd, *J* = 15.3, 5.1 Hz, 1H), 6.72 (dd, *J* = 15.3, 1.6 Hz, 1H), 4.80 (dtd, *J* = 8.2, 5.3, 1.4 Hz, 1H), 4.36 (dd, *J* = 9.4, 5.3 Hz, 1H), 4.27 (dd, *J* = 10.2, 4.8 Hz, 1H), 4.21 (dd, *J* = 8.4, 5.0 Hz, 1H), 3.66 (d, *J* = 3.5 Hz,

2H), 3.56 (dd, $J = 13.7, 5.4$ Hz, 1H), 3.41 (dd, $J = 13.8, 8.6$ Hz, 1H), 3.23 (dd, $J = 14.0, 5.0$ Hz, 1H), 3.04 – 2.98 (m, 4H), 1.75 – 1.64 (m, 2H), 1.61 – 1.52 (m, 4H), 1.02 – 0.88 (m, 12H). ^{13}C NMR (151 MHz, MeOD) δ 174.96, 174.74, 171.89, 168.19, 144.45, 137.81, 132.78, 130.48, 129.64, 128.11, 65.58, 53.81, 53.66, 51.12, 42.88, 42.61, 41.67, 41.59, 41.32, 38.65, 25.98, 25.80, 23.47, 23.37, 21.97, 21.72. LC-MS (linear gradient 10 \rightarrow 90% MeCN, 0.1% TFA, 13.0 min): R_t (min): 5.97 (ESI-MS (m/z): 621.33 ($\text{M}+\text{H}^+$)). HRMS: calculated for $\text{C}_{28}\text{H}_{45}\text{N}_8\text{O}_6\text{S}$ 621.31773 [$\text{M}+\text{H}^+$] $^+$; found 621.31744

N₃Phe-Dap(Gly)-Leu-Leu-VS (12)

This compound was obtained by the general protocol for azide coupling on a 50 μmol scale. Purification by column chromatography (0 \rightarrow 4% MeOH/DCM) provided the Boc-protected product, which was deprotected using the standard procedure for Boc removal. Purification by HPLC (30-50% MeCN, 0.1 % TFA, 10 min gradient) provided the title compound (7.71 mg, 21%) as a white powder after lyophilisation. Isolated with 10% *cis* isomer. Peaks reported correspond to *trans* isomer. ^1H NMR (600 MHz, MeOD) δ 7.33 – 7.23 (m, 5H), 6.83 (dd, $J = 15.2, 5.4$ Hz, 1H), 6.64 (dd, $J = 15.2, 1.5$ Hz, 1H), 4.64 (ddt, $J = 10.3, 5.2, 2.6$ Hz, 1H), 4.53 (t, $J = 6.1$ Hz, 1H), 4.37 (t, $J = 7.6$ Hz, 1H), 4.19 – 4.14 (m, 1H), 3.67 – 3.64 (m, 2H), 3.63 – 3.57 (m, 1H), 3.53 (dd, $J = 13.9, 5.6$ Hz, 1H), 3.23 (dd, $J = 13.9, 5.2$ Hz, 1H), 3.00 (d, $J = 8.9$ Hz, 1H), 2.99 (s, 3H), 1.75 – 1.67 (m, 2H), 1.67 – 1.60 (m, 3H), 1.48 (ddd, $J = 13.9, 9.0, 5.2$ Hz, 1H), 1.00 (d, $J = 6.5$ Hz, 3H), 0.97 (d, $J = 6.6$ Hz, 3H), 0.96 – 0.92 (m, 6H). ^{13}C NMR (151 MHz, MeOD) δ 174.48, 171.94, 171.61, 168.25, 148.38, 137.82, 130.80, 130.41, 129.65, 129.63, 128.13, 65.48, 54.30, 54.19, 53.59, 53.20, 43.12, 42.72, 42.06, 41.75, 41.53, 38.96, 25.93, 25.88, 23.52, 23.34, 21.98, 21.74. LC-MS (linear gradient 10 \rightarrow 90% MeCN, 0.1% TFA, 13.0 min): R_t (min): 5.86 (ESI-MS (m/z): 621.27 ($\text{M}+\text{H}^+$)). HRMS: calculated for $\text{C}_{28}\text{H}_{45}\text{N}_8\text{O}_6\text{S}$ 621.31773 [$\text{M}+\text{H}^+$] $^+$; found 621.31757

N₃Phe-Dap(Gly)-Leu-Dap(Gly)-VS (13)

This compound was obtained by the general protocol for azide coupling on a 50 μmol scale. Purification by column chromatography (0 \rightarrow 4% MeOH/DCM) provided the Boc-protected product, which was deprotected using the standard procedure for Boc removal. Purification by HPLC (10-50% MeCN, 0.1 % TFA, 10 min gradient) provided the title compound (2.93 mg, 6.7%) as a white powder after lyophilisation. ^1H NMR (600 MHz, MeOD) δ 7.36 – 7.22 (m, 5H), 6.84 (dd, $J = 15.3, 5.0$ Hz, 1H), 6.72 (dd, $J = 15.3, 1.6$ Hz, 1H), 4.90 – 4.83 (m, 1H), 4.48 (t, $J = 6.8$ Hz, 1H), 4.30 (dd, $J = 10.6, 4.6$ Hz, 1H), 4.17 (dd, $J = 8.4, 5.5$ Hz, 1H), 3.79 – 3.67 (m, 5H), 3.58 (dd, $J = 13.7, 5.6$ Hz, 1H), 3.42 (dd, $J = 7.5, 4.8$ Hz, 1H), 3.39 (dd, $J = 7.5, 4.8$ Hz, 1H), 3.22 (dd, $J = 13.9, 5.5$ Hz, 1H), 3.04 – 2.97 (m, 4H), 1.76 – 1.63 (m, 2H), 1.59 (ddd, $J = 13.9, 9.4, 4.6$ Hz, 1H), 1.00 (d, $J = 6.5$ Hz, 3H), 0.95 (d, $J = 6.5$ Hz, 3H). ^{13}C NMR (151 MHz, MeOD) δ 174.65, 171.83, 168.44, 168.23, 144.51, 137.73, 132.70, 130.45, 129.64, 128.15, 68.14, 65.38, 54.38, 54.25, 53.72, 50.78, 42.84, 42.58, 41.77, 41.68, 41.54, 41.49, 38.89, 25.92, 23.51, 21.63. LC-MS (linear gradient 10 \rightarrow 90% MeCN, 0.1% TFA, 13.0 min): R_t (min): 4.66 (ESI-MS (m/z): 651.27 ($\text{M}+\text{H}^+$)). HRMS: calculated for $\text{C}_{28}\text{H}_{45}\text{N}_8\text{O}_6\text{S}$ 651.30314 [$\text{M}+\text{H}^+$] $^+$; found 651.30286

N₃Phe-Leu-Leu-His-VS (14)

To a solution of $\text{N}_3\text{Phe-Leu-Leu-His(Trt)-VS}$ **57** (45 mg, 53 μmol , 1 equiv.) in DCM (3 mL) were added TFA (30 μL) and triisopropylsilane (TIPS) (75 μL). After 30 min, TLC showed no formation of product, therefore another 30 μL of TFA was added. After 30 min, still no product formation was observed, therefore TFA (1 mL) and TIPS (75 μL) were added. After stirring for 1 h, TLC analysis revealed completion of the reaction and the reaction mixture was diluted with toluene and concentrated. Purification by column chromatography (1-8% MeOH/DCM) provided the product as a white powder after lyophilisation (28 mg, 38%). Isolated with 7% *cis* isomer. Peaks reported correspond to *trans* isomer. ^1H NMR (600 MHz, MeOD) δ 8.08 (s, 1H), 7.35 – 7.19 (m, 5H), 7.10 (s, 1H), 6.84 (dd, $J = 15.2, 5.1$ Hz, 1H), 6.63 (dd, $J = 15.2, 1.5$ Hz, 1H), 4.90 – 4.85 (m, 1H), 4.41 – 4.34 (m, 1H), 4.28 (dd, $J = 9.8, 5.1$ Hz, 1H), 4.18 (dd, $J = 8.5, 5.0$ Hz, 1H), 3.21 (dd, $J = 14.0, 4.9$ Hz, 1H), 3.09 – 3.03 (m, 1H), 3.00 (dd, $J = 14.3, 8.3$ Hz, 2H), 2.96 (s, 3H), 1.70 – 1.47 (m, 6H), 0.97 (d, $J = 6.4$ Hz, 3H), 0.95 – 0.89 (m, 9H). ^{13}C NMR (151 MHz, MeOD) δ 174.66, 174.39, 171.85, 146.26, 137.82, 135.94, 133.13, 132.14, 130.44, 129.60, 128.05, 118.46, 65.51, 53.73,

53.48, 50.89, 42.71, 41.56, 41.43, 38.62, 31.05, 25.91, 25.79, 23.47, 23.40, 21.90, 21.89. LC-MS (linear gradient 10→90% MeCN, 0.1% TFA, 13.0 min): R_t (min): 6.22 (ESI-MS (m/z): 615.20 (M+H⁺)). HRMS: calculated for C₂₉H₄₃N₈O₅S 615.30716 [M+H]⁺; found 615.30719.

4-hydroxybut-2-yn-1-yl 4-methylbenzenesulfonate (16)

2-butyne-1,4-diol **15** (68.87 g, 800 mmol, 1 equiv.) was dissolved in DCM (2000 mL) and pyridine (129 mL, 1.6 mol), followed by the portion wise addition of 4-toluenesulfonyl chloride (76.2 g, 400 mmol, 0.5 equiv.) over 15 min. Reaction completion was confirmed by TLC (50% EtOAc/pent) after 2 h. The reaction mixture was washed with 1M HCl (3x), brine (3x) and dried over Na₂SO₄, filtered and concentrated. Purification by column chromatography yielded the title compound (60.7 g, 253 mmol, 63%). ¹H NMR (400 MHz, CDCl₃) δ 7.76 (d, J = 8.2 Hz, 2H), 7.34 (d, J = 8.1 Hz, 2H), 4.69 (s, 2H), 4.12 (s, 2H), 3.12 (s, 1H), 2.41 (s, 3H). ¹³C NMR (101 MHz, CDCl₃) δ 145.24, 132.28, 129.72, 127.75, 87.73, 76.72, 57.95, 50.05, 21.31.

1-(tert-butoxycarbonylamino)-4-hydroxy-2-butyne (17)

Alcohol **16** (58.29 g, 243 mmol, 1 equiv.) was dissolved in ammonium hydroxide (450 mL, 25% NH₃ in H₂O), resulting in immediate formation of a white precipitate. TLC (50% EtOAc/pent) confirmed reaction completion after 1h. The ammonium hydroxide was removed *in vacuo* and the mixture co-evaporated with toluene (2x). The resulting solid was dissolved in THF (950 mL) and di-*tert*-butyl dicarbonate (63.53 g, 291 mmol, 1.2 equiv.) was added and the solution was cooled to 0°C. Triethylamine (40.6 mL, 291 mmol, 1.2 equiv.) was added slowly over 20 min and after stirring overnight, the reaction mixture was concentrated, redissolved in DCM (500 mL) and washed with water (3x). The aqueous layer was back extracted twice with DCM and the combined organic layers were washed with brine (1x), dried over Na₂SO₄, filtered and concentrated. Purification by column chromatography (10→25 % EtOAc/n-Pentane) yielded the title compound (19.04 g, 102.8 mmol, 42%). ¹H NMR (400 MHz, CDCl₃) δ 5.25 (s, 1H), 4.26 (s, 2H), 3.95 (s, 2H), 3.71 (s, 1H), 1.45 (s, 9H). ¹³C NMR (101 MHz, CDCl₃) δ 155.76, 81.53, 80.12, 50.58, 30.59, 28.35.

1-(tert-butoxycarbonylamino)-4-bromo-2-butyne (18)

To a solution of alcohol **17** (9.26 g, 50 mmol, 1 equiv.) in DCM (79 mL) at 0°C, triphenylphosphine (19.67 g, 75 mmol, 1.5 equiv.) was added, followed by portion wise addition of tetrabromomethane (3.90 g, 11.8 mmol, 1.5 equiv.). After stirring for 2 h, the reaction mixture was concentrated and purification by column chromatography (1→5% EtOAc/pent) yielded the title compound (8.50 g, 34.2 mmol, 68%). ¹H NMR (400 MHz, CDCl₃) δ 5.00 (s, 1H), 3.99 (s, 2H), 3.92 (s, 2H), 1.46 (s, 9H). ¹³C NMR (101 MHz, CDCl₃) δ 155.31, 83.32, 80.02, 30.67, 28.35, 14.48.

tert-butyl (E)-(4-hydroxybut-2-en-1-yl)carbamate (19)

Alcohol **17** (7.9 g, 42.7 mmol) was dissolved in THF (30 mL) and added drop wise over 15 minutes to a solution of LiAlH₄ (1.95 g, 51.2 mmol, 1.2 equiv.) in THF (400 mL) at 0°C. After completion of addition, the solution was heated to reflux and stirred for 2 h, after which TLC analysis (50% EtOAc/pent) confirmed completion of the reaction. The reaction was quenched with 3M aq. KOH solution until no further gas evolution was observed, diluted with EtOAc (100 mL), washed with 1M HCl (3x), NaHCO₃ (3x), brine (1x) and dried over Na₂SO₄, filtered and concentrated. Purification by column chromatography (10→30 % EtOAc/pent) yielded the title compound as pure *E*-isomer (3.00 g, 16.05 mmol, 38%). ¹H NMR (400 MHz, CDCl₃) δ 5.72 (dt, 2H), 4.89 (s, 1H), 4.09 (dd, J = 4.9, 1.3 Hz, 2H), 3.70 (d, J = 5.1 Hz, 2H), 2.93 (s, 1H), 1.42 (tt, J = 15.5, 5.2 Hz, 9H). ¹³C NMR (101 MHz, CDCl₃) δ 156.03, 130.87, 128.04, 79.51, 62.65, 41.99, 28.44.

1-(tert-butoxycarbonylamino)-4-bromo-2-butene (20)

Alcohol **19** (3.00 g, 16.1 mmol, 1 equiv.) was dissolved in dry DCM (160 mL). Triphenylphosphine (6.31 g, 24.08 mmol, 1.5 equiv.) was added and the solution cooled to 0°C, followed by slow and portion wise addition of the tetrabromomethane (7.99 g, 24.1 mmol, 1.5 equiv.). After stirring for 1 h, the reaction mixture was concentrated

and purification by column chromatography (0→10% EtOAc/pent) yielded the title compound (2.32 g, 9.28 mmol, 58%). ¹H NMR (400 MHz, CDCl₃) δ 6.02 – 5.65 (m, 2H), 4.66 (s, 1H), 3.97 (d, *J* = 6.6 Hz, 2H), 3.79 (s, 2H), 1.47 (s, 9H). ¹³C NMR (101 MHz, CDCl₃) δ 132.22, 127.71, 41.72, 32.15, 28.51.

***tert*-butyl (S,E)-6-((*tert*-butoxycarbonyl)amino)-2-((diphenylmethylene)amino)hex-4-enoate (22)**

Bromide **20** (2.25 g, 8.99 mmol, 1 equiv.), N-(diphenylmethylene)glycine *tert*-butyl ester (**36**) (2.65 g, 8.99 mmol, 1 equiv.) and the CPTC (0.046 g, 0.045 mmol, 0.005 equiv.) were dissolved in toluene/chloroform (31.5 mL, 7/3 v/v) and cooled to 0°C. A 50% (w/w) aqueous KOH solution which had been cooled to 4°C was added drop wise (13.5 mL). The reaction was stirred over two nights at 4°C and the reaction progression was followed by TLC (15% EtOAc/pent). The solution was then diluted with EtOAc, washed with water (1x), brine (1x), dried over Na₂SO₄, filtered and concentrated. Purification by column chromatography (0→10% EtOAc/pent) yielded the title compound as a white solid (2.98 g, 6.44 mmol, 84%, *ee* 79.3%). ¹H NMR (400 MHz, CDCl₃) δ 7.67 – 7.29 (m, 8H), 7.16 (dd, *J* = 7.3, 2.4 Hz, 2H), 5.60 – 5.42 (m, 2H), 4.46 (s, 1H), 3.98 (t, *J* = 6.4 Hz, 1H), 3.65 (s, 2H), 2.60 (t, *J* = 5.4 Hz, 2H), 1.44 (s, 9H), 1.41 (s, 9H). ¹³C NMR (101 MHz, CDCl₃) δ 155.75, 128.56, 128.15, 128.00, 81.23, 66.03, 42.50, 36.59, 28.50, 28.20.

***tert*-butyl (S)-6-((*tert*-butoxycarbonyl)amino)-2-((diphenylmethylene)amino)hex-4-ynoate (23)**

Bromide **18** (1.90 g, 7.67 mmol, 1 equiv.), N-(diphenylmethylene)glycine *tert*-butyl ester **21** (2.27 g, 7.67 mmol, 1 equiv.) and the CPTC (0.039 g, 0.038 mmol, 0.005 equiv.) were dissolved in toluene/chloroform (27 mL, 7/3 v/v) and cooled to 0°C. A 50% (w/w) aqueous KOH solution which had been cooled to 4°C was added drop wise (11.5 mL). The reaction was stirred over two nights at 4°C and the reaction progression was followed by TLC (5% EtOAc/pent). The solution was then diluted with EtOAc, washed with water (1x), brine (1x), dried over Na₂SO₄, filtered and concentrated. Purification by column chromatography (1→10% EtOAc/pent) yielded the title compound as a white solid (2.98 g, 6.44 mmol, 84%, *ee* 80.2%). ¹H NMR (400 MHz, CDCl₃) δ 7.75 – 7.19 (m, 10H), 4.74 (s, 1H), 4.16 (dt, *J* = 9.0, 4.5 Hz, 1H), 3.92 – 3.77 (m, 2H), 2.90 – 2.66 (m, 2H), 1.46 (s, 9H), 1.42 (s, 9H). ¹³C NMR (101 MHz, CDCl₃) δ 171.30, 169.67, 155.19, 139.58, 136.25, 130.34, 128.92, 128.66, 128.38, 128.18, 128.01, 81.47, 80.28, 79.56, 77.87, 64.99, 30.68, 28.32, 28.01, 23.53.

H-Lys(-4-ene)(Boc)-OtBu (24)

Compound **22** (2.74 g, 5.90 mmol, 1 equiv.) was dissolved in THF (33 mL) and cooled to 0°C. A citric acid solution (38 mL, 15% w/w in water) was added and precipitation of a white solid was observed. The ice bath was removed, and the reaction mixture was allowed to warm to rt and was stirred for 2 hours during which time the solution turned clear again. The reaction was followed by TLC (10% EtOAc/pent) and quenched with a sat. K₂CO₃ solution until no further gas evolution was observed (approx. 20 mL). The reaction mixture was diluted with EtOAc, washed with water (2x), brine (1x). The organic layer was dried over Na₂SO₄, filtered, concentrated and purified by column chromatography (0→5% MeOH/DCM) yielding the title compound (yield given over two steps, see synthesis of **26**). ¹H NMR (400 MHz, CDCl₃) δ 5.71 – 5.40 (m, 2H), 4.75 (s, 1H), 3.70 (t, *J* = 5.5 Hz, 2H), 3.40 (t, *J* = 6.0 Hz, 1H), 2.58 – 2.18 (m, 2H), 1.68 (s, 2H), 1.46 (s, 9H), 1.44 (s, 9H). ¹³C NMR (101 MHz, CDCl₃) δ 174.47, 155.76, 130.63, 127.14, 81.18, 79.27, 54.49, 42.34, 37.71, 28.44, 28.12.

H-Lys(-4-yn)(Boc)-OtBu (25)

Compound **23** (5.02 g, 10.9 mmol, 1 equiv.) was dissolved in THF (59 mL) and cooled to 0°C. A citric acid solution (69 mL, 15% w/w in water) was added and precipitation of a white solid was observed. The ice bath was removed, and the reaction mixture was allowed to warm to rt and was stirred for 2 h during which time the solution turned clear again. The reaction was followed by TLC (5% MeOH/DCM) and quenched with a sat. K₂CO₃ solution until no further gas evolution was observed (approx. 20 mL). The reaction mixture was diluted with EtOAc, washed with water (2x), brine (1x). The organic layer was dried over Na₂SO₄, filtered, concentrated and purified by column chromatography (0→5% MeOH/DCM) yielding the title compound (2.94 g, 9.87 mmol, 91%). ¹H NMR

(400 MHz, CDCl_3) δ 4.92 (s, 1H), 3.89 (d, $J = 5.3$ Hz, 2H), 3.48 (t, $J = 5.5$ Hz, 1H), 2.65 – 2.50 (m, 2H), 1.75 (s, 2H), 1.47 (s, 9H), 1.44 (s, 9H). ^{13}C NMR (101 MHz, CDCl_3) δ 173.19, 155.32, 81.53, 79.75, 79.09, 78.75, 53.76, 30.67, 28.39, 28.04, 25.40.

Fmoc-Lys(-4-ene)(Boc)-OtBu (26)

H-Lys-4-ene(Boc)-OtBu **24** (5.90 mmol, 1 equiv.) was dissolved in dry DCM (60 mL) and FmocOSu (2.38 g, 7.08 mmol, 1.2 equiv.) was added followed by the drop wise addition of DiPEA (1.2 mL, 7.08 mmol, 1.2 equiv.). After stirring overnight, the reaction mixture was diluted with EtOAc, washed with 1M HCl (1x), sat. aq. NaHCO_3 (2x) and brine (1x). The organic layer was dried over Na_2SO_4 , filtered and concentrated. Purification by column chromatography (0 \rightarrow 20% EtOAc/pent) yielded the title compound as a white powder (2.56 g, 4.91 mmol, 83% over two steps). ^1H NMR (400 MHz, CDCl_3) δ 7.76 (d, $J = 7.5$ Hz, 2H), 7.60 (d, $J = 7.5$ Hz, 2H), 7.40 (t, $J = 7.5$ Hz, 2H), 7.32 (t, $J = 7.4$ Hz, 2H), 5.63 – 5.44 (m, 2H), 5.39 (d, $J = 8.1$ Hz, 1H), 4.56 (s, 1H), 4.44 – 4.35 (m, 2H), 4.22 (t, $J = 7.0$ Hz, 1H), 3.69 (s, 2H), 2.64 – 2.40 (m, 2H), 1.47 (s, 9H), 1.43 (s, 9H). ^{13}C NMR (101 MHz, CDCl_3) δ 170.83, 155.77, 143.92, 141.42, 131.23, 127.82, 127.18, 125.99, 125.22, 120.10, 82.48, 79.48, 67.06, 53.94, 47.30, 42.36, 35.59, 28.51, 28.18. $[\alpha]_D^{20} = 17.6$ (C=1, CHCl_3). LC-MS (linear gradient 10 \rightarrow 90% MeCN, 0.1% TFA, 13.0 min) Rt (min): 10.95 (ESI-MS (m/z): 523.80 ($\text{M}+\text{H}^+$)). HRMS: calcd. for $\text{C}_{30}\text{H}_{38}\text{N}_2\text{O}_6$, 523.27579 [$\text{M}+\text{H}^+$]; found 523.27997

Fmoc-Lys(-4-yn)(Boc)-OtBu (27)

H-Lys-4-yl(Boc)-OtBu **25** (2.89 g, 9.68 mmol, 1 equiv.) was dissolved in dry DCM (97 mL) and FmocOSu (3.92 g, 11.6 mmol, 1.2 equiv.) was added followed by the drop wise addition of DiPEA (2.0 mL, 11.6 mmol, 1.2 equiv.). After stirring overnight, the reaction mixture was diluted with EtOAc, washed with 1M HCl (1x), sat. aq. NaHCO_3 (2x) and brine (1x). The organic layer was dried over Na_2SO_4 , filtered and concentrated. Purification by column chromatography (0 \rightarrow 20 % EtOAc, n-Pentane) yielded the title compound as a white foam (4.94 g, 9.48 mmol, 98 %). ^1H NMR (400 MHz, CDCl_3) δ 7.80 – 7.74 (m, 2H), 7.62 (d, $J = 7.4$ Hz, 2H), 7.40 (t, $J = 7.5$, 2H), 7.32 (tt, $J = 7.4$, 1.4 Hz, 2H), 5.67 (d, $J = 8.0$ Hz, 1H), 4.68 (s, 1H), 4.44 – 4.34 (m, 3H), 4.24 (t, $J = 7.2$ Hz, 1H), 3.88 (s, 2H), 2.73 (dt, $J = 4.9$, 2.3 Hz, 2H), 1.49 (s, 9H), 1.44 (s, 9H). ^{13}C NMR (101 MHz, CDCl_3) δ 169.57, 155.74, 143.97, 141.39, 127.83, 127.19, 125.27, 120.10, 82.84, 79.51, 77.84, 77.36, 67.25, 53.00, 47.24, 30.76, 28.46, 28.08, 23.41. $[\alpha]_D^{20} = 23.0$ (C=1, CHCl_3). LC-MS (linear gradient 10 \rightarrow 90% MeCN, 0.1% TFA, 13.0 min): Rt (min): 9.22 (ESI-MS (m/z): 520.87 ($\text{M}+\text{H}^+$)). HRMS: calcd. for $\text{C}_{30}\text{H}_{37}\text{N}_2\text{O}_6$ 521.26461 [$\text{M}+\text{H}^+$]; found 521.26459.

Fmoc-Lys(-4-ene)(Boc)-OH (28)

Fmoc-L-Lys-4-ene(Boc)-OtBu **26** (2.48 g, 4.76 mmol, 1 equiv.) was dissolved in 100% TFA (47.6 mL) and stirred for 2 hours, after which TLC analysis (10% EtOAc/pent) showed completion of the reaction, in combination with TLC-MS and HPLC-MS to ensure completion of ester hydrolysis and not only removal of the Boc group. The reaction mixture was concentrated and co-evaporated with toluene (3x). The residue was redissolved in MeCN (48 mL) and Boc_2O (1.25 g, 5.71 mmol, 1.2 equiv.) and DiPEA (1.15 mL, 6.91 mmol, 1.45 equiv.) were added. A white precipitate formed immediately and gas evolution was observed. After stirring overnight, the reaction mixture was concentrated and the residue was dissolved in EtOAc, washed with 0.1 M HCl (2x), water (2x) and brine (2x), dried over Na_2SO_4 , filtered and concentrated. Purification by column chromatography (0 \rightarrow 2% MeOH/DCM) yielded the title compound (1.82 g, 3.90 mmol, 82%). ^1H NMR (400 MHz, CDCl_3) δ 7.74 (t, $J = 7.9$ Hz, 2H), 7.56 (d, $J = 7.9$ Hz, 2H), 7.37 (t, $J = 7.7$ Hz, 2H), 7.31 (d, $J = 8.2$ Hz, 2H), 6.94 (s, 1H), 6.74 (d, $J = 8.6$ Hz, 1H), 5.55 (dt, $J = 15.8$, 9.2 Hz, 2H), 4.60 (s, 1H), 4.43 (q, $J = 12.0$, 11.4 Hz, 2H), 4.23 (t, 1H), 4.13 (t, $J = 6.6$ Hz, 1H), 3.63 (d, $J = 48.0$ Hz, 2H), 2.79 – 2.46 (m, 2H), 1.52 (s, 9H). ^{13}C NMR (101 MHz, CDCl_3) δ 185.56, 155.73, 144.25, 143.86, 141.33, 129.97, 127.65, 119.96, 81.68, 66.59, 53.08, 47.34, 42.76, 34.77, 29.82, 28.49.

Fmoc-Lys(-4-yn)(Boc)-OH (29)

Fmoc-Lys-4-yl(Boc)-OtBu **27** (4.93 g, 9.48 mmol, 1 equiv.) was dissolved in 100% TFA (95 mL) and stirred for 2 h, after which TLC analysis (10 % EtOAc/pent) showed completion of the reaction, in combination with TLC-MS and

HPLC-MS to ensure completion of ester hydrolysis and not only removal of the Boc group. The reaction mixture was concentrated and co-evaporated with toluene (3x). The residue was redissolved in MeCN (95 mL) and Boc₂O (2.48 g, 11.38 mmol, 1.2 equiv.) and DiPEA (2 mL, 11.38 mmol, 1.2 equiv.) were added. A white precipitate formed immediately and gas evolution was observed, and the pH was adjusted until basic by the addition of 1 mL DiPEA. After stirring overnight, the reaction mixture was concentrated and the residue was dissolved in EtOAc, washed with 0.1 M HCl (2x), water (2x) and brine (2x), dried over Na₂SO₄, filtered and concentrated. Purification by column chromatography (0→1% MeOH/DCM) yielded the title compound (2.80 g, 6.02 mmol, 63%). ¹H NMR (400 MHz, CDCl₃) δ 7.73 (d, *J* = 7.5 Hz, 2H), 7.57 (dd, *J* = 17.7, 7.4 Hz, 2H), 7.48 (d, *J* = 4.1 Hz, 1H), 7.36 (d, *J* = 7.5 Hz, 2H), 7.28 (d, *J* = 7.2 Hz, 2H), 4.72 – 4.60 (m, 1H), 4.43 – 4.33 (m, 1H), 4.30 – 4.13 (m, 2H), 3.93 – 3.72 (m, 2H), 2.89 (d, *J* = 4.2 Hz, 2H), 1.51 (s, 9H). ¹³C NMR (101 MHz, CDCl₃) δ 174.93, 157.99, 155.85, 144.33, 143.80, 141.44, 141.35, 127.69, 127.07, 125.22, 119.98, 82.27, 79.67, 77.59, 66.95, 52.55, 47.29, 32.36, 28.46, 23.03.

Fmoc-Lys(-4-ene)(Boc)-N(OMe)Me (30)

The title compound was prepared by the general procedure for peptide coupling on a 0.5 mmol scale. Purification by column chromatography (10→40% EtOAc/pent) yielded the title compound in a quantitative yield. ¹H NMR (400 MHz, CDCl₃) δ 7.76 (d, *J* = 7.5 Hz, 2H), 7.60 (t, *J* = 7.0 Hz, 2H), 7.40 (t, *J* = 7.6, 2H), 7.31 (tdd, *J* = 7.4, 3.0, 1.2 Hz, 2H), 5.64 – 5.51 (m, 3H), 4.80 (q, *J* = 7.0 Hz, 1H), 4.69 – 4.50 (m, 1H), 4.47 – 4.27 (m, 2H), 4.22 (t, *J* = 7.2 Hz, 1H), 3.77 (s, 3H), 3.71 – 3.63 (m, 2H), 3.22 (s, 3H), 2.57 – 2.44 (m, 1H), 2.44 – 2.32 (m, 1H), 1.43 (s, 9H). ¹³C NMR (101 MHz, CDCl₃) δ 173.58, 171.90, 156.04, 143.98, 143.87, 141.38, 130.85, 127.81, 127.17, 126.55, 125.26, 120.08, 67.14, 61.80, 50.79, 47.20, 35.50, 32.21, 28.49.

Fmoc-Lys(-4-yl)(Boc)-N(OMe)Me (31)

The title compound was prepared by the general procedure for peptide coupling on a 3.0 mmol scale. Purification by column chromatography (10→40 % EtOAc/pent) yielded the title compound as a white foam (1.29 g, 2.54 mmol, 85 %). ¹H NMR (400 MHz, CDCl₃) δ 7.73 (d, *J* = 7.5 Hz, 2H), 7.60 (t, *J* = 7.3 Hz, 2H), 7.37 (td, *J* = 7.6, 1.4 Hz, 2H), 7.32 – 7.25 (m, 2H), 6.13 (d, *J* = 8.8 Hz, 1H), 5.04 (bs, 1H), 4.90 (bs, 1H), 4.35 (dd, *J* = 7.4, 1.8 Hz, 2H), 4.21 (t, *J* = 7.1 Hz, 1H), 3.86 (bs, 2H), 3.72 (s, 3H), 3.21 (s, 3H), 2.79 – 2.55 (m, 2H), 1.40 (s, 9H). ¹³C NMR (101 MHz, CDCl₃) δ 170.49, 155.80, 155.25, 143.60, 141.07, 127.57, 126.93, 125.07, 119.83, 79.51, 79.14, 77.84, 77.36, 67.02, 61.52, 49.71, 46.91, 32.01, 30.60, 28.20, 22.74. LC-MS (linear gradient 10→90% MeCN, 0.1% TFA, 13.0 min): Rt (min): 8.20 (ESI-MS (*m/z*): 507.8 (M+H⁺)). HRMS: calcd. for C₂₈H₃₃N₃O₆ 508.24421 [M+H⁺]; found 508.24405. [α]_D²⁰ = 4.4 (C=1, CHCl₃).

Fmoc-Lys(-4-ene)(Boc)-VS (32)

Weinreb amide **30** (255 mg, 0.5 mmol, 1 equiv.) was dissolved in dry Et₂O (5 mL) and cooled to -30°C. LiAlH₄ (2M in THF, 0.25 mL, 0.5 mmol, 1 equiv.) was added drop wise. After 1 h, TLC analysis indicated completion of the reaction. The reaction mixture was quenched with 1M HCl (approx. 2 mL), diluted with EtOAc and wash 1M HCl (2x) and brine (2x). The organic layer was dried over Na₂SO₄, filtered and concentrated and used directly in the next step. Diethyl((methylsulfonyl)methyl)-phosphonate (173 mg, 0.75 mmol, 1.5 equiv.) was dissolved in THF (20 mL) and cooled to 0°C followed by the addition of NaH (60 % w/w in mineral oil, 24 mg, 0.6 mmol, 1.2 equiv.). After stirring for 30 min, the freshly obtained aldehyde in THF (5 mL) was added drop wise to the reaction mixture. After 2.5 h, the reaction was diluted with EtOAc, washed with 1M HCl (1x) and brine (1x). The organic layer was dried over Na₂SO₄, filtered and concentrated. NMR analysis of the crude product indicated significant amounts of aldehyde remaining. Therefore reaction was repeated with 0.7 equiv diethyl((methylsulfonyl)-methyl)-phosphonate and 0.5 equiv NaH. Purification by column chromatography (10→40 % EtOAc, n-Pentane) yielded the title compound (105 mg, 0.2 mmol, 40 %). ¹H NMR (400 MHz, CDCl₃) δ 7.76 (d, *J* = 7.4 Hz, 2H), 7.58 (dd, *J* = 7.3, 3.2 Hz, 2H), 7.40 (t, *J* = 7.3 Hz, 2H), 7.36 – 7.28 (m, 2H), 6.83 (dd, *J* = 15.2, 4.6 Hz, 1H), 6.44 (d, *J* = 15.1 Hz, 1H), 5.65 – 5.40 (m, 2H), 5.31 – 5.10 (m, 1H), 4.80 – 4.59 (m, 1H), 4.54 – 4.30 (m, 3H), 4.20 (q, *J* = 6.6, 5.9 Hz, 1H), 3.68 (q, *J* = 7.1, 6.0 Hz, 2H), 2.91 (s, 3H), 2.46 – 2.22 (m, 2H), 1.43 (s, 9H). ¹³C NMR (101 MHz, CDCl₃) δ 155.66,

146.86, 143.76, 143.60, 141.35, 132.12, 130.06, 127.84, 127.72, 127.12, 125.86, 124.95, 120.07, 66.81, 51.00, 47.20, 42.86, 42.22, 36.69, 28.41.

Fmoc-Lys(-4-yn)(Boc)-VS (33)

Weinreb amide **31** (1.29 g, 2.54 mmol, 1 equiv.) was dissolved in dry Et₂O (26 mL) and cooled to -30°C. LiAlH₄ (2M in THF, 1.3 mL, 2.54 mmol, 1 equiv.) was added drop wise. After < 10 minutes, TLC analysis indicated completion of the reaction. The reaction mixture was quenched with 1M HCl (approx. 10 mL), diluted with EtOAc and washed with 1M HCl (2x) and brine (2x). The organic layer was dried over Na₂SO₄, filtered and concentrated and used directly in the next step. Diethyl((methylsulfonyl)methyl)- phosphonate (0.88 g, 3.81 mmol, 1.5 equiv.) was dissolved in THF (20 mL) and cooled to 0°C followed by the addition of NaH (60 % w/w in mineral oil, 0.12 g, 3.05 mmol, 1.2 equiv.). After stirring for 30 min, the freshly obtained aldehyde in THF (10 mL) was added drop wise to the reaction mixture. After 1 h, TLC (2.5 % MeOH, DCM) indicated completion of the reaction. The reaction was diluted with EtOAc, washed with 1M HCl (1x) and brine (1x). The organic layer was dried over Na₂SO₄, filtered and concentrated. Purification by column chromatography (10→40 % EtOAc, n-Pentane) yielded the title compound (0.94 g, 1.79 mmol, 70 %). ¹H NMR (400 MHz, CDCl₃) δ 7.76 (d, *J* = 7.5 Hz, 2H), 7.60 (t, *J* = 7.3 Hz, 2H), 7.40 (td, *J* = 7.5, 1.2 Hz, 2H), 7.36 – 7.29 (m, 2H), 6.88 (dd, *J* = 15.1, 4.8 Hz, 1H), 6.55 (dt, *J* = 15.1, 1.6 Hz, 1H), 5.58 (d, *J* = 8.6 Hz, 1H), 4.93 (s, 1H), 4.60 (s, 1H), 4.44 (d, *J* = 7.0 Hz, 2H), 4.21 (t, *J* = 6.7 Hz, 1H), 3.87 (s, 2H), 2.94 (s, 3H), 2.75 – 2.41 (m, 2H), 1.44 (s, 9H). ¹³C NMR (101 MHz, CDCl₃) δ 155.56, 145.51, 143.69, 141.38, 130.96, 127.90, 127.20, 125.09, 120.13, 80.70, 77.28, 67.13, 50.02, 47.20, 42.87, 28.42, 24.54.

H-Lys(-4-ene)(Boc)-VS (34)

To a solution of vinyl sulfone **32** (86 mg, 0.16 mmol, 1 equiv.) in MeCN (2 mL) was added diethylamine (0.85 mL). After 1h, TLC analysis (2.5 % MeOH, DCM) showed completion of the reaction and the mixture was diluted with toluene, evaporated to dryness and co-evaporated with toluene (2x). Purification by column chromatography (0→5% MeOH, DCM) yielded the title compound as a yellow oil (37 mg, 0.12 mmol, 75%). ¹H NMR (400 MHz, CDCl₃) δ 6.94 (dd, *J* = 15.0, 4.8 Hz, 1H), 6.60 (dd, *J* = 15.0, 1.3 Hz, 1H), 5.67 – 5.47 (m, 2H), 4.63 (s, 1H), 3.76 – 3.61 (m, 3H), 2.95 (s, 3H), 2.43 – 2.31 (m, 1H), 2.25 – 2.10 (m, 1H), 1.57 (s, 2H), 1.45 (s, 9H). ¹³C NMR (101 MHz, CDCl₃) δ 155.83, 150.89, 131.82, 128.91, 126.93, 51.66, 42.97, 42.36, 39.72, 28.50.

H-Lys(-4-yn)(Boc)-VS (35)

To a solution of vinyl sulfone **33** (0.94 g, 1.79 mmol, 1 equiv.) in MeCN (18 mL) dropwise added diethylamine (8 mL). After 1h, TLC analysis (2.5 % MeOH, DCM) showed completion of the reaction and the mixture was diluted with toluene (30 mL), evaporated to dryness and co-evaporated with toluene (2x). Purification by column chromatography (0→5% MeOH, DCM) yielded the title compound as a yellow oil (0.26 g, 0.84 mmol, 47%). ¹H NMR (400 MHz, CDCl₃) δ 6.94 (dd, *J* = 15.3, 4.8 Hz, 1H), 6.68 (d, *J* = 15.1 Hz, 1H), 5.11 (bs, 1H), 3.89 (s, 2H), 3.76 (d, *J* = 5.9 Hz, 1H), 2.98 (s, 3H), 2.46 (qd, *J* = 16.8, 5.9 Hz, 2H), 1.76 (s, 2H), 1.45 (s, 9H). ¹³C NMR (101 MHz, CDCl₃) δ 155.38, 149.25, 129.66, 79.95, 79.81, 78.24, 50.81, 42.77, 30.52, 28.33, 27.24.

Fmoc-Lys(-4-ene)(Boc)-Leu-OMe (36)

The title compound was prepared by the general procedure for peptide coupling on a 0.5 mmol scale. Column chromatography (0→30% EtOAc/pentane) provided the product (285 mg, 0.48 mmol, 96%). Product isolated with 10% of minor diastereomer. Peaks reported for major diastereomer. ¹H NMR (400 MHz, CDCl₃) δ 7.74 (d, *J* = 7.5 Hz, 2H), 7.57 (d, *J* = 6.3 Hz, 2H), 7.41 – 7.35 (m, 2H), 7.32 – 7.26 (m, 2H), 6.86 (d, *J* = 8.1 Hz, 1H), 5.81 (d, *J* = 8.2 Hz, 1H), 5.65 – 5.49 (m, 2H), 5.00 (t, *J* = 5.8 Hz, 1H), 4.65 – 4.53 (m, 1H), 4.46 – 4.24 (m, 3H), 4.19 (t, *J* = 7.1 Hz, 1H), 3.71 (s, 3H), 3.69 – 3.56 (m, 2H), 2.57 – 2.40 (m, 2H), 1.71 – 1.50 (m, 3H), 1.42 (s, 9H), 0.88 (d, *J* = 4.2 Hz, 6H). ¹³C NMR (101 MHz, CDCl₃) δ 174.32, 173.57, 131.05, 130.99, 127.71, 54.24, 52.29, 50.36, 50.32, 42.34, 41.37, 37.92, 28.42, 24.94, 22.90, 21.84.

Fmoc-Lys(-4-yn)(Boc)-Leu-OMe (37)

The title compound was prepared by the general procedure for peptide coupling on a 0.6 mmol scale. Column chromatography (10→30% EtOAc/pentane) provided the product (220 mg, 0.38 mmol, 76%). ¹H NMR (400 MHz, CDCl₃) δ 7.73 (d, *J* = 7.5 Hz, 2H), 7.57 (dd, *J* = 7.7, 2.9 Hz, 2H), 7.37 (t, *J* = 7.5 Hz, 2H), 7.32 – 7.24 (m, 2H), 6.03 (d, *J* = 7.9 Hz, 1H), 5.28 (s, 1H), 4.73 – 4.58 (m, 1H), 4.51 – 4.27 (m, 3H), 4.19 (t, *J* = 7.1 Hz, 1H), 3.99 – 3.77 (m, 2H), 3.71 (d, *J* = 6.8 Hz, 3H), 2.89 – 2.40 (m, 2H), 1.73 – 1.53 (m, 3H), 1.42 (s, 9H), 0.90 (t, *J* = 5.2 Hz, 6H). ¹³C NMR (101 MHz, CDCl₃) δ 173.24, 169.88, 155.84, 155.49, 143.61, 141.20, 127.71, 127.04, 125.06, 119.96, 79.83, 78.32, 67.27, 53.53, 52.35, 50.92, 46.96, 41.20, 30.71, 28.32, 24.74, 23.28, 22.73, 21.80.

H-Lys(-4-ene)(Boc)-Leu-OMe (38)

Fmoc-L-Lys-4-ene(Boc)-Leu-OMe **36** (273 mg, 0.46 mmol) was deprotected using the standard procedure for Fmoc removal, providing the title compound (161 mg, 0.43 mmol, 94%) after purification by column chromatography (0→3% MeOH, DCM). Product was isolated with 10% of minor diastereomer. Peaks reported for major diastereomer. ¹H NMR (400 MHz, CDCl₃) δ 7.64 (d, *J* = 8.6 Hz, 1H), 5.58 – 5.49 (m, 2H), 4.80 (s, 1H), 4.57 (td, *J* = 8.8, 4.7 Hz, 1H), 3.71 (s, 3H), 3.69 – 3.61 (m, 2H), 3.40 (dd, *J* = 8.3, 4.3 Hz, 1H), 2.53 (dt, *J* = 13.6, 5.0 Hz, 1H), 2.24 (dt, *J* = 13.5, 7.9 Hz, 1H), 1.74 (s, 2H), 1.68 – 1.52 (m, 3H), 1.41 (s, 9H), 0.92 (dd, *J* = 6.1, 3.4 Hz, 6H). ¹³C NMR (101 MHz, CDCl₃) δ 174.32, 173.57, 131.05, 130.99, 127.71, 54.24, 52.29, 50.36, 50.32, 42.34, 41.37, 37.92, 28.42, 24.94, 22.90, 21.84.

H-Lys(-4-yn)(Boc)-Leu-OMe (39)

Fmoc L-Lys-4-yl(Boc)-Leu-OMe **37** (220 mg, 0.38 mmol) was deprotected using the standard procedure for Fmoc removal, providing the title compound (189 mg, 100%) after purification by column chromatography (0→3 % MeOH, DCM). ¹H NMR (400 MHz, CDCl₃) δ 7.74 (d, *J* = 8.7 Hz, 1H), 4.95 (s, 1H), 4.70 – 4.51 (m, 1H), 3.88 (s, 2H), 3.74 (s, 3H), 3.51 (t, *J* = 5.9 Hz, 1H), 2.77 – 2.52 (m, 2H), 1.89 (s, 2H), 1.72 – 1.55 (m, 3H), 1.44 (s, 9H), 1.00 – 0.89 (m, 6H). ¹³C NMR (101 MHz, CDCl₃) δ 173.44, 173.02, 155.37, 79.32, 79.17, 53.66, 52.32, 50.48, 41.43, 30.72, 28.39, 25.38, 24.94, 22.94, 21.84.

N₃Phe-Lys(-4-ene)(Boc)-Leu-OMe (40)

The title compound was prepared by the general procedure for peptide coupling on a 0.38 mmol scale. Column chromatography (0→50% EtOAc/pentane) provided the product (124 mg, 0.23 mmol, 60%). Product was isolated with 10% of minor diastereomer. Peaks reported for major diastereomer. ¹H NMR (400 MHz, CDCl₃) δ 7.39 – 7.24 (m, 5H), 6.99 (d, *J* = 7.3 Hz, 1H), 6.54 (d, *J* = 7.5 Hz, 1H), 5.53 – 5.44 (m, 2H), 4.88 (s, 1H), 4.64 – 4.53 (m, 1H), 4.38 (q, *J* = 7.3 Hz, 1H), 4.24 (dd, *J* = 7.8, 4.2 Hz, 1H), 3.77 (s, 3H), 3.73 – 3.59 (m, 2H), 3.32 (dd, *J* = 14.1, 4.2 Hz, 1H), 3.08 (dd, *J* = 14.0, 7.8 Hz, 1H), 2.46 – 2.37 (m, 1H), 2.37 – 2.26 (m, 1H), 1.64 (dtd, *J* = 16.3, 11.9, 10.4, 6.8 Hz, 3H), 1.46 (s, 9H), 0.95 (t, *J* = 5.3 Hz, 6H). ¹³C NMR (101 MHz, CDCl₃) δ 173.38, 170.12, 168.30, 155.91, 135.90, 131.79, 129.69, 129.48, 128.78, 127.43, 125.83, 65.29, 52.77, 52.55, 51.04, 42.44, 41.17, 38.48, 35.37, 28.52, 24.95, 22.90, 21.91.

N₃Phe-Lys(-4-yn)(Boc)-Leu-OMe (41)

The title compound was prepared by the general procedure for peptide coupling on a 0.23 mmol scale. Column chromatography (0→40% EtOAc/pentane) provided the product (111 mg, 0.21 mmol, 91 %). ¹H NMR (400 MHz, CDCl₃) δ 7.44 – 7.15 (m, 5H), 7.00 (d, *J* = 7.8 Hz, 1H), 5.22 (s, 1H), 4.68 – 4.57 (m, 1H), 4.57 – 4.46 (m, 1H), 4.22 (dd, *J* = 8.0, 4.3 Hz, 1H), 3.99 – 3.78 (m, 2H), 3.75 (s, 3H), 3.30 (dd, *J* = 14.0, 4.3 Hz, 1H), 3.06 (dd, *J* = 14.1, 8.0 Hz, 1H), 2.67 – 2.55 (m, 1H), 2.37 (dd, *J* = 16.7, 8.7 Hz, 1H), 1.75 – 1.56 (m, 3H), 1.43 (s, 9H), 1.00 – 0.89 (m, 6H). ¹³C NMR (101 MHz, CDCl₃) δ 173.29, 169.27, 168.52, 135.82, 129.54, 129.38, 128.80, 128.70, 127.35, 80.21, 78.14, 65.10, 52.49, 51.76, 51.15, 41.27, 38.44, 30.79, 29.73, 28.41, 24.88, 22.86, 22.80, 21.97.

N₃Phe-Lys(-4-ene)(Boc)-Leu-NHNH₂ (42)

Tripeptide **40** (124 mg, 0.23 mmol, 1 equiv.) was dissolved in MeOH (5 mL) and hydrazine monohydrate (0.34 mL, 6.9 mmol, 30 equiv.) was added drop wise. After 3 h, TLC analysis showed completion of the reaction and the reaction mixture was evaporated to dryness and co-evaporated with toluene (3x) yielding the title compound in a quantitative yield. ¹H NMR (400 MHz, MeOD) δ 7.38 – 7.19 (m, 5H), 5.57 – 5.34 (m, 2H), 4.43 – 4.32 (m, 2H), 4.15 (dd, J = 8.6, 5.0 Hz, 1H), 3.60 (qd, J = 16.1, 15.4, 4.4 Hz, 2H), 3.19 (dd, J = 14.0, 5.1 Hz, 1H), 2.97 (dd, J = 13.9, 8.6 Hz, 1H), 2.50 – 2.26 (m, 2H), 1.71 – 1.50 (m, 3H), 1.43 (s, 9H), 0.94 (dd, J = 16.7, 6.4 Hz, 6H). ¹³C NMR (101 MHz, MeOD) δ 173.55, 172.71, 171.39, 158.15, 137.81, 132.12, 130.42, 129.64, 129.58, 128.04, 126.99, 125.99, 120.12, 111.88, 65.35, 54.21, 51.59, 43.01, 41.96, 38.81, 36.08, 28.76, 25.74, 23.33, 22.16.

N₃Phe-Lys(-4-yn)(Boc)-Leu-NHNH₂ (43)

Tripeptide **41** (73 mg, 0.14 mmol, 1 equiv.) was dissolved in MeOH (2 mL) and hydrazine monohydrate (0.2 mL, 4.1 mmol, 30 equiv.) was added drop wise and the solution was then refluxed at 80°C for 1h. The reaction mixture was evaporated to dryness and co-evaporated with toluene (3x) yielding the title compound in a quantitative yield. NMR-analysis could not be performed due to poor solubility in chloroform, methanol and mixture thereof.

Fmoc-Dap(Boc)-N(OMe)Me (45)

The title compound was prepared by the general procedure for peptide coupling on a 0.47 mmol scale, with 2 equiv of *N,O*-dimethylhydroxylamine. Column chromatography (20-40% EtOAc/pentane) provided the product (211 mg, 96%). ¹H NMR (300 MHz, CDCl₃) δ 7.76 (d, J = 7.4 Hz, 2H), 7.67 – 7.55 (m, 2H), 7.40 (t, J = 7.4 Hz, 2H), 7.31 (t, J = 7.6 Hz, 2H), 5.93 (d, J = 6.1 Hz, 1H), 4.96 – 4.83 (m, 1H), 4.83 – 4.69 (m, 1H), 4.39 (d, J = 7.0 Hz, 2H), 4.21 (t, J = 6.9 Hz, 1H), 3.78 (s, 3H), 3.57 (s, 1H), 3.44 (d, J = 13.2 Hz, 1H), 3.22 (s, 3H), 1.43 (s, 9H). ¹³C NMR (75 MHz, CDCl₃) δ 156.16, 143.85, 141.43, 127.82, 127.17, 125.26, 120.09, 120.06, 79.81, 67.17, 61.76, 52.04, 49.86, 47.27, 42.09, 28.43.

Fmoc-Dap(Gly-Boc)-N(OMe)Me (46)

Weinreb amide **44** (211 mg, 0.45 mmol) was deprotected using the standard procedure for Boc removal, followed by peptide coupling with Boc-Gly-OH using the standard procedure for peptide couplings. Column chromatography (60→100% EtOAc/pentane) provided the product (267 mg, 100%). ¹H NMR (400 MHz, CDCl₃) δ 7.75 (d, J = 7.5 Hz, 2H), 7.65 – 7.56 (m, 2H), 7.39 (t, J = 7.4 Hz, 2H), 7.35 – 7.27 (m, 2H), 6.72 (s, 1H), 6.12 (d, J = 6.9 Hz, 1H), 5.20 (s, 1H), 4.85 (s, 1H), 4.37 (d, J = 7.0 Hz, 2H), 4.20 (t, J = 7.0 Hz, 1H), 3.77 (s, 3H), 3.84 – 3.51 (m, 4H), 3.20 (s, 3H), 1.42 (s, 9H). ¹³C NMR (101 MHz, CDCl₃) δ 170.30, 156.42, 143.93, 143.80, 141.40, 141.36, 127.82, 127.17, 125.28, 120.08, 120.06, 80.35, 67.27, 61.82, 51.12, 47.19, 44.40, 41.38, 32.44, 28.38.

Fmoc-Dap(Gly-Boc)-VS (47)

To a solution of Fmoc-Dap(Gly-Boc)-N(OMe)Me **46** (157 mg, 0.3 mmol) at -20°C in THF (4 mL) was added LiAlH₄ (2M in THF, 150 μ L, 1 equiv.) dropwise in 10 min. TLC analysis (3% MeOH in DCM) revealed completion of the reaction and the reaction was quenched by the addition of 1M HCl. EtOAc was added and the layers were separated. The organic layer was washed with brine, dried over Na₂SO₄, filtered and concentrated, providing the crude aldehyde which was directly used in the next step. Diethyl((methylsulfonyl)methyl) phosphonate (1.5 equiv, 0.45 mmol, 104 mg) was dissolved in THF (4 mL) and cooled to 0 °C under an argon atmosphere. NaH (1.3 equiv, 0.39 mmol, 15.6 mg, 60% w/w in mineral oil) was slowly added and the mixture was stirred at 0°C for 30 min. Next, the freshly obtained aldehyde (in THF (5 mL)) was slowly added and the mixture was stirred for 1 h while slowly warming it to RT. After this time TLC analysis indicated complete conversion of the aldehyde. EtOAc was added and the mixture was extracted with 1 M aq. HCl (2x) and brine, dried over Na₂SO₄ and concentrated. Column chromatography (20→100% EA:pent) yielded the title compound (105 mg, 43% (contains 0.4 equiv of Diethyl((methylsulfonyl)methyl) phosphonate based on NMR)). ¹H NMR (400 MHz, MeOD) δ 7.79 (d, J = 7.5 Hz, 2H), 7.65 (d, J = 7.2 Hz, 2H), 7.40 (t, J = 7.4 Hz, 2H), 7.33 (t, J = 7.3 Hz, 2H), 6.82 (dd, J = 15.2, 5.1 Hz, 1H), 6.59 (d,

$J = 15.3$ Hz, 1H), 4.55 – 4.39 (m, 3H), 4.30 – 4.18 (m, 1H), 3.69 (d, $J = 4.9$ Hz, 2H), 3.43 (ddd, $J = 42.5, 13.5, 7.0$ Hz, 2H), 2.99 (s, 3H), 1.45 (s, 9H).

H-Dap(Gly-Boc)-VS (48)

Fmoc-Dap(Gly-Boc)-VS **47** (105 mg, 0.13 mmol) was dissolved in MeCN (2 mL) and cooled to 0°C. Diethylamine (2 mL) was added and after stirring for 1 h, the reaction mixture was concentrated and purified by column chromatography (0→40% MeOH/DCM), providing the title compound (0.13 mmol, 100%). ^1H NMR (400 MHz, MeOD) δ 6.87 (dd, $J = 15.2, 5.4$ Hz, 1H), 6.67 (d, $J = 15.2$ Hz, 1H), 3.85 – 3.69 (m, 3H), 3.50 – 3.23 (m, 2H), 3.00 (s, 3H), 1.45 (s, 9H). ^{13}C NMR (101 MHz, MeOD) δ 173.21, 147.58, 132.23, 80.78, 53.08, 44.80, 44.62, 42.72, 28.69.

Fmoc-Dap(Boc)-Leu-OMe (49)

The title compound was prepared by the general procedure for peptide coupling on a 0.5 mmol scale. Column chromatography (10→50% EtOAc/pentane) provided the product (259 mg, 94%). ^1H NMR (400 MHz, CDCl_3) δ 7.72 (d, $J = 7.5$ Hz, 2H), 7.56 (d, $J = 7.2$ Hz, 2H), 7.35 (t, $J = 7.4$ Hz, 2H), 7.30 – 7.21 (m, 2H), 7.15 (s, 1H), 6.38 (s, 1H), 5.38 (s, 1H), 4.54 (s, 1H), 4.32 (d, $J = 7.0$ Hz, 3H), 4.18 (t, $J = 7.2$ Hz, 1H), 3.67 (s, 3H), 3.49 (s, 2H), 1.58 (dq, $J = 16.8, 8.7, 6.7$ Hz, 3H), 1.40 (s, 9H), 0.87 (d, $J = 5.5$ Hz, 6H). ^{13}C NMR (101 MHz, CDCl_3) δ 173.13, 170.32, 156.72, 143.79, 141.30, 127.80, 127.15, 125.24, 120.03, 80.21, 67.53, 56.15, 52.45, 51.08, 47.05, 42.91, 40.85, 28.35, 24.87, 22.87, 21.77.

Fmoc-Dap(Gly-Boc)-Leu-OMe (50)

Fmoc-Dap(Boc)-Leu-OMe **49** (211 mg, 0.45 mmol) was deprotected using the standard procedure for Boc removal, followed by peptide coupling with Boc-Gly-OH using the standard procedure for peptide couplings. Column chromatography (20→100% EtOAc/pentane) provided the product in a quantitative yield. ^1H NMR (400 MHz, CDCl_3) δ 7.73 (d, $J = 7.5$ Hz, 2H), 7.56 (d, $J = 7.4$ Hz, 3H), 7.47 – 7.40 (m, 1H), 7.37 (t, $J = 7.4$ Hz, 2H), 7.28 (d, $J = 7.5$ Hz, 2H), 6.08 (d, $J = 6.7$ Hz, 1H), 5.73 (t, $J = 5.7$ Hz, 1H), 4.66 – 4.48 (m, 1H), 4.44 – 4.26 (m, 3H), 4.17 (t, $J = 7.0$ Hz, 1H), 3.93 – 3.84 (m, 1H), 3.82 (d, $J = 5.8$ Hz, 1H), 3.75 – 3.62 (m, 4H), 3.31 – 3.19 (m, 1H), 1.75 – 1.58 (m, 3H), 1.40 (s, 9H), 0.88 (d, $J = 5.7$ Hz, 6H). ^{13}C NMR (101 MHz, CDCl_3) δ 174.02, 170.94, 170.50, 155.85, 143.52, 143.47, 140.98, 127.48, 126.85, 124.93, 119.71, 79.90, 67.15, 53.83, 52.36, 51.03, 46.73, 44.26, 41.55, 39.67, 28.06, 24.60, 22.60, 21.15.

H-Dap(Gly-Boc)-Leu-OMe (51)

Fmoc-Dap(Gly-Boc)-Leu-OMe **50** is deprotected using the standard procedure for Fmoc removal, providing the title compound (189 mg, 100%) after purification by column chromatography (50% EtOAc/pent followed by 0→10 % MeOH, EtOAc). Complex NMR due to presence of rotamers. Peaks of major rotamer are reported. ^1H NMR (400 MHz, CDCl_3 , MeOD) δ 4.51 (t, $J = 7.3$ Hz, 1H), 3.79 – 3.72 (m, 5H), 3.58 (t, $J = 6.3$ Hz, 1H), 3.55 – 3.46 (m, 1H), 3.46 – 3.33 (m, 1H), 1.70-1.51 (m, 3H), 1.45 (s, 9H), 1.01 – 0.91 (m, 6H). ^{13}C NMR (101 MHz, MeOD) δ 174.17, 173.40, 171.84, 157.02, 80.38, 54.35, 52.61, 51.24, 44.15, 43.60, 43.50, 40.26, 28.38, 25.06, 22.94, 21.45.

N₃Phe-Dap(Gly-Boc)-Leu-OMe (52)

The title compound was prepared by the general procedure for peptide coupling on a 0.5 mmol scale. Column chromatography (20→80% EtOAc/pentane) provided the product (192 mg, 68%). ^1H NMR (400 MHz, CDCl_3) δ 7.71 (d, $J = 7.8$ Hz, 1H), 7.40 (d, $J = 6.9$ Hz, 2H), 7.31 – 7.20 (m, 5H), 5.83 (t, $J = 5.7$ Hz, 1H), 4.65 – 4.46 (m, 2H), 4.17 (dd, $J = 8.4, 4.0$ Hz, 1H), 3.84 (dd, $J = 16.6, 5.9$ Hz, 1H), 3.72 (s, 3H), 3.77 – 3.66 (m, 2H), 3.27 (dd, $J = 14.1, 4.0$ Hz, 1H), 3.20 – 3.07 (m, 1H), 2.99 (dd, $J = 14.0, 8.6$ Hz, 1H), 1.64 (d, $J = 6.6$ Hz, 3H), 1.40 (s, 9H), 0.97 – 0.82 (m, 6H). ^{13}C NMR (101 MHz, CDCl_3) δ 174.20, 171.13, 170.18, 169.10, 156.43, 136.07, 129.49, 128.73, 127.31, 80.08, 65.14, 52.64, 52.57, 51.39, 44.44, 41.30, 39.98, 38.50, 28.37, 24.92, 22.89, 21.54.

N₃Phe-Dap(Gly-Boc)-Leu-NHNH₂ (53)

N₃Phe-Dap(Gly-Boc)-Leu-OMe **52** (0.34 mmol) was dissolved in MeOH (3 mL), followed by the addition of NH₂⁻ NH₂·H₂O (497 μ L, 10 mmol, 30 equiv.). The reaction mixture was stirred at rt for 4h, concentrated and co-evaporated with toluene (2x) thereby providing the product in a quantitative yield. ¹H NMR (400 MHz, MeOD) δ 7.27 (qd, J = 8.6, 7.7, 4.0 Hz, 5H), 4.51 (t, J = 6.3 Hz, 1H), 4.41 (dd, J = 9.5, 5.5 Hz, 1H), 4.18 (dd, J = 9.0, 4.8 Hz, 1H), 3.83 – 3.65 (m, 2H), 3.52 (tt, J = 13.8, 6.8 Hz, 2H), 3.22 (dd, J = 14.0, 4.7 Hz, 1H), 2.96 (dd, J = 13.9, 9.0 Hz, 1H), 1.75 – 1.51 (m, 3H), 1.44 (s, 9H), 0.95 (d, J = 6.4 Hz, 3H), 0.91 (d, J = 6.4 Hz, 3H). ¹³C NMR (101 MHz, MeOD) δ 173.70, 173.21, 171.64, 171.51, 158.32, 137.81, 130.35, 129.55, 128.01, 80.74, 65.50, 54.37, 51.97, 44.64, 41.81, 41.63, 38.98, 28.70, 25.73, 23.41, 22.02.

Fmoc-His(Trt)-VS (55)

To a solution of Fmoc-His(Trt)-N(OMe)Me **54** (1.99 g, 3 mmol) at 0°C in THF (30 mL) was added LiAlH₄ (2M in THF, 1.8 mL, 3.6 mmol, 1.2 equiv.) dropwise in 10 min. TLC analysis (3% MeOH in DCM) revealed completion of the reaction after 2 h and the reaction was quenched by the addition of 1M HCl. EtOAc was added and the layers were separated. The organic layer was washed with brine, dried over Na₂SO₄, filtered and concentrated, providing the crude aldehyde which was directly used in the next step. Diethyl((methylsulfonyl)methyl) phosphonate (267 mg, 1.26 mmol, 1.5 equiv.) was dissolved in THF (8.5 mL) and cooled to 0 °C under an argon atmosphere. NaH (44 mg, 60% w/w in mineral oil, 1.1 mmol, 1.3 equiv.) was slowly added and the mixture was stirred at 0°C for 45 min. Next, the freshly obtained aldehyde (510 mg, 0.85 mmol, 1 equiv.) in THF (3 mL) was slowly added and the mixture was stirred for 3 h while slowly warming to RT. After this time TLC analysis indicated complete conversion of the aldehyde. EtOAc was added and the mixture was extracted with 1 M aq. HCl (2x) and brine, dried over Na₂SO₄ and concentrated. Column chromatography (twice, 10→80% EA/pent) yielded the title compound (378 mg, 65% (contains 0.2 equiv of Diethyl((methylsulfonyl)methyl) phosphonate based on NMR)). ¹H NMR (400 MHz, CDCl₃) δ 7.78 (d, J = 7.5 Hz, 2H), 7.64 (dt, J = 11.8, 5.8 Hz, 2H), 7.50 – 7.26 (m, 13H), 7.19 – 7.11 (m, 7H), 7.06 (d, J = 7.8 Hz, 1H), 6.85 (dd, J = 15.0, 4.6 Hz, 1H), 6.66 (s, 1H), 6.47 (d, J = 15.0 Hz, 1H), 4.78 (d, J = 5.3 Hz, 1H), 4.47 – 4.33 (m, 2H), 4.33 – 4.20 (m, 1H), 3.04 (dd, J = 14.7, 4.7 Hz, 1H), 2.90 (s, 3H), 2.85 (dd, J = 14.7, 5.2 Hz, 1H).

H-His(Trt)-VS (56)

Fmoc-His(Trt)-VS (266 mg, 0.39 mmol) was dissolved in 1:1 MeCN/diethylamine (5 mL) and cooled to 0°C. After stirring for 1 h, the reaction mixture was concentrated and purified by column chromatography (100% EtOAc, followed by 0→10% MeOH/DCM), providing the title compound (115 mg, 64%). ¹H NMR (400 MHz, CDCl₃) δ 7.42 (d, J = 1.2 Hz, 1H), 7.36 (dd, J = 5.1, 1.7 Hz, 10H), 7.19 – 7.10 (m, 5H), 6.98 (dd, J = 15.0, 4.8 Hz, 1H), 6.65 (s, 1H), 6.62 (dd, J = 15.1, 1.6 Hz, 1H), 4.02 (ddt, J = 6.9, 5.3, 2.7 Hz, 1H), 2.91 (s, 3H), 2.85 (dd, J = 14.3, 5.3 Hz, 1H), 2.67 (dd, J = 14.3, 7.8 Hz, 1H). ¹³C NMR (101 MHz, CDCl₃) δ 150.89, 142.36, 139.04, 136.97, 129.77, 128.90, 128.21, 119.80, 75.40, 51.98, 42.93, 35.61.

N₃Phe-Leu-Leu-His(Trt)-VS (57)

The title compound was obtained by the general protocol for azide coupling on a 100 μ mol scale. Purification by column chromatography (0→2% MeOH/DCM) provided the title compound (45 mg, 53%). ¹H NMR (400 MHz, CDCl₃) δ 8.28 (d, J = 8.1 Hz, 1H), 7.37 (dd, J = 5.2, 1.8 Hz, 9H), 7.34 – 7.27 (m, 4H), 7.27 – 7.22 (m, 2H), 7.16 – 7.05 (m, 6H), 6.86 (d, J = 7.7 Hz, 1H), 6.79 (dd, J = 15.1, 4.6 Hz, 1H), 6.68 – 6.62 (m, 2H), 6.45 (dd, J = 15.1, 1.5 Hz, 1H), 5.01 – 4.91 (m, 1H), 4.56 – 4.46 (m, 1H), 4.43 – 4.34 (m, 1H), 4.31 (dd, J = 7.5, 4.1 Hz, 1H), 3.30 (dd, J = 14.1, 4.1 Hz, 1H), 3.08 (dd, J = 14.1, 7.6 Hz, 1H), 2.98 – 2.91 (m, 1H), 2.90 (s, 3H), 2.80 (dd, J = 14.7, 5.7 Hz, 1H), 1.76 (ddd, J = 13.6, 8.9, 4.7 Hz, 1H), 1.67 – 1.55 (m, 2H), 1.55 – 1.42 (m, 2H), 1.41 – 1.21 (m, 1H), 0.93 (d, J = 6.5 Hz, 6H), 0.79 (d, J = 6.6 Hz, 3H), 0.76 (d, J = 6.5 Hz, 3H). ¹³C NMR (101 MHz, CDCl₃) δ 171.67, 171.64, 169.26, 146.56, 142.19, 138.71, 136.30, 135.81, 130.27, 129.82, 129.73, 129.61, 128.74, 128.29, 128.25, 128.14, 127.36, 120.18, 75.49, 65.43, 52.26, 52.01, 49.86, 42.92, 41.25, 40.36, 38.29, 31.22, 25.04, 24.53, 23.22, 23.12, 21.82, 21.78.

Biochemical experiments

General

Lysates of cells were prepared by treating cell pellets with 4 volumes of lysis buffer containing 50 mM Tris pH 7.5, 2 mM DTT, 5 mM MgCl₂, 10% glycerol, 2 mM ATP, and 0.05% digitonin for 60 min. Protein concentration was determined using Qubit[®] protein assay kit (ThermoFisher). All cell lysate labelling experiments were performed in assay buffer containing 50 mM Tris pH 7.5, 2 mM DTT, 5 mM MgCl₂, 10% glycerol, 2 mM ATP. Cell lysate labelling and competition experiments were performed at 37°C. The probe cocktail consists of: 100 nM Cy5-NC-001, 30 nM BODIPY(FL)-LU-112, 100 nM BODIPY(TMR)-NC-005-VS, used as premixed 10x concentrated cocktail in DMSO which is incubated with cell lysate for 60 min. Prior to fractionation on 12.5% SDS-PAGE (TRIS/glycine), samples were boiled for 3 min in a reducing gel loading buffer. The 7.5x10 cm (L x W) gels were run for 15 min at 80V followed by 120 min at 130V. In-gel detection of (residual) proteasome activity was performed in the wet gel slabs directly on a ChemiDoc™ MP System using Cy2 setting to detect BODIPY(FL), Cy3 settings to detect BODIPY(TMR) and Cy5 settings to detect Cy5.

Competition experiments in cell lysate

Cell lysates (diluted to 10-15 µg total protein in 9 µL buffer) were exposed to the inhibitor (10x stock in DMSO) at indicated concentrations for 1 h at 37 °C, followed by addition of probe cocktail (10x stock, 1.1 µL) and SDS-PAGE as described above.

References

1. Adams, J. The development of proteasome inhibitors as anticancer drugs. *Cancer Cell* **5**, 417-421 (2004).
2. Altun, M. et al. Effects of PS-341 on the activity and composition of proteasomes in multiple myeloma cells. *Cancer Res.* **65**, 7896-901 (2005).
3. Britton, M. et al. Selective inhibitor of proteasome's caspase-like sites sensitizes cells to specific inhibition of chymotrypsin-like sites. *Chem. Biol.* **16**, 1278-1289 (2009).
4. Mirabella, Anne C. et al. Specific cell-permeable inhibitor of proteasome trypsin-like sites selectively sensitizes myeloma cells to bortezomib and carfilzomib. *Chem. Biol.* **18**, 608-618 (2011).
5. Geurink, P.P. et al. Incorporation of non-natural amino acids improves cell permeability and potency of specific inhibitors of proteasome trypsin-like sites. *J. Med. Chem.* **56**, 1262-1275 (2013).
6. Kraus, M. et al. The novel β 2-selective proteasome inhibitor LU-102 synergizes with bortezomib and carfilzomib to overcome proteasome inhibitor resistance of myeloma cells. *Haematologica* (2015).
7. de Bruin, G. et al. A set of activity-based probes to visualize human (immuno)proteasome activities. *Angew. Chem. Int. Ed.*, **13**, 4199-4203 (2016).
8. pKa values obtained from a predictor: <https://epoch.uky.edu/ace/public/pKa.jsp>.
9. Park, H.-g. et al. Highly enantioselective and practical cinchona-derived phase-transfer catalysts for the synthesis of α -amino acids. *Angew. Chem. Int. Ed.* **41**, 3036-3038 (2002).
10. Thimon, C., Panza, L. & Morin, C. Synthesis of a Glycosylated ortho-Carboranyl Amino Acid. *Synlett* **2003**, 1399-1402 (2003).
11. Porter, N.A., Ziegler, C.B., Khouri, F.F. & Roberts, D.H. General synthesis of polyunsaturated fatty acid hydroperoxides involving a novel vinylcyclopropyl bromide ring opening. *J. Org. Chem.* **50**, 2252-2258 (1985).
12. Wender, P.A., Holt, D.A. & Sieburth, S.M. in *Organic Syntheses* (John Wiley & Sons, Inc., 2003).
13. Valverde, I.E. et al. 1,2,3-triazoles as amide bond mimics: triazole scan yields protease-resistant peptidomimetics for tumor targeting. *Angew. Chem. Int. Ed.* **52**, 8957-8960 (2013).
14. de Bruin, G. et al. Structure-based design of β 1i or β 5i specific inhibitors of human immunoproteasomes. *J. Med. Chem.* **57**, 6197-6209 (2014).
15. Huber, Eva M. et al. Immuno- and constitutive proteasome crystal structures reveal differences in substrate and inhibitor specificity. *Cell* **148**, 727-738 (2012).
16. Huber, E.M. et al. Systematic analyses of substrate preferences of 20S proteasomes using peptidic epoxyketone inhibitors. *J. Am. Chem. Soc.* **137**, 7835-7842 (2015).

CHAPTER 10

A native-PAGE FRET assay that reports on mammalian proteasome core particle composition

Introduction

26S proteasomes are responsible for the degradation of the majority of cytoplasmic and nuclear proteins in eukaryotic cells.¹ Proteins destined for degradation are tagged with poly-ubiquitin chains for recognition by 19S (PA700) caps. Subsequently and in an ATP-dependent process, proteasome substrates are unfolded and funnelled through the α -rings to the inner side of 20S proteasome core particles (CP), where they are degraded. CPs are 28-mer multi-protein complexes consisting of four heptameric rings: two outer α -rings onto which 19S caps can dock and two inner β -rings in which the catalytic subunits reside. Each β -ring of the constitutive proteasome (cCP, Figure 1), constitutively expressed in all eukaryotic cells, contains three different active subunits: β 1c (caspase-like, cleaving preferentially after acidic residues), β 2c (trypsin-like, cleaving preferentially after basic residues) and β 5c (chymotrypsin-like, cleaving preferentially after hydrophobic residues). Proteasomes produce oligopeptides varying in length between 3-12 residues.² These are further processed by aminopeptidases and in part escape to the ER lumen, where they bind to major histocompatibility complex class I (MHC-I) heterodimers for antigen presentation. Another type of proteasomes, immunoproteasomes (iCP, Figure 1), are constitutively expressed in bone marrow derived cells and can be induced in other tissues by the inflammatory cytokines, interferon- γ (IFN- γ) and tumour necrosis factor- α (TNF- α).³ iCPs generate peptide pools containing a comparatively (with respect to cCP-produced oligopeptide pools) higher number of peptides prone to bind to MHC-I complexes. This change is mainly caused by the substrate specificity of β 1i, which appears chymotrypsin-like in nature, as compared to the caspase-like nature of β 1c. The cleavage specificity of β 2i and β 5i resembles their cCP counterparts, β 2c and β 5c. Besides 19S caps, CPs can also interact with other proteasome activators including PA28 (or 11S) and PA200.⁴ In addition, hybrid CPs can be simultaneously

bound to 19S, 11S or PA200 to form hybrid proteasomes.⁵ 11S containing proteasome complexes degrade proteins in an ATP-independent manner, are more active and cause generation of peptides that are not suitable for binding to MHC-I. The exact role of 11S caps in the immune system remains elusive.⁴

Constitutive proteasome assembly

In the formation of mammalian constitutive proteasomes, α -rings are assembled first and serve as a scaffold onto which the β -subunits dock.^{6, 7} In this manner $\alpha_7\beta_7$ complexes are formed. These dimerise to form $\alpha_7\beta_7\beta_7\alpha_7$ preholoproteasome cCPs, which, after a number of proteolytic steps, yield fully active cCPs. Correct α -ring formation is mediated by two proteasome assembling chaperones (PACs), heterodimeric protein complexes termed PAC1-PAC2⁸ and PAC3-PAC4.⁹ PAC1-PAC2 binds α_5 and α_7 simultaneously and remains associated until cCP formation nears completion (Figure 1B).⁸ PAC3-PAC4 binds to α_5 and the resulting complex serves as scaffold from which an α -ring emerges.^{7, 9} A fully assembled α -ring next binds to the maturation protein (POMP, or UMP1)¹⁰. Subsequently, β_2 docks onto the α -ring¹¹, followed by β_3 and release of PAC3-PAC4. The resulting assembly is termed a 15S complex and consists of a single α -ring binding to PAC1-PAC2, β_2 and β_3 .¹² Next and in this order β_4 , β_5 , β_6 , β_1 and β_7 are incorporated. The β_7 C-terminal tail then intercalates between β_1 and β_2 of another $\alpha_7\beta_7$ particle, thereby triggering dimerization and formation of a preholoproteasome cCP.¹² Most β -subunits are expressed with N-terminal and/or C-terminal extensions, which function as intramolecular chaperones and are cleaved during the assembly process. The β_{1c} , β_{2c} and β_{5c} subunits are translated with N-terminal propeptides that remain intact until the final stages of proteasome formation.¹³ Autocatalytic removal of both N-terminal and C-terminal propeptides followed by degradation of the chaperones, POMP and PAC1-PAC2 yields functional 20S proteasome cCPs, with the $\beta_{1c}/\beta_{2c}/\beta_{5c}$ catalytic, N-terminal threonine residues revealed at this final stage.^{8, 14}

Immunoproteasome assembly

The assembly of iCP particles is similar to that of cCPs, however with some striking differences. Whereas β_{1c} is incorporated as the second-to-last β -subunit, β_{1i} enters the assembly pathway much earlier and forms an intermediate complex with β_{2i} , β_3 and β_4 (Figure 1C).^{15, 16} β_{5i} has a higher affinity for POMP than β_{5c} and is therefore incorporated preferentially over β_{5c} when both particles are present.¹⁵ In addition, β_{5i} is required for maturation of β_{1i} and β_{2i} .¹⁷ These interdependencies guide a preferential formation of homogenous 20S core particles (iCPs) that contain β_{1i} , β_{2i} and β_{5i} , even though constitutive proteasome catalytic activities (β_{1c} , β_{2c} , β_{5c}) are always present during iCP formation.

Mixed proteasomes

iCPs and cCPs are however not formed exclusively in tissue expressing both active β -subunit sets ($\beta 1c/\beta 2c/\beta 5c$ and $\beta 1i/\beta 2i/\beta 5i$), and mixed proteasomes (mCPs) containing cCP and iCP catalytic subunits can be formed (Figure 1A). Since $\beta 1i$ and $\beta 2i$ both rely on $\beta 5i$ for removal of their N-terminal propeptide, $\beta 5i$ is always present in mCPs in at least one of the two β -rings.

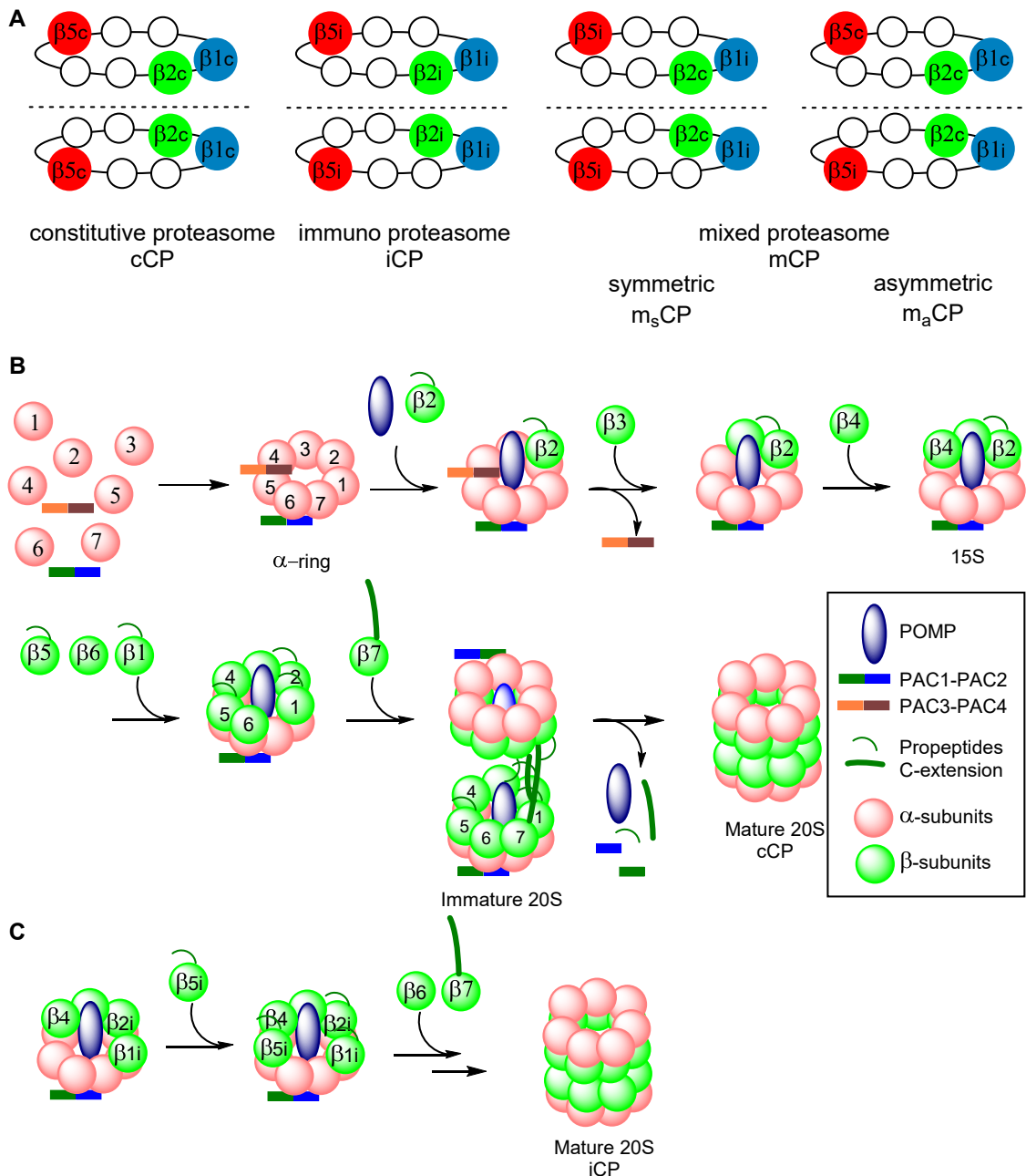


Figure 1. Proteasome subtypes and assembly. A) Schematic representations of cCP, iCP and some m_sCPs and m_aCPs. B) Assembly pathway of cCPs. C) Assembly of the iCP.

Subtype	$\beta 1$	$\beta 2$	$\beta 5$	$\beta 1$	$\beta 2$	$\beta 5$	Subtype	$\beta 1$	$\beta 2$	$\beta 5$	$\beta 1$	$\beta 2$	$\beta 5$
cCP							m_aCP_4						
iCP							m_aCP_5						
m_sCP_1							m_aCP_6						
m_sCP_2							m_aCP_7						
m_sCP_3							m_aCP_8						
m_aCP_1							m_aCP_9						
m_aCP_2							m_aCP_{10}						
m_aCP_3													

Table 1. Theoretical possible proteasome subtypes. With the prerequisite that $\beta 5i$ is always present in a β -ring when $\beta 1i$ and/or $\beta 2i$ are incorporated, 15 subtypes are possible. **Grey:** constitutive proteasome subunit. **White:** immunoproteasome subunit.

Incorporation of $\beta 2i$ and $\beta 1i$ are mutually dependent to some extent, although $\beta 1i$ can be incorporated with $\beta 2c$ and $\beta 2i$ with $\beta 1c$.¹⁷⁻¹⁹ During proteasome assembly, two half proteasomes ($\alpha_7\beta_7$) are joined to form, upon autocatalytic removal of the β -subunit propeptides, mature 20S particles ($\alpha_7\beta_7\beta_7\alpha_7$). In this process, β -rings may have the same β -subunit composition, leading to cCPs, iCPs or symmetric, mixed CPs (m_sCPs). Asymmetric, mixed proteasomes (m_aCPs) are formed when two differently composed $\alpha_7\beta_7$ particles are joined.^{20, 21} Mathematically, different CP particles are possible, however, $\beta 1i$ and $\beta 2i$ can only be incorporated together with $\beta 5i$. Taking this restriction in account, five different β -rings are possible, and thus 15 different proteasome types may exist simultaneously in cells expressing all cCP and iCP subunits (Table 1). Of the 15 possible combinations, mCPs containing either $\beta 5i$ - $\beta 1c$ - $\beta 2c$ or $\beta 5i$ - $\beta 1i$ - $\beta 2c$ β -rings are encountered most often and have been identified in human liver, colon, small intestine and kidney tissues.²² mCPs produce peptide pools distinct from both those produced by cCPs and iCPs, thus adding to the diversity of MHC-I ligands and thereby to a broad CD8⁺ T-cell repertoire. Tumour-specific antigenic peptides^{22, 23} as well as virally encoded antigenic peptides²⁴ have been identified that appear to be produced uniquely by mCPs. A rapid and accurate assay to detect mixed proteasomes and that would report on the nature of their composition would be of considerable use to get insight in the contribution of these in protein turnover and MHC-I antigenic peptide pool production.

Analysis of proteasome composition

Current methods to identify proteasome CP composition are based on either chromatographic separation of proteasome subtypes,^{21, 25} isoelectric focussing electrophoresis,²⁶ or antibody mediated depletion of a β -subunit,²² followed by determination of CP composition by either immunostaining, substrate hydrolysis assays or mass spectrometry analysis of purified proteasomes.²⁷ This chapter describes a native-PAGE

Fluorescence Resonance Energy Transfer (FRET) assay that reports on proteasome CP composition of crude cell lysates. For this purpose proteasome-subunit selective irreversible inhibitors were equipped with suitable fluorophores to yield a panel of activity-based probes (ABPs) for FRET mediated detection of proteasome compositions. FRET is a physical process in which energy is transferred from a donor fluorophore to an acceptor fluorophore via dipole-dipole coupling. This non-radiative energy transfer depends on whether the fluorophores are in close proximity ($>100 \text{ \AA}$); whether there is substantial overlap between the donor emission and acceptor excitation spectra and whether the fluorophores are properly oriented (the dipoles of the fluorophores should be approximately parallel).²⁸ FRET has been widely used to study protein-protein interactions and conformational changes,²⁹ but its potential to determine the composition of protein complexes has not been fully exploited.³⁰ The distances between all active site threonine residues fall well within the FRET range ($<100 \text{ \AA}$)³¹ (Figure 2). This chapter describes the development and use of activity-based probes (ABPs) that target either human $\beta 1c/\beta 1i$, $\beta 2c/\beta 2i$ or $\beta 5c/\beta 5i$ and that are equipped with suitable FRET donor or acceptor fluorophores. With these, in combination with simultaneous selective inhibition of multiple sites, eight distinct CP subunit-combinations, originating from cCPs, iCPs and m_s CPs, were detected using native-PAGE FRET. In addition, ABPs targeting either $\beta 1c$, $\beta 1i$, $\beta 5c$ or $\beta 5i$ were used to discern asymmetric, mixed proteasomes (m_a CPs).

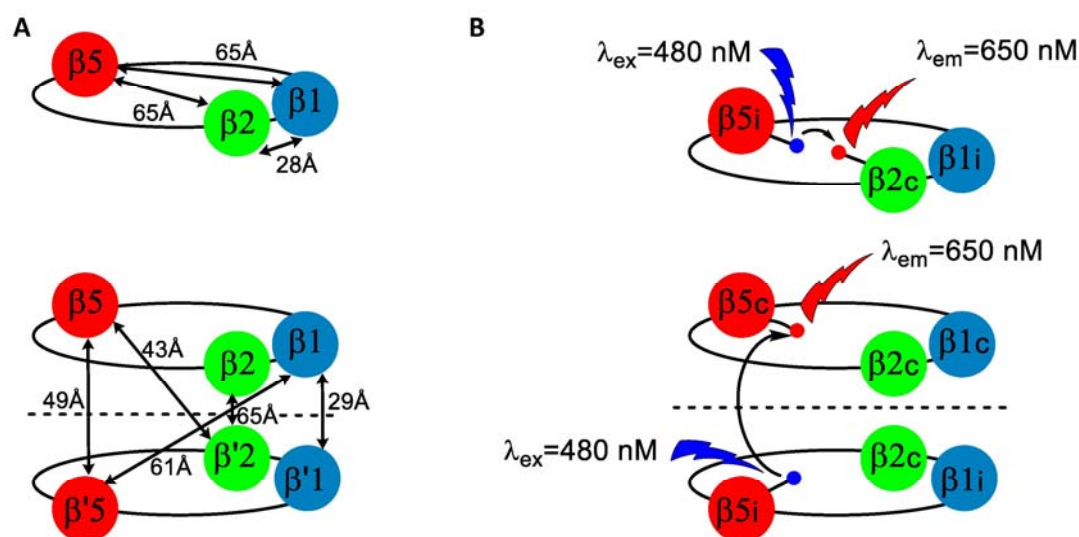


Figure 2. A) Distances between active site Thr residues. B) Examples of intra- (top) and inter- β -ring FRET (bottom) between a donor ABP (small blue sphere, BODIPY-FL fluorophore) and an acceptor ABP (small red sphere, Cy5 fluorophore).

Results

Development of FRET donor and acceptor ABPs

Native-PAGE separation of proteasomes has provided important insights in proteasomal composition, assembly and binding characteristics.³² On native gel, proteasome complexes separate in three bands, corresponding to doubly capped 30S proteasomes, singly capped 26S-proteasomes and 20S proteasome CPs. These complexes are revealed by either Western blotting or in-gel fluorogenic substrate assays.³² Proteasomes containing 11S or PA200 caps have not been investigated using native-PAGE to date. It was reasoned that, in analogy to SDS-PAGE, it should be possible to visualize intact proteasome complexes on native-PAGE using ABPs. Indeed (Figure 3, lane 1-3), clear labelling of both 26S proteasomes and 20S proteasomes was observed in crude cell lysate using either Cy5-NC001 (β 1-selective), BODIPY(FL)-LU112 (β 2-selective) or BODIPY(TMR)-NC005 (β 5-selective; see chapter 3 for the development of these probes). In the first instance it was investigated whether FRET signals emerge from proteasomes exposed to combinations of these probes and next resolved by native-PAGE. For this purpose, lysates were treated with each of the three combinations of two probes simultaneously. Clear FRET signals could be observed for each combination (Figure 3, lane 4-6, Cy2-Cy3, Cy3-Cy5 and Cy2-Cy5 channels) as well as quenching of FRET donor ABPs (Figure 3, Cy2-Cy3 channels, lane 4-6 compared to lane 2-3).

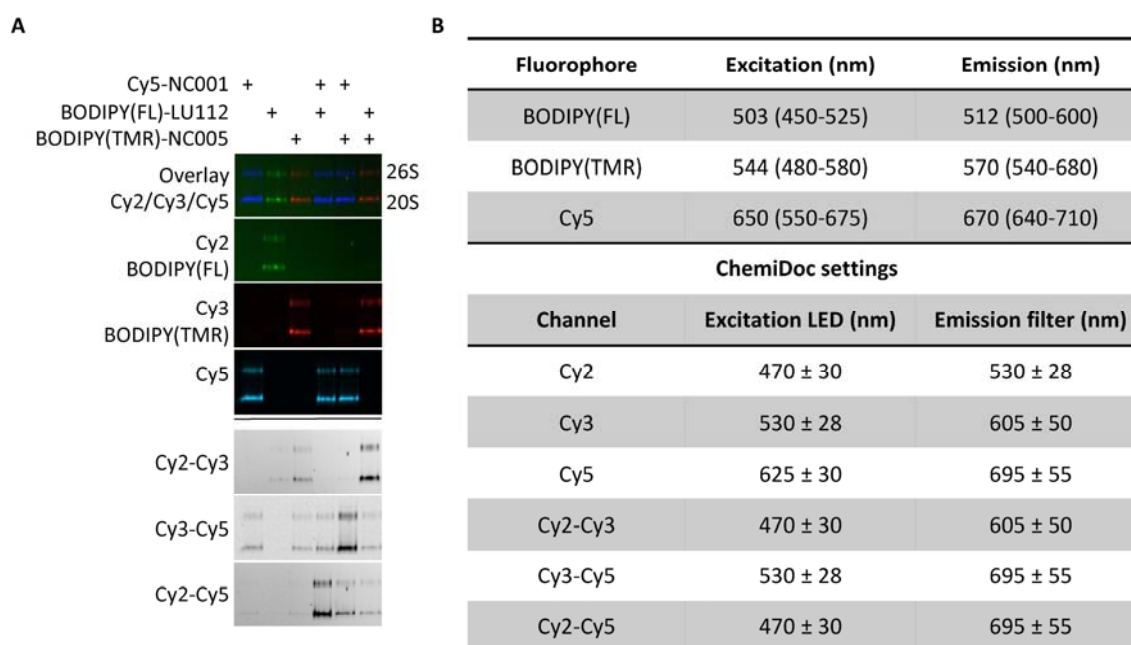


Figure 3. Selection of a suitable FRET donor/acceptor pair. A) Native-PAGE analysis of Raji lysate labelled with individual probes and with three different donor/acceptor pairs. B) Excitation/emission of fluorophores and settings on the ChemiDoc gel imager.

However, due to the spectral overlap with both Cy2 excitation and Cy5 emission, the use of BODIPY(TMR) as either FRET donor or acceptor proved suboptimal (Figure 3, lane 3, Cy2-Cy3 and Cy3-Cy5 channels, notice the background signals). In the Cy2-Cy5 channel, hardly any background signal was observed in the samples treated with BODIPY(FL)- or Cy5-modified probes (Figure 3, lane 1 and 2, Cy2-Cy5). As well, FRET efficiency between these fluorophores appeared close to 100%, indicating near complete quenching of BODIPY(FL) fluorescence. Given these results, it was decided to develop BODIPY(FL) and Cy5 ABPs for each subunit-pair (β 1c/ β 1i, β 2c/ β 2i and β 5c/ β 5i). The structures of all ABPs used in this study are shown in Figure 4. BODIPY(FL)-NC001³³ **2** and BODIPY(FL)-LU112³⁴ **4** have been described previously, whereas Cy5-LU112 **3** was readily synthesised following established procedures (see the experimental section). Cy5-LU015 **5** and BODIPY(FL)-LU015 **6** were used to selectively label β 5c/ β 5i (see chapter 6). Furthermore, in order to study m_aCPs, ABPs selective for a single catalytic subunit, namely BODIPY(FL)-LU001c **7** (β 1c-selective, see chapter 8), Cy5-LU001i **8** (β 1i-selective, see chapter 6), BODIPY(FL)-LU015c **9** (β 5c-selective, see chapter 7) and Cy5-LU035i **10** (β 5i-selective, see chapter 6), were developed. The selectivity window of ABPs **1-10** was assessed in Raji- and HEK cell lysates (ABP **1-6**) and the required concentrations for complete labelling of the respective subunits are indicated in Table 2 (see supplemental Figure 1 for labelling profiles). β 2-selective probes **3** and **4** as well as β 1-selective probe **2** partially label both β 5 subunits at concentrations required for full labelling. To avoid this to happen, the β 5 subunits are to be blocked previous to treatment with **2**, **3** or **4** and this can be accomplished by pre-treatment with either a β 5-selective inhibitor or by β 5 probes **5** or **6** (neither of which are cross-reactive). β 5c selective probe BDP-LU015c **9** partially labels both β 2 subunits, which however can be prevented by pre-treatment with the β 2-selective inhibitor LU102 (**12**) (see chapter 7).

Evaluation of ABPs 1-6 as native-PAGE FRET proteasome probes

From the pool of ABPs **1-6**, six FRET donor/acceptor pairs can be assembled. All these pairs were evaluated in Raji and HEK-293 lysates on their behaviour as FRET couples in a native-PAGE fluorescence readout setting. In the first step, both β 5 subunits were either inhibited with NC-005 **13** (in case FRET signals emerging from ABP labelling of β 1 and β 2 were sought for) or labelled with ABPs **6** or **7** (β 1- β 5 or β 2- β 5 labelling) for 1 hour. Subsequently, β 1 and/or β 2 targeting probes **1**, **2**, **3** and/or **4** were added and the samples were again incubated for 1 hour. One half of each sample was resolved by native-PAGE and the other half by SDS-PAGE. Clear FRET signals and near complete quenching of FRET donor ABPs were observed for each FRET pair (Figure 5A). Following quantification of the fluorescence bands of the acceptor ABPs (Cy2 channel), the FRET efficiencies (E) were calculated, and high FRET efficiencies for each FRET pair (E > 0.8, Figure 5B) were revealed.

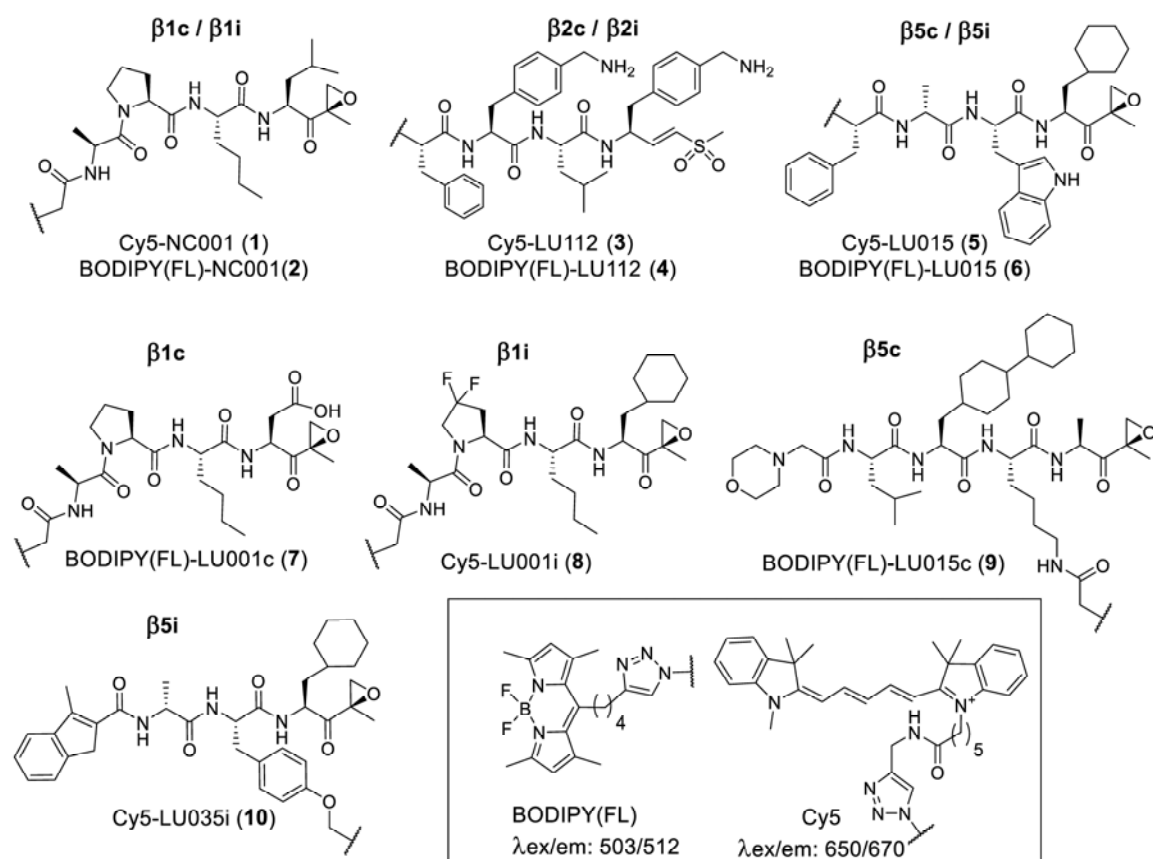
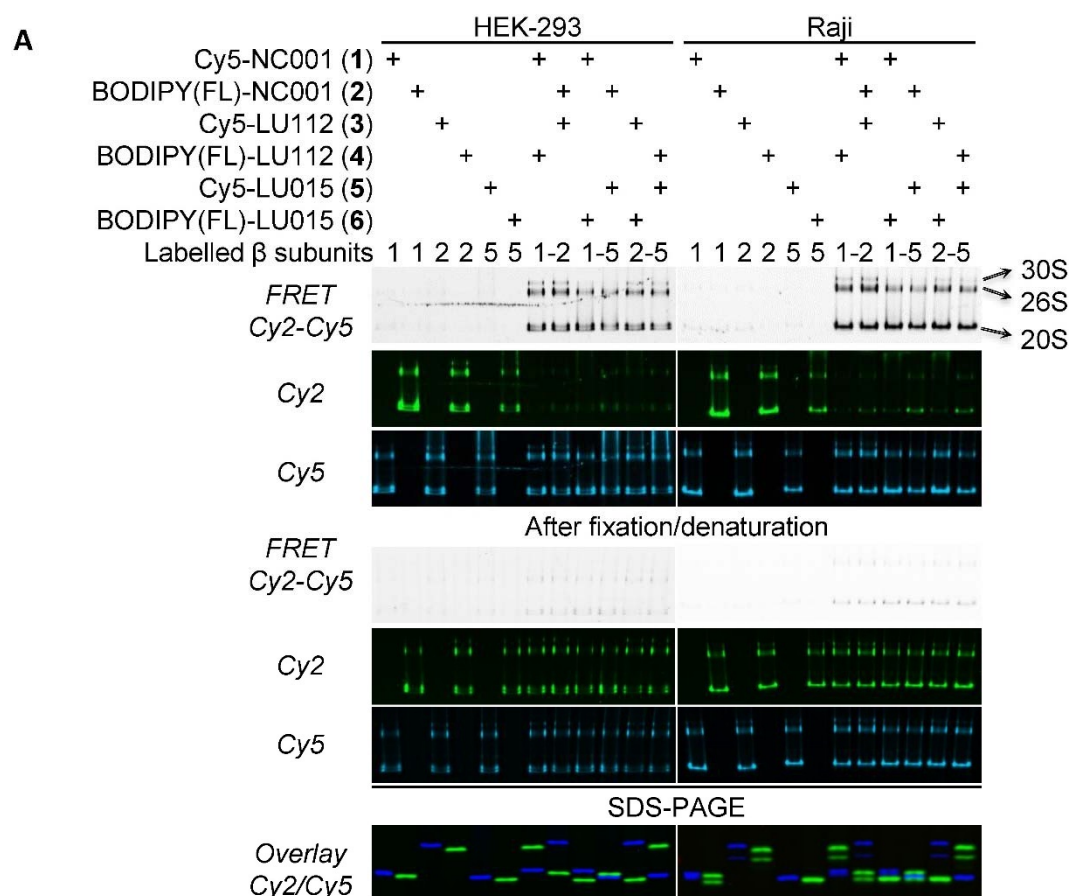


Figure 4. Structures of FRET donor (BODIPY(FL)) and acceptor (Cy5) activity-based probes used in this study.

[ABP] (μM)	Subunit	Raji	HEK (HeLa)	[inhibitor] (μM)	Subunit	Raji (HeLa)
1 Cy5-NC001	$\beta 1c/\beta 1i$	0.3	0.1	11 NC001	$\beta 1c/\beta 1i$	2.5
2 BODIPY(FL)-NC001	$\beta 1c/\beta 1i$	1.0	1.0	12 LU102	$\beta 2c/\beta 2i$	0.3
3 Cy5-LU112	$\beta 2c/\beta 2i$	0.03	0.1	13 NC005	$\beta 5c/\beta 5i$	2.5
4 BODIPY(FL)-LU112	$\beta 2c/\beta 2i$	0.1	0.1	14 LU001c	$\beta 1c$	3.0 (10)
5 Cy5-LU015	$\beta 5c/\beta 5i$	0.3	1.0 (0.3)	15 LU001i	$\beta 1i$	1.0
6 BODIPY(FL)-LU015	$\beta 5c/\beta 5i$	0.3	1.0* (0.3)	16 LU002i	$\beta 2i$	3.0
7 BODIPY-LU001c	$\beta 1c$	0.1	n.d. (0.1)	17 LU005c	$\beta 5c$	1.0 (3)
8 Cy5-LU001i	$\beta 1i$	0.1	n.d. (0.1)	18 LU035i	$\beta 5i$	0.3
9 BODIPY-LU015c	$\beta 5c$	0.3	n.d. (0.3)			
10 Cy5-LU035i	$\beta 5i$	0.1	n.d. (0.1)			

Table 2. Concentrations for full labelling by ABPs or full inhibition by inhibitors for the target subunit(s). n.d.: not determined. * 80% inhibition after 2 h.

Swapping the FRET donor (BODIPY-FL) and acceptor (Cy5) on the subunit-selective ABPs did not result in significant differences in FRET efficiency. In order to verify whether true intra-proteasomal FRET signals are observed, the native-PAGE slab was transferred to a fixing solution (5:4:1 H₂O/MeOH/AcOH) and heated in a microwave oven. This process results in denaturation of the proteins, and separation of the fluorophores. Indeed, after fixation, FRET signals have disappeared almost entirely (Figure 5A), with concomitant return of fluorescence of the donor ABPs.



B

FRET Efficiency $E=1-(F_{DA}/F_D)$				
Donor	Acceptor	Subunits	E (HEK)	E (Raji)
BODIPY(FL)-LU112 (4)	Cy5-NC001 (1)	β_2 - β_1	0.96	0.96
BODIPY(FL)-NC001 (2)	Cy5-LU112 (3)	β_1 - β_2	0.93	0.93
BODIPY(FL)-LU015 (6)	Cy5-NC001 (1)	β_5 - β_1	0.82	0.85
BODIPY(FL)-NC001 (2)	Cy5-LU015 (5)	β_1 - β_5	0.87	0.86
BODIPY(FL)-LU015 (6)	Cy5-LU112 (3)	β_5 - β_2	0.81	0.85
BODIPY(FL)-LU112 (4)	Cy5-LU015 (5)	β_2 - β_5	0.87	0.81

Figure 5. Evaluation of six FRET donor/acceptor pairs in HEK-293 and Raji lysates. A. Native-PAGE and SDS-PAGE analysis. Gels were imaged using Cy2, Cy5 or Cy2-Cy5 settings, see Figure 3B. B. Calculated FRET efficiencies. F_D : Fluorescence intensity donor (lane 2, 4, 6 in Cy2 channel); F_{DA} : FRET intensity donor in presence of acceptor (lane 7-12 in Cy2 channel).

This result confirms the occurrence of intra-proteasomal FRET and the suitability of ABPs **1-6** for native-PAGE FRET analysis of proteasome compositions. Remarkably, mutual differences in fluorescence intensity on native-PAGE between samples treated with a single ABP was observed, while on SDS-PAGE the intensities are similar (Figure 5A, compare lanes 1-6 in both gels). For instance, BODIPY(FL)-NC001 **2** shows the highest fluorescent signal with the intensities for BODIPY(FL)-LU112 **4** and BODIPY(FL)-LU015 being respectively 1.5 and 4 times lower (Figure 5A, compare lane 2, 4 and 6). However, after gel fixation after which all FRET signals were lost, the fluorescence intensity for the three probes became almost equal. These differences may be caused by either self-quenching³⁵ or homo-FRET³⁶, processes that can take place when fluorophores have sufficient overlap in their excitation and emission spectra. Since proteasomes encompass two copies of each subunit (pair), two fluorophores are brought in close proximity, which allows self-quenching or homo-FRET processes to occur. Due to differences in the mutual orientation of- and distances between the two fluorophores, the efficiency of self-quenching of the ABPs may vary, resulting in different fluorescence intensities.

Native-PAGE FRET allows the detection of mixed proteasomes

In order to detect mixed proteasomes by native-PAGE FRET, each donor or acceptor ABP should bind to a single cCP or iCP subunit. The presence of mixed proteasome core particles in a given sample is revealed by FRET when, for instance, a donor ABP is bound to a cCP subunit and an acceptor ABP to an iCP subunit. Selective binding of ABPs **1-6** to a single subunit can be attained by making use of the panel of subunit-selective inhibitors which are described in chapter 3 (see also Table 2). With the exception of LU-002c (targeting β 2c) the selectivity windows for all inhibitors are sufficiently large to allow selective and complete blocking of their target subunits. With the panel of five inhibitors selective for β 1c, β 1i, β 2i, β 5c, or β 5i, eight combinations of two inhibitors can be made. With these and together with ABPs **1-6** eight different proteasome subunit combinations can in theory be detected. Each possible inhibitor combination was assessed in Raji cell lysates using two FRET ABP pairs (see Figure 6). Since both inter- and intra- β -ring FRET can take place, the observed FRET signal is a sum of several possible FRET pathways that emerge from, either, two, three or four ABPs present in a proteasome particle. This complexity essentially precludes the use of relative FRET intensity as a measurement for relative amounts of specific subunit combinations. Interestingly, however, clear FRET signals were observed for each combination, which implies that, next to cCP, iCP and m_s CP particles also m_a CP particles are present. The various ABP couples yield FRET signals of similar intensities, but subtle differences are observed (see Table 3). The FRET intensities derived from either cCP-cCP or iCP-iCP ABP pairs are always higher than those obtained from cCP-iCP probe/inhibitor combinations, a result that

supports the reported preferential formation of pure iCPs and cCPs over mCPs. The high $\beta 2c$ over $\beta 2i$ ratio (see Table 3) is reflected in the relatively high FRET intensities emerging from ABPs bound to $\beta 2c$ - $\beta 1c/\beta 5c$ compared to $\beta 2c$ - $\beta 1i/\beta 5i$, underscoring that $\beta 2c$ is preferentially incorporated together with $\beta 1c$ and $\beta 5c$ (as in cCP and $m_aCP_{1,2 \text{ or } 3}$, see Table 1). The low FRET signal between $\beta 2c$ - $\beta 1i$ (as in m_sCP_2 and $m_aCP_{2,5,8,9}$) reflects the preferential incorporation of $\beta 2i$ together with $\beta 1i$ (as in iCP and $m_aCP_{4,7,9,10}$).

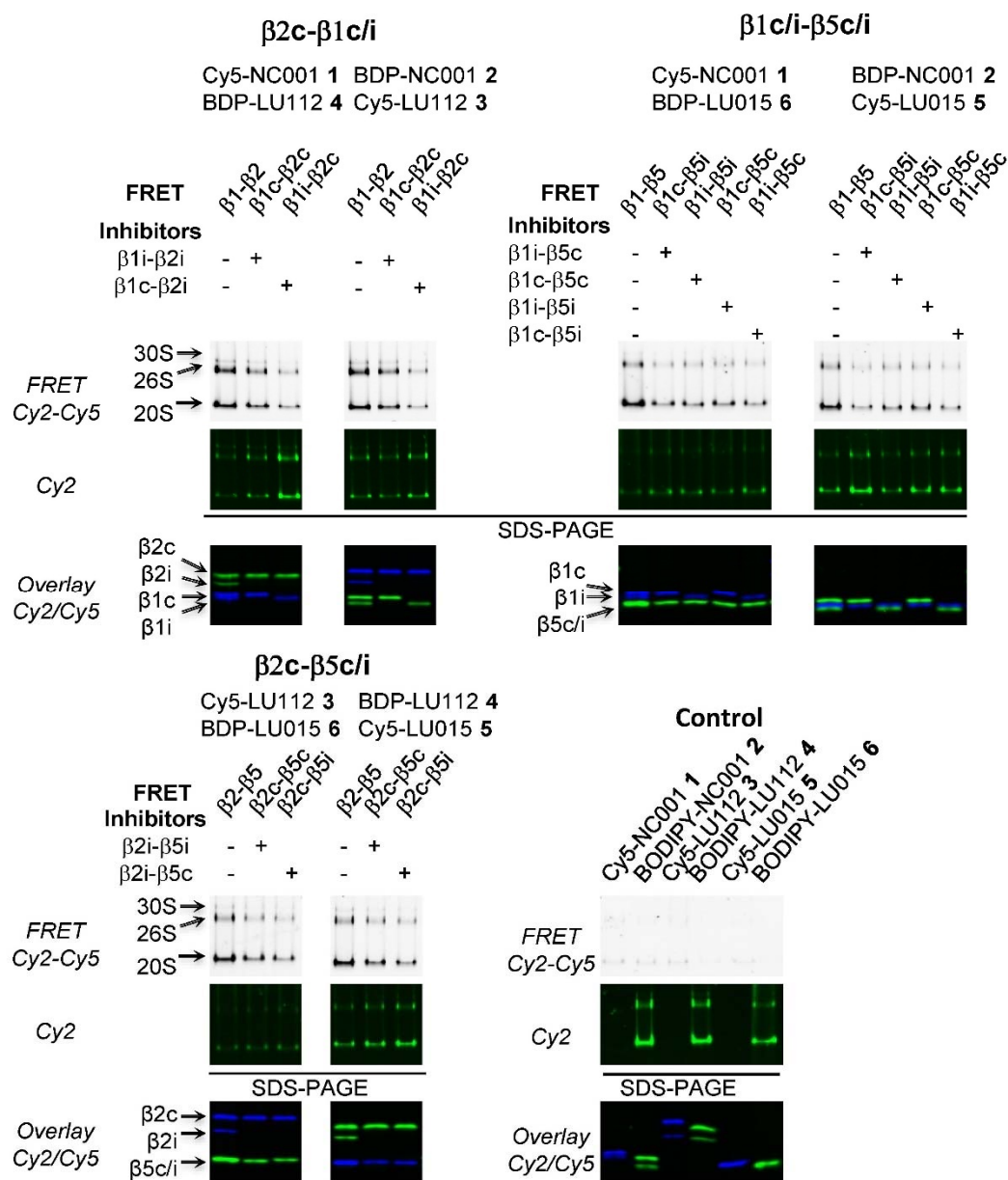


Figure 6. Detection of mixed proteasomes in Raji cell lysates. Samples were pre-incubated with indicated inhibitors, followed by labelling of residual proteasome activity by indicated ABPs. The samples were analysed by native-PAGE and SDS-PAGE.

Subunits		Relative FRET intensity (% of FRET no inhibitor)*		Ratio subunits**
ABPs		Cy5-NC001 – BDP-LU112 (1-4)	BDP-NC001 – Cy5-LU112 (2-3)	
β 1c	β 2c	53	50	β 1c/ β 1i= 1.24±0.03 (55/45)
β 1i	β 2c	18	17	β 2c/ β 2i= 2.28±0.07 (70/30)
ABPs		Cy5-NC001 – BDP-LU015 (1-6)	BDP-NC001 – Cy5-LU015 (2-5)	β 5c/ β 5i= 1.04±0.03 (51/49)
β 1c	β 5i	26	23	
β 1i	β 5i	28	35	
β 1c	β 5c	31	44	
β 1i	β 5c	23	20	
ABPs		Cy5-LU112 – BDP-LU015 (3-6)	BDP-LU112 – Cy5-LU015 (3-5)	
β 2c	β 5c	39	50	
β 2c	β 5i	27	29	

Table 3. Relative FRET intensities in Raji lysates. *Determined by quantification of FRET signals from Figure 6. ** Determined by quantification of SDS-PAGEs from Figure 6.

The FRET intensities for β 1c- β 5c and β 1i- β 5i are higher than those for β 1i- β 5c and β 1c- β 5i, indicating preferential formation of β 1c- β 5c and β 1i- β 5i containing β -rings. Remarkably, a substantial FRET signal was observed for β 1i- β 5c. As β 5i is required for the propeptide removal of β 1i, β 5c cannot be incorporated in the same β -ring together with β 5i, and therefore this result strongly suggests that m_aCP_2 and/or m_aCP_4 are present.

Asymmetric mixed proteasomes (m_aCPs) can be detected using native-PAGE FRET

When applied at appropriate concentrations, ABPs **7**, **8**, **9** and **10** selectively and completely block a single proteasome subunit, namely β 1c, β 1i, β 5c and β 5i respectively. Inclusion of these compounds in the native-PAGE FRET experiments allows labelling of for instance β 1c with a FRET donor and β 1i with a FRET acceptor ABP. FRET signals emerging from samples treated in this way and resolved on native-PAGE, can only be caused by m_aCPs . Clear FRET signals were observed for both FRET pairs **7/8** and **9/10**, confirming the presence of one or more m_aCPs (m_aCP_{1-4} : asymmetric in β 5 composition; $m_aCP_{2,4,5,7,8,10}$: asymmetric in β 1 composition) in Raji cell lysates (see Figure 7). Although relative amounts of m_aCPs could not be established due to lack of appropriate reference samples, this method demonstrates the presence of m_aCPs in a given sample in an unambiguous fashion.

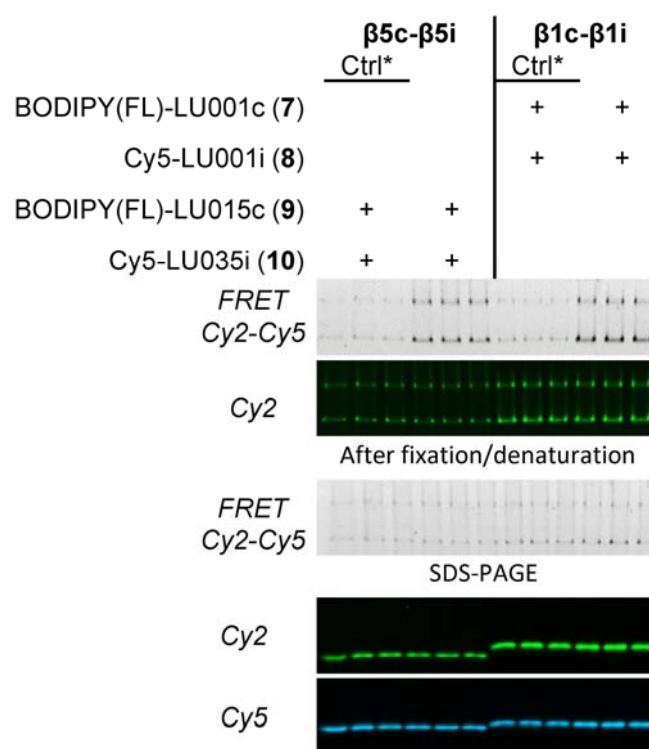


Figure 7. Asymmetric mixed proteasomes in Raji cell lysates. Samples were incubated with a $\beta 2$ -selective inhibitor (LU102, in case of ABPs 9, 10) or a $\beta 5$ -selective inhibitor (NC005, in case of ABPs 7, 7) followed by treatment with various ABPs. *Ctrl: control. Control samples contained twice the amount of protein compared to normal samples and were incubated with LU-102 or NC-005 as for normal samples, followed by incubation with one of the ABPs. Next, remaining proteasome activities were blocked by a mixture of NC001, LU102 and NC005 and the samples treated with ABP 7/8 and 9/10 were mixed. This shows the total background caused by the intrinsic properties of the fluorophores.

Assessment of proteasome composition after induction of iCPs by IFN- γ .

The expression of iCP subunits can be induced by exposure to the inflammatory cytokine interferon- γ (IFN- γ). Dahlmann and co-workers²¹ reported that HeLa cells exposed to IFN- γ express both m_s CPs and m_a CPs. These observations were re-evaluated using the above-described native-PAGE FRET assay. For this, HeLa cells were either exposed to IFN- γ for 24 h or left untreated. Next, both samples were subjected to various inhibitor/ABP combinations and evaluated by native-PAGE FRET as described above. When not exposed to IFN- γ , HeLa cells express only small amounts of $\beta 1i$ and $\beta 5i$ while $\beta 2i$ could not be detected. Following exposure to IFN- γ , a substantial increase of the amount of all iCP subunits was found (Table 4, Figure 8). As expected, non-exposed HeLa cells show high inter-cCP subunit FRET signals. Since the FRET signals emerging from $\beta 5i\text{-}\beta 1c$ are higher than those observed for $\beta 5i\text{-}\beta 1i$, it is likely that the majority of the $\beta 5i$ subunits in these non-exposed cells are present in proteasomes that also contain at least one $\beta 1c$ subunit (as in m_a CP_{1,2,5} and m_s CP₁). As well, substantial $\beta 5i\text{-}\beta 5c$ and $\beta 1i\text{-}\beta 1c$ FRET signals were observed (Figure 9), indicating the

presence of m_aCPs ($m_aCP_{1,2}$: asymmetric in $\beta 5$ composition; $m_aCP_{2,5}$: asymmetric in $\beta 1$ composition). Most likely, the majority of these m_aCPs contain either a single $\beta 5i$ (m_aCP_1), or both one $\beta 5i$ and one $\beta 1i$ in the same β -ring (m_aCP_2), as witnessed by the observed FRET signal between $\beta 5c$ and $\beta 1i$. After exposure to IFN- γ , a dramatic increase in $\beta 5i$ - $\beta 1i$ FRET signal is observed, while $\beta 5i$ - $\beta 1c$, $\beta 5c$ - $\beta 1i$ and $\beta 5c$ - $\beta 1c$ combinations are slightly decreased. This decrease does not necessarily reflect a decrease of the absolute amounts of these subunit-pairs, but is probably caused by the increase in expression and incorporation into proteasome particles of both $\beta 5i$ -subunits and $\beta 1i$ -subunits, with an increased total FRET intensity as the result.

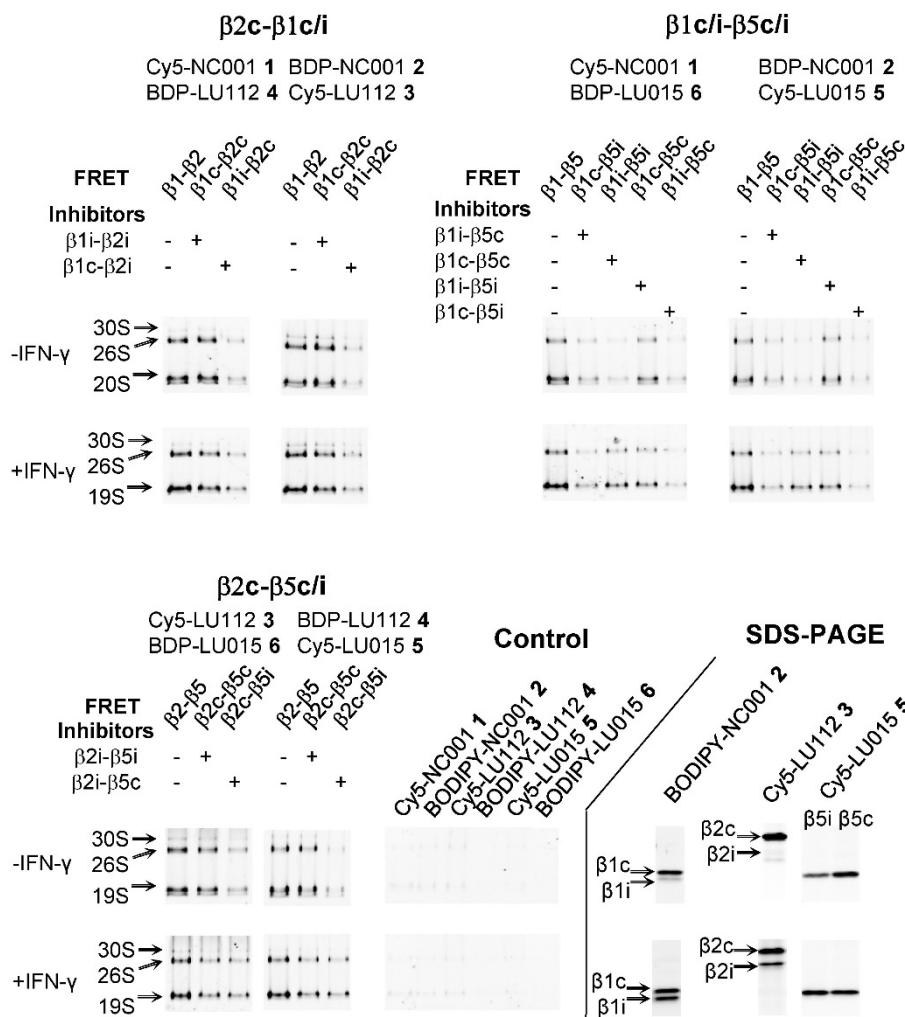


Figure 8. Mixed proteasomes in HeLa cell lysates, with or without exposure to IFN- γ for 24 h. Samples were pre-incubated with indicated inhibitors, followed by labelling of residual proteasome activity by indicated ABPs. SDS-PAGE analysis shows the relative amounts of iCP and cCP subunit before and after exposure to IFN- γ . To label $\beta 5c$ or $\beta 5i$ specifically, either $\beta 5i$ was blocked by LU-035i or $\beta 5c$ by LU-005c.

Subunits		Relative FRET intensity (% of FRET no inhibitor)*				Ratio subunits**
		-IFN- γ	+IFN- γ	-IFN- γ	+IFN- γ	
ABPs		Cy5-NC001-BDP-LU112 (1-4)		BDP-NC001-Cy5-LU112 (2-3)		-IFN- γ
β 1c	β 2c	89	57	102	58	β 1c/ β 1i= 5.52 \pm 0.04 (85/15)
β 1i	β 2c	22	20	20	19	β 2c/ β 2i= 1.00 (100/0)
ABPs		Cy5-NC001-BDP-LU015 (1-6)		BDP-NC001-Cy5-LU015 (2-5)		β 5c/ β 5i= 2.47 \pm 0.12 (72/28)
β 1c	β 5i	29	21	32	22	+IFN- γ
β 1i	β 5i	14	41	13	40	β 1c/ β 1i= 1.44 \pm 0.07 (85/59)
β 1c	β 5c	54	33	67	40	β 2c/ β 2i= 2.72 \pm 0.01 (100/37)
β 1i	β 5c	17	7	15	10	β 5c/ β 5i= 0.98 \pm 0.04 (72/72)
ABPs		Cy5-LU112-BDP-LU015 (3-6)		BDP-LU112-Cy5-LU015 (3-5)		
β 2c	β 5c	72	36	74	47	
β 2c	β 5i	30	30	19	31	

Table 4. Relative FRET intensities in HeLa lysates, before and after exposure to IFN- γ for 24 h. *Determined by quantification of FRET signals from Figure 9. ** Determined by quantification of SDS-PAGES.

Given the long half-life of cCPs (up to 5 days)¹⁵, IFN- γ induced expression of iCP subunits presumably leads to a net increase of the total proteasome amount. When for convenience it is assumed that limited proteasome degradation takes place during the 24 h exposure with IFN- γ , the slight decrease in β 5i- β 1c and β 5c- β 1i-derived FRET signals indicates that no new proteasomes containing these subunit-pairs are formed, that newly expressed β 5i is mainly incorporated together with β 1i and that newly formed CPs are symmetric with respect to their β 1/ β 5 subunit composition. Interestingly, the β 2c- β 5i FRET signals significantly increase (Figure 8) and their intensities become closer to the β 2c- β 5c FRET signals. The same applies to β 1i- β 2c, indicating that β 5i is to some extent incorporated with β 2c, which is also reflected by the lower net increased amount of β 2i (+37%) compared to β 1i and β 5i (both +44%). Altogether it can be concluded that, following exposure to IFN- γ , HeLa cells predominantly produce two distinct proteasome types, namely mCPs featuring β -rings composed of either β 1i- β 2i- β 5i or β 1i- β 2c- β 5i (as in iCP, m_sCP₂ and m_aCP₉). This observation is further confirmed by the lower relative amount of m_aCPs found after exposure to IFN- γ (lower signal/noise ratio compared to no IFN- γ , Figure 9), indicating that the newly formed proteasomes are symmetric with respect to their β 1 and β 5 subunit composition.

Discussion

This chapter describes an in-depth analysis on the use of ABPs to determine the composition of large protein complexes using a native-PAGE FRET assay. Proteasome subunit-pair selective ABPs equipped with suitable FRET donor and acceptor fluorophores were selected, which target β 1c/ β 1i, β 2c/ β 2i or β 5c/ β 5i. Crude cell extracts were treated with combinations of these FRET donor/acceptor ABPs and resolved on native-PAGE, after which FRET signals were measured by fluorescent imaging of the gel.

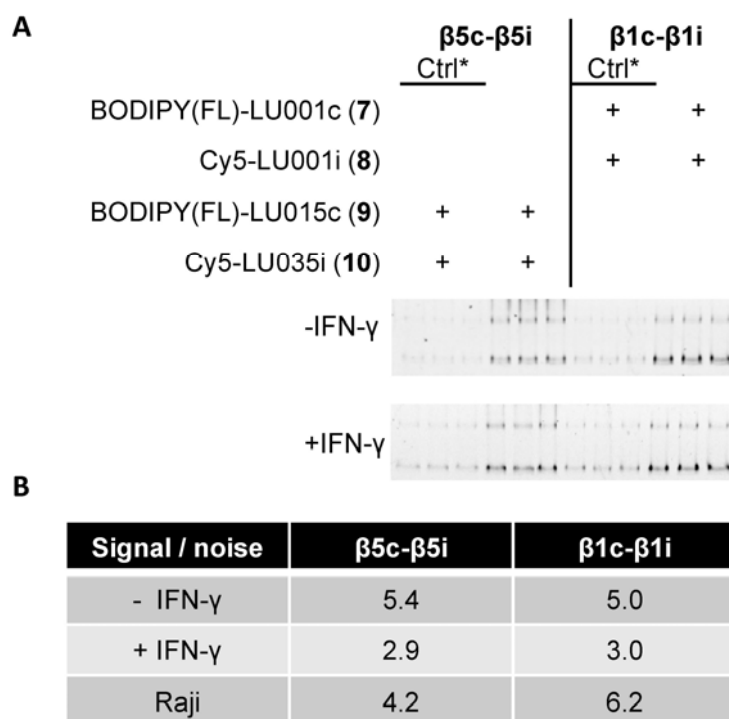


Figure 9. Asymmetric mixed proteasomes in HeLa cell lysates, before and after exposure to IFN- γ for 24 h. A. Samples were incubated with a $\beta 2$ -selective inhibitor (LU102, in case of ABPs **9**, **10**) or a $\beta 5$ -selective inhibitor (NC005, in case of ABPs **7**, **8**) followed by treatment with ABPs. *Ctrl: control. Control samples contained twice the amount of protein compared to normal samples and were incubated with LU-102 or NC-005 as for normal samples, followed by incubation with one of the ABPs. Next, remaining proteasome activity was blocked by a mixture of NC001, LU102 and NC005 and the samples treated with ABP **7/8** and **9/10** were mixed. This shows the total background caused by the intrinsic properties of the fluorophores. B. Signal/noise ratios of m_a CP FRET signals of HeLa cell lysates, before and after exposure to IFN- γ for 24 h, compared to Raji cell lysates.

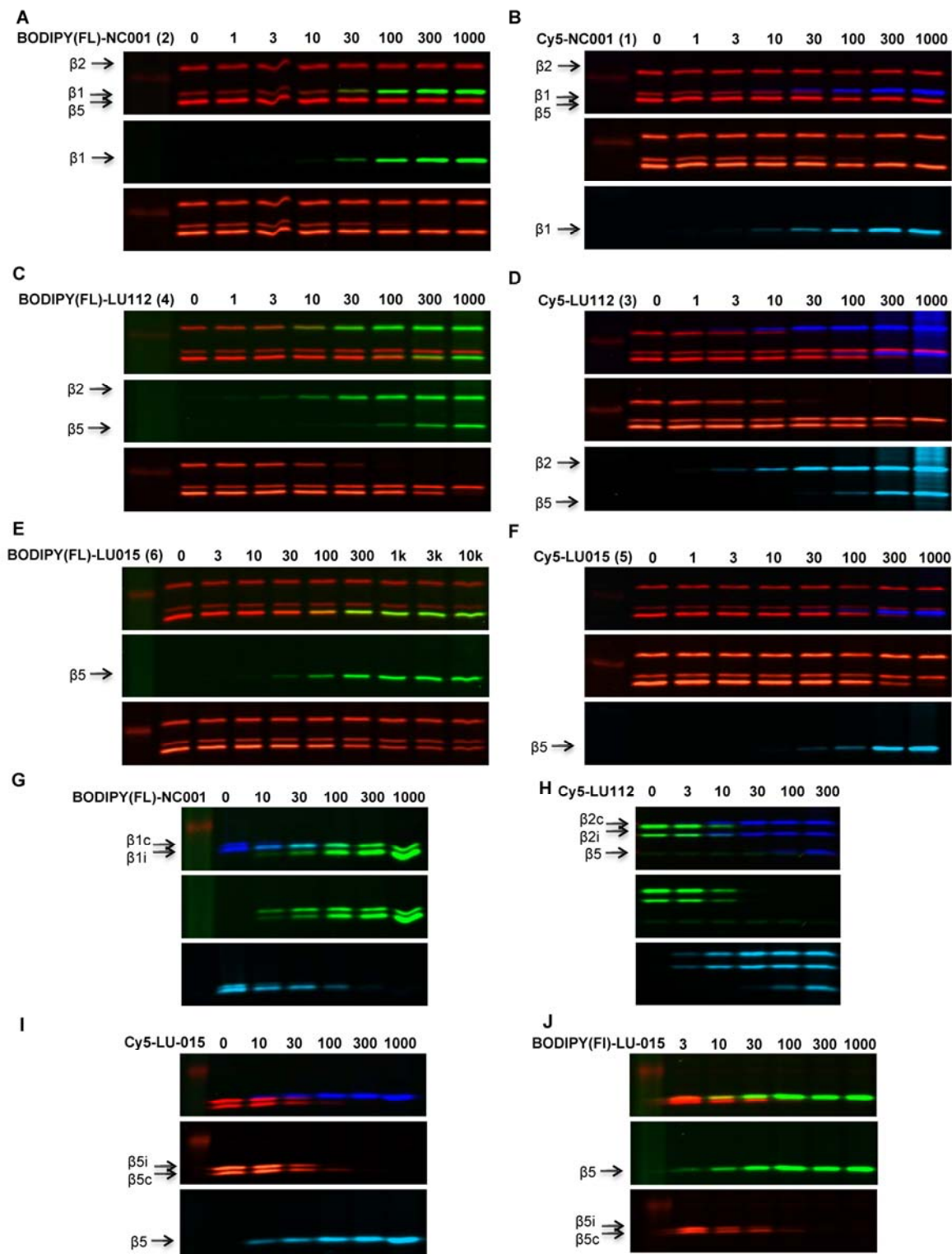
In HEK-293 cells, expressing exclusively cCPs, all FRET pairs gave clear FRET signals with high FRET efficiencies ($E > 0.8$), confirming that $\beta 1c$, $\beta 2c$ and $\beta 5c$ are present in stoichiometric amounts. The assembly pathway of immunoproteasomes favours the formation of CPs that contain only $\beta 1i$, $\beta 2i$ and $\beta 5i$, however, incorporation of both cCP and iCP subunits to form mCPs occurs as well, and in total 15 different 20S proteasomes can exist (see Table 1). Using subunit selective inhibitors, which block $\beta 1c$, $\beta 1i$, $\beta 2i$, $\beta 5c$ or $\beta 5i$, specific FRET signals derived from eight subunit-pairs were obtained. In lysates of Raji cells, which express all six proteasome subunits, FRET signals were observed for iCP-iCP and cCP-cCP subunit-pairs. Interestingly, also FRET signals of all possible iCP-cCP subunit-pairs could be detected, indicating the presence of mCPs. Moreover, using selective $\beta 1c-\beta 1i$ and $\beta 5c-\beta 5i$ targeting FRET donor-acceptor pairs, m_a CPs could be visualized that are asymmetric in their $\beta 1$ and $\beta 5$ subunits. Altogether, these results indicate a complex mixture of proteasome subtypes in Raji cells. Although this method does not provide the exact composition and neither absolute quantity of the different proteasome subtypes, relative FRET intensities do provide

semi-quantitative information regarding the presence of the different subunit-pairs. In Raji cells, iCP-iCP and cCP-cCP subunit-pairs show higher relative FRET intensities compared to iCP-cCP subunit-pairs for $\beta 1$ - $\beta 5$, indicating preferential formation of $\beta 1i$ - $\beta 5i$ and $\beta 1c$ - $\beta 5c$ containing β -rings. Compared to Raji cells, IFN- γ exposed HeLa cells do show much lower relative FRET intensities of $\beta 1$ - $\beta 5$ iCP-cCP subunit-pairs, and the relative FRET intensities indicate preferential formation of proteasomes containing β -rings composed of $\beta 5i$ - $\beta 1i$ - $\beta 2i$ and $\beta 5i$ - $\beta 1i$ - $\beta 2c$. Interestingly, both Raji- and IFN- γ exposed HeLa cells express similar amounts of all subunits, indicating that more mCPs are formed when all subunits are constitutively expressed compared to induction of iCP subunits in otherwise low iCP expressing cells. Remarkably, Dahlmann and co-workers identified CPs asymmetric in their $\beta 1$ subunit composition in IFN- γ exposed HeLa cells, while the non-exposed HeLa in their hands did not express detectable amount of immunoproteasome subunits.²¹ However, in this study it was found that after IFN- γ exposure HeLa cells predominantly express proteasome containing β -rings symmetric in their $\beta 1$ subunit composition. Dahlmann and co-workers used $\beta 1c$ -ZZ transfected HeLa cells to allow specific precipitation of $\beta 1$ -ZZ by binding to IgG and subsequent analysis of subunit composition of precipitated proteasomes. This might result in higher $\beta 1c$ -ZZ than normal $\beta 1c$ expression, causing higher incorporation of $\beta 1c$ -ZZ in newly formed proteasomes resulting in asymmetric proteasome formation.

Compared to existing methods to determine proteasome composition, the method described in this chapter has several advantages. For instance, van den Eynde and co-workers²² used subunit depletion and subsequent immunoblotting to determine proteasome composition. Alternatively, they calculated the quantity of mCPs based on the assumption that $\beta 5i$ can be incorporated as the only iCP subunit or together with $\beta 1i$, but that $\beta 2i$ is always incorporated together with $\beta 1i$ and $\beta 5i$. However, in these approaches asymmetric proteasomes are not taken into account and therefore several proteasome subtypes are possibly overlooked. This FRET-based approach, besides being more sensitive, is also much faster, straightforward and less time consuming than the methods relying on chromatographic separation of proteasomes. The measurement of FRET signals in-native PAGE also represents a major improvement the methodology developed by Kim and co-workers.³⁰ In this method, FRET signals were measured in a plate reader, which required removal of unbound probes by filtration. Moreover, whereas detect $\beta 5c$ - $\beta 1i$ FRET signals were detected, the detection of other subunit-pairs was hampered by the lack of truly subunit selective probes and inhibitors. Importantly, their method to prove $\beta 5c$ - $\beta 1i$ containing proteasomes is highly questionable, since a $\beta 5i$ selective probe (LKSCy5³⁷) was claimed to selectively label $\beta 5c$ and a $\beta 1c$ / $\beta 1i$ targeting probe (UKPCy3) was used to selectively label $\beta 1i$ in RPMI-8226 cells and no selective inhibitors were applied to inhibit $\beta 5i$ and $\beta 1c$.

In conclusion, the native-PAGE FRET assay described in this chapter adds to existing methods that allow the assessment of proteasome core particle composition. The method provides semi-quantitative insights in the abundance of ten different proteasome subunit-pairs and can do so in any crude cell extract.

Supporting Figure



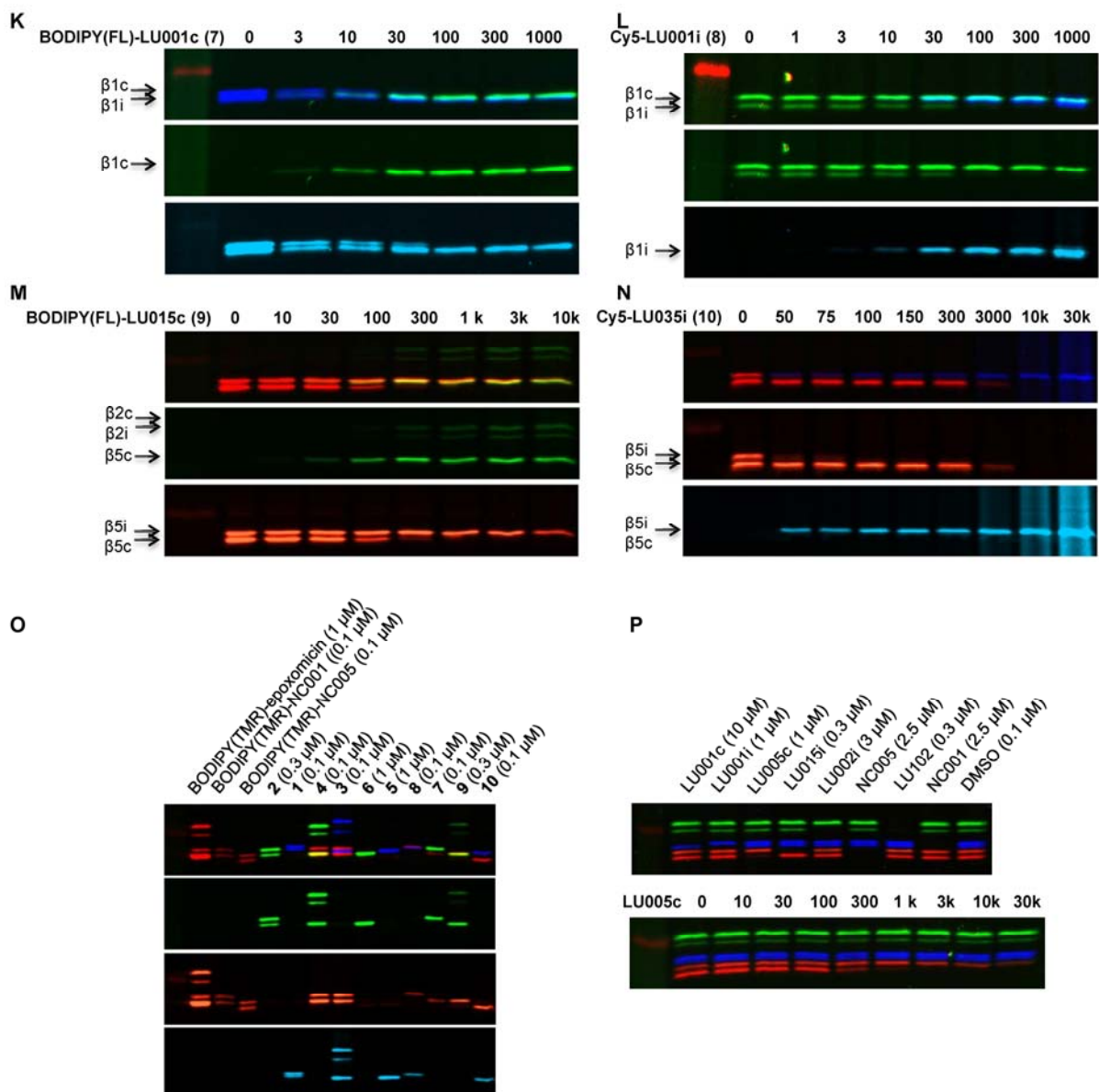


Figure S1. Labelling profiles of ABPs in HEK-293 (A-F) and Raji (G-N) to determine optimal probe concentrations, as indicated in Table 1 and verification of ABP labelling and selective inhibition by inhibitors in IFN- γ treated HeLa cells. For labelling profiles of Cy5-NC001 and BODIPY(FL)-LU112, see chapter 3. Upper gels picture is overlay of Cy2/Cy3, Cy3/Cy5 or Cy2/Cy5 channels. BODIPY(FL): depicted green; BODIPY(TMR): depicted red; Cy5: depicted blue. A-F. HEK-293 cell lysates were treated with indicated concentrations of ABP 1-6, followed by labelling of residual proteasome activity by labelling of residual β 1 activity by BODIPY(TMR)-epoxomicin (1 μ M); G-N. Raji cell lysates were treated with indicated concentrations of ABPs followed by labelling of: residual β 1 activity by Cy5-NC001 (0.1 μ M) (G, K) or BODIPY(FL)-NC001 (L); residual β 2 activity by BODIPY(FL)-LU112 (0.03 μ M) (H); residual β 5 activity by BODIPY(TMR)-NC005 (0.1 μ M) (I,J,M,N). O. Labelling of HeLa cell lysates by ABPs 1-10 at indicated concentrations followed by labelling of residual β 1 activity by BODIPY(TMR)-NC001 (0.1 μ M) in case of β 1 selective ABPs; residual β 2 activity by BODIPY(TMR)-epoxomicin (1 μ M) in case of β 2 selective ABPs and β 5 activity by BODIPY(TMR)-NC005 (0.1 μ M) in case of β 1 selective ABPs. P. Verification of selective inhibition by inhibitors in IFN- γ treated HeLa cells.

Experimental

Synthetic procedures

General procedures

Acetonitrile (ACN), dichloromethane (DCM), N,N-dimethylformamide (DMF), methanol (MeOH), diisopropylethylamine (DiPEA) and trifluoroacetic acid (TFA) were of peptide synthesis grade, purchased at Biosolve, and used as received. All general chemicals (Fluka, Acros, Merck, Aldrich, Sigma, Iris Biotech) were used as received. Column chromatography was performed on Screening Devices b.v. Silica Gel, with a particle size of 40–63 μm and pore diameter of 60 \AA . TLC analysis was conducted on Merck aluminium sheets (Silica gel 60 F254). Compounds were visualized by UV absorption (254 nm), by spraying with a solution of $(\text{NH}_4)_6\text{Mo}_7\text{O}_{24}\cdot 4\text{H}_2\text{O}$ (25 g/L) and $(\text{NH}_4)_4\text{Ce}(\text{SO}_4)_4\cdot 2\text{H}_2\text{O}$ (10 g/L) in 10% sulphuric acid, a solution of KMnO_4 (20 g/L) and K_2CO_3 (10 g/L) in water, or ninhydrin (0.75 g/L) and acetic acid (12.5 mL/L) in ethanol, where appropriate, followed by charring at ca. 150 $^\circ\text{C}$. ^1H and ^{13}C NMR spectra were recorded on an AV-600 (600 MHz) spectrometer. Chemical shifts are given in ppm (δ) relative to CD_3OD as internal standard. High resolution mass spectra were recorded by direct injection (2 μL of a 2 μM solution in water/acetonitrile 50/50 (v/v) and 0.1% formic acid) on a mass spectrometer (Thermo Finnigan LTQ Orbitrap) equipped with an electrospray ion source in positive mode (source voltage 3.5 kV, sheath gas flow 10, capillary temperature 250 $^\circ\text{C}$) with resolution $R = 60,000$ at m/z 400 (mass range $m/z = 150\text{--}2,000$) and dioctylphthalate ($m/z = 391.28428$) as a “lock mass”. The high resolution mass spectrometer was calibrated prior to measurements with a calibration mixture (Thermo Finnigan). LC-MS analysis was performed on a Finnigan Surveyor HPLC system with a Gemini C_{18} 50 \times 4.60 mm column (detection at 200–600 nm), coupled to a Finnigan LCQ Advantage Max mass spectrometer with ESI. The applied buffers were H_2O , ACN and 1.0% aq. TFA. Method: xx \rightarrow xx% MeCN, 13.0 min (0 \rightarrow 0.5 min: 10% MeCN; 0.5 \rightarrow 8.5 min: gradient time; 8.5 \rightarrow 10.5 min: 90% MeCN; 10.5 \rightarrow 13.0 min: 10% MeCN). HPLC purification was performed on a Gilson HPLC system coupled to a Phenomenex Gemini 5 μm 250 \times 10 mm column and a GX281 fraction collector. LU112(Boc)³⁴, ABPs **1**³⁸, **2**³³, **4**³⁴; **5**, **6**, **8**, **10** (chapter 6); **7** (chapter 8); **9** (chapter 7) were synthesized as reported before. Subunit selective inhibitors are described in chapter 3.

Cy5-LU112 (3)

To a degassed solution of LU-112(Boc) (7.2 mg, 7.8 μmol) and Cy5-alkyne (5.2 mg) in DMF (0.8 mL) under an argon atmosphere was added $\text{CuSO}_4\cdot 5\text{H}_2\text{O}$ (0.5 equiv., 3.9 μmol (100 μL from degassed stock solution of 39 $\mu\text{mol}/\text{mL}$) and NaAsc (0.75 equiv., 5.9 μmol (100 μL from degassed stock solution of 59 $\mu\text{mol}/\text{mL}$)). After stirring overnight, the reaction mixture was concentrated and purified by column chromatography (0–2–5% MeOH in DCM). The Boc-protected compound was then treated with 1:1 TFA/DCM for 15 min, followed by concentration and purification by HPLC (C_{18} , 30–50% MeCN, 0.1% TFA, 10 min gradient) provided the product as a blue powder after lyophilisation (2.03 mg, 1.4 μmol , 18%). ^1H NMR (600 MHz, MeOD) δ 8.24 (t, $J = 13.0$ Hz, 2H), 7.82 (s, 1H), 7.49 (d, $J = 7.3$ Hz, 2H), 7.45 – 7.37 (m, 4H), 7.35 (d, $J = 8.1$ Hz, 2H), 7.32 – 7.23 (m, 5H), 7.23 – 7.10 (m, 5H), 7.06 (d, $J = 6.8$ Hz, 2H), 6.79 (dd, $J = 15.2, 5.5$ Hz, 1H), 6.67 – 6.49 (m, 2H), 6.27 (dd, $J = 13.7, 7.7$ Hz, 2H), 5.50 (dd, $J = 10.1, 5.6$ Hz, 1H), 4.82 – 4.78 (m, 1H), 4.62 (dd, $J = 10.3, 4.6$ Hz, 1H), 4.58 (s, 2H), 4.40 – 4.32 (m, 2H), 4.30 (dd, $J = 9.8, 5.1$ Hz, 1H), 4.09 (t, $J = 7.5$ Hz, 2H), 4.05 (d, $J = 7.7$ Hz, 3H), 3.61 (s, 3H), 3.49 – 3.39 (m, 1H), 3.24 – 3.13 (m, 1H), 3.12 – 2.96 (m, 2H), 2.92 (s, 3H), 2.86 (dd, $J = 14.0, 10.3$ Hz, 1H), 2.24 (t, $J = 7.4$ Hz, 2H), 1.88 – 1.78 (m, 2H), 1.77 – 1.65 (m, 12H), 1.65 – 1.54 (m, 3H), 1.47 (dt, $J = 11.6, 6.7$ Hz, 3H), 1.37 – 1.23 (m, 2H), 0.93 (dd, $J = 31.8, 6.3$ Hz, 6H). ^{13}C NMR (151 MHz, MeOD) δ 175.78, 175.51, 174.55, 174.32, 172.98, 169.46, 155.59, 155.43, 146.51, 146.15, 144.21, 143.56, 142.62, 142.53, 139.60, 139.39, 136.85, 133.10, 132.83, 131.99, 131.32, 130.94, 130.25, 130.04, 129.97, 129.75, 129.63, 128.20, 126.56, 126.35, 126.20, 123.80, 123.43, 123.29, 111.97, 111.88, 104.45, 104.16, 65.97, 55.92, 53.78, 52.64, 50.52, 44.74, 44.06,

44.03, 42.78, 41.84, 40.14, 39.09, 38.39, 36.56, 35.53, 31.53, 28.18, 27.96, 27.78, 27.42, 26.50, 25.90, 23.41, 21.96. HRMS: calculated $C_{72}H_{90}N_{11}O_6S$ 1236.67908[M]⁺; found 1236.67920. LC-MS (linear gradient 10 → 90% MeCN/H₂O, 0.1% TFA, 13.0 min):R_t (min): 6.22 (ESI-MS (m/z): 1236.67 (M⁺)).

Biochemical experiments

General

Lysates of cells were prepared by treating cell pellets with 4 volumes of lysis buffer containing 50 mM Tris pH 7.5, 2 mM DTT, 5 mM MgCl₂, 10% glycerol, 2 mM ATP, and 0.05% digitonin for 60 min. Protein concentration was determined using Qubit[®] protein assay kit (ThermoFisher). All cell lysate labelling experiments were performed in assay buffer containing 50 mM Tris pH 7.5, 2 mM DTT, 5 mM MgCl₂, 10% glycerol, 2 mM ATP. Cell lysate labelling and competition experiments were performed at 37°C. Incubation times were always 1 hour. Prior to fractionation on 12.5% SDS-PAGE (TRIS/glycine), samples were boiled for 3 min in a reducing gel loading buffer. The 7.5x10 cm (L x W) gels were run for 15 min at 80V followed by 120 min at 130V. NativePAGE[™] Novex[™] 3-12% Bis-Tris Protein Gels, 1.0 mm, 15-well, NativePAGE[™] Running Buffer (20X) and NativePAGE[™] Sample Buffer (4X) were obtained from ThermoFisher. Native gels were run for 115 min at 150V. In-gel detection of (residual) proteasome activity was performed in the wet gel slabs directly on a ChemiDoc[™] MP System using Cy2 setting to detect BODIPY(FL), Cy3 settings to detect BODIPY(TMR) and Cy5 settings to detect Cy5. FRET signal were detected using manual settings as indicated in Figure 3B.

FRET experiments

Final concentrations of ABPs and inhibitors are indicated in Table 1.

FRET with probes 1-6: Cell lysates (40 µg/sample, 18 µL) were treated with inhibitors (1 µL of 20x stocks in DMSO, inhibitors were premixed in case of multiple inhibitors) or DMSO. Samples for β1-β2 FRET were treated with NC005. After 1 h incubation, β5 selective ABPs **5** or **6** were added to the appropriate samples (1 µL of 20x stocks in DMSO) and the samples were incubated for 1 h (2 h for HEK), followed by the addition of β1 selective ABPs **1**, **2**, **3**, and/or **4** (1 µL of 20x stocks in DMSO). After incubation for 1 h, 8 µL of each samples was transferred for SDS-PAGE analysis. Another 8 µL was transferred for native-PAGE analysis, to which was added 4 µL NativePAGE sample buffer. Gels were run as described in the general section.

FRET with probes 7-10 (asymmetric proteasomes): Cell lysates (20 µg/sample, 18 µL) were first treated with LU102 (to inhibit β2 in the samples for β5c-β5i FRET) or NC005 (to inhibit β5 in the samples for β1c-β1i FRET) for 1 h. Subsequently, either ABPs **7** and **8** or **9** and **10** were added (1 µL of 20x stocks in DMSO) and the samples were incubated for 1 h. For the control samples, two separate vials for each sample containing cell lysates (40 µg/sample, 18 µL) were first treated with LU102 (to inhibit β2 in the samples for β5c-β5i FRET) or NC005 (to inhibit β5 in the samples for β1c-β1i FRET) for 1 h. To the first vial, ABPs **7** or **9** were added and to the second vial ABPs **8** or **10**. After incubation for 1 h, NC005 (to samples containing ABPs **7** or **8**, to inhibit residual β5 activities) or NC001 (to samples containing ABPs **7** or **8**, to inhibit residual β1 activities) were added and after incubation for 1 h, the samples containing ABPs **7/8** and **9/10** were mixed. The control samples contain the same amount of proteasome subunits labelled by the ABPs, however, the probes are not bound to the same CPs, thereby providing total background FRET signal, caused by the individual ABPs. All samples were analysed by SDS-PAGE and native-PAGE as described above.

Immunoproteasome induction in HeLa cells

HeLa cells were cultured in DMEM media supplemented with 10% fetal calf serum, GlutaMAX[™], penicillin, streptomycin in a 5% CO₂ humidified incubator. 3x10⁶ cells were seeded in a 10 cm dish and the cells were left to attach for 6 h, followed by the addition of IFN-γ (100 u/mL). The cells were grown for 24 h, and harvest by trypsin treatment, and washed with PBS. Lysates were prepared as described in the general section.

References

1. Hershko, A. & Ciechanover, A. The ubiquitin system. *Annu. Rev. Biochem.* **67**, 425-79 (1998).
2. Kisselev, A.F., Akopian, T.N., Woo, K.M. & Goldberg, A.L. The sizes of peptides generated from protein by mammalian 26 and 20 S proteasomes: implications for understanding the degradative mechanism and antigen presentation. *J. Biol. Chem.* **274**, 3363-3371 (1999).
3. Ferrington, D.A. & Gregerson, D.S. Immunoproteasomes: structure, function, and antigen presentation. *Prog. Mol. Biol. Transl. Sci.* **109**, 75-112 (2012).
4. McCarthy, M.K. & Weinberg, J.B. The immunoproteasome and viral infection: a complex regulator of inflammation. *Front. Microbiol.* **6**, doi: 10.3389/fmicb.2015.00021 (2015).
5. Tanaka, K. & Kasahara, M. The MHC class I ligand-generating system: roles of immunoproteasomes and the interferon-gamma-inducible proteasome activator PA28. *Immunol. Rev.* **163**, 161-176 (1998).
6. Murata, S., Yashiroda, H. & Tanaka, K. Molecular mechanisms of proteasome assembly. *Nat. Rev. Mol. Cell. Biol.* **10**, 104-115 (2009).
7. Kunjappu, M.J. & Hochstrasser, M. Assembly of the 20S proteasome. *Biochim. Biophys. Acta* **1843**, 2-12 (2014).
8. Hirano, Y. et al. A heterodimeric complex that promotes the assembly of mammalian 20S proteasomes. *Nature* **437**, 1381-1385 (2005).
9. Kusmierczyk, A.R., Kunjappu, M.J., Funakoshi, M. & Hochstrasser, M. A multimeric assembly factor controls the formation of alternative 20S proteasomes. *Nat. Struct. Mol. Biol.* **15**, 237-244 (2008).
10. Witt, E. et al. Characterisation of the newly identified human Ump1 homologue POMP and analysis of LMP7(β 5i) incorporation into 20 S proteasomes. *J. Mol. Biol.* **301**, 1-9 (2000).
11. Hirano, Y. et al. Dissecting β -ring assembly pathway of the mammalian 20S proteasome. *EMBO J.* **27**, 2204-2213 (2008).
12. Li, X., Kusmierczyk, A.R., Wong, P., Emili, A. & Hochstrasser, M. β -Subunit appendages promote 20S proteasome assembly by overcoming an Ump1-dependent checkpoint. *EMBO J.* **26**, 2339-2349 (2007).
13. Chen, P. & Hochstrasser, M. Autocatalytic subunit processing couples active site formation in the 20S proteasome to completion of assembly. *Cell* **86**, 961-972 (1996).
14. Ramos, P.C., Höckendorff, J., Johnson, E.S., Varshavsky, A. & Dohmen, R.J. Ump1p is required for proper maturation of the 20S proteasome and becomes its substrate upon completion of the assembly. *Cell* **92**, 489-499 (1998).
15. Heink, S., Ludwig, D., Kloetzel, P.-M. & Krüger, E. IFN- γ -induced immune adaptation of the proteasome system is an accelerated and transient response. *Proc. Natl. Acad. Sci.* **102**, 9241-9246 (2005).
16. Nandi, D., Woodward, E., Ginsburg, D.B. & Monaco, J.J. Intermediates in the formation of mouse 20S proteasomes: implications for the assembly of precursor beta subunits. *EMBO J.* **16**, 5363-5375 (1997).
17. Griffin, T.A. et al. Immunoproteasome assembly: cooperative incorporation of interferon γ (IFN- γ)-inducible subunits. *J. Exp. Med.* **187**, 97-104 (1998).
18. De, M. et al. β 2 subunit propeptides influence cooperative proteasome assembly. *J. Biol. Chem.* **278**, 6153-6159 (2003).
19. Groettrup, M., Standera, S., Stohwasser, R. & Kloetzel, P.M. The subunits MECL-1 and LMP2 are mutually required for incorporation into the 20S proteasome. *Proc. Natl. Acad. Sci.* **94**, 8970-8975 (1997).
20. Dahlmann, B., Ruppert, T., Kuehn, L., Merforth, S. & Kloetzel, P.-M. Different proteasome subtypes in a single tissue exhibit different enzymatic properties. *J. Mol. Biol.* **303**, 643-653 (2000).
21. Klare, N., Seeger, M., Janek, K., Jungblut, P.R. & Dahlmann, B. Intermediate-type 20 S proteasomes in HeLa cells: "asymmetric" subunit composition, diversity and adaptation. *J. Mol. Biol.* **373**, 1-10 (2007).
22. Guillaume, B. et al. Two abundant proteasome subtypes that uniquely process some antigens presented by HLA class I molecules. *Proc. Natl. Acad. Sci.* **107**, 18599-18604 (2010).

23. Guillaume, B. et al. Analysis of the processing of seven human tumor antigens by intermediate proteasomes. *J. Immunol.* **189**, 3538-3547 (2012).
24. Zanker, D., Waithman, J., Yewdell, J.W. & Chen, W. Mixed proteasomes function to increase viral peptide diversity and broaden antiviral CD8(+) T cell responses. *J. Immunol.* **191**, 52-59 (2013).
25. Dahlmann, B., Ruppert, T., Kloetzel, P.M. & Kuehn, L. Subtypes of 20S proteasomes from skeletal muscle. *Biochimie* **83**, 295-299 (2001).
26. Drews, O. et al. Mammalian proteasome subpopulations with distinct molecular compositions and proteolytic activities. *Mol. Cell. Proteomics* **6**, 2021-2031 (2007).
27. Pelletier, S. et al. Quantifying cross-tissue diversity in proteasome complexes by mass spectrometry. *Molecular BioSystems* **6**, 1450-1453 (2010).
28. Chirio-Lebrun, M.-C. & Prats, M. Fluorescence resonance energy transfer (FRET): theory and experiments. *Biochem. Educ.* **26**, 320-323 (1998).
29. Piston, D.W. & Kremers, G.-J. Fluorescent protein FRET: the good, the bad and the ugly. *Trends Biochem. Sci.* **32**, 407-414.
30. Park, J.E. et al. A FRET-based approach for identification of proteasome catalytic subunit composition. *Mol. BioSyst.* **10**, 196-200 (2014).
31. Borissenko, L. & Groll, M. 20S Proteasome and its Inhibitors: crystallographic knowledge for drug development. *Chem. Rev.* **107**, 687-717 (2007).
32. Elsasser, S., Schmidt, M. & Finley, D. in *Methods Enzymol.* 353-363 (Academic Press, 2005).
33. Verdoes, M. et al. A panel of subunit-selective activity-based proteasome probes. *Org. Biomol. Chem.* **8**, 2719-2727 (2010).
34. Geurink, P.P. et al. Incorporation of non-natural amino acids improves cell permeability and potency of specific inhibitors of proteasome trypsin-like sites. *J. Med. Chem.* **56**, 1262-1275 (2013).
35. Meer, B.W.v.d., III, G.C. & Chen, S.-Y.S. Resonance energy transfer. Theory and data. *VCH Publishers, New York*, 5-33 (1994).
36. Bader, A.N. et al. Homo-FRET imaging as a tool to quantify protein and lipid clustering. *ChemPhysChem* **12**, 475-483 (2011).
37. Sharma, L.K. et al. Activity-based near-infrared fluorescent probe for LMP7: a chemical proteomics tool for the immunoproteasome in living cells. *ChemBioChem* **13**, 1899-1903 (2012).
38. de Bruin, G. et al. A set of activity-based probes to visualize human (immuno)proteasome activities. *Angew. Chem. Int. Ed.* **55**, 4199-4203 (2016).

Enantioselective synthesis of adamantylalanine and carboranylalanine and their incorporation into the proteasome inhibitor bortezomib*

Introduction

The ubiquitin proteasome system (UPS) is responsible for the degradation of 80-90% of the proteins in eukaryotic cells. E1-E2-E3 enzymes can modify a protein destined for degradation with a poly-ubiquitin chain, which is recognized by the 19S cap of the 26S proteasome. The 19S cap removes the ubiquitin chain and unfolds the protein, which is then translocated in the 20S core particle (CP), where proteolysis takes place.¹ The hollow cylindrical shaped CP is composed out of four heptameric rings: two outer α -rings and two inner β -rings. The catalytic activities reside within the β -subunits: β 1 (caspase-like, cleaves after acidic residues), β 2 (trypsin-like, cleaves after basic residues) and β 5 (chymotrypsin-like, cleaves after hydrophobic residues). Next to the constitutively expressed cCP (β 1c, β 2c and β 5c) subunits, immune cells also express β -subunits with slightly altered substrate specificities (iCP: β 1i, β 2i and β 5i).² Two proteasome inhibitors (PIs) are currently used in the clinic for the treatment of multiple myeloma (MM) and mantle cell lymphoma, namely bortezomib (Btz, Figure 1) and carfilzomib (Cfz), and several PIs are being evaluated in clinical trials.³ PIs can provide useful information on the substrate specificity of each β subunit. The S1 and S3 pockets mainly determine the substrate specificities for each β -subunit. Large (aromatic) ring structures are well tolerated by the S1 pocket of β 5i and β 2i and the S3 pocket of β 5c and β 5i.^{4,5} However, introducing an adamantylalanine at P1 resulted in complete loss of activity.⁵ The crystal structure of bortezomib in complex with yeast proteasome showed a spacious, solvent exposed S2 pocket, in which the P2 phenylalanine lacked interactions with the protein.⁶

* de Bruin, G.; Mock E.D. *et al.* Enantioselective synthesis of adamantylalanine and carboranylalanine and their incorporation into the proteasome inhibitor bortezomib, *Chem. Comm.* **52**, 4064 - 4067 (2016)

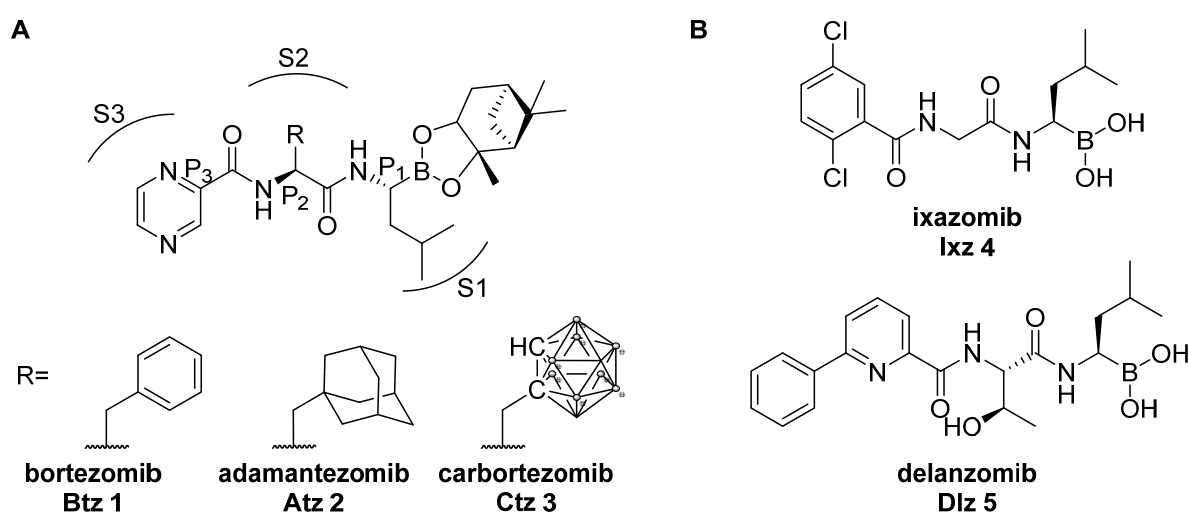


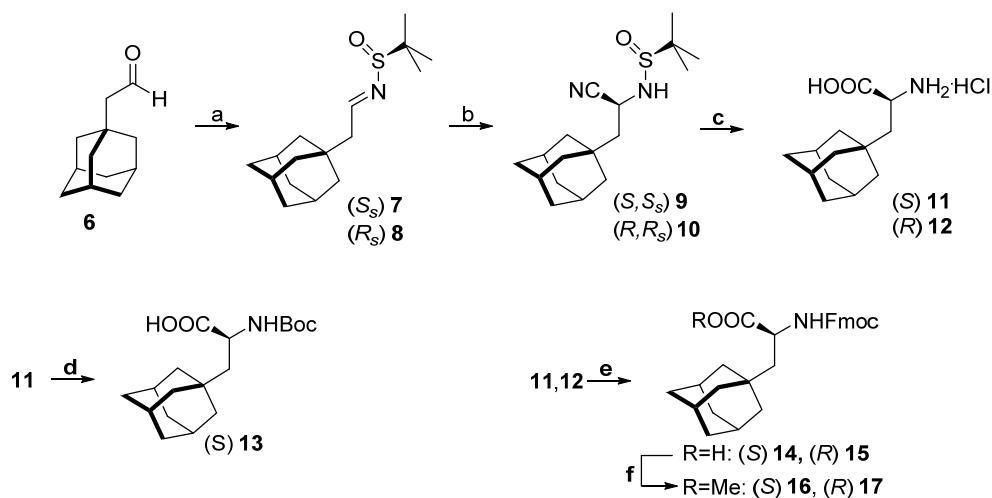
Figure 1. A) Structures of bortezomib **1** and the analogues adamantezomib **2** and carbortezomib **3** that are synthesized in this study. Enzyme pockets (S1, S2 and S3) and inhibitor residues (P1, P2 and P3) are indicated. B) Structures of boronic acid PIs currently in clinical trials: ixazomib **4** and delanzomib **5**.

Interestingly, ixazomib **4** (Ixz, P2: glycine) and to a lesser extent delanzomib **5** (Dlz, P2: threonine) (Fig. 1B) both show higher off-rates compared to Btz.⁷ The high off-rate of Ixz is arguably responsible for its improved pharmacokinetic and pharmacodynamic properties.⁸ This observation raised the question whether more sterically demanding moieties at P2 would affect binding properties of boronic acid PIs. To investigate this, Btz analogues were designed in which phenylalanine is replaced by adamantylalanine or *ortho*-carboranylalanine, leading to ‘adamantezomib’ (Atz) **2** and ‘carbortezomib’ (Ctz) **3** respectively. Carborane has roughly the same molecular volume as adamantane (148 Å vs. 136 Å), but is more hydrophobic.⁹ Given their electronic structure, carboranes can be considered ‘super-aromatic’ and are therefore used as isosteres for phenyl groups. Due to their lipophilicity and stability, carboranes are often exploited to improve cell-permeability of lead compounds, and as a pharmacophore for hydrophobic interactions with receptors and proteins.⁹ In addition, carboranes have been used in boron-neutron capture therapy (BNCT), a binary anti-cancer therapy based on the reaction between boron-10 and thermal neutrons, leading to high energy α -particles and lithium ions. When delivered in sufficient concentrations to the tumour, the energy released will ensure selective cell death in the tumour tissue.^{10, 11} In this chapter, new synthetic routes towards adamantylalanine and carboranylalanine are described, which provided both amino acids in good yields and enantiomeric purity. These amino acids were incorporated in the Btz sequence and evaluated the resulting peptidic boronic esters as proteasome inhibitors.

Results and discussion

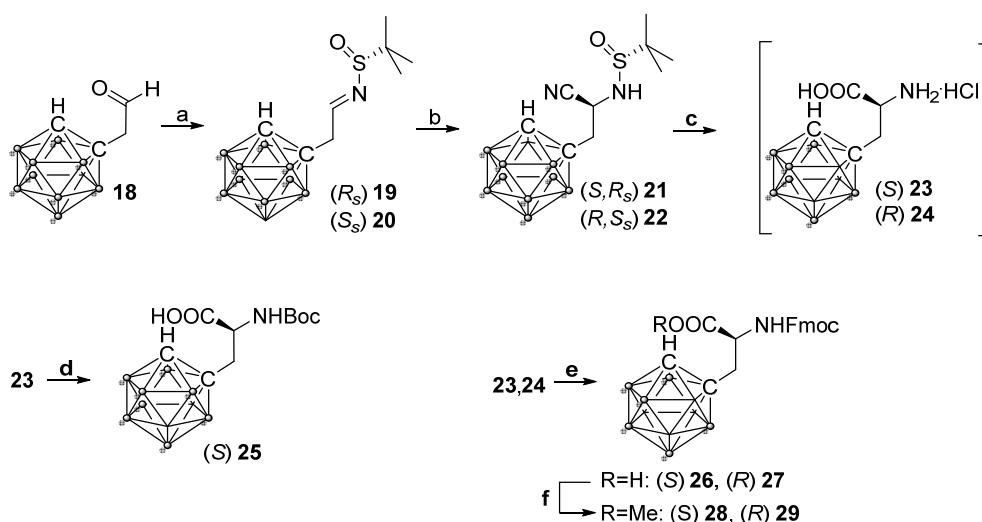
Synthesis

Two chiral auxiliaries have been reported in the asymmetric synthesis of adamantylalanine, namely (*S*)- α -methylbenzylamine¹² (poor enantiomeric excess) and sulfonamido-isobornane.¹³ In addition, a moderate enantioselective conjugate addition of an adamantyl Grignard reagent to an optically active carbamatoacrylate has been reported¹⁴ as well as the use of a chiral quaternary ammonium salt.¹⁵ Also, various routes towards carboranylalanine have been reported, either starting from the highly toxic decaborane (the reaction of decaborane with propargyl glycine, recently optimized by Toppino *et al.*¹⁶) or starting from *ortho*-carborane, using either Evans' oxazolidinone¹⁷ or Oppolzer's chiral camphorsultam¹⁸ as the chiral auxiliaries. In this chapter, Ellman's *N*-*tert*-butylsulfonamide is used as the chiral auxiliary and the key step is the asymmetric Strecker reaction of a chiral imine.¹⁹ The synthesis of adamantylalanine commenced with the condensation of aldehyde **6** with (*R*)- or (*S*)-*N*-*tert*-butyl-sulfonamide under Dean-Stark conditions providing imines **7** and **8** (Scheme 1).



Scheme 1. Synthesis of (protected) adamantylalanine. Reagents and conditions: a. (*R*)- or (*S*)-*N*-*tert*-butyl-sulfonamide, toluene, 50°C, 100 mbar, **7** (*S_S*): 89%; **8** (*R_S*): 90%; b. Et_2AlCN , *i*PrOH, THF, **9** (*S, S_S*): 66%; **10** (*R, R_S*): 62%; *de*: 92%, >99% after crystallization; c. 6N HCl, reflux, **11** (*S*): 98%; **12** (*R*): 96%; d. Boc_2O , Na_2CO_3 , H_2O , dioxane, 80%; e. FmocOSu , Na_2CO_3 , H_2O , dioxane, **14** (*S*): 89%; **15** (*R*): 89%; f. TMSCH_2N_2 , MeOH, **16** (*S*): 93%, 97.4 *ee*; **17** (*R*): 99%, 96.6 *ee*.

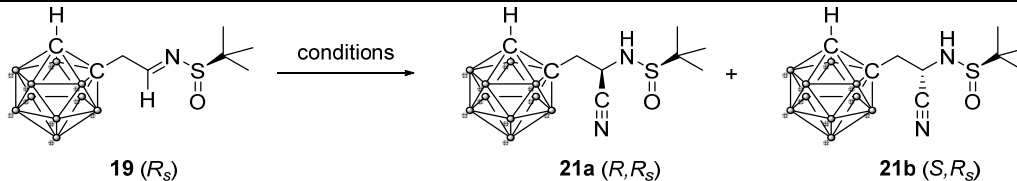
The asymmetric Strecker reaction using ethylisopropoxyaluminiumcyanide²⁰ (obtained by reacting Et_2AlCN with *i*PrOH) as the cyanide delivery agent yielded *syn* products **9** and **10** in 92% diastereomeric excess (*de*), which could be further increased by crystallization to >99% *de*. Subsequent hydrolysis under strong aqueous acidic conditions hydrolysed the nitrile and cleaved the chiral auxiliary, thereby providing amino acids **10** and **11** in high yield and purity.



Scheme 2. Synthesis of (protected) *ortho*-carboranylanine. Reagents and conditions: a. *R*- or *S*-*N*-*tert*-butyl-sulfinamide, CuSO₄, DCM, **19** (*R*_s): 94%; **20** (*S*_s): 94%; b. CsF, TMSCN, DMF -50°C, **21** (*S*,*R*_s): 48%; **10** (*R*,*S*_s): 54%; *de*: 86%, >99% after crystallization; c. 6N HCl, reflux; d. Boc₂O, Et₃N, H₂O, THF, 85%; e. FmocOSu, Et₃N, H₂O, THF, (*S*): 94%; **15** (*R*): 81%; f. EDC·HCl, HOBT, MeOH, DCM, **28** (*S*): 79%, 85.5 *ee*; **29** (*R*): 78%, 90.5 *ee*.

Boc or Fmoc protection of adamantylalanine proceeded without any problem yielding compounds **13** (Boc), **14** and **15** (Fmoc). Fmoc protected compounds **14** and **15** were converted to the corresponding methyl esters **16** and **17** to allow chiral HPLC analysis, which revealed excellent enantiomeric excess (*ee*) for both enantiomers. Since condensation of carboranyl aldehyde **18**²¹ with *N*-*tert* butylsulfinamide under Dean-Stark conditions resulted in significant enamine formation, the reaction was performed at room temperature in presence of an excess of CuSO₄, which dramatically increased the yield and prevented enamine formation (Scheme 2). Using the same conditions for the asymmetric Strecker reaction as used for the adamantylalanine synthesis resulted in a much lower diastereomeric ratio (*dr*) (Table 1, entry 1). Lewis acid catalyzed cyanation with Sc(OTf)₃ and TMSCN led to similar *syn* selectivity (Table 1, entry 2). The use of a catalytic amount of the Lewis base TBA-Ac at -78°C provided product **21b** in a good *dr*, (8:92, *syn*/*anti*, note the preference for *anti*-addition, Table 1, entry 3).²² In order to further improve the *dr*, conditions reported by Li *et al.*, who used TMSCN and equimolar CsF at -50°C in *n*-hexane giving *syn*-addition, or in THF giving *anti* addition, were used.²³ As imine **19** is not soluble in *n*-hexane, the reaction was performed in THF, giving only poor selectivity with a slight preference for *anti*-addition product **21b** (Table 1, entry 4). Using a DMF/THF mixture at -60°C improved the *dr* (Table 1, entry 5). When only DMF was used at -50°C, the highest yield and *dr* (3:97, *syn*/*anti*; 7:93 at larger scale) was obtained (Table 1, entries 6/7). Upon crystallization diastereomerically pure cyanosulfonamide **21b** was isolated in a reasonable yield. In the same manner sulfinimine **20** gave the mirror image **22**. The X-ray crystals structure confirmed the absolute stereochemistry of **21b** and **22** (Figure 2).²⁴

Incorporation of adamantylalanine and carboranylalanine into bortezomib

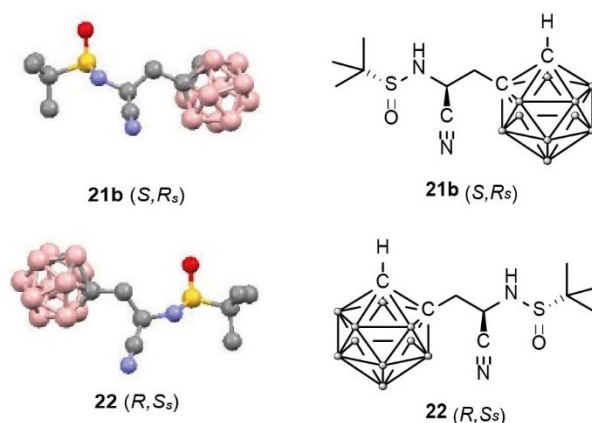


Entry	Reagents	Solvent	Temp (°C)	Yield (%)	dr (18a/18b) ^a
1	Et ₂ AlCN, iPrOH	THF	-78 to rt	78	71 : 29
2	TMSCN, Sc(OTf) ₃	DCM	0 to rt	52	76 : 24
3	TMSCN, TBA-Ac ^b	DMF/THF (2:1)	-78	88	8 : 92
4	TMSCN, CsF ^c	THF	-50	n.d.	40 : 60
5	TMSCN, CsF ^c	DMF/THF (2:1)	-60	n.d.	7 : 93
6	TMSCN, CsF ^c	DMF	-50	92	3 : 97
7	TMSCN, CsF ^d	DMF	-50	98 (48) ^e	7 : 93 (1 < 99)
8	TMSCN, CsF ^c	Tol	-10	n.d.	67 : 33
9	TMSCN, CsF ^c	CH ₂ Cl ₂	-10	n.d.	72 : 28

^a The diastereomeric ratio was determined by ¹H-NMR, by comparing the integral of the CH_α. ^b 10 mol% TBA-Ac was added. ^c Conditions: 0.20 mmol **19**, 1.05 eq TMSCN, 1.05 eq CsF, 0.2M ^d Conditions: 3.5 mmol **19**, 2.2 eq TMSCN, 1.3 eq CsF, 0.2M ^e Between parentheses = yield of diastereomerically pure product after crystallization. n.d. = not determined.

Table 1. Optimization of the asymmetric Strecker reaction for the synthesis of carboranylalanine

Treatment of **21b** and **22** in refluxing aqueous 6N HCl yielded (*S*)- and (*R*)- carboranylalanine **23/24**, which could be converted into their Boc or Fmoc protected analogues without difficulties. Chiral HPLC analysis revealed excellent enantiomeric excess for both enantiomers. Both Boc-adamantylalanine and Boc-carboranylalanine were incorporated at the P2 position of Btz, using similar procedures as described before (see experimental).^{25, 26} It was decided to leave the pinanediol protection in place, since it has been reported that boronic esters of this kind show similar activity as unprotected boronic acids.²⁵


Figure 2. X-ray crystal structures of (*S,R_S*)-cyanosulfonamide **21b and (*R,S_S*)-cyanosulfonamide **22**.**

Biological evaluation

The activity against all the cCP and iCP subunits was assessed by competitive activity-based protein profiling (ABPP) in lysate of Raji cells (human B-lymphoblastic cell line expressing all six active β subunits). In addition, the cell permeability and efficiency of proteasome inhibition was evaluated in living RPMI-8226 cells (MM cell line). Residual proteasome activity after incubation with inhibitors is labelled by the recently published activity-based probe (ABP) cocktail⁷ (see chapter 2), which provides full resolution of all six active β subunits on SDS-PAGE (Figure 3). In Raji cell lysates, Atz closely resembles the activity of Btz, while Ctz shows slightly higher IC_{50} values for all $\beta 1$ and $\beta 5$ sites. All three inhibitors show a slight preference for $\beta 1i$ and $\beta 5i$ over their constitutive counterparts (Figure 3B). Evaluation in living RPMI-8226 cells showed similar potency of Atz and Ctz compared to Btz indicating good cell permeability (Figure 3). Interestingly, Atz and Ctz show a 4-5 fold preference for $\beta 5i$ over $\beta 5c$, while Btz, Dlx and Cfx inhibit $\beta 5c$ and $\beta 5i$ with equal potency and Ixz shows only a <2 fold preference for $\beta 5i$.

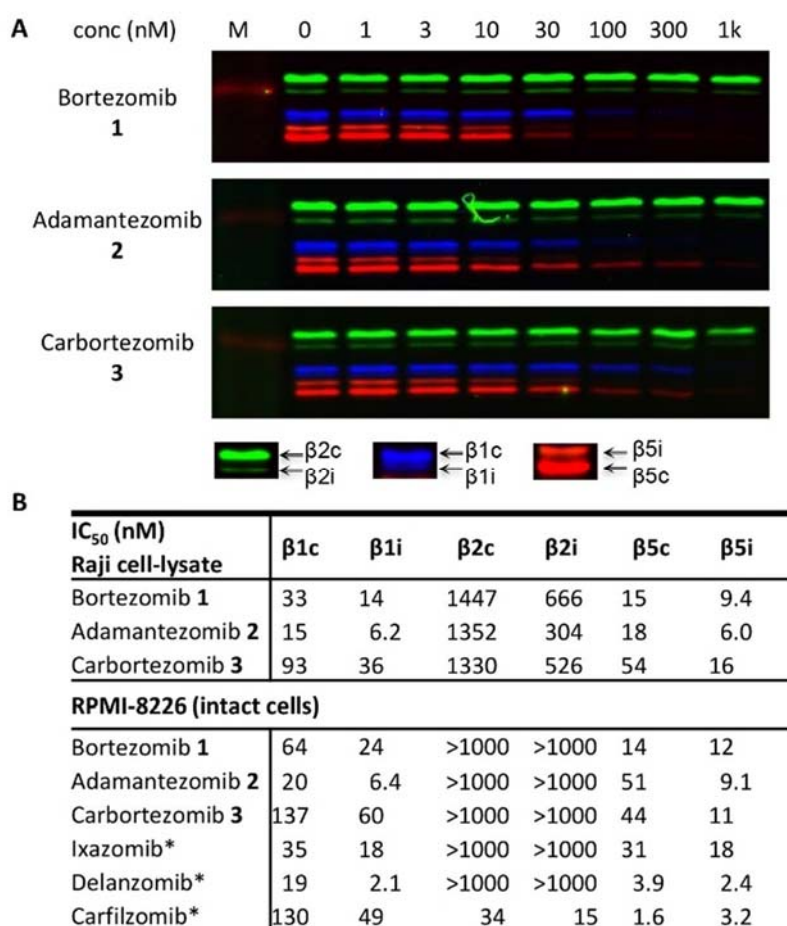


Figure 3. Determination of inhibitory potency of Btz 1, adamantezomib 2, and carbortemib 3 by ABPP. A) Inhibitory profiles in intact RPMI-8226 cells after 1 h treatment. B) IC_{50} values as determined by ABPP in Raji cell lysates and RPMI-8226 intact cells. M=protein marker. * IC_{50} values of ixazomib, delanzomib and carfilzomib have been determined by ABPP before.⁷

In addition, Ctz shows lower- and Atz higher potency towards the $\beta 1$ subunits compared to Btz, whereas all inhibitors show a preference for $\beta 1i$ over $\beta 1c$. To gain more insight in the off-rate of Atz and Ctz, a wash-out experiment was performed in which Atz and Ctz were compared to Btz (low off-rate) and Ixz (high off-rate).^{7,8}

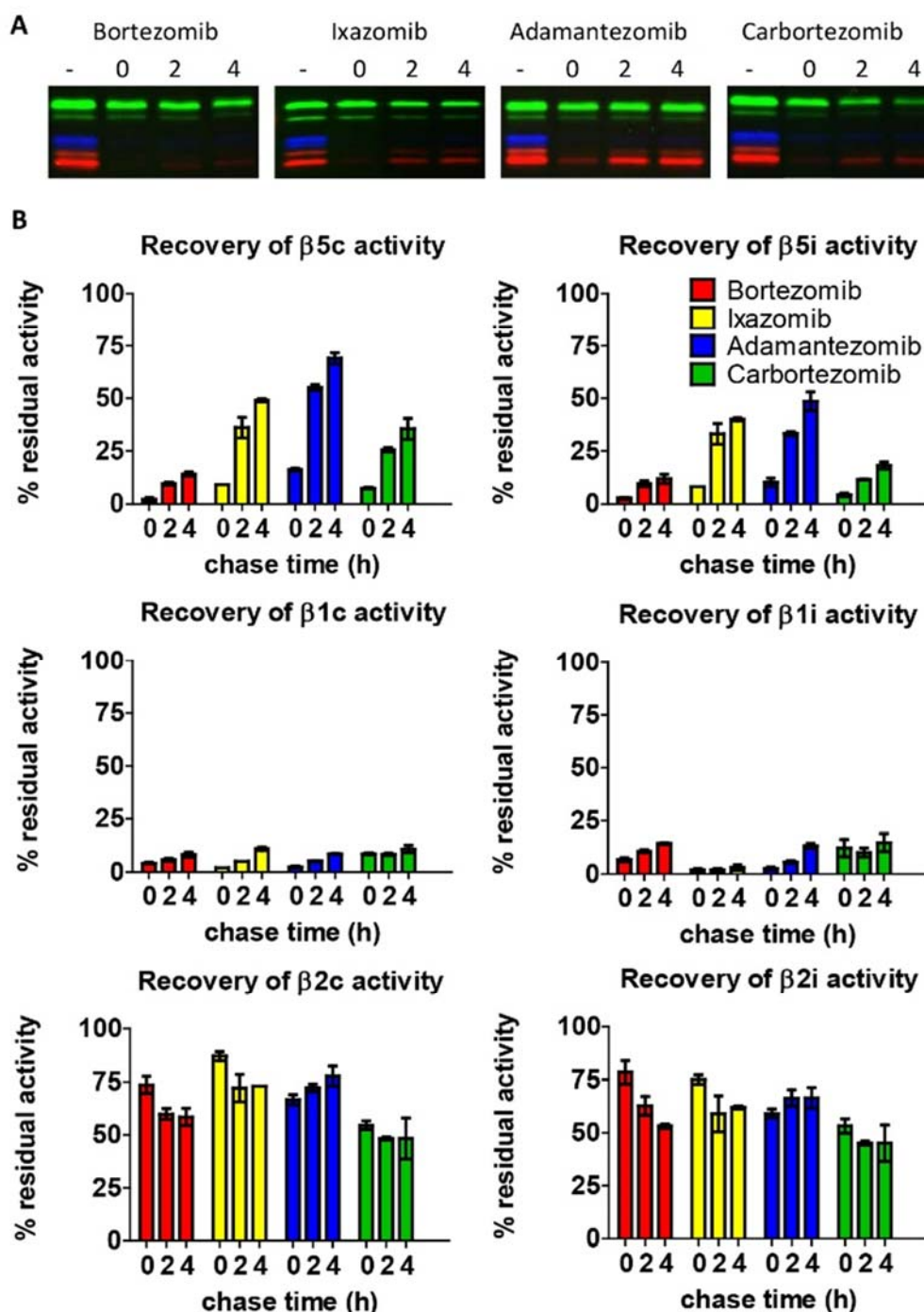


Figure 4. Inhibitor washout experiments. A) Inhibitory profiles of Btz 1, Ixz, Atz 2 and Ctz 3 in RPMI-8226 cells, which were treated with inhibitors for 1h, followed by washing of the cells and chase for 0, 2, or 4 h. B) Graphs show recovery for $\beta 5c$ and $\beta 5i$. Error bars show \pm SEM values. Quantifications of gel intensities have been corrected for gel loading (Coomassie). Wash-out data of Ixz used as determined before, see chapter 2.⁷

RPMI-8226 cells were incubated with the inhibitors in order to block the $\beta 1$ and $\beta 5$ sites.²⁷ Subsequently, the cells were washed and chased for multiple hours. The $\beta 5$ sites show faster recovery when inhibited by Atz and Ctz, compared to Btz (Figure 4). Interestingly, Atz not only shows a much higher off-rate than Ctz for both $\beta 5$ sites, it also shows faster recovery of the $\beta 5$ activities than Ixz (69% vs. 49% for $\beta 5c$ after 4h). Remarkably, the off-rate of all compounds appears to be higher for $\beta 5c$ than $\beta 5i$ while the $\beta 1$ subunits show comparable low recovery of activity for all inhibitors. The higher off-rate for $\beta 5c$ increases the $\beta 5i$ selectivity of Atz and Ctz. These data suggest that large P2 residues destabilize the inhibitor-proteasome- $\beta 5$ -subunit complexes.

Conclusion

This chapter describes new enantioselective synthetic routes for adamantylalanine and *ortho*-carboranylalanine. Incorporation of these amino acids at the P2 site of Btz led to potent proteasome inhibitors, with high off-rates and $\beta 5i$ selectivity. Atz and Ctz could thus be used to selectively block $\beta 5i$ with minimal co-inhibition of $\beta 5c$. The incorporation of adamantylalanine or carboranylalanine at the P2 site of boronic acid PIs could be an important design parameter for the development of iCP selective PIs with similar pharmacodynamic and pharmacokinetic properties as Ixz. Finally, considering that carboranes are non-toxic and biologically stable, Ctz might also find its application in BNCT.

Experimental

Synthetic procedures

General procedures

Acetonitrile (ACN), dichloromethane (DCM), N,N-dimethylformamide (DMF), methanol (MeOH), diisopropylethylamine (DiPEA) and trifluoroacetic acid (TFA) were of peptide synthesis grade, purchased at Biosolve, and used as received. All general chemicals (Fluka, Acros, Merck, Aldrich, Sigma, Iris Biotech) were used as received. Traces of water were removed from reagents used in reactions that require anhydrous conditions by co-evaporation with toluene. Column chromatography was performed on Screening Devices b.v. Silica Gel, with a particle size of 40-63 μm and pore diameter of 60 \AA . TLC analysis was conducted on Merck aluminium sheets (Silica gel 60 F254). Compounds were visualized by UV absorption (254 nm), by spraying with a solution of $(\text{NH}_4)_6\text{Mo}_7\text{O}_{24}\cdot 4\text{H}_2\text{O}$ (25 g/L) and $(\text{NH}_4)_4\text{Ce}(\text{SO}_4)_4\cdot 2\text{H}_2\text{O}$ (10 g/L) in 10% sulfuric acid, a solution of KMnO_4 (20 g/L) and K_2CO_3 (10 g/L) in water, or ninhydrin (0.75 g/L) and acetic acid (12.5 mL/L) in ethanol, where appropriate, followed by charring at ca. 150 $^\circ\text{C}$. ^1H and ^{13}C -NMR spectra were recorded on a Bruker AV-400 (400 MHz) or AV-600 (600 MHz) spectrometer. Chemical shifts are given in ppm (δ) relative to tetramethylsilane, CD_3OD or CDCl_3 as internal standard. High resolution mass spectra were recorded by direct injection (2 μL of a 2 μM solution in water/acetonitrile 50/50 (v/v) and 0.1% formic acid) on a mass spectrometer (Thermo Finnigan LTQ Orbitrap) equipped with an electrospray ion source in positive mode (source voltage 3.5 kV, sheath gas flow 10, capillary temperature 250 $^\circ\text{C}$) with resolution $R = 60,000$ at m/z 400 (mass range $m/z = 150\text{--}2,000$) and dioctylphthalate ($m/z = 391.28428$) as a "lock mass". The high resolution mass spectrometer was calibrated prior to measurements with a calibration mixture (Thermo Finnigan). LC-MS analysis was performed on a Finnigan Surveyor HPLC system with a Gemini C_{18} 50 \times 4.60 mm column (detection at 200–600 nm) coupled to a Finnigan LCQ Advantage Max mass spectrometer with ESI. The applied buffers were H_2O , MeCN and 1.0% TFA in H_2O (0.1% TFA end concentration). Methods used are: 10 \rightarrow 90% MeCN, 15.0 min (0 \rightarrow 0.5 min: 10% MeCN; 0.5 \rightarrow 10.5 min: gradient time; 10.5 \rightarrow 12.5 min: 90% MeCN; 12.5 \rightarrow 15.0 min: 90% \rightarrow 10% MeCN), HPLC purification was performed on a Gilson HPLC system coupled to a C_4 Phenomenex Gemini 5 μm 250 \times 10 mm column and a GX281 fraction collector. Chiral HPLC analysis was performed using a Daicell Chiralcel OD column (250 \times 5.4 mm) or a Chiralpak AD (250 \times 5.4 mm), using hexane/isopropanol solvent mixtures, flowrate: 1 mL/min. All tested compounds are >95% pure on the basis of LC-MS and NMR. (1R)-4-(1-chloro-3-methyl(butyl)-2,9,9-trimethyl-3,5-dioxo-4-bora-tricyclo[6.1.1.0 $_{2,6}$]decane²⁸, boronoleucine pinanediol ester²⁶ and bortezomib²⁸ were synthesized according to literature procedures.

Synthesis of (Fmoc/Boc-adamantylalanine(-OMe)

(S,E)-N-(2-(adamantan-1-yl)ethylidene)-tert-butyl-sulfinamide (7)

A solution of adamantylacetaldehyde (1.42 g, 8 mmol, 1 equiv.) and (S)-tert-butylsulfinamide (1.06 g, 8.8 mmol, 1.1 equiv.) in toluene (50 mL) was rotated overnight under continuous removal of water using a rotary evaporator (50 $^\circ\text{C}$, 100 mbar). After concentration, the crude product was purified by column chromatography (0 \rightarrow 10% EtOAc:toluene) providing the title compound (2.02 g, 7.1 mmol, 90%). $[\alpha]_D^{20} = +253.8$ (C=1, CHCl_3). ^1H NMR (400 MHz, CDCl_3) δ 8.09 (t, $J = 5.9$ Hz, 1H), 2.34 – 2.14 (m, 2H), 1.93 (s, 3H), 1.72 – 1.46 (m, 12H), 1.16 (s, 9H). ^{13}C NMR (101 MHz, CDCl_3) δ 168.37, 56.42, 50.17, 42.56, 42.18, 36.60, 33.50, 28.50, 28.42, 22.36. HRMS: calcd. for $\text{C}_{16}\text{H}_{28}\text{NOS}$ 282.18861 $[\text{M}+\text{H}]^+$; found 282.18854.

(R,E)-N-(2-(adamantan-1-yl)ethylidene)- tert-butyl-sulfinamide (8)

A solution of adamantylacetaldehyde (1.78 g, 10 mmol, 1 equiv.) and (*R*)-*tert*-butylsulfinamide (1.33 g, 11 mmol, 1.1 equiv.) in toluene (50 mL) was rotated overnight under continuous removal of water using a rotary evaporator (50°C, 100 mbar). After concentration, the crude product was purified by column chromatography (0→10% EtOAc:toluene) providing the title compound (2.50 g, 8.9 mmol, 89%). $[\alpha]_D^{20} = -242.6$ (C=1, CHCl₃). ¹H NMR (400 MHz, CDCl₃) δ 8.09 (t, *J* = 5.9 Hz, 1H), 2.24 (m, 2H), 1.93 (s, 3H), 1.72 – 1.50 (m, 12H), 1.16 (s, 9H). ¹³C NMR (101 MHz, CDCl₃) δ 168.34, 56.41, 50.17, 42.57, 42.19, 36.64, 36.60, 33.50, 28.51, 28.42, 22.36. HRMS: calcd. for C₁₆H₂₈NOS 282.18861 [M+H]⁺; found 282.18849.

(S)-N-((S)-2-(adamantan-1-yl)-1-cyanoethyl)- tert-butyl-sulfinamide (9)

Et₂AlCN (1M in toluene, 28.3 mmol, 28.3 mL, 1.5 equiv.) was added to THF (55 mL), followed by the addition of *i*PrOH (57 mmol, 4.3 mL, 3 equiv.) resulting in some discolouration of the mixture, from red to slightly yellow. After stirring for 15 min, the Et₂AlCN/*i*PrOH solution was added in 25 min to a solution of sulfinamide **7** (5.32 g, 18.9 mmol, 1 equiv.) in THF (120 mL) at -78 °C. After stirring for 30 min at -78 °C, the reaction mixture was let to warm up to RT. After stirring for 3 hour at RT, TLC showed full consumption of starting material. The reaction mixture was cooled to -78 °C and quenched by the addition of 10% NaHCO₃ (40 mL). After warming up to RT, the mixture was diluted by NaHCO₃ and extracted with EtOAc (3x). The combined organic layers were dried over Na₂SO₄, filtered and concentrated. Column chromatography (10→40% EtOAc:PE) provided the title compound (4.97 g, 16.1 mmol, 85%) as a 96:4 mixture of diastereomers. Recrystallization from DCM:n-hexane provided enantiomerically pure product (3.85 g, 12.5 mmol, 66%). $[\alpha]_D^{20} = +25.8$ (C=1, CHCl₃). ¹H NMR (400 MHz, CDCl₃) δ 4.17 (td, *J* = 8.3, 5.2 Hz, 1H), 3.84 (d, *J* = 8.2 Hz, 1H), 2.01 – 1.93 (m, 3H), 1.84 (dd, *J* = 14.3, 8.3 Hz, 1H), 1.76 – 1.51 (m, 13H), 1.22 (s, 9H). ¹³C NMR (101 MHz, CDCl₃) δ 120.80, 57.03, 49.44, 42.33, 41.74, 36.74, 32.41, 28.45, 22.57. HRMS: calcd. for C₁₇H₂₉N₂OS 309.19951 [M+ H]⁺; found 309.19955

(R)-N-((R)-2-(adamantan-1-yl)-1-cyanoethyl)- tert-butyl-sulfinamide (10)

Et₂AlCN (1M in toluene, 11.85 mmol, 11.85 mL, 1.5 equiv.) was added to THF (24 mL), followed by the addition of *i*PrOH (23.7 mmol, 1.61 mL, 3 equiv.) resulting in some discolouration of the mixture, from red to slightly yellow. After stirring for 15 min, the Et₂AlCN/*i*PrOH solution was added in 25 min to a solution of sulfinamide **8** (2.29 g, 7.9 mmol, 1 equiv.) in THF (55 mL) at -78 °C. After stirring for 30 min at -78 °C, the reaction mixture was let to warm up to RT. After stirring for 1 hour at RT, TLC showed full consumption of starting material. The reaction mixture was cooled to -78 °C and quenched by the addition of 10% NaHCO₃ (20 mL). After warming up to RT, the mixture was diluted by NaHCO₃ and extracted with EtOAc (3x). The combined organic layers were dried over Na₂SO₄, filtered and concentrated. Column chromatography (10→30% EtOAc:PE) provided the title compound (1.86 g, 6.0 mmol, 77%) as a 96:4 mixture of diastereomers. Recrystallization from DCM:n-hexane provided enantiomerically pure product (1.51 g, 4.9 mmol, 62%). $[\alpha]_D^{20} = -25.8$ (C=1, CHCl₃). ¹H NMR (400 MHz, CDCl₃) δ 4.15 (td, *J* = 8.3, 5.2 Hz, 1H), 4.04 (d, *J* = 8.4 Hz, 1H), 1.95 (m, 3H), 1.82 (dd, *J* = 14.3, 8.2 Hz, 1H), 1.73 – 1.49 (m, 13H), 1.20 (s, 9H). ¹³C NMR (101 MHz, CDCl₃) δ 120.86, 56.97, 49.33, 42.25, 41.75, 36.69, 32.33, 28.39, 22.55. HRMS: calcd. for C₁₇H₂₉N₂OS 309.19951 [M+ H]⁺; found 309.19958

(S)-3-(adamantan-1-yl)-2-aminopropanoic acid hydrochloride (11)

Compound **9** (3.85 g, 12.5 mmol) was dissolved in 6N HCl (400 mL) and refluxed at 130 °C overnight. The reaction mixture was cooled on ice, resulting in precipitation of the product. The precipitate was collected by filtration, washed with ice-cold water and dried under vacuum yielding the title product as a white solid (3.17 g, 12.2 mmol, 98%). $[\alpha]_D^{20} = +16.8$ (C=1, MeOH). ¹H NMR (400 MHz, MeOD) δ 3.98 (t, *J* = 5.6 Hz, 1H), 2.00 (s, 3H), 1.89 – 1.38 (m, 14H). ¹³C NMR (101 MHz, MeOD) δ 172.97, 49.85, 46.40, 42.93, 37.71, 33.31, 29.91. HRMS: calcd. for C₁₃H₂₂NO₂ [M+ H]⁺ 224.16451; found 224.16451.

(R)-3-(adamantan-1-yl)-2-aminopropanoic acid (12)

Compound **10** (1.40 g, 4.5 mmol) was dissolved in 6N HCl (140 mL) and refluxed at 130°C overnight. The reaction mixture was cooled on ice, resulting in precipitation of the product. The precipitate was collected by filtration, washed with ice-cold water and dried under vacuum yielding the title product as a white solid (1.13 g, 4.4 mmol, 96%). $[\alpha]_D^{20} = -16.6$ (C=1, MeOH). $^1\text{H NMR}$ (400 MHz, MeOD) δ 3.98 (t, $J = 5.5$ Hz, 1H), 2.00 (s, 3H), 1.89 – 1.37 (m, 14H). $^{13}\text{C NMR}$ (101 MHz, MeOD) δ 172.97, 49.87, 46.41, 42.94, 37.71, 33.32, 29.92. HRMS: calcd. for $\text{C}_{13}\text{H}_{22}\text{NO}_2$ $[\text{M} + \text{H}]^+$ 224.16451; found 224.16454.

(S)-N-Boc-adamantylalanine-OMe (13)

To a solution of (*S*)-adamantylalanine **11** (1.0 g, 3.85 mmol, 1 equiv.) in H_2O (4.5 mL) at 0 °C was added Na_2CO_3 (466 mg, 8.01 mmol, 2.1 equiv.). After 5 min, Boc_2O (1.68 g, 7.7 mmol, 2.0 equiv.) in dioxane (13.2 mL) was added. After stirring overnight, LC-MS analysis showed incomplete conversion. Therefore, another 2 equiv.)alent Boc_2O (1.68 g, 7.7 mmol) in dioxane (9 mL) was added and after 2 h, LC-MS showed complete consumption of the starting material. The reaction mixture was diluted with H_2O and acidified to pH=4 using 0.5N HCl, followed by extraction with EtOAc (3x). The combined organic layers were washed with brine (1x), dried over Na_2SO_4 and concentrated. Purification by column chromatography (0→5% MeOH/DCM) yielded the title compound (998 mg, 3.08 mmol, 80%). $[\alpha]_D^{20} = -4.2$ (C=0.1, CHCl_3). $^1\text{H NMR}$ (400 MHz, CDCl_3) δ 10.66 (s, 1H), 6.02 (s, 0.3H), 4.89 (d, $J = 8.4$ Hz, 0.7H), 4.38 (t, $J = 7.7$ Hz, 0.7H), 4.18 (s, 0.3H), 1.98 (s, 3H), 1.91 – 1.10 (m, 23H). $^{13}\text{C NMR}$ (101 MHz, CDCl_3) δ 178.98, 155.28, 80.05, 49.75, 46.78, 42.24, 36.78, 32.59, 28.50, 28.31. HRMS: calcd. for $\text{C}_{18}\text{H}_{30}\text{NO}_4$ 324.21693 $[\text{M} + \text{H}]^+$; found 324.21695

(S)-N-Fmoc-adamantylalanine (14)

To a solution of (*S*)-adamantylalanine **11** (260 mg, 1 mmol, 1 equiv.) in H_2O (4.5 mL) and dioxane (3.3 mL) were added Fmoc-OSu (371 mg, 1.1 mmol, 1.1 equiv.) and Na_2CO_3 (222 mg, 2.1 mmol, 2.1 equiv.). After stirring overnight, the reaction mixture was diluted with H_2O and acidified to pH=2 using 1N HCl, followed by extraction with EtOAc (3x). The combined organic layers were washed with brine (1x), dried over Na_2SO_4 and concentrated. Purification by column chromatography (0→2% MeOH/DCM) yielded the title compound (350 mg, 0.89 mmol, 89%). $[\alpha]_D^{20} = -5.6$ (C=1, CHCl_3). $^1\text{H NMR}$ (400 MHz, CDCl_3) δ 9.83 (bs, 1H), 7.76 (d, $J = 7.4$ Hz, 2H), 7.60 (t, $J = 8.1$ Hz, 2H), 7.39 (t, $J = 7.0$ Hz, 2H), 7.30 (t, $J = 7.3$ Hz, 2H), 5.19 (d, $J = 8.8$ Hz, 1H), 4.58 – 4.33 (m, 3H), 4.24 (t, $J = 7.0$ Hz, 1H), 1.98 (s, 3H), 1.80 – 1.22 (m, 14H). $^{13}\text{C NMR}$ (101 MHz, CDCl_3) δ 178.87, 155.93, 143.99, 143.79, 141.40, 127.80, 127.15, 125.22, 125.14, 120.07, 67.19, 50.28, 47.27, 46.66, 42.43, 36.88, 32.78, 28.62. HRMS: calcd. for $\text{C}_{28}\text{H}_{32}\text{NO}_4$ $[\text{M} + \text{H}]^+$ 446.23258; found 446.23254.

(R)-N-Fmoc-adamantylalanine (15)

To a solution of *R*-adamantylalanine **12** (260 mg, 1 mmol, 1 equiv.) H_2O (4.5 mL) and dioxane (3.3 mL) were added Fmoc-OSu (371 mg, 1.1 mmol, 1.1 equiv.) and Na_2CO_3 (222 mg, 2.1 mmol, 2.1 equiv.). After stirring overnight, the reaction mixture was diluted with H_2O and acidified to pH=2 using 1N HCl, followed by extraction with EtOAc (3x). The combined organic layers were washed with brine (1x), dried over Na_2SO_4 and concentrated. Purification by column chromatography (0→2% MeOH/DCM) yielded the title compound (350 mg, 0.89 mmol, 89%). $[\alpha]_D^{20} = +5.6$ (C=1, CHCl_3). $^1\text{H NMR}$ (400 MHz, CDCl_3) δ 9.16 (bs, 1H), 7.78 (d, $J = 7.5$ Hz, 2H), 7.66 – 7.58 (m, 2H), 7.41 (t, $J = 7.5$ Hz, 2H), 7.31 (dd, $J = 14.8, 7.4$ Hz, 2H), 5.28 – 5.01 (m, 1H), 4.58 – 4.39 (m, 3H), 4.27 (t, $J = 6.8$ Hz, 1H), 2.01 (s, 3H), 1.82 – 1.28 (m, 14H). $^{13}\text{C NMR}$ (101 MHz, CDCl_3) δ 178.11, 156.11, 144.10, 143.99, 141.57, 127.85, 127.21, 125.17, 125.13, 120.10, 67.43, 50.54, 47.53, 46.87, 42.63, 37.05, 32.86, 28.84. HRMS: calcd. for $\text{C}_{28}\text{H}_{32}\text{NO}_4$ $[\text{M} + \text{H}]^+$ 446.23258; found 446.23257.

(S)-N-Fmoc-adamantylalanine-OMe (16)

To a solution of Fmoc protected adamantyl-alanine **14** (50 mg, 0.11 mmol, 1 equiv.) in MeOH (1 mL) was added slowly added TMSCH_2N_2 (2M in hexanes, added until solution stayed clear, 7 equiv.) in total). After concentration

of the reaction mixture, the crude product was purified by column chromatography (0→10% EtOAc/PE) providing the title product (48 mg, 0.10 mmol, 93%). *ee*: 97.4% (as determined by chiral HPLC using 90:10 hexane/isopropanol, Chiralcell OD). $[\alpha]_D^{20} = -5.8$ ($C=0.5$, CHCl_3). $^1\text{H NMR}$ (400 MHz, CDCl_3) δ 7.77 (d, $J = 7.5$ Hz, 2H), 7.60 (t, $J = 7.8$ Hz, 2H), 7.40 (t, $J = 7.5$ Hz, 2H), 7.35 – 7.28 (m, 2H), 5.11 (d, $J = 8.9$ Hz, 1H), 4.53 – 4.33 (m, 3H), 4.24 (t, $J = 7.1$ Hz, 1H), 3.73 (s, 3H), 1.97 (s, 3H), 1.77 – 1.29 (m, 14H). HRMS: calcd. for $\text{C}_{29}\text{H}_{34}\text{NO}_4$ 460.24824 $[\text{M}+\text{H}]^+$; found 460.24820.

(R)-N-Fmoc-adamantylalanine-OMe (17)

To a solution of Fmoc protected adamantylalanine **15** (50 mg, 0.11 mmol, 1 equiv.) in MeOH (1 mL) was added slowly added TMSCH_2N_2 (2M in hexanes, added until solution stayed clear, 9 equiv. in total). After concentration of the reaction mixture, the crude product was purified by column chromatography (0→10% EtOAc/PE) providing the title product (50 mg, 0.11 mmol, 99%). *ee*: 96.6% (as determined by chiral HPLC using 90:10 hexane/isopropanol, Chiralcell OD). $[\alpha]_D^{20} = +5.6$ ($C=0.5$, CHCl_3). $^1\text{H NMR}$ (400 MHz, CDCl_3) δ 7.76 (d, $J = 7.5$ Hz, 2H), 7.60 (t, $J = 7.6$ Hz, 2H), 7.40 (t, $J = 7.5$ Hz, 2H), 7.31 (td, $J = 7.5, 1.0$ Hz, 2H), 5.10 (d, $J = 8.9$ Hz, 1H), 4.55 – 4.32 (m, 3H), 4.24 (t, $J = 7.1$ Hz, 1H), 3.73 (s, 3H), 1.97 (s, 3H), 1.76 – 1.14 (m, 14H). $^{13}\text{C NMR}$ (101 MHz, CDCl_3) δ 174.21, 155.60, 143.97, 143.78, 141.32, 127.69, 127.05, 125.12, 125.06, 119.98, 67.00, 52.36, 50.29, 47.22, 46.91, 42.39, 36.82, 32.64, 28.56. HRMS: calcd. for $\text{C}_{29}\text{H}_{34}\text{NO}_4$ 460.24824 $[\text{M}+\text{H}]^+$; found 460.24823.

Synthesis of (Fmoc/Boc-carboranylalanine(-OMe)

(R,E)-N-[2-(1',2'-Dicarba-closo-dodecaboranyl)ethylidene]-tert-butyl-sulfinamide (19)

To a solution of aldehyde **18** (0.96 g, 5.18 mmol, 1 equiv.) in dry DCM (25 mL) was added (*R*)-tert-butylsulfinamide (0.69 g, 5.7 mmol, 1.1 equiv.) and anhydrous CuSO_4 (2.65 g, 16.6 mmol, 3.2 equiv.) at rt under an argon atmosphere. TLC showed complete conversion of starting material after stirring overnight. The suspension was vacuum filtrated over a Whatman glass microfiber filter, washed with DCM and concentrated under reduced pressure. Flash column chromatography (5% → 30% EtOAc in pentane) afforded the sulfinimine **19** as a white powder (1.41 g, 4.88 mmol, 94%). $[\alpha]_D^{20} = -231.4$ ($c = 1.0$, DCM). $^1\text{H NMR}$ (400 MHz, CDCl_3) δ 7.93 (t, $J = 5.3$ Hz, 1H), 3.84 (s, 1H), 3.54 – 3.29 (m, 2H), 3.16 – 1.48 (m, 10H), 1.21 (s, 9H). $^{13}\text{C NMR}$ (101 MHz, CDCl_3) δ 162.29, 69.85, 60.55, 57.73, 42.69, 22.55. $^{11}\text{B NMR}$ (128 MHz, CDCl_3) δ -1.82, -4.92, -8.87, -11.31, -12.69. HRMS (m/z): calcd. for $\text{C}_8\text{H}_{24}\text{B}_{10}\text{NOS}$ 290.25777 $[\text{M}+\text{H}]^+$, found 290.25791.

(S, E)-N-[2-(1',2'-Dicarba-closo-dodecaboranyl)ethylidene]-tert-butyl-sulfinamide (20)

To a solution of aldehyde **18** (2.65 g, 14.2 mmol, 1 equiv.) in dry DCM (70 mL) was added (*S*)-tert-butylsulfinamide (1.89 g, 15.6 mmol, 1.1 equiv.) and anhydrous CuSO_4 (7.25 g, 45.4 mmol, 3.2 equiv.) at rt under an argon atmosphere. TLC showed complete conversion of starting material after stirring overnight. The suspension was vacuum filtrated over a Whatman glass microfiber filter, washed with DCM and concentrated under reduced pressure. Flash column chromatography (10% → 50% EtOAc in pentane) afforded the sulfinimine **20** as a white powder (3.86 g, 13.3 mmol, 94%). $[\alpha]_D^{20} = +239.0^\circ$ ($c = 1.0$, DCM). $^1\text{H NMR}$ (400 MHz, CDCl_3) δ 7.94 (t, $J = 5.3$ Hz, 1H), 3.82 (s, 1H), 3.51 – 3.28 (m, 2H), 3.21 – 1.50 (m, 10H), 1.21 (s, 9H). $^{13}\text{C NMR}$ (101 MHz, CDCl_3) δ 162.29, 69.84, 60.52, 57.76, 42.72, 22.58. $^{11}\text{B NMR}$ (128 MHz, CDCl_3) δ -1.87, -4.94, -8.91, -11.36, -12.78. HRMS (m/z): calcd. for $\text{C}_8\text{H}_{24}\text{B}_{10}\text{NOS}$ $[\text{M}+\text{H}]^+$ 290.25777, found 290.25797.

(S₁)-(+)-N-[(R)-1-Cyano-2-(1',2'-dicarba-closo-dodecaboranyl)ethyl]-tert-butylsulfinamide (21)

Sulfinamide **19** (1.74 g, 6.00 mmol, 1 equiv.) was dissolved in dry DMF (30 mL) and cooled to -50°C under an argon atmosphere. CsF (hygroscopic!) (1.00 g, 6.60 mmol, 1.1 equiv.) was added, followed by the dropwise addition of TMSCN (0.83 mL, 6.60 mmol, 1.1 equiv.). The mixture turned bright yellow and stirring was kept at -50°C . After 24 h additional CsF (0.27 g, 1.80 mmol, 0.3 equiv.) was added as well as TMSCN (0.23 mL, 1.80 mmol, 0.3 equiv.). TMSCN (0.3 equiv.) was added two times more after 43 h and 67 h until TLC showed complete

conversion of the starting material after 71 h. The reaction was quenched with a sat. aq. NH_4Cl solution (50 mL) and water (100 mL) was added. The aqueous layer was extracted with EtOAc (3 x 150 mL) and the combined organic layers were washed with brine (1 x 400 mL), dried over MgSO_4 , filtrated and concentrated by rotary evaporation. The product was co-evaporated three times with toluene to remove leftover DMF and purified by flash column chromatography (30% \rightarrow 60% EtOAc in pentane) to yield cyanosulfonamide **21** (1.77 g, 5.58 mmol, 93%) as a pale yellow powder in a diastereomeric ratio of 93:7 (anti/syn, determined by ^1H NMR). Recrystallization from EtOH/pentane at -20°C afforded cyanosulfonamide **21** as white crystals (1.03 g, 3.24 mmol, 54%) as a single diastereomer ($de \geq 99\%$). $[\alpha]_D^{20} = +62.1^\circ$ ($c = 2.2$, MeOH). ^1H NMR (400 MHz, MeOD) δ 4.71 (s, 1H), 4.51 (dd, $J = 9.1, 5.0$ Hz, 1H), 3.00 (dd, $J = 15.4, 9.2$ Hz, 1H), 2.90 (dd, $J = 15.4, 5.0$ Hz, 1H), 3.21 – 1.43 (m, 10H), 1.25 (s, 9H). ^{13}C NMR (101 MHz, MeOD) δ 119.19, 72.20 (b), 63.72, 58.24, 48.08, 42.22, 22.68. ^{11}B NMR (128 MHz, MeOD) δ -2.38, -5.01, -9.35, -11.70, -12.75. HRMS (m/z): calcd. for $\text{C}_9\text{H}_{24}\text{B}_{10}\text{N}_2\text{OS}$ $[\text{M}+\text{H}]^+$ 317.26863, found 317.26900.

(*R*,)-(+)-*N*-[(*S*)-1-Cyano-2-(1',2'-dicarba-closo-dodecaboranyl)ethyl]-*tert*-butylsulfonamide (22**)**

Sulfonamide **20** (1.01 g, 3.50 mmol, 1 equiv.) was dissolved in dry DMF (18 mL) and cooled to -50°C under an argon atmosphere. CsF (hygroscopic!) (0.69 g, 4.60 mmol, 1.3 equiv.) was added, followed by the dropwise addition of TMSCN (0.57 mL, 4.60 mmol, 1.3 equiv.). The mixture turned bright yellow and stirring was kept at -50°C . After 24 h additional TMSCN (0.13 mL, 1.10 mmol, 0.3 equiv.) was added and stirring was maintained at -50°C for two days. TMSCN (0.3 equiv.) was added two times more after 92 h and 97 h until TLC showed complete conversion of the starting material after 99 h. The reaction was quenched with a sat. aq. NH_4Cl solution (30 mL) and water (60 mL) was added. The aqueous layer was extracted with EtOAc (3 x 100 mL) and the combined organic layers were washed with brine (1 x 300 mL), dried over MgSO_4 , filtrated and concentrated by rotary evaporation, which gave cyanosulfonamide **22** (1.09 g, 3.43 mmol, 98%) as an orange/yellow solid which was pure according to ^1H -NMR-analysis in a diastereomeric ratio of 93:7 (anti/syn, determined by ^1H NMR). Recrystallization from EtOH/pentane at -20°C afforded cyanosulfonamide **22** as yellow crystals (0.54 g, 1.69 mmol, 48%) as a single diastereomer ($de \geq 99\%$). $[\alpha]_D^{20} = -59.4^\circ$ ($c = 2.2$, MeOH). ^1H NMR (400 MHz, MeOD) δ 4.70 (s, 1H), 4.50 (dd, $J = 9.1, 5.0$ Hz, 1H), 3.00 (dd, $J = 15.4, 9.2$ Hz, 1H), 2.89 (dd, $J = 15.4, 5.0$ Hz, 1H), 3.20 – 1.47 (m, 10H), 1.25 (s, 9H). ^{13}C NMR (101 MHz, MeOD) δ 119.17, 72.15, 63.68, 58.21, 48.03, 42.18, 22.68. ^{11}B NMR (128 MHz, MeOD) δ -2.36, -4.97, -9.33, -11.71, -12.71. HRMS (m/z): calcd. for $\text{C}_9\text{H}_{25}\text{B}_{10}\text{N}_2\text{OS}$ $[\text{M}+\text{H}]^+$ 317.26863, found 317.26905.

(*S*)-(-)-*N*-Boc-*o*-carboranylalanine (25**)**

Cyanosulfonamide **21** (520 mg, 1.64 mmol, 1 equiv.) was dissolved in 6N HCl (aq., 10 mL) at rt and refluxed overnight. The mixture was co-evaporated three times with toluene to remove all solvent to afford unprotected amino acid as the HCl salt **23**. Subsequently, the amino acid was redissolved in THF/water (8 mL, 1:1) at rt under an argon atmosphere and Boc_2O (537 mg, 2.46 mmol, 1.5 equiv.) and Et_3N (0.69 mL, 4.92 mmol, 3 equiv.) were added and the mixture was stirred overnight. The solvent was removed under reduced pressure and co-evaporated with toluene (3x). Flash column chromatography (100% DCM \rightarrow 20% MeOH in DCM) gave the Boc protected amino acid **25** as an off-white powder (462 mg, 1.39, 85%). $[\alpha]_D^{20} = -19.7^\circ$ ($c = 2.3$, MeOH). ^1H NMR (400 MHz, MeOD) δ 4.52 (s, 1H), 4.15 (d, $J = 8.8$ Hz, 1H), 2.92 (d, $J = 15.2$ Hz, 1H), 2.64 (dd, $J = 15.0, 10.6$ Hz, 1H), 3.14 – 1.56 (m, 10H), 1.46 (s, 9H). ^{13}C NMR (101 MHz, MeOD) δ 157.67, 80.90, 74.51, 63.18, 54.60, 39.55, 28.71. ^{11}B NMR (128 MHz, MeOD) δ -2.64, -5.55, -9.57, -11.40, -13.00. HRMS (m/z): calcd. for $\text{C}_{10}\text{H}_{26}\text{B}_{10}\text{NO}_4 + \text{CH}_3\text{CN}$ $[\text{M}+\text{CH}_3\text{CN}+\text{H}]^+$ 373.31270, found 373.31299.

(*S*)-(-)-*N*-Fmoc-*o*-carboranylalanine (26**)**

Boc-carboranylalanine **25** (166 mg, 0.50 mmol, 1 equiv.) was dissolved in 4M HCl in dioxane (2.5 mL, 10 mmol, 20 equiv.) at rt and stirred for 1.5 h. The mixture was co-evaporated three times with toluene to remove all solvents to afford the unprotected amino acid as the HCl salt. Subsequently, the amino acid (80 mg, 0.30 mmol,

1 equiv.) was redissolved in THF/water (3 mL, 1:1) at 0°C under an argon atmosphere and FmocOSu (121 mg, 0.36 mmol, 1.2 equiv.) and Et₃N (125 μL, 0.90 mmol, 3 equiv.) were added. After 1h at 0°C the mixture was stirred overnight at rt. The reaction was acidified with 0.1M HCl (30 mL) and extracted with EtOAc (3 x 30 mL). The combined organic layers were washed with brine (1 x 100 mL), dried over MgSO₄ and concentrated. Flash column chromatography (5% → 20% MeOH in DCM) gave the Fmoc protected amino acid **26** as a clear oil (128 mg, 0.28 mmol, 94%). $[\alpha]_D^{20} = -9.6^\circ$ ($c = 2.3$, CHCl₃). ¹H NMR (400 MHz, CDCl₃) δ 9.75 (s, 1H), 7.74 (d, $J = 7.5$ Hz, 2H), 7.61 – 7.43 (m, 2H), 7.38 (t, $J = 7.4$ Hz, 2H), 7.28 (t, $J = 7.3$ Hz, 2H), 5.59 – 5.31 (m, 1H), 4.53 – 4.43 (m, 1H), 4.43 – 4.33 (m, 1H), 4.33 – 4.21 (m, 1H), 4.17 (t, $J = 5.6$ Hz, 1H), 3.68 (s, 1H), 2.99 (s, 12H), 2.89 (d, $J = 13.6$ Hz, 1H), 2.66 – 2.53 (m, 1H). ¹³C NMR (101 MHz, CDCl₃) δ 174.17, 156.21, 143.47, 143.32, 141.39, 128.05, 127.29, 125.00, 120.23, 77.48, 77.16, 76.84, 71.69, 67.59, 61.26, 53.67, 47.04, 38.58. ¹¹B NMR (128 MHz, CDCl₃) δ -2.01, -5.15, -9.15, -11.57. HRMS (m/z): calcd. for C₂₀H₂₈B₁₀NO₄ [M+H]⁺ 454.30261, found 454.30215.

(R)-(+)-N-Fmoc-o-carboranylalanine (27)

Cyanosulfonamide **22** (250 mg, 0.80 mmol, 1 equiv.) was dissolved in 6M HCl (aq., 8 mL) at rt and refluxed overnight. The mixture was co-evaporated three times with toluene to remove all solvents to afford the unprotected amino acid as the HCl salt. Subsequently, the amino acid (106 mg, 0.40 mmol, 1 equiv.) was redissolved in THF/water (4 mL, 1:1) at 0°C under an argon atmosphere and FmocOSu (160 mg, 0.47 mmol, 1.2 equiv.) and Et₃N (167 μL, 1.2 mmol, 3 equiv.) were added. After 1h at 0°C the mixture was stirred overnight at rt. The reaction was acidified with 0.1M HCl (40 mL) and extracted with EtOAc (3 x 40 mL). The combined organic layers were washed with brine (1 x 100 mL), dried over MgSO₄ and concentrated. Flash column chromatography (5% → 20% MeOH in DCM) gave the Fmoc protected amino acid **27** as a clear oil (147 mg, 0.32 mmol, 81%). $[\alpha]_D^{20} = +9.5^\circ$ ($c = 2.0$, CHCl₃). ¹H NMR (400 MHz, CDCl₃) δ 7.93 (s, 1H), 7.73 (d, $J = 7.5$ Hz, 2H), 7.51 (d, $J = 6.8$ Hz, 2H), 7.37 (t, $J = 7.5$ Hz, 2H), 7.27 (t, $J = 7.4$ Hz, 2H), 5.63 – 5.46 (m, 1H), 4.52 – 4.40 (m, 1H), 4.40 – 4.28 (m, 1H), 4.28 – 4.19 (m, 1H), 4.19 – 4.09 (m, 1H), 3.67 (s, 1H), 3.10 – 1.42 (m, 10H), 2.86 (d, $J = 14.5$ Hz, 1H), 2.55 (dd, $J = 15.3, 8.9$ Hz, 1H). ¹³C NMR (101 MHz, CDCl₃) δ 173.75, 156.34, 143.49, 143.31, 141.39, 128.07, 127.30, 125.00, 120.24, 77.48, 77.16, 76.84, 71.80, 67.60, 61.28, 53.66, 47.02, 38.54. ¹¹B NMR (128 MHz, CDCl₃) δ -2.02, -5.06, -9.13, -11.49. ESI-HRMS (m/z): calcd. for C₂₀H₂₈B₁₀NO₄ [M+H]⁺ 454.30261, found 454.30206.

(S)-(-)-N-Fmoc-o-carboranylalanine methyl ester (28)

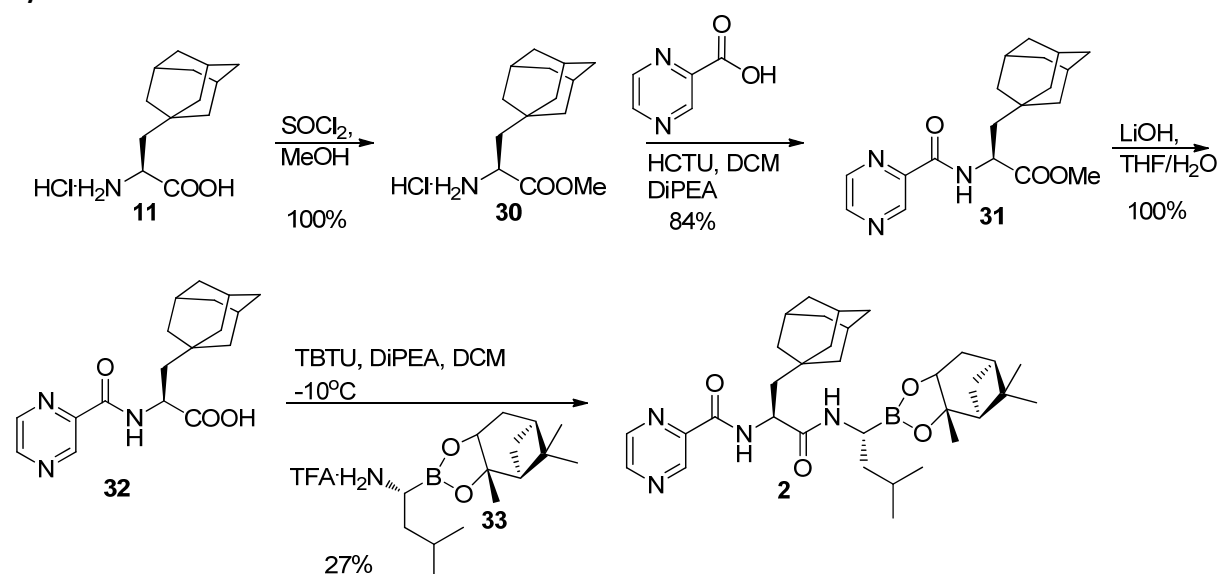
Fmoc-carboranylalanine **26** (114 mg, 0.25 mmol, 1 equiv.) was dissolved in DCM (2 mL) at 0°C under an argon atmosphere. HOBt (46 mg, 0.33 mmol, 1.3 equiv.), EDC·HCl (62 mg, 0.33 mmol, 1.3 equiv.) and MeOH (0.5 mL) were added and the reaction was stirred at rt overnight. The mixture was diluted with EtOAc (25 mL) and washed with 0.1M HCl (2 x 25 mL), sat. aq. NaHCO₃ (2 x 25 mL) and brine (1 x 25 mL), dried over MgSO₄ and concentrated. Flash column chromatography (10% → 40% EtOAc in pentane) gave the fully protected amino acid **28** as a clear oil (92 mg, 0.20 mmol, 79%). $[\alpha]_D^{20} = -10.0^\circ$ ($c = 1.6$, CHCl₃). *ee*: 90.6% (as determined by chiral HPLC using 90:10 hexane/isopropanol, Chiralpak AD). ¹H NMR (400 MHz, CDCl₃) δ 7.76 (d, $J = 7.5$ Hz, 2H), 7.56 (d, $J = 6.3$ Hz, 2H), 7.40 (t, $J = 7.4$ Hz, 2H), 7.31 (t, $J = 7.4$ Hz, 2H), 5.37 (d, $J = 8.2$ Hz, 1H), 4.57 – 4.46 (m, 1H), 4.46 – 4.37 (m, 1H), 4.31 (s, 1H), 4.20 (t, $J = 6.3$ Hz, 1H), 3.77 (s, 1H), 3.73 (s, 3H), 3.03 – 1.46 (m, 10H), 2.91 (d, $J = 14.6$ Hz, 1H), 2.61 (dd, $J = 14.9, 7.9$ Hz, 1H). ¹³C NMR (101 MHz, CDCl₃) δ 170.54, 155.79, 143.61, 143.49, 141.44, 127.97, 127.25, 125.00, 120.19, 77.48, 77.16, 76.84, 71.72, 67.31, 60.96, 53.56, 53.31, 47.15, 39.07. ¹¹B NMR (128 MHz, CDCl₃) δ -2.09, -5.01, -9.14, -11.41, -12.71. HRMS (m/z): calcd. for C₂₁H₃₀B₁₀NO₄ [M+H]⁺ 468.31830, found 468.31741.

(R)-(+)-N-Fmoc-o-carboranylalanine methyl ester (29)

Fmoc-carboranylalanine **27** (102 mg, 0.22 mmol, 1 equiv.) was dissolved in DCM (2 mL) at 0°C under an argon atmosphere. HOBt (40 mg, 0.29 mmol, 1.3 equiv.), EDC·HCl (56 mg, 0.29 mmol, 1.3 equiv.) and MeOH (0.5 mL) were added and the reaction was stirred at rt overnight. The mixture was diluted with EtOAc (25 mL) and washed with 0.1M HCl (2 x 25 mL), sat. aq. NaHCO₃ (2 x 25 mL) and brine (1 x 25 mL), dried over MgSO₄ and concentrated. Flash column chromatography (10% → 40% EtOAc in pentane) gave the fully protected amino acid **29** as a clear

oil (80 mg, 0.17 mmol, 78%). $[\alpha]_D^{20} = +10.6^\circ$ ($c = 1.6$, CHCl_3). *ee*: 86.6% (as determined by chiral HPLC using 90:10 hexane/isopropanol, Chiralpak AD). $^1\text{H NMR}$ (400 MHz, CDCl_3) δ 7.76 (d, $J = 7.5$ Hz, 2H), 7.56 (d, $J = 6.5$ Hz, 2H), 7.40 (t, $J = 7.4$ Hz, 2H), 7.31 (t, $J = 7.4$ Hz, 2H), 5.38 (d, $J = 8.3$ Hz, 1H), 4.56 – 4.46 (m, 1H), 4.45 – 4.37 (m, 1H), 4.36 – 4.26 (m, 1H), 4.20 (t, $J = 6.4$ Hz, 1H), 3.77 (s, 1H), 3.74 (s, 3H), 3.13 – 1.36 (m, 10H), 2.91 (d, $J = 13.2$ Hz, 1H), 2.61 (dd, $J = 15.4, 8.0$ Hz, 1H). $^{13}\text{C NMR}$ (101 MHz, CDCl_3) δ 170.58, 155.78, 143.60, 143.48, 141.43, 127.97, 127.25, 125.00, 120.19, 77.48, 77.16, 76.84, 71.70, 67.31, 60.96, 53.54, 53.32, 47.13, 39.06. $^{11}\text{B NMR}$ (128 MHz, CDCl_3) δ -2.08, -4.98, -9.15, -11.40, -12.64. HRMS (m/z): calcd. for $\text{C}_{21}\text{H}_{30}\text{B}_{10}\text{NO}_4$ $[\text{M}+\text{H}]^+$ 468.31830, found 468.31784.

Synthesis of adamantezomib



Scheme 3. Synthesis of adamantezomib **2** starting from enantiopure *S*-adamantylalanine

(*S*)-methyl 3-(adamantan-1-yl)-2-aminopropanoate hydrochloride (**30**)

To a solution of (*S*)-adamantylalanine **11** (519 mg, 2 mmol, 1 equiv.) in MeOH (10 mL) was added SOCl_2 (435 μL , 6 mmol, 3 equiv.). After refluxing for 3 hours, the solvent was removed by evaporation providing the product in a quantitative yield. $^1\text{H NMR}$ (400 MHz, MeOD) δ 4.07 (t, $J = 5.0$ Hz, 1H), 3.84 (s, 3H), 1.99 (s, 3H), 1.89 – 1.65 (m, 7H), 1.63 – 1.49 (m, 7H). $^{13}\text{C NMR}$ (101 MHz, MeOD) δ 171.89, 53.79, 49.95, 46.16, 42.78, 37.64, 33.16, 29.80.

(*S*)-methyl 3-(adamantan-1-yl)-2-(pyrazine-2-carboxamido)propanoate (**31**)

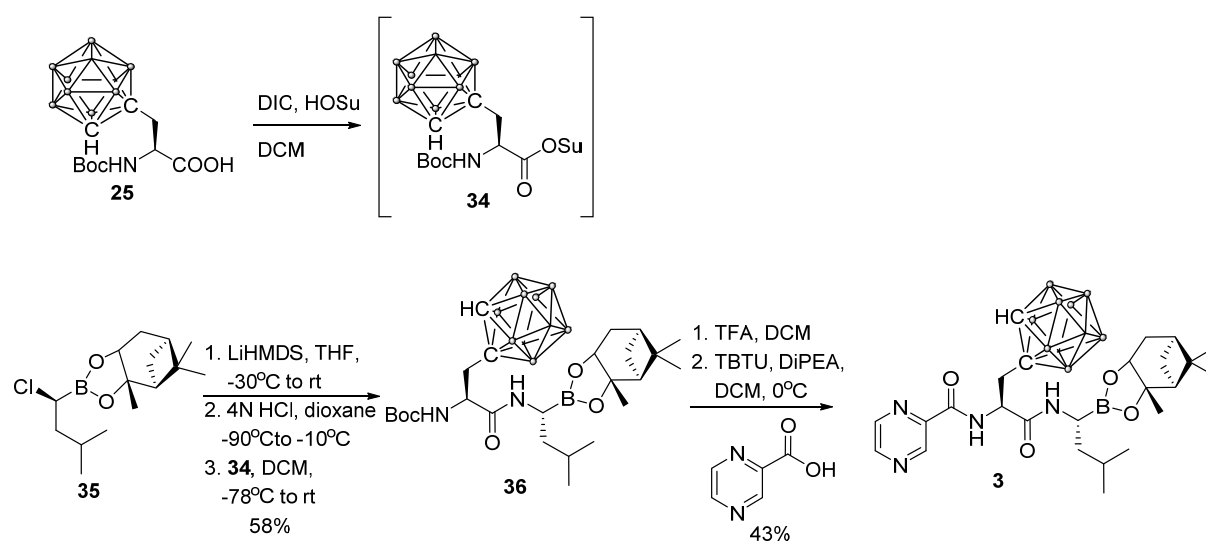
To a solution of pyrazinecarboxylic acid (74 mg, 0.6 mmol, 1.2 equiv.) and HCTU (248 mg, 0.6 mmol, 1.2 equiv.) in DCM was added DiPEA (304 μL , 1.75 mmol, 3.5 equiv.). After stirring for 5 min, methylester **30** (137 mg, 0.5 mmol, 1 equiv.) was added and the resulting mixture was stirred for 3 hours. The reaction mixture was evaporated and dissolved in EtOAc and washed with 0.1N HCl (2x) and sat. NaHCO_3 (2x), dried over Na_2SO_4 and concentrated. Column chromatography (30→50% EtOAc:PE) provided the title compound (144 mg, 0.42 mmol, 84%). $^1\text{H NMR}$ (400 MHz, CDCl_3) δ 9.36 (d, $J = 1.1$ Hz, 1H), 8.73 (d, $J = 2.4$ Hz, 1H), 8.59 – 8.47 (m, 1H), 8.01 (d, $J = 8.5$ Hz, 1H), 4.82 (td, $J = 8.8, 3.3$ Hz, 1H), 3.71 (s, 3H), 1.91 (s, 3H), 1.74 (dd, $J = 14.6, 3.3$ Hz, 1H), 1.58 (dt, $J = 31.6, 11.9$ Hz, 13H). $^{13}\text{C NMR}$ (101 MHz, CDCl_3) δ 173.48, 162.48, 147.53, 144.54, 144.05, 142.79, 52.56, 48.50, 46.83, 42.31, 36.78, 32.73, 28.51. HRMS (m/z): calcd. for $\text{C}_{18}\text{H}_{26}\text{N}_3\text{O}_3$ $[\text{M}+\text{H}]^+$ 330.18122, found 330.18118

(S)-3-(adamantan-1-yl)-2-(pyrazine-2-carboxamido)propanoic acid (32)

To a solution of methyl ester **31** (144 mg, 0.42 mmol) in THF (5 mL) was added LiOH (11 mg, 0.46 mmol, 1.1 equiv.) in H₂O (1 mL). After 1.5 hours, 4 mg LiOH was added since TLC-analysis showed remaining starting material. After 15 min, TLC-analysis showed complete conversion of starting material and the reaction mixture was diluted by the addition of EtOAc. 1N HCl was added and the mixture was extracted with EtOAc (2x). The combined organic layers were dried over Na₂SO₄, filtered and concentrated, providing the title compound in a quantitative yield. ¹H NMR (400 MHz, CDCl₃) δ 10.47 (bs, 1H), 9.36 (s, 1H), 8.76 (s, 1H), 8.56 (s, 1H), 8.06 (d, *J* = 8.2 Hz, 1H), 4.83 (s, 1H), 1.91 (s, 3H), 1.83 (d, *J* = 14.0 Hz, 1H), 1.69 – 1.45 (m, 13H). ¹³C NMR (101 MHz, CDCl₃) δ 174.70, 162.44, 146.97, 144.08, 143.96, 142.95, 48.36, 46.42, 42.11, 36.59, 32.61, 29.57, 28.33.

(1S, 2S, 3R, 5S) - Pinanediol - N - pyrazinoyl - L - adamantylalanine - L - boronoleucine 'Adamantezomib' (2)

To a solution of TBTU (35.3 mg, 0.11 mmol, 1.1 equiv.), boronoleucine **33** (33.7 mg, 0.1 mmol, 1 equiv.) and dipeptide **32** in DCM at -10°C was added DiPEA (52.3 μL, 0.3 mmol, 3 equiv.). After stirring for 2 hours at -10°C, TLC analysis (5% MeOH:DCM) indicated complete conversion of starting material. The reaction mixture was concentrated and the residue was dissolved in EtOAc, washed with 0.1N HCl (2x), sat. NaHCO₃ (2x) and brine, dried over Na₂SO₄, filtered and concentrated. Column chromatography (0→2% MeOH:DCM) followed by HPLC purification (C4, 50-90% MeCN, 0.1% TFA, 10 min gradient) provided the title compound (15.67 mg, 0.027 mmol, 27%). ¹H NMR (600 MHz, CDCl₃) δ 9.40 (d, *J* = 1.3 Hz, 1H), 8.79 (d, *J* = 2.4 Hz, 1H), 8.56 (dd, *J* = 2.3, 1.6 Hz, 1H), 8.05 (d, *J* = 8.6 Hz, 1H), 6.44 (d, *J* = 4.7 Hz, 1H), 4.71 (td, *J* = 8.0, 4.9 Hz, 1H), 4.31 (dd, *J* = 8.8, 2.0 Hz, 1H), 3.21 (dt, *J* = 9.1, 5.9 Hz, 1H), 2.33 (ddt, *J* = 13.9, 8.8, 2.3 Hz, 1H), 2.22 – 2.15 (m, 1H), 2.02 – 1.94 (m, 5H), 1.92 (tt, *J* = 5.8, 3.1 Hz, 1H), 1.85 (dt, *J* = 14.5, 2.6 Hz, 1H), 1.73 – 1.60 (m, 7H), 1.59 – 1.56 (m, 6H), 1.56 – 1.43 (m, 3H), 1.40 (s, 3H), 1.30 (s, 3H), 1.27 (d, *J* = 10.8 Hz, 1H), 0.89 (t, *J* = 6.4 Hz, 6H), 0.86 (s, 3H). ¹³C NMR (151 MHz, CDCl₃) δ 172.68, 162.78, 147.62, 144.54, 144.15, 142.89, 85.74, 77.84, 51.58, 48.62, 45.93, 42.55, 40.17, 39.78, 38.32, 36.96, 35.75, 32.41, 28.74, 28.67, 27.29, 26.51, 25.75, 24.21, 23.14, 22.26. LC-MS (linear gradient 50 → 90% MeCN, 0.1% TFA, 15 min): R_t (min): 9.30 (ESI-MS (m/z): 577.20. HRMS (m/z): calcd. for C₃₃H₅₀BN₄O₄ [M+ H]⁺ 577.39196, found 577.39203

Synthesis of carbortezomib

Scheme 4. Synthesis of carbortezomib **3** starting from enantiopure L-N-Boc-carboranylalanine

(1S,2S,3R,5S)-Pinanediol -N- Boc-L-carboranylalanine-L-borono-leucine (36)

(S)-N-Boc carboranylalanine **25** (83 mg, 0.25 mmol, 1.25 equiv.) in dry CH₂Cl₂ (0.2M) under an argon atmosphere at rt, was treated with N-hydroxysuccinimide (52 mg, 0.45 mmol, 2.25 equiv.) and N,N'-diisopropylcarbodiimide (57 mg, 0.45 mmol, 2.25 equiv.). The mixture was stirred until TLC showed complete conversion of the starting material, after 6 h, yielding the crude OSu ester. Separately, chloroboronate **35** (57 mg, 0.2 mmol, 1 equiv.) was dissolved in dry THF (0.2M) at -30 °C under an argon atmosphere and treated with LiHMDS (0.26 mL, 1M in THF, 1.3 equiv.). The mixture was slowly warmed to rt and re-cooled to -90 °C when TLC indicated complete conversion of the starting material typically after 5 h. HCl (0.23 mL, 4N in 1,4-dioxane, 4.5 equiv.) was added and the reaction was allowed to warm to -10°C. The mixture was cooled again to -80 °C and DiPEA (12 equiv.) was added, followed by the crude OSu ester solution. The reaction was stirred overnight and allowed to warm up to rt. The mixture was filtrated over a Whatmann glass microfiber filter and concentrated by rotary evaporation. Column chromatography (10% → 30% EtOAc in pentane) afforded dipeptide **36** as a colourless oil (67 mg, 0.12 mmol, 58%). ¹H NMR (400 MHz, MeOD) δ 4.55 (s, 1H, C_{carb}H), 4.34 (dd, J = 9.6, 3.5 Hz, 1H), 4.21 (dd, J = 8.5, 1.7 Hz, 1H), 3.03 – 1.58 (m, 10H), 2.87 – 2.76 (m, 2H), 2.62 (dd, J = 15.6, 9.7 Hz, 1H), 2.40 – 2.30 (m, 1H), 2.19 – 2.11 (m, 1H), 1.96 (t, J = 5.5 Hz, 1H), 1.91 – 1.85 (m, 1H), 1.79 (dt, J = 14.3, 2.6 Hz, 1H), 1.75 – 1.67 (m, 1H), 1.46 (s, 9H), 1.42 – 1.32 (m, 6H), 1.29 (s, 3H), 0.92 (dd, J = 6.5, 3.6 Hz, 6H), 0.88 (s, 3H). ¹³C NMR (101 MHz, MeOD) δ 175.22, 156.99, 85.16, 81.27, 77.82, 73.91, 63.32, 53.23, 52.88, 41.16), 41.12, 40.97 (HSQC confirmed), 39.56, 39.21, 37.22, 29.49, 28.68, 27.68, 27.33, 26.61, 24.54, 23.43, 22.48. ¹¹B NMR (128 MHz, MeOD) δ 21.56, -2.51, -5.57, -9.57, -11.81, -13.11. HRMS (m/z): calcd. for C₂₅H₅₁B₁₁N₂O₅ [M+ H]⁺ 579.49725, found 579.49817.

(1S, 2S, 3R, 5S) - Pinanediol - N - pyrazinoyl - L - carboranylalanine - L - boronoleucine 'carbortezomib' (3)

Dipeptide **52** (23 mg, 40 μmol, 1 equiv.) was dissolved in dry DCM/TFA (1:1, 1.5 mL) at rt under an argon atmosphere. After 40 min the solvents were removed by co-evaporation with toluene (3x) and the deprotected dipeptide re-dissolved in dry DCM (1.5 mL) and cooled to 0 °C. 2-Pyrazinecarboxylic acid (8 mg, 60 μmol, 1.5 equiv.), TBTU (20 mg, 60 μmol, 1.5 equiv.) and DiPEA (20 μL, 120 μmol, 3 equiv.) were added and the mixture was stirred for 1 h at 0 °C. The DCM was removed by rotary evaporation and redissolved in EtOAc (20 mL). The organic layer was washed with 0.1M aq. HCl (2 x 20 mL), 2% aq. NaCO₃ (2 x 20 mL) and brine (1 x 20 mL). The EtOAc layer was then dried over MgSO₄, filtrated and concentrated by rotary evaporation. Flash column chromatography (20 → 50% EtOAc in pentane) followed by HPLC purification (C₁₈, 80→86% MeCN, 0.1 % TFA, 12 min gradient) and lyophilisation, afforded the title compound **3** as a white powder (10.08 mg, 17.24 μmol, 43%). ¹H NMR at 303 K (600 MHz, MeOD) δ 9.26 (d, J = 1.3 Hz, 1H), 8.82 (d, J = 2.4 Hz, 1H), 8.76 – 8.68 (m, 1H), 4.86 (dd, J = 8.8, 4.3 Hz, 1H), 4.59 (s, 1H), 4.25 (dd, J = 8.7, 1.9 Hz, 1H), 3.04 (dd, J = 15.8, 4.3 Hz, 1H), 2.97 – 2.88 (m, 2H), 2.78 – 1.57 (m, 10H), 2.38 – 2.32 (m, 1H), 2.19 – 2.13 (m, 1H), 1.95 (t, J = 5.5 Hz, 1H), 1.90 – 1.85 (m, 1H), 1.79 (dt, J = 14.3, 2.5 Hz, 1H), 1.69 (dtt, J = 20.5, 13.3, 6.6 Hz, 1H), 1.47 – 1.36 (m, 2H), 1.35 (s, 3H), 1.35 – 1.32 (m, 1H), 1.29 (s, 3H, C_qCH₃CH₃), 0.91 – 0.84 (m, 9H). ¹³C NMR (151 MHz, MeOD) δ 173.52, 165.38, 148.92, 145.71, 144.99, 144.86, 85.72, 78.23, 73.97, 63.65, 53.15, 52.35, 41.13, 40.94, 40.28, 39.30, 39.24, 37.03, 29.35, 27.63, 27.30, 26.60, 24.47, 23.28, 22.52. ¹¹B NMR (128 MHz, MeOD) δ 22.40, -2.51, -5.47, -9.54, -11.59, -12.94. LC-MS (linear gradient 50 → 90% MeCN, 0.1% TFA, 15 min): R_t (min): 9.81 (ESI-MS (m/z): 585.20. HRMS : calcd. for C₂₅H₄₆B₁₁N₄O₄ [M+ H]⁺ 585.46237, found 585.46251.

Biochemical methods

General methods

Lysates of cells were prepared by treating cell pellets with 4 volumes of lysis buffer containing 50 mM Tris pH 7.5, 2 mM DTT, 5 mM MgCl₂, 10% glycerol, 2 mM ATP, and 0.05% digitonin for 15-60 min. Protein concentration was determined using Qubit[®] protein assay kit (Thermofisher). All cell lysate labelling experiments were performed in assay buffer containing 50 mM Tris pH 7.5, 2 mM DTT, 5 mM MgCl₂, 10% glycerol, 2 mM ATP. Cell lysate labelling and competition experiments were performed at 37°C. The 10x concentrated ABP cocktail is composed of: 1 μM Cy5-NC-001, 0.3 μM BODIPY(FL)-LU-112, 1 μM BODIPY(TMR)-NC-005-VS, mixed in DMSO. Prior to fractionation on 12.5% SDS-PAGE (TRIS/glycine), samples were boiled for 3 min in a reducing gel loading buffer. The 7.5x10 cm (L x W) gels were run for 15 min at 80V followed by 120 min at 130V. In-gel fluorescence in the wet gel slabs was directly detected on a ChemiDoc[™] MP System using Cy2 setting to detect BODIPY(FL)-LU-112, Cy3 settings to detect BODIPY(TMR)-NC-005-VS and Cy5 settings to detect Cy5-NC-001.

Competition experiments in cell lysate

Cell lysates (diluted to 10-15 μg total protein in 9 μL buffer) were exposed to the inhibitors (10x stock in DMSO) at indicated concentrations for 1 h at 37 °C, followed by addition of probe cocktail (1.1 μL) and SDS-PAGE as described in general methods. Intensities of bands were measured by fluorescent densitometry and divided by the intensity of bands in mock-treated extracts. Average values of three independent experiments were plotted against inhibitor concentrations. IC₅₀ (inhibitor concentrations giving 50% inhibition) values were calculated using GraphPad Prism software.

Competition experiments in living RPMI-8226 cells

RPMI-8226 were cultured in RPMI-1640 media supplemented with 10% fetal calf serum, GlutaMAX[™], penicillin, streptomycin in a 5% CO₂ humidified incubator. 5-8 × 10⁵ cells/mL were exposed to inhibitors for 1 h at 37 °C. Cells were harvested and washed twice with PBS. Cell pellets were treated with lysis buffer on ice for 15 min, followed by centrifugation at 14000 rpm for 10 min. Proteasome inhibition in the obtained cell lysates was determined using the method described above (60 min incubation with ABP cocktail). Intensities of bands were measured by fluorescent densitometry and divided by the intensity of bands in mock-treated extracts. Average values of three independent experiments were plotted against inhibitor concentrations. IC₅₀ (inhibitor concentrations giving 50% inhibition) values were calculated using GraphPad Prism software.

Inhibitor washout experiments

5 × 10⁵ RPMI-8226 cells were treated with 1 μM of inhibitor (1% DMSO end concentration) at 37°C. After 1 h, the cells were washed with medium (2x) and incubated at 37°C for 0, 2 or 4 hours. The cells were harvested and washed with PBS, lysed in standard lysis buffer for 15 min, followed by centrifugation at 14000 rpm for 5 min. Proteasome inhibition in the obtained cell lysates was determined using the method described above (30 min incubation with ABP cocktail). Intensities of bands were measured by fluorescent densitometry and divided by the intensity of bands in mock-treated extracts and corrected for gel loading using Coomassie staining. Average values of three independent experiments are reported.

References

1. Hershko, A. & Ciechanover, A. The ubiquitin system. *Annu. Rev. Biochem.* **67**, 425-79 (1998).
2. Ferrington, D.A. & Gregerson, D.S. Immunoproteasomes: structure, function, and antigen presentation. *Prog. Mol. Biol. Transl. Sci.* **109**, 75-112 (2012).
3. Zhang, J., Wu, P. & Hu, Y. Clinical and marketed proteasome inhibitors for cancer treatment. *Curr. Med. Chem.* **20**, 2537-51 (2013).
4. Huber, E M. et al. Immuno- and constitutive proteasome crystal structures reveal differences in substrate and inhibitor specificity. *Cell* **148**, 727-738 (2012).
5. de Bruin, G. et al. Structure-based design of beta1i or beta5i specific inhibitors of human immunoproteasomes. *J. Med. Chem.* **57**, 6197-209 (2014).
6. Groll, M., Berkers, C.R., Ploegh, H.L. & Ovaa, H. Crystal structure of the boronic acid-based proteasome inhibitor bortezomib in complex with the yeast 20S proteasome. *Structure* **14**, 451-456.
7. de Bruin, G. et al. A set of activity-based probes to visualize human (immuno)proteasome activities. *Angewa. Chem. Int. Ed.* **13**, 4199-4203 (2016).
8. Kupperman, E. et al. Evaluation of the proteasome inhibitor MLN9708 in preclinical models of human cancer. *Cancer. Res.* **70**, 1970-80 (2010).
9. Scholz, M. & Hey-Hawkins, E. Carbaboranes as pharmacophores: properties, synthesis, and application strategies. *Chem. Rev.* **111**, 7035-7062 (2011).
10. Barth, R.F., Coderre, J.A., Vicente, M.G.H. & Blue, T.E. Boron neutron capture therapy of cancer: Current status and future prospects. *Clin. Cancer Res.* **11**, 3987-4002 (2005).
11. Moss, R.L. Critical review, with an optimistic outlook, on Boron Neutron Capture Therapy (BNCT). *Appl. Radiat. Isotopes* **88**, 2-11 (2014).
12. Do, K.Q., Thanei, P., Caviezel, M. & Schwyzer, R. The synthesis of (S)-(+)-2-Amino-3-(1-adamantyl)-propionic acid (L-(+)-Adamantylalanine, Ada) as a 'fat' or 'super' analogue of leucine and phenylalanine. *Helv. Chim. Acta* **62**, 956-964 (1979).
13. Oppolzer, W., Pedrosa, R. & Moretti, R. Asymmetric syntheses of alpha-amino-acids from alpha-halogenated 10-Sulfonamido-isobornyl esters. *Tetrahedron Lett.* **27**, 831-834 (1986).
14. Lander, P.A. & Hegedus, L.S. Asymmetric-synthesis of alpha-amino-acids by copper-catalyzed conjugate addition of grignard-reagents to optically-active carbamatoacrylates. *J. Am. Chem. Soc.* **116**, 8126-8132 (1994).
15. Cho, D.H. & Jang, D.O. Enantioselective radical addition reactions to the C=N bond utilizing chiral quaternary ammonium salts of hypophosphorous acid in aqueous media. *Chem. Comm.*, 5045-5047 (2006).
16. Toppino, A. et al. A carborane-derivative "click" reaction under heterogeneous conditions for the synthesis of a promising lipophilic MRI/GdBNCT agent. *Chem-Eur. J.* **19**, 720-727 (2013).
17. Radel, P.A. & Kahl, S.B. Enantioselective synthesis of L- and D-carboranylalanine. *J. Org. Chem.* **61**, 4582-4588 (1996).
18. Malmquist, J. & Sjöberg, S. Asymmetric synthesis of p-carboranylalanine (p-Car) and 2-methyl-o-carboranylalanine (Me-o-Car). *Tetrahedron* **52**, 9207-9218 (1996).
19. Robak, M.T., Herbage, M.A. & Ellman, J.A. Synthesis and applications of tert-butanesulfonamide. *Chem. Rev.* **110**, 3600-3740 (2010).
20. Mabic, S. & Cordi, A.A. Synthesis of enantiomerically pure ethylenediamines from chiral sulfinimines: a new twist to the Strecker reaction. *Tetrahedron* **57**, 8861-8866 (2001).
21. Dozzo, P., Kasar, R.A. & Kahl, S.B. Simple, high-yield methods for the synthesis of aldehydes directly from o-, m-, and p-carborane and their further conversions. *Inorg. Chem.* **44**, 8053-8057 (2005).
22. Takahashi, E., Fujisawa, H., Yanai, T. & Mukaiyama, T. Lewis base-catalyzed diastereoselective strecker-type reaction between trimethylsilyl cyanide and chiral sulfinimines. *Chem. Lett.* **34**, 604-605 (2005).

23. Li, B.-F. et al. Highly diastereoselective strecker reaction of enolizable aliphatic sulfinimines. *J. Org. Chem.* **68**, 6264-6267 (2003).
24. CCDC numbers: **21b**: 1442382; **22**: 1442383. Details of crystal data and refinement can be found in the supplementary information.
25. Verdoes, M. et al. Mixing of peptides and electrophilic traps gives rise to potent, broad-spectrum proteasome inhibitors. *Org. Biomol. Chem.* **5**, 1416-1426 (2007).
26. Ivanov, A.S., Zhalnina, A.A. & Shishkov, S.V. A convergent approach to synthesis of bortezomib: the use of TBTU suppresses racemization in the fragment condensation. *Tetrahedron* **65**, 7105-7108 (2009).
27. Due to partial dissociation of the inhibitors during cell lysis and labelling by ABPs, at t=0 blockage of the β 1 and β 5 appears to be <100%.
28. Verdoes, M. et al. A fluorescent broad-spectrum proteasome inhibitor for labeling proteasomes in vitro and in vivo. *Chem. Biol.* **13**, 1217-1226 (2006).

CHAPTER 12

Summary and future prospects

In this thesis the development of new tools to monitor and control proteasome activities are described. Proteasomes are multi-protein, multi-catalytic complexes responsible for the degradation of 80-90% of the proteins inside eukaryotic cells. Proteasomes contain a cylindrical 20S core particle (CP) and one or two 19S regulatory particles (RP). Proteins destined for degradation are tagged with a poly-ubiquitin chain, which is recognized by the 19S RP. Following ubiquitin removal and protein unfolding, the protein is translocated to the CP where the actual protein degradation takes place. The CP consists of four heptameric rings, two outer α -rings and two inner β -rings, with the catalytic subunits residing in the latter. The constitutive proteasome core particle (cCP), which is expressed in all mammalian tissues, contains three catalytically active subunits, namely β 1c (caspase-like, cleaving preferentially after acidic amino acids), β 2c (trypsin-like, cleaving preferentially after basic amino acids) and β 5c (chymotrypsin-like, cleaving preferentially after hydrophobic amino acids). Lymphoid cells, as well as cells that have been exposed to inflammatory cytokines express another proteasome core particle known as the immunoproteasome (iCP). In iCPs, β 1c, β 2c and β 5c are replaced by β 1i, β 2i and β 5i, respectively. The iCP catalytic activities have altered substrates preferences and iCP generated peptides have an averaged higher affinity for major histocompatibility complex class I (MHC-I), thus the iCP plays a major role in the immune system. In addition to cCPs and iCPs, mixed proteasomes (mCPs) may exist, in which both constitutive proteasome and immunoproteasome catalytic activities are found. Finally, thymic epithelial cells express thymoproteasomes (tCP), which play an important role in positive T-cell selection. In tCPs β 5i is replaced by β 5t in otherwise unchanged iCPs.

Proteasome inhibition is cytotoxic for certain types of cancer and is thought to lead to suppression of (auto)-immune diseases. Therefore, the proteasome is an important drug target in the field of oncology and immunology. Currently, several proteasome inhibitors are in use or in development for treatment of multiple myeloma and mantle cell lymphoma. Moreover, some iCP selective inhibitors are currently in clinical trials for the treatment of

auto-immune diseases. While in their development, $\beta 5$ subunits were considered as the most important target, all clinically used proteasome inhibitors appear to inhibit both $\beta 5c$ and $\beta 5i$, along with several other cCP/iCP catalytic activities. Indeed, in the last decade it has become clear that co-inhibition of additional proteasome catalytic subunits sensitizes cells to $\beta 5$ inhibition and is able to overcome resistance. For this reason, but also with the aim to unravel the contribution of the various catalytic subunits to protein turnover and MHC-I mediated antigen presentation, much research has been focussed on the discovery of proteasome catalytic subunit selective inhibitors. Associated with this, there is an increased interest in methods that allow simultaneous measurement of multiple proteasome catalytic activities. Such assays could aid the development of subunit selective inhibitors and determination of the proteasome composition in cell lines and (diseased) tissues. Related to this, methods to determine the presence and composition of mCPs have been developed. Briefly, the research described in this thesis reports on the development of new subunit-selective inhibitors and activity-based probes (ABPs), on the development of an assay to simultaneously monitor all cCP and iCP catalytic activities and on the development of a method that reports on CP catalytic active subunit composition. The tools that stem from the work described in this thesis can now be used to unravel the role of each individual catalytic subunit in a chemical genetics setting (selective and (near) complete inhibition of each individual subunit), and to clarify the role of mCPs, in, for instance, antigen presentation and cancer. Furthermore, these tools could possibly serve as leads in the discovery of agents for future treatment of cancer and autoimmune diseases.

Chapter 1 discusses the catalytic mechanism employed by proteasome active sites and the rationale behind proteasome inhibitors. **Chapter 2** presents an overview of the methods available to measure proteasome activity that have been developed to date. All methods rely either on the hydrolysis of substrates or on activity-based protein profiling (ABPP) and all methods have proven their worth in the search for new proteasome inhibitors, in determining the (relative) activity of the proteasome and in providing insight in the proteasome composition of a given biological sample.

Chapter 3 describes the development of a set of tools that enables monitoring and controlling the six catalytic activities of both human constitutive proteasomes and human immunoproteasomes. A cocktail of three ABPs, targeting either $\beta 1c/\beta 1i$ (Cy5-NC-001), $\beta 2c/\beta 2i$ (BODIPY(FL)-LU112) or $\beta 5c/\beta 5i$ (BODIPY(TMR)-NC-005), and each equipped with an orthogonal (in terms of excitation/emission) fluorophore was assembled.

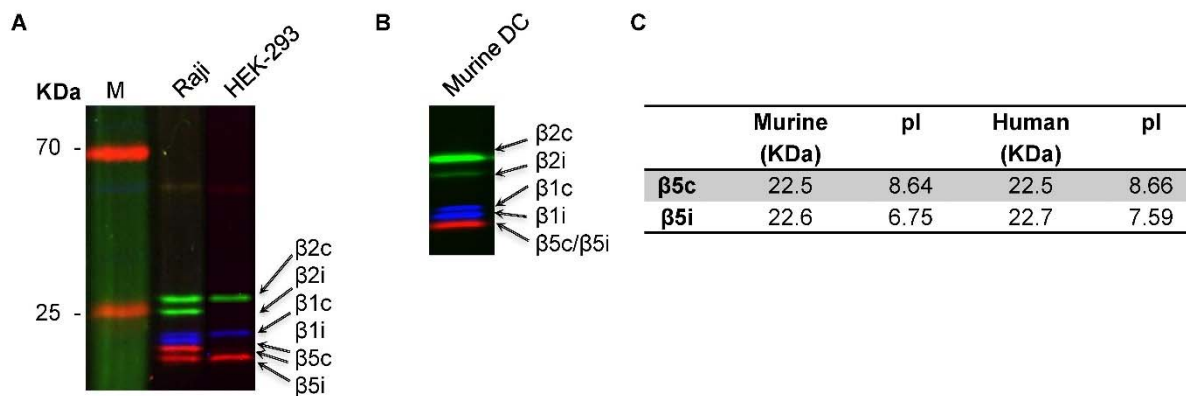


Figure 1. Proteasome ABP cocktail provides full separation of human cCP and iCP subunits on SDS-PAGE. Raji- or HEK-293 cell lysates (A) or murine dendritic cell (DC) lysates (B) were treated with the ABP cocktail, followed by SDS-PAGE and fluorescence imaging of the wet gel slabs. C) Molecular weight and pI values of human and murine $\beta 5c$ and $\beta 5i$.

On SDS-PAGE, this cocktail provided full resolution of all six catalytic subunits of the human (immuno)proteasome modified by these probes (Figure 1A). This assay enables straightforward screening of putative proteasome inhibitors and rapid assessment of the proteasome composition of cell lines and patient samples, with respect to the relative abundance of each subunit. Using this cocktail, proteasome inhibitors selective for, either $\beta 1c$, $\beta 2c$, $\beta 2i$ or $\beta 5c$ were identified. Moreover, primary malignant haematological cells were revealed to express predominately iCP subunits; this in contrast to for instance multiple myeloma cell lines that express about equal levels of cCP and iCP subunits. Based on this observation, acute lymphoid leukemia (ALL) patient cells were treated with a combination of $\beta 1i$ and $\beta 5i$ inhibitors, which proved to be highly cytotoxic. Thus, selective iCP inhibition may be a valuable strategy to limit side effects associated with proteasome inhibitors currently used in the clinic in treating haematological cancers, especially since most cells have no or low expression of iCP subunits.

Since the $\beta 5c/\beta 5i$ selective ABP BODIPY(TMR)-NC-005 does not separate murine $\beta 5c$ and $\beta 5i$ on SDS-PAGE, this probe cannot be used to determine the individual activity of these subunits in murine cell lines or tissues (Figure 1B). Murine $\beta 5c$ and $\beta 5i$ are slightly smaller compared to their human counterparts, and differ slightly in pI values and either of these differences, or a combination thereof, may be at the basis of the subtly different behaviour on SDS-PAGE (Figure 1C). The use of the ABPP assay described in Chapter 2 is thus limited to human cell lines or patient samples when full assessment of all cCP and iCP activities is desired. This is disadvantageous since often mouse models are used for *in vivo* studies. Interestingly, other $\beta 5c/\beta 5i$ targeting ABPs, such as BODIPY-epoxomicin^{1, 2} and the probes described in chapter 6, are also not able to separate human $\beta 5c$ and $\beta 5i$ on SDS-PAGE, indicating that the nature of the fluorophore or inhibitor influences the resolution of the

subunits modified by these on SDS-PAGE. It would therefore be interesting to evaluate $\beta 5c/\beta 5i$ selective inhibitors equipped with different fluorophores, such as Cy3, Cy5, TAMRA and rhodamine in murine samples and compare these with human samples. Given the difference in pI values between human and murine $\beta 5i$, another solution to this problem might be to change the pH of the resolving gel. Furthermore, the percentage acrylamide and cross-links, size of the gel and the voltage at which the gel is resolved could be varied in order to find conditions which enable separation of murine $\beta 5c$ and $\beta 5i$.

While this assay enables rapid screening of putative proteasome inhibitors, high-throughput screening (HTS) of large compound libraries is not possible due to the gel-based format. To overcome this shortcoming, a fluorescence polarization competitive ABPP assay (FluoPol-ABPP) assay may be considered. Fluorescence polarization is used to study molecular interactions and is a measure of the apparent size of a fluorophore. The underlying principle is the slow tumbling rate of large molecules and high tumbling rate of small molecules. Small fluorophore containing molecules, such as ABPs, excited with plane-polarized light rotate in the excited state, resulting in the emission of depolarized light (low fluorescence polarization). Larger molecules, such as an ABP bound to a protein, rotate much slower, thereby emitting highly polarized light (high fluorescence polarization).³ Cravatt *et al.* have pioneered the application of FluoPol-ABPP in HTS.⁴ They developed an assay to screen for inhibitors of retinoblastoma-binding protein-9 (RBBP9) which was found to covalently interact with fluorophosphonate (FP)-rhodamine, a broad-spectrum serine hydrolase ABP. Based on these results, it might be possible to develop a proteasome FluoPol-ABPP, as depicted in Figure 2. However, several hurdles have to be taken. In FluoPol-ABPP assays, often μM concentrations of purified enzyme and nM concentration of ABP are needed in order ensure full binding of ABPs, thereby providing low background.⁴⁻⁶ However, given the size of the proteasome, this would require large amounts of purified 20S proteasome, which is rather expensive. Therefore, it would be desirable to perform proteasome FluoPol-ABPP in crude cell lysates with preferably also lower ABP concentrations. The probes described in chapter 3 are equipped with different fluorophores, and therefore it should be possible to monitor the activity of $\beta 1$, $\beta 2$ and $\beta 5$ simultaneously by FluoPol-ABPP. Fluorescence quenching will however likely occur (see chapter 10) in native samples, and a denaturation step is likely necessary following a competitive ABPP with the three probes and before fluorescence polarization is measured.

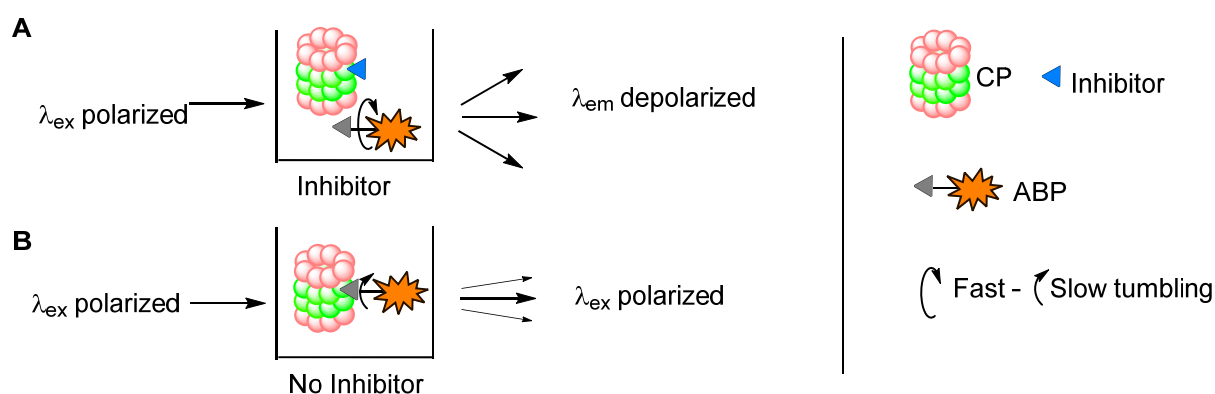


Figure 2. Proteasome FluoPol-ABPP. A) In presence of an inhibitor the ABP cannot bind, and the fast tumbling rate causes depolarization of the emitted light. B) In absence of an inhibitor, the ABP binds to the proteasome, resulting in slow rotation of the fluorophore, hence emission of highly polarized light.

Chapter 4 reports on a systematic analysis of substrate specificities of human cCPs and iCPs and yeast proteasome (yCP). For this, 18 oligopeptide epoxyketones (EK) were synthesized. The focused peptide library was assembled from Ala, Leu, Asp, Glu, Phe, Tyr, Ile or Val at P1; Ala or Leu at P2 and Leu or Pro at P3, and an acetyl N-cap. yCP crystals were soaked with the epoxyketones and X-ray structures were determined. This study provided detailed insight in substrate specificities of human proteasome subunits and yielded design parameters for subunit selective inhibitors. Interestingly, Val and Ile at P1 are highly disfavoured by all active sites of yeast and human proteasomes. Both yeast $\beta 1$ and human $\beta 1c$ prefer Asp, and not so much Glu, at P1, confirming that ‘caspase-like’ describes the specificity of $\beta 1(c)$ more accurately than the traditional ‘peptidyl-glutamyl peptide hydrolysing’. Implementation of the obtained knowledge led to the development of the $\beta 1c$ selective inhibitor LU-001c, as described in chapter 8. As expected, due to mutations in its S1 pocket, $\beta 1i$ prefers hydrophobic residues (Leu, Phe) at P1. The study also yielded a structural basis for the $\beta 1c/\beta 1i$ preference of inhibitors bearing Pro at P3. Compounds bearing Ala at P1 and Leu at P3 proved highly $\beta 5c$ selective (hardly any $\beta 5i$ inhibition observed), a result that was capitalized on in the development of $\beta 5c$ selective inhibitors (chapter 7). Interestingly, Glu at P1 in Ac-LAE-EK showed 30-fold selectivity for $\beta 2c$ over $\beta 2i$, although with moderate potency (IC_{50} : 3.6 μM). It may well be that the Asp53Glu mutation in $\beta 2i$, which prevents hydrogen bonding to the Glu side chain of Ac-LAE-EK, causes this observed $\beta 2c$ selectivity. These results may be exploited to further improve the moderate $\beta 2c$ selective inhibitor LU-002c described in chapter 3 (LU-002c, (IC_{50} : 0.08 μM , selectivity: 20x). Although both compounds bear an Ala residue at P2, it is unlikely that in case of Ac-LAE-EK this causes $\beta 2c$ selectivity, this because none of the other epoxyketone with Ala at P2 proved to be $\beta 2c$ selective.

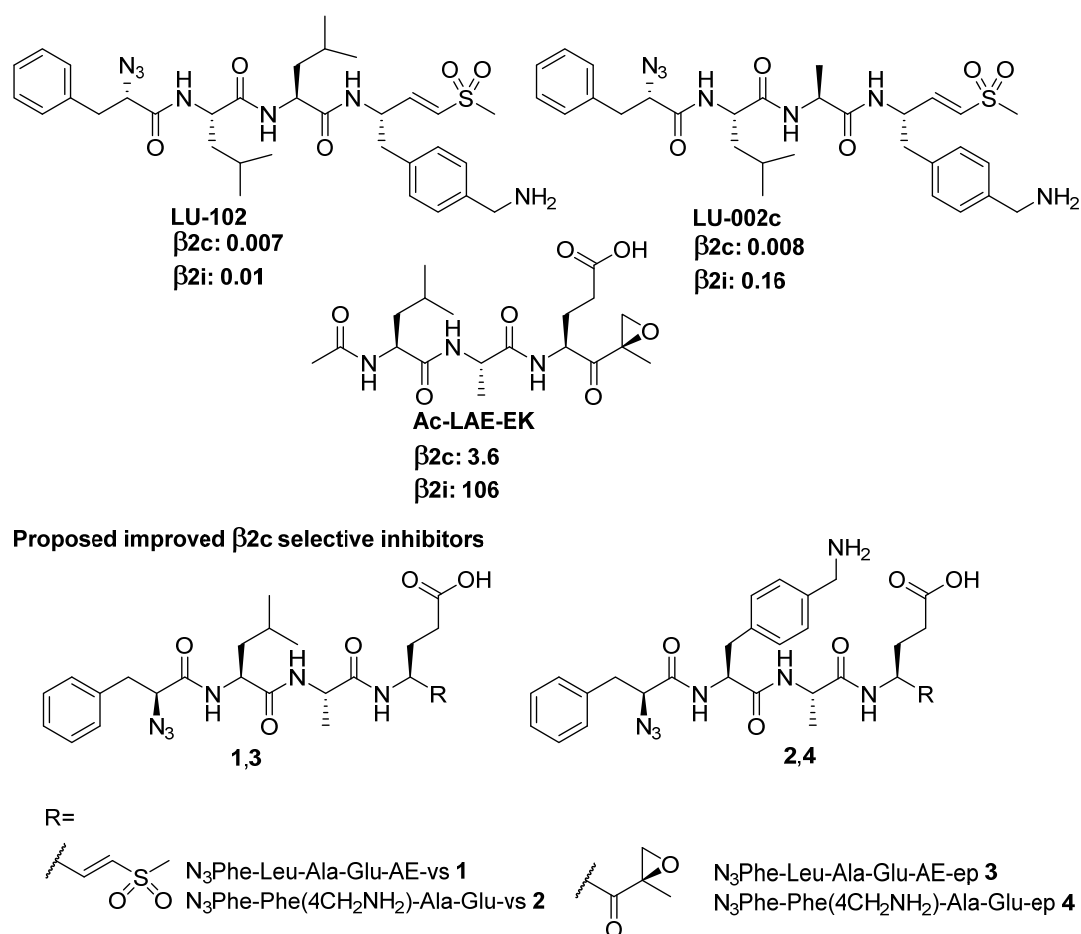


Figure 3. Structures of $\beta 2c/\beta 2i$ selective inhibitor LU-102, $\beta 2c$ selective inhibitors LU-002c and Ac-LAE-EK and proposed improved $\beta 2c$ selective inhibitors 1-4.

However, since in LU-002c, the P2 Ala does cause $\beta 2c$ selectivity, selectivity of an inhibitor is likely in part guided by the combination of amino acids present in this inhibitor. Considering this, several compounds can be proposed which may turn out to have improved $\beta 2c$ selectivity compared to LU-002c and Ac-LAE-EK (Figure 3). Addition of a P4 residue could increase the potency of P1 Glu containing compounds **1** and **3**. Since LU-002c is equipped with a vinyl sulfone warhead and Ac-LAE-EK contains an epoxyketone, both warheads should be evaluated to determine their influence on selectivity. As has been shown previously⁷, a basic residue at P3 does increase $\beta 2c/\beta 2i$ selectivity and potency and could thus further increase the potency of P1 Glu containing compounds. These considerations suggest that compounds **2** and **4** would be interesting targets to prepare and evaluate.

Chapter 5 describes the design and synthesis of improved $\beta 1i$ and $\beta 5i$ selective inhibitors. Incorporation of larger groups at P1 resulted in improved selectivity of existing $\beta 5i$ selective inhibitors, which was the expected result given the structural data on murine cCP and iCP in complex with the literature $\beta 5i$ -selective inhibitor, PR-957. Guided by these proteasome-

inhibitor structures, a focussed compound library was assembled featuring a number of bulky, hydrophobic residues at P1, specifically 1-naphthyl, 2-naphthyl, biphenyl, cyclohexyl and adamantyl. Taking the PR-957 structure and substituting the P1 phenylalanine for cyclohexylalanine (Cha) (LU-005i) yielded a compound featuring a five-fold improved β 5i selectivity compared to the parent compound. Substituting the P1 Phe residue in PR-924 (another β 5i selective inhibitor) for Cha resulted in the most selective β 5i inhibitor known to date (LU-015i, 500-fold selective for β 5i over β 5c, Figure 4). In a related study, analogues of the β 1 selective inhibitor NC-001, bearing different Pro residues at P3, were synthesized. Of these, in particular 4,4-F₂-Pro was found to induce β 1i selectivity. Moreover, β 5i selective inhibitors with either Phe or Cha at P1 were found to be selective for β 1i over β 1c. Combining these two findings led to the highly potent and selective β 1i inhibitor LU-001i (Figure 4).

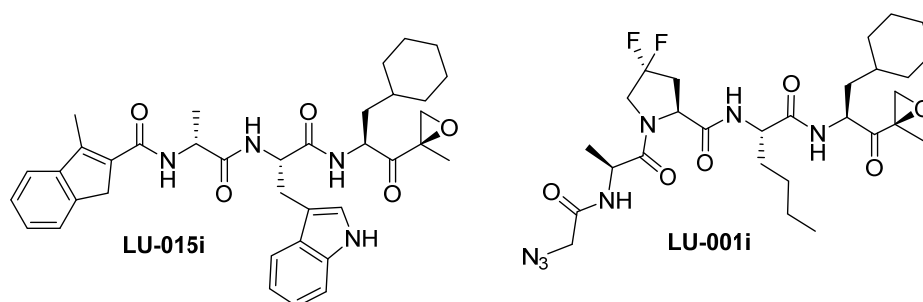


Figure 4. Structures of LU-015i (β 5i-selective) and LU-001i (β 1i selective).

The selective inhibitors described in chapter 5 were used to develop ABPs selective for β 5i or β 1i, as is described in **chapter 6**. LU-001i was converted to Cy5-LU-001i (Figure 5) through copper catalysed azide-alkyne cycloaddition (click) with Cy5-alkyne. In order to obtain a β 5i selective ABP, first the 3-methylindene cap of LU-015i was substituted for azido phenylalanine. However, attachment of a fluorophore at the azide provided ABPs with poor selectivity.

The S2 binding pocket of β 5i (and all other active subunits) is spacious and solvent exposed. This allows the introduction of reporter moieties at the P2 position of subunit-selective inhibitors. Substituting the methyltyrosine at P2 position in the β 5i-selective inhibitor LU-035i for a fluorescently labelled tyrosine residue gave Cy5-LU-035i (Figure 5), which proved to be potent and selective for β 5i. Both Cy5-LU-001i and Cy5-LU-035i can be used to completely block and tag their targeting subunits, with the other subunits remaining uncompromised.

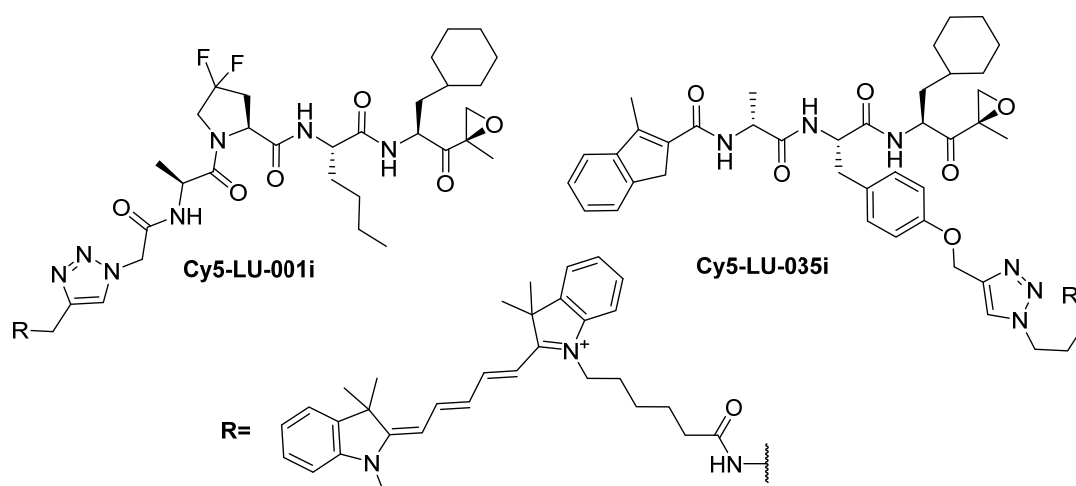


Figure 5. Structures of iCP subunit selective probes Cy5-LU-001i (β 1i selective) and Cy5-LU-035i (β 5i selective).

Chapter 7 details the development of highly selective β 5c targeting inhibitors. Now, crystal structures of murine cCP and iCP in complex with PR-957 guided the design of β 5c selective inhibitors. In this study, a focussed library of compounds, containing different bulky amino acids at the P3 position of the otherwise unchanged N₃Phe-xxx-Phe-Leu-EK sequence was prepared and evaluated. The compound featuring a Cha residue at P3 proved to be a low nanomolar β 5c inhibitor with some ten-fold selectivity for β 5c over β 5i. Various other compounds also proved to be β 5c selective, but were considerably less potent. Since it was previously established that P1 Ala is well tolerated by β 5c but not by β 5i (see chapter 4), a series of compounds was synthesized bearing an Ala at P1 and bulky amino acids at P3. The compound with Cha at P3 and Ala at P1 showed impeccable β 5c over β 5i selectivity, although β 2c/ β 2i are also targeted. At the same time, it was noted that compounds bearing a P3 biphenylalanine (BiPhe) are highly disfavoured by β 2c/ β 2i. Therefore, bicyclohexylalanine (BiCha, synthesized by hydrogenation of BiPhe, thus yielding a mixture of *cis/trans*-isomers – something to resolve as well in the future) was incorporated at P3 together with Ala at P1. The resulting compound (LU-005c) proved to be highly β 5c selective (over β 5i), did not target β 2c/ β 2i and can thus be considered as the most β 5c selective inhibitor known to date (Figure 6). Unfortunately, while LU-005c displayed high potency and β 5c selectivity in lysates, its *in situ* potency is drastically lower. Arguably, the compound is too lipophilic to cross the cell membrane. Substitution of the P4 azidophenylalanine residue by Leu, which was then N-capped with a 2-morpholino acetate moiety, resulted in compound LU-015c. Although this compound showed reduced selectivity compared to LU-005c, it showed increased cell permeability and allows full blockage of β 5c without inhibition of other subunits. Introduction of a BODIPY(FL) fluorophore at the P2 position of LU-015c yielded the β 5c-selective ABP, (BODIPY(FL)-LU-015i), with good selectivity for β 5c over β 5i, however, accompanied by significant β 2c/ β 2i labelling.

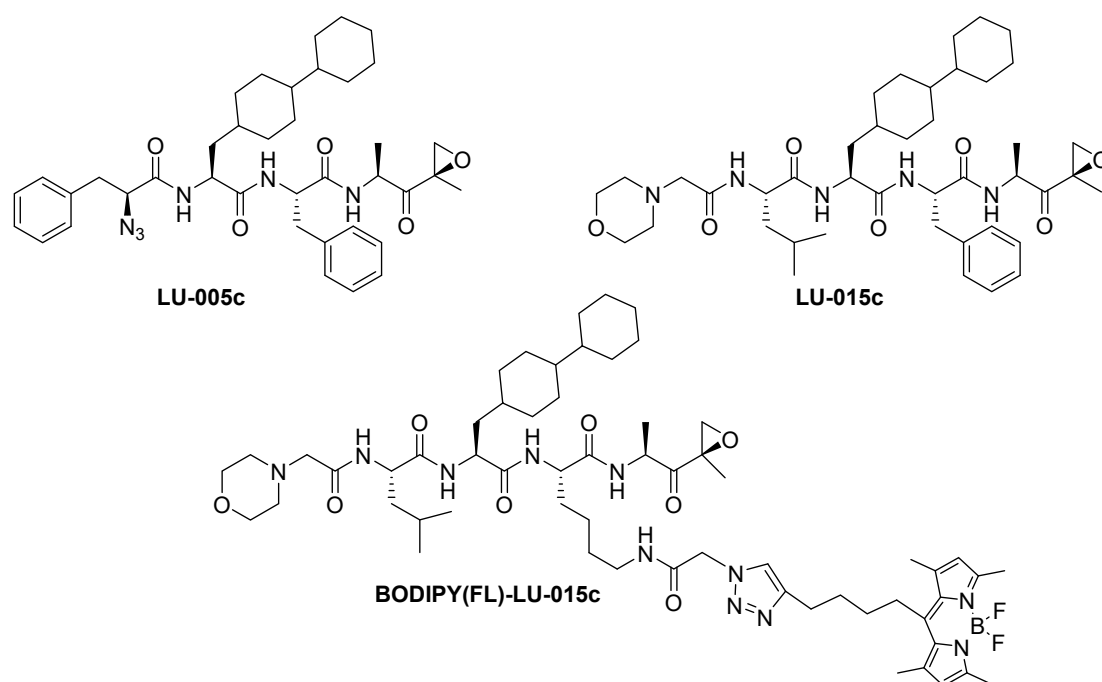


Figure 6. Structures of $\beta 5c$ selective inhibitors LU-005c and LU-015c and $\beta 5c$ selective ABP BODIPY(FL)-LU-015c

Chapter 8 describes the development of a potent, highly selective $\beta 1c$ inhibitor. From the systematic study described in chapter 4 it became apparent that $\beta 1c$ can be selectively targeted by the P1 Asp bearing compound Ac-PAD-EK (Figure 7). However, the apparent IC_{50} value in Raji lysate was rather high (1.4 μM for $\beta 1c$, >100 μM for all other subunits). Therefore, Asp epoxyketone was incorporated at P1 in the highly optimized $\beta 1$ targeting sequence of NC-001, resulting in compound LU-001c (Figure 7). The P4 residues (Ala) and extended P2 residues (Nle) may provide additional interactions and stabilization of the inhibitor, thereby enhancing the potency of LU-001c compared to Ac-PAD-EK. Indeed, the apparent IC_{50} value of LU-001c was found to be 20-fold lower (0.07 μM), while all other subunits remained unmodified up to 100 μM concentrations. LU-001c is equipped with a N-terminal azide moiety, which enabled the attachment of BODIPY-FL using click chemistry. In this way the highly potent and $\beta 1c$ targeting ABP BODIPY(FL)-LU-001c (Figure 7) was obtained, which can be used to completely block $\beta 1c$, without modifying other active proteasome subunits.

At neutral pH, the carboxylic acid moiety of LU-001c is negatively charged, rendering this compound cell impermeable thus precluding its use in intact cells. To overcome this limitation, a prodrug approach could be employed in which the carboxylic acid is protected as an ester. After cell membrane penetration, the ester protecting group is expected to be hydrolysed by esterases thereby liberating the active inhibitors.⁸

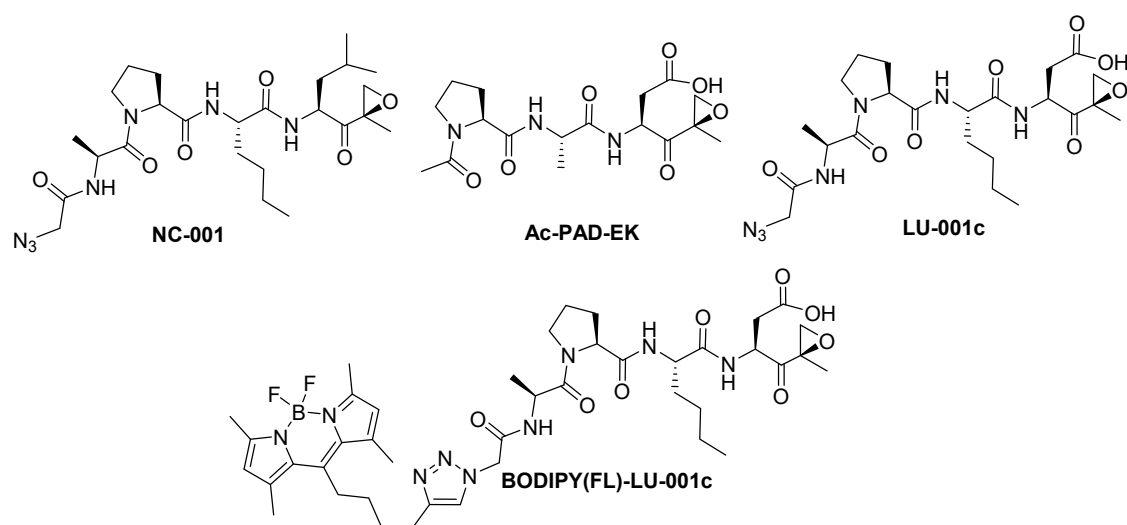
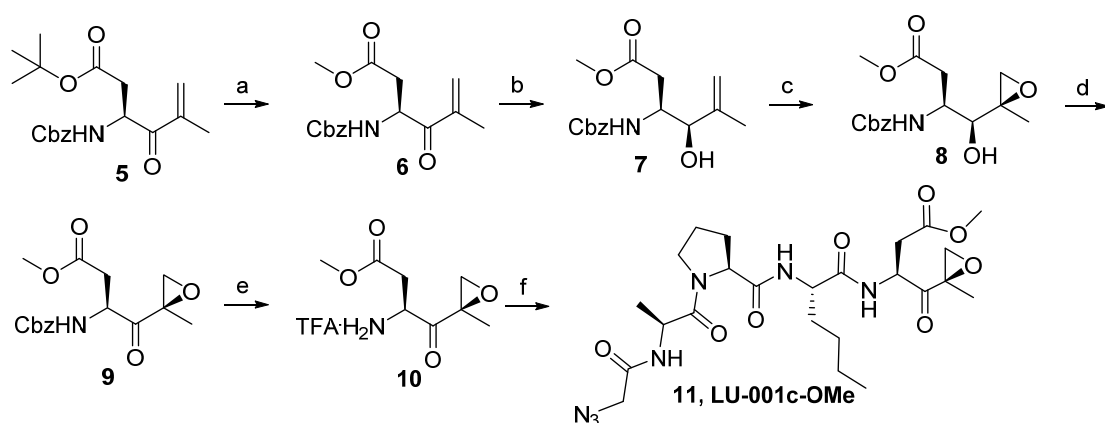


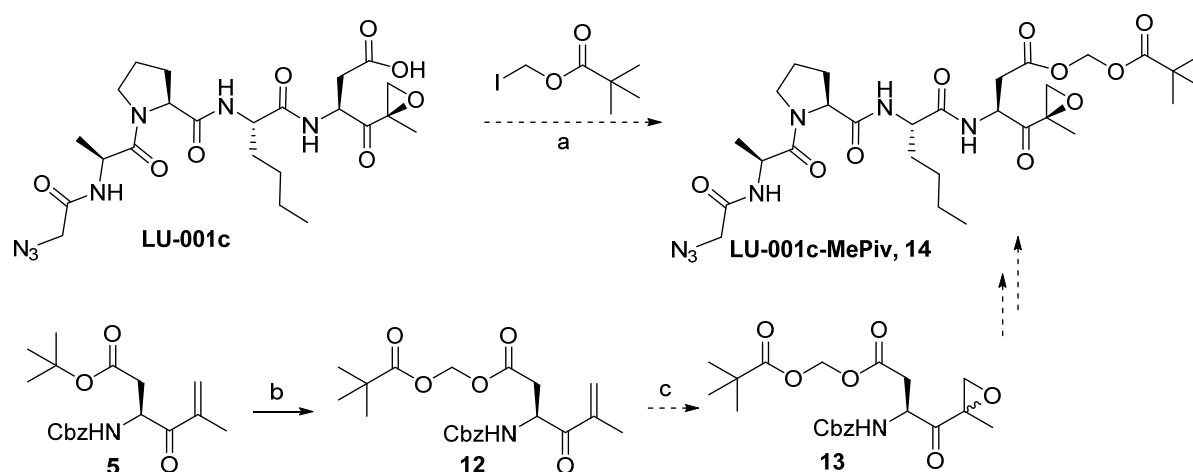
Figure 7. Structures of NC-001, Ac-PAD-EK, LU-001c and BODIPY(FL)-LU-001c

To explore this strategy, a methyl ester analogue of LU-001c was synthesized. For this, *tert*-butyl ester protected building block **5** was deprotected using TFA and the resulting carboxylic acid was converted to methyl ester **6** (Scheme 1). Luche reduction provided alcohol **7**, which was epoxidized to yield compound **8** as a mixture of two diastereomers, which could be separated using column chromatography. The major isomer was oxidized to provide epoxyketone **9**, which was hydrogenated to remove the Cbz protecting group. Finally, azide coupling provided compound **11**. The minor diastereomer of compound **8** was also taken further in the synthesis, however, biological evaluation of the resulting final compound showed impaired activity, indicating wrong epoxyketone stereochemistry.



Scheme 1. Synthesis of LU-001c-OMe (**11**). Reagents and conditions: a. 1. TFA; 2. DMAP, EDC, MeOH, 43%; b. $\text{CeCl}_3 \cdot 7\text{H}_2\text{O}$, NaBH_4 , MeOH, 0°C , 79%; c. $\text{VO}(\text{acac})_2$, $t\text{BuOOH}$, DCM, 0°C , 22%; d. DMP, DCM, 0°C , 70%; e. TFA, Pd/C, MeOH, H_2 ; f. $\text{N}_3\text{Gly-Ala-Pro-Nle-NHNH}_2$, $t\text{BuONO}$, HCl, DiPEA, DMF, -30°C , 18%.

Evaluation of LU-001c-OMe **11** in Raji lysates showed loss of selectivity and reduced potency for β 1c (IC_{50} : β 1c 0.46 μ M; β 1i: 0.95 μ M) indicating that hydrolysis of the methyl ester does not occur in lysates. Unfortunately, also in living RPMI-8226 cells the methyl ester is not hydrolysed, even not after a three hour treatment as is indicated by the high IC_{50} value for both β 1c/ β 1i (both 10 μ M). Nevertheless, LU-001c was found to be completely cell impermeable, indicating that protecting the carboxylic acid as ester does improve cell permeability. Possibly, the methyl ester is too hindered for esterase-mediated hydrolysis. In literature studies, (acyloxy)alkyl esters have been used to overcome the slow cleavage rate of alkyl ester β -lactam antibiotics.⁹ Cleavage of (acyloxy)alkyl esters is initiated at the distal ester moiety, followed by spontaneous elimination of the 'central' aldehyde providing the free carboxylic acid. To investigate (acyloxy)alkyl esters as prodrugs in β 1c inhibitors, the methyl pivalate ester (MePiv) can be taken as starting point (Scheme 2). The *tert*-butyl moiety provides additional hydrophobicity, which may increase cell permeability. The additional steric bulk may also prevent proteasome inhibition by the unprocessed compound. It has been attempted to perform a Luche reduction of compound **12**, however this proved to be unsuccessful. Therefore, it is proposed to directly epoxidize **12** after which the resulting mixture of diastereomers may be separated during final HPLC purification.¹⁰ Alternatively, LU-001c-MePiv **14** may be synthesized by alkylation of LU-001c with iodomethyl pivalate (Scheme 2).



Scheme 2. Proposed synthesis of LU-001c-MePiv. Reagents and conditions: a. DiPEA, DCM or DMF; b. 1. TFA; 2. Iodomethylpivalate, DiPEA, DCM; c. H₂O₂, H₂O, benzonitrile, DiPEA, MeOH, 0-4 °C.

The presence of a basic residue at P1, which may be accompanied by another basic residue at P3, in proteasome inhibitors induces $\beta 2c/\beta 2i$ selectivity. LU-102 (P1: Phe(4CH₂NH₂)) is the most potent and cell permeable $\beta 2c/\beta 2i$ selective inhibitor known to date, but shows a 30-fold increased apparent IC₅₀ value in living cells compared to cell lysates. This is likely caused by the positive charge on the benzylamine moiety, which impairs cell permeability. Introduction of an amine moiety with a pK_a value closer to physiological pH will lead to a less charged inhibitor, possibly resulting in an improved cell permeability. **Chapter 9** describes the synthesis and evaluation of compounds with various lysine analogues with reduced pK_a values at P1 and/or P3. In addition, histidine was explored as basic residue at P1. Allylic (pK_a 9.7) and propargylic (pK_a 8.9) ϵ -amine lysine analogues were synthesized via chiral phase transfer catalyzed alkylation of a glycine-based template. However, while most compounds proved to be $\beta 2c/\beta 2i$ selective, all displayed a severe loss of potency compared to LU-102 (Figure 8A). Interestingly, both P1 allylic and propargylic amine containing compounds showed similar potency and $\beta 2c/\beta 2i$ selectivity, indicating that lower pK_a values are tolerated. It seems therefore that the loss of potency can be explained by the shorter distance between the amine and the peptide backbone in lysine (analogues) compared to arginine in the first generation $\beta 2c/\beta 2i$ selective inhibitors¹¹ and to the benzylamine moiety in LU-102.⁷ It would therefore be desirable to explore more bulky, basic amino acids with a similar distance between the α -carbon and the amino-group as 4-aminomethyl-Phe of LU-102 to ensure optimal positioning of the amine group of the inhibitor and Asp53 of $\beta 2c$ and Glu53 of $\beta 2i$. Examples of such amino acids are homo-lysine analogues containing an allylic- or propargylic amine (Figure 8B).

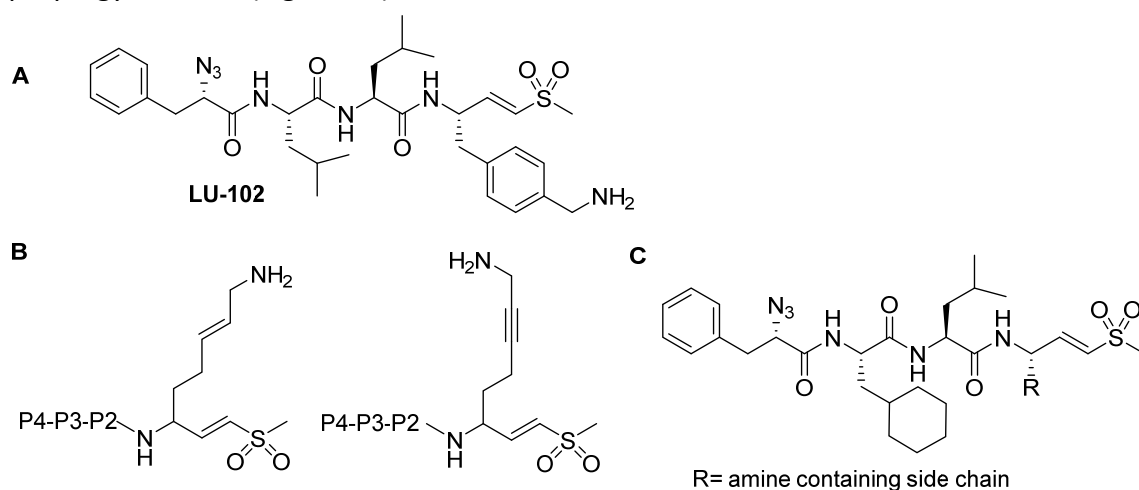


Figure 8. Structures of (proposed) $\beta 2c/\beta 2i$ selective inhibitors. A) Structure of LU-102. B) Structures of homo-lysine analogues with reduced pK_a values compared to lysine. C) Incorporation of cyclohexylalanine at P3 in $\beta 2c/\beta 2i$ selective inhibitors may increase potency and cell permeability.

Since cyclohexylalanine at P3 is well tolerated by $\beta 2c/\beta 2i$ (see chapter 6), its incorporation at the P3 position might improve the potency of $\beta 2$ selective inhibitors. Moreover, the lipophilic nature of the cyclohexyl moiety may increase cell permeability (Figure 8c).

From the panel of proteasome inhibitors with large residues at P3, as described in chapter 7, various compounds appeared to possess some $\beta 2i$ selectivity. This appeared in particular to hold for compounds featuring a *tert*-butyl serine residue at P3. The $\beta 2i$ selective inhibitor LU-002i (see chapter 3) shows good selectivity, however, is only moderately potent. Since LU-002i bears an alanine at P3, and the S3 pocket of $\beta 2c$ and $\beta 2i$ are rather spacious, *tert*-butyl serine at P3 may provide additional interactions, which may enhance the potency for $\beta 2i$ but to a lesser extent for $\beta 2c$ (Figure 9).

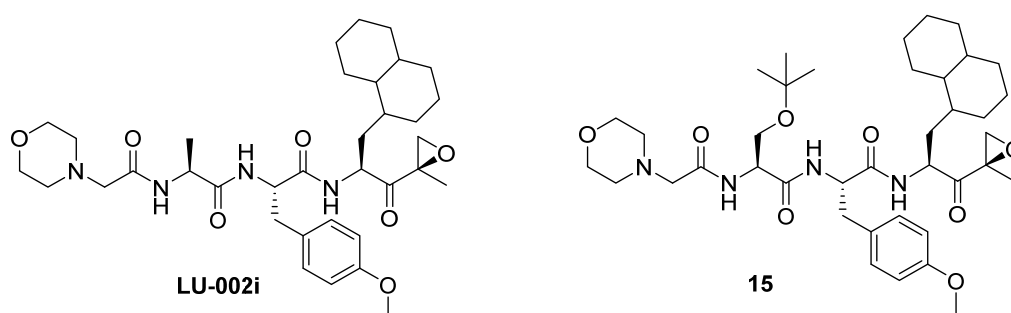


Figure 9. Structure of $\beta 2i$ selective inhibitor LU-002i and proposed inhibitor 15. Incorporation of a P3 *tert*-butyl serine may result in enhanced potency and/or selectivity for $\beta 2i$

During proteasome assembly the formation of pure cCP and iCP is favoured when all six catalytic subunits are expressed. However, also mixed proteasomes (mCPs) have been shown to exist in various tissues. In **chapter 10** a new assay is described, which provides insight in the proteasome composition of a given cell lysate. Since proteasome active sites are all in close proximity to each other, fluorescence resonance energy transfer (FRET) can take place between FRET donor and acceptor ABPs that are bound to separate active sites. When a cell lysate is separated on native PAGE, CPs stay intact and FRET signals emerge after fluorescent imaging of the wet gel slab. The optimal FRET donor-acceptor pair for this purpose was found to be the BODIPY(FL) (donor) and Cy5 (acceptor) fluorophores, which displayed close to 100% high FRET efficiency with minimal background. A set of ten ABPs equipped with either BODIPY(FL) or Cy5 and selective for either $\beta 1c/\beta 1i$, $\beta 2c/\beta 2i$, $\beta 5c/\beta 5i$, $\beta 1c$, $\beta 1i$, $\beta 5c$ or $\beta 5i$ was synthesised (as described in previous chapters). This set of ABPs was complemented by five proteasome inhibitors, each selective for a single catalytic subunit ($\beta 1c$, $\beta 1i$, $\beta 2i$, $\beta 5c$ or $\beta 5i$) and each with sufficient selectivity windows to allow full blockage of their target subunit without inhibition of the other five active subunits. When two of these inhibitors are used together, eight different subunit pairs can be blocked. By selecting the appropriate FRET ABP pair and selective inhibitor pair, FRET signals derived from eight

distinct subunit combinations were obtained. For instance, following inhibition of $\beta 1c$ and $\beta 5i$ using selective inhibitors, $\beta 1c/\beta 1i$ and $\beta 5c/\beta 5i$ targeting ABPs can only label $\beta 1i$ and $\beta 5c$. In case a FRET signal is observed, this indicates the presence of $\beta 1i/\beta 5c$ containing mCPs. CPs contain two β -rings, which do not have to be the same in subunits composition. Proteasome CPs containing different β -rings are termed asymmetric mixed proteasomes (m_a CPs). Using $\beta 1c$, $\beta 1i$, $\beta 5c$ and $\beta 5i$ selective ABPs, proteasomes asymmetric with respect to their $\beta 1$ and $\beta 5$ subunit composition could be visualized. For instance, when a sample is treated with a $\beta 1c$ targeting donor ABP and a $\beta 1i$ targeting acceptor ABP, an observed FRET signal reveals the presence of CPs asymmetric in their $\beta 1$ subunit composition.

The native PAGE FRET assay was used to analyse the proteasome composition of lysates from Raji cells, which constitutively express all six catalytic subunits. Furthermore, lysates of HeLa cells, which express mainly constitutive proteasome subunits were studied in comparison with lysates of HeLa cells in which immunoproteasome subunit expression was induced by a 24 h exposure to IFN- γ . Interestingly, although Raji cells and IFN- γ treated HeLa cells express similar ratios of constitutive proteasome subunit and immunoproteasome subunits, the relative FRET signals derived from mCPs were much higher in Raji cell lysates. This observation indicates that after immunoproteasome induction predominantly iCPs are formed, whereas in cells continuously expressing all six catalytic subunits the levels of mCPs are substantially higher.

The native PAGE FRET assay is not suitable for rapid screening of multiple samples, because running a native gel is rather time consuming. To overcome this limitation, a proteasome-capture-FRET assay can be envisioned, in which the total proteasome content of a cell lysate is captured on an anti- $\alpha 2$ coated 96-well plate (Figure 10). After removal of unbound proteins by washing of the wells, proteasome inhibitors are to be added, followed by the addition of FRET probes. Following removal of the unbound FRET probes by washing steps, the FRET signal is to be measured using a plate reader. Alternatively, anti- β subunit antibodies coated to a 96 well plate can be used to determine the composition of a subpopulation of proteasomes.

Compared to bortezomib, the recently approved (by the FDA) drug ixazomib exhibits a high off-rate for in particular $\beta 5c$ and $\beta 5i$ (see chapter 3). This feature may be at the basis of the reputedly improved pharmacodynamic and pharmacokinetic properties of ixazomib. Ixazomib bears a glycine at P2, thus no amino acid side chains for interaction with the proteasome subunit, which may be the reason behind the comparable higher instability of the ixazomib-proteasome complex. All proteasome subunit have spacious, solvent exposed S2 pockets. This invites the question whether large, sterically demanding moieties at P2 would affect the binding properties of boronic acid proteasome inhibitors.

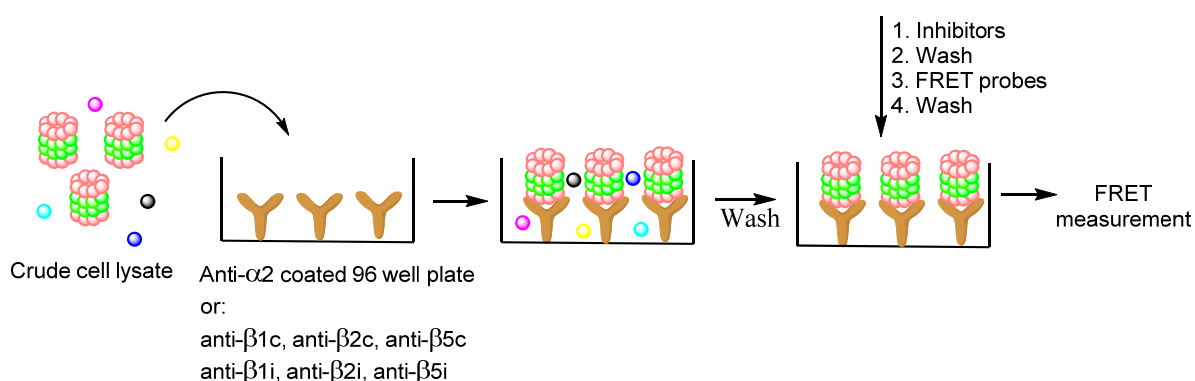


Figure 10. Proposed proteasome-capture-FRET assay

In **Chapter 11** the incorporation of adamantylalanine and carboranylalanine at the P2 position of bortezomib is described. Carboranes are considered to be ‘super-aromatic’, are highly hydrophobic and have been used as phenyl isosters. Besides this, carboranes are currently explored in boron-neutron capture therapy (BNCT), a potential anti-cancer therapy. A new enantioselective synthesis of both amino acids was developed, making use of Ellman’s *N-tert*-butylsulfinamide as the chiral auxiliary and as key step an asymmetric Strecker reaction. Both amino acids could be synthesized as Fmoc building blocks in good yields and with high enantiomeric excess. The incorporation of these amino acids at the P2 position of bortezomib provided adamantezomib and carbortezomib. Both inhibitors displayed similar inhibition profiles and potencies compared to bortezomib, indicating that large residues are well tolerated at P2. However, both adamantezomib and carbortezomib showed a slight preference for β 1i and β 5i compared to β 1c and β 5c. In addition, both inhibitors show higher off-rates for β 5c/ β 5i compared to bortezomib, indicating that large P2 substituents cause destabilization of the boronic acid- β 5 complex. While the off-rate of carbortezomib was found to be lower than ixazomib, adamantezomib displayed a higher off-rate. Moreover, the off-rate of both compounds appeared to be higher for β 5c compared to β 5i, which increases their β 5i selectivity. Therefore, adamantylalanine or carboranylalanine at P2 could be an important design parameter for the development of immunoproteasome selective inhibitors that have similar pharmacodynamic and pharmacokinetic properties as ixazomib.

All proteasome inhibitors described in this thesis target the non-primed site of active β -subunits. However, some inhibitors are bound by both the primed and non-primed sites, such as homobelactosin C¹², UK-101¹³ and α -keto phenylamides¹⁴ (Figure 11). These inhibitors have only a small moiety binding to the primed site (UK-101 and α -keto phenylamides) or to the non-primed site (homobelactosin C). In order to study the substrate preferences of the primed pockets, extended vinyl sulfones are proposed (Scheme 3).

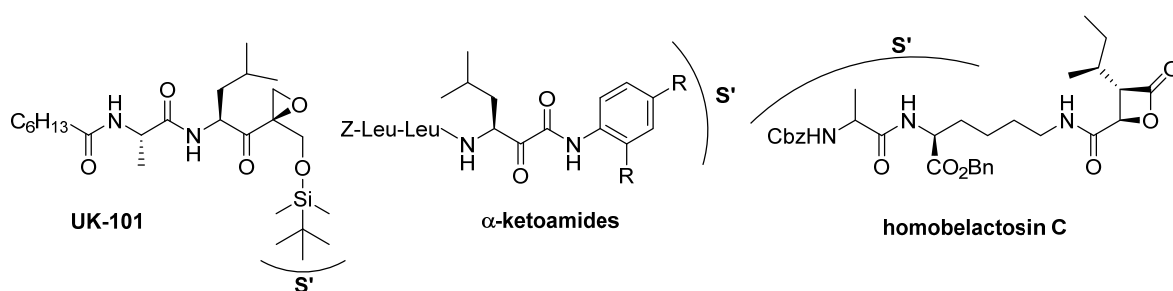
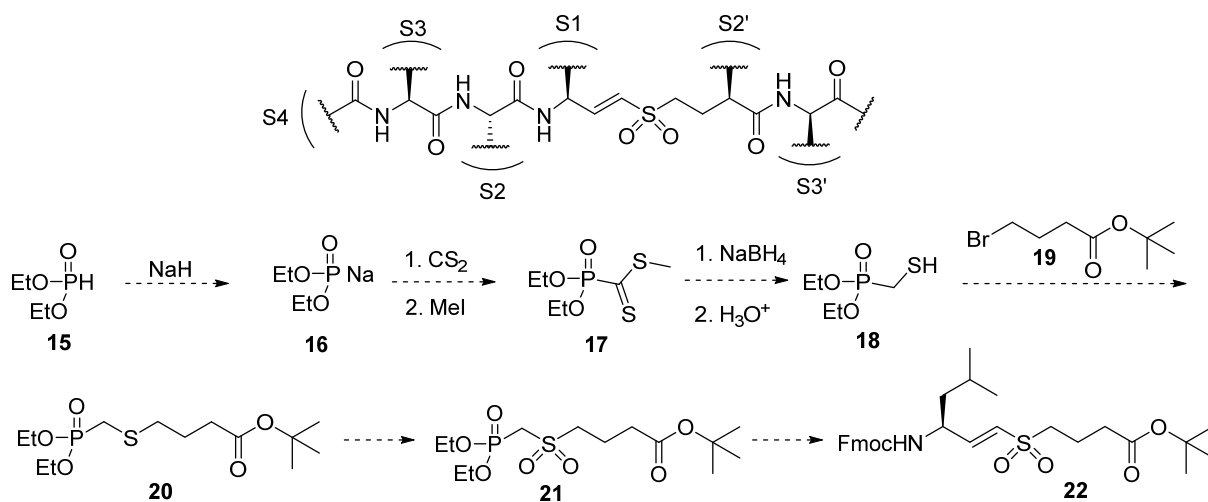


Figure 11. Structures of primed site targeting proteasome inhibitors. S' = primed site.

Epoxyketones are considered to be unsuited for this purpose, since the methyl group does not point into the direction of the primed site.¹⁵ Scheme 3 shows a proposed structure of an extended vinyl sulfone. The amino acids at S1, S2 and S3 can be chosen to tune subunit selectivity. Initially, the S2' residue can be omitted to simplify the synthesis and in a later stage the S2' and S3' can be varied in order to explore the subunit preferences. For initial studies, key building block **22** is required, which bears orthogonally protected amine and carboxylic acids residues for sequential N- and C- terminal functionalization. A putative synthesis of **22** is shown in scheme 3. *In situ* generated sodium diethylphosphonate **16** can be reacted with carbondisulfide followed by the addition of methyl iodide to give compound **17**.¹⁶ Subsequent reduction and acidic hydrolysis¹⁷ will provide free thiol **18**, which can be reacted with bromide **19**. Phosphonate **20** can be oxidized to sulfone **21**, which can be reacted in a Horner-Wadsworth-Emmons reaction with Fmoc-leucinal. Initially, a focussed library with fixed S1-S4 (for instance Ac-LLL-) and varying S2'-S3' substituents could be synthesized and evaluated for their inhibitory potency and subunit selectivity on Raji lysates. In case certain amino acids at S2'-S3' induce subunit selectivity, these may be combined with known subunit-selectivity inducing amino acids at S1-S4. This may result in subunit selective inhibitors with improved potency and selectivity windows compared to existing ones.



Scheme 3. Structure of proposed extended vinyl sulfones and proposed synthesis of key intermediate **22**.

Experimental

Synthetic procedures

General procedures

Acetonitrile (ACN), dichloromethane (DCM), N,N-dimethylformamide (DMF), methanol (MeOH), diisopropylethylamine (DiPEA) and trifluoroacetic acid (TFA) were of peptide synthesis grade, purchased at Biosolve, and used as received. All general chemicals (Fluka, Acros, Merck, Aldrich, Sigma, Iris Biotech) were used as received. Column chromatography was performed on Screening Devices b.v. Silica Gel, with a particle size of 40–63 μm and pore diameter of 60 \AA . TLC analysis was conducted on Merck aluminium sheets (Silica gel 60 F254). Compounds were visualized by UV absorption (254 nm), by spraying with a solution of $(\text{NH}_4)_6\text{Mo}_7\text{O}_{24}\cdot 4\text{H}_2\text{O}$ (25 g/L) and $(\text{NH}_4)_4\text{Ce}(\text{SO}_4)_4\cdot 2\text{H}_2\text{O}$ (10 g/L) in 10% sulphuric acid, a solution of KMnO_4 (20 g/L) and K_2CO_3 (10 g/L) in water, or ninhydrin (0.75 g/L) and acetic acid (12.5 mL/L) in ethanol, where appropriate, followed by charring at ca. 150 $^\circ\text{C}$. ^1H and ^{13}C NMR spectra were recorded on an AV-400 (400 MHz) or on a AV-600 (600 MHz) spectrometer. Chemical shifts are given in ppm (δ) relative to CD_3OD as internal standard. High resolution mass spectra were recorded by direct injection (2 μL of a 2 μM solution in water/acetonitrile 50/50 (v/v) and 0.1% formic acid) on a mass spectrometer (Thermo Finnigan LTQ Orbitrap) equipped with an electrospray ion source in positive mode (source voltage 3.5 kV, sheath gas flow 10, capillary temperature 250 $^\circ\text{C}$) with resolution $R = 60,000$ at m/z 400 (mass range $m/z = 150\text{--}2,000$) and dioctylphthalate ($m/z = 391.28428$) as a "lock mass". The high resolution mass spectrometer was calibrated prior to measurements with a calibration mixture (Thermo Finnigan). LC-MS analysis was performed on a Finnigan Surveyor HPLC system with a Gemini C_{18} 50×4.60 mm column (detection at 200–600 nm), coupled to a Finnigan LCQ Advantage Max mass spectrometer with ESI. The applied buffers were H_2O , ACN and 1.0% aq. TFA. Method: xx \rightarrow xx% MeCN, 13.0 min (0 \rightarrow 0.5 min: 10% MeCN; 0.5 \rightarrow 8.5 min: gradient time; 8.5 \rightarrow 10.5 min: 90% MeCN; 10.5 \rightarrow 13.0 min: 10% MeCN). HPLC purification was performed on a Gilson HPLC system coupled to a Phenomenex Gemini $5\mu\text{m}$ 250×10 mm column and a GX281 fraction collector.

Methyl (S)-3-(((benzyloxy)carbonyl)amino)-5-methyl-4-oxohex-5-enoate (6)

Tert-butyl ester **5** (1.0 mmol, 347 mg) was dissolved in TFA. After 30 minutes the reaction mixture was concentrated and co-evaporated with toluene (3x). The crude product was dissolved in MeOH (10 mL) followed by the addition of DMAP (0.1 mmol, 12 mg) and EDC-HCl (2.0 mmol, 383 mg). After one hour the crude product was concentrated, redissolved in EtOAc, washed with 1M HCl, NaHCO_3 (2x), dried over Na_2SO_4 , filtered and concentrated. The product was purified by column chromatography (5 \rightarrow 20% EtOAc/Pent) and concentrated yielding the title compound (133 mg, 43%). ^1H NMR (400 MHz, Chloroform-*d*) δ 7.33 (d, $J = 3.9$ Hz, 5H), 6.09 (s, 1H), 5.98 – 5.83 (m, 2H), 5.31 (dt, $J = 8.4, 5.7$ Hz, 1H), 5.09 (s, 2H), 3.64 (s, 3H), 2.86 (dd, $J = 15.9, 5.5$ Hz, 1H), 2.70 (dd, $J = 15.9, 5.7$ Hz, 1H), 1.90 (s, 3H). ^{13}C NMR (101 MHz, CDCl_3) δ 198.45, 170.94, 155.64, 141.89, 136.18, 128.53, 128.21, 128.09, 126.29, 67.09, 52.02, 51.47, 37.49, 17.95.

Methyl (3S,4R)-3-(((benzyloxy)carbonyl)amino)-4-hydroxy-5-methylhex-5-enoate (7)

Methyl ester **6** (0.43 mmol, 133 mg) was dissolved in MeOH (4.3 mL) and $\text{CeCl}_3\cdot 7\text{H}_2\text{O}$ (0.69 mmol, 257 mg) was added. When the reaction mixture became clear, it was cooled to 0 $^\circ\text{C}$. NaBH_4 (0.56 mmol, 21 mg) was added portion wise and after 15 minutes the reaction mixture was quenched by the addition of AcOH. The mixture was co-evaporated with toluene and redissolved in EtOAc/ H_2O . The two layers were separated and the water layer was extracted with EtOAc (2x). The combined organic layers were washed with brine, dried over Na_2SO_4 , filtered and concentrated. Further purification was performed by column chromatography (10 \rightarrow 40% EtOAc/Pent) yielding the title compound in a 6:4 mixture of diastereoisomers (105 mg, 79%). ^1H NMR (400

MHz, CDCl₃) δ 7.33 – 7.28 (m, 5H), 5.65 (d, *J* = 8.3 Hz, 0.6 H), 5.45 (d, *J* = 8.2 Hz, 0.4 H), 5.08 – 4.95 (m, 4H), 4.20 – 4.15 (m, 2H), 3.65 – 3.63 (m, 3H), 2.72 – 2.53 (m, 3H), 1.76 (s, 3H). ¹³C NMR (101 MHz, CDCl₃) δ 172.98, 156.07, 144.64, 144.40, 136.44, 128.56, 128.53, 128.20, 128.15, 128.12, 128.04, 112.64, 112.33, 76.52, 75.75, 66.87, 51.97, 51.93, 50.14, 36.94, 33.57, 18.88.

Methyl (3S,4S)-3-(((benzyloxy)carbonyl)amino)-4-hydroxy-4-((R)-2-methyloxiran-2-yl)butanoate (8).

To a solution of alkene **7** (1.0 mmol, 307 mg) in DCM (10 mL) at 0°C, VO(acac)₂ (0.1 mmol, 27 mg) and tBuOOH (5.5 M in decane, 3.0 mmol, 545 μL) were added. After two hours the reaction mixture was concentrated and redissolved in EtOAc, washed with NaHCO₃ (2x), H₂O and brine, dried over Na₂SO₄, filtered and concentrated followed by column chromatography (10→40% EtOAc/Pent) yielding the desired compound (70 mg, 22%). ¹H NMR (400 MHz, CDCl₃) δ 7.35 – 7.28 (m, 5H), 5.74 (d, *J* = 9.3 Hz, 1H), 5.10 (s, 2H), 4.30 – 4.23 (m, 1H), 3.84 (d, *J* = 3.5 Hz, 1H), 3.64 (s, 3H), 2.91 (d, *J* = 4.5 Hz, 1H), 2.75 (s, 1H), 2.57 (dd, *J* = 13.8, 5.3 Hz, 3H), 1.39 (s, 3H). ¹³C NMR (101 MHz, CDCl₃) δ 172.08, 155.79, 136.40, 128.57, 128.22, 128.16, 73.20, 66.93, 57.37, 51.95, 50.06, 49.84, 34.39, 18.38.

Methyl (S)-3-(((benzyloxy)carbonyl)amino)-4-((R)-2-methyloxiran-2-yl)-4-oxobutanoate (9)

Epoxide **8** (0.2 mmol, 70 mg) was dissolved in DCM (2 mL) and cooled to 0°C. Dess-Martin periodane (0.8 mmol, 339 mg) was added as a suspension in DCM. After four hours the reaction mixture was quenched by the addition of NaHCO₃. The two layers were separated and the water layer extracted with DCM. The combined organic layers were washed with NaHCO₃ and brine, dried over Na₂SO₄, filtered and concentrated. The product was further purified by column chromatography (5→20% EtOAc/Pent) obtaining the title compound (44 mg, 70%). ¹H NMR (400 MHz, CDCl₃) δ 7.38 – 7.30 (m, 5H), 5.73 (d, *J* = 7.6 Hz, 1H), 5.11 – 5.04 (m, 2H), 4.61 – 4.56 (m, 1H), 3.67 (s, 3H), 3.15 (d, *J* = 4.6 Hz, 1H), 2.95 – 2.83 (m, 3H), 1.55 (s, 3H). ¹³C NMR (101 MHz, CDCl₃) δ 205.99, 170.57, 155.81, 136.13, 128.65, 128.33, 128.17, 67.18, 59.50, 52.55, 52.26, 51.07, 36.59, 16.99. $[\alpha]_D^{20} = -133^\circ$ (c = 0.6, CHCl₃).

(S)-4-methoxy-1-((R)-2-methyloxiran-2-yl)-1,4-dioxobutan-2-aminium 2,2,2-trifluoroacetate (10)

To a solution of epoxyketone **9** (70 μmol, 23 mg) in MeOH (5 mL) were added TFA (84 μmol, 6.4 μL) and Pd/C (10 mg). After two hours of stirring under a H₂ atmosphere the reaction mixture was filtered, concentrated and co-evaporated with toluene yielding the title compound (16 mg, 76%), which was directly used in the next step.

N₃Gly-Ala-Pro-Nle-Asp(OMe)-EK (11)

To a solution of N₃Gly-Ala-Pro-Nle-NHNH₂ (48 μmol, 19 mg) in DMF (2 mL) at -30°C were added HCl (4M in dioxane, 270 μmol, 68 μL) and tBuONO (110 μmol, 13 μL). After stirring for three hours, deprotected epoxyketone **10** (53 μmol, 16 mg) in DMF and DiPEA (480 μmol, 84 μL) were added. The mixture was allowed to react overnight while warming up to room temperature. The mixture was diluted in DCM, washed with water (2x) and brine, dried over MgSO₄, filtered and concentrated. Column chromatography (1→4% MeOH/DCM) and HPLC (32→36% MeCN/H₂O, 12 min.) yielded the desired compound as a white solid after lyophilisation (4.7 mg, 18%). ¹H NMR (600 MHz, MeOD) δ 4.78 – 4.75 (m, 1H), 4.61 – 4.58 (m, 1H), 4.51 – 4.41 (m, 1H), 4.21 – 4.12 (m, 1H), 3.89 – 3.83 (m, 1H), 3.79 – 3.73 (m, 1H), 3.69 – 3.56 (m, 1H), 3.32 (s, 3H), 3.21 – 3.15 (m, 2H), 2.92 – 2.88 (m, 2H), 2.81 – 2.65 (m, 2H), 2.30 – 2.15 (m, 1H), 2.08 – 1.94 (m, 3H), 1.79 – 1.72 (m, 1H), 1.63 – 1.56 (m, 1H), 1.47 – 1.44 (m, 3H), 1.41 – 1.37 (m, 1H), 1.37 – 1.10 (m, 8H), 0.94 – 0.83 (m, 3H). ¹³C NMR (151 MHz, MeOD) δ 207.08, 174.26, 174.15, 173.24, 171.91, 169.89, 61.77, 61.47, 60.32, 56.29, 54.68, 53.23, 52.58, 52.47, 50.28, 48.65, 36.25, 32.79, 30.44, 28.92, 28.24, 26.02, 23.44, 17.04, 16.80, 14.26. HRMS: calculated C₂₄H₃₈N₇O₈ 552.27819 [M+H]⁺; found 552.27762.

(pivaloyloxy)Methyl (S)-3-(((benzyloxy)carbonyl)amino)-5-methyl-4-oxohex-5-enoate (12).

Tert-butyl ester **5** (2.4 mmol, 820 mg) was dissolved in TFA. After 30 minutes the reaction mixture was concentrated and co-evaporated with toluene (2x). The product was redissolved in DMF (24 mL) and DiPEA (7.2 mmol, 1.23 mL, 3 equiv.) was slowly added. Iodomethyl pivalate (1.16 g, 4.8 mmol, 2 equiv.) was added and the mixture was allowed to react overnight. The reaction mixture was dissolved in EtOAc, washed with 1M HCl (2x), NaHCO₃ (2x), dried over Na₂SO₄, filtered and concentrated. Column chromatography (5→20% EtOAc/Pent) yielded the title compound (854 mg, 89%). ¹H NMR (400 MHz, CDCl₃) δ 7.46 – 7.20 (m, 5H), 6.09 (s, 1H), 5.92 (d, *J* = 8.3 Hz, 1H), 5.88 (s, 1H), 5.70 (s, 2H), 5.35 – 5.28 (m, 1H), 5.09 (s, 2H), 2.92 (dd, *J* = 16.2, 5.7 Hz, 1H), 2.73 (dd, *J* = 16.2, 5.3 Hz, 1H), 1.89 (s, 3H), 1.20 (s, 9H). ¹³C NMR (101 MHz, CDCl₃) δ 197.92, 177.00, 169.33, 155.56, 141.71, 136.08, 128.49, 128.18, 128.04, 126.39, 79.55, 67.09, 51.19, 38.69, 37.14, 26.79, 17.90.

Biochemical methods

General

Lysates of cells were prepared by treating cell pellets with 4 volumes of lysis buffer containing 50 mM Tris pH 7.5, 2 mM DTT, 5 mM MgCl₂, 10% glycerol, 2 mM ATP, and 0.05% digitonin for 15–60 min. Protein concentration was determined using Qubit[®] protein assay kit (Thermo Fisher). All cell lysate labelling experiments were performed in assay buffer containing 50 mM Tris pH 7.5, 2 mM DTT, 5 mM MgCl₂, 10% glycerol, 2 mM ATP. Cell lysate labelling and competition experiments were performed at 37°C. Prior to fractionation on 12.5% SDS-PAGE (TRIS/glycine), samples were boiled for 3 min in a reducing gel loading buffer. The 7.5x10 cm (L x W) gels were run for 15 min at 80V followed by 120 min at 130V. In-gel detection of (residual) proteasome activity was performed in the wet gel slabs directly on a ChemiDoc™ MP System using Cy2 setting to detect BODIPY(FL)-LU-112, BODIPY(FL)-epoxomicin and BODIPY(FL)-NC-001, Cy3 settings to detect BODIPY(TMR)-NC-005-VS and BODIPY(TMR)-epoxomicin and Cy5 settings to detect Cy5-NC-001. When the probes were used as a mixture the following concentrations were used: 100 nM Cy5-NC-001, 30 nM BODIPY(FL)-LU-112, 100 nM BODIPY(TMR)-NC-005-VS, as premixed 10x concentrated cocktail in DMSO which was incubated with cell lysate for 60 min, unless stated otherwise.

Competition experiments in cell lysate

Cell lysates (diluted to 10–15 μg total protein in 9 μL buffer) were exposed to the inhibitors (10x stock in DMSO) at indicated concentrations for 1 h at 37 °C, followed by addition of probe cocktail (10x stock, 1.1 μL) and SDS-PAGE as described in general methods.

Competition experiments in living RPMI-8226 cells

RPMI-8226 were cultured in RPMI-1640 media supplemented with 10% fetal calf serum, GlutaMAX™, penicillin, streptomycin in a 5% CO₂ humidified incubator. 5–8 × 10⁵ cells/mL were exposed to inhibitors for 1 h at 37 °C. Cells were harvested and washed twice with PBS. Cell pellets were treated with lysis buffer on ice for 15 min, followed by centrifugation at 14000 rpm for 5 min. Proteasome inhibition in the obtained cell lysates was determined using the method described above. Intensities of bands were measured by fluorescent densitometry and divided by the intensity of bands in mock-treated extracts. Average values of three independent experiments were plotted against inhibitor concentrations. IC₅₀ (inhibitor concentrations giving 50% inhibition) values were calculated using GraphPad Prism software.

References

1. Screen, M. et al. Nature of pharmacophore influences active site specificity of proteasome inhibitors. *J. Biol. Chem.* **285**, 40125-40134 (2010).
2. Verdoes, M. et al. Acetylene functionalized BODIPY dyes and their application in the synthesis of activity based proteasome probes. *Bioorg. Med. Chem. Lett.* **17**, 6169-6171 (2007).
3. Owicki, J.C. Fluorescence polarization and anisotropy in high throughput screening: perspectives and primer. *J. Biomol. Screen.* **5**, 297-306 (2000).
4. Bachovchin, D.A., Brown, S.J., Rosen, H. & Cravatt, B.F. Identification of selective inhibitors of uncharacterized enzymes by high-throughput screening with fluorescent activity-based probes. *Nat. Biotech.* **27**, 387-394 (2009).
5. Wolf, E.V. et al. A new class of rhomboid protease inhibitors discovered by activity-based fluorescence polarization. *PLoS ONE* **8**, e72307 (2013).
6. Lewallen, D.M. et al. A fluoPol-ABPP PAD2 high-throughput screen identifies the first calcium site inhibitor targeting the PADs. *ACS Chem. Biol.* **9**, 913-921 (2014).
7. Geurink, P.P. et al. Incorporation of non-natural amino acids improves cell permeability and potency of specific inhibitors of proteasome trypsin-like sites. *J. Med. Chem.* **56**, 1262-1275 (2013).
8. Huttunen, K.M., Raunio, H. & Rautio, J. Prodrugs—from serendipity to rational design. *Pharm. Rev.* **63**, 750-771 (2011).
9. Maag, H. in *Prodrugs: Challenges and rewards Part 1* (eds. Stella, V.J. et al.) 703-729 (Springer New York, New York, NY, 2007).
10. Sin, N. et al. Total synthesis of the potent proteasome inhibitor epoxomicin: a useful tool for understanding proteasome biology. *Bioorg. Med. Chem. Lett.* **9**, 2283-2288 (1999).
11. Mirabella, Anne C. et al. Specific cell-permeable inhibitor of proteasome trypsin-like sites selectively sensitizes myeloma cells to bortezomib and carfilzomib. *Chem. Biol.* **18**, 608-618 (2011).
12. Groll, M., Larionov, O.V., Huber, R. & de Meijere, A. Inhibitor-binding mode of homobelactosin C to proteasomes: New insights into class I MHC ligand generation. *Proc. Natl. Acad. Sci.* **103**, 4576-4579 (2006).
13. Ho, Y.K., Bargagna-Mohan, P., Wehenkel, M., Mohan, R. & Kim, K.-B. LMP2-specific inhibitors: chemical genetic tools for proteasome biology. *Chem. Biol.* **14**, 419-430 (2007).
14. Voss, C. et al. α -Keto phenylamides as P1'-extended proteasome inhibitors. *ChemMedChem* **9**, 2557-2564 (2014).
15. Huber, Eva M. et al. Immuno- and constitutive proteasome crystal structures reveal differences in substrate and onhibitor specificity. *Cell* **148**, 727-738 (2012).
16. Grisley, J.D. Notes- the reactions of sodium dialkyl phosphonates with carbonyl sulfide and with carbon disulfide. *J. Org. Chem.* **26**, 2544-2546 (1961).
17. Makomo, H., Masson, S. & Saquet, M. Reductions of phosphonodithioformates: syntheses of β -phosphonyl thiols and hemidithioacetals. *Tetrahedron* **50**, 10277-10288 (1994).

Samenvatting

Dit proefschrift beschrijft de ontwikkeling van nieuwe chemische tools om proteasoom activiteit te kunnen beïnvloeden en zichtbaar te maken. Proteasomen zijn grote eiwit complexen met meerdere katalytische activiteiten die verantwoordelijk zijn voor de afbraak van 80-90% van de eiwitten in eukaryotische cellen. Een eiwit dat afgebroken moet worden, wordt gelabeld met meerdere ubiquitine moleculen die vervolgens worden herkend door proteasomen. Eenmaal ter plaatse aangekomen wordt de ubiquitine-keten verwijderd, waarna het eiwit wordt ontvouwen en afgebroken door de verschillende proteolytische activiteiten in het proteasoom. Alle cellen bevatten zogeheten constitutieve proteasomen (cCPs), welke drie verschillende katalytisch actieve eenheden bevatten, namelijk β 1c (caspase-achtig, knipt na zure aminozuren), β 2c (trypsine-achtig, knipt na basische aminozuren) en β 5c (chymotrypsine-achtig, knipt na hydrofobe aminozuren). Proteasomen breken eiwitten af tot korte peptiden, die verder in de cel afgebroken worden tot losse aminozuren. Een klein deel van de peptiden wordt aan de buitenkant van de cel gepresenteerd aan het immuunsysteem. Dit proces wordt ook wel antigeen-presentatie genoemd. Het immuunsysteem herkent lichaamsvreemde peptiden op de buitenkant van de cel en kan hiertegen een immuunreactie opwekken. Immune cellen en cellen die blootgesteld zijn aan bepaalde ontstekingsfactoren (cytokinen) brengen ook immunoproteasomen (iCPs) tot expressie. In immunoproteasomen zijn β 1c, β 2c en β 5c vervangen door β 1i, β 2i en β 5i. Peptiden die door immunoproteasomen worden geproduceerd, ondergaan verbeterde antigeen-presentatie. Op deze manier speelt het proteasoom een belangrijke rol in het immuunsysteem. Naast constitutieve- en immunoproteasomen bestaan er ook proteasomen waarin eenheden van beide typen in voorkomen, zogenaamde gemengde proteasomen (mCPs). Remming van het proteasoom is cytotoxisch voor sommige tumorcellen en zou (auto)-immuun ziekten kunnen onderdrukken. Om deze redenen is het proteasoom een belangrijk doelwit voor medicijn ontwikkeling binnen de oncologie en de immunologie. Op dit moment worden verschillende proteasoom remmers gebruikt en ontwikkeld voor de behandeling van multipel myeloom (ziekte van Kahler) en mantelcel lymfoom. Ook zijn er immunoproteasoom selectieve remmers in de klinische testfase voor de behandeling van auto-immuun ziekten. Tijdens de

ontwikkeling van deze medicijnen werden de β 5 eenheden beschouwd als de belangrijkste katalytische activiteiten die geremd moeten worden. Echter, het is gebleken dat deze medicijnen ook de andere eenheden (gedeeltelijk) remmen. De laatste jaren heeft onderzoek uitgewezen dat het remmen van ander katalytische actieve eenheden tumorcellen gevoeliger maakt voor β 5 remming en dat dit resistentie tegen proteasoom remmers kan overwinnen. Om deze reden en ook met het doel om de rol van elk type eenheid in de afbraak van eiwitten en antigen-presentatie te kunnen bestuderen, wordt er veel onderzoek gedaan naar eenheid-selectieve proteasoom remmers. Veel proteasoom remmers bestaan uit een elektrofiële val, die covalent aan het katalytische actieve residu van de proteasoom eenheid bindt, en een peptide sequentie, die zorgt voor herkenning en initiële binding van de remmer aan de eenheid. Hiermee samenhangend is er ook veel interesse in methoden die het gelijktijdig meten van alle proteasoom katalytische activiteiten mogelijk maken. Zulke methoden zouden de ontwikkeling van eenheid selectieve remmers en het bepalen van de samenstelling van proteasomen in cellijnen en (zieke) weefsels kunnen ondersteunen en bevorderen. Dit proefschrift beschrijft de ontwikkeling van verschillende eenheid selectieve remmers en 'activity-based probes' (ABPs). De ABPs beschreven in dit proefschrift zijn fluorescent gelabelde verbindingen die covalent en onomkeerbaar binden aan een katalytische actieve eenheden, waardoor de katalytische actieve eenheden zichtbaar gemaakt kunnen worden. Verder beschrijft dit proefschrift een methode om, gebruikmakende van eenheid selectieve ABPs, de activiteit van alle katalytisch actieve constitutieve- en immunoproteasoom eenheden gelijktijdig te kunnen meten. Ook wordt er een methode beschreven om de samenstelling van proteasomen te kunnen bestuderen met als doel om gemengde proteasomen aan te kunnen tonen. De tools die voort zijn gekomen uit het onderzoek beschreven in dit proefschrift kunnen worden gebruikt om zowel de rol van elke katalytisch actieve eenheid als de rol van gemengde proteasomen te bestuderen in bijvoorbeeld antigen-presentatie en kanker. De selectieve remmers kunnen mogelijk gebruikt worden als leidende structuren voor het ontwikkelen van medicijnen voor verdere behandeling van kanker en auto-immuun ziekten.

In **hoofdstuk 1** wordt het katalytische mechanisme van eiwit afbraak door het proteasoom en het concept en mechanisme van proteasoom remmers besproken. In **hoofdstuk 2** wordt een overzicht gegeven van alle mogelijke methoden om proteasoom activiteit te meten. Deze methoden zijn gebaseerd op de hydrolyse van substraten of op het gebruik van ABPs. De methoden zijn en worden gebruikt in de zoektocht naar nieuwe proteasoom remmers, voor het bepalen van proteasoom activiteit en voor het geven van inzicht in de samenstelling van proteasomen.

Hoofdstuk 3 beschrijft de ontwikkeling van een methode om alle zes de katalytische activiteiten van humane constitutieve- en immunoproteasomen gelijktijdig te kunnen meten. Een cocktail van drie ABPs is samengesteld, elk uitgerust met een verschillende fluorescente groep, en met als doelwit $\beta 1c/\beta 1i$ (Cy5-NC-001), $\beta 2c/\beta 2i$ (BODIPY(FL)-LU112) of $\beta 5c/\beta 5i$ (BODIPY(TMR)-NC-005). Op SDS-PAGE verschaftte deze cocktail volledige scheiding van alle humane (immuno)-proteasoom eenheden die gemodificeerd waren met deze ABPs. Deze methode maakt het snel screenen van mogelijk proteasoom remmers mogelijk evenals het snel bepalen van de relatieve hoeveelheid van de zes katalytisch actieve eenheden in cellijnen of monsters afkomstig van patiënten. Door gebruik te maken van deze methode werd aangetoond dat kwaadaardige bloedcellen voornamelijk immunoproteasoom eenheden tot expressie brengen. Dit in tegenstelling tot bijvoorbeeld multipel myeloom cellijnen die ongeveer gelijke hoeveelheden van constitutieve- en immunoproteasoom eenheden tot expressie brengen. Gebaseerd op deze observatie werden acute lymfatische leukemie (ALL) cellen afkomstig van patiënten behandeld met een combinatie van $\beta 5i$ en $\beta 1i$ selectieve remmers, wat zeer cytotoxisch bleek te zijn. Hieruit kan geconcludeerd worden dat het selectief remmen van het immunoproteasoom een goede strategie kan zijn om bijwerkingen van proteasoom remmers te verminderen, omdat de meeste lichaamcellen lage of geen immunoproteasoom expressie hebben.

Hoofdstuk 4 beschrijft een systematische analyse van de substraat specificiteit van humane constitutieve- en immunoproteasomen en gist proteasomen. Voor deze studie werden 18 oligopeptiden uitgerust met een epoxyketon als elektrofiel val gesynthetiseerd. Op de eerste positie ten opzichte van het epoxyketon (P1) werden alanine (Ala), leucine (Leu), asparagine zuur (Asp), glutamine zuur (Glu), fenylalanine (Phe), tyrosine (Tyr), isoleucine (Ile) of valine (Val) ingebouwd; op P2 Ala of Leu; op P3 proline (Pro) of Leu. Gist proteasoom kristallen werden behandeld met deze remmers en kristal structuren werden bepaald. Deze studie verschaftte nuttige inzichten in de substraat specificiteit van humane proteasoom eenheden en leverde ontwerp parameters op voor nieuwe eenheid selectieve remmers. Een van de verrassende vindingen was dat alle eenheden Val en Ile op P1 niet tolereren. Verder werd gevonden dat gist $\beta 1$ en humane $\beta 1c$ Asp op P1 prefereren boven Glu. Zoals verwacht, als gevolg van mutaties in $\beta 1i$ ten opzichte van $\beta 1c$, geeft $\beta 1i$ de voorkeur aan hydrofobe residuen op P1 (Phe of Leu). Ook verschaftte deze studie een verklaring voor de $\beta 1$ selectiviteit van remmers met Pro op P3. Verder werd gevonden dat Ala op P1 in combinatie met Leu op P3 zorgt voor $\beta 5c$ selectiviteit en dat Glu op P1 in combinatie met Leu op P3 resulteert in $\beta 2c$ selectiviteit.

Hoofdstuk 5 beschrijft het ontwerp en de synthese van verbeterde β 1i en β 5i selectieve remmers. Gebaseerd op de kristalstructuren van constitutieve proteasomen en immunoproteasomen van de muis in complex met de β 5i selectieve remmer PR-957 werd de hypothese gesteld dat het inbouwen van grotere groepen op P1 zou leiden tot verbeterde β 5i selectiviteit. Een kleine bibliotheek van verbindingen gebaseerd op PR-957 (P1: Phe) met grote residuen op P1 werd gesynthetiseerd. De verbinding met cyclohexylalanine (Cha) op P1 liet een vijfvoudige toename in selectiviteit zien ten opzichte van PR-957. Het inbouwen van Cha op P1 in PR-924 (een andere β 5i selectieve remmer) resulteerde in de meest selectieve β 5i remmer top op heden bekend (LU-015i). In een gerelateerde studie werden analogen van de β 1 selectieve remmer NC-001 gesynthetiseerd. Eerst werden verschillende Pro analogen ingebouwd op P3, wat leidde tot de ontdekking dat 4,4-F₂-Pro β 1i selectiviteit induceert. Tijdens de ontwikkeling van β 5i selectieve remmers werd gevonden dat verbindingen met Phe en vooral Cha op P1 selectief waren voor β 1i ten opzichte van β 1c. Het combineren van deze vindingen leidde tot de zeer selectieve en potente β 1i remmer met Cha op P1 en 4,4-F₂-Pro op P3 (LU-001i).

In **hoofdstuk 6** worden de β 1i en β 5i selectieve remmers uit hoofdstuk 5 als uitgangspunt genomen voor de ontwikkeling van β 1i en β 5i selectieve ABPs. LU-001i bevatte al een azide functionaliteit en kon daardoor gemakkelijk omgezet worden tot Cy5-LU-001i, door middel van een koper gekatalyseerde azide-alkyn cycloadditie reactie ('click' chemie) met Cy5 alkyne. LU-015i bevatte geen azide en daarom werd er een N-terminale azide ingebouwd, gevolgd door een click-reactie met een fluorofoor. Dit resulteerde echter in ABPs met lage selectiviteit. Daarom werd er een Cy5 fluorofoor op de P2 positie van LU-015i ingebouwd. Dit resulteerde in de potente en β 5i selectieve ABP Cy5-LU-015i. Zowel Cy-LU-001i als Cy5-LU-015i kunnen gebruikt worden om selectief β 1i respectievelijk β 5i te modificeren, zonder dat de andere eenheden gelabeld worden.

Hoofdstuk 7 beschrijft de ontwikkeling van selectieve β 5c remmers. In deze studie werden verschillende grote aminozuren op P3 ingebouwd in de verder onveranderde N₃Phe-xxx-Leu-Leu-EK sequentie. De verbinding met Cha op P3 bleek een laag nanomolaire β 5c remmer te zijn met een tienvoudige selectiviteit voor β 5c ten opzichte van β 5i. Enkele andere verbindingen bleken ook β 5c selectief te zijn, maar deze waren veel minder potent. Zoals beschreven in hoofdstuk 4 wordt Ala op P1 getolereerd door β 5c maar niet door β 5i. Daarom werd een serie verbindingen gemaakt met Ala op P1 en grote aminozuren op P3. De verbinding met Cha op P3 en Ala op P1 liet zeer hoge β 5c selectiviteit zien, hoewel β 2c/ β 2i ook geremd werden. Deze verbindingen lieten ook zien dat biphenylalanine (BiPhe) op P3 niet getolereerd wordt door β 2c/ β 2i. Daarom werd bicyclohexylalanine (BiCha) (gesynthetiseerd door hydrogenatie van BiPhe, resulterend in een mengsel van *cis/trans*-

isomeren) ingebouwd op P3 met Ala op P1. Deze verbinding (LU-005c) liet zeer hoge $\beta 5c$ selectiviteit zien, maar bleek helaas niet bruikbaar in levende cellen. Als gevolg van de zeer hydrofobe eigenschappen kan LU-005c waarschijnlijk de celmembraan niet passeren. Substitutie van de N-terminale N_3Phe door Leu, gevolgd door koppeling van 2-morpholinoacetaat als N-cap resulteerde in LU-015c. Hoewel LU-015c minder selectief bleek dan LU-005c, was LU-015c wel beter cel permeabel en kan deze verbinding gebruikt worden om $\beta 5c$ volledig te remmen zonder dat de andere eenheden beïnvloed worden in zowel levende cellen als in cel extracten. Op de P2 positie van LU-015c werd een BODIPY(FL) fluorofoor ingebouwd, wat resulteerde in een ABP (BODIPY(FL)-LU-015c) die selectief is voor $\beta 5c$ ten opzichte van $\beta 5i$, hoewel $\beta 2c/\beta 2i$ ook gedeeltelijk gemodificeerd werden door deze ABP.

Hoofdstuk 8 beschrijft de ontwikkeling van een potente en zeer selectieve $\beta 1c$ remmer. Vanuit de systematische studie beschreven in hoofdstuk 4 werd het duidelijk dat $\beta 1c$ selectief kan worden geremd door de P1 Asp bevattende verbinding Ac-PAD-EK. Deze verbinding was echter niet heel potent en daarom voor verbetering vatbaar. Om dit te bewerkstelligen werd Asp ingebouwd op P1 in de geoptimaliseerde sequentie van de $\beta 1$ selectieve remmer NC-001, wat resulteerde in de selectieve en veel potentere verbinding LU-001c (20x potenter dan Ac-PAD-EK). Deze verbetering kan verklaard worden door de aanwezigheid van een P4 residu (Ala) en een verlengd P2 residu (norleucine, Nle) in LU-001c vergeleken met Ac-PAD-EK (geen P4 residu en Ala op P2). Deze extra groepen bieden mogelijk extra interacties tussen de remmer en de $\beta 1c$ eenheid waardoor de remmer beter gestabiliseerd wordt. LU-001c is negatief geladen bij fysiologische pH en daarom niet cel permeabel. LU-001c is uitgerust met een N-terminale azide groep en kon daarom gemakkelijk omgezet worden in een ABP door een 'click' reactie met BODIPY(FL)-alkyn. De resulterende ABP (BODIPY(FL)-LU-001c) kon gebruikt worden om $\beta 1c$ volledig te labelen zonder dat andere eenheden gemodificeerd worden.

De aanwezigheid van een basisch residu op P1 of P1 en P3 in proteasoom remmers resulteert in $\beta 2c/\beta 2i$ selectiviteit. LU-102 (P1: 4-aminomethylfenylalanine) is de meest potente en cel permeabele $\beta 2c/\beta 2i$ selectieve remmer die bekend is. LU-102 is echter 30 keer minder potent in levende cellen vergeleken met zijn activiteit in cellysaat. Dit kan waarschijnlijk verklaard worden door de positieve lading van de benzylamine groep die slechte membraan permeabiliteit veroorzaakt. Het inbouwen van basische groepen met een pK_a dicht bij de fysiologische pH zal vermoedelijke resulteren in verbindingen met verbeterde cel permeabiliteit. **Hoofdstuk 9** beschrijft de synthese en evaluatie van verbindingen met verschillende lysine analogen met verlaagde pK_a waarden op P1 en/of P3. Ook werd histidine ingebouwd op P1. Allylisch (pK_a 9.7) en propargylisch (pK_a 8.9) ϵ -amine lysine analogen werden gesynthetiseerd via de chirale fase transfer gekatalyseerde

alkylering van een glycine-gebaseerde template. De meeste gesynthetiseerde verbindingen waren $\beta 2c/\beta 2i$ selectief, echter alle verbindingen waren veel minder potent dan LU-102. Interessant genoeg lieten zowel de P1 allylisch amine als propargylisch amine bevattende verbindingen vergelijkbare potentie zien, wat er op wijst dat lagere pK_a waarden wel getolereerd worden door $\beta 2c/\beta 2i$. Dat deze verbindingen zoveel minder potent zijn kan waarschijnlijk verklaard worden door de kortere afstand tussen de amine en het α -koolstof atoom in de lysine analogen vergeleken met arginine in de eerste generatie $\beta 2c/\beta 2i$ selectieve remmers en de benzylamine groep in LU-102.

Wanneer cellen zowel constitutieve- als immunoproteasoom eenheden tot expressie brengen worden niet alleen zuivere cCPs en iCPs gevormd, maar ook proteasomen die beide type eenheden bevatten. Deze zogenaamde gemengde proteasomen (mCPs) zijn aangetoond in verschillende weefsels. In **hoofdstuk 10** wordt een nieuwe methode beschreven die inzicht geeft in de samenstelling van proteasomen in cellysaat. Omdat de afstand tussen de katalytisch actieve eenheden klein genoeg is kan er fluorescentie resonantie energie transfer (FRET) plaatsvinden tussen FRET donor en acceptor ABPs die gebonden zijn aan verschillende actieve eenheden. Proteasomen blijven intact wanneer een cel extract wordt gescheiden op native PAGE en FRET signalen kunnen zichtbaar gemaakt worden door het fluorescent scannen van de gel. Het optimale FRET donor-acceptor paar voor deze toepassing bleek BODIPY(FL) als donor en Cy5 als acceptor te zijn. Dit FRET-paar liet een FRET efficiëntie zien van bijna 100% en minimale achtergrond. Een set van tien ABPs, uitgerust met BODIPY(FL) of Cy5 en selectief voor $\beta 1c/\beta 2i$, $\beta 2c/\beta 2i$, $\beta 5c/\beta 5i$, $\beta 1c$, $\beta 1i$, $\beta 5c$ of $\beta 5i$ werd ontwikkeld (zoals beschreven in de voorgaande hoofdstukken). Deze set van ABPs werd aangevuld met vijf eenheid selectieve remmers (selectief voor $\beta 1c$, $\beta 1i$, $\beta 2i$, $\beta 5c$ of $\beta 5i$). Met behulp van deze selectieve remmers kunnen acht verschillende eenheid-paren worden geremd, wanneer twee van deze remmers tegelijkertijd worden gebruikt. Door steeds een geschikt FRET ABP paar en twee selectieve remmers te selecteren kunnen FRET signalen van acht verschillende eenheid paren verkregen worden. Bijvoorbeeld, wanneer een monster eerst behandeld wordt met een $\beta 1c$ en $\beta 5i$ selectieve remmer en vervolgens met een FRET ABP paar selectief voor $\beta 1c/\beta 1i$ en $\beta 5c/\beta 5i$, dan worden alleen $\beta 1i$ en $\beta 5c$ gelabeld. Wanneer nu een FRET signaal verkregen wordt, dan duidt dit op de aanwezigheid van $\beta 1i/\beta 5c$ bevattende proteasomen. Proteasomen bevatten twee β -ringen waarvan de samenstelling niet noodzakelijk hetzelfde hoeft te zijn. Proteasomen die verschillende β -ringen bevatten worden ook wel asymmetrische gemengde proteasomen (m_a CPs) genoemd. Gebruikmakend van $\beta 1c$, $\beta 1i$, $\beta 5c$ en $\beta 5i$ selectieve ABPs konden proteasomen die asymmetrisch zijn wat betreft de samenstelling van de $\beta 1$ en $\beta 5$ eenheden zichtbaar gemaakt worden. Bijvoorbeeld, wanneer een monster behandeld wordt met een $\beta 1c$ selectieve donor ABP en

β 1i selectieve acceptor ABP en er wordt een FRET signaal waargenomen, dan duidt dit op proteasomen die asymmetrisch zijn wat betreft de β 1 eenheden. De native PAGE FRET methode is gebruikt om de proteasoom samenstelling van het extract van Raji cellen, die continue alle zes katalytische eenheden tot expressie brengen, te analyseren. Verder is ook het extract van HeLa cellen, die voornamelijk constitutieve proteasoom eenheid tot expressie brengen, geanalyseerd en vergeleken met het extract van HeLa cellen waarin immunoproteasoom eenheid expressie was geïnduceerd door blootstelling aan IFN- γ gedurende 24 uur. Hoewel Raji cellen en IFN- γ behandelde HeLa cellen vergelijkbare ratio's van constitutieve- en immunoproteasoom eenheden tot expressie brengen, waren de relatieve FRET signalen afkomstig van mCPs in Raji cel extract significant hoger. Dit wijst erop dat na inductie van immunoproteasoom expressie voornamelijk iCPs worden gevormd, terwijl in cellen die continue alle zes de eenheden tot expressie brengen meer mCPs gevormd worden.

Vergeleken met bortezomib heeft het recent goedgekeurde (door de FDA) medicijn ixazomib een hoge off-rate voor β 5c en β 5i (zie hoofdstuk 3). Deze eigenschap ligt waarschijnlijk ten grondslag aan de sterk verbeterde farmacodynamische en farmacokinetische eigenschappen van ixazomib ten opzichte van bortezomib. Ixazomib heeft een glycine op P2 en dus geen aminozuur zijketen die kan interacteren met de proteasoom eenheid, wat de reden zou kunnen zijn voor de instabiliteit van het ixazomib-proteasoom complex. Alle proteasoom eenheden hebben grote, aan oplosmiddel blootgestelde S2-pockets. Dit leidde tot de vraag of grote sterische groepen op P2 de binding van boorzuur bevattende proteasoom remmers zou kunnen beïnvloeden. In **hoofdstuk 11** wordt het inbouwen van adamantylalanine en carboranylalanine op de P2 positie van bortezomib beschreven. Carboranen worden beschouwd als 'super-aromatisch', zijn zeer hydrofoob en zijn toegepast als fenyl-groep isosteren. Daarnaast worden carboranen momenteel onderzocht in boor-neutronenvangst therapie (BNCT), een mogelijk anti-kanker therapie. Voor beide aminozuren is een nieuwe enantioselectieve synthese ontwikkeld die gebruik maakt van Ellman's N-*tert*-butylsulfonamide als chiraal hulpmiddel, met als cruciale stap een asymmetrische Strecker reactie. Beide aminozuren werden gesynthetiseerd als Fmoc bouwstenen met goede opbrengsten en in hoge enantiomere overmaat. Het inbouwen van deze aminozuren op de P2 positie resulteerde in adamantezomib en carbortezomib. Beide remmers lieten een met bortezomib overeenkomende proteasoom remming zien, wat er op wijst dat grote substituenten op P2 worden getolereerd. Hoewel, in tegenstelling tot bortezomib, lieten zowel adamantezomib als carbortezomib (geringe) selectiviteit voor β 1i en β 5i ten opzichte van β 1c en β 5c zien. Daarnaast lieten beide remmers een hogere off-rate zien voor β 5c/ β 5i vergeleken met bortezomib, wat er op wijst dat grote substituenten op P2 het β 5 eenheid-

inhibitor complex destabiliseert. Terwijl de off-rate van carbortezomib lager was dan ixazomib, liet adamantezomib een hogere off-rate zien. De off-rate van beide verbindingen bleek hoger voor $\beta5c$ dan voor $\beta5i$, wat de selectiviteit voor $\beta5i$ verhoogt. Derhalve zou het inbouwen van adamantylalanine of carboranylalanine op P2 een belangrijke design parameter kunnen zijn voor de ontwikkeling van immunoproteasoom selectieve remmers met overeenkomende farmacodynamische en farmacokinetische eigenschappen als ixazomib.

List of publications

- 1. Proteasome subunit selective activity-based probes report on proteasome core particle composition in a native-PAGE FRET assay**
de Bruin, G.; Florea, B.I.; Overkleeft, H.S.; *manuscript in preparation.*
- 2. Structure-based design of β 5c selective inhibitors of human constitutive proteasomes**
Xin, B.T.; de Bruin, G.; Huber, E. M.; Besse, A.; Florea, B.I.; Filippov, D.V.; van der Marel, G.A.; Kisselev, A.F; van der Stelt, M.; Driessen, C.; Groll, M.; Overkleeft, H. S.; *manuscript in preparation.*
- 3. Towards β 2 selective inhibitors with reduced basicity**
de Bruin, G.; Wesseling, C.M.J.; Ward, D.J.; van Rooden, E.J.; Florea, B.I.; van der Marel, G. A. Overkleeft, H.S.; *manuscript in preparation.*
- 4. Tools and strategies to monitor and quantify proteasome activities**
de Bruin, G.; Florea, B.I.; Overkleeft, H.S.; *manuscript in preparation.*
- 5. Enantioselective synthesis of adamantylalanine and carboranylalanine and their incorporation into the proteasome inhibitor bortezomib**
de Bruin, G.; Mock, E.; Hoogendoorn, S.; van den Nieuwendijk, A. M. C. H.; Mazurek, J.; van der Marel, G. A.; Florea, B. I.; Overkleeft, H. S., *Chemical Communications* **2016**, 52 (21), 4064-4067.
- 6. 5-Methylpyridin-2-one into peptide vinyl sulfones and peptide epoxyketones is detrimental for proteasome inhibition**
Xin, B.-T.; de Bruin, G.; Plomp, J.-W.; Florea, B. I.; van der Marel, G. A.; Overkleeft, H. S., *European Journal of Organic Chemistry* **2016**, 6, 1132-1144.

- 7. A set of activity-based probes to visualize human (immuno)proteasome activities**
de Bruin, G.; Xin, B. T.; Kraus, M.; van der Stelt, M.; van der Marel, G. A.; Kisselev, A. F.; Driessen, C.; Florea, B. I.; Overkleeft, H. S., *Angewandte Chemistry International Edition* **2016**, 55 (13), 4199-4203.
- 8. Systematic analyses of substrate preferences of 20S proteasomes using peptidic epoxyketone inhibitors**
de Bruin, G.; Huber, E. M.; Heinemeyer, W.; Paniagua Soriano, G.; Overkleeft, H. S.; Groll, M., *Journal of the American Chemical Society* **2015**, 137, 7835-7842.
- 9. The novel β 2-selective proteasome inhibitor LU-102 decreases phosphorylation of I kappa B and induces highly synergistic cytotoxicity in combination with ibrutinib in multiple myeloma cells**
Kraus, J.; Kraus, M.; Liu, N.; Besse, L.; Bader, J.; Geurink, P.; de Bruin, G.; Kisselev, A.; Overkleeft, H.; Driessen, C., *Cancer Chemotherapy and Pharmacology*, **2015**, 76 (2), 383-396.
- 10. The novel β 2-selective proteasome inhibitor LU-102 synergizes with bortezomib and carfilzomib to overcome proteasome inhibitor resistance of myeloma cells**
Kraus, M.; Bader, J.; Geurink, P. P.; Weyburne, E. S.; Mirabella, A. C.; Silzle, T.; Shabaneh, T. B.; van der Linden, W. A.; de Bruin, G.; Haile, S. R.; van Rooden, E.; Appenzeller, C.; Li, N.; Kisselev, A. F.; Overkleeft, H.; Driessen, C., *Haematologica* **2015**, 100 (10), 1350–1360
- 11. Structure-based design of β 1i or β 5i specific inhibitors of human immunoproteasomes**
de Bruin, G.; Huber, E. M.; Xin, B.-T.; van Rooden, E. J.; Al-Ayed, K.; Kim, K.-B.; Kisselev, A. F.; Driessen, C.; van der Stelt, M.; van der Marel, G. A.; Groll, M.; Overkleeft, H. S., *Journal of Medicinal Chemistry* **2014**, 57 (14), 6197-6209.
- 12. Toward understanding induction of oxidative stress and apoptosis by proteasome inhibitors**
Paniagua Soriano, G.; de Bruin, G.; Overkleeft, H. S.; Florea, B. I., *T. Antioxidants & Redox Signaling* **2014**, 21 (17), 2419-2443.
- 13. Activity-based proteasome profiling in medicinal chemistry and chemical biology**
de Bruin, G.; Li, N.; Paniagua, G.; Willems, L.; Xin, B.-T.; Verdoes, M.; Geurink, P.; Linden, W. v. d.; Stelt, M. v. d.; Marel, G. v. d.; Overkleeft, H.; Florea, B., *In Concepts and Case Studies in Chemical Biology*, Wiley-VCH Verlag GmbH & Co. KGaA, **2014**, 177-190

14. Proteasome inhibitors with photocontrolled activity

Hansen, M. J.; Velema, W. A.; de Bruin, G.; Overkleeft, H. S.; Szymanski, W.; Feringa, B. L., *ChemBioChem* **2014**, *15* (14), 2053-2057.

15. Exploring dual electrophiles in peptide-based proteasome inhibitors: carbonyls and epoxides

Xin, B.-T.; de Bruin, G.; Verdoes, M.; Filippov, D. V.; van der Marel, G. A.; Overkleeft, H. S., *Organic & Biomolecular Chemistry* **2014**, *12* (30), 5710-5718.

16. A combined solid- and solution-phase approach provides convenient access to analogues of the calcium-dependent lipopeptide antibiotics

Hart, P. t.; Kleijn, L. H. J.; de Bruin, G.; Oppedijk, S. F.; Kemmink, J.; Martin, N. I., *Organic & Biomolecular Chemistry* **2014**, *12* (6), 913-918.

17. Scalable synthesis of γ -thiolysine starting from lysine and a side by side comparison with δ -thiolysine in non-enzymatic ubiquitination

Merkx, R.; de Bruin, G.; Kruithof, A.; van den Bergh, T.; Snip, E.; Lutz, M.; El Oualid, F.; Ovaa, H., *Chemical Science* **2013**, *4* (12), 4494-4498.

18. Incorporation of non-natural amino acids improves cell permeability and potency of specific inhibitors of proteasome trypsin-like sites

Geurink, P. P.; van der Linden, W. A.; Mirabella, A. C.; Gallastegui, N.; de Bruin, G.; Blom, A. E. M.; Voges, M. J.; Mock, E. D.; Florea, B. I.; van der Marel, G. A.; Driessen, C.; van der Stelt, M.; Groll, M.; Overkleeft, H. S.; Kisselev, A. F., *Journal of Medicinal Chemistry* **2013**, *56* (3), 1262-1275.

19. A concise preparation of the non-proteinogenic amino acid L-kynurenine

Kleijn, L. H. J.; Müskens, F. M.; Oppedijk, S. F.; de Bruin, G.; Martin, N. I., *Tetrahedron Letters* **2012**, *53* (47), 6430-6432.

Curriculum Vitae

Nederlands

Gerjan de Bruin werd geboren op 7 januari 1988 te Nunspeet. Hij behaalde in 2006 het Gymnasium diploma (profiel Natuur & Gezondheid) aan de 'Jacobus Fruijtjer Scholengemeenschap' te Apeldoorn. In datzelfde jaar begon hij aan de bachelor opleiding Scheikunde aan de Universiteit van Utrecht, welke hij in 2009 *cum laude* afrondde. Tijdens de bachelor opleiding heeft hij zich gespecialiseerd in de richting van organische chemie en biochemie.

In 2009 begon hij met de master *Drug Innovation* aan de Universiteit van Utrecht, in het kader waarvan hij twee onderzoekstages voltooide. Het *major research project* voerde hij uit onder de supervisie van dr. N.I. Martin en prof. dr. R.M.J. Liskamp in de vakgroep *Medicinal Chemistry & Chemical Biology* in Utrecht. Tijdens dit onderzoek synthetiseerde hij verschillende cyclische peptiden en onnatuurlijk aminozuren met als doel het ophelderen van het werkingsmechanisme van het peptidisch antibioticum daptomycine. Het *minor research project* heeft hij gedaan bij het Nederlands Kanker Instituut (NKI) in de vakgroep *Cell Biology II* onder de supervisie van dr. R. Merkx en prof. dr. H. Ovaa. In dit onderzoek werd de synthese van di-ubiquitine moleculen door middel van natieve chemische ligatie geoptimaliseerd. In 2011 behaalde hij het Master of Science diploma *cum laude*.

In september 2011 begon hij als promovendus aan de Universiteit Leiden in de vakgroep Bio-organische Synthese. Het onderzoek vond plaats onder supervisie van prof. dr. H.S. Overkleeft, prof. dr. G.A. van der Marel en dr. B.I. Florea. Op verschillende nationale en internationale conferenties werden delen van het onderzoek gepresenteerd. Zo gaf hij mondelinge presentaties op de COST *Chemical Proteomics Meeting* in Berlijn (Duitsland, 2013) en Oxford (Engeland, 2015), op het *Dutch Peptide Symposium* in Utrecht (2014) en op de nationale chemische conferentie CHAINS in Veldhoven (2015). Binnen de Universiteit Leiden gaf hij presentaties als onderdeel van de *Chemical Biology Lectures* (2015) en *This Weeks Discoveries* (2016). In 2015 werd hij genomineerd als 'Onderzoeker van het Jaar' van de Faculteit der Wiskunde en Natuurwetenschappen van de Universiteit Leiden.

Curriculum Vitae

English

Gerjan de Bruin was born on January 7th 1988 in Nunspeet, the Netherlands. He obtained his high school diploma (Gymnasium) at the 'Jacobus Fruijtjer Scholengemeenschap' in Apeldoorn (major Nature & Health) in 2006. In the same year he started with the bachelor's program Chemistry at Utrecht University, which he completed with distinction in 2009. During the bachelor education he specialized in organic chemistry and biochemistry.

In 2009 he started the master's program Drug Innovation at Utrecht University, as part of which he did two research internships. He performed his Major Research Project under the supervision of dr. N.I. Martin and prof. dr. R.M.J. Liskamp in the group of Medicinal Chemistry & Chemical Biology. During this research he synthesized several cyclic peptides and unnatural amino acids with the aim to elucidate the mechanism of action of the peptidic antibiotic daptomycin. Subsequently, he performed his Minor Research Project at the Dutch Cancer Institute (NKI) in the Cell Biology II group under the supervision of dr. R. Merckx and prof. dr. H. Ovaa. In this research the synthesis of di-ubiquitins via native chemical ligation was optimized. In 2011 he obtained his Master of Science degree with distinction.

In September 2011, he started as PhD-student at Leiden University in the Bio-organic Synthesis group. The research was conducted under the supervision of prof. dr. H.S. Overkleeft, prof. dr. G.A. van der Marel en dr. B.I. Florea. Parts of the research have been presented on various conferences. He gave oral presentations at the COST Chemical Proteomics Meeting in Berlin (Germany, 2013) and Oxford (England, 2015), at the Dutch Peptide Symposium in Utrecht (2014) and at the Dutch national chemistry conference CHAINS in Veldhoven (2015). At Leiden University, he gave presentations as part of the Chemical Biology Lectures (2015) and This Weeks Discoveries (2016). In 2015 he was nominated as 'Researcher of the Year' of the Faculty of Science of Leiden University.